SYNAPTIC LOSS AND NEURODEGENERATION

EDITED BY: Marie-Ève Tremblay and Jaichandar (Jai) Subramanian
PUBLISHED IN: Frontiers in Cellular Neuroscience and
Frontiers in Molecular Neuroscience

frontiers Research Topics

ISSN 1664-8714
ISBN 978-2-88966-878-6
DOI 10.3389/978-2-88966-878-6

About Frontiers

Frontiers is more than just an open-access publisher of scholarly articles: it is a pioneering approach to the world of academia, radically improving the way scholarly research is managed. The grand vision of Frontiers is a world where all people have an equal opportunity to seek, share and generate knowledge. Frontiers provides immediate and permanent online open access to all its publications, but this alone is not enough to realize our grand goals.

Frontiers Journal Series

The Frontiers Journal Series is a multi-tier and interdisciplinary set of open-access, online journals, promising a paradigm shift from the current review, selection and dissemination processes in academic publishing. All Frontiers journals are driven by researchers for researchers; therefore, they constitute a service to the scholarly community. At the same time, the Frontiers Journal Series operates on a revolutionary invention, the tiered publishing system, initially addressing specific communities of scholars, and gradually climbing up to broader public understanding, thus serving the interests of the lay society, too.

Dedication to Quality

Each Frontiers article is a landmark of the highest quality, thanks to genuinely collaborative interactions between authors and review editors, who include some of the world's best academicians. Research must be certified by peers before entering a stream of knowledge that may eventually reach the public - and shape society; therefore, Frontiers only applies the most rigorous and unbiased reviews.
Frontiers revolutionizes research publishing by freely delivering the most outstanding research, evaluated with no bias from both the academic and social point of view. By applying the most advanced information technologies, Frontiers is catapulting scholarly publishing into a new generation.

What are Frontiers Research Topics?

Frontiers Research Topics are very popular trademarks of the Frontiers Journals Series: they are collections of at least ten articles, all centered on a particular subject. With their unique mix of varied contributions from Original Research to Review Articles, Frontiers Research Topics unify the most influential researchers, the latest key findings and historical advances in a hot research area! Find out more on how to host your own Frontiers Research Topic or contribute to one as an author by contacting the Frontiers Editorial Office: frontiersin.org/about/contact

SYNAPTIC LOSS AND NEURODEGENERATION

Topic Editors:
Marie-Ève Tremblay, University of Victoria, Canada
Jaichandar (Jai) Subramanian, University of Kansas, United States

Citation: Tremblay, M.-È., Subramanian, J., eds. (2021). Synaptic Loss and Neurodegeneration. Lausanne: Frontiers Media SA. doi: 10.3389/978-2-88966-878-6

Table of Contents

frontiers in Cellular Neuroscience

EDITORIAL
published: 21 April 2021
doi: 10.3389/fncel.2021.681029

Editorial: Synaptic Loss and Neurodegeneration

Jaichandar Subramanian[1]* *and Marie-Ève Tremblay*[2,3,4,5,6]*

[1] Department of Pharmacology & Toxicology, University of Kansas, Lawrence, KS, United States, [2] Axe Neurosciences, Centre de Recherche du CHU de Québec, Université Laval, Québec City, QC, Canada, [3] Neurology and Neurosurgery Department, McGill University, Montréal, QC, Canada, [4] Department of Molecular Medicine, Université Laval, Québec City, QC, Canada, [5] Division of Medical Sciences, University of Victoria, Victoria, BC, Canada, [6] Department of Biochemistry and Molecular Biology, The University of British Columbia, Vancouver, BC, Canada

Keywords: synaptic loss, neurodegenerative diseases, glial cells, astrocytes, microglia, multiphoton imaging, periphery, gut microbiome

Editorial on the Research Topic

Synaptic Loss and Neurodegeneration

Synapse loss is associated with sensory, motor, and cognitive impairments in a variety of neurodegenerative conditions, such as major depressive disorder, schizophrenia, Alzheimer's disease, Huntington's disease, and amyotrophic lateral sclerosis, as well as aging. Loss of excitatory synapses is the strongest correlate for cognitive impairments in Alzheimer's disease. Despite the overwhelming evidence for synapse loss in contributing to disease etiology, very little is known about the mechanisms involved. Introducing disease linked mutations in model organisms has provided an entry point to address the mechanisms of synaptic dysfunction. Though this has led to many exciting discoveries, our current understanding has not reached the threshold required to develop translational approaches to treat synaptic abnormalities. To shine some light on this very important topic, this Research Topic provides a collection of primary research articles, reviews as well as mini reviews, and a perspective article, on different aspects of synaptic dysfunction in the context of neurodegenerative diseases.

The emerging roles of microglia and astrocytes in synaptic loss are first discussed in a series of reviews and mini-reviews. Lee and Chung cover the recent developments on the physiological roles of glial cells at synapses, and propose that synaptic loss can be initiated by a misregulation of normal glial functions. Henstridge et al. (2016) next synthesizes the recent literature on the contribution of glial cells to excitatory/inhibitory imbalance, in the context of prevalent neurodegenerative diseases: Alzheimer's disease, Parkinson's disease, amyotrophic lateral sclerosis, and multiple sclerosis. Focusing on Alzheimer's disease, Ziegler-Waldkirch and Meyer-Luehmann further summarize the roles of microglia and astrocytes in synaptic loss in genetic mouse models, and discuss the current therapeutic avenues. Pons and Rivest also cover important therapeutic avenues of macrophage colony-stimulating factor and its receptor expressed by peripheral monocytes, macrophages and microglia, in Alzheimer's disease, multiple sclerosis, glioma, and brain injury.

In complement, Subramanian et al. review the role of cell-intrinsic calcium dyshomeostasis and cell-extrinsic activities of microglia in the mechanisms underlying synaptic loss in genetic mouse models of Alzheimer's disease. Chang et al. further discuss the involvement of neuronal hyperpolarization-activated cyclic nucleotide-gated channels in major depressive disorder, Parkinson's disease, Alzheimer's disease, amyotrophic lateral sclerosis, and spinal muscular atrophy. Pradhan et al. summarize the evidence for an altered brain derived neurotrophic signaling in amyotrophic lateral sclerosis and provide insights into its modulation as a neuroprotective strategy. Liu et al. additionally expose the current state of knowledge on the pathophysiological roles of

OPEN ACCESS

Edited and reviewed by:
Maria Angeles Arevalo, Cajal Institute (CSIC), Spain

***Correspondence:**
Jaichandar Subramanian
jaichandar@ku.edu
Marie-Ève Tremblay
evetremblay@uvic.ca

Specialty section:
This article was submitted to Non-Neuronal Cells, a section of the journal Frontiers in Cellular Neuroscience

Received: *15 March 2021*
Accepted: *22 March 2021*
Published: *21 April 2021*

Citation:
Subramanian J and Tremblay M-È (2021) Editorial: Synaptic Loss and Neurodegeneration. Front. Cell. Neurosci. 15:681029. doi: 10.3389/fncel.2021.681029

neuron- and glial-derived exosomes in different diseases of the central nervous system and their application as non-invasive biomarkers in the cerebrospinal fluid and peripheral body fluids. In a perspective article, Zhao et al. discuss the interaction between the periphery and the central nervous system, particularly focused on the gut microbiome and its modulation of neurofilaments and synaptic signaling proteins upon bacterial infection.

A series of primary research articles also unravel mechanisms of synaptic loss in different pathological conditions using different model organisms, from drosophila to rodents. In particular, Chen et al. reveal an altered synaptic vesicle release and calcium influx at single presynaptic terminals of cortical neurons in a knockin mouse model of Huntington's disease. Spring et al. provide results from fourteen different drosophila lines expressing spinal muscular atrophy patient-derived mutations, showing a comprehensive modeling of the disease features including locomotor decline. Kriebel et al. propose a novel model of age-related decline in synaptic connectivity, involving a partial inhibition of the mitochondrial respiratory chain, *in vitro* and *in vivo* in rats. Lastly, Hui et al. (2018) uncover partial sex differences in microglial phagocytic activity, excitatory, and inhibitory synaptic density, as well as inhibitory synaptic tone and excitatory synaptic transmission in a mouse model of maternal immune activation.

In conclusion, this special issue provides different perspectives on the neuronal, glial, and peripheral mechanisms involved in synaptic loss across a wide range of neurodegenerative disease conditions, including major depressive disorder, Parkinson's disease, Alzheimer's disease, amyotrophic lateral sclerosis, multiple sclerosis, spinal muscular atrophy, glioma, and brain injury. Novel model organisms also are proposed and shown to provide insights into the mechanisms at play in Huntington's disease, spinal muscular atrophy, cognitive aging, and maternal immune activation, which is associated with the onset of various neuropsychiatric disorders and neurodegenerative diseases in human.

AUTHOR CONTRIBUTIONS

JS and M-ÈT wrote the manuscript. Both authors contributed to the article and approved the submitted version.

FUNDING

M-ÈT is a Canada Research Chair Tier II in Neurobiology of Aging and Cognition. This work was supported by grants from the Canadian Institutes of Health Research (CIHR; Foundation Grant, 353750) and Natural Sciences and Engineering Research Council of Canada (NSERC; Discovery Grant, RGPIN-05308-2014) to M-ÈT and the National Institutes of Health (R01AG064067) to JS.

REFERENCES

Henstridge, C. M., Pickett, E., and Spires-Jones, T. L. (2016). Synaptic pathology: a shared mechanism in neurological disease. *Ageing Res.* Rev. 28, 72–84. doi: 10.1016/j.arr.2016.04.005

Hui, C., St-Pierre, A., El Hajj, H., Remy, Y., Hébert, S. S., Luheshi, G. N., et al. (2018). Prenatal immune challenge in mice leads to partly sex-dependent behavioral, microglial, and molecular abnormalities associated with schizophrenia. *Front. Mol. Neurosci.* 11:13. doi: 10.3389/fnmol.2018.00013

Conflict of Interest: The authors declare that the research was conducted in the absence of any commercial or financial relationships that could be construed as a potential conflict of interest.

frontiers in Cellular Neuroscience

MINI REVIEW
published: 11 December 2018
doi: 10.3389/fncel.2018.00473

The Role of Glial Cells and Synapse Loss in Mouse Models of Alzheimer's Disease

Stephanie Ziegler-Waldkirch[1,2] *and Melanie Meyer-Luehmann*[1,2]*

[1]*Department of Neurology, Medical Center—University of Freiburg, Freiburg, Germany,* [2]*Faculty of Medicine, University of Freiburg, Freiburg, Germany*

Synapse loss has detrimental effects on cellular communication, leading to network disruptions within the central nervous system (CNS) such as in Alzheimer's disease (AD). AD is characterized by a progressive decline of memory function, cognition, neuronal and synapse loss. The two main neuropathological hallmarks are amyloid-β (Aβ) plaques and neurofibrillary tangles. In the brain of AD patients and in mouse models of AD several morphological and functional changes, such as microgliosis and astrogliosis around Aβ plaques, as well as dendritic and synaptic alterations, are associated with these lesions. In this review article, we will summarize the current literature on synapse loss in mouse models of AD and discuss current and prospective treatments for AD.

Keywords: Alzheimer's disease, amyloid plaques, glial cells, synapse loss, microglia, astrocytes

OPEN ACCESS

Edited by:
Marie-Eve Tremblay,
Laval University, Canada

Reviewed by:
Silvia Di Angelantonio,
La Sapienza University of Rome, Italy
Viola Nordström,
German Cancer Research Center (DKFZ), Germany

***Correspondence:**
Melanie Meyer-Luehmann
melanie.meyer-luehmann@uniklinik-freiburg.de

Received: *18 September 2018*
Accepted: *20 November 2018*
Published: *11 December 2018*

Citation:
Ziegler-Waldkirch S and Meyer-Luehmann M (2018) The Role of Glial Cells and Synapse Loss in Mouse Models of Alzheimer's Disease. Front. Cell. Neurosci. 12:473. doi: 10.3389/fncel.2018.00473

SYNAPSE LOSS IN NEURODEGENERATION

Synapse loss has harmful effects on cellular communication, leading to network disruption in the central nervous system (CNS). The communication of billions of neurons within the mammalian brain generates and controls memory, thoughts and emotions. In a neuronal network with different cells, the transfer of information is coordinated at specialized compartments such as the synapse. Synapses are contact points between two neurons, where they communicate by passing ions or neurotransmitter across the synaptic cleft. Synapses can have excitatory or inhibitory effects on the target cells, depending on the released signals. The formed synapses are not rigid but rather dynamic and can either strengthen, shrink or even get lost. Considering the critical role of synapses under physiological conditions, it is not surprising that a severe loss of synaptic integrity can cause substantial disorders such as neurodegenerative diseases (Dudai and Morris, 2013).

Neurodegenerative diseases are disorders of the CNS or the peripheral nervous system characterized by the progressive structural and functional degeneration of neurons, leading to mental or movement problems. The most common form of neurodegenerative diseases is Alzheimer's disease (AD) which currently affects 46 million people worldwide (Prince, 2015). Over a century ago Alois Alzheimer first described the defining lesions (Stelzmann et al., 1995), the two main hallmarks of AD, extracellular amyloid-β (Aβ) plaques and intraneuronal aggregates of hyperphosphorylated tau protein, so-called neurofibrillary tangles. Aβ is released from the amyloid precursor protein (APP) by cleavage of β- and γ-secretases (Haass, 2004) and accumulates in the extracellular space of the brain to diffuse or dense-core plaques (Serrano-Pozo et al., 2011). Intravital imaging studies of APP transgenic mice confirmed that smaller dense-core plaques can cluster together, thus forming lager plaques (McCarter et al., 2013) that are associated with neuronal and synapse loss (Tsai et al., 2004; Spires et al., 2005), increased neurite curvature (Garcia-Alloza et al., 2006; Meyer-Luehmann et al., 2008), impaired neuronal activity in dendritic segments

(Meyer-Luehmann et al., 2009), dystrophic neurites (D'Amore et al., 2003; Tsai et al., 2004) and the accumulation of glial cells (Bolmont et al., 2008; Meyer-Luehmann et al., 2008; Kuchibhotla et al., 2009; Delekate et al., 2014). However, memory impairments and cognitive decline are most likely caused by synapse dysfunction and synapse loss rather than due to mere neuronal loss or the accumulation of Aβ plaques and neurofibrillary tangles (Terry et al., 1991; Masliah et al., 1994; Koffie et al., 2011). Electron microscopy and immunohistochemical stainings for synaptic markers revealed significant reductions in synaptic density in the cortex and hippocampus (Scheff et al., 1990; Terry et al., 1991; Masliah, 2001). Although the cause of synapse loss has not yet been fully elucidated, most likely both lesions, Aβ and tau, contribute to neurodegeneration.

Besides aging, new genetic risk factors for AD were reported recently in GWAS, such as ApoJ/Clusterin, PICALM, complement receptor 1 (CR1), TREM2 and sialic-binding immunoglobulin (Ig)-like lectin CD33 (Lambert et al., 2009; Naj et al., 2011; Hollingworth et al., 2012; Guerreiro et al., 2013; Jonsson et al., 2013). Interestingly, some of these genes are involved in Aβ production or clearance (Harold et al., 2009; Lambert et al., 2009), or are part of immune-related pathways. During development, synapse elimination was shown to be dependent on microglia phagocytosis that was mediated by C1q and C3 (Stevens et al., 2007). Recently, it was also demonstrated that in young pre-depositing hAPP mice this "developmental synaptic pruning pathway" is activated and leads to synapse loss (Hong et al., 2016).

Aβ plaque formation follows a nucleation-dependent polymerization, where monomers form dimers, oligomers, protofibrils and amyloid fibrils (Harper and Lansbury, 1997; Kumar and Walter, 2011). Aβ peptides are 36–43 amino acids in length, whereas Aβ42 is the most neurotoxic fragment, with the highest affinity to aggregate and represents the main component of senile Aβ plaques. Soluble Aβ oligomers are the most neurotoxic species that have been shown to impair long-term potentiation (LTP) (Walsh et al., 2002; Shankar et al., 2008) and enhance long-term depression (LTD) (Li et al., 2009), resulting in weakening of synapses. LTP has been related to the formation of new dendritic spines, increases of postsynaptic densities and the enlargement of spine heads (Maletic-Savatic et al., 1999; Nägerl et al., 2004). In contrast, LTD has been associated with spine shrinkage and loss (Nägerl et al., 2004). Other studies reported that the non-fibrillar forms of Aβ can affect learned behaviors in rodents (Cleary et al., 2005; Lesné et al., 2006; Freir et al., 2011). Recently, it was demonstrated that lower molecular weight oligomers are highly bioactive molecules that inhibit synaptic plasticity, alter cell-surface receptor levels and induce microglial inflammatory response (Yang et al., 2017). Soluble oligomers extracted from AD brains disrupt LTP and synaptic function *in vitro* and impair cognition when injected into healthy mice *in vivo* (Walsh et al., 2002; Cleary et al., 2005; Shankar et al., 2007). *In vivo* imaging studies revealed a loss of dendritic spines around plaques as a result of altered structural plasticity (Spires et al., 2005), whereas increased spine density and synaptic markers were obtained upon the removal of soluble oligomers (Spires-Jones et al., 2009). Together, these results support the idea that soluble forms of Aβ are toxic to synapses.

In mouse models of AD, synapse loss is primarily found around dense-core Aβ plaques (Koffie et al., 2009), whereas no synapses are lost in the vicinity of diffuse plaques (Masliah et al., 1990), thus indicating that dense-core Aβ plaques release toxic soluble Aβ oligomers into the surrounding tissue (Takahashi et al., 2004; Koffie et al., 2009), leading first to synaptic dysfunction and finally to complete synapse loss. In several mouse models of AD, synapse numbers are significantly decreased compared to non-transgenic control mice already at pre-depositing stages (Hsia et al., 1999; Mucke et al., 2000; Shankar et al., 2009; Harris et al., 2010).

The role of tau in synapse loss is less well established. During the course of AD tau gets hyperphosphorylated and accumulates in the somata and dendrites of neurons (Grundke-Iqbal et al., 1986). The intracellular aggregates of hyperphosphorylated tau form inclusions and neuropil threads, both of which are strongly related to neuronal apoptosis (Spires-Jones et al., 2009). In human AD brains and in mouse models of tauopathy, tangle bearing neurons comprise fewer synapses onto their somata and express less synaptic proteins compared to healthy neurons (Callahan et al., 1999; Ginsberg et al., 2000). The overexpression of mutant P301L in rTg4510 mice led to altered synaptic function and synapse loss (Crimins et al., 2011).

GLIAL CELLS

Neuronal synapse formation is based on the interplay between neurons and glial cells. Microglia, the immune cells of the brain parenchyma, regulate synapse formation (Parkhurst et al., 2013) and synapse engulfment via the complement system, which is part of the innate immune system (Wu et al., 2015). In contrast, astrocytes provide nutrients to neurons, take up and release neurotransmitters and provide structural support for neurons (Verkhratsky et al., 2010; Clarke and Barres, 2013). Oligodendrocytes are myelin-forming cells guaranteeing a fast movement of action potentials through axons. Recently, a new cell population was defined as oligodendrocyte precursor cells or NG2-glia (Dimou and Gallo, 2015). In the hippocampus synaptic transmission occurs between NG2-glia and axons. Furthermore, NG2-glia can receive direct excitatory and inhibitory synaptic input from neurons mediated by the neurotransmitters glutamate and GABA. However, the functional role of this neuron to glia synapse is not yet entirely understood (Lin and Bergles, 2004; Bergles et al., 2010). The discovery of NG2-neuron synapses offers the possibility to further investigate the relationship between NG2-glia and neurons in the brain. Interestingly, during their differentiation step from NG2-glia to more mature stages (oligodendrocytes), these cells lose their synapses with neurons (De Biase et al., 2010). Due to the dearth of data, we will focus in this review more on the role of microglia and astrocytes and synapse loss.

MICROGLIA

Microglia mediated synapse loss, or synapse pruning is an important physiological process for proper brain maturation during development. Understanding microglia function in healthy conditions can further help to get insights into their contribution to synapse loss and dysfunction early in disease. Microglia constantly extend and retract their processes and scan their local environment, thereby exploring the entire brain volume (Nimmerjahn et al., 2005). Several studies confirmed that microglia directly contact synaptic elements, thus affecting many synapses (Tremblay et al., 2010; Paolicelli et al., 2011; Schafer et al., 2012). Recent work has also shown that disruption of microglia function resulted in deficient synaptic pruning that was associated with weak synaptic transmission leading to functional connectivity deficits (Paolicelli et al., 2011; Zhan et al., 2014). Furthermore, this microglia-mediated synaptic elimination was shown to be dependent on neuronal activity (Schafer et al., 2012). In addition, depletion of microglia led to a reduction in motor-learning-dependent synapse formation (Parkhurst et al., 2013), implicating microglia in sculpting synaptic connectivity.

Aβ plaques in human AD brains and in mouse models of AD are surrounded by microglia (Meyer-Luehmann et al., 2008; Serrano-Pozo et al., 2013) with impaired process extension (**Figure 1A**). Microglia cells can be classified into three main types based on their morphology: ramified, hypertrophic and amoeboid. Ramified microglia are found in plaque-free areas of the brain, whereas hypertrophic and amoeboid microglia with short, thick and poorly ramified processes are typically associated with senile plaques (Brawek et al., 2014). Interestingly, microglia are not only the resident monocytes in the brain but are also present in the retina, where Aβ deposits have been reported as well in AD patients and AD mice (Ning et al., 2008; Grimaldi et al., 2018). Similar to the brain, the retina of late-symptomatic AD mice contains less ramified microglia when compared to wildtype (WT) controls (Grimaldi et al., 2018). Recently, with the help of advanced technologies, more microglial phenotypes have been described. By comparing microglia cells from WT and 5xFAD transgenic mice using single-cell RNA-sequencing, disease associated microglia (DAM) co-localizing with Aβ plaques were identified (Keren-Shaul et al., 2017). Though, their precise role in synapse clearance and remodeling requires further investigation (Deczkowska et al., 2018). Moreover, an electron microscopy study defined "dark" microglia that are under steady state conditions rarely present but become prevalent in mouse models with AD pathology. Those "dark" microglia are predominantly active at synapses with condensed, electron-dense cytoplasm and nucleoplasm (Bisht et al., 2016). Ultimately, another study depicted the switch of microglia from a homeostatic to a neurodegenerative phenotype by gene expression analyses (Krasemann et al., 2017). However, the exact function of microglia in the context of AD is still not understood. In any case, they play either a beneficial or detrimental role in AD pathology, including the degradation of Aβ or the stimulation of neurotoxicity through inflammatory cytokine release (Wyss-Coray and Rogers, 2012). Several genes expressed or enriched in microglia appeared to be involved in Aβ clearance, including CD33 (Griciuc et al., 2013). Furthermore, members of the classical-complement-cascade, Clusterin and CR1 have been linked to late onset AD (Jun et al., 2010; Fonseca et al., 2016). The best characterized molecules involved in synapse removal by microglia are components of the complement cascade that is upregulated in AD brains. Furthermore, Aβ and tau aggregates can induce microglial and complement activation (Rogers et al., 1992; Shen et al., 2001). A recent study implicates microglia, complement and immune-related pathways as early mediators

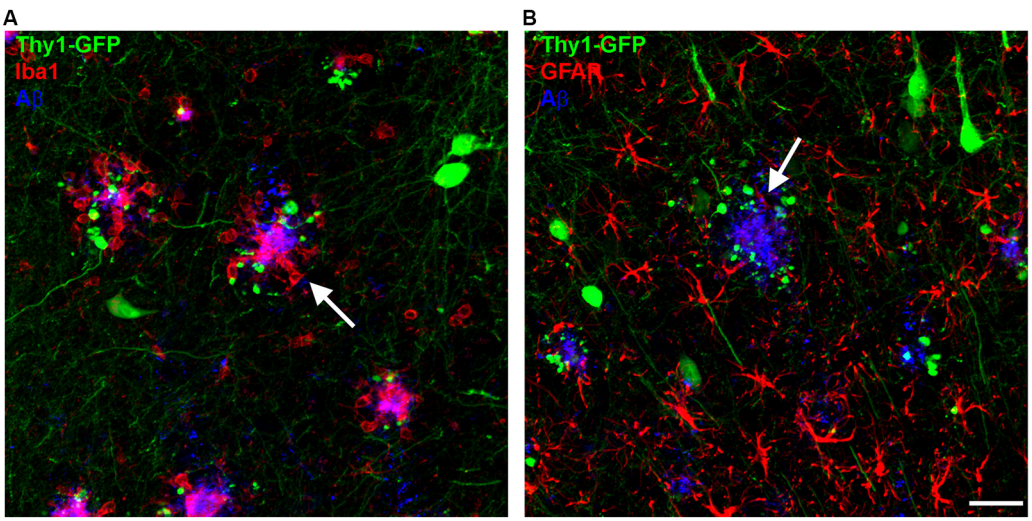

FIGURE 1 | Microglia and astrocytes cluster around amyloid-β (Aβ) plaques (white arrows) in the brains of amyloid precursor protein (APP) transgenic mice. **(A)** Microglia (Iba1, red) can be found closely associated with Aβ plaques (6E10, blue), with dystrophic neurites appearing in the vicinity of Aβ plaques (GFP). **(B)** Reactive astrocytes (GFAP, red) can be found in close proximity to Aβ plaques (6E10, blue). Scale bar represents 10 μm.

of synaptic dysfunction (Hong et al., 2016). In the hippocampus of AD mice, the complement proteins C1q and C3 were upregulated and connected with synapses at pre-depositing stages, causing extended engulfment of synaptic elements (Hong et al., 2016). Furthermore, inhibition of C1q, C3 and CR3 rescued synapse loss and synaptic dysfunction in young hAPP mice indicating that microglia are involved in early synapse loss in pre-depositing mice. In addition, C1q-deficient mice that were crossed to Tg2576 mice displayed less astrogliosis and Aβ plaques, suggesting a detrimental role of the complement pathway (Fonseca et al., 2004). Together, these data indicate that pathways responsible for synaptic pruning during development are activated in AD that eventually lead to synapse loss (Stephan et al., 2012; Hong et al., 2016). Interestingly, depletion of microglia (30%) in 3xTg AD mice improved cognition but did not alter Aβ plaque load, suggesting that microglia might play a role in cognitive dysfunction independent of Aβ pathology (Dagher et al., 2015). Alternatively, it has been proposed that Aβ binds to postsynaptic glutamatergic receptors leading to synapse inactivation (Decker et al., 2010; Li et al., 2011). Microglia might then be recruited to the Aβ tagged synapse and induce the removal of this complex.

ASTROCYTES

Astrocytes represent the most abundant cell type in the brain. They are involved in synapse formation and elimination, synaptic plasticity and activity. Due to their essential role in brain function it is likely that astrocyte dysfunction results in progression of neurodegenerative diseases. Similar to microglia, reactive astrocytes surround senile Aβ plaques in the brain of AD patients and in mouse models of AD. They become reactive as indicated by their hypertrophic processes and increased expression of GFAP (Wisniewski and Wegiel, 1991; Sofroniew, 2009) (**Figure 1B**). On the one hand, astrocytes are able to degrade and phagocytose Aβ and reduce Aβ mediated neurotoxicity (Wyss-Coray et al., 2003), but on the other hand they induce microglia activation by releasing proinflammatory factors (Wyss-Coray and Rogers, 2012). Vice versa, a subtype of reactive astrocytes (A1) that is abundant in the AD brain, is induced by neuroinflammatory microglia (Liddelow et al., 2017). As AD pathology progresses, reactive astrocytes upregulate the adenosine receptor A2A, thereby leading to long-term memory loss due to affected astrocyte-synapse interactions. In addition, conditional genetic removal of the A2A-receptor enhanced memory function in hAPP mice (Orr et al., 2015). These findings suggest that increased levels of astrocytic A2A receptor due to AD pathology might contribute to memory loss. Moreover, resting Ca^{2+} levels are enhanced in AD mice and more frequent Ca^{2+} transients and intracellular Ca^{2+} waves are present, all of which can lead to the release of gliotransmitters (glutamate, ATP, GABA) (Kuchibhotla et al., 2009; Henneberger et al., 2010; Lee et al., 2010; Woo et al., 2012). Furthermore, production of GABA by reactive astrocytes is increased in APPPS1 mice, though inhibition of GABA production or release from reactive astrocytes fully recovers spike probability, synaptic plasticity, learning and memory loss in these mice (Jo et al., 2014).

Further investigations of neuron-glia signaling pathways and their disruption in neurodegenerative diseases are necessary for the development of new successful therapies that are promising due to the early involvement of glia in the disease process.

THERAPEUTIC APPROACHES

Although our knowledge regarding the mechanism underlying AD pathogenesis has improved over the last decades, there is still no cure available. Moreover, open questions concerning memory and synapse loss, as well as gliosis and related neuronal damage, still remain (De Strooper and Karran, 2016).

Most current therapeutic approaches focused on the reduction of Aβ levels and Aβ plaque load by inhibiting or modifying the generation of Aβ. Other attempts tried to target the tau protein instead (Roberson et al., 2007; Ittner et al., 2010). The reduction of endogenous WT murine tau by 50% circumvented synaptic and behavioral deficits in hAPP mice, without affecting Aβ plaque load (Roberson et al., 2007). Although the mechanism by which Aβ-mediated cognitive deficits are prevented without diminishing Aβ levels remains elusive. *In vivo* imaging of 3xTg-AD mice revealed spine loss on dystrophic dendrites positive for hyperphosphorylated tau in areas without plaques (Bittner et al., 2010). Further investigations on the function of tau in mouse models of AD will provide insights regarding the role of tau in AD.

Prime targets for AD therapies are β- and γ-secretase inhibitors. Numerous inhibitors currently undergo clinical trials (May et al., 2011; Lucas et al., 2012; Wang et al., 2014; Yan and Vassar, 2014). Therefore, several studies have tested β- and γ-secretase inhibitors in mouse models of AD. *In vivo* 2-photon imaging allows to explore structural plasticity of synapses in living mice, even for long-time periods (Grutzendler et al., 2002; Tsai et al., 2004; Spires et al., 2005; Fuhrmann et al., 2007; Liebscher and Meyer-Luehmann, 2012; Liebscher et al., 2014) and the effect of administered drugs on the plasticity of spines and synapses can be directly monitored. Two different γ-secretase inhibitors, DAPT and LY450139, were tested in WT and APP-KO mice on structural plasticity of dendritic spines. Bittner et al. (2009) could show that APP-KO mice have an increased spine density and that γ-secretase inhibition reduces the number of spines in an APP-dependent manner. Other studies performed *in vivo* 2-photon imaging and followed dendritic spines and axonal boutons over the course of several weeks in APPS1 mice. Pre- and postsynaptic structures showed an enhanced instability in the vicinity of Aβ plaques (Grutzendler and Gan, 2007; Spires-Jones et al., 2007; Liebscher et al., 2014). Four weeks treatment with a γ-secretase inhibitor (ELN594) efficiently reduced Aβ plaque formation and growth and stabilized spines near plaques (Liebscher et al., 2014).

Unfortunately, the inhibition of BACE1 is known for its mechanism-based side-effects. Conditional deletion of BACE1 in 5xFAD mice resulted in reduced Aβ plaque load and improved synaptic function, determined by LTP and contextual fear conditioning experiments (Hu et al., 2018). However, ablation

of BACE1 in mice is not without issues, as those mice exhibit abnormal astrogenesis, neurogenesis, hyperactivities, impaired axonal growth and altered LTP (Vassar, 2014). Pharmacological inhibition of BACE1 slowed down plaque formation and reduced dendritic spine formation via Seizure Protein 6 in long-term *in vivo* imaging experiments (Filser et al., 2015; Peters et al., 2018; Zhu et al., 2018). Further studies are needed to elucidate how side-effects can be reduced to a minimum e.g., by partial inhibition of BACE1 (Fukumoto et al., 2002; Zhao et al., 2007).

The oligomeric form of Aβ is often considered as the toxic form. Immunotherapy against Aβ oligomers had little effect on synapse loss in the vicinity of Aβ plaques but abolished synapse loss further away from plaques (Dorostkar et al., 2014), suggesting that synapse loss is not primarily mediated by oligomers. In another study, switching off oligomer production resulted in improved cognitive and synaptic impairment (Fowler et al., 2014). However, despite these promising results in preclinical studies, removing toxic Aβ species from the brain with active immunization failed in clinical trials (Hyman, 2011).

To date, it remains an open question whether such Aβ lowering strategies will be successful. Therefore, alternative treatment options should be considered. Mice exposed to an environmental enrichment developed enhanced numbers of new dendritic spines, excitatory synapses and dendritic branches on pyramidal neurons (Mora et al., 2007). Environmental enrichment has also been shown to ameliorate Aβ plaque load, synapse loss and impaired synaptic plasticity (Lazarov et al., 2005; Cracchiolo et al., 2007; Herring et al., 2009; Ziegler-Waldkirch et al., 2018a,b). In a non-pharmacological approach, housing in an environmental enrichment reduced Aβ plaque load by activating phagocytic microglia in 5xFAD transgenic mice (Ziegler-Waldkirch et al., 2018a). Furthermore, adult neurogenesis was revived and cognitive deficits caused by induced Aβ plaque deposits were rescued (Ziegler-Waldkirch et al., 2018a). Future research on the microglia function and dysfunction in CNS disorders, such as pruning, regulating plasticity and neurogenesis will undoubtedly play a predominant role in the search for an effective cure.

CONCLUSION

Besides the physical degeneration of synapses in AD and other neurodegenerative diseases, it is unclear which role glial cells play during the process of synapse loss. Further research will hopefully provide more insights into the role of glial cells and their contribution to synapse loss, in particular at earlier pre-depositing stages when synapses are already vulnerable. Future preclinical treatment approaches should combine pharmacological, non-pharmacological and behavioral studies.

AUTHOR CONTRIBUTIONS

SZ-W and MM-L contributed equally to this work, wrote the manuscript, read and approved the final manuscript.

FUNDING

This work was supported by the Deutsche Forschungsgemeinschaft (DFG) ME 3542/2-1 (MM-L). The article processing charge was funded by the German Research Foundation (DFG) and the University of Freiburg in the funding programme Open Access Publishing.

REFERENCES

Bergles, D. E., Jabs, R., and Steinhäuser, C. (2010). Neuron-glia synapses in the brain. *Brain Res. Rev.* 63, 130–137. doi: 10.1016/j.brainresrev.2009.12.003

Bisht, K., Sharma, K. P., Lecours, C., Sánchez, M. G., El Hajj, H., Milior, G., et al. (2016). Dark microglia: a new phenotype predominantly associated with pathological states. *Glia* 64, 826–839. doi: 10.1002/glia.22966

Bittner, T., Fuhrmann, M., Burgold, S., Jung, C. K. E., Volbracht, C., Steiner, H., et al. (2009). γ-secretase inhibition reduces spine density *in vivo* via an amyloid precursor protein-dependent pathway. *J. Neurosci.* 29, 10405–10409. doi: 10.1523/JNEUROSCI.2288-09.2009

Bittner, T., Fuhrmann, M., Burgold, S., Ochs, S. M., Hoffmann, N., Mitteregger, G., et al. (2010). Multiple events lead to dendritic spine loss in triple transgenic Alzheimer's disease mice. *PLoS One* 5:e15477. doi: 10.1371/journal.pone.0015477

Bolmont, T., Haiss, F., Eicke, D., Radde, R., Mathis, C. A., Klunk, W. E., et al. (2008). Dynamics of the microglial/amyloid interaction indicate a role in plaque maintenance. *J. Neurosci.* 28, 4283–4292. doi: 10.1523/JNEUROSCI.4814-07.2008

Brawek, B., Schwendele, B., Riester, K., Kohsaka, S., Lerdkrai, C., Liang, Y., et al. (2014). Impairment of *in vivo* calcium signaling in amyloid plaque-associated microglia. *Acta Neuropathol.* 127, 495–505. doi: 10.1007/s00401-013-1242-2

Callahan, L. M., Vaules, W. A., and Coleman, P. D. (1999). Quantitative decrease in synaptophysin message expression and increase in cathepsin D message expression in Alzheimer disease neurons containing neurofibrillary tangles. *J. Neuropathol. Exp. Neurol.* 58, 275–287. doi: 10.1097/00005072-199903000-00007

Clarke, L. E., and Barres, B. A. (2013). Emerging roles of astrocytes in neural circuit development. *Nat. Rev. Neurosci.* 14, 311–321. doi: 10.1038/nrn3484

Cleary, J. P., Walsh, D. M., Hofmeister, J. J., Shankar, G. M., Kuskowski, M. A., Selkoe, D. J., et al. (2005). Natural oligomers of the amyloid-β protein specifically disrupt cognitive function. *Nat. Neurosci.* 8, 79–84. doi: 10.1038/nn1372

Cracchiolo, J. R., Mori, T., Nazian, S. J., Tan, J., Potter, H., and Arendash, G. W. (2007). Enhanced cognitive activity—over and above social or physical activity—is required to protect Alzheimer's mice against cognitive impairment, reduce Aβ deposition, and increase synaptic immunoreactivity. *Neurobiol. Learn. Mem.* 88, 277–294. doi: 10.1016/j.nlm.2007.07.007

Crimins, J. L., Rocher, A. B., Peters, A., Shultz, P., Lewis, J., and Luebke, J. I. (2011). Homeostatic responses by surviving cortical pyramidal cells in neurodegenerative tauopathy. *Acta Neuropathol.* 122, 551–564. doi: 10.1007/s00401-011-0877-0

D'Amore, J. D., Kajdasz, S. T., McLellan, M. E., Bacskai, B. J., Stern, E. A., and Hyman, B. T. (2003). *In vivo* multiphoton imaging of a transgenic mouse model of Alzheimer disease reveals marked thioflavine-S-associated alterations in neurite trajectories. *J. Neuropathol. Exp. Neurol.* 62, 137–145. doi: 10.1093/jnen/62.2.137

Dagher, N. N., Najafi, A. R., Kayala, K. M. N., Elmore, M. R. P., White, T. E., Medeiros, R., et al. (2015). Colony-stimulating factor 1 receptor inhibition prevents microglial plaque association and improves cognition in 3xTg-AD mice. *J. Neuroinflammation* 12:139. doi: 10.1186/s12974-015-0366-9

De Biase, L. M., Nishiyama, A., and Bergles, D. E. (2010). Excitability and synaptic communication within the oligodendrocyte lineage. *J. Neurosci.* 30, 3600–3611. doi: 10.1523/JNEUROSCI.6000-09.2010

De Strooper, B., and Karran, E. (2016). The cellular phase of Alzheimer's disease. *Cell* 164, 603–615. doi: 10.1016/j.cell.2015.12.056

Decker, H., Lo, K. Y., Unger, S. M., Ferreira, S. T., and Silverman, M. A. (2010). Amyloid-β peptide oligomers disrupt axonal transport through an NMDA

receptor-dependent mechanism that is mediated by glycogen synthase kinase 3β in primary cultured hippocampal neurons. *J. Neurosci.* 30, 9166–9171. doi: 10.1523/JNEUROSCI.1074-10.2010

Deczkowska, A., Keren-Shaul, H., Weiner, A., Colonna, M., Schwartz, M., and Amit, I. (2018). Disease-associated microglia: a universal immune sensor of neurodegeneration. *Cell* 173, 1073–1081. doi: 10.1016/j.cell.2018.05.003

Delekate, A., Füchtemeier, M., Schumacher, T., Ulbrich, C., Foddis, M., and Petzold, G. C. (2014). Metabotropic P2Y1 receptor signalling mediates astrocytic hyperactivity *in vivo* in an Alzheimer's disease mouse model. *Nat. Commun.* 5:5422. doi: 10.1038/ncomms6422

Dimou, L., and Gallo, V. (2015). NG2-glia and their functions in the central nervous system. *Glia* 63, 1429–1451. doi: 10.1002/glia.22859

Dorostkar, M. M., Burgold, S., Filser, S., Barghorn, S., Schmidt, B., Anumala, U. R., et al. (2014). Immunotherapy alleviates amyloid-associated synaptic pathology in an Alzheimer's disease mouse model. *Brain J. Neurol.* 137, 3319–3326. doi: 10.1093/brain/awu280

Dudai, Y., and Morris, R. G. M. (2013). Memorable trends. *Neuron* 80, 742–750. doi: 10.1016/j.neuron.2013.09.039

Filser, S., Ovsepian, S. V., Masana, M., Blazquez-Llorca, L., Brandt Elvang, A., Volbracht, C., et al. (2015). Pharmacological inhibition of BACE1 impairs synaptic plasticity and cognitive functions. *Biol. Psychiatry* 77, 729–739. doi: 10.1016/j.biopsych.2014.10.013

Fonseca, M. I., Chu, S., Pierce, A. L., Brubaker, W. D., Hauhart, R. E., Mastroeni, D., et al. (2016). Analysis of the putative role of CR1 in Alzheimer's disease: genetic association, expression and function. *PLoS One* 11:e0149792. doi: 10.1371/journal.pone.0149792

Fonseca, M. I., Zhou, J., Botto, M., and Tenner, A. J. (2004). Absence of C1q leads to less neuropathology in transgenic mouse models of Alzheimer's disease. *J. Neurosci.* 4, 6457–6465. doi: 10.1523/JNEUROSCI.0901-04.2004

Fowler, S. W., Chiang, A. C. A., Savjani, R. R., Larson, M. E., Sherman, M. A., Schuler, D. R., et al. (2014). Genetic modulation of soluble Aβ rescues cognitive and synaptic impairment in a mouse model of Alzheimer's disease. *J. Neurosci.* 34, 7871–7885. doi: 10.1523/JNEUROSCI.4749-14.2014

Freir, D. B., Fedriani, R., Scully, D., Smith, I. M., Selkoe, D. J., Walsh, D. M., et al. (2011). Aβ oligomers inhibit synapse remodelling necessary for memory consolidation. *Neurobiol. Aging* 32, 2211–2218. doi: 10.1016/j.neurobiolaging.2010.01.001

Fuhrmann, M., Mitteregger, G., Kretzschmar, H., and Herms, J. (2007). Dendritic pathology in prion disease starts at the synaptic spine. *J. Neurosci.* 27, 6224–6233. doi: 10.1523/JNEUROSCI.5062-06.2007

Fukumoto, H., Cheung, B. S., Hyman, B. T., and Irizarry, M. C. (2002). β-secretase protein and activity are increased in the neocortex in Alzheimer disease. *Arch. Neurol.* 59, 1381–1389. doi: 10.1001/archneur.59.9.1381

Garcia-Alloza, M., Dodwell, S. A., Meyer-Luehmann, M., Hyman, B. T., and Bacskai, B. J. (2006). Plaque-derived oxidative stress mediates distorted neurite trajectories in the Alzheimer mouse model. *J. Neuropathol. Exp. Neurol.* 65, 1082–1089. doi: 10.1097/01.jnen.0000240468.12543.af

Ginsberg, S. D., Hemby, S. E., Lee, V. M., Eberwine, J. H., and Trojanowski, J. Q. (2000). Expression profile of transcripts in Alzheimer's disease tangle-bearing CA1 neurons. *Ann. Neurol.* 48, 77–87. doi: 10.1002/1531-8249(200007)48:1<77::aid-ana12>3.3.co;2-1

Griciuc, A., Serrano-Pozo, A., Parrado, A. R., Lesinski, A. N., Asselin, C. N., Mullin, K., et al. (2013). Alzheimer's disease risk gene CD33 inhibits microglial uptake of amyloid β. *Neuron* 78, 631–643. doi: 10.1016/j.neuron.2013.04.014

Grimaldi, A., Brighi, C., Peruzzi, G., Ragozzino, D., Bonanni, V., Limatola, C., et al. (2018). Inflammation, neurodegeneration and protein aggregation in the retina as ocular biomarkers for Alzheimer's disease in the 3xTg-AD mouse model. *Cell Death Dis.* 9:685. doi: 10.1038/s41419-018-0740-5

Grundke-Iqbal, I., Iqbal, K., Tung, Y. C., Quinlan, M., Wisniewski, H. M., and Binder, L. I. (1986). Abnormal phosphorylation of the microtubule-associated protein tau (tau) in Alzheimer cytoskeletal pathology. *Proc. Natl. Acad. Sci. U S A* 83, 4913–4917. doi: 10.1073/pnas.83.13.4913

Grutzendler, J., and Gan, W.-B. (2007). Long-term two-photon transcranial imaging of synaptic structures in the living brain. *CSH Protoc.* 2007:pdb.prot4766. doi: 10.1101/pdb.prot4766

Grutzendler, J., Kasthuri, N., and Gan, W.-B. (2002). Long-term dendritic spine stability in the adult cortex. *Nature* 420, 812–816. doi: 10.1038/nature01276

Guerreiro, R., Wojtas, A., Bras, J., Carrasquillo, M., Rogaeva, E., Majounie, E., et al. (2013). TREM2 variants in Alzheimer's disease. *N. Engl. J. Med.* 368, 117–127. doi: 10.1056/NEJMoa1211851

Haass, C. (2004). Take five—BACE and the γ-secretase quartet conduct Alzheimer's amyloid β-peptide generation. *EMBO J.* 23, 483–488. doi: 10.1038/sj.emboj.7600061

Harold, D., Abraham, R., Hollingworth, P., Sims, R., Gerrish, A., Hamshere, M. L., et al. (2009). Genome-wide association study identifies variants at CLU and PICALM associated with Alzheimer's disease. *Nat. Genet.* 41, 1088–1093. doi: 10.1038/ng.440

Harper, J. D., and Lansbury, P. T. Jr. (1997). Models of amyloid seeding in Alzheimer's disease and scrapie: mechanistic truths and physiological consequences of the time-dependent solubility of amyloid proteins. *Annu. Rev. Biochem.* 66, 385–407. doi: 10.1146/annurev.biochem.66.1.385

Harris, J. A., Devidze, N., Halabisky, B., Lo, I., Thwin, M. T., Yu, G.-Q., et al. (2010). Many neuronal and behavioral impairments in transgenic mouse models of Alzheimer's disease are independent of caspase cleavage of the amyloid precursor protein. *J. Neurosci.* 30, 372–381. doi: 10.1523/JNEUROSCI.5341-09.2010

Henneberger, C., Papouin, T., Oliet, S. H. R., and Rusakov, D. A. (2010). Long-term potentiation depends on release of D-serine from astrocytes. *Nature* 463, 232–236. doi: 10.1038/nature08673

Herring, A., Ambrée, O., Tomm, M., Habermann, H., Sachser, N., Paulus, W., et al. (2009). Environmental enrichment enhances cellular plasticity in transgenic mice with Alzheimer-like pathology. *Exp. Neurol.* 216, 184–192. doi: 10.1016/j.expneurol.2008.11.027

Hollingworth, P., Sweet, R., Sims, R., Harold, D., Russo, G., Abraham, R., et al. (2012). Genome-wide association study of Alzheimer's disease with psychotic symptoms. *Mol. Psychiatry* 17, 1316–1327. doi: 10.1038/mp.2011.125

Hong, S., Beja-Glasser, V. F., Nfonoyim, B. M., Frouin, A., Li, S., Ramakrishnan, S., et al. (2016). Complement and microglia mediate early synapse loss in Alzheimer mouse models. *Science* 352, 712–716. doi: 10.1126/science.aad8373

Hsia, A. Y., Masliah, E., McConlogue, L., Yu, G. Q., Tatsuno, G., Hu, K., et al. (1999). Plaque-independent disruption of neural circuits in Alzheimer's disease mouse models. *Proc. Natl. Acad. Sci. U S A* 96, 3228–3233. doi: 10.1073/pnas.96.6.3228

Hu, X., Das, B., Hou, H., He, W., and Yan, R. (2018). BACE1 deletion in the adult mouse reverses preformed amyloid deposition and improves cognitive functions. *J. Exp. Med.* 215, 927–940. doi: 10.1084/jem.20171831

Hyman, B. T. (2011). Amyloid-dependent and amyloid-independent stages of Alzheimer disease. *Arch. Neurol.* 68, 1062–1064. doi: 10.1001/archneurol.2011.70

Ittner, L. M., Ke, Y. D., Delerue, F., Bi, M., Gladbach, A., van Eersel, J., et al. (2010). Dendritic function of tau mediates amyloid-β toxicity in Alzheimer's disease mouse models. *Cell* 142, 387–397. doi: 10.1016/j.cell.2010.06.036

Jo, S., Yarishkin, O., Hwang, Y. J., Chun, Y. E., Park, M., Woo, D. H., et al. (2014). GABA from reactive astrocytes impairs memory in mouse models of Alzheimer's disease. *Nat. Med.* 20, 886–896. doi: 10.1038/nm.3639

Jonsson, T., Stefansson, H., Steinberg, S., Jonsdottir, I., Jonsson, P. V., Snaedal, J., et al. (2013). Variant of TREM2 associated with the risk of Alzheimer's disease. *N. Engl. J. Med.* 368, 107–116. doi: 10.1056/NEJMoa1211103

Jun, G., Naj, A. C., Beecham, G. W., Wang, L.-S., Buros, J., Gallins, P. J., et al. (2010). Meta-analysis confirms CR1, CLU, and PICALM as alzheimer disease risk loci and reveals interactions with APOE genotypes. *Arch. Neurol.* 67, 1473–1484. doi: 10.1001/archneurol.2010.201

Keren-Shaul, H., Spinrad, A., Weiner, A., Matcovitch-Natan, O., Dvir-Szternfeld, R., Ulland, T. K., et al. (2017). A unique microglia type associated with restricting development of Alzheimer's disease. *Cell* 169, 1276–1290. doi: 10.1016/j.cell.2017.05.018

Koffie, R. M., Hyman, B. T., and Spires-Jones, T. L. (2011). Alzheimer's disease: synapses gone cold. *Mol. Neurodegener.* 6:63. doi: 10.1186/1750-1326-6-63

Koffie, R. M., Meyer-Luehmann, M., Hashimoto, T., Adams, K. W., Mielke, M. L., Garcia-Alloza, M., et al. (2009). Oligomeric amyloid β associates with postsynaptic densities and correlates with excitatory synapse loss near senile plaques. *Proc. Natl. Acad. Sci. U S A* 106, 4012–4017. doi: 10.1073/pnas.0811698106

Krasemann, S., Madore, C., Cialic, R., Baufeld, C., Calcagno, N., El Fatimy, R., et al. (2017). The TREM2-APOE pathway drives the transcriptional phenotype

of dysfunctional microglia in neurodegenerative diseases. *Immunity* 47, 566.e9–581.e9. doi: 10.1016/j.immuni.2017.08.008

Kuchibhotla, K. V., Lattarulo, C. R., Hyman, B. T., and Bacskai, B. J. (2009). Synchronous hyperactivity and intercellular calcium waves in astrocytes in Alzheimer mice. *Science* 323, 1211–1215. doi: 10.1126/science.1169096

Kumar, S., and Walter, J. (2011). Phosphorylation of amyloid β (Aβ) peptides—a trigger for formation of toxic aggregates in Alzheimer's disease. *Aging* 3, 803–812. doi: 10.18632/aging.100362

Lambert, J.-C., Heath, S., Even, G., Campion, D., Sleegers, K., Hiltunen, M., et al. (2009). Genome-wide association study identifies variants at CLU and CR1 associated with Alzheimer's disease. *Nat. Genet.* 41, 1094–1099. doi: 10.1038/ng.439

Lazarov, O., Robinson, J., Tang, Y.-P., Hairston, I. S., Korade-Mirnics, Z., Lee, V. M.-Y., et al. (2005). Environmental enrichment reduces Aβ levels and amyloid deposition in transgenic mice. *Cell* 120, 701–713. doi: 10.1016/j.cell.2005.01.015

Lee, S., Yoon, B.-E., Berglund, K., Oh, S.-J., Park, H., Shin, H.-S., et al. (2010). Channel-mediated tonic GABA release from glia. *Science* 330, 790–796. doi: 10.1126/science.1184334

Lesné, S., Koh, M. T., Kotilinek, L., Kayed, R., Glabe, C. G., Yang, A., et al. (2006). A specific amyloid-β protein assembly in the brain impairs memory. *Nature* 440, 352–357. doi: 10.1038/nature04533

Li, S., Hong, S., Shepardson, N. E., Walsh, D. M., Shankar, G. M., and Selkoe, D. (2009). Soluble oligomers of amyloid β protein facilitate hippocampal long-term depression by disrupting neuronal glutamate uptake. *Neuron* 62, 788–801. doi: 10.1016/j.neuron.2009.05.012

Li, S., Jin, M., Koeglsperger, T., Shepardson, N. E., Shankar, G. M., and Selkoe, D. J. (2011). Soluble Aβ oligomers inhibit long-term potentiation through a mechanism involving excessive activation of extrasynaptic NR2B-containing NMDA receptors. *J. Neurosci.* 31, 6627–6638. doi: 10.1523/JNEUROSCI.0203-11.2011

Liddelow, S. A., Guttenplan, K. A., Clarke, L. E., Bennett, F. C., Bohlen, C. J., Schirmer, L., et al. (2017). Neurotoxic reactive astrocytes are induced by activated microglia. *Nature* 541, 481–487. doi: 10.1038/nature21029

Liebscher, S., and Meyer-Luehmann, M. (2012). A peephole into the brain: neuropathological features of Alzheimer's disease revealed by *in vivo* two-photon imaging. *Front. Psychiatry* 3:26. doi: 10.3389/fpsyt.2012.00026

Liebscher, S., Page, R. M., Käfer, K., Winkler, E., Quinn, K., Goldbach, E., et al. (2014). Chronic γ-secretase inhibition reduces amyloid plaque-associated instability of pre- and postsynaptic structures. *Mol. Psychiatry* 19, 937–946. doi: 10.1038/mp.2013.122

Lin, S.-C., and Bergles, D. E. (2004). Synaptic signaling between neurons and glia. *Glia* 47, 290–298. doi: 10.1002/glia.20060

Lucas, F., Fukushima, T., and Nozaki, Y. (2012). Novel BACE1 inhibitor, E2609, lowers Aβ levels in the cerebrospinal fluid and plasma in nonhuman primates. *Alzheimers Dement.* 8:P224. doi: 10.1016/j.jalz.2012.05.2022

Maletic-Savatic, M., Malinow, R., and Svoboda, K. (1999). Rapid dendritic morphogenesis in CA1 hippocampal dendrites induced by synaptic activity. *Science* 283, 1923–1927. doi: 10.1126/science.283.5409.1923

Masliah, E. (2001). Recent advances in the understanding of the role of synaptic proteins in Alzheimer's disease and other neurodegenerative disorders. *J. Alzheimers Dis.* 3, 121–129. doi: 10.3233/jad-2001-3117

Masliah, E., Mallory, M., Hansen, L., DeTeresa, R., Alford, M., and Terry, R. (1994). Synaptic and neuritic alterations during the progression of Alzheimer's disease. *Neurosci. Lett.* 174, 67–72. doi: 10.1016/0304-3940(94)90121-x

Masliah, E., Terry, R. D., Mallory, M., Alford, M., and Hansen, L. A. (1990). Diffuse plaques do not accentuate synapse loss in Alzheimer's disease. *Am. J. Pathol.* 137, 1293–1297.

May, P. C., Dean, R. A., Lowe, S. L., Martenyi, F., Sheehan, S. M., Boggs, L. N., et al. (2011). Robust central reduction of amyloid-β in humans with an orally available, non-peptidic β-secretase inhibitor. *J. Neurosci.* 31, 16507–16516. doi: 10.1523/JNEUROSCI.3647-11.2011

McCarter, J. F., Liebscher, S., Bachhuber, T., Abou-Ajram, C., Hübener, M., Hyman, B. T., et al. (2013). Clustering of plaques contributes to plaque growth in a mouse model of Alzheimer's disease. *Acta Neuropathol.* 126, 179–188. doi: 10.1007/s00401-013-1137-2

Meyer-Luehmann, M., Mielke, M., Spires-Jones, T. L., Stoothoff, W., Jones, P., Bacskai, B. J., et al. (2009). A reporter of local dendritic translocation shows plaque- related loss of neural system function in APP-transgenic mice. *J. Neurosci.* 29, 12636–12640. doi: 10.1523/JNEUROSCI.1948-09.2009

Meyer-Luehmann, M., Spires-Jones, T. L., Prada, C., Garcia-Alloza, M., de Calignon, A., Rozkalne, A., et al. (2008). Rapid appearance and local toxicity of amyloid-β plaques in a mouse model of Alzheimer's disease. *Nature* 451, 720–724. doi: 10.1038/nature06616

Mora, F., Segovia, G., and del Arco, A. (2007). Aging, plasticity and environmental enrichment: structural changes and neurotransmitter dynamics in several areas of the brain. *Brain Res. Rev.* 55, 78–88. doi: 10.1016/j.brainresrev.2007.03.011

Mucke, L., Masliah, E., Yu, G.-Q., Mallory, M., Rockenstein, E. M., Tatsuno, G., et al. (2000). High-level neuronal expression of $a\beta_{1-42}$ in wild-type human amyloid protein precursor transgenic mice: synaptotoxicity without plaque formation. *J. Neurosci.* 20, 4050–4058. doi: 10.1523/JNEUROSCI.20-11-04050.2000

Nägerl, U. V., Eberhorn, N., Cambridge, S. B., and Bonhoeffer, T. (2004). Bidirectional activity-dependent morphological plasticity in hippocampal neurons. *Neuron* 44, 759–767. doi: 10.1016/j.neuron.2004.11.016

Naj, A. C., Jun, G., Beecham, G. W., Wang, L.-S., Vardarajan, B. N., Buros, J., et al. (2011). Common variants at MS4A4/MS4A6E, CD2AP, CD33 and EPHA1 are associated with late-onset Alzheimer's disease. *Nat. Genet.* 43, 436–441. doi: 10.1038/ng.801

Nimmerjahn, A., Kirchhoff, F., and Helmchen, F. (2005). Resting microglial cells are highly dynamic surveillants of brain parenchyma *in vivo*. *Science* 308, 1314–1318. doi: 10.1126/science.1110647

Ning, A., Cui, J., To, E., Ashe, K. H., and Matsubara, J. (2008). Amyloid-β deposits lead to retinal degeneration in a mouse model of Alzheimer disease. *Invest. Ophthalmol. Vis. Sci.* 49, 5136–5143. doi: 10.1167/iovs.08-1849

Orr, A. G., Hsiao, E. C., Wang, M. M., Ho, K., Kim, D. H., Wang, X., et al. (2015). Astrocytic adenosine receptor A_{2A} and G_s-coupled signaling regulate memory. *Nat. Neurosci.* 18, 423–434. doi: 10.1038/nn.3930

Paolicelli, R. C., Bolasco, G., Pagani, F., Maggi, L., Scianni, M., Panzanelli, P., et al. (2011). Synaptic pruning by microglia is necessary for normal brain development. *Science* 333, 1456–1458. doi: 10.1126/science.1202529

Parkhurst, C. N., Yang, G., Ninan, I., Savas, J. N., Yates, J. R. III., Lafaille, J. J., et al. (2013). Microglia promote learning-dependent synapse formation through brain-derived neurotrophic factor. *Cell* 155, 1596–1609. doi: 10.1016/j.cell.2013.11.030

Peters, F., Salihoglu, H., Rodrigues, E., Herzog, E., Blume, T., Filser, S., et al. (2018). BACE1 inhibition more effectively suppresses initiation than progression of β-amyloid pathology. *Acta Neuropathol.* 135, 695–710. doi: 10.1007/s00401-017-1804-9

Prince, M. J. (2015). *World Alzheimer Report 2015: The Global Impact of Dementia*. Available online at: https://www.alz.co.uk/research/world-report-2015 [Accessed on August 29, 2018].

Roberson, E. D., Scearce-Levie, K., Palop, J. J., Yan, F., Cheng, I. H., Wu, T., et al. (2007). Reducing endogenous tau ameliorates amyloid β-induced deficits in an Alzheimer's disease mouse model. *Science* 316, 750–754. doi: 10.1126/science.1141736

Rogers, J., Schultz, J., Brachova, L., Lue, L. F., Webster, S., Bradt, B., et al. (1992). Complement activation and β-amyloid-mediated neurotoxicity in Alzheimer's disease. *Res. Immunol.* 143, 624–630.

Schafer, D. P., Lehrman, E. K., Kautzman, A. G., Koyama, R., Mardinly, A. R., Yamasaki, R., et al. (2012). Microglia sculpt postnatal neural circuits in an activity and complement-dependent manner. *Neuron* 74, 691–705. doi: 10.1016/j.neuron.2012.03.026

Scheff, S. W., DeKosky, S. T., and Price, D. A. (1990). Quantitative assessment of cortical synaptic density in Alzheimer's disease. *Neurobiol. Aging* 11, 29–37. doi: 10.1016/0197-4580(90)90059-9

Serrano-Pozo, A., Frosch, M. P., Masliah, E., and Hyman, B. T. (2011). Neuropathological alterations in Alzheimer disease. *Cold Spring Harb. Perspect. Med.* 1:a006189. doi: 10.1101/cshperspect.a006189

Serrano-Pozo, A., Muzikansky, A., Gómez-Isla, T., Growdon, J. H., Betensky, R. A., Frosch, M. P., et al. (2013). Differential relationships of reactive astrocytes and microglia to fibrillar amyloid deposits in Alzheimer disease. *J. Neuropathol. Exp. Neurol.* 72, 462–471. doi: 10.1097/nen.0b013e3182933788

Shankar, G. M., Bloodgood, B. L., Townsend, M., Walsh, D. M., Selkoe, D. J., and Sabatini, B. L. (2007). Natural oligomers of the Alzheimer amyloid-β protein induce reversible synapse loss by modulating an NMDA-type

glutamate receptor-dependent signaling pathway. *J. Neurosci.* 27, 2866–2875. doi: 10.1523/JNEUROSCI.4970-06.2007

Shankar, G. M., Leissring, M. A., Adame, A., Sun, X., Spooner, E., Masliah, E., et al. (2009). Biochemical and immunohistochemical analysis of an Alzheimer's disease mouse model reveals the presence of multiple cerebral Aβ assembly forms throughout life. *Neurobiol. Dis.* 36, 293–302. doi: 10.1016/j.nbd.2009.07.021

Shankar, G. M., Li, S., Mehta, T. H., Garcia-Munoz, A., Shepardson, N. E., Smith, I., et al. (2008). Amyloid-β protein dimers isolated directly from Alzheimer's brains impair synaptic plasticity and memory. *Nat. Med.* 14, 837–842. doi: 10.1038/nm1782

Shen, Y., Lue, L., Yang, L., Roher, A., Kuo, Y., Strohmeyer, R., et al. (2001). Complement activation by neurofibrillary tangles in Alzheimer's disease. *Neurosci. Lett.* 305, 165–168. doi: 10.1016/S0304-3940(01)01842-0

Sofroniew, M. V. (2009). Molecular dissection of reactive astrogliosis and glial scar formation. *Trends Neurosci.* 32, 638–647. doi: 10.1016/j.tins.2009.08.002

Spires, T. L., Meyer-Luehmann, M., Stern, E. A., McLean, P. J., Skoch, J., Nguyen, P. T., et al. (2005). Dendritic spine abnormalities in amyloid precursor protein transgenic mice demonstrated by gene transfer and intravital multiphoton microscopy. *J. Neurosci.* 25, 7278–7287. doi: 10.1523/JNEUROSCI.1879-05.2005

Spires-Jones, T. L., Meyer-Luehmann, M., Osetek, J. D., Jones, P. B., Stern, E. A., Bacskai, B. J., et al. (2007). Impaired spine stability underlies plaque-related spine loss in an Alzheimer's disease mouse model. *Am. J. Pathol.* 171, 1304–1311. doi: 10.2353/ajpath.2007.070055

Spires-Jones, T. L., Stoothoff, W. H., de Calignon, A., Jones, P. B., and Hyman, B. T. (2009). Tau pathophysiology in neurodegeneration: a tangled issue. *Trends Neurosci.* 32, 150–159. doi: 10.1016/j.tins.2008.11.007

Stelzmann, R. A., Schnitzlein, H. N., and Murtagh, F. R. (1995). An English translation of Alzheimer's 1907 paper, "Über eine eigenartige Erkankung der Hirnrinde". *Clin. Anat.* 8, 429–431. doi: 10.1002/ca.980080612

Stephan, A. H., Barres, B. A., and Stevens, B. (2012). The complement system: an unexpected role in synaptic pruning during development and disease. *Annu. Rev. Neurosci.* 35, 369–389. doi: 10.1146/annurev-neuro-061010-113810

Stevens, B., Allen, N. J., Vazquez, L. E., Howell, G. R., Christopherson, K. S., Nouri, N., et al. (2007). The classical complement cascade mediates CNS synapse elimination. *Cell* 131, 1164–1178. doi: 10.1016/j.cell.2007.10.036

Takahashi, R. H., Almeida, C. G., Kearney, P. F., Yu, F., Lin, M. T., Milner, T. A., et al. (2004). Oligomerization of Alzheimer's β-amyloid within processes and synapses of cultured neurons and brain. *J. Neurosci.* 24, 3592–3599. doi: 10.1523/JNEUROSCI.5167-03.2004

Terry, R. D., Masliah, E., Salmon, D. P., Butters, N., DeTeresa, R., Hill, R., et al. (1991). Physical basis of cognitive alterations in Alzheimer's disease: synapse loss is the major correlate of cognitive impairment. *Ann. Neurol.* 30, 572–580. doi: 10.1002/ana.410300410

Tremblay, M.-E., Riad, M., and Majewska, A. (2010). Preparation of mouse brain tissue for immunoelectron microscopy. *J. Vis. Exp.* 41:e2021. doi: 10.3791/2021

Tsai, J., Grutzendler, J., Duff, K., and Gan, W.-B. (2004). Fibrillar amyloid deposition leads to local synaptic abnormalities and breakage of neuronal branches. *Nat. Neurosci.* 7, 1181–1183. doi: 10.1038/nn1335

Vassar, R. (2014). BACE1 inhibitor drugs in clinical trials for Alzheimer's disease. *Alzheimers Res. Ther.* 6:89. doi: 10.1186/s13195-014-0089-7

Verkhratsky, A., Olabarria, M., Noristani, H. N., Yeh, C.-Y., and Rodriguez, J. J. (2010). Astrocytes in Alzheimer's disease. *Neurother. J. Am. Soc. Exp. Neurother.* 7, 399–412. doi: 10.1016/j.nurt.2010.05.017

Walsh, D. M., Klyubin, I., Fadeeva, J. V., Cullen, W. K., Anwyl, R., Wolfe, M. S., et al. (2002). Naturally secreted oligomers of amyloid β protein potently inhibit hippocampal long-term potentiation *in vivo*. *Nature* 416, 535–539. doi: 10.1038/416535a

Wang, H., Megill, A., Wong, P. C., Kirkwood, A., and Lee, H.-K. (2014). Postsynaptic target specific synaptic dysfunctions in the CA3 area of BACE1 knockout mice. *PLoS One* 9:e92279. doi: 10.1371/journal.pone.0092279

Wisniewski, H. M., and Wegiel, J. (1991). Spatial relationships between astrocytes and classical plaque components. *Neurobiol. Aging* 12, 593–600. doi: 10.1016/0197-4580(91)90091-w

Woo, D. H., Han, K.-S., Shim, J. W., Yoon, B.-E., Kim, E., Bae, J. Y., et al. (2012). TREK-1 and Best1 channels mediate fast and slow glutamate release in astrocytes upon GPCR activation. *Cell* 151, 25–40. doi: 10.1016/j.cell.2012.09.005

Wu, Y., Dissing-Olesen, L., MacVicar, B. A., and Stevens, B. (2015). Microglia: dynamic mediators of synapse development and plasticity. *Trends Immunol.* 36, 605–613. doi: 10.1016/j.it.2015.08.008

Wyss-Coray, T., Loike, J. D., Brionne, T. C., Lu, E., Anankov, R., Yan, F., et al. (2003). Adult mouse astrocytes degrade amyloid-β *in vitro* and *in situ*. *Nat. Med.* 9, 453–457. doi: 10.1038/nm838

Wyss-Coray, T., and Rogers, J. (2012). Inflammation in Alzheimer disease-a brief review of the basic science and clinical literature. *Cold Spring Harb. Perspect. Med.* 2:a006346. doi: 10.1101/cshperspect.a006346

Yan, R., and Vassar, R. (2014). Targeting the β secretase BACE1 for Alzheimer's disease therapy. *Lancet Neurol.* 13, 319–329. doi: 10.1016/S1474-4422(13)70276-X

Yang, T., Li, S., Xu, H., Walsh, D. M., and Selkoe, D. J. (2017). Large soluble oligomers of amyloid β-protein from Alzheimer brain are far less neuroactive than the smaller oligomers to which they dissociate. *J. Neurosci.* 37, 152–163. doi: 10.1523/JNEUROSCI.1698-16.2016

Zhan, Y., Paolicelli, R. C., Sforazzini, F., Weinhard, L., Bolasco, G., Pagani, F., et al. (2014). Deficient neuron-microglia signaling results in impaired functional brain connectivity and social behavior. *Nat. Neurosci.* 17, 400–406. doi: 10.1038/nn.3641

Zhao, J., Fu, Y., Yasvoina, M., Shao, P., Hitt, B., O'Connor, T., et al. (2007). β-site amyloid precursor protein cleaving enzyme 1 levels become elevated in neurons around amyloid plaques: implications for Alzheimer's disease pathogenesis. *J. Neurosci.* 27, 3639–3649. doi: 10.1523/JNEUROSCI.4396-06.2007

Zhu, K., Peters, F., Filser, S., and Herms, J. (2018). Consequences of pharmacological BACE inhibition on synaptic structure and function. *Biol. Psychiatry* 84, 478–487. doi: 10.1016/j.biopsych.2018.04.022

Ziegler-Waldkirch, S., d'Errico, P., Sauer, J.-F., Erny, D., Savanthrapadian, S., Loreth, D., et al. (2018a). Seed-induced Aβ deposition is modulated by microglia under environmental enrichment in a mouse model of Alzheimer's disease. *EMBO J.* 37, 167–182. doi: 10.15252/embj.201797021

Ziegler-Waldkirch, S., Marksteiner, K., Stoll, J., d'Errico, P., Friesen, M., Eiler, D., et al. (2018b). Environmental enrichment reverses Aβ pathology during pregnancy in a mouse model of Alzheimer's disease. *Acta Neuropathol. Commun.* 6:44. doi: 10.1186/s40478-018-0549-6

Conflict of Interest Statement: The authors declare that the research was conducted in the absence of any commercial or financial relationships that could be construed as a potential conflict of interest.

frontiers in Cellular Neuroscience

REVIEW
published: 20 December 2018
doi: 10.3389/fncel.2018.00499

New Therapeutic Avenues of mCSF for Brain Diseases and Injuries

*Vincent Pons and Serge Rivest **

Neuroscience Laboratory, Centre Hospitalier Universitaire (CHU) de Québec Research Center and Department of Molecular Medicine, Faculty of Medicine, Laval University, Quebec, QC, Canada

Macrophage colony-stimulating factor (mCSF) is a cytokine known to promote the recruitment of macrophages inducing the release of CCL2, a chemokine mobilizing monocytes to sites of inflammation. Additionally, it induces microglia/macrophage proliferation and the polarization of these cells towards a M2-like phenotype, impairing their ability to release pro-inflammatory factors and toxic mediators, while favoring the release of mediators promoting tissue repair. Another important player is the mCSF receptor CSFR1, which is highly expressed in monocytes, macrophages and microglia. Here, we discuss the new interesting therapeutic avenue of the mCSF/CSFR1 axis on brain diseases. More specifically, mCSF cascade might stimulate the survival/proliferation of oligodendrocytes, enhance the immune response as well as modulate the release of growth factors and the phagocytic activity of immune cells to remove myelin debris and toxic proteins from the brain.

Keywords: mCSF, microglia, brain diseases, innate immune response, phagocytosis

OPEN ACCESS

Edited by:
Jaichandar Subramanian,
University of Kansas, United States

Reviewed by:
Andrew MacLean,
Tulane University School of Medicine, United States
Luísa V. Lopes,
Universidade de Lisboa, Portugal

Helena Brigas,
Universidade de Lisboa, Portugal, in collaboration with reviewer LL

***Correspondence:**
Serge Rivest
serge.rivest@crchudequebec.ulaval.ca

Received: *28 August 2018*
Accepted: *03 December 2018*
Published: *20 December 2018*

Citation:
Pons V and Rivest S (2018) New Therapeutic Avenues of mCSF for Brain Diseases and Injuries. Front. Cell. Neurosci. 12:499. doi: 10.3389/fncel.2018.00499

INTRODUCTION

Macrophage colony-stimulating factor (mCSF) is an hematopoietic cytokine expressed in a wide range of cells and tissues, namely the kidney, brain, liver, retina, spleen, lung, adipose tissue, skin and joints (Ryan, 2001; Nandi, 2006). It stimulates progenitor cells from bone marrow (Stanley, 1976) and takes a role in the development, proliferation and maintenance of mononuclear phagocytes such as monocytes, dendritic cells, microglia and osteoclasts (Chitu et al., 2016). mCSF signals through a tyrosine kinase family receptor, CSFR1 also known as CD115, which also binds interleukin-34 (IL-34) that plays similar roles (Ségaliny et al., 2015). In addition to be involved in the development and support of innate immune cells, mCSF/CSFR1 activity is involved in various pathologies such as ovarian cancer, breast cancer, rheumatoid arthritis and cutaneous lupus (Toy et al., 2009; Achkova and Maher, 2016). The mCSF/CSFR1 axis is a therapeutic target to regulate the inflammatory and pathological processes, including cancer, rheumatoid arthritis and cutaneous lupus. CSFR1 monoclonal antibody or antagonist has been shown to suppress the inflammatory response in a phase II clinical trial on rheumatoid arthritis (Garcia et al., 2013). mCSF-deficient mice exhibit numerous phenotypic defects, namely toothless, skeletal defects (Naito et al., 1997), reduced body weight, deficit in tissue macrophages and osteoclasts as well as neurological abnormalities (Nandi et al., 2012) indicating a major role played by this ligand on these populations of cells. In the brain this cytokine is secreted by neurons, astrocytes and microglia and is involved in the brain development (Nandi et al., 2012). In this regard, mCSF-deficient animals have severe brain deficits with specific abnormalities within the cerebral cortex.

mCSF has also a critical role on the activity, survival, maintenance, proliferation and differentiation of microglial cells, which are resident immune cells in the brain. It has been proposed that microglia are derived from progenitors that originate from the neuroectoderm and/or the mesoderm, which colonize the brain from the early embryonic stage, and throughout the fetal development stage (Soulet and Rivest, 2008). They are the only cell type that expresses the CSFR1 in the brain (Erblich et al., 2011). A conditional deletion of CSFR1 specifically in microglia leads to a severe depletion of these innate immune cells in the brain (Elmore et al., 2014). Taken together, these data point towards a major role of the mCSF/CSFR1 axis within microglia as a crucial neuroprotective mechanism in the brain during normal and pathological conditions.

mCSF IN PATHOLOGICAL CONDITIONS

mCSF has the ability to polarize microglia towards both pro-inflammatory (M1) and anti-inflammatory (M2) directions depending on the microenvironment and other inflammatory molecules (Hamilton et al., 2014). The presence of IL-1, tumor necrosis factor (TNF), reactive oxygen species (ROS) and nitric oxide (NO) creates a powerful pro-inflammatory medium, whereas IL-10, arginase 1, transforming growth factor β (TGF-β) are rather anti-inflammatory and contribute to the effects of mCSF to restrict neuroinflammation in brain injuries and diseases. (Cherry et al., 2014).

Neurodegenerative diseases are associated with a robust microglial response, which is known to have both beneficial and detrimental properties depending on the disease, animal models, duration and environmental factors (Aguzzi et al., 2013). In many diseases, microglia are becoming a key target for therapeutic purposes since they can eliminate toxic elements from the brain and set the conditions for repair and remyelination. The mCSF/CSFR1 axis is consequently a very interesting new therapeutic avenue and has also been used as diagnostic tools in neuropathologies (Hume and MacDonald, 2012). In this regard, low levels of mCSF were measured in patients with presymptomatic Alzheimer's disease (AD) or mild cognitive impairment (MCI), which together with low levels of other hematopoietic cytokines predicted the rapid evolution of the disease toward a dementia diagnosis 2–6 years later (Ray et al., 2007; Laske et al., 2010). In multiple sclerosis (MS) patients, despite the tremendous increase in macrophages/microglia within the lesions, the relative number of these cells expressing mCSF or CSFR1 decreased (Werner et al., 2002). Consequently, a lower level of mCSF/CSFR1 in the bloodstream and the brain seems to be predictive a the disease evolution.

ALZHEIMER'S DISEASE (AD)

AD is a progressive neurodegenerative disease and the most common form of dementia with close to 50 million affected individuals in the world. One proposed hypothesis of the disease onset and progression is the failure of microglia to clear amyloid-beta (Aβ) due to their poor phagocytic properties when compared to macrophages. The consequence is the Aβ accumulation (both soluble and insoluble) that provokes neurological disorder, cognitive decline and neurodegeneration (Masters et al., 2015). On the other hand, the harmful role of microglia is due to the production of pro-inflammatory cytokines, NO and ROS among other secreted factors in presence of Aβ (Combs et al., 2001). Although microglia have ability to clear Aβ at the early stage of AD, this phagocytic response seems to deteriorate with time explaining the overflow of Aβ accumulation while the diseases is progressing (ElAli and Rivest, 2016). Such impaired role of microglial cells to clear this toxic protein appears crucial in AD etiology. As mentioned, mCSF plays important roles in the activation state of microglia, especially to improve their phagocytic properties with very limited pro-inflammatory activities (Mitrasinovic et al., 2003). Intraperitoneal weekly injections of mCSF beginning before the apparition of symptoms prevent amyloid burden and neurological decline in the APPswe/PS1 mouse model of AD (Boissonneault et al., 2009). Even more interesting is the fact that such a treatment was able to stabilize the disease then improve the cognition and memory when started late after the first symptoms. The main conclusion of this study was that mCSF was able to trigger microglia proliferation, improve their phagocytic activities to Aβ and prevent its toxicity to neuronal elements (Boissonneault et al., 2009).

In another study supporting the neuroprotective role of mCSF, Mitrasinovic and colleagues used microglial cell line overexpressing CSFR1 in the presence of Aβ in the culture medium (Mitrasinovic, 2003). Such a preparation was able to activate microglia and improve Aβ phagocytosis. One of the challenges is to control the chronic inflammatory reaction, which has frequently been associated with the detrimental role of these cells in that disease. Of interest is that such a response does not take place in the brain of mCSF-treated animals such as in the case of lipopolysaccharide (LPS)-treated mice that exhibit of strong and robust pro-inflammatory reaction together with an increased phagocytosis. Of note, a chronic systemic LPS administration in APP_{swe}/PS1 mice leads to higher Aß deposit (Lee et al., 2008). In contrast, Michaud et al. (2013) used a detoxified LPS called monophosphoryl lipid A (MLP) that triggers a low inflammatory response while inducing a strong phagocytic microglial reaction in APP_{swe}/PS1 mice and improvement of AD-related pathologies. This provides clear evidence that a strong inflammatory response by microglia is not necessary to improve their efficiency to clear Aβ. The challenge remains to mastering the inflammatory/anti-inflammatory phenotype depending on stage of AD and to maintain efficient responses to clear Aβ in a chronic manner to prevent or delay the symptoms.

MULTIPLE SCLEROSIS (MS)

MS is an autoimmune disorder with consequences as axon demyelination and chronic inflammation of the CNS (Thompson et al., 2018). The demyelinating processes leave

many myelin debris, which can be cleared by microglia and infiltrating macrophages later in the pathology (Huizinga et al., 2012). A proper activation of microglia enhances myelin clearance and allows the oligodendrocyte precursor cell (OPC) differentiation and oligodendrocyte survival, that improve remyelination (Kotter, 2006). As for the case of amyloid, microglia need to be activated to phagocyte the myelin debris and we recently provided solid evidence that mCSF plays a key role in such activation process (Laflamme et al., 2018). A number of animal models are available to mimic MS, namely cuprizone-induced demyelination and Experimental Autoimmune Encephalomyelitis (EAE). The well-characterized, very reproducible and non-invasive cuprizone model allows to study cellular and molecular mechanisms involved in the demyelination (DM)/remyelination (RM) process, while excluding the autoimmune component (Denic et al., 2011). Indeed, continued exposition to dietary cuprizone, a copper-chelating toxin, leads to oligodendrocyte apoptosis and demyelination among vulnerable brain structures, such as the corpus callosum and cerebral cortex. Few days after replacing cuprizone by normal food, RM is observed in those structures (Matsushima and Morell, 2006; Gudi et al., 2014). Our previous study brought us to deepen the role of microglia and other parenchymal cells such as oligodendrocytes in the cascade of events that leads to DM/RM events (Lampron et al., 2015). For this reason, in this study, exogenous mCSF was administered to mice that received dietary cuprizone (Laflamme et al., 2018). mCSF is a cytokine well-known to stimulate cell survival, proliferation and differentiation of myeloid cells (Hamilton, 2008; Otero et al., 2009). Moreover, it modulates microglial phenotype towards an anti-inflammatory one (Ushach and Zlotnik, 2016), reducing the expression of antigen presenting proteins (Smith et al., 2013) and promoting the release of trophic factors (Smith et al., 2013). Herein, we investigated the effect of exogenous mCSF on the activity of microglia and oligodendrocytes over the course of cuprizone intoxication. Since mCSF is expressed constitutively, we utilized a conditional model in which its mCSF receptor (CSF1R) is deleted in microglia selectively, to better understand the role of the endogenous cytokine.

mCSF-treated mice exhibited reduced myelin loss during the demyelination phase, together with an increased number of microglia and OPCs in lesion sites (Laflamme et al., 2018). Tamoxifen-induced conditional deletion of the mCSF receptor in microglia from cuprizone-fed mice caused aberrant myelin debris accumulation in the corpus callosum and reduced microglial phagocytic response. mCSF therefore plays a key role in stimulating myelin clearance by brain innate immune cells, which is a prerequisite for proper remyelination and myelin repair processes. Microglial cells synthetize the growth factor IGF-1 that may be involved in the remyelination process. IGF-1 would play a role in oligodendrocyte survival and OPC differentiation, but the mechanism remains unclear and needs to be further investigated (Laflamme et al., 2018).

Although the cuprizone model allowed us to study the de/remyelination and the interactions between microglia, oligodendrocytes and the environment, it is not a model to study the inflammation and peripheral immune cell invasion. For this aspect of the disease, EAE is used. In this model, there is a chronic inflammatory response together with a robust activation of microglia, DM, synaptic dysfunctions and perturbation in the axonal transport (Rasmussen et al., 2007). mCSF inhibition in EAE animals improved recovery, suppressed the production of pro-inflammatory molecules and decreased the number of infiltrating immune cells (Uemura et al., 2008). The dual role of the cytokine in these two different models may be explained by critical contribution of infiltrating cells in the pathology of EAE mice. Although there is also infiltration of monocytes in the brain of cuprizone fed mice, these cells do not contribute to the neuropathology of cuprizone-treated animals (Lampron et al., 2015). Consequently, inhibiting mCSF function seems beneficial in a model that depends on blood brain barrier damages and massive infiltration of immune cells, whereas it is the opposite in a model depending on the ability of microglia to clear myelin debris, such as in the case of cuprizone.

GLIOMA

Glioma is a tumor that begins within the population of glial cells in the CNS. The tumor-associated cytokines are correlated with the grade of the cancer (Balkwill and Mantovani, 2001). In high-grade gliomas, macrophages with an anti-inflammatory profile are predominant. mCSF, IL-10, TGFβ are reported to be highly expressed by the tumor and its microenvironment compared to low grade gliomas (De et al., 2016). These results suggest that tumor-derived mCSF induces a shift of microglia/macrophages towards the M2 phenotype, which influences tumor growth. Evaluation of the proportion of M2 microglia/macrophages and mCSF expression in tumor tissue would be useful for the assessment of microglia/macrophage proliferative activity and the prognosis of patients with gliomas. Injecting mCSF in rats bearing tumors has two effects depending on the dose. A low dose of mCSF has no effect regarding the tumor progression and cell recruitment, whereas an high dose of mCSF has a significant anti-tumor effect against glioma (Matsuoka et al., 1994). Similar anti-tumor effects were reported in other cancers, such as sarcoma, melanoma and lung cancer. Another study in mCSF-deficient mice (mice op/op) has shown a comparable number of Iba1 cells in tumor-bearing brain and a comparable state of activation in both wild type and op/op groups of mice (Sielska et al., 2013). Inhibition of mCSF signaling pathway by blocking the CSFR1 on microglia prevents the glioblastoma invasion and tumor-associated microglia (Coniglio et al., 2012). Glioblastoma cells from human patient express mCSF which triggers microglia M2 profile that is involved in tumor progression (Komohara et al., 2008; Pollard, 2009). Despite conflicting data, it seems that inhibiting of the mCSF/CSFR1 pathway would be the angle to treat glioblastoma.

BRAIN INJURY

A massive proliferation and infiltration of innate immune cells takes place during CNS injury and microglia are the main

effector of this response (Donat et al., 2017). Such a cellular response is mainly mediated by the release of cytokines in the microenvironment of the injury. mCSF inhibition was found to prevent significantly such a cellular movement together with microglial proliferation, an increase number of neuron death and exacerbation of the injury. These observations unravel another example of the beneficial role played by mCSF and the importance of these resident immune cells in the brain. Neuronal protection from excitotoxic and teratogen reaction followed by brain injury was also observed in organotypic co-culture media with transfected microglia overexpressing CSFR1. Microglia activation by mCSF improved neuronal survival in the co-culture *in vitro* system (Mitrasinovic, 2005). It was also shown that the cytokine is secreted by neurons in early phases then by microglia on later phases around necrosis in an *in vivo* model of focal brain injury in rats (Takeuchi et al., 2001), mCSF-induced microglial proliferation promotes tissue repair, nerve regeneration and inhibits production of pro-inflammatory cytokines (Xu et al., 2017). It is also important to mention that activated microglia are not strictly polarized into pro-inflammatory or anti-inflammatory profiles, but into a mixed phenotype resulting in a complex signaling between the actors of neuroinflammation. Indeed, gene expression analyses have unraveled such a mixed signature of M1/M2 microglia following brain injury (Rosi, 2016).

CLINICAL STUDIES

mCSF/CSFR1 axis is a therapeutic target to regulate the inflammation and innate immune cell proliferation and differentiation that play both beneficial and detrimental roles in neuropathologic processes depending on the disease and model (Hamilton et al., 2017). Drugs were developed against the ligand or the receptor in various diseases namely cancer, rheumatoid arthritis and cutaneous lupus. It is targeted with monoclonal antibodies or antagonists, which block the action of the ligand on its binding site. It is the principal strategy used in cancer therapy. Monoclonal antibodies have also been developed against mCSF. Based on preclinical data, inhibition of the mCSF/CSFR1 axis may not be a good strategy and can be deleterious in inflammatory or neurodegenerative diseases (Hamilton et al., 2017). On the other hand, such a strategy seems to have beneficial effects on pain alleviation where microglia have to be inhibited in contrast to the diseases discussed above.

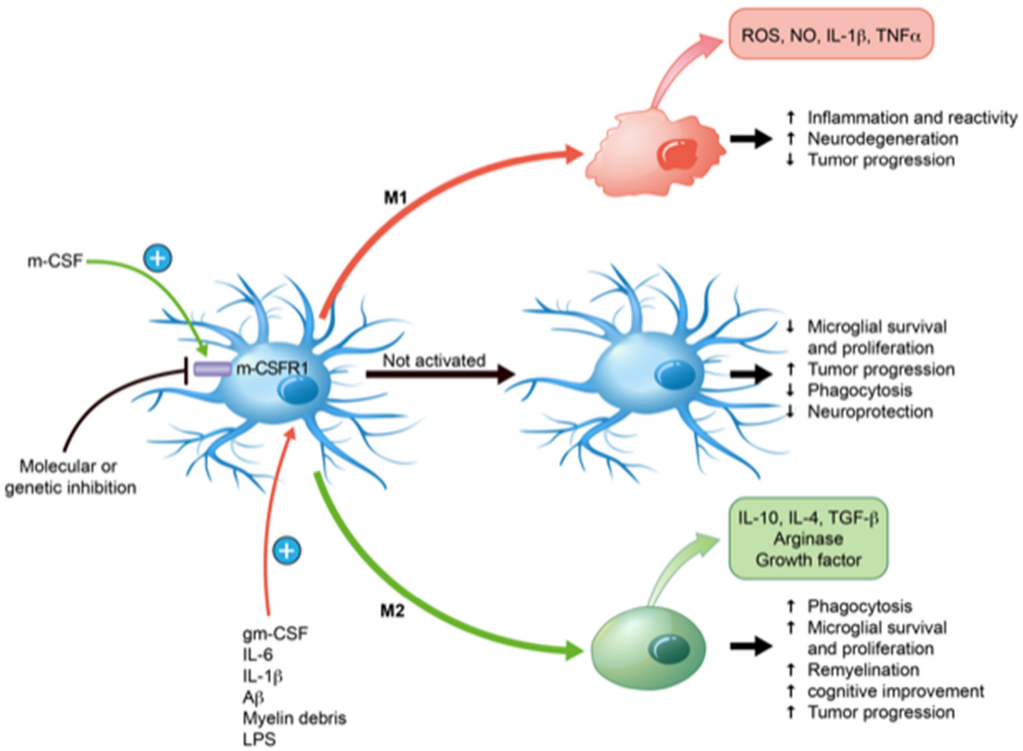

FIGURE 1 | Effects of macrophage colony-stimulating factor (mCSF) on microglial polarization and functions. mCSF has the ability to polarize microglia into pro-inflammatory (M1) or anti-inflammatory (M2) depending on the environment and cytokine production. They may also remain inactivated. Their states of activation have direct consequences on their specific functions, such as phagocytosis, neuroprotection, inflammation, etc. M1 takes place in response to granulocyte-mCSF (gmCSF), interleukin-6 (IL-6), IL-1β, lipopolysaccharide (LPS), amyloid β (Aβ) and myelin debris. M1 profile shows anti-tumor progression and induces neuroinflammation with the production of reactive oxygen species (ROS), nitric oxide (NO), IL-1β and tumor necrosis factor-α (TNF-α) that may contribute to neurodegeneration. M2 profile occurs in response to mCSF, which induces remyelination, improves phagocytosis, diminishes inflammation together with the production of IL-10, IL-4, arginase, transforming growth factor β (TGF-β). These may promote neurorepair and tumor progression. Inhibition of mCSF with specific molecules or genetic construction inhibits microglia and blocking its receptor causes a marked microglial depletion.

CONCLUSION

mCSF/CSFR1 has a pivotal role in healthy brain and neurodegenerative pathologies. It is synthetized by neurons, astrocytes and microglia. Such a mCSF/CSFR1 signaling helps microglia clearing myelin debris, support neurons, clear toxic proteins and maintaining microglia (**Figure 1**). Many groups have studied the role of the mCSF/CSFR1 axis in the brain. It appears essential in brain development, synaptic landscape, infection resolution and neuronal maintenance. In some neurodegenerative diseases, mCSF and microglia are highly beneficial, especially in mouse model of AD to clear amyloid, prevent its toxicity to neurons and improve cognitive impairment. mCSF-activated microglia help clearing myelin debris and set the conditions for remyelination and repair. mCSF injections have beneficial effects on remyelination, oligodendrocyte survival and OPC differentiation in cuprizone-fed mice. mCSF is not always benefic, inhibition of mCSF reduces immune cell infiltration and inflammation in the EAE model that mimics the massive invasion of systemic immune cells in the CNS. In the same line, mCSF deficiency prevents tumor invasion in glioblastoma.

Taken together, these studies underline a great potential of this hematopoietic cytokine and the need to modulate the mCSF/CSFR1 axis in pre-clinical models of brain diseases, although this has to be validated in clinical settings. Many clinical trials have used mCSF inhibitors or a monoclonal antibody against CSFR1 in last years, most of them concern cancer or rheumatoid arthritis. The different effects of the molecule may be due to several factors. A better understanding of the exact role of mCSF in different neuropathologies is needed to develop strategies for the use of mCSF as new therapeutic perspectives. Different time points in the disease progression as well as the model used clearly influence the effects of the cytokine. In addition, some findings have demonstrated physiological differences between young and elderly humans, which may depend on the unalike characteristics of microglia in young and old animals. As mentioned, CSFR1 conditional gene deletion mice are quite useful to study the role of the receptor in neuropathologies and these needed studies will certainly help investigating the role of the mCSF/CSFR1 axis in clinical settings.

AUTHOR CONTRIBUTIONS

VP and SR wrote the manuscript together.

FUNDING

This work was supported by the Canadian Institutes in Health Research (CIHR; grant no. 143279) and les Fonds de Recherche du Québec-Santé (FRQS) *via* the research center funding grant. SR was supported by a Canada Research Chair in Neuroimmunology.

REFERENCES

Achkova, D., and Maher, J. (2016). Role of the colony-stimulating factor (CSF)/CSF-1 receptor axis in cancer. *Biochem. Soc. Trans.* 44, 333–341. doi: 10.1042/bst20150245

Aguzzi, A., Barres, B. A., and Bennett, M. L. (2013). Microglia: scapegoat, saboteur, or something else? *Science* 339, 156–161. doi: 10.1126/science.1227901

Balkwill, F., and Mantovani, A. (2001). Inflammation and cancer: back to virchow? *Lancet* 357, 539–545. doi: 10.1016/S0140-6736(00)04046-0

Boissonneault, V., Filali, M., Lessard, M., Relton, J., Wong, G., and Rivest, S. (2009). Powerful beneficial effects of macrophage colony-stimulating factor on -amyloid deposition and cognitive impairment in Alzheimer's disease. *Brain* 132, 1078–1092. doi: 10.1093/brain/awn331

Cherry, J. D., Olschowka, J. A., and O'Banion, M. (2014). Neuroinflammation and M2 microglia: the good, the bad and the inflamed. *J. Neuroinflammation* 11:98. doi: 10.1186/1742-2094-11-98

Chitu, V., Gokhan, Ş., Nandi, S., Mehler, M. F., and Richard Stanley, E. (2016). Emerging roles for CSF-1 receptor and its ligands in the nervous system. *Trends Neurosci.* 39, 378–393. doi: 10.1016/j.tins.2016.03.005

Combs, C. K., Karlo Colleen, J., Kao, S.-C., and Landreth, G. E. (2001). β-amyloid stimulation of microglia and monocytes results in TNFα-dependent expression of inducible nitric oxide synthase and neuronal apoptosis. *J. Neurosci.* 21, 1179–1188. doi: 10.1523/JNEUROSCI.21-04-01179.2001

Coniglio, S. J., Eugenin, E., Dobrenis, K., Stanley Richard, E., West, B. L., Symons, M. H., et al. (2012). Microglial stimulation of glioblastoma invasion involves epidermal growth factor receptor (EGFR) and colony stimulating factor 1 receptor (CSF-1R) signaling. *Mol. Med.* 18, 519–527. doi: 10.2119/molmed.2011.00217

De, I., Steffen, M. D., Clark, P. A., Patros, C. J., Sokn, E., Bishop, S. M., et al. (2016). CSF1 overexpression promotes high-grade glioma formation without impacting the polarization status of glioma-associated microglia and macrophages. *Cancer Res.* 76, 2552–2560. doi: 10.1158/0008-5472.can-15-2386

Denic, A., Johnson, A. J., Bieber, A. J., Warrington, A. E., Rodriguez, M., and Pirko, I. (2011). The relevance of animal models in multiple sclerosis research. *Pathophysiology* 18, 21–29. doi: 10.1016/j.pathophys.2010.04.004

Donat, C. K., Scott, G., Gentleman, S. M., and Sastre, M. (2017). Microglial activation in traumatic brain injury. *Front. Aging Neurosci.* 9:208. doi: 10.3389/fnagi.2017.00208

ElAli, A., and Rivest, S. (2016). Microglia in Alzheimer's disease: a multifaceted relationship. *Brain Behav. Immun.* 55, 138–150. doi: 10.1016/j.bbi.2015.07.021

Elmore, M. R. P., Najafi, A. R., Koike, M. A., Dagher, N. N., Spangenberg, E. E., Rice, R. A., et al. (2014). Colony-stimulating factor 1 receptor signaling is necessary for microglia viability, unmasking a microglia progenitor cell in the adult brain. *Neuron* 82, 380–397. doi: 10.1016/j.neuron.2014.02.040

Erblich, B., Zhu, L., Etgen, A. M., Dobrenis, K., and Pollard, J. W. (2011). Absence of colony stimulation factor-1 receptor results in loss of microglia, disrupted brain development and olfactory deficits. *PLoS One* 6:e26317. doi: 10.1371/journal.pone.0026317

Garcia, S., Hartkamp, L. M., Tang, M. W., van Es, I., Lin, H., Long, L., et al. (2013). THU0042 colony-stimulating factor (CSF) receptor 1 blockade overcomes overlapping effects of M-CSF and interleukin-34 on myeloid differentiation and gene expression to reduce inflammation in human and murine models of rheumatoid arthritis. *Ann. Rheum. Dis.* 72:A178. doi: 10.1136/annrheumdis-2013-eular.570

Gudi, V., Gingele, S., Skripuletz, T., and Stangel, M. (2014). Glial response during cuprizone-induced de- and remyelination in the CNS: lessons learned. *Front. Cell. Neurosci.* 8:73. doi: 10.3389/fncel.2014.00073

Hamilton, J. A., Cook, A. D., and Tak, P. P. (2017). Anti-colony-stimulating factor therapies for inflammatory and autoimmune diseases. *Nat. Rev. Drug Discov.* 16, 53–70. doi: 10.1038/nrd.2016.231

Hamilton, T. A., Zhao, C., Pavicic, P. G., and Datta, S. (2014). Myeloid colony-stimulating factors as regulators of macrophage polarization. *Front. Immunol.* 5:554. doi: 10.3389/fimmu.2014.00554

Hamilton, J. A. (2008). Colony-stimulating factors in inflammation and autoimmunity. *Nat. Rev. Immunol.* 8, 533–544. doi: 10.1038/nri2356

Huizinga, R., van der Star, B. J., Kipp, M., Jong, R., Gerritsen, W., Clarner, T., et al. (2012). Phagocytosis of neuronal debris by microglia is associated with

neuronal damage in multiple sclerosis. *Glia* 60, 422–431. doi: 10.1002/glia.22276

Hume, D. A., and MacDonald, K. P. A. (2012). Therapeutic applications of macrophage colony-stimulating factor-1 (CSF-1) and antagonists of CSF-1 receptor (CSF-1R) signaling. *Blood* 119, 1810–1820. doi: 10.1182/blood-2011-09-379214

Komohara, Y., Ohnishi, K., Kuratsu, J., and Takeya, M. (2008). Possible involvement of the M2 anti-inflammatory macrophage phenotype in growth of human gliomas. *J. Pathol.* 216, 15–24. doi: 10.1002/path.2370

Kotter, M. R. (2006). Myelin impairs CNS remyelination by inhibiting oligodendrocyte precursor cell differentiation. *J. Neurosci.* 26, 328–332. doi: 10.1523/jneurosci.2615-05.2006

Laflamme, N., Cisbani, G., Préfontaine, P., Srour, Y., Bernier, J., St-Pierre, M.-K., et al. (2018). mCSF-induced microglial activation prevents myelin loss and promotes its repair in a mouse model of multiple sclerosis. *Front. Cell Neurosci.* 12:178. doi: 10.3389/fncel.2018.00178

Lampron, A., Larochelle, A., Laflamme, N., Préfontaine, P., Plante, M.-M., Sánchez, M. G., et al. (2015). Inefficient clearance of myelin debris by microglia impairs remyelinating processes. *J. Exp. Med.* 212, 481–495. doi: 10.1084/jem.20141656

Laske, C., Stransky, E., Hoffmann, N., Maetzler, W., Straten, G., G.Eschweiler, W., et al. (2010). Macrophage colony-stimulating factor (M-CSF) in plasma and CSF of patients with mild cognitive impairment and Alzheimers disease. *Curr. Alzheimer Res.* 7, 409–414. doi: 10.2174/156720510791383813

Lee, J., Lee, Y., Yuk, D., Choi, D., Ban, S., Oh, K., et al. (2008). Neuro-inflammation induced by lipopolysaccharide causes cognitive impairment through enhancement of beta-amyloid generation. *J. Neuroinflammation* 5:37. doi: 10.1186/1742-2094-5-37

Masters, C. L., Bateman, R., Blennow, K., Rowe, C. C., Sperling, R. A., and Cummings, J. L. (2015). Alzheimer's disease. *Nat. Rev. Dis. Primers* 1:15056. doi: 10.1038/nrdp.2015.56

Matsuoka, T., Uozumi, T., Kurisu, K., Maeda, H., Kawamoto, K., and Monden, S. (1994). Antitumor effects of human recombinant macrophage colony-stimulating factor against rat brain tumors. *Biotherapy* 8, 51–62. doi: 10.1007/bf01878121

Matsushima, G. K., and Morell, P. (2006). The neurotoxicant, cuprizone, as a model to study demyelination and remyelination in the central nervous system. *Brain Pathol.* 11, 107–116. doi: 10.1111/j.1750-3639.2001.tb00385.x

Michaud, J.-P., Halle, M., Lampron, A., Theriault, P., Prefontaine, P., Filali, M., et al. (2013). Toll-like receptor 4 stimulation with the detoxified ligand monophosphoryl lipid a improves Alzheimer's disease-related pathology. *Proc. Natl. Acad. Sci. U S A* 110, 1941–1946. doi: 10.1073/pnas.1215165110

Mitrasinovic, O. (2003). Microglial overexpression of the m-CSF receptor augments phagocytosis of opsonized Aβ. *Neurobiol. Aging* 24, 807–815. doi: 10.1016/s0197-4580(02)00237-3

Mitrasinovic, O. M. (2005). Microglia overexpressing the macrophage colony-stimulating factor receptor are neuroprotective in a microglial-hippocampal organotypic coculture system. *J. Neurosci.* 25, 4442–4451. doi: 10.1523/jneurosci.0514-05.2005

Mitrasinovic, O. M., Vincent, V. A. M., Simsek, D., and Murphy, G. M. (2003). Macrophage colony stimulating factor promotes phagocytosis by murine microglia. *Neurosci. Lett.* 344, 185–188. doi: 10.1016/s0304-3940(03)00474-9

Naito, M., Umeda, S., Takahashi, K., and Shultz, L. D. (1997). Macrophage differentiation and granulomatous inflammation in osteopetrotic mice (Op/Op) defective in the production of CSF-1. *Mol. Reprod. Dev.* 46, 85–91. doi: 10.1002/(sici)1098-2795(199701)46:1<85::aid-mrd13>3.0.co;2-2

Nandi, S. (2006). Developmental and functional significance of the csf-1 proteoglycan chondroitin sulfate chain. *Blood* 107, 786–795. doi: 10.1182/blood-2005-05-1822

Nandi, S., Gokhan, S., Dai, X.-M., Wei, S., Enikolopov, G., Lin, H., et al. (2012). The CSF-1 receptor ligands IL-34 and CSF-1 exhibit distinct developmental brain expression patterns and regulate neural progenitor cell maintenance and maturation. *Dev. Biol.* 367, 100–113. doi: 10.1016/j.ydbio.2012.03.026

Otero, K., Turnbull, I. R., Poliani, P. L., Vermi, W., Cerutti, E., Aoshi, T., et al. (2009). Macrophage colony-stimulating factor induces the proliferation and survival of macrophages via a pathway involving DAP12 and β-catenin. *Nat. Immunol.* 10, 734–743. doi: 10.1038/ni.1744

Pollard, J. W. (2009). Trophic macrophages in development and disease. *Nat. Rev. Immunol.* 9, 259–270. doi: 10.1038/nri2528

Rasmussen, S., Wang, Y., Kivisäkk, P., Bronson, R. T., Meyer, M., Imitola, J., et al. (2007). Persistent activation of microglia is associated with neuronal dysfunction of callosal projecting pathways and multiple sclerosis-like lesions in relapsing-remitting experimental autoimmune encephalomyelitis. *Brain* 130, 2816–2829. doi: 10.1093/brain/awm219

Ray, S., Britschgi, M., Herbert, C., Takeda-Uchimura, Y., Boxer, A., Blennow, K., et al. (2007). Classification and prediction of clinical Alzheimer's diagnosis based on plasma signaling proteins. *Nat. Med.* 13, 1359–1362. doi: 10.1038/nm1653

Rosi, S. (2016). A polarizing view on posttraumatic brain injury inflammatory response. *Brain Circ.* 2, 126–128. doi: 10.4103/2394-8108.192517

Ryan, G. R. (2001). Rescue of the colony-stimulating factor 1 (CSF-1)-nullizygous mouse (Csf1op/Csf1op) phenotype with a CSF-1 transgene and identification of sites of local CSF-1 synthesis. *Blood* 98, 74–84. doi: 10.1182/blood.v98.1.74

Ségaliny, A. I., Brion, R., Brulin, B., Maillasson, M., Charrier, C., Téletchéa, S., et al. (2015). IL-34 and M-CSF form a novel heteromeric cytokine and regulate the M-CSF receptor activation and localization. *Cytokine* 76, 170–181. doi: 10.1016/j.cyto.2015.05.029

Sielska, M., Przanowski, P., Wylot, B., Gabrusiewicz, K., Maleszewska, M., Kijewska, M., et al. (2013). Distinct roles of CSF family cytokines in macrophage infiltration and activation in glioma progression and injury response: GM-CSF in glioma pathology. *J. Pathol.* 230, 310–321. doi: 10.1002/path.4192

Smith, A. M., Gibbons, H. M., Oldfield, R. L., Bergin, P. M., Mee, E. W., Curtis, M. A., et al. (2013). M-CSF increases proliferation and phagocytosis while modulating receptor and transcription factor expression in adult human microglia. *J. Neuroinflammation* 10:85. doi: 10.1186/1742-2094-10-85

Soulet, D., and Rivest, S. (2008). Microglia. *Curr. Biol.* 18, R506–R508. doi: 10.1016/j.cub.2008.04.047

Stanley, E. R. (1976). Factors regulating macrophage production and growth: identity of colony- stimulating factor and macrophage growth factor. *J. Exp. Med.* 143, 631–647. doi: 10.1084/jem.143.3.631

Takeuchi, A., Miyaishi, O., Kiuchi, K., and Isobe, K.-I. (2001). Macrophage colony-stimulating factor is expressed in neuron and microglia after focal brain injury. *J. Neurosci. Res.* 65, 38–44. doi: 10.1002/jnr.1125

Thompson, A. J., Baranzini, S. E., Geurts, J., Hemmer, B., and Ciccarelli, O. (2018). Multiple sclerosis. *Lancet* 391, 1622–1936. doi: 10.1016/S0140-6736(18)30481-1

Toy, E. P., Azodi, M., Folk, N. L., Zito, C. M., Zeiss, C. J., and Chambers, S. K. (2009). Enhanced ovarian cancer tumorigenesis and metastasis by the macrophage colony-stimulating factor. *Neoplasia* 11, 136–144. doi: 10.1593/neo.81150

Uemura, Y., Ohno, H., Ohzeki, Y., Takanashi, H., Murooka, H., Kubo, K., et al. (2008). The selective M-CSF receptor tyrosine kinase inhibitor ki20227 suppresses experimental autoimmune encephalomyelitis. *J. Neuroimmunol.* 195, 73–80. doi: 10.1016/j.jneuroim.2008.01.015

Ushach, I., and Zlotnik, A. (2016). Biological role of granulocyte macrophage colony-stimulating factor (GM-CSF) and macrophage colony-stimulating factor (M-CSF) on cells of the myeloid lineage. *J. Leukoc. Biol.* 100, 481–489. doi: 10.1189/jlb.3RU0316-144R

Werner, K., Bitsch, A., Bunkowski, S., Hemmerlein, B., and Brück, W. (2002). The relative number of macrophages/microglia expressing macrophage colony-stimulating factor and its receptor decreases in multiple sclerosis lesions: M-CSF/M-CSFR expression in MS. *Glia* 40, 121–129. doi: 10.1002/glia.10120

Xu, C., Fu, F., Li, X., and Zhang, S. (2017). Mesenchymal stem cells maintain the microenvironment of central nervous system by regulating the polarization of macrophages/microglia after traumatic brain injury. *Int. J. Neurosci.* 127, 1124–1135. doi: 10.1080/00207454.2017.1325884

Conflict of Interest Statement: The authors declare that the research was conducted in the absence of any commercial or financial relationships that could be construed as a potential conflict of interest.

frontiers in Molecular Neuroscience

ORIGINAL RESEARCH
published: 24 December 2018
doi: 10.3389/fnmol.2018.00478

Altered Synaptic Vesicle Release and Ca^{2+} Influx at Single Presynaptic Terminals of Cortical Neurons in a Knock-in Mouse Model of Huntington's Disease

*Sidong Chen[1†], Chenglong Yu[1†], Li Rong[1], Chun Hei Li[1], Xianan Qin[2], Hoon Ryu[3] and Hyokeun Park[1,2,4]**

[1]Division of Life Science, The Hong Kong University of Science and Technology, Kowloon, Hong Kong, [2]Department of Physics, The Hong Kong University of Science and Technology, Kowloon, Hong Kong, [3]Department of Neurology, Boston University School of Medicine, Boston, MA, United States, [4]State Key Laboratory of Molecular Neuroscience, The Hong Kong University of Science and Technology, Kowloon, Hong Kong

Huntington's disease (HD) is an inherited neurodegenerative disorder caused by the abnormal expansion of CAG repeats in the *huntingtin* (*HTT*) gene, which leads to progressive loss of neurons starting in the striatum and cortex. One possible mechanism for this selective loss of neurons in the early stage of HD is altered neurotransmission at synapses. Despite the recent finding that presynaptic terminals play an important role in HD, neurotransmitter release at synapses in HD remains poorly understood. Here, we measured synaptic vesicle release in real time at single presynaptic terminals during electrical field stimulation. We found the increase in synaptic vesicle release at presynaptic terminals in primary cortical neurons in a knock-in mouse model of HD (zQ175). We also found the increase in Ca^{2+} influx at presynaptic terminals in HD neurons during the electrical stimulation. Consistent with increased Ca^{2+}-dependent neurotransmission in HD neurons, the increase in vesicle release and Ca^{2+} influx was rescued with Ca^{2+} chelators or by blocking N-type voltage-gated Ca^{2+} channels, suggesting N-type voltage-gated Ca^{2+} channels play an important role in HD. Taken together, our results suggest that the increased synaptic vesicles release due to increased Ca^{2+} influx at presynaptic terminals in cortical neurons contributes to the selective neurodegeneration of these neurons in early HD and provide a possible therapeutic target.

Keywords: Huntington's disease, synaptic vesicle release, calcium influx, real-time imaging, presynaptic terminal

OPEN ACCESS

Edited by:
Jaichandar (Jai) Subramanian, University of Kansas, United States

Reviewed by:
Anna Fejtova, Universitätsklinikum Erlangen, Germany
Anthony John Hannan, Florey Institute of Neuroscience and Mental Health, Australia

****Correspondence:***
Hyokeun Park
hkpark@ust.hk

[†]These authors have contributed equally to this work

Received: *12 July 2018*
Accepted: *06 December 2018*
Published: *24 December 2018*

Citation:
Chen S, Yu C, Rong L, Li CH, Qin X, Ryu H and Park H (2018) Altered Synaptic Vesicle Release and Ca^{2+} Influx at Single Presynaptic Terminals of Cortical Neurons in a Knock-in Mouse Model of Huntington's Disease. Front. Mol. Neurosci. 11:478. doi: 10.3389/fnmol.2018.00478

INTRODUCTION

Huntington's disease (HD) is an autosomal dominant neurodegenerative disorder caused by an increase in CAG trinucleotide repeats in the *huntingtin* (*HTT*) gene, giving rise to an expanded polyglutamine (polyQ) domain in the N-terminal of the encoded HTT protein (MacDonald et al., 1993). The main clinical symptoms of HD include severe involuntary motor dysfunction, psychiatric disturbance, cognitive impairment, and eventual death (Dayalu and Albin, 2015). Although the *HTT* gene is ubiquitously expressed throughout the human body, the medium spiny

neurons (MSNs) in the striatum and the pyramidal neurons in the cortex are most vulnerable neurons in HD (Vonsattel and DiFiglia, 1998).

It has been suggested that the selective loss of these neurons in HD may be associated with altered synaptic transmission (Klapstein et al., 2001; Cepeda et al., 2003; Li et al., 2003; Smith et al., 2005; Raymond et al., 2011; Tyebji and Hannan, 2017; Virlogeux et al., 2018), reduced support of brain-derived neurotrophic factor (BDNF; Zuccato and Cattaneo, 2009, 2014; Park, 2018; Yu et al., 2018), mitochondrial dysfunction (Carmo et al., 2018; Franco-Iborra et al., 2018), and altered Ca^{2+} regulation (Bezprozvanny, 2009; Miller and Bezprozvanny, 2010; Raymond, 2017). In particular, altered synaptic transmission has been investigated as a pathogenic mechanism and as a possible therapeutic target in HD (Raymond, 2017; Tyebji and Hannan, 2017). Some studies have focused on postsynaptic terminals, which are generally related to neuronal death in the striatum (Raymond, 2017). For example, increased activity of extrasynaptic N-methyl-D-aspartate receptors (NMDARs) was suggested to lead to the degeneration of striatal neurons (Milnerwood et al., 2010; Botelho et al., 2014; Plotkin et al., 2014). An increased intracellular Ca^{2+} concentration due to increased NMDAR activity and/or other Ca^{2+} sources, including the $InsP_3R1$ (inositol 1,4,5-trisphosphate receptor type 1) and store-operated Ca^{2+} entry, was also suggested to underlie the striatal neurodegeneration in HD (Tang et al., 2003, 2004; Wu et al., 2016). Activation of the NMDAR can be induced by the release of neurotransmitters from presynaptic terminals (Blanton et al., 1990; Atasoy et al., 2008). In this respect, it is interesting to note that mutant HTT protein has been reported to alter the exocytosis of presynaptic vesicles (DiFiglia et al., 1995; Morton et al., 2001; Romero et al., 2008; Joshi et al., 2009). Recently, reconstituted corticostriatal synapses formed in microfluidics devices showed that presynaptic terminals from cortical neurons contribute to HD (Virlogeux et al., 2018). However, the release of neurotransmitters at single presynaptic terminals as an input of corticostriatal synapses in HD remains poorly understood.

Using real-time imaging of single presynaptic terminals containing FM 1–43-labeled synaptic vesicles, we measured synaptic vesicle release in real time at single presynaptic terminals during electrical field stimulation. We found the increase in synaptic vesicle release at presynaptic terminals in primary cortical neurons in a knock-in mouse model of HD (zQ175). We also found the increase in Ca^{2+} influx at presynaptic terminals in HD neurons during the electrical stimulation. The increased release and Ca^{2+} influx in cortical neurons of heterozygous zQ175 were reduced by loading the neurons with BAPTA-AM (a Ca^{2+} chelator) or treating neurons with ω-conotoxin GVIA (a selective N-type voltage-gated Ca^{2+} channel blocker).

MATERIALS AND METHODS

Mice

The HD knock-in mice (zQ175) were obtained from Jackson Laboratories and were maintained in the Animal and Plant Care Facility at the Hong Kong University of Science and Technology (HKUST). Heterozygous mice were used for breeding. All procedures were approved by the Department of Health, Government of Hong Kong.

Primary Cultures of Cortical Neurons

HD and wild-type (WT) cortical neurons were obtained from primarily neocortical tissue of postnatal day 0 (P0) heterozygous pups and littermates. Approximately 10^5 neurons were cultured on each glass coverslip in 24-well plates as described previously (Liu and Tsien, 1995). Three days after plating the neurons (days in vitro 3, DIV3), 20 μM 5-Fluoro-2'-deoxyuridine (FUDR, Sigma) was added to inhibit the proliferation of glia (Leow-Dyke et al., 2012). The neurons were incubated at 37°C in humidified air containing 5% CO_2 for at least 14 days, and imaging and patch-clamp experiments were performed between DIV14 and DIV21.

Immunofluorescence

Cultured cortical neurons were fixed in 4% paraformaldehyde in phosphate-buffered saline (PBS) at room temperature for 10 min. After washing three times with ice-cold 0.1 M PBS, the neurons were permeabilized with PBS containing 0.1% Triton X-100 at room temperature for 10 min. After washing and blocking, 50 μl of primary antibody mixtures containing polyclonal anti-microtubule-associated protein 2 [anti-MAP2; 1:500; Ab5392 (Abcam)] together with the monoclonal anti-vesicular glutamate transporter 1 [anti-VGLUT1; 1:500; MAB5502 (Millipore)], monoclonal anti-glutamic acid decarboxylase 67 [anti-GAD67; 1:500; MAB5406 (Millipore)], monoclonal anti-GFAP [1:500; MAB360 (Millipore)], monoclonal anti-polyQ [1:500; MAB1574 (Millipore)], or monoclonal anti-ubiquitin [1:200; ab7780 (Abcam)] were added to each coverslip, and the neurons were incubated in a cold room overnight. The following day, Alexa 546-conjugated (A11040, Abcam) and Alexa 647-conjugated secondary antibodies (A31571, Abcam) were added. After washing with PBS three times, 50 μl DAPI (300 nM) was added to each coverslip, and the coverslips were mounted on glass slides. Fluorescence images were obtained using a Zeiss LSM 710 microscope. The percentage of VGLUT1 positive neuron was calculated by 100 × [(the number of VGLUT1-positive cells)/(the number of MAP2-positive cells)]. The percentage of GAD67-positive neurons was calculated by 100 × [(the number of GAD67-positive cells)/(the number of MAP2-positive cells)]. The percentage of GFAP-positive cells was calculated by 100 × [(the number of GFAP-positive cells)/(the number of MAP2-positive cells + the number of GFAP-positive cells)]. The number of VGLUT1-positive, GAD67-positive, and GFAP-positive cells was calculated in a blinded fashion.

Imaging of FM 1–43-Labeled Synaptic Vesicles

FM 1–43 was loaded into synaptic vesicles in cultured cortical neurons by applying 1-ms field stimuli at 10 Hz for 120 s in the presence of 16 μM FM 1–43 (T35356, Thermo Fisher Scientific) at 37°C using a parallel platinum electrode connected to an SD9 Grass Stimulator (Grass Technologies). The chamber was

perfused for 10 min with ACSF solution containing (in mM): 120 NaCl, 4 KCl, 2 $CaCl_2$, 2 $MgCl_2$, 10 D-Glucose, and 10 HEPES (300–310 mOsm, pH 7.2–7.4 with NaOH). The experiments were performed similarly as described previously (Zhang et al., 2007; Park et al., 2012). Time-lapse images were acquired for 200 s at 1 Hz with an exposure time of 0.1 s using an iXon Ultra EMCCD camera (Andor camera). The experimental setup was made up of several pieces of equipment as described previously (Alsina et al., 2017). The stimulator, beam shutter, and EMCCD camera were synchronized with a trigger from the camera *via* a Digidata 1550 (Molecular Devices). Clampex (Molecular Devices) was used to generate the stimulation protocol. An inverted IX-73 microscope (Olympus) was used with a 100× UPlanSApo oil-immersion objective (Olympus). A 532-nm laser (CrystaLaser) was used to illuminate FM 1–43 with a dichroic mirror (ZT532rdc) and emission filter (ET595/50m). The normalized fluorescence of FM 1–43 was calculated as the fluorescence intensity in a region of interest (ROI) relative to the mean of resting fluorescence intensity in that ROI during the first 20 s (F/F_0). The fluorescence intensity in a ROI was analyzed using MetaMorph software (Molecular Devices) and the normal fluorescence was calculated using customer-made MATLAB (MathWorks, Inc.) program. Average traces of normalized fluorescence were calculated using the average signal from all analyzed individual boutons. Fluorescence loss was calculated by subtracting the average normalized intensity in the final 60 s after stimulation and is expressed as a percentage. The time constant of FM 1–43 destaining was calculated by fitting the data from 20 s through 140 s to an exponential decay using a custom-written MATLAB program. The fitting with $R > 0.8$ was included for comparison of time constants of FM 1–43 destaining between WT and HD cortical neurons.

Electrophysiology

The paired-pulse ratio (PPR) between two evoked excitatory postsynaptic currents (eEPSCs) was measured in cultured cortical neurons after DIV14. Neurons were voltage clamped in the whole-cell configuration and recorded using a MultiClamp 700B amplifier (Molecular Devices) and a Digidata 1440a digitizer (Molecular Devices). Recordings were performed at room temperature under continuous perfusion of ACSF solution. Glass pipettes with a resistance of 3–5 MΩ were filled with an intracellular solution containing (in mM): 140 K-gluconate, 2 $MgCl_2$, 0.5 EGTA, 10 HEPES, and 0.5 Mg-ATP (300–310 mOsm, pH 7.3 with NaOH). The recorded neuron was held at −70 mV, and the stimulating electrode was positioned 100–200 μm from the recorded neuron. Two consecutive stimuli were applied at increasing intervals of 50, 100, 150, and 200 ms. PPR was calculated as the ratio between the second eEPSC amplitude and the first eEPSC amplitude.

Ca^{2+} Imaging

We performed Ca^{2+} imaging at single presynaptic terminals in cultured neurons using Cal-520-AM (21130, AAT Bioquest). A stock solution of 1 mM Cal-520-AM was prepared in dimethyl sulfoxide (DMSO) and stored at −20°C. The stock solution of Cal-520-AM was added to the culture medium at the final concentration of 1 μM, and neurons were incubated for 30 min. During the incubation, neurons were also incubated with FM 4–64 (T13320, Thermo Fisher Scientific) at a final concentration of 10 μM to label presynaptic terminals (Gaffield and Betz, 2006). Loaded neurons were then transferred to the imaging chamber and perfused continuously with ACSF for more than 20 min before imaging. FM 4–64 fluorescence was imaged using the frame-transfer mode for 10 frames with a 532-nm laser (CrystaLaser) with a dichroic mirror (ZT532rdc) and emission filter (ET665lp). Cal-520 fluorescence was acquired using a 488-nm laser (CrystaLaser) with a dichroic mirror (ZT488rdc) and emission filter (ET525/50m). Time-lapse imaging of Cal-520 was acquired similar to FM 1–43 imaging. Continuous imaging of Cal-520 with high temporal resolution was performed using a frame-transfer mode of 10 Hz (exposure time of 0.1 s) during 0.1 Hz external stimulation. The concentration of Ca^{2+} was estimated by the relative changes in fluorescence intensity relative to baseline fluorescence of Cal-520 ($\Delta F/F_0$).

FM 1–43 Destaining in the Presence of BAPTA-AM

FM 1–43 was loaded into synaptic vesicles as described above; 2 min after loading, the chamber was perfused with ACSF at 37°C containing 200 nM BAPTA-AM (B1205, Thermo Fisher Scientific) for 10 min. FM 1–43 imaging was then performed as described above. Data was analyzed as described above.

FM 1–43 Destaining in the Presence of ω-Conotoxin GVIA or ω-Agatoxin IVA

FM 1–43 was loaded into synaptic vesicles as described above; 2 min after loading, the chamber was perfused with ACSF for 10 min. The perfusion solution was then switched to ACSF containing 100 nM ω-conotoxin GVIA (C-300, Alomone Labs) or 200 nM ω-agatoxin GVIA (STA-500, Alomone Labs); 2 min later, FM 1–43 imaging was performed as described above. Data was analyzed as described above.

Ca^{2+} Imaging in the Presence of ω-Conotoxin GVIA

Neurons were loaded with Cal-520-AM and FM 4–64 as described above. After perfusion with ACSF for more than 20 min, the perfusion solution was then switched to ACSF containing 100 nM ω-conotoxin GVIA; 2 min later, FM 4–64 and Cal-520 imaging was performed as described above. Data was analyzed as described above.

Ca^{2+} Imaging in the Presence of Calciseptine, AP5, and NBQX

Neurons were loaded with Cal-520-AM and FM 4–64 as described above. After perfusion for >20 min with ACSF containing 1 μM calciseptine, 50 μM AP5, and 10 μM NBQX, FM 4–64 and Cal-520 imaging was performed as described above. Data were analyzed as described above.

Analysis

MetaMorph (Molecular Devices) was used to calculate fluorescence of FM 1–43 and Cal-520 within the ROIs. All data are presented as the mean ± SEM. Differences between HD and WT neurons were determined using the independent two-tailed Student's *t*-test or the Kolmogorov–Smirnov (K-S) test (SPSS, IBM Corp.). The effect of the toxins of voltage-gated Ca^{2+} channels on the release of FM 1–43 on genotypes was analyzed using two-way ANOVA analysis (SPSS, IBM Corp.). Differences with $p < 0.05$ were considered significant.

RESULTS

Excitatory Neurons Are Predominant in Primary Cortical Neurons

The loss of neurons in HD has been suggested to be associated with altered synaptic transmission (Raymond, 2017; Tyebji and Hannan, 2017). However, the release of neurotransmitters at single presynaptic terminals in HD has not been investigated in detail. To examine whether synaptic transmission is altered at single presynaptic terminals in HD neurons, we measured the release of synaptic vesicles at single presynaptic terminals in dissociated cortical neurons cultured from zQ175 mice, a recently developed knock-in mouse model of HD that is more relevant to human HD than other models in terms of genetic context and recapitulating the late onset, slow natural progression, and neuropathology of HD patients. Previous studies showed that the volume of the striatum and cortex decreases beginning at 4 months of age in heterozygous mice, and behavioral deficits appear at 4.5 months (Heikkinen et al., 2012; Menalled et al., 2012).

First, we measured the relative proportion of excitatory neurons in dissociated cortical neurons by plating low-density WT and HD cortical neurons isolated from P0 littermates; the neurons were then cultured until mature, functional synapses were formed. After DIV14, the cultured neurons were fixed and immunostained for MAP2 (a neuron-specific marker) and VGLUT1 (a marker for excitatory synapses). **Figure 1A** shows representative confocal images of WT and HD cortical neurons co-stained for MAP2 and VGLUT1. Our analysis between

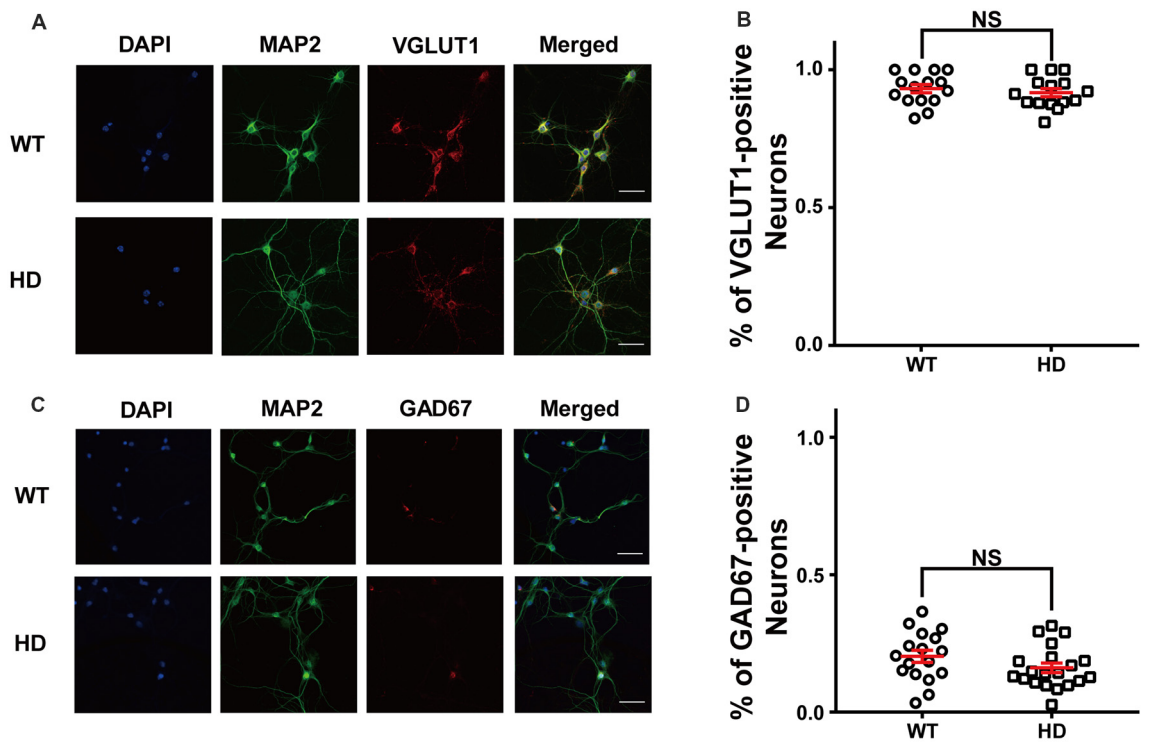

FIGURE 1 | The majority of cultured cortical neurons are excitatory. **(A)** Representative confocal images of wild-type (WT) and Huntington's disease (HD) cultured cortical neurons isolated from WT and heterozygous zQ175 mice immunostained for microtubule-associated protein 2 (MAP2; green) and vesicular glutamate transporter 1 (VGLUT1; an excitatory neuronal marker; red); the nuclei were counterstained with DAPI (blue). The scale bar represents 40 μm. **(B)** The percent of VGLUT1-positive neurons in WT and HD cortical neurons. The percentage of VGLUT1-positive neurons were higher than 90% regardless of genotype, indicating that the vast majority of neurons are excitatory. The percentage between WT and HD showed no significant differences ($p = 0.0225$, from independent two-tailed Student's *t*-test). **(C)** Representative confocal images of cultured neurons WT and HD cortical neurons immunostained for MAP2 (green) and glutamic acid decarboxylase 67 (GAD67; an inhibitory neuronal marker; red); the nuclei were counterstained with DAPI (blue). Scale bar represents 40 μm. **(D)** The percent of GAD67-positive neurons in WT and HD neurons. The percentage of GAD67-positive neurons between WT and HD showed no significant differences ($p = 0.136$; independent two-tailed Student's *t*-test). In this and subsequent figures, data are presented as the mean ± SEM. NS, not significant.

MAP2 and VGLUT1 immunoreactivity (**Figure 1B**) revealed that the vast majority of primary cultured cortical neurons are excitatory (i.e., VGLUT1-positive), with no significant difference between WT and HD neurons [93 ± 1.5% (N = 14) vs. 92 ± 1.5% (N = 15), p = 0.225 from independent two-tailed Student's t-test]. We also co-stained neurons for MAP2 and GAD67 (a marker for inhibitory neurons) in order to measure the proportion of inhibitory neurons in our cultures (**Figure 1C**). Our analysis confirms that only a minority of neurons are inhibitory, with no significant difference between WT and HD neurons [20 ± 2.2% (N = 17) vs. 16 ± 1.7% (N = 20), p = 0.136 from independent two-tailed Student's t-test; **Figure 1D**]. We also measured the number of glial cells in our primary cultures and found that glial cells represent approximately 12% of the cells in both WT and HD neurons (12 ± 1.6% vs. 11 ± 1.5%, respectively; N = 10; p = 0.774, independent two-tailed Student's t-test; **Supplementary Figure S1**). We also looked for the presence of inclusion bodies (a pathological hallmark of HD) in our culture system using antibodies against polyQ and ubiquitin; however, no such aggregates were observed (**Supplementary Figure S2**). Taken together, our immunostaining results indicate that the majority of cultured mouse cortical neurons are excitatory, consistent with previous reports (Gabbott and Somogyi, 1986; Hendry et al., 1987).

Synaptic Vesicle Release Is Increased in HD Cortical Neurons

Next, we examined whether the mutant HTT protein affects the release of synaptic vesicles at presynaptic terminals of cortical neurons. We loaded presynaptic vesicles with FM 1–43 (a membrane-impermeable lipophilic styryl dye) using electrical field stimulation. We then measured the decrease in FM 1–43 fluorescence at single presynaptic terminals during electrical field stimulation (Betz and Bewick, 1992; Ryan et al., 1993; Gaffield and Betz, 2006; Yu et al., 2016). The loading protocol consisted of a train of 1,200 1-ms stimuli delivered at 10 Hz for 120 s, which labels the total recycling pool of synaptic vesicles (Zhang et al., 2007, 2009; Park et al., 2012), followed by extensive washing with ACSF to remove extracellular and plasma membrane-bound FM 1–43, thereby enabling us to specifically monitor FM 1–43-loaded vesicles.

Figure 2A shows typical fluorescence images of cultured WT (**Figure 2A1**) and HD (**Figure 2A2**) neurons after extensive washing, showing FM 1–43-loaded presynaptic vesicles (Ryan et al., 1993; Henkel et al., 1996). Fluorescence intensity of the FM 1–43 signal was calculated at fixed ROI (Harata et al., 2001; Jordan et al., 2005), each of which encompasses a single isolated FM 1–43-bright spot called a bouton, likely representing a single presynaptic terminal. To exclude synapses that were labeled by spontaneous neuronal activity and nonspecific labeling with FM 1–43, isolated boutons that showed destaining upon electrical field stimulation were used to measure synaptic vesicle release.

The density of functional presynaptic terminals was calculated by counting boutons labeled with FM 1–43 at the presynaptic terminal. The average bouton density was similar between cultured WT and HD cortical neurons (0.59 ± 0.008 boutons·μm^{-1} and 0.59 ± 0.014 boutons·μm^{-1}, respectively; N = 5 experiments/genotype; p = 0.803), suggesting that the presence of the mutant HTT protein does not alter the number of functional presynaptic terminals in cortical neurons.

Next, we used electrical field stimulation to destain FM 1–43-loaded synaptic vesicles and measured vesicle release using real-time imaging of single presynaptic terminals. The release of vesicular FM 1–43 was reflected as a decrease in FM 1–43 intensity in each ROI. **Figure 2B** displays a time course of normalized fluorescence intensity in WT (**Figure 2B1**) and HD (**Figure 2B2**) cortical neurons at individual boutons during electrical field stimulation with 1,200 electrical pulses, which trigger the release of synaptic vesicles from the total recycling pool at the level of single boutons (Zhang et al., 2007, 2009; Welzel et al., 2011; Park et al., 2012; Yu et al., 2016). The normalized fluorescence intensity was calculated as the ratio of the intensity in the ROI with respect to the average intensity before stimulation (i.e., baseline fluorescence). As expected, our stimulation protocol induced the rapid release of FM 1–43 in individual presynaptic terminals in both WT and HD neurons. The degree of fluorescence loss at individual presynaptic terminals in cortical neurons was highly variable; consistent with previous reports (Murthy et al., 1997; Branco and Staras, 2009; Daniel et al., 2009), the coefficient of variation (CV) was 23% and 19% in WT and HD neurons, respectively. Nevertheless, the total loss of fluorescence was significantly higher in HD neurons compared to WT neurons [59 ± 1.3% (n = 62 boutons, N = 8 experiments for HD) vs. 42 ± 1.4% (n = 60 boutons, N = 7 for WT), p = 4.27E-15 from independent two-tailed Student's t-test; **Figure 2C**] during the electrical stimulation to trigger the release of synaptic vesicles from the total recycling pool. Given that relative release probability (P_r) is proportional to the relative release of lipophilic dyes (Murthy et al., 1997; Branco et al., 2008; Branco and Staras, 2009; Daniel et al., 2009), our finding of increased fluorescence loss at presynaptic terminals of HD neurons likely indicates that in HD, cortical neurons have a higher release probability compared to WT neurons.

In addition to measuring total fluorescence loss, we also measured the kinetics of vesicle release by fitting the time course of fluorescence loss with an exponential time constant (Richards et al., 2005; Daniel et al., 2009). As shown in **Figure 2D**, the time constant of FM 1–43 destaining was significantly smaller in HD neurons compared to WT neurons [39.9 ± 2.5 s (n = 57 boutons) for HD vs. 53.8 ± 6.5 s (n = 54 boutons) for WT, p = 0.0448 from independent two-tailed Student's t-test], suggesting faster vesicle release at presynaptic terminals of HD cortical neurons. Taken together, these results indicate that cortical neurons expressing the mutant HTT protein have increased neurotransmission compared to WT neurons under similar stimulation conditions.

Next, we measured whether inhibitory neurotransmission is altered in inhibitory synapses by measuring the release

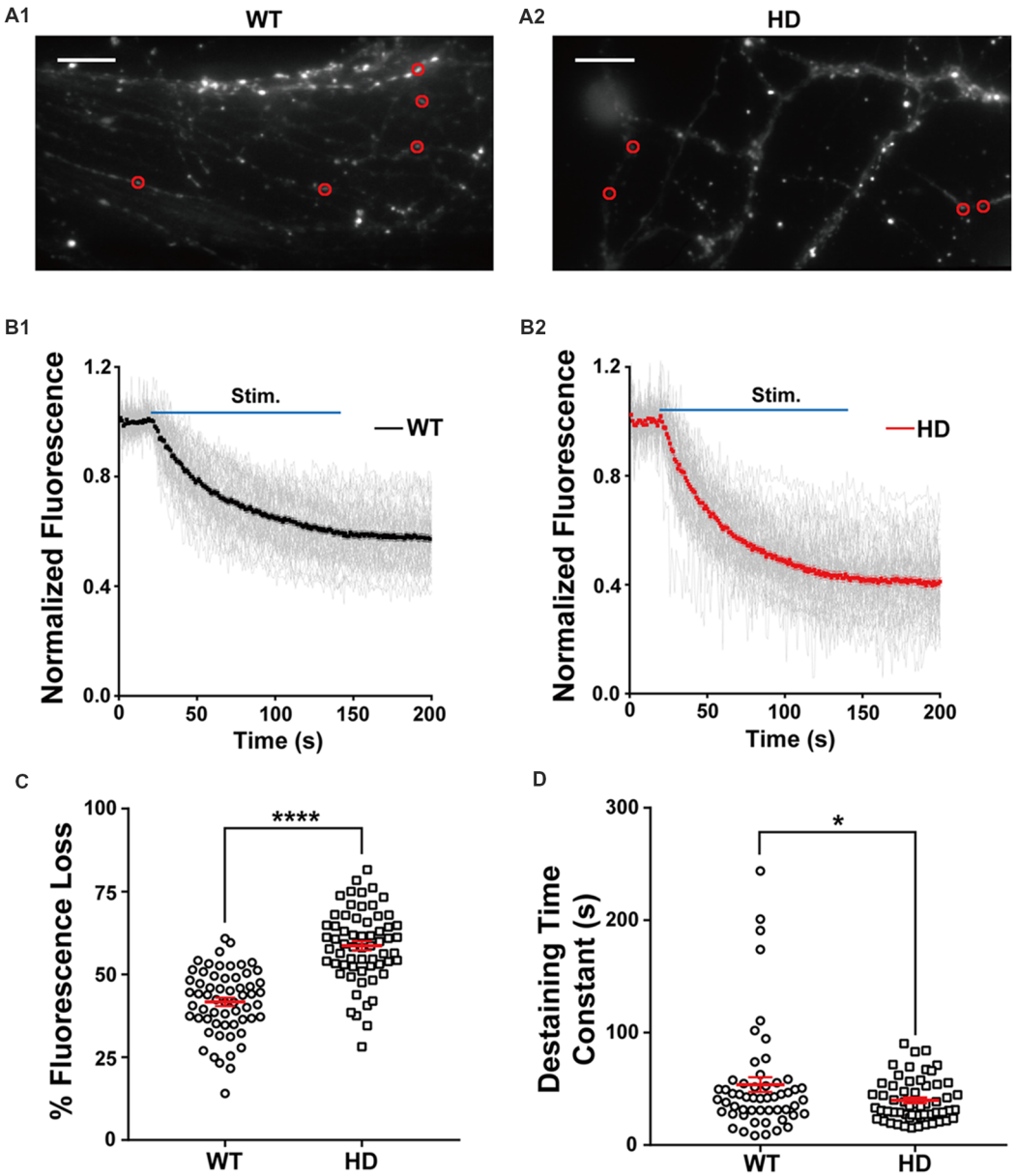

FIGURE 2 | HD cortical neurons have increased synaptic vesicle release. **(A1,A2)** Representative images of WT and HD cortical neurons loaded with FM 1–43. The red circles indicate the regions of interest (ROIs) representing presynaptic terminals that were analyzed for FM 1–43 release. The scale bars represent 10 μm. **(B1,B2)** Traces of normalized fluorescence intensity showing FM 1–43 destaining during 1,200 1-ms field stimuli applied at 10 Hz for 120 s in WT (n = 60 boutons, N = 7 experiments) and HD cortical neuron (n = 62 boutons, N = 8 experiments). **(C)** The percent fluorescence loss of FM 1–43 staining in WT and HD cortical neurons. **(D)** The time constant of FM 1–43 destaining in WT and HD cortical neurons. *$p < 0.05$ and ****$p < 0.0001$ (independent two-tailed Student's t-test).

of VGAT-cypHer5e, a fluorescent marker that selectively labels inhibitory synaptic vesicles (Hua et al., 2011). In contrast with our FM 1–43 results, WT and HD neurons were similar with respect to VGAT-cypHer5e fluorescence loss (**Supplementary Figure S3**), suggesting that inhibitory neurotransmission is not altered in cortical neurons expressing mutant HTT proteins. Given the relatively small number of inhibitory neurons in our cortical cultures and no alteration in the inhibitory neurotransmission in HD cortical neurons, we conclude that the mutant HTT protein primarily affects excitatory neurotransmission in cortical neurons.

Synapses in HD Cortical Neurons Have Paired-Pulsed Depression

Next, we investigated in further detail the release probability in HD cortical neurons of zQ175 knock-in mice by recording eEPSCs in a postsynaptic neuron (**Figure 3A**); eEPSCs were

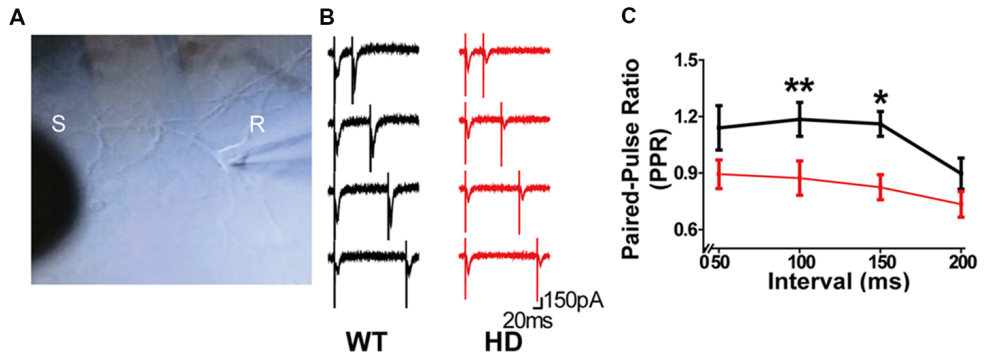

FIGURE 3 | Synapses in HD cortical neurons exhibit paired-pulse depression. **(A)** Example image of cultured cortical neurons, showing the stimulating electrode (S) and recording electrode (R). **(B)** Representative traces of evoked excitatory postsynaptic currents (eEPSPs) recorded in WT and HD cortical neurons. From top to bottom, the interval between the two stimuli was 50, 100, 150, and 200 ms. **(C)** The paired-pulse ratio (PPR) was measured as the amplitude of the second EPSP divided by the first EPSP and is plotted against the interval between stimuli. $*p < 0.05$ and $**p < 0.01$ [Kolmogorov–Smirnov (K-S) test; $n = 15$ per genotype].

evoked using a monopolar silver wire electrode, and the currents were then used to calculate the PPR. **Figure 3B** shows example recordings of a WT and HD neuron with increasing paired-pulse intervals. Given that the amplitude of an EPSC is largely dependent upon the number of synaptic vesicles released upon presynaptic stimulation, the ratio between the second EPSC amplitude and the first EPSC is widely used as a measure of release probability (Dobrunz and Stevens, 1997). Specifically, neurons with low release probability tend to have a larger available pool for the second stimulation, giving rise to paired-pulse facilitation (Debanne et al., 1996; Murthy et al., 1997). Therefore, the measured PPR is inversely correlated to release probability (Dobrunz and Stevens, 1997; Murthy et al., 1997).

Using the four pulse intervals shown in **Figure 3B** (i.e., 50, 100, 150, and 200 ms), we calculated the PPR for WT and HD neurons (**Figure 3C**). Our analysis ($n = 15$ per genotype) revealed that HD synapses have significantly smaller PPR values with a 100-ms ($p = 0.005$ from K-S test) and 150-ms ($p = 0.017$ from K-S test) interval between the first and second pulses compared with WT neurons. Moreover, the PPR in HD synapses was smaller than 1.0 at all interval tests, consistent with paired-pulse depression. Taken together, these data suggest that presynaptic terminals in HD cortical neurons of heterozygous zQ175 mice have increased release probability, consistent with our FM 1–43 results.

Presynaptic Ca^{2+} Influx Is Increased in HD Cortical Neurons

Ca^{2+} influx into the presynaptic terminal triggers the release of neurotransmitter *via* the Ca^{2+}-dependent fusion of synaptic vesicles (Luebke et al., 1993; Südhof, 2012). Moreover, the cumulative increase in presynaptic Ca^{2+} influx during high-frequency stimulation enhances the recruitment of synaptic vesicles for fusion (Wang and Kaczmarek, 1998; Hosoi et al., 2007). Thus, Ca^{2+} influx at presynaptic terminals is a key factor in determining the strength of neurotransmission (Murthy et al., 1997; Ermolyuk et al., 2012; Körber and Kuner, 2016).

To investigate whether the increase in neurotransmission in HD neurons is mediated by an increase in presynaptic Ca^{2+} influx, we measured presynaptic Ca^{2+} transient during electrical field stimulation of neurons loaded with Cal-520-AM, an ultrasensitive fluorescence-based Ca^{2+} indicator well-suited for measuring Ca^{2+} level in subcellular compartments (Tada et al., 2014; Lock et al., 2015). Representative images of cultured WT and HD neurons co-loaded with FM 4–64 (to label presynaptic terminals) and Cal-520 are shown in **Figure 4A**. The fluorescence signal of Cal-520 was used to measure Ca^{2+} transients specifically at presynaptic terminals. Presynaptic Ca^{2+} was measured as the fluorescence change relative to resting fluorescence ($\Delta F/F_0$), which normalizes various factors, including differences in dye loading, in order to minimize possible artifacts associated with measuring raw fluorescence intensity (Chen et al., 2013; Lock et al., 2015). Average traces of $\Delta F/F_0$ in Cal-520-loaded WT and HD cortical neurons are shown in **Figure 4B**. Applying 1,200 field stimuli caused a significantly larger peak intensity in $\Delta F/F_0$ in presynaptic terminals of HD neurons compared to WT neurons [8.1 ± 0.17 (n = 571 boutons, N = 17 experiments for HD) vs. 6.7 ± 0.21 (n = 474 boutons, N = 16 experiments for WT), p = 1.51E-7, K-S test; **Figure 4C**], which indicates a significantly larger increase of Ca^{2+} influx in the presynaptic terminals of HD neurons during electrical field stimulation.

Next, we measured the entire increase in presynaptic Ca^{2+} during field stimulation by calculating the area under the curve for $\Delta F/F_0$ (Atucha et al., 2003; Reznichenko et al., 2012). The area under the curve for $\Delta F/F_0$ in the presynaptic terminals of HD neurons was significantly larger than that in WT terminals (714 ± 14.8 for HD vs. 559 ± 19.3 for WT, p = 1.37E-10; **Figure 4D**), implying that significantly more Ca^{2+} entered the presynaptic terminals in HD neurons compared with WT neurons during field stimulation. Moreover, presynaptic terminals of HD neurons had significantly more Ca^{2+} following field stimulation (170 ± 5.2 for HD vs. 126 ± 6.4 for WT, p = 1.10E-7; **Figure 4E**). These results suggest that HD cortical neurons of heterozygous zQ175 mice have increased Ca^{2+}

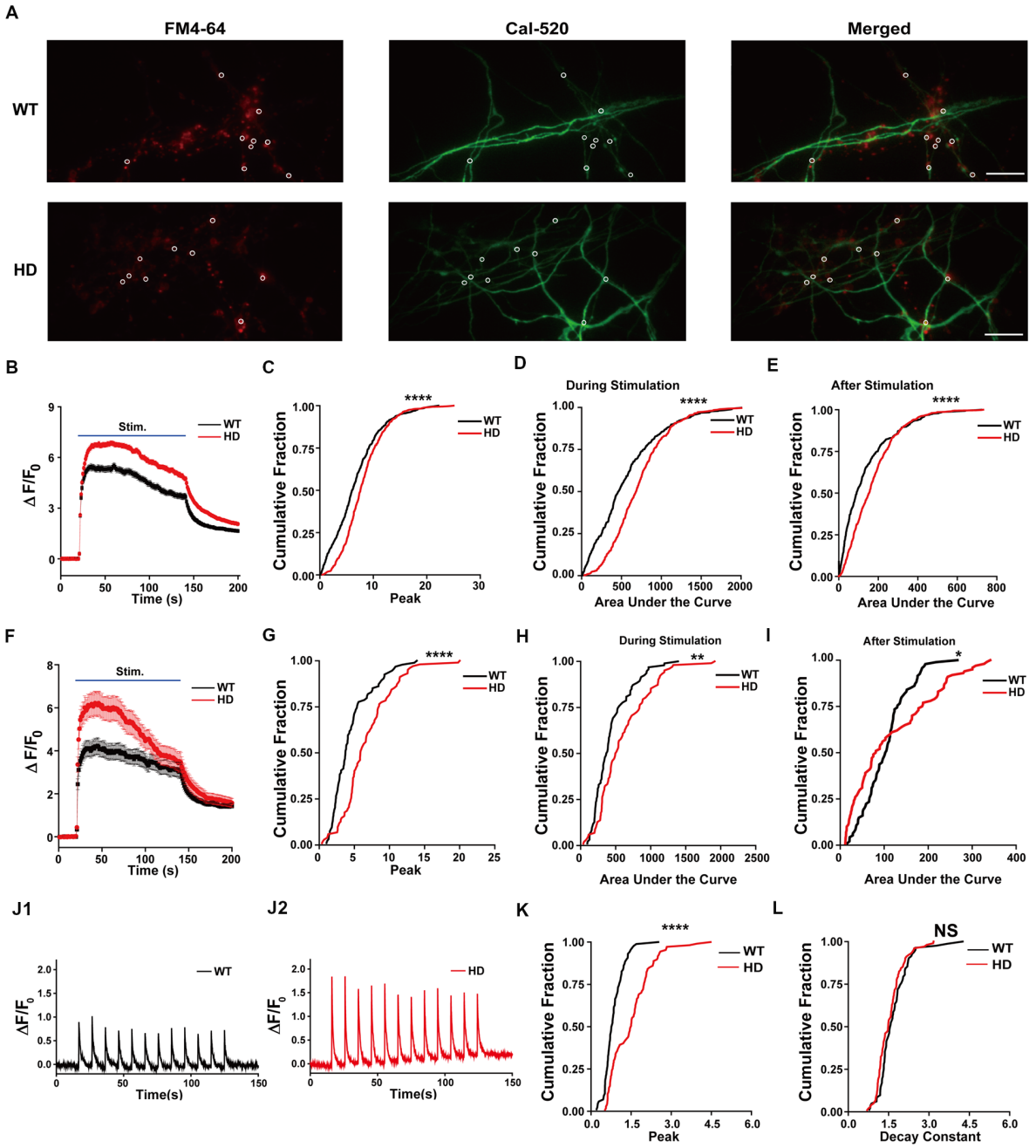

FIGURE 4 | HD cortical neurons increase presynaptic Ca^{2+} influx. **(A)** Representative images of WT and HD cortical neurons loaded with FM 4–64 (to label presynaptic terminals) and Cal-520 (an ultrasensitive fluorescence-based Ca^{2+} indicator). Cal-520 fluorescence was measured at FM 4–64-positive puncta (white circles) as the change in fluorescence relative to baseline fluorescence ($\Delta F/F_0$). The scale bar represents 10 μm. **(B)** Average $\Delta F/F_0$ traces measured before, during, and after field stimulation with 1,200 1-ms pulses delivered at 10 Hz for 120 s; n = 474 boutons in WT (N = 16 experiments) and n = 571 boutons in HD neurons (N = 15 experiments). **(C)** The peak $\Delta F/F_0$ of Cal-520 during the electrical stimulation. **(D)** Area under the curve of fluorescence change ($\Delta F/F_0$) during the stimulation. **(E)** Area under the curve of fluorescence change ($\Delta F/F_0$) after stimulation. **(F)** Average $\Delta F/F_0$ traces measured before, during, and after field stimulation with 1,200 1-ms pulses delivered at 10 Hz for 120 s in the presence of 50 μM AP5, 10 μM NBQX, and 1 μM calciseptine; n = 94 boutons in WT (N = 6 experiments) and n = 102 boutons in HD neurons (N = 9 experiments). **(G)** The peak $\Delta F/F_0$ of Cal-520 in the presence of 50 μM AP5, 10 μM NBQX, and 1 μM calciseptine during the electrical stimulation. **(H)** Area under the curve of fluorescence change ($\Delta F/F_0$) in the presence of 50 μM AP5, 10 μM NBQX, and 1 μM calciseptine during the stimulation. **(I)** Area under the curve of fluorescence change ($\Delta F/F_0$) in the presence of 50 μM AP5, 10 μM NBQX, and 1 μM calciseptine after stimulation. **(J)** Representative traces of $\Delta F/F_0$ traces measured at 10 Hz imaging frequency before, during, and after stimulation with 12 1-ms pulses delivered at 0.1 Hz for 120 s in WT (n = 86 boutons and N = 7 experiments; **J1**) and HD (n = 107 boutons and N = 6 experiments) neurons **(J2)**. **(K)** Peak of $\Delta F/F_0$ measured after a single stimulus, averaged for single boutons. **(L)** Decay constant of $\Delta F/F_0$ after a single stimulus averaged for single boutons in WT (n = 86 boutons and N = 7 experiments) and HD (n = 107 boutons and N = 6 experiments) neurons. *$p < 0.05$, **$p < 0.01$, ****$p < 0.0001$ and NS, not significant (K-S test).

influx, which may suggest a possible mechanism underlying the increased excitatory activity in HD. To confirm that the measured $\Delta F/F_0$ represents Ca^{2+} influx in presynaptic terminals, we repeated these experiments in the presence of 50 μM AP5 (an NMDA receptor antagonist), 10 μM NBQX (an AMPA receptor antagonist), and 1 μM calciseptine (an L-type voltage-gated Ca^{2+} channels blocker). The peak response, the area under the curve measured during 1,200 stimuli, and the area under the curve measured after the 1,200 stimuli were unaffected by the presence of these blockers (**Figures 4F–I**). Moreover, all of these parameters differed significantly WT an HD neurons (**Figures 4F–I**). These results confirm that we indeed measured Ca^{2+} in presynaptic terminals.

In order to examine the detailed mechanism underlying the increased Ca^{2+} influx in HD neurons, we also measured Ca^{2+} influx with high temporal resolution imaging. **Figure 4J** shows exemplar traces of $\Delta F/F_0$ measured using 10 Hz imaging while stimulating at 0.1 Hz in WT (**Figure 4J1**) and HD (**Figure 4J2**) neurons. The traces of $\Delta F/F_0$ show that the signal returned to baseline within 10 s of stimulation. We also measured the peak intensity of $\Delta F/F_0$ and the decay constant in response to a single stimulus. We found that the average peak $\Delta F/F_0$ after a single stimulus was significantly higher in HD neurons than in WT neurons [1.50 ± 0.075 for HD (n = 107 boutons, N = 6 experiments) vs. 0.85 ± 0.040 for WT (n = 86 boutons, N = 7 experiments), respectively, p < 1.0E-17, K-S test; **Figure 4K**], indicating that more Ca^{2+} ions enter the presynaptic terminals of HD neurons compared to WT neurons. The addition of more Ca^{2+} influx after each stimulus in the HD neurons led to the significantly larger influx of Ca^{2+} during 1,200 external stimuli shown in **Figure 4C**. Next, to investigate whether the clearance of Ca^{2+} is altered in HD neurons, we calculated the decay constant of $\Delta F/F_0$ by fitting the decay phase of $\Delta F/F_0$ to an exponential function. We found that the decay constant was similar between HD and WT neurons [1.54 ± 0.049 s for HD (n = 102 boutons) vs. 1.68 ± 0.064 s for WT (n = 82 boutons), p = 0.11, K-S test; **Figure 4L**], suggesting that Ca^{2+} clearance is not altered in HD neurons. The increased peak intensity in HD neurons, together with no change in Ca^{2+} clearance, suggests a possible association between the mutant HTT protein and voltage-gated Ca^{2+} channels during electrical stimulation.

Loading HD Neurons With BAPTA-AM (a Ca^{2+} Chelator) Prevents Increased Synaptic Vesicle Release

Next, we directly examined the role of presynaptic Ca^{2+} on neurotransmission in HD cortical neurons by loading neurons with the membrane-permeable Ca^{2+} chelator BAPTA-AM (Tsien, 1981) and measuring vesicle fusion in single FM 1–43-loaded presynaptic terminals. We used 200 nM BAPTA for these experiments, as this chelator has been reported to protect neurons against excitotoxicity (Tymianski et al., 1993, 1994; Abdel-Hamid and Tymianski, 1997). As shown in **Figure 5A**, HD cortical neurons loaded with BAPTA-AM had significantly reduced the release of vesicles compared to control HD neurons (loaded with DMSO); this reduction was reflected in both the significant average fluorescence loss [37.9 ± 2.0% (n = 32 boutons, N = 6 experiments with BAPTA-AM) vs. 57.8 ± 3.0% (n = 25 boutons, N = 5 experiments with DMSO), p = 1.33E-7, independent two-tailed Student's t-test; **Figure 5B**] and the increased time constant of FM 1–43 destaining [80.6 ± 12.4 s (n = 16 boutons) with BAPTA-AM vs. 34.4 ± 4.4 s (n = 21 boutons) with DMSO, p = 0.000428; **Figure 5C**]. Interestingly, loading HD neurons with BAPTA reduced fluorescence loss to WT levels [37.9 ± 2.0% vs. 41.7 ± 1.4% (WT), respectively]. The application of BAPTA-AM to WT neurons also decreased the fluorescence loss [23.1 ± 1.0% (n = 40 boutons, N = 5 experiments with BAPTA-AM) vs. 42.2 ± 1.5% (n = 32 boutons, N = 5 experiments with DMSO), p = 8.29E-17; **Figures 5D,E**], but did not decrease the destaining time constant [42.4 ± 6.2 s (n = 25 boutons with BAPTA-AM) vs. 39.9 ± 2.2% (n = 26 boutons with DMSO), p = 0.59, independent two-tailed Student's t-test; **Figure 5F**]. These results indicate that restricting Ca^{2+} influx at presynaptic terminals prevents the increased neurotransmission in HD cortical neurons of heterozygous zQ175 mice.

Blocking N-type Voltage-Gated Ca^{2+} Channels Prevents Increased Synaptic Vesicle Release and Presynaptic Ca^{2+} Influx in HD Neurons

Evoked vesicle fusion requires presynaptic Ca^{2+} influx through voltage-gated Ca^{2+} channels, which are coupled to the fusion machinery at presynaptic terminals (Vázquez and Sánchez-Prieto, 1997; Simms and Zamponi, 2014). In the central nervous system, presynaptic Ca^{2+} influx is mediated primarily by N-type ($Ca_v2.2$) and P/Q-type ($Ca_v2.1$) voltage-gated Ca^{2+} channels (Zamponi, 2003; Catterall, 2011). However, several reports have suggested that N-type voltage-gated Ca^{2+} channels can be affected by mutant HTT protein. That is, mutant HTT proteins were reported to modulate N-type voltage-gated Ca^{2+} channels by their interaction with N-type voltage-gated Ca^{2+} channels and binding proteins (Miller et al., 2003; Swayne et al., 2005; Silva et al., 2017), or the expression level of N-type voltage-gated Ca^{2+} channels in the plasma membrane (Silva et al., 2017). To test the role of N-type voltage-gated Ca^{2+} channels in the increased Ca^{2+} influx and neurotransmission measured in HD cortical neurons, we treated HD neurons with 100 nM ω-conotoxin GVIA (a highly selective blocker of N-type voltage-gated Ca^{2+} channels). We found that ω-conotoxin GVIA decreased the release of FM 1–43 during field stimulation (**Figure 6A**), reflected by a significant decrease in fluorescence loss [53.6 ± 1.9% (n = 36 boutons, N = 4 experiments without ω-conotoxin GVIA) vs. 34.8 ± 1.5% (n = 31 boutons, N = 5 experiments with ω-conotoxin GVIA), p = 7.18E-10, independent two-tailed Student's t-test; **Figure 6B**]. Treatment with ω-conotoxin GVIA also significantly increased the time constant of FM 1–43 destaining [24.5 ± 2.0 s (n = 35 boutons without ω-conotoxin GVIA) vs. 43.3 ± 4.4 s (n = 22 boutons with ω-conotoxin GVIA), p = 0.000063; **Figure 6C**].

We also treated WT neurons with ω-conotoxin GVIA and measured the release of FM 1–43 during field stimulation

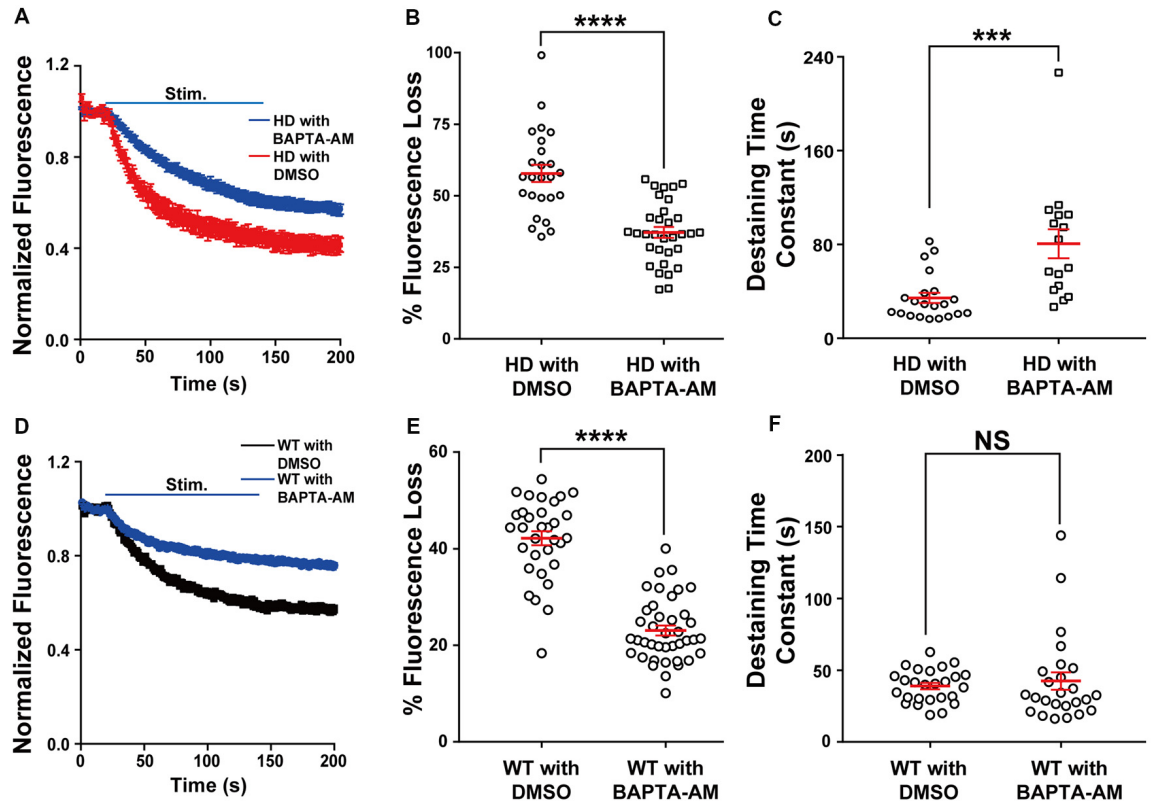

FIGURE 5 | Loading HD and WT neurons with BAPTA-AM reduces the increased release of synaptic vesicles. **(A)** Average traces of normalized FM 1–43 fluorescence intensity in HD neurons loaded with BAPTA-AM (n = 32 boutons, N = 6 experiments) or vehicle dimethyl sulfoxide (DMSO; n = 25 boutons, N = 5 experiments). Where indicated, the neurons were stimulated with 1,200 1-ms field stimuli delivered at 10 Hz for 120 s. **(B)** The percent fluorescence loss of FM 1–43 in control-treated and BAPTA-AM-loaded HD cortical neurons. **(C)** The time constant of FM 1–43 destaining in control-treated and BAPTA-AM-loaded HD cortical neurons. **(D)** Average traces of normalized FM 1–43 fluorescence intensity in WT neurons loaded with BAPTA-AM (n = 40 boutons, N = 5 experiments) or vehicle (DMSO; n = 32 boutons, N = 5 experiments). Where indicated, the neurons were stimulated with 1,200 1-ms field stimuli delivered at 10 Hz for 120 s. **(E)** The percent fluorescence loss of FM 1–43 in control-treated and BAPTA-AM-loaded WT cortical neurons. **(F)** The time constant of FM 1–43 destaining in control-treated and BAPTA-AM-loaded WT cortical neurons. NS, not significant, ***$p < 0.001$, and ****$p < 0.0001$ (independent two-tailed Student's t-test).

(**Figure 6A**). We found a significant decrease in fluorescence loss of FM 1–43 with ω-conotoxin GVIA [45.0 ± 1.3% (n = 49 boutons, N = 5 experiments without ω-conotoxin GVIA) vs. 34.5 ± 2.0% (n = 29 boutons, N = 4 experiments with ω-conotoxin GVIA), p = 0.000019; **Figures 6A,B**]. However, the effect of application of ω-conotoxin GVIA on fluorescence loss of HD neurons was significantly different compared with WT neurons (p = 0.0339, two-way ANOVA analysis). In addition, application of ω-conotoxin GVIA in WT cortical neurons did not significantly affect the time constant of FM 1–43 destaining in WT cortical neurons [52.1 ± 4.5 s (n = 45 boutons without ω-conotoxin GVIA) vs. 38.4 ± 6.2 s (n = 23 boutons with ω-conotoxin GVIA), p = 0.0814; **Figure 6C**], suggesting that blocking N-type voltage-gated Ca^{2+} channels does not affect vesicle release kinetics in WT cortical neurons. The effect of application of ω-conotoxin GVIA on vesicle release kinetics of HD neurons was significantly different compared with WT neurons (p = 0.0006, two-way ANOVA analysis).

In addition, treating HD neurons with ω-conotoxin GVIA reduced the increase in presynaptic Ca^{2+} influx (**Figure 7A**); treating HD neurons with ω-conotoxin GVIA significantly reduced both the peak increase in $\Delta F/F_0$ [4.9 ± 0.17 (n = 254 boutons, N = 6 experiments without ω-conotoxin GVIA) vs. 4.1 ± 0.21 (n = 162 boutons, N = 6 experiments with ω-conotoxin GVIA), p = 0.00232, K-S test; **Figure 7B**] and the area under the curve during the field stimulation [435 ± 15.6 without ω-conotoxin GVIA vs. 383 ± 21.6 with ω-conotoxin GVIA, p = 0.047; **Figure 7C**].

Next, we tested whether the decreased Ca^{2+} influx during 1,200 external stimuli in HD neurons in the presence of ω-conotoxin GVIA is caused by decreased Ca^{2+} influx by a single stimulus, we used high temporal resolution imaging to measure the average peak $\Delta F/F_0$ in response to a single stimulus. The application of ω-conotoxin GVIA to HD neurons decreased the average peak $\Delta F/F_0$ significantly [1.50 ± 0.075 for HD without ω-conotoxin GVIA (**Figure 7E1**; n = 107 boutons, N = 6 experiments) vs. 0.80 ± 0.042 for HD with ω-conotoxin GVIA (**Figure 7E2**; n = 86 boutons, N = 5 experiments), p = 2.1E-13, independent two-tailed Student's t-test; **Figures 7E,F**]. The application of ω-conotoxin GVIA to WT neurons also decreased

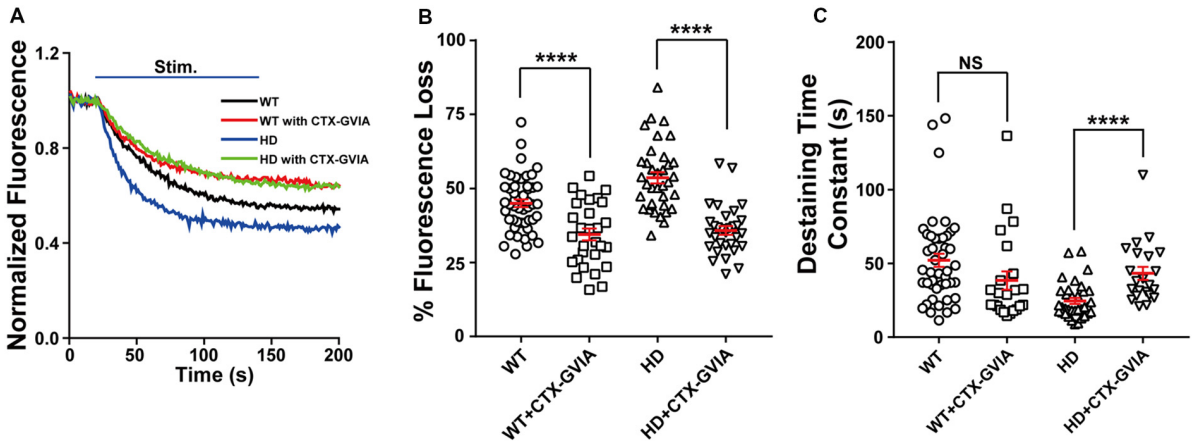

FIGURE 6 | Blocking N-type voltage-gated Ca^{2+} channels reduces the increased release of synaptic vesicles in HD cortical neurons. **(A)** Average traces of normalized FM 1–43 fluorescence intensity in untreated HD (n = 36 boutons, N = 4 experiments) and WT cortical neurons (n = 49 boutons, N = 5 experiments), HD (n = 31 boutons, N = 5 experiments) and WT cortical neurons (n = 29 boutons, N = 4 experiments) treated with 100 nM ω-conotoxin GVIA (Ctx-GVIA). Where indicated, 1,200 1-ms field stimuli were delivered at 10 Hz for 120 s. **(B)** The percent fluorescence loss of FM 1–43 in untreated and ω-conotoxin GVIA-treated HD and WT neurons. The average change in fluorescence loss in response to ω-conotoxin GVIA treatment was considerably smaller in WT cortical neurons (10.5%) compared with HD neurons (17.8%). **(C)** The time constant of FM 1–43 destaining in untreated and ω-conotoxin GVIA-treated HD and WT cortical neurons. The destaining rates of FM 1–43 in WT cortical neurons with ω-conotoxin GVIA were not significantly different from those without ω-conotoxin GVIA ($p > 0.08$). NS, not significant, and ****$p < 0.0001$ (independent two-tailed Student's t-test).

the average peak $\Delta F/F_0$ significantly [0.85 ± 0.040 for WT without ω-conotoxin GVIA (**Figure 7D1**; n = 86 boutons, N = 7 experiments) vs. 0.73 ± 0.032 for WT with ω-conotoxin GVIA (**Figure 7D2**; n = 84 boutons, N = 5 experiments), p = 0.028, independent two-tailed Student's t-test; **Figures 7D,F**], but the effect was significantly smaller in WT neurons than in HD neurons (p = 4.2E-8, two-way ANOVA). We also calculated the decay constant of $\Delta F/F_0$ by fitting the of $\Delta F/F_0$ traces to an exponential function. The decay constants in HD and WT neurons were unaffected by the presence of ω-conotoxin GVIA [1.54 ± 0.049 s without ω-conotoxin GVIA (n = 102 boutons, N = 6 experiments) vs. 1.56 ± 0.066 s with ω-conotoxin GVIA (n = 81 boutons, N = 5 experiments) for HD, p = 0.89; 1.68 ± 0.064 s without ω-conotoxin GVIA (n = 82 boutons, N = 7 experiments) vs. 1.53 ± 0.077 s with ω-conotoxin GVIA (n = 82 boutons, N = 5 experiments) for WT, p = 0.12, independent two-tailed Student's t-test; **Figure 7G**], suggesting that the clearance of Ca^{2+} in neurons is not affected by the presence of ω-conotoxin GVIA in either HD or WT neurons. These results indicate that N-type voltage-gated Ca^{2+} channels likely play an important role in the increased Ca^{2+} influx in HD cortical neurons of heterozygous zQ175.

Given that P/Q-type voltage-gated Ca^{2+} channels are also a major source of Ca^{2+} influx at presynaptic terminals, driving synaptic transmission (Wheeler et al., 1994), we also examined the role of P/Q-type voltage-gated Ca^{2+} channels in the increased synaptic vesicle release in HD cortical neurons by measuring FM 1–43 destaining in the absence and presence of 200 nM ω-agatoxin IVA (a selective blocker of P/Q-type voltage-gated Ca^{2+} channels). Application of ω-agatoxin IVA decreased fluorescence loss in WT (**Figure 8A1**) and HD (**Figure 8A2**) cortical neurons significantly compared with untreated ones (**Figures 8A,B**). However, the decrease of FM 1–43 in the presence of ω-agatoxin IVA was similar regardless of genotype [18.8% (WT) vs. 20.3% (HD), **Figure 8B**] and the effect of ω-agatoxin on fluorescence loss of HD neurons was not significantly different compared with WT neurons (p = 0.669, two-way ANOVA analysis). Moreover, ω-agatoxin IVA did not affect the time constant of FM 1–43 destaining in both WT and HD neurons significantly (**Figure 8C**) and the effect of ω-agatoxin IVA on vesicle release kinetics of HD neurons was not significantly different compared WT neurons (p = 0.741, two-way ANOVA analysis). Taken together, these results suggest that N-type voltage-gated Ca^{2+} channels—and not P/Q-type voltage-gated Ca^{2+} channels—play an important role in the increased release of synaptic vesicles at presynaptic terminals of HD cortical neurons in heterozygous zQ175 mice.

DISCUSSION

It has been suggested that synaptic dysfunction (i.e., "synaptopathy") is involved in many neurodegenerative diseases, including Alzheimer's disease and HD (Li et al., 2003; Bae and Kim, 2017; Tyebji and Hannan, 2017). Recent work in the field of HD suggests that altered synaptic transmission may play an important role in the pathogenesis of HD (Li et al., 2003; Sepers and Raymond, 2014; Raymond, 2017; Tyebji and Hannan, 2017). The altered synaptic function in corticostriatal synapses is a prodromal symptom and can trigger the death of vulnerable striatal neurons in HD. The mechanism that underlies altered synaptic transmission at presynaptic terminals in HD neurons remains elusive. In particular, the release of synaptic vesicles at single presynaptic terminals is poorly understood. Here, we

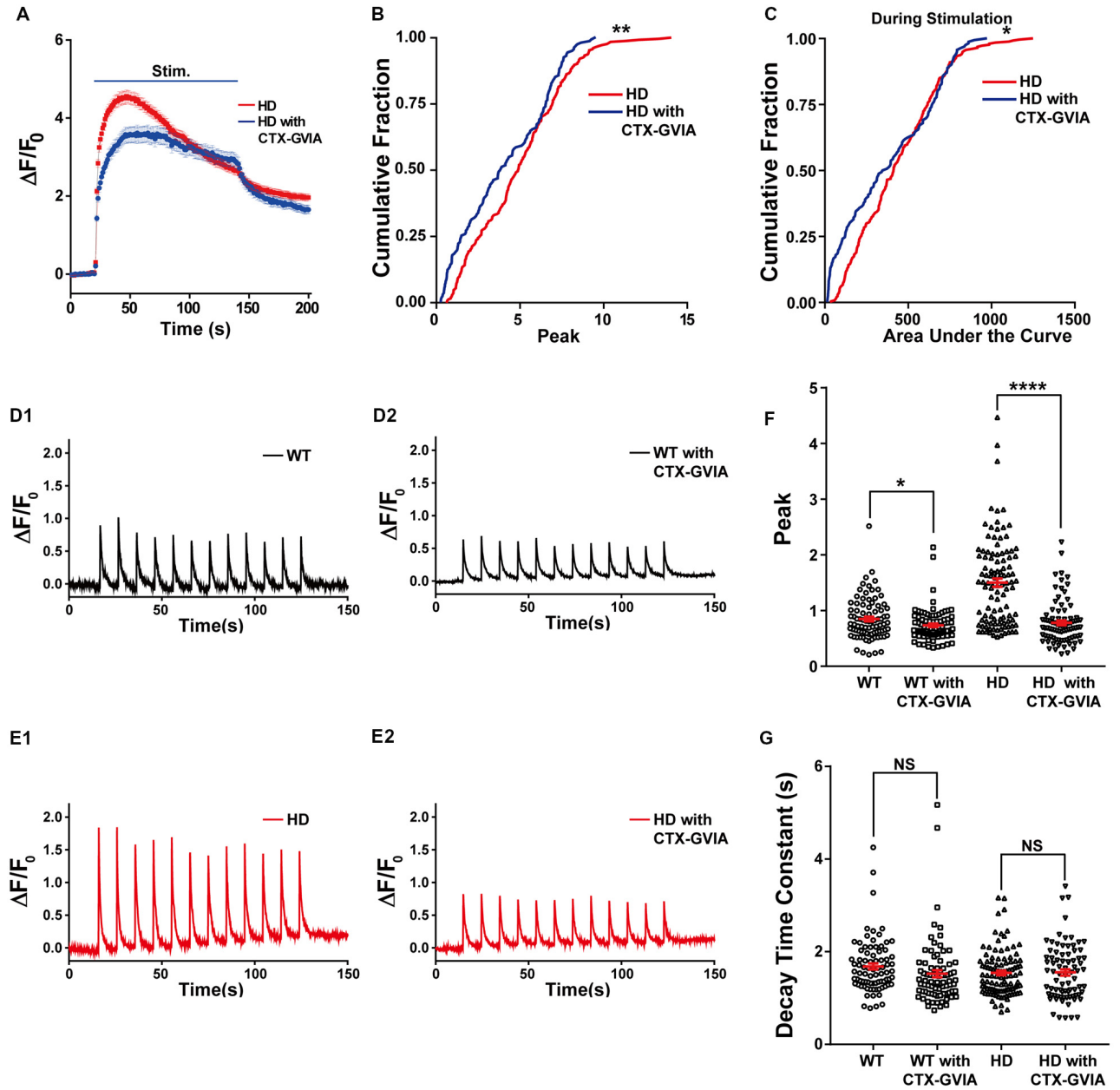

FIGURE 7 | Blocking N-type voltage-gated Ca^{2+} channels reduces Ca^{2+} influx in HD cortical neurons. **(A)** Average $\Delta F/F_0$ traces of Cal-520 measured in the untreated (n = 254 boutons, N = 6 experiments) and ω-conotoxin GVIA-treated HD neurons (n = 162 boutons, N = 6 experiment). Where indicated, 1,200 1-ms field stimuli were delivered at 10 Hz for 120 s. **(B)** The peak $\Delta F/F_0$ of Cal-520 during electrical stimulation in the untreated and ω-conotoxin GVIA-treated HD neurons. $^{**}p < 0.01$ (K-S test). **(C)** The area under the curve of Cal-520 during electrical stimulation in the untreated and ω-conotoxin GVIA-treated HD neurons. $^{*}p < 0.05$ (K-S test). **(D)** Representative traces of $\Delta F/F_0$ traces measured at 10 Hz imaging frequency before, during, and after stimulation with 12 1-ms pulses delivered at 0.1 Hz for 120 s in WT neurons in the absence **(D1)** or presence of ω-conotoxin GVIA **(D2)**. **(E)** Representative traces of $\Delta F/F_0$ traces measured at 10 Hz imaging frequency before, during, and after stimulation with 12 1-ms pulses delivered at 0.1 Hz for 120 s in HD neurons in the absence **(E1)** or presence of ω-conotoxin GVIA **(E2)**. **(F)** Peak of $\Delta F/F_0$ measured after a single stimulus, averaged for single boutons of WT and HD neurons in the presence or absence of ω-conotoxin GVIA (CTX-GVIA). $^{*}p < 0.05$ and $^{****}p < 0.0001$ (independent two-tailed Student's t-test). **(G)** Decay constant of $\Delta F/F_0$ after a single stimulus averaged for single boutons in WT and HD neurons in the presence or absence of ω-conotoxin GVIA (CTX-GVIA). NS, not significant (independent two-tailed Student's t-test).

performed real-time measurements of synaptic vesicles release at single presynaptic terminals in primary cultured HD cortical neurons obtained from a knock-in mouse model of HD (zQ175). We found that compared to WT neurons, HD cortical neurons of heterozygous zQ175 mice have increased release of synaptic vesicles and presynaptic Ca^{2+} influx. We also found that the increased neurotransmission and presynaptic Ca^{2+} influx were significantly reduced by loading the neurons with BAPTA-AM

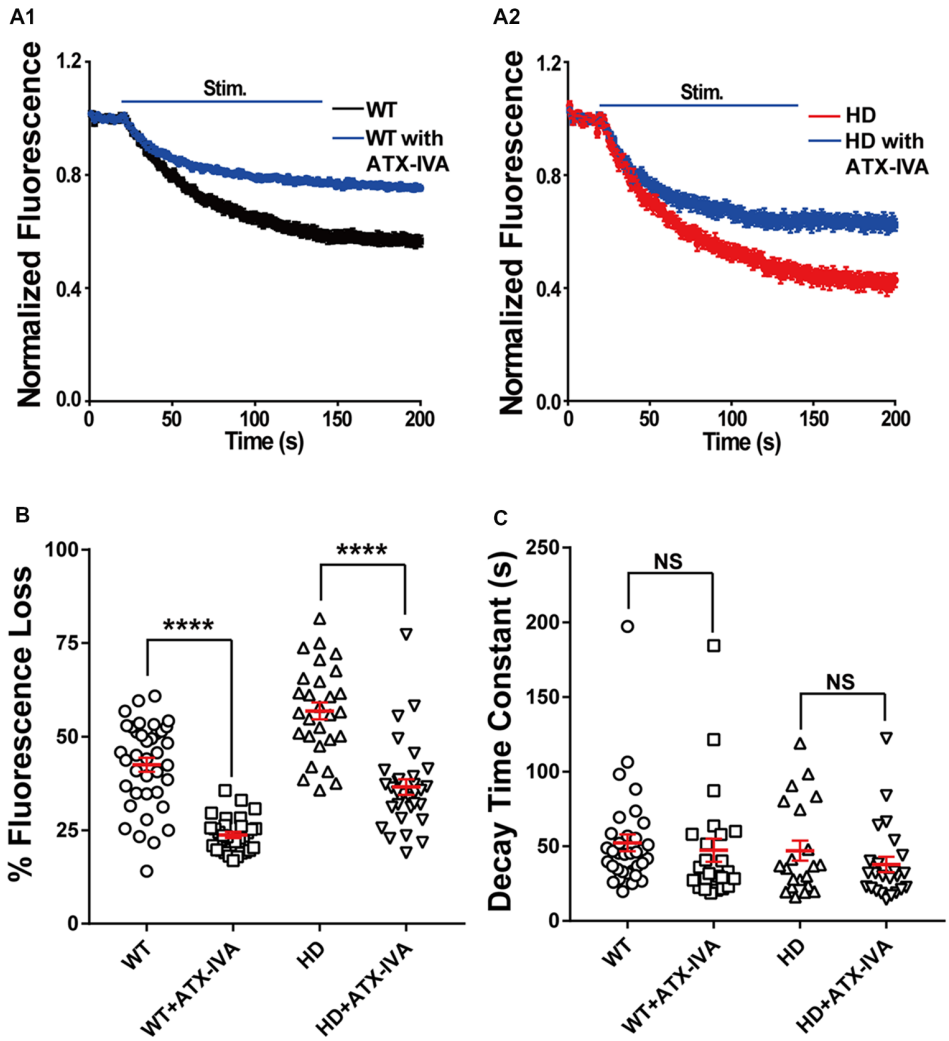

FIGURE 8 | Blocking P/Q-type voltage-gated Ca^{2+} channels does not affect the increased release of synaptic vesicles in HD cortical neurons compared to WT neurons. **(A)** Average traces of normalized FM 1–43 fluorescence intensity in untreated (n = 36 boutons, N = 4 experiments) and 200 nM ω-agatoxin IVA(ATX-IVA)-treated WT neurons (n = 31 boutons, N = 5 experiments; **A1**), and untreated (n = 36 boutons, N = 4 experiments) and 200 nM ω-agatoxin IVA(ATX-IVA)-treated HD neurons (n = 31 boutons, N = 5 experiments; **A2**). Where indicated, a train of 1,200 1-ms field stimuli was applied at 10 Hz for 120 s. **(B)** The percent loss of FM 1–43 fluorescence measured in WT and HD neurons in the presence or absence of ATX-IVA. Note that ω-agatoxin IVA caused a similar change in percent fluorescence loss in WT and HD neurons (18.7% and 20.3%, respectively). **(C)** The time constant of FM1–43 destaining measured in WT and HD neurons in the presence or absence of ATX-IVA. ****$p < 0.0001$ and NS, not significant (independent two-tailed Student's t-test).

(a Ca^{2+} chelator) or treating neurons with ω-conotoxin GVIA (a highly selective N-type voltage-gated Ca^{2+} channel blocker).

Our finding of increased neurotransmission in primary cultured cortical neurons of a knock-in model of HD (zQ175) is consistent with previous reports of increased neurotransmission in acute cortical slices from presymptomatic YAC128 mice (Joshi et al., 2009) and at the neuromuscular junction in R6/1 mice (Rozas et al., 2011), two mouse models of HD. Our results are also consistent with increased neurotransmitter release in a *Drosophila* model of HD (Romero et al., 2008) and the recent report of increased glutamate release in striatal synaptosomes isolated from 6-month-old 140Q knock-in mice (Valencia et al., 2013).

Intracellular Ca^{2+} regulates a wide range of signaling pathways (Brini et al., 2014). Altered Ca^{2+} regulation in neurons has been reported in many neurodegenerative diseases, including Alzheimer's disease, Parkinson's disease, and HD (Bezprozvanny, 2009). With respect to HD, increased somatic Ca^{2+} transients were reported in striatal neurons in several HD mouse models (Tang et al., 2005; Fernandes et al., 2007; Rosenstock et al., 2010). Here, we report that Ca^{2+} influx at single presynaptic terminals is increased in HD cortical neurons of heterozygous zQ175 mice, and this increased Ca^{2+} influx is associated with increased neurotransmission. Together with other reports suggesting that mutant HTT proteins modulate N-type voltage-gated Ca^{2+} channels through their

interaction with N-type voltage-gated Ca^{2+} channels and their binding proteins (Miller et al., 2003; Swayne et al., 2005; Silva et al., 2017), our results suggest that N-type voltage-gated Ca^{2+} channels, play an important role in the increased presynaptic Ca^{2+} influx and synaptic vesicle release in cortical neurons from HD mice. However, it is possible that other Ca^{2+} channels may contribute to the increased Ca^{2+} influx in HD neurons (Silva et al., 2017). Several other mechanisms, including $InsP_3R1$ and store-operated Ca^{2+} entry (SOCE), may increase the level of Ca^{2+} inside HD neurons (Miller and Bezprozvanny, 2010; Raymond, 2017). Therefore, additional experiments are needed to better understand the mechanism underlying increased presynaptic Ca^{2+} influx in cortical neurons in HD. In particular, investigating the effects of increased presynaptic Ca^{2+} influx, including one from N-type voltage-gated Ca^{2+} channels, on the neurodegeneration of HD neurons will contribute to identifying potential therapeutic targets for HD.

Although our data suggest that increased presynaptic Ca^{2+} influx contributes to the increased neurotransmission in zQ175 mice, we cannot exclude the possibility that other mechanisms might play a role, including the binding of mutant HTT protein to regulatory proteins that control vesicle fusion. For example, the mutant HTT protein can bind vesicular proteins (DiFiglia et al., 1995; Liévens et al., 2002), thereby increasing neurotransmitter release (Valencia et al., 2013).

Based on our findings, we propose a model in which increased excitatory neurotransmission in cortical neurons due to increased presynaptic Ca^{2+} influx *via* the interaction of N-type voltage Ca^{2+} channels with mutant HTT proteins can increase the activation of NMDARs, thereby inducing excitotoxicity in cortical and striatal neurons, ultimately leading to the progressive loss of these neurons in HD. Importantly, this model may explain the vulnerability of MSNs in the indirect pathway; these MSNs would be particularly susceptible to increased excitatory neurotransmission, as they are more depolarized than MSNs in the direct pathway from the cortex (Gertler et al., 2008) and are therefore more excitable. Thus, our model may explain the increased firing (Kreitzer and Malenka, 2007; Cepeda et al., 2008) and increased vulnerability (Cepeda et al., 2008) of MSNs in the indirect pathway in HD. Our model also suggests that the increase in excitatory neurotransmission causes the hyperactivity of MSNs that proceeds neural degeneration and death (Raymond et al., 2011). In addition, our model provides a possible explanation for the recent report about the contribution of presynaptic terminals from cortical neurons to HD at reconstituted corticostriatal synapses (Virlogeux et al., 2018); the increased release of excitatory neurotransmitters from the presynaptic terminals of cortical neurons may lead to degeneration of striatal neurons. Future experiments of corticostriatal synapses and organotypic slices at different ages of mice will help to identify the detailed mechanisms about how increased excitatory neurotransmission contribute to neurodegeneration of MSNs as HD progresses.

In summary, we report the real-time measurements of synaptic vesicle release and Ca^{2+} influx at single presynaptic terminals during electrical field stimulation in primary cortical neurons obtained from a transgenic knock-in mouse model of HD (zQ175). We found that HD cortical neurons from heterozygous zQ175 mice had increased neurotransmission and presynaptic Ca^{2+} influx compared to WT neurons. These increases were reduced by treating the neurons with an intracellular Ca^{2+} chelator or by pharmacologically blocking N-type voltage-gated Ca^{2+} channels, thereby providing a possible new therapeutic target for HD. Our findings also suggest that the increase in neurotransmission and/or presynaptic Ca^{2+} influx may underlie the excitotoxicity in vulnerable neurons in HD and the eventual loss of these neurons.

AUTHOR CONTRIBUTIONS

SC, CY, and HP designed the experiments. SC, CY, LR and CL performed the experiments. SC, CY, and XQ provided the analysis programs. SC, CY, HR and HP wrote the manuscript.

FUNDING

This work was supported by the Research Grants Council, University Grants Committee of Hong Kong (Grants 26101117, 16101518, A-HKUST603/17 and N_HKUST613/17) and the Innovation and Technology Commission (ITCPD/17-9).

ACKNOWLEDGMENTS

We thank Min Zhang for help with immunostaining and members of Park lab for helpful discussion and comments. We thank Dr. Curtis Barrett for critically reading the manuscript and for providing constructive comments.

SUPPLEMENTARY MATERIAL

The Supplementary Material for this article can be found online at: https://www.frontiersin.org/articles/10.3389/fnmol.2018.00478/full#supplementary-material

REFERENCES

Abdel-Hamid, K. M., and Tymianski, M. (1997). Mechanisms and effects of intracellular calcium buffering on neuronal survival in organotypic hippocampal cultures exposed to anoxia/aglycemia or to excitotoxins. *J. Neurosci.* 17, 3538–3553. doi: 10.1523/jneurosci.17-10-03538.1997

Alsina, A., Lai, W. M., Wong, W. K., Qin, X., Zhang, M., and Park, H. (2017). Real-time subpixel-accuracy tracking of single mitochondria in neurons reveals heterogeneous mitochondrial motion. *Biochem. Biophys. Res. Commun.* 493, 776–782. doi: 10.1016/j.bbrc.2017.08.103

Atasoy, D., Ertunc, M., Moulder, K. L., Blackwell, J., Chung, C., Su, J., et al. (2008). Spontaneous and evoked glutamate release activates two populations of NMDA receptors with limited overlap. *J. Neurosci.* 28, 10151–10166. doi: 10.1523/JNEUROSCI.2432-08.2008

Atucha, N., Iyu, D., De Rycker, M., Soler, A., and Garcia-Estan, J. (2003). Altered calcium regulation in freshly isolated aortic smooth muscle cells

from bile duct-ligated rats: role of nitric oxide. *Cell Calcium* 33, 129–135. doi: 10.1016/s0143-4160(02)00206-3

Bae, J. R., and Kim, S. H. (2017). Synapses in neurodegenerative diseases. *BMB Rep.* 50, 237–246. doi: 10.5483/bmbrep.2017.50.5.038

Betz, W. J., and Bewick, G. S. (1992). Optical analysis of synaptic vesicle recycling at the frog neuromuscular junction. *Science* 255, 200–203. doi: 10.1126/science.1553547

Bezprozvanny, I. (2009). Calcium signaling and neurodegenerative diseases. *Trends Mol. Med.* 15, 89–100. doi: 10.1016/j.molmed.2009.01.001

Blanton, M. G., Lo Turco, J. J., and Kriegstein, A. R. (1990). Endogenous neurotransmitter activates N-methyl-D-aspartate receptors on differentiating neurons in embryonic cortex. *Proc. Natl. Acad. Sci. U S A* 87, 8027–8030. doi: 10.1073/pnas.87.20.8027

Botelho, E. P., Wang, E., Chen, J. Y., Holley, S., Andre, V., Cepeda, C., et al. (2014). Differential synaptic and extrasynaptic glutamate-receptor alterations in striatal medium-sized spiny neurons of aged YAC128 Huntington's disease mice. *PLoS Curr.* 6:ecurrents.hd.34957c4f8bd7cb1f5ec47381dfc811c3 doi: 10.1371/currents.hd.34957c4f8bd7cb1f5ec47381dfc811c3

Branco, T., and Staras, K. (2009). The probability of neurotransmitter release: variability and feedback control at single synapses. *Neuroscience* 10, 373–383. doi: 10.1038/nrn2634

Branco, T., Staras, K., Darcy, K. J., and Goda, Y. (2008). Local dendritic activity sets release probability at hippocampal synapses. *Neuron* 59, 475–485. doi: 10.1016/j.neuron.2008.07.006

Brini, M., Calì, T., Ottolini, D., and Carafoli, E. (2014). Neuronal calcium signaling: function and dysfunction. *Cell. Mol. Life Sci.* 71, 2787–2814. doi: 10.1007/s00018-013-1550-7

Carmo, C., Naia, L., Lopes, C., and Rego, A. C. (2018). Mitochondrial dysfunction in Huntington's disease. *Adv. Exp. Med. Biol.* 1049, 59–83. doi: 10.1007/978-3-319-71779-1_3

Catterall, W. A. (2011). Voltage-gated calcium channels. *Cold Spring Harb. Perspect. Biol.* 3:a003947. doi: 10.1101/cshperspect.a003947

Cepeda, C., André, V. M., Yamazaki, I., Wu, N., Kleiman-Weiner, M., and Levine, M. S. (2008). Differential electrophysiological properties of dopamine D1 and D2 receptor-containing striatal medium-sized spiny neurons. *Eur. J. Neurosci.* 27, 671–682. doi: 10.1111/j.1460-9568.2008.06038.x

Cepeda, C., Hurst, R. S., Calvert, C. R., Hernández-Echeagaray, E., Nguyen, O. K., Jocoy, E., et al. (2003). Transient and progressive electrophysiological alterations in the corticostriatal pathway in a mouse model of Huntington's disease. *J. Neurosci.* 23, 961–969. doi: 10.1523/jneurosci.23-03-00961.2003

Chen, T. W., Wardill, T. J., Sun, Y., Pulver, S. R., Renninger, S. L., Baohan, A., et al. (2013). Ultrasensitive fluorescent proteins for imaging neuronal activity. *Nature* 499, 295–300. doi: 10.1038/nature12354

Daniel, J. A., Galbraith, S., Iacovitti, L., Abdipranoto, A., and Vissel, B. (2009). Functional heterogeneity at dopamine release sites. *J. Neurosci.* 29, 14670–14680. doi: 10.1523/JNEUROSCI.1349-09.2009

Dayalu, P., and Albin, R. L. (2015). Huntington disease: pathogenesis and treatment. *Neurol. Clin.* 33, 101–114. doi: 10.1016/j.ncl.2014.09.003

Debanne, D., Guérineau, N. C., Gahwiler, B. H., and Thompson, S. M. (1996). Paired-pulse facilitation and depression at unitary synapses in rat hippocampus: quantal fluctuation affects subsequent release. *J. Physiol.* 491, 163–176. doi: 10.1113/jphysiol.1996.sp021204

DiFiglia, M., Sapp, E., Chase, K., Schwarz, C., Meloni, A., Young, C., et al. (1995). Huntingtin is a cytoplasmic protein associated with vesicles in human and rat brain neurons. *Neuron* 14, 1075–1081. doi: 10.1016/0896-6273(95)90346-1

Dobrunz, L. E., and Stevens, C. F. (1997). Heterogeneity of release probability, facilitation and depletion at central synapses. *Neuron* 18, 995–1008. doi: 10.1016/s0896-6273(00)80338-4

Ermolyuk, Y. S., Alder, F. G., Henneberger, C., Rusakov, D. A., Kullmann, D. M., and Volynski, K. E. (2012). Independent regulation of basal neurotransmitter release efficacy by variable Ca^{2+} influx and bouton size at small central synapses. *PLoS Biol.* 10:e1001396. doi: 10.1371/journal.pbio.1001396

Fernandes, H. B., Baimbridge, K. G., Church, J., Hayden, M. R., and Raymond, L. A. (2007). Mitochondrial sensitivity and altered calcium handling underlie enhanced NMDA-induced apoptosis in YAC128 model of Huntington's disease. *J. Neurosci.* 27, 13614–13623. doi: 10.1523/JNEUROSCI.3455-07.2007

Franco-Iborra, S., Vila, M., and Perier, C. (2018). Mitochondrial quality control in neurodegenerative diseases: focus on Parkinson's disease and Huntington's disease. *Front. Neurosci.* 12:342. doi: 10.3389/fnins.2018.00342

Gabbott, P. L., and Somogyi, P. (1986). Quantitative distribution of GABA-immunoreactive neurons in the visual cortex (area 17) of the cat. *Exp. Brain Res.* 61, 323–331. doi: 10.1007/bf00239522

Gaffield, M. A., and Betz, W. J. (2006). Imaging synaptic vesicle exocytosis and endocytosis with FM dyes. *Nat. Protoc.* 1, 2916–2921. doi: 10.1038/nprot.2006.476

Gertler, T. S., Chan, C. S., and Surmeier, D. J. (2008). Dichotomous anatomical properties of adult striatal medium spiny neurons. *J. Neurosci.* 28, 10814–10824. doi: 10.1523/jneurosci.2660-08.2008

MacDonald, M. E., Ambrose, C. M., Duyao, M. P., Datson, N., Shaw, D., and Harper, P. S. (1993). A novel gene containing a trinucleotide repeat that is expanded and unstable on Huntington's disease chromosomes. *Cell* 72, 971–983. doi: 10.1016/0092-8674(93)90585-e

Harata, N., Ryan, T. A., Smith, S. J., Buchanan, J., and Tsien, R. W. (2001). Visualizing recycling synaptic vesicles in hippocampal neurons by FM 1–43 photoconversion. *Proc. Natl. Acad. Sci. U S A* 98, 12748–12753. doi: 10.1073/pnas.171442798

Heikkinen, T., Lehtimäki, K., Vartiainen, N., Puoliväli, J., Hendricks, S. J., Glaser, J. R., et al. (2012). Characterization of neurophysiological and behavioral changes, MRI brain volumetry and 1H MRS in zQ175 knock-in mouse model of Huntington's disease. *PLoS One* 7:e50717. doi: 10.1371/journal.pone.0050717

Hendry, S. H., Schwark, H. D., Jones, E. G., and Yan, J. (1987). Numbers and proportions of GABA-immunoreactive neurons in different areas of monkey cerebral cortex. *J. Neurosci.* 7, 1503–1519. doi: 10.1523/jneurosci.07-05-01503.1987

Henkel, A. W., Lübke, J., and Betz, W. J. (1996). FM1–43 dye ultrastructural localization in and release from frog motor nerve terminals. *Proc. Natl. Acad. Sci. U S A* 93, 1918–1923. doi: 10.1073/pnas.93.5.1918

Hosoi, N., Sakaba, T., and Neher, E. (2007). Quantitative analysis of calcium-dependent vesicle recruitment and its functional role at the calyx of Held synapse. *J. Neurosci.* 27, 14286–14298. doi: 10.1523/jneurosci.4122-07.2007

Hua, Y., Sinha, R., Thiel, C. S., Schmidt, R., Hüve, J., Martens, H., et al. (2011). A readily retrievable pool of synaptic vesicles. *Nat. Neurosci.* 14, 833–839. doi: 10.1038/nn.2838

Jordan, R., Lemke, E. A., and Klingauf, J. (2005). Visualization of synaptic vesicle movement in intact synaptic boutons using fluorescence fluctuation spectroscopy. *Biophys. J.* 89, 2091–2102. doi: 10.1529/biophysj.105.061663

Joshi, P. R., Wu, N. P., André, V. M., Cummings, D. M., Cepeda, C., Joyce, J. A., et al. (2009). Age-dependent alterations of corticostriatal activity in the YAC128 mouse model of Huntington disease. *J. Neurosci.* 29, 2414–2427. doi: 10.1523/jneurosci.5687-08.2009

Klapstein, G. J., Fisher, R. S., Zanjani, H., Cepeda, C., Jokel, E. S., Chesselet, M. F., et al. (2001). Electrophysiological and morphological changes in striatal spiny neurons in R6/2 Huntington's disease transgenic mice. *J. Neurophysiol.* 86, 2667–2677. doi: 10.1152/jn.2001.86.6.2667

Körber, C., and Kuner, T. (2016). Molecular machines regulating the release probability of synaptic vesicles at the active zone. *Front. Synaptic Neurosci.* 8:5. doi: 10.3389/fnsyn.2016.00005

Kreitzer, A. C., and Malenka, R. C. (2007). Endocannabinoid-mediated rescue of striatal LTD and motor deficits in Parkinson's disease models. *Nature* 445, 643–647. doi: 10.1038/nature05506

Leow-Dyke, S., Allen, C., Denes, A., Nilsson, O., Maysami, S., Bowie, A. G., et al. (2012). Neuronal toll-like receptor 4 signaling induces brain endothelial activation and neutrophil transmigration *in vitro*. *J. Neuroinflamm.* 9:230. doi: 10.1186/1742-2094-9-230

Li, J.-Y., Plomann, M., and Brundin, P. (2003). Huntington's disease: a synaptopathy? *Trends Mol. Med.* 9, 414–420. doi: 10.1016/j.molmed.2003.08.006

Liévens, J. C., Woodman, B., Mahal, A., and Bates, G. P. (2002). Abnormal phosphorylation of synapsin I predicts a neuronal transmission impairment

in the R6/2 Huntington's disease transgenic mice. *Mol. Cell. Neurosci.* 20, 638–648. doi: 10.1006/mcne.2002.1152

Liu, G., and Tsien, R. W. (1995). Synaptic transmission at single visualized hippocampal boutons. *Neuropharmacology* 34, 1407–1421. doi: 10.1016/0028-3908(95)00143-t

Lock, J. T., Parker, I., and Smith, I. F. (2015). A comparison of fluorescent Ca^{2+} indicators for imaging local Ca^{2+} signals in cultured cells. *Cell Calcium* 58, 638–648. doi: 10.1016/j.ceca.2015.10.003

Luebke, J. I., Dunlap, K., and Turner, T. J. (1993). Multiple calcium channel types control glutamatergic synaptic transmission in the hippocampus. *Neuron* 11, 895–902. doi: 10.1016/0896-6273(93)90119-c

Menalled, L. B., Kudwa, A. E., Miller, S., Fitzpatrick, J., Watson-Johnson, J., Keating, N., et al. (2012). Comprehensive behavioral and molecular characterization of a new knock-in mouse model of Huntington's disease: zQ175. *PLoS One* 7:e49838. doi: 10.1371/journal.pone.0049838

Miller, B. R., and Bezprozvanny, I. (2010). Corticostriatal circuit dysfunction in Huntington's disease: intersection of glutamate, dopamine and calcium. *Future Neurol.* 5, 735–756. doi: 10.2217/fnl.10.41

Miller, L. C., Swayne, L. A., Chen, L., Feng, Z. P., Wacker, J. L., Muchowski, P. J., et al. (2003). Cysteine string protein (CSP) inhibition of N-type calcium channels is blocked by mutant huntingtin. *J. Biol. Chem.* 278, 53072–53081. doi: 10.1074/jbc.m306230200

Milnerwood, A. J., Gladding, C. M., Pouladi, M. A., Kaufman, A. M., Hines, R. M., Boyd, J. D., et al. (2010). Early increase in extrasynaptic NMDA receptor signaling and expression contributes to phenotype onset in Huntington's disease mice. *Neuron* 65, 178–190. doi: 10.1016/j.neuron.2010.01.008

Morton, A. J., Faull, R. L., and Edwardson, J. M. (2001). Abnormalities in the synaptic vesicle fusion machinery in Huntington's disease. *Brain Res. Bull.* 56, 111–117. doi: 10.1016/s0361-9230(01)00611-6

Murthy, V. N., Sejnowski, T. J., and Stevens, C. F. (1997). Heterogeneous release properties of visualized individual hippocampal synapses. *Neuron* 18, 599–612. doi: 10.1016/s0896-6273(00)80301-3

Park, H. (2018). Cortical axonal secretion of BDNF in the striatum is disrupted in the mutant-huntingtin knock-in mouse model of Huntington's disease. *Exp. Neurobiol.* 27, 217–225. doi: 10.5607/en.2018.27.3.217

Park, H., Li, Y., and Tsien, R. W. (2012). Influence of synaptic vesicle position on release probability and exocytotic fusion mode. *Science* 335, 1362–1366. doi: 10.1126/science.1216937

Plotkin, J. L., Day, M., Peterson, J. D., Xie, Z., Kress, G. J., Rafalovich, I., et al. (2014). Impaired TrkB receptor signaling underlies corticostriatal dysfunction in Huntington's disease. *Neuron* 83, 178–188. doi: 10.1016/j.neuron.2014.05.032

Raymond, L. A. (2017). Striatal synaptic dysfunction and altered calcium regulation in Huntington disease. *Biochem. Biophys. Res. Commun.* 483, 1051–1062. doi: 10.1016/j.bbrc.2016.07.058

Raymond, L. A., André, V. M., Cepeda, C., Gladding, C. M., Milnerwood, A. J., and Levine, M. S. (2011). Pathophysiology of Huntington's disease: time-dependent alterations in synaptic and receptor function. *Neuroscience* 198, 252–273. doi: 10.1016/j.neuroscience.2011.08.052

Reznichenko, L., Cheng, Q., Nizar, K., Gratiy, S. L., Saisan, P. A., Rockenstein, E. M., et al. (2012). *In vivo* alterations in calcium buffering capacity in transgenic mouse model of synucleinopathy. *J. Neurosci.* 32, 9992–9998. doi: 10.1523/jneurosci.1270-12.2012

Richards, D. A., Bai, J., and Chapman, E. R. (2005). Two modes of exocytosis at hippocampal synapses revealed by rate of FM1–43 efflux from individual vesicles. *J. Cell Biol.* 168, 929–939. doi: 10.1083/jcb.200407148

Romero, E., Cha, G. H., Verstreken, P., Ly, C. V., Hughes, R. E., Bellen, H. J., et al. (2008). Suppression of neurodegeneration and increased neurotransmission caused by expanded full-length huntingtin accumulating in the cytoplasm. *Neuron* 57, 27–40. doi: 10.1016/j.neuron.2007.11.025

Rosenstock, T. R., Bertoncini, C. R., Teles, A. V., Hirata, H., Fernandes, M. J., and Smaili, S. S. (2010). Glutamate-induced alterations in Ca^{2+} signaling are modulated by mitochondrial Ca^{2+} handling capacity in brain slices of R6/1 transgenic mice. *Eur. J. Neurosci.* 32, 60–70. doi: 10.1111/j.1460-9568.2010.07268.x

Rozas, J. L., Gómez-Sánchez, L., Tomás-Zapico, C., Lucas, J. J., and Fernández-Chacón, R. (2011). Increased neurotransmitter release at the neuromuscular junction in a mouse model of polyglutamine disease. *J. Neurosci.* 31, 1106–1113. doi: 10.1523/JNEUROSCI.2011-10.2011

Ryan, T. A., Reuter, H., Wendland, B., Schweizer, F. E., Tsien, R. W., and Smith, S. J. (1993). The kinetics of synaptic vesicle recycling measured at single presynaptic boutons. *Neuron* 11, 713–724. doi: 10.1016/0896-6273(93)90081-2

Sepers, M. D., and Raymond, L. A. (2014). Mechanisms of synaptic dysfunction and excitotoxicity in Huntington's disease. *Drug Discov. Today* 19, 990–996. doi: 10.1016/j.drudis.2014.02.006

Silva, F. R., Miranda, A. S., Santos, R. P., Olmo, I. G., Zamponi, G. W., Dobransky, T., et al. (2017). N-type Ca^{2+} channels are affected by full-length mutant huntingtin expression in a mouse model of Huntington's disease. *Neurobiol. Aging* 55, 1–10. doi: 10.1016/j.neurobiolaging.2017.03.015

Simms, B. A., and Zamponi, G. W. (2014). Neuronal voltage-gated calcium channels: structure, function and dysfunction. *Neuron* 82, 24–45. doi: 10.1016/j.neuron.2014.03.016

Smith, R., Brundin, P., and Li, J. Y. (2005). Synaptic dysfunction in Huntington's disease: a new perspective. *Cell. Mol. Life Sci.* 62, 1901–1912. doi: 10.1007/s00018-005-5084-5

Südhof, T. C. (2012). Calcium control of neurotransmitter release. *Cold Spring Harb. Perspect. Biol.* 4:a011353. doi: 10.1101/cshperspect.a011353

Swayne, L. A., Chen, L., Hameed, S., Barr, W., Charlesworth, E., Colicos, M. A., et al. (2005). Crosstalk between huntingtin and syntaxin 1A regulates N-type calcium channels. *Mol. Cell. Neurosci.* 30, 339–351. doi: 10.1016/j.mcn.2005.07.016

Tada, M., Takeuchi, A., Hashizume, M., Kitamura, K., and Kano, M. (2014). A highly sensitive fluorescent indicator dye for calcium imaging of neural activity *in vitro* and *in vivo*. *Eur. J. Neurosci.* 39, 1720–1728. doi: 10.1111/ejn.12476

Tang, T. S., Slow, E., Lupu, V., Stavrovskaya, I. G., Sugimori, M., Llinás, R., et al. (2005). Disturbed Ca^{2+} signaling and apoptosis of medium spiny neurons in Huntington's disease. *Proc. Natl. Acad. Sci. U S A* 102, 2602–2607. doi: 10.1073/pnas.0409402102

Tang, T. S., Tu, H., Orban, P. C., Chan, E. Y., Hayden, M. R., and Bezprozvanny, I. (2004). HAP1 facilitates effects of mutant huntingtin on inositol 1,4,5-trisphosphate-induced Ca^{2+} release in primary culture of striatal medium spiny neurons. *Eur. J. Neurosci.* 20, 1779–1787. doi: 10.1111/j.1460-9568.2004.03633.x

Tang, T. S., Tu, H., Wang, Z., and Bezprozvanny, I. (2003). Modulation of type 1 inositol (1,4,5)-trisphosphate receptor function by protein kinase a and protein phosphatase 1α. *J. Neurosci.* 23, 403–415. doi: 10.1523/JNEUROSCI.23-02-00403.2003

Tsien, R. Y. (1981). A non-disruptive technique for loading calcium buffers and indicators into cells. *Nature* 290, 527–528. doi: 10.1038/290527a0

Tyebji, S., and Hannan, A. J. (2017). Synaptopathic mechanisms of neurodegeneration and dementia: insights from Huntington's disease. *Prog. Neurobiol.* 153, 18–45. doi: 10.1016/j.pneurobio.2017.03.008

Tymianski, M., Charlton, M. P., Carlen, P. L., and Tator, C. H. (1994). Properties of neuroprotective cell-permeant Ca^{2+} chelators: effects on $[Ca^{2+}]$i and glutamate neurotoxicity *in vitro*. *J. Neurophysiol.* 72, 1973–1992. doi: 10.1152/jn.1994.72.4.1973

Tymianski, M., Wallace, M. C., Spigelman, I., Uno, M., Carlen, P. L., Tator, C. H., et al. (1993). Cell-permeant Ca^{2+} chelators reduce early excitotoxic and ischemic neuronal injury *in vitro* and *in vivo*. *Neuron* 11, 221–235. doi: 10.1016/0896-6273(93)90180-y

Valencia, A., Sapp, E., Kimm, J. S., McClory, H., Ansong, K. A., Yohrling, G., et al. (2013). Striatal synaptosomes from $Hdh^{140Q/140Q}$ knock-in mice have altered protein levels, novel sites of methionine oxidation, and excess glutamate release after stimulation. *J. Huntingtons Dis.* 2, 459–475. doi: 10.3233/JHD-130080

Vázquez, E., and Sánchez-Prieto, J. (1997). Presynaptic modulation of glutamate release targets different calcium channels in rat cerebrocortical nerve terminals. *Eur. J. Neurosci.* 9, 2009–2018. doi: 10.1111/j.1460-9568.1997.tb01369.x

Virlogeux, A., Moutaux, E., Christaller, W., Genoux, A., Bruyère, J., Fino, E., et al. (2018). Reconstituting corticostriatal network on-a-chip reveals the contribution of the presynaptic compartment to Huntington's disease. *Cell Rep.* 22, 110–122. doi: 10.1016/j.celrep.2017.12.013

Vonsattel, J. P., and DiFiglia, M. (1998). Huntington disease. *J. Neuropathol. Exp. Neurol.* 57, 369–384. doi: 10.1097/00005072-199805000-00001

Wang, L. Y., and Kaczmarek, L. K. (1998). High-frequency firing helps replenish the readily releasable pool of synaptic vesicles. *Nature* 394, 384–388. doi: 10.1038/28645

Welzel, O., Henkel, A. W., Stroebel, A. M., Jung, J., Tischbirek, C. H., Ebert, K., et al. (2011). Systematic heterogeneity of fractional vesicle pool sizes and release rates of hippocampal synapses. *Biophys. J.* 100, 593–601. doi: 10.1016/j.bpj.2010.12.3706

Wheeler, D. B., Randall, A., and Tsien, R. W. (1994). Roles of N-type and Q-type Ca^{2+} channels in supporting hippocampal synaptic transmission. *Science* 264, 107–111. doi: 10.1126/science.7832825

Wu, J., Ryskamp, D. A., Liang, X., Egorova, P., Zakharova, O., Hung, G., et al. (2016). Enhanced store-operated calcium entry leads to striatal synaptic loss in a Huntington's disease mouse model. *J. Neurosci.* 36, 125–141. doi: 10.1523/JNEUROSCI.1038-15.2016

Yu, C., Li, C. H., Chen, S., Yoo, H., Qin, X., and Park, H. (2018). Decreased BDNF release in cortical neurons of a knock-in mouse model of Huntington's disease. *Sci. Rep.* 8:16976. doi: 10.1038/s41598-018-34883-w

Yu, C., Zhang, M., Qin, X., Yang, X., and Park, H. (2016). Real-time imaging of single synaptic vesicles in live neurons. *Front. Biol.* 11, 109–118. doi: 10.1007/s11515-016-1397-z

Zamponi, G. W. (2003). Regulation of presynaptic calcium channels by synaptic proteins. *J. Pharmacol. Sci.* 92, 79–83. doi: 10.1254/jphs.92.79

Zhang, Q., Cao, Y.-Q., and Tsien, R. W. (2007). Quantum dots provide an optical signal specific to full collapse fusion of synaptic vesicles. *Proc. Natl. Acad. Sci. U S A* 104, 17843–17848. doi: 10.1073/pnas.0706906104

Zhang, Q., Li, Y., and Tsien, R. W. (2009). The dynamic control of kiss-and-run and vesicular reuse probed with single nanoparticles. *Science* 323, 1448–1554. doi: 10.1126/science.1167373

Zuccato, C., and Cattaneo, E. (2009). Brain-derived neurotrophic factor in neurodegenerative diseases. *Nat. Rev. Neurol.* 5, 311–322. doi: 10.1038/nrneurol.2009.54

Zuccato, C., and Cattaneo, E. (2014). Huntington's disease. *Handb. Exp. Pharmacol.* 220, 357–409. doi: 10.1007/978-3-642-45106-5_14

Conflict of Interest Statement: The authors declare that the research was conducted in the absence of any commercial or financial relationships that could be construed as a potential conflict of interest.

frontiers in Cellular Neuroscience

MINI REVIEW
published: 13 February 2019
doi: 10.3389/fncel.2019.00042

Glial Control of Synapse Number in Healthy and Diseased Brain

*Eunbeol Lee and Won-Suk Chung**

Department of Biological Sciences, Korea Advanced Institute of Science and Technology (KAIST), Daejeon, South Korea

Glial cells are emerging as crucial players that mediate development and homeostasis of the central nervous system (CNS). In particular, glial cells are closely associated with synapses, and control synapse formation, function, plasticity, and elimination during the stages of development and adulthood. Importantly, it is now increasingly evident that abnormal glial function can be an active inducer of the initiation and progression of various neurodegenerative diseases. Here, we discuss recent developments on the physiological roles of glial cells in the brain, and propose that synapse loss, which is a common characteristic of several neurodegenerative diseases, can be initiated by mis-regulation of normal glial function.

Keywords: astrocytes, microglia, synapse loss, Alzheimer's disease, neurodegenerative diseases

INTRODUCTION

Glial cells, non-neuronal central nervous system (CNS) cells, are not simply passive support cells for neurons, but active players in neuronal network formation and information processing. The fine processes of astrocytes and microglia closely associate with synapses and affect synapse formation and elimination during development. Even after initial establishment of a neural circuit, glial cells continue to participate in regulation of synapse number and modulation of synaptic function and plasticity. Due to their crucial roles in synapses, it is not surprising that mis-regulation of glial function has recently been revealed to be one of the initiating factors for onset and progression of various neurodegenerative diseases (Phatnani and Maniatis, 2015; Liddelow and Barres, 2017; Li and Barres, 2018).

Synapse loss is one of the most common, and earliest, pathophysiological features of neurodegenerative disease progression. In Alzheimer's disease (AD), where amyloid β (Aβ) plaques accumulate in the brain, surrounded by reactive glial cells, synapses are weakened and undergo specific loss long before neuronal cell death (Perry and Holmes, 2014; Phatnani and Maniatis, 2015; Ransohoff, 2016). Previously, it was thought that this early synapse loss was mainly due to the direct effects of Aβ oligomers and fibrils on neuronal Aβ receptors or secondary neuroinflammation. However, recent studies have revealed that it is reactive glial cells that actually drive the initial synapse loss in AD (Hong et al., 2016; Shi Q. et al., 2017; Dejanovic et al., 2018; Litvinchuk et al., 2018).

In this review, we summarize the roles of astrocytes and microglia in synapse formation and elimination, and review/propose how mis-regulation of glial function leads to synapse loss in various neurodegenerative diseases (**Figure 1**).

OPEN ACCESS

Edited by:
Marie-Eve Tremblay, Laval University, Canada

Reviewed by:
Schuichi Koizumi, University of Yamanashi, Japan
Annalisa Buffo, University of Turin, Italy

****Correspondence:***
Won-Suk Chung
wonsuk.chung@kaist.ac.kr

Received: *23 November 2018*
Accepted: *25 January 2019*
Published: *13 February 2019*

Citation:
Lee E and Chung W-S (2019) Glial Control of Synapse Number in Healthy and Diseased Brain. Front. Cell. Neurosci. 13:42. doi: 10.3389/fncel.2019.00042

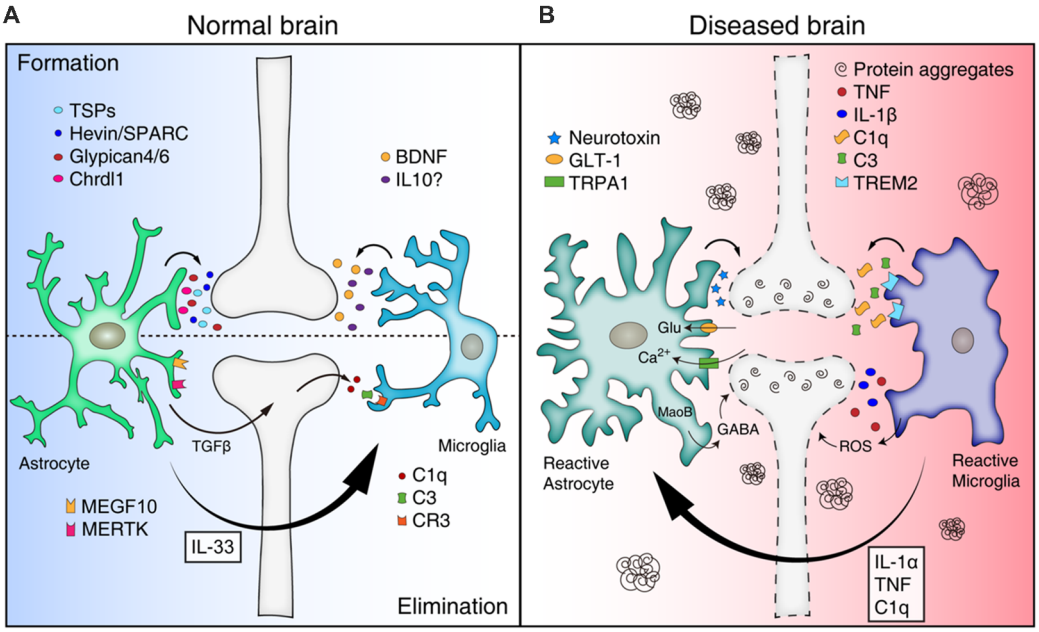

FIGURE 1 | Mis-regulation of glial function can lead to synapse loss in neurodegenerative diseases. **(A)** Astrocytes and microglia release a number of synaptogenic factors [for example, thrombospondins (TSPs), Hevin/SPARC, Glypican 4/6, Chrdl1 from astrocytes, and brain-derived neurotrophic factor (BDNF) and interleukin 10 (IL10) from microglia], regulating synapse formation. Astrocytes can mediate synapse pruning through MEGF10, MERTK phagocytic pathways whereas microglia contribute to synapse elimination through complement cascades [C1q, C3, and complement receptor 3 (CR3)]. Astrocytes also can regulate microglia-mediated synapse elimination by secreting transforming growth factor beta (TGFβ) and IL33. **(B)** In neurodegenerative diseases, reactive astrocytes and microglia are found around protein aggregates [such as amyloid β (Aβ) plaques, α-synuclein aggregates] and mediate synapse loss through various mechanisms. Reactive astrocytes may be induced by cytokines (IL-1α, TNF, and C1q) secreted from reactive microglia in pathological conditions, and produce neurotoxic factors that kill synapses and neurons. In addition, reactive astrocytes in Alzheimer's disease (AD) show increased expression of glutamate transporter-1 (GLT-1), increased activity of transient receptor potential A1 (TRPA1) channels, and increased release of γ-aminobutyric acid (GABA), leading to aberrant neuronal excitability and synaptic function. Similar to astrocytes, reactive microglia can participate in neuronal damage and synapse loss through inflammatory signaling [such as TNF, IL-1β, and reactive oxygen species (ROS)]. Microglia mediate aberrant synapse loss in AD brains through complement mediators (especially C1q and C3) and triggering receptor expressed on myeloid cells 2 (TREM2).

THE ROLE OF GLIA IN SYNAPSE FORMATION

During CNS development, glial cells participate in regulating synapse number by inducing proper formation and elimination (Ullian et al., 2001). Over the past decades, the molecular mechanisms of glia-mediated synapse formation and elimination have been revealed.

Through *in vitro* culture of neurons, with or without astrocytes, it was initially found that astrocytes induced synapse formation by secreting several distinct molecules. When retinal ganglion cells (RGCs) were cultured in astrocyte-conditioned media (ACM), the number of synapses were increased both structurally and functionally. Later, thrombospondins (TSPs), especially TSP1 and TSP2, were found to be one of the synaptogenic proteins in the ACM. Despite effects on the formation of structural synapses, TSP1/2-induced synapses are postsynaptically silent due to their lack of functional α-amino-3-hydroxy-5-methyl-4-isoxazole propionic acid receptors (AMPARs; Christopherson et al., 2005; Eroglu et al., 2009). Along with TSPs, astrocytes express a number of matricellular proteins, such as hevin and SPARC, which modulate cell-cell and cell-matrix interactions (Eroglu, 2009). Hevin induces structurally normal and postsynaptically silent excitatory synapses, similar to TSP-induced synapses. In contrast, SPARC, a hevin homolog, antagonizes hevin and blocks synapse formation (Kucukdereli et al., 2011). Recently, it was discovered that hevin plays a role in bridging synaptic adhesion molecules neurexin 1α (NRX1α) and neuroligins (NL; Singh et al., 2016), which are localized in pre- and post-synaptic compartments, respectively (Graf et al., 2004). NLs and NRX1α, which alone are interaction-incompatible partners, can associate when transcellularly-linked by hevin. This complex can then recruit more NL1 and NMDAR to synapses (Singh et al., 2016).

So, how do astrocytes increase functional synapses? Through biochemical fractionation of ACM, glypican 4 (Gpc4) and glypican 6 (Gpc6) have been identified as functional synaptogenic molecules that strengthen glutamatergic synapses by recruiting GluA1-containing AMPARs (Allen et al., 2012). Astrocyte-secreted Gpc4 appears to upregulate release of neuronal pentraxins 1 (NP1) through interactions with presynaptic type 2a receptor protein tyrosine phosphatases δ (RPTPδ). Subsequently, NP1 binds postsynaptic AMPARs to recruit GluA1 and induce functional synapse formation (Farhy-Tselnicker et al., 2017). Astrocyte-expressed pentraxin 3 (PTX3) has been also reported to promote functionally-active CNS

synapses (Fossati et al., 2019). PTX3, whose activity is regulated by TSP1, increases the surface levels and synaptic clustering of AMPARs through remodeling the perineuronal network, and a β1-integrin/ERK pathway. Chordin-like 1 (Chrdl1) has recently been shown to be another synaptogenic molecule, from astrocytes, that can induce maturation of functional synapses by increasing synaptic GluA2 AMPA receptors. Chrdl1 expression is limited to cortical astrocytes *in vivo*, and is necessary and sufficient to increase GluA2 clustering, resulting in formation of active synapses *in vitro* and *in vivo* (Blanco-Suarez et al., 2018). In addition, astrocyte-derived apolipoprotein E (APOE), which forms lipoprotein particles, with cholesterol and other lipids, has been reported to enhance presynaptic glutamatergic function (Mauch et al., 2001).

Several recent studies have suggested that microglia may also participate in inducing structural synapses. Microglia, the resident macrophages of the CNS, constantly survey and make contacts with synapses in the normal adult brain. Interestingly, when microglia were depleted by diphtheria toxin, synapse formation was disrupted, but synapse elimination rate was unchanged. Removal of brain-derived neurotrophic factor (BDNF), specifically from microglia, recapitulated this phenotype, suggesting that synapse formation is mediated by microglial BDNF (Parkhurst et al., 2013). Additionally, microglial cytokines, such as interleukin 10 (IL-10), have been shown to induce synapse formation (Lim et al., 2013). Using *in vivo* multiphoton imaging, a recent report found that microglial contact induces neuronal Ca^{2+} transients and actin accumulation, inducing filopodia formation from the dendritic branches (Miyamoto et al., 2016).

Thus, astrocytes and microglia regulate synapse formation through various mechanisms. How these different molecules engage in crosstalk, and whether neural activity/injury response controls their expression, are important questions for understanding how synapse dynamics are regulated by glial cells in healthy and diseased brains. Aberrant increases in synapse formation during development or after injury may cause hyperactive neural circuits and increased chances of epilepsy (Liuzzi and Lasek, 1987). In contrast, defective glia-mediated synapse formation could impair synaptic turnover and homeostasis, contributing to synapse loss in neurodegenerative diseases, as well as defective synaptic plasticity.

THE ROLE OF GLIA IN SYNAPSE ELIMINATION THROUGH PHAGOCYTOSIS

To maintain proper synapse numbers, unnecessary synapses need to be eliminated during development and adulthood. Many studies have suggested that excess synapses are eliminated by neuronal activity-dependent competition (Ramiro-Cortés and Israely, 2013; Bian et al., 2015). Surprisingly, glial cells, especially astrocytes and microglia, have been shown to mediate this elimination. Astrocytes express several phagocytic receptors, such as MEGF10 (an ortholog of *Drosophila* Draper and *C. elegans* CED-1) and MERTK [a member of the Tyro-Axl-MerTK (TAM) family of receptor tyrosine kinase], and participate in eliminating synapses in the developing brain. RGCs in developing mice deficient in both *Megf10* and *Mertk* pathways show a failure of the normal refinement of connections and retain excess functional synapses with neurons in the dorsal lateral geniculate nucleus (Chung et al., 2013). This finding suggests that astrocytes actively participate in eliminating live synapses rather than simply cleaning up dead synaptic debris. Although microglia have traditionally been thought to be the major glial cells mediating synapse elimination in development, this study shows astrocytes also play a critical role. Astrocytes appear to continuously engulf both excitatory and inhibitory synapses throughout the brain during adulthood as well, suggesting that the synaptic architecture of our brains is constantly being remodeled by astrocytes in response to our experiences.

In addition to synapse elimination *via* direct phagocytosis, astrocytes also contribute to synapse elimination *via* inositol 1,4,5-triphosphate receptor type 2 (IP3R2) and *P2ry1* dependent signaling (Yang et al., 2016), as well as *via* microglia-mediated phagocytosis. Microglia mediate synapse pruning through the classical complement cascade (Schafer et al., 2012). C1q, the cascade initiating protein, is expressed by microglia and subsets of neurons (Stephan et al., 2013), and localizes to unwanted synapses for opsonization (Stevens et al., 2007). Synapse-associated C1q, then activates a downstream complement cascade and mediates microglia-dependent synapse elimination through complement receptor 3 (CR3)-mediated phagocytosis (Schafer et al., 2012). Interestingly, C1q expression in neurons is regulated by transforming growth factor (TGF)-β secreted from astrocytes (Bialas and Stevens, 2013). Additionally, it has recently been shown that microglial synapse engulfment during development is regulated by interleukin-33 (IL-33) secreted from astrocytes (Vainchtein et al., 2018), further suggesting a close interplay between astrocytes and microglia in eliminating synapses.

CX3CR1s (fractalkine receptors), expressed by microglia, also play important roles in synapse elimination. Microglia respond to neuronal fractalkine by increasing intracellular calcium transients *in vitro* and *in vivo* (Harrison et al., 1998). In *Cx3cr1*-knockout mice, migration and recruitment of microglia to the brain were impaired, resulting in an increased immature synapse population, which appeared to be responsible for weak functional synaptic connectivity and impaired social interaction in the knockout mice (Fuhrmann et al., 2010; Paolicelli et al., 2011; Hoshiko et al., 2012; Zhan et al., 2014).

REACTIVE GLIOSIS IN RESPONSE TO THE INJURED AND DISEASED BRAIN

Reactive gliosis is observed under various conditions, such as infection, ischemia, trauma, and neurodegeneration, and usually involves hypertrophy and proliferation of glial cells and changes in gene expression. Reactive glial cells release various molecules, including chemokines, cytokines, and neurotrophic factors, that can exhibit either neuroprotective or neurotoxic effects (Sofroniew and Vinters, 2010). Although reactive gliosis was previously believed to be

a secondary response to neuroinflammation, recent studies suggest that glial cells react differently depending on injury stimulus, and that gliosis can initiate neurodegeneration (Jonsson et al., 2013; Hong et al., 2016; Sekar et al., 2016).

In general, it is believed that reactive microglia can exhibit more than two polarization states, such as M1 and M2. M1-like microglia upregulate inflammatory signaling, such as TNF, IL-1β, and reactive oxygen species (ROS) signaling. In contrast, M2-like microglia express anti-inflammatory molecules, such as TGF-β1, IL-4, and IL-10. By converting their gene expression status, reactive microglia participate not only in neuronal damage and synapse loss, but also regeneration and tissue remodeling through phagocytosis (Block et al., 2007; Boche et al., 2013; Simon et al., 2017). For example, M1-like microglia led to decrease in dendritic spine density in hippocampal neurons *in vivo* and *in vitro* by producing extracellular vesicles (EVs) containing a set of miRNAs that regulate the expression of synaptic proteins. Among them, miR-146a-5p controls the expression of synaptotagmin1 and neuroligin1 in EV-receiving neurons. In contrast, M2-like microglia appear to have opposite effects by producing EVs depleted of miR-146a-5p (Prada et al., 2018).

Similar to microglia, reactive astrocytes isolated from mice with transient ischemia induced by occlusion of the middle cerebral artery (MCAO) or treated with lipopolysaccharide (LPS) differentially expressed certain genes categories depending on injury type. Genes related to metabolic activity, cell-cycle, and transcription factors (e.g., Klf5 and Klf6) were selectively increased in middle cerebral artery (MCAO)-induced reactive astrocytes (A2 astrocytes), whereas genes related to immune response, antigen processing/presentation, and complement pathway were upregulated in lipopolysaccharide (LPS)-induced reactive astrocytes (A1 astrocytes; Zamanian et al., 2012). Subsequent work has revealed that A1 astrocytes can be induced by a combination of cytokines (IL-1α, TNF, and C1q) released by reactive microglia. This study also showed that A1 astrocytes not only lose their ability to induce synapse formation and elimination, but also produce neurotoxic factors that kill neurons and oligodendrocytes (Liddelow et al., 2017). In comparison to signals inducing A1 astrocytes, little is known about the upstream inductive signals that drives A2 astrocytes. Reactive astrocytes after transient ischemic injury can transform into efficient phagocytes, clearing neuronal and synaptic debris through ATP-binding cassette transporter A1 (ABCA1)-dependent mechanisms (Morizawa et al., 2017). Furthermore, astrocytes perform neuroprotective functions through downregulating the $P2Y_1$ purinergic receptor after traumatic brain injury. Downregulation of $P2Y_1$ enhances extension of astrocytic processes and accelerates reactive astrogliosis accompanied by upregulation of glial fibrillary acidic protein (GFAP) and phosphorylation of STAT3. Accelerated activation of astrocytes helps diminish scar formation following injury (Shinozaki et al., 2017). Thus, these astrocytes, which presumably associated with the A2 type, may promote CNS recovery and repair (Bush et al., 1999; Gao et al., 2005; Hayakawa et al., 2014).

GLIA-SYNAPSE INTERACTIONS IN NEURODEGENERATIVE DISEASE

In many neurodegenerative diseases, synapse loss is a common, early sign of disease progression. As we discussed in the previous section, glia play central roles in normal synapse formation and elimination. In this section, we discuss how glial cells also participate in synapse loss in neurodegenerative diseases, especially AD and Parkinson's disease (PD).

AD is the most common cause of dementia. Its pathology includes extracellular accumulation of Aβ plaques and intracellular, neurofibrillary tangles of hyperphosphorylated tau protein. Aβ, produced by proteolytic cleavage of amyloid precursor protein (APP), self-aggregates to form oligomers, protofibrils, or other fibrils. Soluble Aβ oligomers have been shown to induce synapse loss, tau phosphorylation, and reactive gliosis of astrocytes and microglia (Tomiyama et al., 2010; Mitew et al., 2013; Forny-Germano et al., 2014). Oligomeric Aβ surrounding senile plaques contributes to significant synapse loss in AD mouse models (Koffie et al., 2009). Although the mechanism is not fully understood, it is thought that Aβ oligomers induce overstimulation of NMDA receptors, leading to abnormal redox events and Ca^{2+} upregulation (Tu et al., 2014). Additionally, Aβ oligomers reduce synaptic adhesion by disrupting neural cell adhesion molecule 2 (NCAM2), leading to synapse loss in the AD hippocampus (Leshchyns'ka et al., 2015).

In AD brains, reactive astrocytes and microglia are found around Aβ plaques and can play beneficial or harmful roles in disease progression (Nagele et al., 2003; Olabarria et al., 2010; Simpson et al., 2010). Reactive astrocytes can internalize Aβ *in vitro* and *in vivo* (Wyss-Coray et al., 2003; Pihlaja et al., 2008), although the molecular mechanism and biological impact of this clearance are unclear. In contrast, evidence from aged AD mouse brains shows that astrocytic processes are tightly associated with Aβ plaques, but do not engulf them. Interestingly, reactive astrocytes found in AD brains seem to follow an A1 astrocyte fate, with neuroinflammatory gene expression patterns (Liddelow et al., 2017; Shi Y. et al., 2017). Since A1 astrocytes are less capable of phagocytosing neuronal material, it is possible that reactive astrocytes in AD brains become less able to engulf Aβ plaque during disease progression. Therefore, boosting the phagocytic capacity of astrocytes for Aβ plaques could lower Aβ burden in the CNS. Consistent with this hypothesis, transplantation of wild-type (WT) astrocytes into AD mouse brain results in more efficient removal of Aβ plaques compared to non-transplanted controls (Pihlaja et al., 2011). Moreover, since reactive astrocytes in AD show characteristics of A1 astrocytes, they may produce synaptic and neurotoxic factors, similar to cases of neuroinflammation and brain injury. Identifying such factors may be an important step in preventing reactive astrocyte-induced synapse loss in AD.

In AD, reactive astrocytes also directly affect synaptic function and dynamics. These astrocytes exhibit reduced expression of glutamine synthetase and glutamate transporter-1 (GLT-1; Robinson, 2001; Zumkehr et al., 2015), directly inducing aberrant neuronal excitability and synaptic function, which can lead to synapse loss. It has been suggested that reactive astrocytes can affect synaptic dysfunction through hyper-production and release of inhibitory gliotransmitter γ-aminobutyric acid (GABA). Impaired presynaptic release and spike probability, synaptic plasticity, and learning and memory were rescued by inhibiting the GABA-producing enzyme, MaoB, in AD astrocytes (Jo et al., 2014). Soluble Aβ oligomers also induce astrocytic calcium hyperactivity by activating transient receptor potential A1 (TRPA1) channels, leading to neuronal hyperactivity (Lee et al., 2014; Bosson et al., 2017). Since astrocytic calcium transients may control astrocyte-synapse interaction (Henneberger et al., 2010; Shigetomi et al., 2013; Bazargani and Attwell, 2016), dysregulation of calcium transients in AD astrocytes could be an initiating factor for synapse loss.

Similar to astrocytes, microglia are located around Aβ plaques in both human and mouse AD brains (Perlmutter et al., 1990; Bolmont et al., 2008; Grathwohl et al., 2009). It was recently found that the complement cascade that microglia use for pruning unnecessary synapses in the developing brains is responsible for synapse loss in AD brains. In Aβ overproducing AD mouse models, expression of complement mediators, especially C1q and C3, is highly upregulated, mediating aberrant synapse phagocytosis by microglia (Hong et al., 2016; Shi Q. et al., 2017). Blocking complement activation by an antibody blocking C1q function or introduction of $C3^{KO}$ and $C3R^{KO}$ to this AD model mouse background were sufficient to prevent early synapse loss, establishing a direct role of microglial phagocytosis in AD-associated synapse loss. A recent report also showed that in Tau-P301S transgenic mice, a C1q-blocking antibody can also prevent aberrant microglial synapse removal and rescue synaptic density (Dejanovic et al., 2018; Litvinchuk et al., 2018).

Recent studies have shown that triggering receptor expressed on myeloid cells 2 (TREM2) also plays an important role in microglia-mediated synapse elimination. Several phospholipids, including phosphatidylinositol, phosphatidylcholine, and lipoproteins (APOE, LDL, CLU/apoj), as well as Aβ, have been suggested as potential TREM2 ligands. Activation of TREM2 receptors changes microglial gene expression related to inflammatory signals and phagocytosis (Colonna, 2003). In developing brains, TREM2 maintains the phagocytic capacity of microglia and mediates normal synapse pruning (Filipello et al., 2018). Interestingly, TREM2 also mediates Aβ-induced, microglial cytokine expression and Aβ clearance through phagocytosis (Zhao et al., 2018). Determining exact functions of TREM2 in AD would be necessary in understanding the role of microglia in mediating synapse loss in AD.

PD is another common neurodegenerative disease with loss of nigrostriatal dopaminergic neurons. Abnormal intraneuronal and intraneuritic deposits of fibrillary, α-synuclein aggregates are thought to be the main cause of PD. Aggregates of α-synuclein have been found at presynaptic terminals in PD, resulting in synaptic degeneration (Schulz-Schaeffer, 2010). Previous studies demonstrated that α-synuclein induces microglial activation (Austin et al., 2006; Lee E.-J. et al., 2010) and influences microglial phagocytic activity. Park et al. (2008) showed that microglial phagocytosis was enhanced by monomeric α-synuclein, but inhibited by aggregated α-synuclein. It has been also suggested that microglia clear α-synuclein through a C1q-dependent pathway (Depboylu et al., 2011).

In PD brains, α-synuclein also stimulates reactive astrogliosis, and α-synuclein inclusions have been found in astrocytes (Wakabayashi et al., 2000; Lee H.-J. et al., 2010; Braidy et al., 2013). These studies suggest that astrocytes can uptake α-synuclein, although the physiological role of this process is unclear. Recently, it has been shown that inhibiting microglia-mediated conversion of astrocytes into A1 astrocytes significantly alleviate synaptic/neuronal loss in PD mouse models (Yun et al., 2018). Furthermore, microglia in PD show changes in expression of innate immunity genes, such as progranulin, NF-κB, and TDP-43, which may further impact microglial phagocytosis and synapse elimination (Kao et al., 2011; Frakes et al., 2014; Lui et al., 2016; Spiller et al., 2018). Therefore, similar to AD, synapse and neuronal loss in PD may be triggered by reactive microglia and astrocytes. Further studies are necessary to determine whether modulating glial function can prevent α-synuclein accumulation and synapse/neuronal loss in PD.

CONCLUSIONS AND PERSPECTIVES

We here describe recent findings that glial cells, especially astrocytes and microglia, regulate synapse dynamics in normal and neurodegenerative diseases. In the past, neurodegeneration studies have focused mainly on neurons; however, recent studies suggest that abnormal interactions between glia and synapses can initiate many pathophysiological aspects of synapse loss. In diseased brains, glial cells lose their normal functions for proper synapse formation, function, plasticity, and elimination. Furthermore, these cells acquire new, deleterious functions to drive synapse and neuronal loss. In both cases, understanding the exact molecular mechanisms responsible for glia–mediated synapse loss is an important step in developing therapeutic strategies for neurodegenerative diseases. In addition, determining what initiates reactive gliosis in each disease, and whether we can prevent these processes are equally important questions. Astrocytes and microglia may participate in synapse formation and elimination with different degrees in various development and disease conditions. In normal physiological conditions, since major portion of synapses are in direct contact with astrocytic processes, astrocytes may respond more efficiently than microglia in regulating neuronal activity-dependent changes in synaptic density. In contrast, microglia may play dominant roles in eliminating synapses in the diseased conditions due to the significant upregulation of phagocytic machineries after reactive gliosis. How astrocytes and microglia

differentially and cooperatively control synapse number in the healthy and diseased brain would be additional fascinating subjects to investigate. Current advances in establishing gene expression databases of disease-affected human brains, as well as in understanding normal glial function in synapse regulation will aid this discovery.

AUTHOR CONTRIBUTIONS

Both authors listed have made a substantial, direct and intellectual contribution to the work, and approved it for publication.

FUNDING

This work was supported by the National Research Foundation of Korea (NRF) grant funded by the Korean government (MSIP; NRF-2016M3C7A1905391, NRF-2016R1C1B3006969 and NRF-2018R1A4A1020922; W-SC). W-SC is also supported by Cure Alzheimer's Fund.

ACKNOWLEDGMENTS

We thank all members in Chung's laboratory for helpful discussion.

REFERENCES

Allen, N. J., Bennett, M. L., Foo, L. C., Wang, G. X., Chakraborty, C., Smith, S. J., et al. (2012). Astrocyte glypicans 4 and 6 promote formation of excitatory synapses via GluA1 AMPA receptors. *Nature* 486, 410–414. doi: 10.1038/nature11059

Austin, S. A., Floden, A. M., Murphy, E. J., and Combs, C. K. (2006). α-synuclein expression modulates microglial activation phenotype. *J. Neurosci.* 26, 10558–10563. doi: 10.1523/JNEUROSCI.1799-06.2006

Bazargani, N., and Attwell, D. (2016). Astrocyte calcium signaling: the third wave. *Nat. Neurosci.* 19, 182–189. doi: 10.1038/nn.4201

Bialas, A. R., and Stevens, B. (2013). TGF-β signaling regulates neuronal C1q expression and developmental synaptic refinement. *Nat. Neurosci.* 16, 1773–1782. doi: 10.1038/nn.3560

Bian, W. J., Miao, W. Y., He, S. J., Qiu, Z., and Yu, X. (2015). Coordinated spine pruning and maturation mediated by inter-spine competition for cadherin/catenin complexes. *Cell* 162, 808–822. doi: 10.1016/j.cell.2015.07.018

Blanco-Suarez, E., Liu, T. F., Kopelevich, A., and Allen, N. J. (2018). Astrocyte-secreted chordin-like 1 drives synapse maturation and limits plasticity by increasing synaptic GluA2 AMPA receptors. *Neuron* 100, 1116.e13–1132.e13. doi: 10.1016/j.neuron.2018.09.043

Block, M. L., Zecca, L., and Hong, J. S. (2007). Microglia-mediated neurotoxicity: uncovering the molecular mechanisms. *Nat. Rev. Neurosci.* 8, 57–69. doi: 10.1038/nrn2038

Boche, D., Perry, V. H., and Nicoll, J. A. (2013). Review: activation patterns of microglia and their identification in the human brain. *Neuropathol. Appl. Neurobiol.* 39, 3–18. doi: 10.1111/nan.12011

Bolmont, T., Haiss, F., Eicke, D., Radde, R., Mathis, C. A., Klunk, W. E., et al. (2008). Dynamics of the microglial/amyloid interaction indicate a role in plaque maintenance. *J. Neurosci.* 28, 4283–4292. doi: 10.1523/JNEUROSCI.4814-07.2008

Bosson, A., Paumier, A., Boisseau, S., Jacquier-Sarlin, M., Buisson, A., and Albrieux, M. (2017). TRPA1 channels promote astrocytic Ca^{2+} hyperactivity and synaptic dysfunction mediated by oligomeric forms of amyloid-β peptide. *Mol. Neurodegener.* 12:53. doi: 10.1186/s13024-017-0194-8

Braidy, N., Gai, W. P., Xu, Y. H., Sachdev, P., Guillemin, G. J., Jiang, X. M., et al. (2013). Uptake and mitochondrial dysfunction of α-synuclein in human astrocytes, cortical neurons and fibroblasts. *Transl. Neurodegener.* 2:20. doi: 10.1186/2047-9158-2-20

Bush, T. G., Puvanachandra, N., Horner, C. H., Polito, A., Ostenfeld, T., Svendsen, C. N., et al. (1999). Leukocyte infiltration, neuronal degeneration and neurite outgrowth after ablation of scar-forming, reactive astrocytes in adult transgenic mice. *Neuron* 23, 297–308. doi: 10.1016/s0896-6273(00)80781-3

Christopherson, K. S., Ullian, E. M., Stokes, C. C., Mullowney, C. E., Hell, J. W., Agah, A., et al. (2005). Thrombospondins are astrocyte-secreted proteins that promote CNS synaptogenesis. *Cell* 120, 421–433. doi: 10.1016/j.cell.2004.12.020

Chung, W. S., Clarke, L. E., Wang, G. X., Stafford, B. K., Sher, A., Chakraborty, C., et al. (2013). Astrocytes mediate synapse elimination through MEGF10 and MERTK pathways. *Nature* 504, 394–400. doi: 10.1038/nature12776

Colonna, M. (2003). TREMs in the immune system and beyond. *Nat. Rev. Immunol.* 3, 445–453. doi: 10.1038/nri1106

Dejanovic, B., Huntley, M. A., De Mazière, A., Meilandt, W. J., Wu, T., Srinivasan, K., et al. (2018). Changes in the synaptic proteome in tauopathy and rescue of tau-induced synapse loss by C1q antibodies. *Neuron* 100, 1322.e7–1336.e7. doi: 10.1016/j.neuron.2018.10.014

Depboylu, C., Schäfer, M. K., Arias-Carrión, O., Oertel, W. H., Weihe, E., and Höglinger, G. U. (2011). Possible involvement of complement factor C1q in the clearance of extracellular neuromelanin from the substantia nigra in Parkinson disease. *J. Neuropathol. Exp. Neurol.* 70, 125–132. doi: 10.1097/nen.0b013e31820805b9

Eroglu, C. (2009). The role of astrocyte-secreted matricellular proteins in central nervous system development and function. *J. Cell Commun. Signal.* 3, 167–176. doi: 10.1007/s12079-009-0078-y

Eroglu, C., Allen, N. J., Susman, M. W., O'Rourke, N. A., Park, C. Y., Ozkan, E., et al. (2009). Gabapentin receptor α2delta-1 is a neuronal thrombospondin receptor responsible for excitatory CNS synaptogenesis. *Cell* 139, 380–392. doi: 10.1016/j.cell.2009.09.025

Farhy-Tselnicker, I., van Casteren, A. C. M., Lee, A., Chang, V. T., Aricescu, A. R., and Allen, N. J. (2017). Astrocyte-secreted glypican 4 regulates release of neuronal pentraxin 1 from axons to induce functional synapse formation. *Neuron* 96, 428.e13–445.e13. doi: 10.1016/j.neuron.2017.09.053

Filipello, F., Morini, R., Corradini, I., Zerbi, V., Canzi, A., Michalski, B., et al. (2018). The microglial innate immune receptor TREM2 is required for synapse elimination and normal brain connectivity. *Immunity* 48, 979.e8–991.e8. doi: 10.1016/j.immuni.2018.04.016

Forny-Germano, L., Lyra e Silva, N. M., Batista, A. F., Brito-Moreira, J., Gralle, M., Boehnke, S. E., et al. (2014). Alzheimer's disease-like pathology induced by amyloid-β oligomers in nonhuman primates. *J. Neurosci.* 34, 13629–13643. doi: 10.1523/JNEUROSCI.1353-14.2014

Fossati, G., Pozzi, D., Canzi, A., Mirabella, F., Valentino, S., Morini, R., et al. (2019). Pentraxin 3 regulates synaptic function by inducing AMPA receptor clustering via ECM remodeling and β1-integrin. *EMBO J.* 38:e99529. doi: 10.15252/embj.201899529

Frakes, A. E., Ferraiuolo, L., Haidet-Phillips, A. M., Schmelzer, L., Braun, L., Miranda, C. J., et al. (2014). Microglia induce motor neuron death via the classical NF-kappaB pathway in amyotrophic lateral sclerosis. *Neuron* 81, 1009–1023. doi: 10.1016/j.neuron.2014.01.013

Fuhrmann, M., Bittner, T., Jung, C. K., Burgold, S., Page, R. M., Mitteregger, G., et al. (2010). Microglial Cx3cr1 knockout prevents neuron loss in a mouse model of Alzheimer's disease. *Nat. Neurosci.* 13, 411–413. doi: 10.1038/nn.2511

Gao, Q., Li, Y., and Chopp, M. (2005). Bone marrow stromal cells increase astrocyte survival via upregulation of phosphoinositide 3-kinase/threonine protein kinase and mitogen-activated protein kinase kinase/extracellular signal-regulated kinase pathways and stimulate astrocyte trophic factor gene expression after anaerobic insult. *Neuroscience* 136, 123–134. doi: 10.1016/j.neuroscience.2005.06.091

Graf, E. R., Zhang, X., Jin, S. X., Linhoff, M. W., and Craig, A. M. (2004). Neurexins induce differentiation of GABA and glutamate postsynaptic specializations via neuroligins. *Cell* 119, 1013–1026. doi: 10.1016/j.cell.2004.11.035

Grathwohl, S. A., Kalin, R. E., Bolmont, T., Prokop, S., Winkelmann, G., Kaeser, S. A., et al. (2009). Formation and maintenance of Alzheimer's disease β-amyloid plaques in the absence of microglia. *Nat. Neurosci.* 12, 1361–1363. doi: 10.1038/nn.2432

Harrison, J. K., Jiang, Y., Chen, S., Xia, Y., Maciejewski, D., McNamara, R. K., et al. (1998). Role for neuronally derived fractalkine in mediating interactions between neurons and CX3CR1-expressing microglia. *Proc. Natl. Acad. Sci. U S A* 95, 10896–10901. doi: 10.1073/pnas.95.18.10896

Hayakawa, K., Pham, L. D., Arai, K., and Lo, E. H. (2014). Reactive astrocytes promote adhesive interactions between brain endothelium and endothelial progenitor cells via HMGB1 and β-2 integrin signaling. *Stem Cell Res.* 12, 531–538. doi: 10.1016/j.scr.2013.12.008

Henneberger, C., Papouin, T., Oliet, S. H., and Rusakov, D. A. (2010). Long-term potentiation depends on release of D-serine from astrocytes. *Nature* 463, 232–236. doi: 10.1038/nature08673

Hong, S., Beja-Glasser, V. F., Nfonoyim, B. M., Frouin, A., Li, S., Ramakrishnan, S., et al. (2016). Complement and microglia mediate early synapse loss in Alzheimer mouse models. *Science* 352, 712–716. doi: 10.1126/science.aad8373

Hoshiko, M., Arnoux, I., Avignone, E., Yamamoto, N., and Audinat, E. (2012). Deficiency of the microglial receptor CX3CR1 impairs postnatal functional development of thalamocortical synapses in the barrel cortex. *J. Neurosci.* 32, 15106–15111. doi: 10.1523/JNEUROSCI.1167-12.2012

Jo, S., Yarishkin, O., Hwang, Y. J., Chun, Y. E., Park, M., Woo, D. H., et al. (2014). GABA from reactive astrocytes impairs memory in mouse models of Alzheimer's disease. *Nat. Med.* 20, 886–896. doi: 10.1038/nm.3639

Jonsson, T., Stefansson, H., Steinberg, S., Jonsdottir, I., Jonsson, P. V., Snaedal, J., et al. (2013). Variant of TREM2 associated with the risk of Alzheimer's disease. *N. Engl. J. Med.* 368, 107–116. doi: 10.1056/NEJMoa1211103

Kao, A. W., Eisenhut, R. J., Martens, L. H., Nakamura, A., Huang, A., Bagley, J. A., et al. (2011). A neurodegenerative disease mutation that accelerates the clearance of apoptotic cells. *Proc. Natl. Acad. Sci. U S A* 108, 4441–4446. doi: 10.1073/pnas.1100650108

Koffie, R. M., Meyer-Luehmann, M., Hashimoto, T., Adams, K. W., Mielke, M. L., Garcia-Alloza, M., et al. (2009). Oligomeric amyloid β associates with postsynaptic densities and correlates with excitatory synapse loss near senile plaques. *Proc. Natl. Acad. Sci. U S A* 106, 4012–4017. doi: 10.1073/pnas.0811698106

Kucukdereli, H., Allen, N. J., Lee, A. T., Feng, A., Ozlu, M. I., Conatser, L. M., et al. (2011). Control of excitatory CNS synaptogenesis by astrocyte-secreted proteins Hevin and SPARC. *Proc. Natl. Acad. Sci. U S A* 108, E440–E449. doi: 10.1073/pnas.1104977108

Lee, L., Kosuri, P., and Arancio, O. (2014). Picomolar amyloid-β peptides enhance spontaneous astrocyte calcium transients. *J. Alzheimers Dis.* 38, 49–62. doi: 10.3233/jad-130740

Lee, H.-J., Suk, J. E., Patrick, C., Bae, E. J., Cho, J. H., Rho, S., et al. (2010). Direct transfer of α-synuclein from neuron to astroglia causes inflammatory responses in synucleinopathies. *J. Biol. Chem.* 285, 9262–9272. doi: 10.1074/jbc.M109.081125

Lee, E.-J., Woo, M. S., Moon, P. G., Baek, M. C., Choi, I. Y., Kim, W. K., et al. (2010). α-synuclein activates microglia by inducing the expressions of matrix metalloproteinases and the subsequent activation of protease-activated receptor-1. *J. Immunol.* 185, 615–623. doi: 10.4049/jimmunol.0903480

Leshchyns'ka, I., Liew, H. T., Shepherd, C., Halliday, G. M., Stevens, C. H., Ke, Y. D., et al. (2015). Aβ-dependent reduction of NCAM2-mediated synaptic adhesion contributes to synapse loss in Alzheimer's disease. *Nat. Commun.* 6:8836. doi: 10.1038/ncomms9836

Li, Q., and Barres, B. A. (2018). Microglia and macrophages in brain homeostasis and disease. *Nat. Rev. Immunol.* 18, 225–242. doi: 10.1038/nri.2017.125

Liddelow, S. A., and Barres, B. A. (2017). Reactive astrocytes: production, function, and therapeutic potential. *Immunity* 46, 957–967. doi: 10.1016/j.immuni.2017.06.006

Liddelow, S. A., Guttenplan, K. A., Clarke, L. E., Bennett, F. C., Bohlen, C. J., Schirmer, L., et al. (2017). Neurotoxic reactive astrocytes are induced by activated microglia. *Nature* 541, 481–487. doi: 10.1038/nature21029

Lim, S. H., Park, E., You, B., Jung, Y., Park, A. R., Park, S. G., et al. (2013). Neuronal synapse formation induced by microglia and interleukin 10. *PLoS One* 8:e81218. doi: 10.1371/journal.pone.0081218

Litvinchuk, A., Wan, Y. W., Swartzlander, D. B., Chen, F., Cole, A., Propson, N. E., et al. (2018). Complement C3aR inactivation attenuates tau pathology and reverses an immune network deregulated in tauopathy models and Alzheimer's disease. *Neuron* 100, 1337.e5–1353.e5. doi: 10.1016/j.neuron.2018.10.031

Liuzzi, F. J., and Lasek, R. J. (1987). Astrocytes block axonal regeneration in mammals by activating the physiological stop pathway. *Science* 237, 642–645. doi: 10.1126/science.3603044

Lui, H., Zhang, J., Makinson, S. R., Cahill, M. K., Kelley, K. W., Huang, H. Y., et al. (2016). Progranulin deficiency promotes circuit-specific synaptic pruning by microglia via complement activation. *Cell* 165, 921–935. doi: 10.1016/j.cell.2016.04.001

Mauch, D. H., Nagler, K., Schumacher, S., Göritz, C., Müller, E. C., Otto, A., et al. (2001). CNS synaptogenesis promoted by glia-derived cholesterol. *Science* 294, 1354–1357. doi: 10.1126/science.294.5545.1354

Mitew, S., Kirkcaldie, M. T., Dickson, T. C., and Vickers, J. C. (2013). Altered synapses and gliotransmission in Alzheimer's disease and AD model mice. *Neurobiol. Aging* 34, 2341–2351. doi: 10.1016/j.neurobiolaging.2013.04.010

Miyamoto, A., Wake, H., Ishikawa, A. W., Eto, K., Shibata, K., Murakoshi, H., et al. (2016). Microglia contact induces synapse formation in developing somatosensory cortex. *Nat. Commun.* 7:12540. doi: 10.1038/ncomms12540

Morizawa, Y. M., Hirayama, Y., Ohno, N., Shibata, S., Shigetomi, E., Sui, Y., et al. (2017). Reactive astrocytes function as phagocytes after brain ischemia via ABCA1-mediated pathway. *Nat. Commun.* 8:28. doi: 10.1038/s41467-017-00037-1

Nagele, R. G., D'Andrea, M. R., Lee, H., Venkataraman, V., and Wang, H. Y. (2003). Astrocytes accumulate A β 42 and give rise to astrocytic amyloid plaques in Alzheimer disease brains. *Brain Res.* 971, 197–209. doi: 10.1016/s0006-8993(03)02361-8

Olabarria, M., Noristani, H. N., Verkhratsky, A., and Rodríguez, J. J. (2010). Concomitant astroglial atrophy and astrogliosis in a triple transgenic animal model of Alzheimer's disease. *Glia* 58, 831–838. doi: 10.1002/glia.20967

Paolicelli, R. C., Bolasco, G., Pagani, F., Maggi, L., Scianni, M., Panzanelli, P., et al. (2011). Synaptic pruning by microglia is necessary for normal brain development. *Science* 333, 1456–1458. doi: 10.1126/science.1202529

Park, J. Y., Paik, S. R., Jou, I., and Park, S. M. (2008). Microglial phagocytosis is enhanced by monomeric α-synuclein, not aggregated α-synuclein: implications for Parkinson's disease. *Glia* 56, 1215–1223. doi: 10.1002/glia.20691

Parkhurst, C. N., Yang, G., Ninan, I., Savas, J. N., Yates, J. R., Lafaille, J. J., et al. (2013). Microglia promote learning-dependent synapse formation through brain-derived neurotrophic factor. *Cell* 155, 1596–1609. doi: 10.1016/j.cell.2013.11.030

Perlmutter, L. S., Barron, E., and Chui, H. C. (1990). Morphologic association between microglia and senile plaque amyloid in Alzheimer's disease. *Neurosci. Lett.* 119, 32–36. doi: 10.1016/0304-3940(90)90748-x

Perry, V. H., and Holmes, C. (2014). Microglial priming in neurodegenerative disease. *Nat. Rev. Neurol.* 10, 217–224. doi: 10.1038/nrneurol.2014.38

Phatnani, H., and Maniatis, T. (2015). Astrocytes in neurodegenerative disease. *Cold Spring Harb. Perspect. Biol.* 7:a020628. doi: 10.1101/cshperspect.a020628

Pihlaja, R., Koistinaho, J., Kauppinen, R., Sandholm, J., Tanila, H., and Koistinaho, M. (2011). Multiple cellular and molecular mechanisms are involved in human Aβ clearance by transplanted adult astrocytes. *Glia* 59, 1643–1657. doi: 10.1002/glia.21212

Pihlaja, R., Koistinaho, J., Malm, T., Sikkilä, H., Vainio, S., and Koistinaho, M. (2008). Transplanted astrocytes internalize deposited β-amyloid peptides in a transgenic mouse model of Alzheimer's disease. *Glia* 56, 154–163. doi: 10.1002/glia.20599

Prada, I., Gabrielli, M., Turola, E., Iorio, A., D'Arrigo, G., Parolisi, R., et al. (2018). Glia-to-neuron transfer of miRNAs via extracellular vesicles: a new mechanism underlying inflammation-induced synaptic alterations. *Acta Neuropathol.* 135, 529–550. doi: 10.1007/s00401-017-1803-x

Ramiro-Cortés, Y., and Israely, I. (2013). Long lasting protein synthesis- and activity-dependent spine shrinkage and elimination after synaptic depression. *PLoS One* 8:e71155. doi: 10.1371/journal.pone.0071155

Ransohoff, R. M. (2016). How neuroinflammation contributes to neurodegeneration. *Science* 353, 777–783. doi: 10.1126/science.aag2590

Robinson, S. R. (2001). Changes in the cellular distribution of glutamine synthetase in Alzheimer's disease. *J. Neurosci. Res.* 66, 972–980. doi: 10.1002/jnr.10057

Schafer, D. P., Lehrman, E. K., Kautzman, A. G., Koyama, R., Mardinly, A. R., Yamasaki, R., et al. (2012). Microglia sculpt postnatal neural circuits in an activity and complement-dependent manner. *Neuron* 74, 691–705. doi: 10.1016/j.neuron.2012.03.026

Schulz-Schaeffer, W. J. (2010). The synaptic pathology of α-synuclein aggregation in dementia with Lewy bodies, Parkinson's disease and Parkinson's disease dementia. *Acta Neuropathol.* 120, 131–143. doi: 10.1007/s00401-010-0711-0

Sekar, A., Bialas, A. R., de Rivera, H., Davis, A., Hammond, T. R., Kamitaki, N., et al. (2016). Schizophrenia risk from complex variation of complement component 4. *Nature* 530, 177–183. doi: 10.1038/nature16549

Shi, Q., Chowdhury, S., Ma, R., Le, K. X., Hong, S., Caldarone, B. J., et al. (2017). Complement C3 deficiency protects against neurodegeneration in aged plaque-rich APP/PS1 mice. *Sci. Transl. Med.* 9:eaaf6295. doi: 10.1126/scitranslmed.aaf6295

Shi, Y., Yamada, K., Liddelow, S. A., Smith, S. T., Zhao, L., Luo, W., et al. (2017). ApoE4 markedly exacerbates tau-mediated neurodegeneration in a mouse model of tauopathy. *Nature* 549, 523–527. doi: 10.1038/nature24016

Shigetomi, E., Jackson-Weaver, O., Huckstepp, R. T., O'Dell, T. J., and Khakh, B. S. (2013). TRPA1 channels are regulators of astrocyte basal calcium levels and long-term potentiation via constitutive D-serine release. *J. Neurosci.* 33, 10143–10153. doi: 10.1523/JNEUROSCI.5779-12.2013

Shinozaki, Y., Shibata, K., Yoshida, K., Shigetomi, E., Gachet, C., Ikenaka, K., et al. (2017). Transformation of astrocytes to a neuroprotective phenotype by microglia via P2Y1 receptor downregulation. *Cell Rep.* 19, 1151–1164. doi: 10.1016/j.celrep.2017.04.047

Simon, D. W., McGeachy, M. J., Bayir, H., Clark, R. S. B., Loane, D. J., and Kochanek, P. M. (2017). The far-reaching scope of neuroinflammation after traumatic brain injury. *Nat. Rev. Neurol.* 13:572. doi: 10.1038/nrneurol.2017.116

Simpson, J. E., Ince, P. G., Lace, G., Forster, G., Shaw, P. J., Matthews, F., et al. (2010). Astrocyte phenotype in relation to Alzheimer-type pathology in the ageing brain. *Neurobiol. Aging* 31, 578–590. doi: 10.1016/j.neurobiolaging.2008.05.015

Singh, S. K., Stogsdill, J. A., Pulimood, N. S., Dingsdale, H., Kim, Y. H., Pilaz, L. J., et al. (2016). Astrocytes assemble thalamocortical synapses by bridging NRX1α and NL1 via hevin. *Cell* 164, 183–196. doi: 10.1016/j.cell.2015.11.034

Sofroniew, M. V., and Vinters, H. V. (2010). Astrocytes: biology and pathology. *Acta Neuropathol.* 119, 7–35. doi: 10.1007/s00401-009-0619-8

Spiller, K. J., Restrepo, C. R., Khan, T., Dominique, M. A., Fang, T. C., Canter, R. G., et al. (2018). Microglia-mediated recovery from ALS-relevant motor neuron degeneration in a mouse model of TDP-43 proteinopathy. *Nat. Neurosci.* 21, 329–340. doi: 10.1038/s41593-018-0083-7

Stephan, A. H., Madison, D. V., Mateos, J. M., Fraser, D. A., Lovelett, E. A., Coutellier, L., et al. (2013). A dramatic increase of C1q protein in the CNS during normal aging. *J. Neurosci.* 33, 13460–13474. doi: 10.1523/JNEUROSCI.1333-13.2013

Stevens, B., Allen, N. J., Vazquez, L. E., Howell, G. R., Christopherson, K. S., Nouri, N., et al. (2007). The classical complement cascade mediates CNS synapse elimination. *Cell* 131, 1164–1178. doi: 10.1016/j.cell.2007.10.036

Tomiyama, T., Matsuyama, S., Iso, H., Umeda, T., Takuma, H., Ohnishi, K., et al. (2010). A mouse model of amyloid β oligomers: their contribution to synaptic alteration, abnormal tau phosphorylation, glial activation, and neuronal loss *in vivo*. *J. Neurosci.* 30, 4845–4856. doi: 10.1523/JNEUROSCI.5825-09.2010

Tu, S., Okamoto, S., Lipton, S. A., and Xu, H. (2014). Oligomeric Aβ-induced synaptic dysfunction in Alzheimer's disease. *Mol. Neurodegener.* 9:48. doi: 10.1186/1750-1326-9-48

Ullian, E. M., Sapperstein, S. K., Christopherson, K. S., and Barres, B. A. (2001). Control of synapse number by glia. *Science* 291, 657–661. doi: 10.1126/science.291.5504.657

Vainchtein, I. D., Chin, G., Cho, F. S., Kelley, K. W., Miller, J. G., Chien, E. C., et al. (2018). Astrocyte-derived interleukin-33 promotes microglial synapse engulfment and neural circuit development. *Science* 359, 1269–1273. doi: 10.1126/science.aal3589

Wakabayashi, K., Hayashi, S., Yoshimoto, M., Kudo, H., and Takahashi, H. (2000). NACP/α-synuclein-positive filamentous inclusions in astrocytes and oligodendrocytes of Parkinson's disease brains. *Acta Neuropathol.* 99, 14–20. doi: 10.1007/pl00007400

Wyss-Coray, T., Loike, J. D., Brionne, T. C., Lu, E., Anankov, R., Yan, F., et al. (2003). Adult mouse astrocytes degrade amyloid-β *in vitro* and *in situ*. *Nat. Med.* 9, 453–457. doi: 10.1038/nm838

Yang, J., Yang, H., Liu, Y., Li, X., Qin, L., Lou, H., et al. (2016). Astrocytes contribute to synapse elimination via type 2 inositol 1,4,5-trisphosphate receptor-dependent release of ATP. *Elife* 5:e15043. doi: 10.7554/eLife.15043

Yun, S. P., Kam, T. I., Panicker, N., Kim, S., Oh, Y., Park, J. S., et al. (2018). Block of A1 astrocyte conversion by microglia is neuroprotective in models of Parkinson's disease. *Nat. Med.* 24, 931–938. doi: 10.1038/s41591-018-0051-5

Zamanian, J. L., Xu, L., Foo, L. C., Nouri, N., Zhou, L., Giffard, R. G., et al. (2012). Genomic analysis of reactive astrogliosis. *J. Neurosci.* 32, 6391–6410. doi: 10.1523/JNEUROSCI.6221-11.2012

Zhan, Y., Paolicelli, R. C., Sforazzini, F., Weinhard, L., Bolasco, G., Pagani, F., et al. (2014). Deficient neuron-microglia signaling results in impaired functional brain connectivity and social behavior. *Nat. Neurosci.* 17, 400–406. doi: 10.1038/nn.3641

Zhao, Y., Wu, X., Li, X., Jiang, L. L., Gui, X., Liu, Y., et al. (2018). TREM2 is a receptor for β-amyloid that mediates microglial function. *Neuron* 97, 1023.e7–1031.e7. doi: 10.1016/j.neuron.2018.01.031

Zumkehr, J., Rodriguez-Ortiz, C. J., Cheng, D., Kieu, Z., Wai, T., Hawkins, C., et al. (2015). Ceftriaxone ameliorates tau pathology and cognitive decline via restoration of glial glutamate transporter in a mouse model of Alzheimer's disease. *Neurobiol. Aging* 36, 2260–2271. doi: 10.1016/j.neurobiolaging.2015.04.005

Conflict of Interest Statement: The authors declare that the research was conducted in the absence of any commercial or financial relationships that could be construed as a potential conflict of interest.

frontiers in Cellular Neuroscience

REVIEW
published: 26 February 2019
doi: 10.3389/fncel.2019.00063

Glial Contribution to Excitatory and Inhibitory Synapse Loss in Neurodegeneration

Christopher M. Henstridge[1,2], *Makis Tzioras*[1,2] *and Rosa C. Paolicelli*[3]*

[1]Centre for Discovery Brain Sciences, The University of Edinburgh, Edinburgh, United Kingdom, [2]Dementia Research Institute UK, The University of Edinburgh, Edinburgh, United Kingdom, [3]Department of Physiology, University of Lausanne, Lausanne, Switzerland

Synapse loss is an early feature shared by many neurodegenerative diseases, and it represents the major correlate of cognitive impairment. Recent studies reveal that microglia and astrocytes play a major role in synapse elimination, contributing to network dysfunction associated with neurodegeneration. Excitatory and inhibitory activity can be affected by glia-mediated synapse loss, resulting in imbalanced synaptic transmission and subsequent synaptic dysfunction. Here, we review the recent literature on the contribution of glia to excitatory/inhibitory imbalance, in the context of the most common neurodegenerative disorders. A better understanding of the mechanisms underlying pathological synapse loss will be instrumental to design targeted therapeutic interventions, taking in account the emerging roles of microglia and astrocytes in synapse remodeling.

OPEN ACCESS

Edited by:
Jaichandar Subramanian, University of Kansas, United States

Reviewed by:
Rodrigo A. Cunha, Universidade de Coimbra, Portugal
Marco Fuenzalida, Universidad de Valparaíso, Chile

***Correspondence:**
Rosa C. Paolicelli
rosachiara.paolicelli@unil.ch

Received: 18 November 2018
Accepted: 08 February 2019
Published: 26 February 2019

Citation:
Henstridge CM, Tzioras M and Paolicelli RC (2019) Glial Contribution to Excitatory and Inhibitory Synapse Loss in Neurodegeneration. Front. Cell. Neurosci. 13:63. doi: 10.3389/fncel.2019.00063

Keywords: microglia, astrocytes, neurodegeneration, synapse loss, E/I imbalance

INTRODUCTION

The prevalence of neurodegenerative disorders has been rapidly increasing over the past decades. These untreatable and often lethal conditions including Alzheimer's disease (AD), Parkinson's disease (PD), amyotrophic lateral sclerosis (ALS) and multiple sclerosis (MS), affect over 100 million people worldwide (Prince et al., 2013; Browne et al., 2014; Baxter et al., 2015). Despite differences in age of onset and genetic risk factors associated with the disease, common pathophysiological features can be identified, including synaptic and glial dysfunction, as well as cognitive impairments. Synapse loss is an early occurring hallmark in many neurodegenerative disorders, which correlates best with the appearance and progression of cognitive decline (DeKosky and Scheff, 1990; Terry et al., 1991; Koffie et al., 2011; Spires-Jones and Hyman, 2014). Abnormal glial function is also recognized as an early pathological feature commonly observed in neurodegenerative disease (Verkhratsky et al., 2014). However, for a long time, the prevailing neuro-centric view of pathogenesis has led to the underestimation of key roles for non-neuronal cells in the brain, primarily glia, which were instead considered as mere bystanders or secondary responders in the pathological process. Only in the last decade, with the advent of new genetic, molecular and pharmacological tools, have significant steps forward been made towards our understanding of glial function, revealing a central role for these cells in disease (Verkhratsky et al., 2014).

From the Greek word "glue," glia in the central nervous system (CNS) include three major cell subsets: astrocytes, microglia and oligodendrocytes. While the latter are mainly responsible for the

formation of myelin and for providing metabolic support to axons (Baumann and Pham-Dinh, 2001; Simons and Nave, 2015), microglia and astrocytes cover a variety of functions, ranging from trophic support to refinement and coordination of neural networks (Reemst et al., 2016; Allen and Lyons, 2018). Microglia are the resident macrophages of the CNS and constitute about 10%–15% of all the brain cells. Historically, they have been regarded exclusively as innate immune cells, considered to be "activated" only during infection or injury. In the last decade, however, several new physiological roles for microglia have been described, revealing a much broader scenario for the multifaceted tasks performed by these cells (Tremblay et al., 2011; Sierra et al., 2014; Paolicelli and Ferretti, 2017). Astrocytes are the more abundant glial cell in the CNS; their processes closely enwrap synapses, and their role in regulating synaptogenesis, neurotransmitter recycling and synaptic transmission is well established (Parpura et al., 1994; Vesce et al., 1999; Panatier et al., 2011; Chever et al., 2016). In addition, they play key roles in maintaining the blood–brain barrier, providing trophic and metabolic support to neurons (Pellerin et al., 2007; Sofroniew and Vinters, 2010). Since the recent recognition of a role for glia in refining synaptic connections, intense investigations have been devoted to elucidate the molecular mechanisms of glia-meditated synapse elimination, particularly in the context of neurodegeneration. The majority of neurodegenerative disorders fall into the category of "proteinopathies," because of the characteristic accumulation of toxic protein aggregates (Ross and Poirier, 2004; Soto and Pritzkow, 2018). In such diseases, pathological proteins often accumulate at the synapse (Koffie et al., 2009, 2012; Henstridge et al., 2018), thus causing synaptic dysfunction and likely rendering the synapses vulnerable and primed for removal (Walsh et al., 2002; Geracitano et al., 2003; Pieri et al., 2003; Shankar et al., 2007; Crimins et al., 2012). In the case of AD, for instance, amyloid β (Aβ) peptide accumulates at the synaptic site long before its extracellular aggregation in plaques, and it is associated with alterations in synaptic structures, both in mouse and in human studies (Gylys et al., 2004; Almeida et al., 2005; Sokolow et al., 2012; Takahashi et al., 2013).

Synapse elimination could occur *via* autonomous pathways within the damaged neuron, due to localized caspases or necrotic signals (Wishart et al., 2006; Ertürk et al., 2014) or *via* active non-cell-autonomous removal of synapses by surrounding glial cells (Hong et al., 2016; Vasek et al., 2016; Paolicelli et al., 2017). Evidence for either scenario or even a combination of both exists. In this review article, we will primarily focus on glial-dependent synapse loss and revise the recent literature providing evidence for glial contribution to excitatory-inhibitory network dysfunction in pathological states.

SYNAPSE REMODELING IN DEVELOPMENT AND DISEASE

The term synapse, from the Greek συυάψις, meaning "conjunction," refers to the physical point of contact between two neurons, and thus defines the anatomical site of information exchange between an axonal input and the recipient dendritic spine (Harris and Weinberg, 2012). Synapses are highly dynamic sub-cellular structures, as they can be rapidly formed or eliminated during plasticity-mediated processes (Engert and Bonhoeffer, 1999; Matsuzaki et al., 2001). They represent the structural basis of long-term potentiation (LTP), essential for memory formation (Matsuzaki et al., 2004). Evidence of the highly dynamic nature of synapses has been provided by advances in live imaging techniques, showing that dendritic spines rapidly appear and disappear as a result of experience-dependent plasticity upon sensory experience, and learning processes (Toni et al., 1999; Lendvai et al., 2000; Holtmaat and Svoboda, 2009; Fu et al., 2012). During early development, immature neural circuits undergo synaptic refinement, in which activity-dependent competition between synapses ultimately results in the elimination of inappropriate connections and brain plasticity, while strong synapses are reinforced (Penn et al., 1998; Lichtman and Colman, 2000; Hua and Smith, 2004; Torborg and Feller, 2005; Mikuni et al., 2013; Fields et al., 2014; Robin et al., 2018). Importantly, the proposed mechanism of the strongest "winning inputs" (Personius and Balice-Gordon, 2000) is consistent across a number of models, namely the neuromuscular junction (NMJ; Wang et al., 2014), the Purkinje fibers in the cerebellum (Mason and Gregory, 1984; Hashimoto and Kano, 2003; Kakegawa et al., 2015) and the retino-thalamic system (Hong and Chen, 2011), suggesting that activity-dependent remodeling of synapses is a conserved process across the central and peripheral nervous system. *In vivo* imaging studies recently showed that monocular deprivation (MD) increases dendritic spine elimination in the developing mouse visual cortex, with no effects on synapse formation (Zhou et al., 2017). Interestingly, binocular deprivation (BD), which entirely suppresses competition between the two eyes, failed to induce synapse elimination, and resulted by contrast in enlarged dendritic spine size (Zhou et al., 2017).

The high dynamic remodeling of synapses not only occurs during early developmental stages, but also persists across the entire lifespan (Peretti et al., 2015). Live imaging of cortical regions largely supports the experience-dependent plasticity of dendritic spines in the adult mouse brain (Xu et al., 2009; Yang and Zhou, 2009). *In vivo* imaging of the hippocampus, a highly plastic structure, has been made possible only recently, upon novel methods of cortical tissue resection (Pilz et al., 2016). Such studies have provided evidence for network plasticity with new spines formed and eliminated in the CA1 *stratum radiatum*, with an impressive-previously underscored- spine turnover of ∼40% within 4 days (Gu et al., 2014; Pfeiffer et al., 2018).

While synapse elimination in the context of brain development and experience-dependent plasticity is a physiological process (Wolff and Missler, 1993; Kamiyama et al., 2006), its later and dysregulated occurrence is recognized as an early pathological feature of neurodegenerative diseases (DeKosky and Scheff, 1990; Henstridge et al., 2018). Indeed, one of the earliest hallmarks of neurodegeneration is the loss of presynaptic terminals and dendritic spines, which represents the major correlate of cognitive impairment (Terry et al., 1991; Scheff et al., 2006, 2014). Structural and

functional alterations of synapses, culminating in synapse loss, are associated with sensory, motor, and cognitive impairments observed in a variety of neurodegenerative disorders, ranging from AD to motor neuron diseases (MND), and often precede clinical manifestations (Selkoe, 2002; Henstridge et al., 2018). Yet, the causes and the molecular mechanisms leading to pathological synapse loss have not been fully elucidated (Henstridge et al., 2016). On one hand, the regenerative capacity of synapses seems to be significantly reduced in the disease state, as shown in prion-infected and AD mouse models (Peretti et al., 2015); on the other hand, aberrant synaptic pruning or lack of trophic support by surrounding glia cells can contribute to the drastic reduction in synapse number.

CONTRIBUTION OF GLIA TO SYNAPSE ELIMINATION

Recent literature highlights glial cells as active participants in the process of neural circuits refinement (**Figure 1**). Microglia and astrocytes contribute to accurate network formation by directly pruning redundant synapses during early development, and thus shaping brain connectivity (Paolicelli et al., 2011; Chung et al., 2013; Hakim et al., 2014; Zhan et al., 2014; Risher et al., 2014; Filipello et al., 2018). In addition, glia can also act indirectly to induce effects on synaptic function, *via* the release of soluble modulators (Chung et al., 2015). Compelling evidence shows that synapse elimination by glia is important in the activity-dependent wiring of

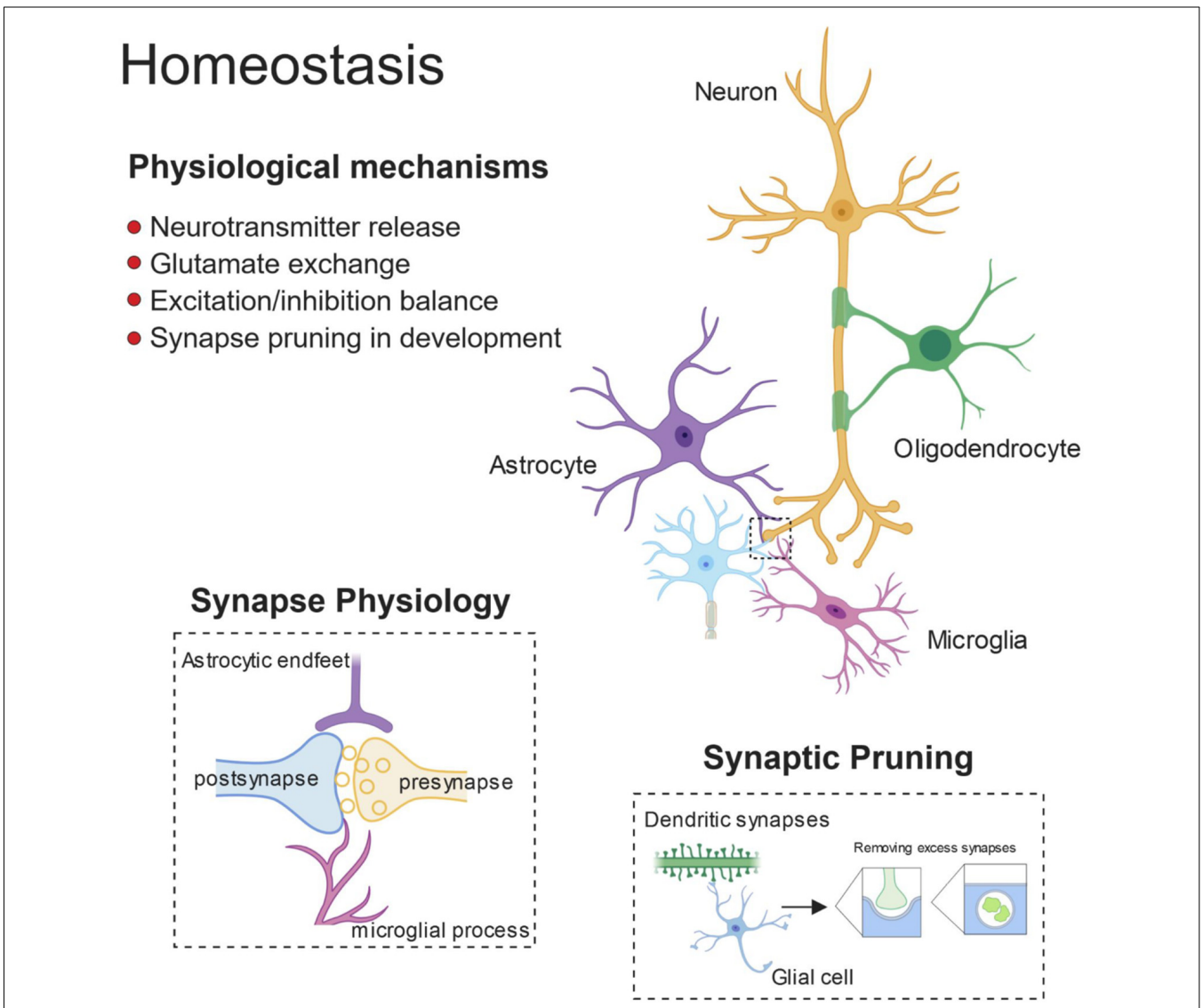

FIGURE 1 | Glial control of synaptic homoeostasis. Synapses exists as tri- or even quad-partite structures with glial processes in direct contact with neuronal components. Glia play important roles in regulating efficient neurotransmitter release and clearance, as well as providing trophic factors to ensure healthy function. Furthermore, during development glia prune away excess synapses and by doing so, fine-tune the excitatory/inhibitory balance within developing neuronal networks.

the brain, with microglia and astrocytes selectively removing the weaker synapses upon input competition (Schafer et al., 2012; Chung et al., 2013; Sipe et al., 2016; Yang et al., 2016). For example, the visual system is a well-characterized model for experience-dependent synaptic refinement (Wiesel and Hubel, 1963), and thus, the developing retino-thalamic system has been frequently used for studying competition of synaptic inputs, which project from the retinal ganglion cells (RGCs) to the relay neurons in the dorsal later geniculate nucleus (dLGN), and then to the primary visual cortex. This model has been influential in revealing that microglia are active players in experience-dependent remodeling of neural circuits (Tremblay et al., 2010; Schafer et al., 2012; Sipe et al., 2016). Sensory deprivation, by closure of one eye, during the visual critical period results in enhanced engulfment of synaptic terminals by microglia and astrocytes (Chung et al., 2013; Sipe et al., 2016), whereas BD, achieved by pharmacological blockade, drastically reduces astrocyte-mediated synaptic pruning, further confirming that active competition of synaptic inputs is required for glial-dependent synapse remodeling (Chung et al., 2013). Several pathways have been implicated in this process, including fractalkine signaling (Cx3cr1/Cx3cl1), DAP12/triggering receptor expressed on myeloid cells 2 (TREM2) signaling and the complement pathway for synapse elimination by microglia (Paolicelli et al., 2011; Schafer et al., 2012; Filipello et al., 2018), and MEGF10 and MERTK for astrocyte-mediated synapse engulfment (Chung et al., 2013). Dysfunctional regulation of such pathways or intrinsic defects in glia are possible causes for the pathological synaptic pruning observed in neurodegeneration. Indeed, a growing body of evidence indicates that glia-mediated synapse removal becomes dysregulated in aging and disease. A prominent hypothesis is that an increased activation of the complement cascade, associated with neurodegenerative disorders, enhances complement deposition on synaptic terminals, priming the synapses for removal and thus mediating aberrant synapse elimination. In support of this, distinct animal models of neurodegeneration (discussed below) exhibit upregulated levels of complement C3 and C1q, and subsequent synapse loss (Fonseca et al., 2004; Michailidou et al., 2015, 2017; Shi et al., 2015, 2017; Lui et al., 2016). Also, injection of Aβ peptide in wild-type mice was shown to increase the levels of complement molecules, and in turn to promote synapse engulfment by microglia (Hong et al., 2016). A consistent role for complement in opsonizing synapses for removal has been shown in ageing models, with complement C3-deficient mice protected from age-related hippocampal decline (Shi et al., 2015). Complement upregulation was also reported upon viral infection. However, while such increase is critical for mediating microglial removal of presynaptic terminals in the hippocampus of West Nile Virus (WNV) infected mice (Vasek et al., 2016), it appears dispensable in IFN-γ mediated microglial synaptic stripping upon lymphocytic choriomeningitis viral infection (Di Liberto et al., 2018). Type I IFN signaling instead mediates synapse elimination by microglia in a mouse model of systemic lupus erythematosous (SLE), an incurable autoimmune disease (Bialas et al., 2017).

Purinergic signaling also plays crucial roles in microglia-mediated synapse refinement. ATP is a major signaling molecule, that acts as a danger signal once released extracellularly and profoundly affects microglial function (George et al., 2015; Rodrigues et al., 2015). Microglial processes are rapidly directed towards sources of ATP through the activation of P2Y12 receptors (Davalos et al., 2005). Activity-dependent synapse remodeling in the developing mouse visual cortex has been shown to strongly rely on such purinergic pathways in microglia, as knockout mice exhibited defective ocular dominance plasticity (Sipe et al., 2016). In addition, calcium-mediated purinergic receptors regulate microglial phagocytoses during postnatal brain development (Sunkaria et al., 2016).

Microglia not only sense and respond to ATP, but they can also serve as a source of purines, which modulate synaptic plasticity, thus representing an alternative mechanism for microglia-induced synaptic refinement (George et al., 2016).

Also, intrinsic glia dysfunction caused by genetic mutations can lead to aberrant synapse elimination. Loss of progranulin was shown to promote synaptic pruning by microglia, in a C1q-dependent manner (Lui et al., 2016). We have reported evidence for enhanced synapse engulfment, in the motor/somatosensory cortex of mice selectively lacking microglial TDP-43 (Paolicelli et al., 2017).

Other immune-related molecules such as CD47, have been recently described to work as "spare me" signals, and to protect synapses from excessive microglia-mediated pruning (Lehrman et al., 2018).

An interesting aspect that warrants further investigation is the cross-talk between microglia and astrocytes. Collecting evidence indicates that microglia can modulate astrocytic function, and conversely astrocytes can regulate microglial phenotypes (Jha et al., 2018). Microglial derived ATP, for instance, acts through the astrocytic receptor P2Y1, thus modulating excitatory neurotransmission and providing neuroprotection (Pascual et al., 2012; Shinozaki et al., 2014). Microglia can also induce neurotoxic astrocytes through the release of C1q, tumor necrosis factor-α (TNF-α), and interleukin-1α (IL-1α) (Liddelow et al., 2017). Recent findings show that astrocytic NF-kB activation induce a Wnt-dependent microglial proliferation, identifying astrocytes as important regulator of microglial expansion (Ouali Alami et al., 2018). Astrocyte-mediated synapse elimination has been shown to occur soon after acute sleep deprivation, before microglia-mediated remodeling, which is engaged only subsequently, if sleep deprivation is prolonged for several hours (Bellesi et al., 2017). It is thus tempting to speculate that astrocytes and microglia can act together in coordination, to ensure efficient synapse remodeling. Fine-tuned communication between microglia and astrocytes is crucial for proper brain functioning. Thus, a better understanding of the cellular processes involved in this cross-talk will be essential to elucidate the role of glia in the diseased brain.

Lifestyle factors related to dementia, such as nutrition, sleep quality and stress, are heavily implicated in glia-mediated synapse loss and cognitive decline (Cope et al., 2018; Rajendran and Paolicelli, 2018). On the other hand, large-scale human genetic studies have identified glia-specific genes as genetic

risk factor in a range of neurological conditions from autism (Voineagu et al., 2011) to AD (Karch and Goate, 2015; Gosselin et al., 2017). Taken together, all this evidence reveals glia as a common link between many of the world's most impenetrable diseases.

IMBALANCE BETWEEN EXCITATION AND INHIBITION IN PATHOLOGICAL STATES

The balance between the excitatory and inhibitory control of synaptic activity needs to be tightly maintained to ensure proper functioning and plasticity of neural circuits (Hensch and Fagiolini, 2005; Harauzov et al., 2010). Pre-synaptic terminals of excitatory synapses release glutamate as their major neurotransmitter, and are thus defined glutamatergic. Glutamate is received at the post-synapse by the ionotropic [N-methyl-D-aspartate receptors (NMDARs) and 2-amino-3-3-hydroxy-5-methyl-isoxazol-4-yl propanoic acid receptors (AMPARs)] and metabotropic (mGluR) glutamate receptors. On the other hand, pre-synaptic terminals at inhibitory synapses primarily release γ-aminobutyric acid (GABA), and are thus defined GABAergic. GABA is post-synaptically received by ionotropic ($GABA_AR$) and metabotropic ($GABA_BR$) GABA receptors. In terms of spatial organization, glutamatergic synapses are located almost exclusively on dendritic spines, whereas GABAergic synapses can be spread along the dendritic shaft, somata, and axon initial segments (Fritschy and Brünig, 2003; Penzes et al., 2011).

Excitatory neurons increase or decrease the accumulation of glutamate receptors at synaptic sites in response to changes in their own firing rates, through what has been defined as homeostatic synaptic scaling (Turrigiano et al., 1998; Turrigiano and Nelson, 2004; Turrigiano, 2008). The aim is to stabilize neuronal firing by adjusting its own synaptic strength to compensate for perturbations in surrounding neural activity (Ibata et al., 2008).

Network synchrony and oscillatory brain rhythms are promoted and controlled by the activity of inhibitory GABAergic interneurons across the entire lifespan, with important cross-talks with astrocytes modulating synaptic efficacy (Buzsáki et al., 2004; Klausberger and Somogyi, 2008; Perea et al., 2016; Sardinha et al., 2017; Mederos et al., 2018). Indeed, in the early stages of several brain disorders, impairment in inhibitory transmission combined with possible defects in homeostatic synaptic scaling at excitatory synapses might drastically compromise the excitation/inhibition (E/I) balance (Palop and Mucke, 2016). Defective inhibition or aberrant excitation in brain development has been associated with severe alteration in the E/I ratio (observed in ASD for example) and considered to be causally linked to behavioral abnormalities (Rubenstein and Merzenich, 2003; Gao and Penzes, 2015; Nelson and Valakh, 2015). In support of this, modulation of prefrontal cortex E/I by optogenetics has recently been shown to rescue deficits in social behavior, in a mouse model of autism (Selimbeyoglu et al., 2017). Nevertheless, in other cases with memory alterations, selective changes of glutamatergic synaptic markers, have been reported without evident changes of GABAergic synaptic markers, in models of childhood epilepsy, diabetic encephalopathy and repeated stress, supporting the complexity of this topic (Cognato et al., 2010; Duarte et al., 2012; Canas et al., 2014; Kaster et al., 2015).

In neurodegeneration, such as in AD, network activities are altered even decades before clinical disease onset and are associated with diverse cognitive manifestations (Palop and Mucke, 2016). To date, the mechanisms and pathophysiological consequences of these alterations, which include activation and deactivation deficits of neural circuits, are poorly understood. Importantly, recent findings suggest that network activities can be experimentally or behaviorally manipulated to improve cognitive function in AD mouse models (Sanchez et al., 2012; Busche et al., 2015), and even in patients at risk of AD (Bakker et al., 2012, 2015). Overall, impairments in inhibitory connections, with consequent hyperexcitation, are emerging as potential mechanisms underlying cognitive dysfunction in several neurodegenerative diseases. On the other hand, selective increase in inhibition, *via* pharmacogenetic activation of parvalbumin interneurons, was recently shown to have beneficial effects, preventing stress-induced synapse loss *in vivo* (Chen et al., 2018).

Considering the complexity of our brain, it is easy to imagine that the fine-tuned balance between excitation and inhibition is not simply the net output of neuronal firing, but is rather the result of a highly regulated cross-talk amongst numerous cell types that are able to sense synaptic activity and to assist neurons to dynamically and appropriately adjust synapse strength and number. In this scenario, glial cells, such as astrocytes and microglia, which are known to closely interact with neural networks, can directly contribute to homeostatic synaptic scaling. Indeed, it has been proposed that glia participate directly in the homeostatic, activity-dependent regulation of synaptic connectivity through the release of TNF-α, a cytokine known to increase the cell surface expression of AMPA receptors (Stellwagen and Malenka, 2006). Similarly, several other molecules released by microglia and astrocytes might exert a direct regulation of plasticity by affecting receptor composition at the synapse, such as BDNF and IL1β (Parkhurst et al., 2013; Rizzo et al., 2018).

In addition to mechanisms mediated by release of soluble factors, it would be important to investigate whether refinement of synaptic connections by glial synaptic pruning also occurs to reinforce synaptic scaling. Growing evidence indicates that microglia are capable of sensing synaptic activity and act as key players in homeostatic regulation of neural firing (Li et al., 2012; Béchade et al., 2013; Ji et al., 2013). Lipopolysaccharide (LPS) injection in mice promotes transient but selective microglia-mediated removal of inhibitory synapses, which ultimately results in neuroprotection by suppressing inhibition and increasing synchronic neural firing (Chen et al., 2014). LPS-driven inflammation has profound effects on synaptic transmission (Pickering and O'Connor, 2007). Recent studies show that short-term LPS stimulation of microglia in spinal cord specifically decreases inhibitory glycinergic post-synaptic currents (Cantaut-Belarif et al., 2017). It is thus plausible to speculate that loss of excitatory synapses could be counteracted by microglia through removal of inhibitory inputs. On the other hand, astrocytes are much less motile, but their processes

are more stably associated with synapses, and even considered a constant synaptic element, forming the so-called "tripartite synapse" (Araque et al., 1999). Interestingly, perturbations in astrocytic function lead to selective reduction in inhibitory, but not excitatory currents, as a consequence of rapid GABA depletion induced by downregulation of the glutamine synthetase enzyme (Ortinski et al., 2010).

Astrocytes also play critical roles in activity-dependent synapse elimination, as previously discussed. In the light of such observations, glia cells represent the perfect candidates for monitoring and eventually restoring E/I networks balance, through selective remodeling of excitatory or inhibitory inputs.

Overall, a dysregulated ratio between excitation and inhibition has significant implications in behavioral outputs associated with neurodevelopmental and neurodegenerative disorders, however the exact molecular and cellular processes at the origin of such dysfunction are yet to be elucidated. In the following paragraphs we will review the recent literature, highlighting possible links between glia-mediated synaptic remodeling and dysregulation of the E/I network balance in neurodegeneration.

ALZHEIMER'S DISEASE

AD is the most common cause of dementia in the elderly, and despite its increasing prevalence there are no effective treatments available. The rare familial form of AD involves mutations of the amyloid precursor protein gene (APP) and Presenilins 1 and 2 (PSEN1 and PSEN2), which cleave APP to form Aβ species (Hardy and Higgins, 1992; Chávez-Gutiérrez et al., 2012). Late-onset (LOAD), or sporadic AD accounts for more than 95% of the Alzheimer's cases, but has no clear etiology. With ageing being the strongest risk factor, several genetic polymorphisms in various gene loci have been associated with increased AD risk, such the Apolipoprotein E4 (ApoE4) allele or the R47H mutation in Trem2 (Roses, 1996; Guerreiro et al., 2013; Jonsson et al., 2013). AD is characterized by deposition of extracellular Aβ plaques, intracellular neurofibrillary tau tangles (NFTs), and progressive neurodegeneration accompanied by cognitive decline (Spires-Jones and Hyman, 2014). Several studies have focused on the pathological role of Aβ oligomeric species as a major player in neuronal and network dysfunction at early stages of the disease progression, thus providing a broad range of causative mechanisms (Cleary et al., 2005; Shankar et al., 2008; Li et al., 2011). For instance, Aβ can cause E/I imbalance through disruption of fast-spiking GABAergic inputs (Ren et al., 2018). Mutations in the APP leading to increase in Aβ oligomerization (E693 Osaka mutation; Tomiyama et al., 2010) have also been shown to cause selective GABAergic depletion in recessive familial AD (Umeda et al., 2017). Many of the LOAD risk genes, including APOE and TREM2, involve the brain's immune system and the majority of them are highly enriched in microglia (Gosselin et al., 2017), suggesting glial cells are causally implicated in the pathogenesis of AD, and thus might be important players in the E/I imbalance observed already in the early stages (Henstridge et al., 2019).

The microglial and astrocyte reactivity in AD and their physiological role in synaptic pruning has inspired a new wave of research into glial-mediated synapse loss in AD as a driver of network dysfunction (Serrano-Pozo et al., 2013; Rodriguez et al., 2014). **Figure 2** summarizes the role of glia in mediating synaptic refinement in AD.

Other immune cells, such as lymphocytes and neutrophils may play important roles in the onset and progression of AD, also interacting with resident glia cells (Town et al., 2005; Xie and Yang, 2015; Ferretti et al., 2016).

Microglia and Astrocytes in Synapse Loss in AD

It is well established that excitatory synapses are vulnerable in AD. Specifically, oligomeric Aβ (oAβ) not only induces synaptotoxicity but also synaptic weakening through prolonged long-term depression (LTD) and impaired LTP (Shankar et al., 2008; Li et al., 2009; Wu et al., 2010). In turn, glutamatergic signaling deficits in AD can range from NMDA and AMPAR internalization causing synaptic weakening (Zhang et al., 2003; Snyder et al., 2005) to NMDA-mediated glutamate excitotoxicity (Esposito et al., 2013). Recent reports suggest that other mechanisms of synapse dysfunction, such as the upregulation of adenosine A2A receptor might even occur before and independent of defective glutamate receptors, in a mouse model of AD (Viana da Silva et al., 2016).

Most studies demonstrating synapse loss by microglia have focused on the engulfment of pre- and post-synaptic markers, by co-localization approaches, with a preferential focus on excitatory synapses. The role of complement, in virtue of its role in mediating synaptic pruning during development, has been extensively investigated in the context of synapse elimination in AD. Indeed, in two amyloidopathy models of AD (Tg2576 and APP/PS1) crossed with C1q knockout mice, lack of C1q protected against synaptophysin loss in the hippocampus of aged mice (Fonseca et al., 2004). Similarly, more recent work has shown increased co-localization of C1q with excitatory post-synaptic densities-95 (PSD-95) in the J20 APP-overexpressing mouse model, as well as in transgenic APPsw/PSEN1DE9 mice, and also following injections of oAβ (Hong et al., 2016; Bie et al., 2019). Synaptotoxicity and LTP impairments induced by oAβ were also prevented in C1q knockout mice or upon administration of C1q neutralizing antibodies, suggesting C1q is critical for synaptic elimination (Hong et al., 2016; Bie et al., 2019). A proposed mechanism for C1q upregulation in hippocampal synapses is *via* metabotropic glutamate receptor signaling (mGluR1; Bie et al., 2019), which has been shown to be involved in synaptic LTD upon amyloid challenge (Chen et al., 2013). Overall, upregulation in complement molecules is associated with higher internalization of synaptic markers by microglia and with overall synaptic loss. In agreement with these outcomes, APP/PS1 mice lacking C3 showed a milder pro-inflammatory biochemical and morphological profile, reduced Aβ-associated microgliosis and astrogliosis, and greater levels of pre-synaptic (synaptophysin, VGLUT1) and excitatory post-synaptic (homer, PSD-95) markers compared to APP/PS1 mice expressing

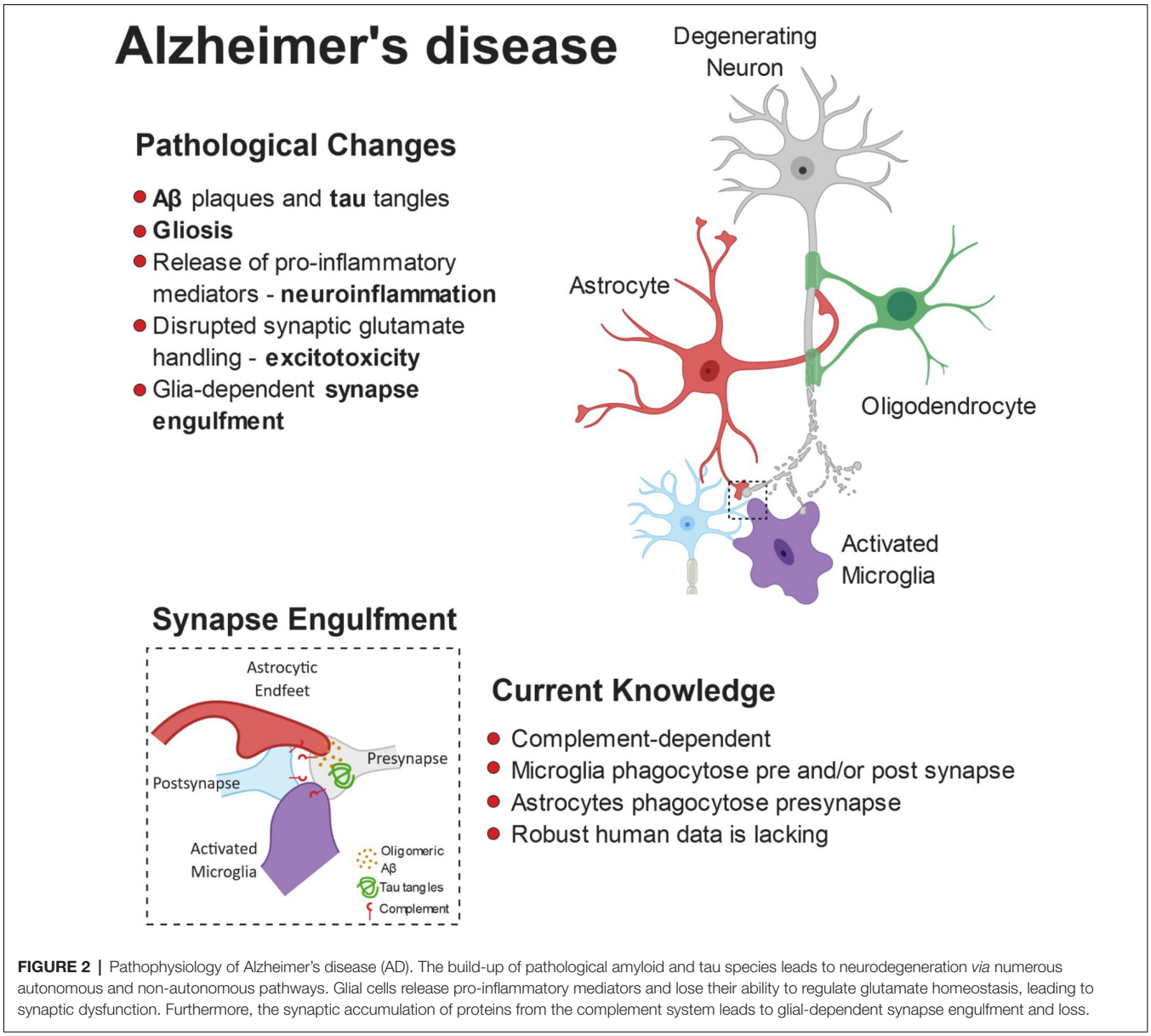

FIGURE 2 | Pathophysiology of Alzheimer's disease (AD). The build-up of pathological amyloid and tau species leads to neurodegeneration *via* numerous autonomous and non-autonomous pathways. Glial cells release pro-inflammatory mediators and lose their ability to regulate glutamate homeostasis, leading to synaptic dysfunction. Furthermore, the synaptic accumulation of proteins from the complement system leads to glial-dependent synapse engulfment and loss.

C3 normally (Shi et al., 2017). Importantly, C3 absence in 16-month-old APP/PS1 mice, spared cognitive deficits as shown by enhanced spatial memory. This suggests that in AD, healthy synapses that would not normally require physiological elimination may be aberrantly targeted by the complement system for elimination, partly eliciting the cognitive decline seen in AD.

Secretion of pro-inflammatory mediators by microglia is likely to occur concomitantly to phagocytosis, contributing to the AD-related synapse loss. Prolonged exposure to TNF-α in a triple transgenic AD-like model (3xTg) induced neuronal loss, microgliosis and upregulated C3 as well as intracellular Aβ levels (Janelsins et al., 2008). In the TgCRND8 AD mouse model, C3 was also upregulated in response to another potent pro-inflammatory cytokine, IFN-γ (Chakrabarty et al., 2010). Additionally, in culture assays, microglial IL-6 and nitric oxide (NO) have direct synaptotoxic effects on neurons (Azevedo et al., 2013). Therefore, microglia not only can directly mediate synapse elimination, but can also prime synapses for removal through released soluble factors.

The presence of the allele E4 for APOE (a major cholesterol carrier) is the strongest genetic risk factor influencing susceptibility to LOAD and it is associated with increased synapse loss (Koffie et al., 2009, 2012; Liu et al., 2013; Tzioras et al., 2018) as well as complement activation (McGeer et al., 1997). Transcriptomic studies have heavily implicated microglial APOE as a common facilitator of many AD-associated conditions, including amyloidosis, tauopathy, ageing and inflammation (Kang et al., 2018; Lin et al., 2018; Ulrich et al., 2018). Specifically, microglia close to Aβ plaques develop a disease associated phenotype and upregulate *Apoe* expression in a TREM2 dependent pathway (Keren-Shaul et al., 2017;

Krasemann et al., 2017). APOE4 expressing mice also exhibit increased hippocampal gliosis and decreased levels of both synaptophysin and excitatory postsynaptic proteins (Zhu et al., 2012). Crossing APOE4 mice to the 5xFAD AD-like mouse model resulted in exacerbated Aβ-associated gliosis, presence of dystrophic neurites and IL-1β neuroinflammation (Rodriguez et al., 2014). Moreover, in human *post mortem* brains, the *APOE4* genotype is associated with an increase in microglial markers of activation including CD68, MSR-A and CD64 and decrease in homeostatic Iba1 (Minett et al., 2016). It is, therefore, compelling to hypothesize that, in carriers of the *APOE4* allele, microglia might be more prone to mediate pathological synapse loss.

Astrocytes and their many functions have been extensively studied in the context of AD (González-Reyes et al., 2017; Liddelow and Barres, 2017; Perez-Nievas and Serrano-Pozo, 2018), albeit their role in synapse loss is less clear. Both human and mouse studies have reported upregulation of reactive astrocyte signatures (GFAP) in the presence of an *APOE4* allele (Overmyer et al., 1999; Ophir et al., 2003; Belinson and Michaelson, 2009; Shi et al., 2017). In a recent study, induced pluripotent stem cells from APOE4 AD patients were differentiated into astrocytes and were then genetically modified using CRISPR-Cas9 to generate an *APOE3* genotype (Lin et al., 2018). This approach revealed that APOE4 to APOE3 conversion is sufficient to rescue the impaired phagocytic ability of astrocytes towards Aβ (Lin et al., 2018). Interestingly, and unexpectedly, an allele-dependent role for APOE was also shown in respect to mediating synapse elimination, with APOE2 enhancing and APOE4 decreasing the rate of synaptic pruning by astrocytes (Chung et al., 2016). This apparent controversy might be explained if we assume that homeostatic elimination of damaged synapses occurs constantly in the healthy brain. Thus, one could speculate that ApoE4 carrier would be impaired in such glia-mediated "homeostatic synapse remodeling."

Only recently there was evidence of reactive astrocytes engulfing synapses in AD, with electron microscopy showing dystrophic VGLUT1-positive terminals being cleared by astrocytic endfeet in the hippocampus of APP/PS1 mice and in late stages of AD (Gomez-Arboledas et al., 2018). Whether this clearing mechanism is exacerbated in AD and contributes to excessive synaptic elimination is still under debate. The decreased phagocytic ability of reactive and APOE4-expressing astrocytes in development introduces new questions as to how these cells change in the context of AD and thus contribute to neurodegeneration.

Glia Implications in E/I Imbalance in AD

Mounting evidence from mouse model studies suggest that, in the amyloid-depositing brain, functional impairments of local neuronal circuits lead to disruption in the E/I balance, which then result in large-scale networks defects (Busche et al., 2008; Busche and Konnerth, 2016; Palop and Mucke, 2016). Loss of inhibitory interneurons results in impaired oscillatory rhythm (Ramos et al., 2006; Baglietto-Vargas et al., 2010; Verret et al., 2012) leading to epileptiform activity (Vossel et al., 2016) and network hyperexcitability (Brown et al., 2018) in a subset of AD patients. Some studies have reported reduction of inhibitory pre-synaptic VGAT and GAT1 peri-somatic terminals on pyramidal neurons close to plaques, both in AD *post mortem* cases and aged APP/PS1 mice (Garcia-Marin et al., 2009). Others have found no such loss of inhibitory synapses in neither the same APP/PS1 model nor AD cases at comparable pathological stages; conversely, excitatory VGLUT1 boutons were found to be significantly reduced (Mitew et al., 2013; Canas et al., 2014). In the same study, Aβ was also suggested to increase astrocyte GABA synthesis, highlighting a possible implication of astrocytes as a source of E/I imbalance in AD (Mitew et al., 2013). Microglia, too, may play an active role in compromising the equilibrium of excitatory vs. inhibitory synaptic transmission in AD, by promoting loss of selective synapses (i.e., glutamatergic vs. GABAergic). Evidence for microglia engulfing excitatory inputs in AD mouse models have been provided (Hong et al., 2016; Paolicelli et al., 2017), however, evidence for the engulfment of inhibitory connections is still lacking. Whether microglia can directly contribute to E/I imbalance in AD is currently under debate, and further studies are required to investigate this possibility. A clear implication of microglia in the AD brain has been recently underscored by the use of PET tracers *in vivo*, which are capable of specifically revealing the microglial component of neuroinflammation (Edison et al., 2018; Horti et al., 2019).

PARKINSON'S DISEASE

PD is a neurodegenerative disorder characterized by massive degeneration of nigro-striatal dopaminergic neurons, which leads to progressive motor and cognitive symptoms. It is the second most common neurodegenerative disease and affects 2%–3% of the population over the age of 65 years (Poewe et al., 2017). The general term "parkinsonism" refers to the ensemble of movement disorders defined by the appearance of bradykinesia, rigidity or tremor. Cognitive impairment, in addition, is an important non-motor symptom of PD, with a mean duration from clinical disease onset to dementia of about 10 years (Aarsland et al., 2011; Selnes et al., 2017). A key neuropathological hallmark of the PD brain is the abnormal deposition of intraneuronal (Lewy bodies) and intraneuritic (Lewy neurites) fibrillary aggregates, mainly composed of α-synuclein (α-syn) and referred to as Lewy pathology. α-syn inclusions, initially thought to be limited to the substantia nigra pars compacta of the striatum, have been associated with the primary cause of neuronal loss in PD (Desplats et al., 2009). However, *post mortem* brain examinations of patients affected by PD revealed that Lewy pathology is not only confined to the striatum, but also affects other well-defined brain regions, possibly following a progressive spreading pattern (Del Tredici et al., 2002; Beach et al., 2009; Colom-Cadena et al., 2017). Staging of Lewy pathology in PD was first proposed by Braak et al. (2003), based on histological examinations showing the anatomical caudo-rostral progression of disease over time. Accumulating *in vitro* and *in vivo* evidence indicates that α-syn can undergo toxic conformational changes, spread from cell to cell, and initiate the formation of pathological aggregates, in a prion-like manner (Kordower et al., 2008; Li et al., 2008; Luk et al., 2012;

Masuda-Suzukake et al., 2013). Together with the progressive stages of the disease, these data are in support of the spreading hypothesis, according to which Lewy pathology arises in specific brain nuclei and spreads to other structures through synaptic connections (Recasens and Dehay, 2014).

Transgenic animal models with α-syn overexpression exhibit neuronal dysfunction in the absence of cell loss, indicating that disruptions of synaptic transmission occur as an initial event, preceding α-syn-induced neuronal cell death (Janezic et al., 2013; Phan et al., 2017). Experimental evidence in fact shows that synaptic dysfunction is caused by presynaptic accumulation of α-syn aggregates, which impair axonal transport by affecting key proteins governing synaptic vesicle release (Kramer and Schulz-Schaeffer, 2007; Bellucci et al., 2012; Anichtchik et al., 2013).

Early synaptic dysfunction in PD has been supported by genetic evidence, with recently identified mutations in genes involved in clathrin-dependent synaptic vesicle endocytosis (SVE), such as DNAJC6 (auxilin) and SYNJ-1 (synaptojanin 1), in patients with juvenile and early-onset atypical parkinsonism (Nguyen and Krainc, 2018). In these models, a central role for glia cell have been also proposed, although causative mechanisms still await further supportive evidence (Teismann et al., 2003).

Microglia and Astrocyte-Mediated Synapse Impairment in PD

Synapse loss in PD correlates with the pathological deposition of α-syn at the pre-synaptic site. Indeed, prolonged exposure to α-syn oligomers in hippocampal slices was shown to regulate synaptic transmission and impair LTP by activating NMDARs (Diógenes et al., 2012). Most of the studies aimed at elucidating the cellular basis of PD, have focused so far on mechanisms of neuronal dysfunction; however, PD-related genes are also expressed in astrocytes and microglia. Thus, it is likely that dysregulation of such genes may contribute to disease onset and progression *via* glia-mediated processes. Astrocytic roles in glucose metabolism are well described, and mutations in Parkin, PINK1, DJ-1 and LRKK2, associated with PD, have been shown to affect astrocytes function (Choi et al., 2013).

Parkin is a ubiquitin ligase largely implicated in PD, however its role in modulating glial specific function has just started to be unraveled. Recent studies show that parkin loss exacerbates inflammation and promotes survival of activated microglia by inhibiting necroptosis, thus contributing to chronic neuroinflammation (Dionísio et al., 2018), whereas in astrocytes it induces endoplasmic reticulum stress. Whether such effects can negatively impact on synaptic function and mediate synapse loss, however, remains to be elucidated. Similarly, novel evidence for DJ-1 modulation of glial function are emerging. DJ-1, encoded by *PARK7* gene, is a ubiquitously-expressed multifunctional protein which regulates anti-oxidant and anti-apoptotic gene expression (Canet-Avilés et al., 2004). DJ-1 knockdown in astrocytes was shown to impair astrocyte-mediated neuroprotection in primary neurons (Mullett and Hinkle, 2009; Kim et al., 2016), whereas astrocytic over-expression of DJ-1 prevented oxidative stress and mitochondrial dysfunction, leading to enhanced neuronal survival *in vitro* and *in vivo* (De Miranda et al., 2018; Frøyset et al., 2018). On the other hand, DJ-1 has been also shown to modulate microglial function, with its deficiency impairing autophagy, reducing α-syn phagocytosis and inducing a constitutive pro-inflammatory activation (Meiser et al., 2016; Nash et al., 2017). Mutations in LRKK2, another multifunctional protein associated with late-onset familial PD, has been shown to affect basic glial function. For instance, pathogenic mutations impair lysosomal function in astrocytes (Henry et al., 2015), and attenuate motility in microglia, preventing efficient response to brain damage (Choi et al., 2015). Altogether, these findings support the implication of glial dysfunction in the synaptic impairment occurring in PD.

Glial Contribution to E/I Imbalance in PD

The pathophysiology of PD is characterized, among other features, by a prominent imbalance within striatal activity. Dopamine (DA) has excitatory effects on the projections from the striatum to the internal segment of globus pallidus (GP), defined as the direct pathway, acting through D1 receptors (D1Rs). The same neurotransmitter, however, exerts inhibitory effects on the projection from the striatum to the external segment of GP through D2Rs, or indirect pathway (Surmeier et al., 2007). Loss of DA, therefore, has complex consequences on multiple levels. Several studies in rodents, using both pathogenic 6-hydroxydopamine (6-OHDA) and 1-methyl-4-phenyl-1,2,3,6-tetrahydropyridine (MPTP) models, have shown that the progressive loss of striatal DA leads to a significant loss of glutamatergic synapses on medium spiny neurons (MSNs) of the dorsal striatum (Ingham et al., 1989; Zaja-Milatovic et al., 2005; Day et al., 2006), and that dendritic spines are decreased and enlarged specifically in the direct pathway neurons (Nishijima et al., 2014). Overall, the loss of dopaminergic input from the substantia nigra alters the equilibrium between excitatory and inhibitory control from the basal ganglia to the motor cortex.

Recent studies have highlighted the existence of subpopulations of astrocytes, with circuit-specific roles in the basal ganglia (Martín et al., 2015). Considering that both the direct and indirect pathways are fundamental for motor control, and are associated with motor deficits in PD and Huntington's diseases, the selective regulation of specific synapses by astrocytes may be involved in the coordinated activity of these networks in the striatal function, therefore, pointing to astrocytes as central players in these disorders (Martín et al., 2015).

However, whether and how glia cells contribute to the E/I imbalance in PD remains elusive.

It has recently been proposed that microglia may compensate for dopaminergic neuron loss through selective elimination of glutamatergic synapses from the subthalamic nucleus (Aono et al., 2017). By using the 6-OHDA-induced experimental Parkinsonism rat model, the authors showed a specific increase of activated microglia in the substantia nigra pars reticulata (SNr), engulfing excitatory pre- and post-synaptic elements. These findings suggest that microglia may be involved in a negative feedback in the indirect pathway of the basal ganglia

to compensate for the loss of dopaminergic neurons in PD pathology (Aono et al., 2017). A central role for astrocytes has also been proposed in the PD brain, based on the observation that loss of DA neurons in the substantia nigra is associated with increased density of activated astrocytes (Hirsch et al., 2006; Gomide and Chadi, 2005; McGeer and McGeer, 2008). Only recently, however, it has been shown that striatal astrocytes engulf dopaminergic debris in the 6-OHDA model (Morales et al., 2017). Interestingly, α-syn was observed within astrocytic processes already 4 h after 6-OHDA administration, whereas the amyloid precursor protein (APP), found at synapses and accumulated in bulb-like structures of degenerating axons, was never found inside astrocytes. These findings suggest a selective engulfment of synaptic terminals by astrocytes, rather than a non-specific clearance of cellular debris (Morales et al., 2017). The contribution of microglia and astrocytes to synapse loss observed in PD is summarized in **Figure 3**.

AMYOTROPHIC LATERAL SCLEROSIS (ALS)

ALS is caused by the breakdown of upper and lower motor neurons leading to the progressive weakness and atrophy of muscle, often resulting in respiratory failure and death within a few years of diagnosis. It is the most common form of MND, yet we still do not have a unifying theory of disease pathogenesis. Most cases (90%) are sporadic, with the remaining 10% due to known mutations in a growing number of disease-associated genes, such as c9orf72, SOD1, FUS and TDP-43 (Renton et al., 2014). Mounting evidence suggests that disconnection of the neuromuscular synapse occurs very early in the disease, with an initial toxic insult at the synapse, leading to disconnection of axons from their target cell, axonal breakdown and ultimately neuron death. This model led to the popular "dying back" hypothesis of disease progression (Frey et al., 2000; Fischer et al., 2004; Pun et al., 2006). This process has been described at both peripheral synapses at the NMJ and synapses in the CNS, however the toxic insult at either site has yet to be identified. An alternative theory is the "dying forward" hypothesis, which posits that breakdown of primary motor neurons in the brain leads to subsequent loss of secondary motor neurons in the periphery, and thus muscular denervation. Cortical hyperexcitability has been observed early in ALS brains using a number of imaging techniques and it is known that chronic hyperexcitability results in excitotoxicity, leading to motor neuron loss (Bae et al., 2013). In strong support of hyperexcitability as an important feature, the most widely prescribed drug for ALS, Riluzole, acts by dampening excitatory synaptic activity in the brain (Doble, 1996). Given the complex heterogeneity of ALS, it is likely that both dying forward and dying back processes occur in disease, however, regardless the nature of the predominant process, they ultimately converge on synaptic dysfunction. Cell autonomous and non-autonomous pathways have been studied in both pathogenic pathways, with glia strongly implicated in ALS progression.

Synaptic Alterations in ALS

ALS has historically been considered exclusively a motor neuron disease, with much of the early research focused on the central and peripheral components of the motor system. Recent studies, however, have revealed that ALS is a multi-system disorder, displaying striking genetic, pathological and clinical overlap with frontotemporal dementia (FTD; Ling et al., 2013). Approximately 15% of ALS cases receive a co-morbid diagnosis of FTD and another 30%–40% present with milder cognitive and behavioral changes, reminiscent of symptoms (Strong et al., 2017). Given that synapse loss is the strongest correlate with cognitive decline in AD (Terry et al., 1991), it is interesting to note that synapse loss also associates with cognitive decline in ALS (Henstridge et al., 2018), suggesting that synapse loss may be a common feature of cognitive change in diverse neurodegenerative diseases (Henstridge et al., 2016).

Betz cells are giant pyramidal neurons located in layer V of the primary motor cortex where they project mono-synaptically onto lower motor neurons within the spinal cord. They receive synaptic input primarily from the premotor cortex, which is important for the planning and execution of complex movement. Research has shown that synapses onto anatomically-normal Betz cells are dysmorphic in the brains of ALS patients (Sasaki and Iwata, 1999). Furthermore, diverse animal models of ALS have revealed a common feature of pre-symptomatic loss of cortical synapses (Qiu et al., 2014; Fogarty et al., 2015, 2016). Lower motor neurons within the spinal cord exhibit a lower density of axo-somatic synapses in ALS (Sasaki and Maruyama, 1994a,b), suggesting a disconnection between upper and lower motor neurons. At the periphery, loss of NMJ synapses represent one of the first anatomical changes in ALS models, occurring long before disease symptoms (Frey et al., 2000; Fischer et al., 2004; Pun et al., 2006). Collectively, these studies show that synaptic connections throughout the motor system are vulnerable early in disease.

Microglia-Dependent Loss of Central Synapses in ALS

Mutations in superoxide dismutase 1 (SOD1), an antioxidizing enzyme, are associated with ALS.

Animal models overexpressing human mutated SOD1, display pre-symptomatic changes to cortical motor neurons, resulting in intrinsic hyperexcitability (Saba et al., 2016) and an early loss of inhibitory interneurons (Clark et al., 2017). Thus, it appears in SOD1 animal models of ALS, both intrinsic hyperexcitability and decreased inhibitory control play a role in cortical pathophysiology. Recent human studies using novel neurophysiological techniques have also suggested that imbalance between intracortical excitatory and inhibitory systems leads to hyperexcitability (Van den Bos et al., 2018). Many diverse ALS models exhibit pre-symptomatic synapse loss. SOD1 models present with early spine loss in the motor cortex, which worsens with disease progression (Fogarty et al., 2015; Saba et al., 2016). Mice overexpressing mutated forms of two RNA-DNA binding proteins commonly associated with ALS display overt synaptic defects: TDP-43 A315T mice have progressive loss of spines from P60–P90 compared to wild

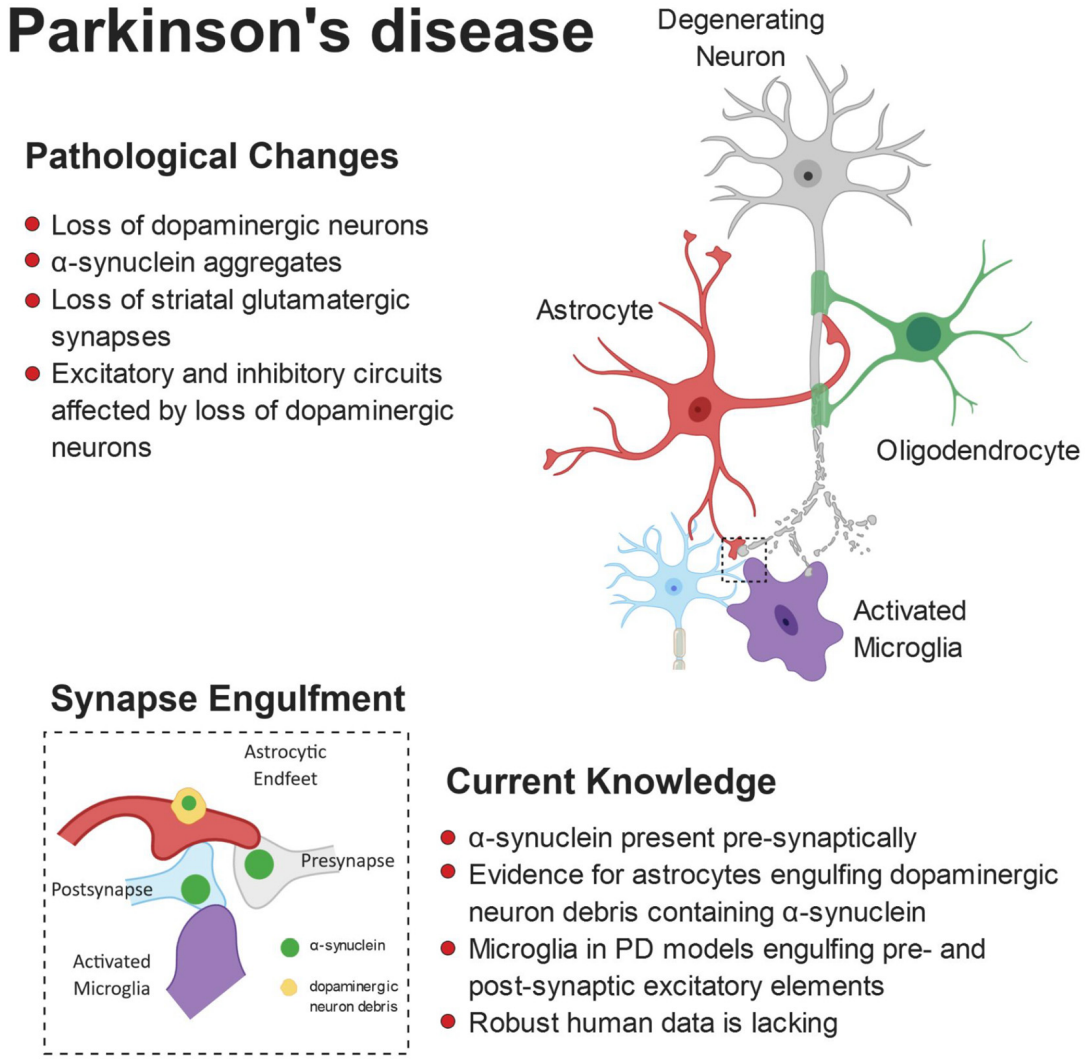

FIGURE 3 | Pathophysiology of Parkinson's disease (PD). Anatomically, PD is characterized by a loss of striatal dopaminergic neurons. This can lead to disruption of excitatory and inhibitory circuits, resulting in the clinical motor symptoms. Loss of glutamatergic synapses is apparent in the striatum and aggregates of α-synuclein (α-syn) are observed in the brains of patients. Furthermore, evidence suggests α-syn accumulates at the synapse, where both astrocytes and microglia have been shown to engulf α-syn-containing synaptic material.

type mice (Handley et al., 2017) and FUS R521G mice have a significantly lower density of mature spines in the cortex at P18 (Sephton et al., 2014). While cell autonomous changes can influence neuronal morphology, glial cells also have the ability to significantly influence both excitatory and inhibitory synaptic systems *via* the release of toxic mediators or by direct phagocytosis of neuronal compartments, as described above. The study of microgliosis in human ALS tissue has mostly been confined to *post mortem* studies, which tend to show an increase in microglia number (Kawamata et al., 1992; Brettschneider et al., 2012). However, some studies have shown increased microglial activity in live human ALS brain, using PET imaging (Turner et al., 2004; Zürcher et al., 2015). Microglial activation is consistently detected in the motor cortex however one study also detected an increase in the dorsolateral prefrontal cortex and thalamus (Turner et al., 2004). Interestingly, microgliosis appears to associate with disease severity (Turner et al., 2004; Brettschneider et al., 2012; Zürcher et al., 2015), with a recent study suggesting microgliosis is specifically associated with rapid disease progression (Gorter et al., 2018). Taking a data-driven approach, another recent work uncovered networks of genes that associate with motor neuron pathology in human ALS brain. The study found that most genes within the top scoring network, are expressed in microglia (Cooper-Knock et al., 2017). Furthermore, TREM2 levels in the cerebrospinal fluid (CSF) of ALS patients was higher than controls and TREM2 levels positively correlated with disease duration in late stage ALS (Cooper-Knock et al., 2017). This supports previous work which found an increased expression of TREM2 mRNA in human and SOD1 mouse spinal cord, and also implicated a rare variant in

TREM2 (p.R47H) as a risk factor for developing ALS (Cady et al., 2014). Therefore, it is clear that microglia have an important role to play in ALS pathogenesis (Geloso et al., 2017), but what effect are microglia having on surrounding neurons? An intricate mouse study utilizing cell-type specific expression of mutant SOD1 G93A, placed microglia in a central role for mediating ALS progression. Removing mutant SOD1 from microglia, thus returning them to a wild-type state, had no effect on disease onset, but significantly slowed late stage progression (Boillée et al., 2006). This is supported by recent work (Frakes et al., 2014) showing that a toxic microglial gain of function exerts a pathological effect on neurons in ALS. Our recent work has uncovered a potential mechanism by which activated, inflammatory microglia may exert degenerative effects on neurons. TDP-43 is the main pathological hallmark of ALS, with protein aggregates found in almost 100% of ALS cases (Neumann et al., 2006; Ling et al., 2013). Debate surrounds whether this leads to a pathological loss of normal function or a toxic gain of function, however, when TDP-43 is specifically knocked-out of microglial cells in mice, we found that they convert to a hyper-phagocytic phenotype and ingest surrounding synapses (Paolicelli et al., 2017). This links TDP-43 pathology to microglial activation and synapse loss. In human ALS brain, the presence of TDP-43 pathology in the frontal cortex is associated with a higher burden of microglial activity as evidenced by increased CD68 expression (Brettschneider et al., 2012; Paolicelli et al., 2017). Furthermore, the presence of TDP-43 in the frontal cortex was associated with lower synapse number in one study (Henstridge et al., 2018) and cognitive impairment in another (Brettschneider et al., 2012). Taken together, these studies place TDP-43 pathology and activated microglia at the sites of synapse loss in the ALS brain, resulting in a breakdown of neuronal function and clinical manifestation of ALS.

The evidence above clearly states that synapse loss is a prominent feature in human ALS brain and in diverse ALS models. However, does a similar synaptic breakdown occur around lower motor neurons within the spinal cord? A number of early studies assessing synaptic coverage of spinal motor neurons in human *post mortem* tissue described synapse loss and altered morphology in remaining synapses (Matsumoto et al., 1994; Sasaki and Maruyama, 1994a,b; Ince et al., 1995). Similar findings are evident in the SOD1 G93A mouse model, with decreased synapses onto motor neurons in the spinal cord and decreased spine density of spinal motor neurons (Zang et al., 2005; Fogarty et al., 2017). In the same mouse model, another study found a decrease in total synapse number onto brainstem motor neurons that manifested as a small increase in excitatory synapses and a larger decrease of inhibitory terminals (Sunico et al., 2011). Taken together it is clear that synapses are lost in the brainstem and spinal cord in ALS. At approximately the same time as spines are being lost in the SOD1 G93A mouse model, microglia are proliferating in the rat SOD1 G93A model (Graber et al., 2010). However, to the best of our knowledge no studies to date have assessed whether microglia may be stripping synapses in the spinal cord.

A recent study has found that microglia in the spinal cord may play a neuroprotective role. When human TDP-43 was over-expressed exclusively in neurons, microgliosis in the spinal cord was mild, but when the TDP-43 was switched off with doxycycline treatment, microglia became inflamed, proliferated and selectively engulfed neuronally-derived TDP-43 (Spiller et al., 2018). This has been recently confirmed in a zebrafish model of human TDP-43 over-expression, in which microglia actively phagocytose degenerating spinal cord neurons expressing TDP-43 (Svahn et al., 2018). Taken together, these studies suggest that TDP-43 in stressed neurons may act as a signal to attract phagocytic microglia to clear away aggregated TDP-43. With this in mind, it is interesting to note that TDP-43 aggregates have been observed in human synapses (Henstridge et al., 2018) and may act as a microglial "eat me" signal in the same way complement appears to in AD.

Microglia can also exert indirect effects on neuronal and synaptic function by the release of numerous signaling molecules. There is a wealth of literature describing the increased expression of proinflammatory mediators in ALS models and patients, ranging from elevated blood levels of TNF-a in human blood to increased chemokine MCP-1 expression in SOD1 mouse models (reviewed in Philips and Robberecht, 2011). Many of these excreted molecules can directly affect neuronal physiology, such as NO, reactive oxygen species (ROS) and cytokines (Henkel et al., 2009), further supporting a role for microglia ALS-related synapse dysfunction.

Astrocyte-Dependent Loss of Central Synapses in ALS

Glutamate is the major excitatory neurotransmitter in the brain and its levels need to be tightly controlled at the synapse to prevent excitotoxicity. Astrocytes play a major role by actively taking up excess glutamate using glutamate transporters, EEAT1 and EEAT2 (also known as GLAST and GLT-1, respectively). In SOD1 models, GLT-1 levels decrease as disease progresses (Bruijn et al., 1997) and this finding is consistent in human ALS spinal cord and brain (Rothstein et al., 1995). These early studies suggest that a failure in astrocytic control of synaptic glutamate may result in excitotoxicity and network imbalance, supported by a study that knocked out glial GLT-1 using oligonucleotides and discovered that animals developed a progressive motor paralysis (Rothstein et al., 1996). Interestingly, crossing the SOD G93A mouse with an EAAT2 over-expressing mouse delayed axonal dystrophy and motor neuron loss but did not affect onset of paralysis or life span (Guo et al., 2003). Despite this less than positive outcome, a pharmacological approach (beta-lactam antibiotic, ceftriaxone) to stimulate GLT-1 expression in SOD1 G93A mice at symptom onset, led to delayed loss of muscle strength and body weight and prolonged life by 10 days (Rothstein et al., 2005). Ceftriaxone was tested in a recent clinical trial and provided some excitement after a successful Phase 2, however it failed to show clinical efficacy in Phase 3 (Cudkowicz et al., 2014). It was not determined if the drug affected EAAT2 expression or function in the participants, so further work is required to assess the value in targeting glial glutamate transporters in ALS. Astrocytes also play an important trophic role through the uptake of glucose from the blood stream, which they convert into lactate and pass to neurons for the

generation of glutamate (Pellerin and Magistretti, 1994; Pellerin et al., 1998). Lactate is shuttled from the astrocyte to the neuron in a pathway requiring the glutamate transporters mentioned above, however pre-symptomatic SOD1 G93A mice have a significantly lower amount of lactate in spinal cord homogenates and a decreased expression of GLAST (Ferraiuolo et al., 2011). This suggests a disruption in the astrocyte-neuron lactate shuttle, potentially rendering the neurons hypometabolic.

Small heat shock proteins (HSPBs) are important chaperones that reduce protein misfolding and aid in misfolded protein degradation. A recent study has found that in human ALS spinal cord, rapidly progressing disease was associated with increased HSPB5 and HSPB8 in astrocytes (Gorter et al., 2018). Furthermore, a recent rat model with restricted mutant human TDP-43 (M337V) expression in astrocytes, displayed a progressive paralysis due to loss of motor neurons in the spinal cord (Tong et al., 2013). This strongly supports an important role for glia-derived toxicity in ALS. These studies suggest that astrocytes may become overwhelmed with misfolded protein stressors in ALS, which could affect their trophic support of neurons and synapses. While it is clear that astrocytes have an important role to play in the synaptic pathology of ALS, there are currently no studies that we are aware of showing astrocytic ingestion of synaptic terminals. It will be important to discover if astrocytes are restricted to indirect effects on synaptic dysfunction or whether they can physically strip synapses and dystrophic dendrites as observed in other diseases.

Cross-talk between astrocytes and microglia also appear to play a critical role in ALS pathogenesis. In the SOD1 G93A mouse, specific knock out of SOD1 G93A from astrocytes, thus reverting them back to wild-type, had no effect on ALS onset but significantly delayed microglial activation and slowed late-stage disease (Yamanaka et al., 2008). This suggests that in ALS not only do microglia and astrocytes affect neuronal physiology alone, they also regulate the function of one another. **Figure 4** shows a schematic representation of microglial and astrocytic roles in synapse loss in ALS.

Glia-Dependent Loss of Peripheral Synapses in ALS

The NMJ exists as a tripartite structure, consisting of the motor nerve ending, the postsynaptic muscle cell and non-myelinating perisynaptic Schwann cells (PSCs; Ko and Robitaille, 2015). These specialized glial cells are critical for the maintenance and remodeling of adult NMJs, actively phagocytosing damaged nerve terminals and guiding regenerating nerves to their correct target (Ko and Robitaille, 2015). Active uptake of degenerating axonal components by Schwann cells involves the initial formation of "axosomes," aggregates of synaptic proteins and membrane fragments that are released by the axonal tip (Bishop et al., 2004). Phagocytic behavior of PSCs is induced by signals released from degenerating motor neuron axons, resulting in engulfment of synaptic terminals at the NMJ (Duregotti et al., 2015). Interestingly, in a toxin-induced neuropathy model, the toxic signals (H_2O_2, mitochondrial DNA and cytochrome C) are released from mitochondria within the degenerating motor nerves, supporting the role of mitochondrial dysfunction in ALS (Duregotti et al., 2015; Smith et al., 2017). Furthermore, the expression of numerous receptors and signaling molecules involved in regulating PSC activity is under the control of the RNA-binding protein TDP-43 (Narayanan et al., 2013), suggesting that TDP-43 dysfunction can significantly impact the activity of Schwann cells at the NMJ.

Given the important role of the complement system in synapse loss in AD, it is interesting to note that components of the complement system are found at the NMJ in SOD1 mouse models and human tissue (Heurich et al., 2011; Bahia El Idrissi et al., 2016). It will be interesting to discover if these proteins tag the synaptic terminals for engulfment, in a similar glial-dependent process as described in AD above. Paradoxically, a recent study has shown that C1q deletion exacerbates disease progression and synapse loss in a SOD1 mouse model, revealing that further study is required to understand the role of complement at peripheral synaptic function (Lobsiger et al., 2013).

While these intriguing studies provide a glimpse of the normal function of PSCs, little is known about their role in disease. For example, it would be important to know if disease-associated changes in PSC activity resulted in aberrant synapse loss or whether their trophic role is disrupted in disease, leading to pathogenic processes.

MULTIPLE SCLEROSIS

MS is an autoimmune disease characterized by oligodendroglial dysfunction (Kotter et al., 2006; Miron et al., 2013) and T-cell driven inflammation (Korn et al., 2007; Aggelakopoulou et al., 2016), resulting in demyelination of gray and white matter tracts. Loss of the myelin sheath makes axons less capable of propagating electrical signals to the synapse and renders them more vulnerable to degeneration. Typically, affected individuals present with motor deficits but signs of cognitive decline are also evident in some patients (Rao et al., 1991; Chiaravalloti and DeLuca, 2008). Due to the demyelinating nature of MS and because the white matter is myelin-rich, changes in the gray matter have been largely over-looked, particularly in respect to synapses. Dendritic cortical spine loss, independent of cortical demyelination and axon loss, has emerged as a pathological feature of some MS patients (Nistico et al., 2014; Jürgens et al., 2016), which may explain the cognitive deficits (Di Filippo et al., 2018). The role of microglia and astrocytes as active players in MS-associated synaptic stripping (**Figure 5**) has been implied by multiple *post-mortem* studies but quantitative and mechanistic evidence is still elusive.

Microglial and Astrocyte Contribution to Synapse Loss in MS

Hippocampal microgliosis is a common feature in MS models as well as in human *post-mortem* samples, highlighting microglia yet again as a potential driver of synaptic loss in disease. Primarily, there are fewer pre-synaptic terminals in demyelinated MS cases (MS-D) compared to myelinated (MS-M) and control cases in various regions of the hippocampus, including CA3 and CA1 (Michailidou et al., 2015). Moreover, the researchers found

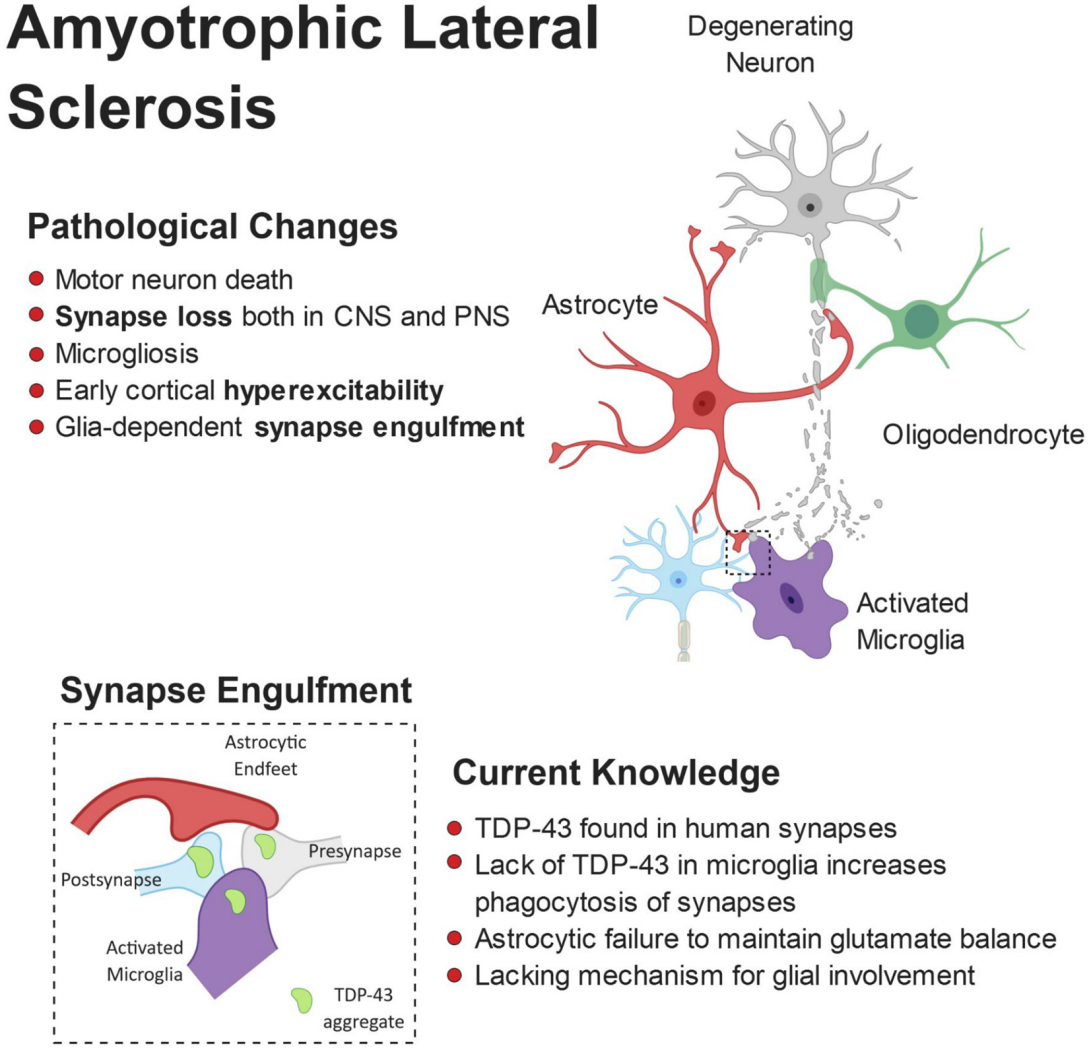

FIGURE 4 | Pathophysiology of amyotrophic lateral sclerosis (ALS). ALS is characterized by the breakdown of motor neurons in the motor cortex and spinal cord. Gliosis and cortical hyperexcitability are early features of the ALS brain and aggregates of TDP-43 are found in almost all patients. TDP-43 has been found at human synapses in ALS and the removal of TDP-43 from microglia leads to hyperphagocytic cells that engulf synapses. Microglia have been shown to engulf neuronally-derived TDP43. Interestingly, synapse loss is an early feature of ALS and observed in both the central and peripheral nervous systems.

that the levels of C1q and C3 are increased in the MS-D cases, and have shown, but not quantified, activated microglia containing pre-synaptic elements, suggesting that complement molecules—once again—may act as a synapse removal tag. C3d-expressing microglial clusters are seen in chronic MS lesions rather than the acute phases of demyelination, indicating C3d may not play a role in the initial synaptic degeneration seen in MS-D. Moreover, in the gray matter of MS *post-mortem* cases, C1q-positive neurons show dysmorphic nuclei, typical of cell stress, when adjacent to activated microglia clusters (Watkins et al., 2016). Together, these studies suggest a model in which C1q may act as a tag for early synaptic engulfment in MS, while neuronal C3d is internalized by microglia during phagocytosis of degenerating neuronal and synaptic debris in later phases of the disease. In addition, other members of the classical complement cascade need to be considered. Specifically, administration of oligonucleotides against C6 partially rescued the synaptophysin depletion found in experimental autoimmune encephalomyelitis (EAE) mouse model for MS. Reduction in C6 also led to decreases in the levels of IL-1β, microgliosis, myelin damage, and C9 of the membrane attack complex (MAC; Michailidou et al., 2018). Interestingly, C9 showed a strong negative correlation to synaptophysin, meaning high levels of C9 correlate with lower levels of pre-synaptic terminals. Given that the MAC can activate subsequent pathological mediators like the NLRP3 inflammasome in microglia (Laudisi et al., 2013), which allows maturation and release of IL-1β (Jo et al., 2016), it makes sense that there are lowers levels of inflammation and gliosis when C6 is inhibited. Furthermore, it has been previously discussed in the context of AD that other pro-inflammatory

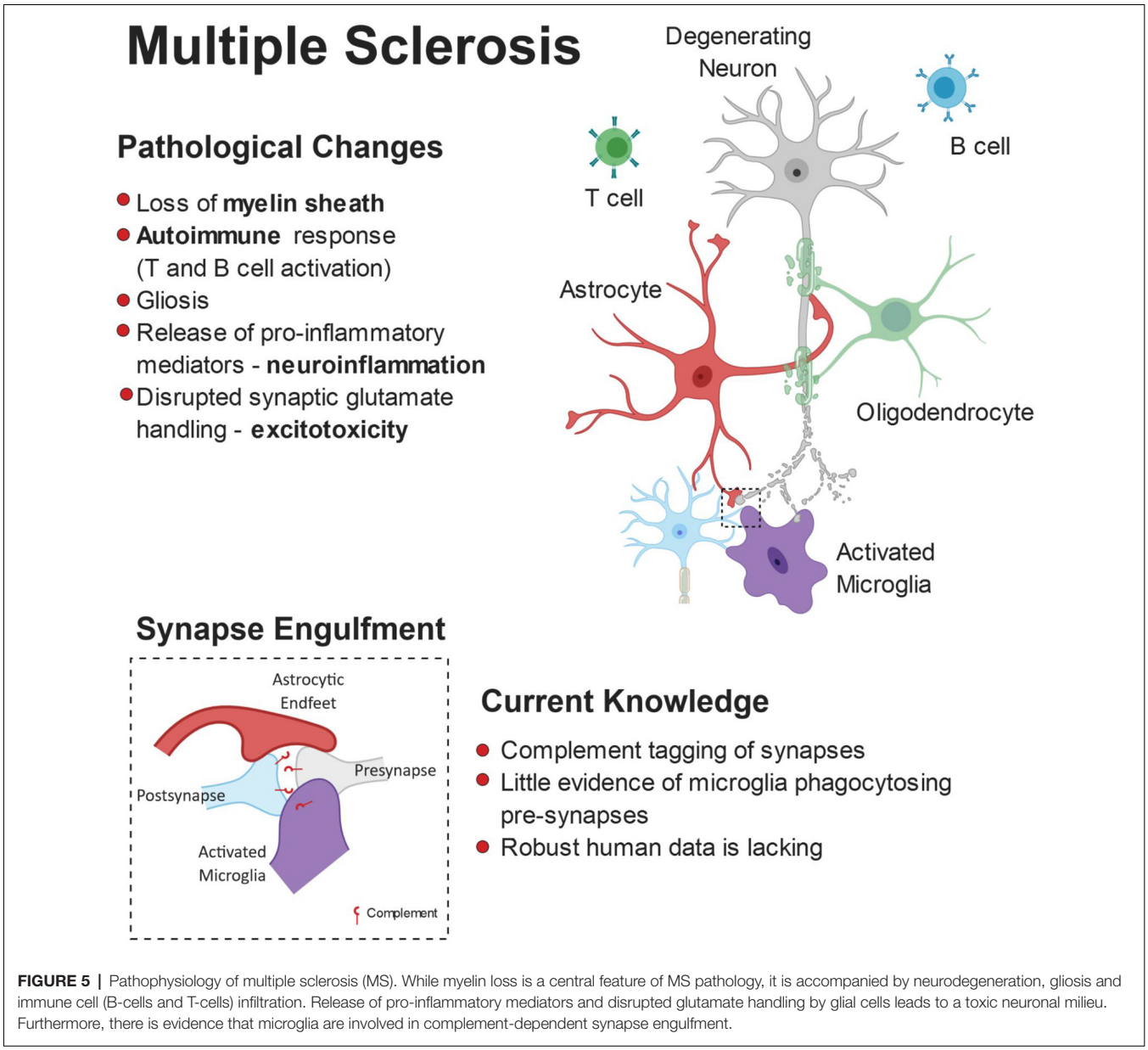

FIGURE 5 | Pathophysiology of multiple sclerosis (MS). While myelin loss is a central feature of MS pathology, it is accompanied by neurodegeneration, gliosis and immune cell (B-cells and T-cells) infiltration. Release of pro-inflammatory mediators and disrupted glutamate handling by glial cells leads to a toxic neuronal milieu. Furthermore, there is evidence that microglia are involved in complement-dependent synapse engulfment.

cytokines secreted by microglia have synaptotoxic effects, providing an alternative pathway to non-contact dependent synapse loss. Astrocytes can also contribute to glutamate excitotoxicity in MS as they reduce the levels of their glutamate transporters, EAAT1 and EAAT2, in MS-D lesions (Dutta et al., 2011), allowing excess levels of glutamate to surround synapses.

E/I Imbalance in MS and Possible Implication of Glia

Evidence of E/I imbalance has been reported in MS animal models, particularly the EAE model. Electrophysiological experiments have shown decreased excitatory post-synaptic potentials (EPSPs) in the CA1 of the hippocampus and impaired LTP in EAE mice, leading to cognitive impairments mediated by IL-1β driven inflammation (Kim et al., 2012; Di Filippo et al., 2013). This functional impairment may arise due to the downregulation of GluN2B NMDAR subunits in EAE mice. In contrast, there is evidence for inflammation-associated increase of LTP and reduction of LTD in EAE mice, displaying overall circuit hyperexcitation (Nistico et al., 2014). In favor of this, a magnetic resonance spectroscopy study found increased levels of glutamate in demyelinated brain areas of MS patients (Srinivasan et al., 2005), implicating excitatory imbalance as a pathological substrate for myelin damage, preceding synapse loss (Dutta et al., 2011). Specifically, oligodendroglia are vulnerable to glutamate excitotoxicity as they express NMDARs (Pérez-Otaño et al., 2016) which are required for activity-dependent myelination and plasticity (Lundgaard et al., 2013). Therefore, initial hyperexcitability could result in oligodendroglial

dysfunction and demyelination, ultimately rendering synapses weaker and more vulnerable to elimination, leading to later LTP impairments.

However, other studies have reported synapse reduction occurring independently of demyelination (Jürgens et al., 2016; Albert et al., 2017).

Researchers also found increased, rather than decreased, spine density in the somatosensory cortex of EAE mice, associated with increased VGLUT1 levels and disrupted PV+ interneuron connectivity (Potter et al., 2016). The altered excitatory-inhibitory balance in the cortex of these mice was associated with increased density of Iba1+ microglia, however no evidence of cause-effect was reported (Potter et al., 2016).

The synaptic terminals assessed in the above MS and EAE studies are exclusively pre-synaptic with no distinction of excitatory or inhibitory nature. Loss of inhibitory signaling causes E/I imbalance, which has already been described here in the context of dementias but applies to MS as well. Indeed, GABA levels are reduced in the CSF of patients with MS, indicating decreased inhibition (Manyam et al., 1980). More recently, RNA sequencing from gray matter of motor cortices in MS patients showed downregulation of multiple genes that are critical to interneuron function (Dutta et al., 2006). Namely, there was downregulation of GAD67, an enzyme required for GABA synthesis pre-synaptically, and of the GABA receptor subunits α1 and β3 which are essential for GABA function post-synaptically. Furthermore, parvalbumin (PV) and cholecystokinin (CCK) levels were found to be lower in MS than controls, with PV-positive interneurons reduced by 30% in MS gray matter (Dutta et al., 2006).

Reduction of axosomatic synaptic terminals was recently reported in the cerebellum of MS patients, associated with increased levels of reactive astrocytes and microglia, specifically in the dentate nucleus (Albert et al., 2017). In this study, ultrastructural examination by electron microscopy revealed evidence for astrocyte-mediated synaptic stripping (Albert et al., 2017).

Altogether, these findings point toward a consistent alteration in the E/I balance in MS and encourage further investigation to better elucidating the role of glia mediated-synapse loss.

CONCLUSION

Here, we have summarized the contributions of glial cells in some of the most common neurodegenerative diseases, highlighting evidence for their role in synapse remodeling. In disease, glia-mediated synaptic refinement likely represents an attempt to counteract network dysfunction occurring in the early stages of the disease. In this scenario, glia selectively remove excitatory or inhibitory connections in specific brain regions, to compensate for disease-associated changes in synaptic input. On the other hand, intrinsic dysfunction of glia cells, due for instance to genetic mutations, could also play a critical causative role in the pathogenesis of the diseases, acting as a primary trigger for E/I imbalance, by inducing excessive synaptic pruning (**Figure 6**). It is tempting to speculate that similar mechanisms could occur in response to shifts

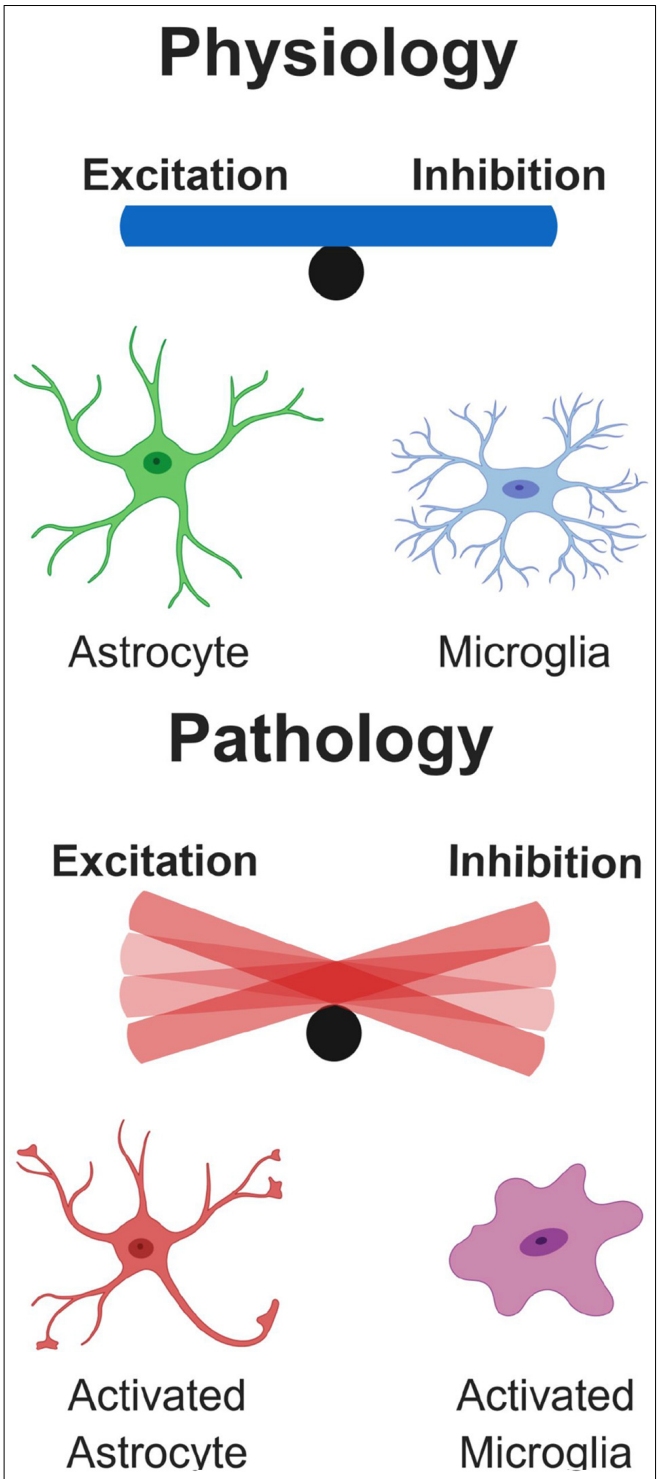

FIGURE 6 | Glial Influence on excitatory/inhibitory balance. Under physiological conditions, glial cells play important roles in the control of neuronal physiology, resulting in a well-controlled balance of excitatory/inhibitory neuronal networks. However, under pathological conditions as described in some of the diseases here, glial cells become hyperactive and damage surrounding neurons. This results in a dramatic tip of the balance depending on whether excitatory or inhibitory cells are disproportionally affected in the network.

in E/I balance in the developing brain, where glia-mediated synaptic alterations may lead to long lasting structural and functional defects, thus promoting the risk of developing psychiatric disorders and depression later in life (Durieux et al., 2015; Rial et al., 2015). Thus, deeper insight into the process of synapse remodeling mediated by glia cells, both in physiological and pathological conditions, will be essential for designing effective therapeutics to prevent, or at least halt synapse elimination. Such therapeutic interventions include an attenuation of the microglial response in AD pathology. For example, in two separate models of AD, the APPswe/PS1 and the 5xFAD, inhibiting the colony stimulating factor-1 receptor (CSF1R) markedly reduced microglial proliferation, rescuing synapse loss and cognitive deficits (Olmos-Alonso et al., 2016; Spangenberg et al., 2016). Importantly, in neither of these studies did pharmacological inhibition of microglia influence Aβ-plaque load, suggesting that microglial activation in AD can be synaptotoxic, *via* non-Aβ mediated mechanisms. However, whether this synaptic and cognitive rescue was due to attenuating microglial driven inflammation is unclear. Microglial neurotoxic and synaptotoxic cytokine release in prodromal stages of the disease is likely to coincide with complement deposition and aberrant phagocytosis. Complement molecules deposited at synapses have been reported to be work as a powerful "eat me" signal in several distinct neurodegenerative disorders. However, synapse elimination in pathological contexts could also be seen as a beneficial process, at least in the initial stages, aimed at re-establishing the E/I balance. Critical information will be provided by clinical trials currently testing a humanized anti-C1q antibody in neurodegeneration, after its safety was recently proven in both animal models and human cohorts (Lansita et al., 2017).

Given that early synapse loss is a common phenotype in many neurodegenerative diseases, it raises the exciting possibility that a greater understanding of glia-mediated synapse loss may lead to a single therapeutic strategy that targets many of the world's most devastating diseases.

AUTHOR CONTRIBUTIONS

CH, MT and RP revised the literature and wrote the manuscript.

FUNDING

This work was funded and supported by the University of Lausanne, the University of Edinburgh, Edinburgh Neuroscience, the UK Dementia Research Institute, Alzheimer's Research UK, Alzheimer's Society, the Medical Research Council, and by a Starting Grant from the European Research Council to RP (Grant 804949). CH is a member of the Euan Macdonald Centre and funded by MND Scotland. Figures were created with BioRender.

REFERENCES

Anichtchik, O., Calo, L., and Spillantini, M. G. (2013). Synaptic dysfunction in synucleinopathies. *CNS Neurol Disord Drug Targets* 12, 1094–1100. doi: 10.2174/18715273113129990114

Aarsland, D., Brønnick, K., and Fladby, T. (2011). Mild cognitive impairment in Parkinson's disease. *Curr. Neurol. Neurosci. Rep.* 11, 371–378. doi: 10.1007/s11910-011-0203-1

Aggelakopoulou, M., Kourepini, E., Paschalidis, N., Simoes, D. C., Kalavrizioti, D., Dimisianos, N., et al. (2016). ERβ-dependent direct suppression of human and murine Th17 cells and treatment of established central nervous system autoimmunity by a neurosteroid. *J. Immunol.* 197, 2598–2609. doi: 10.4049/jimmunol.1601038

Albert, M., Barrantes-Freer, A., Lohrberg, M., Antel, J. P., Prineas, J. W., Palkovits, M., et al. (2017). Synaptic pathology in the cerebellar dentate nucleus in chronic multiple sclerosis. *Brain Pathol.* 27, 737–747. doi: 10.1111/bpa.12450

Allen, N. J., and Lyons, D. A. (2018). Glia as architects of central nervous system formation and function. *Science* 362, 181–185. doi: 10.1126/science.aat0473

Almeida, C. G., Tampellini, D., Takahashi, R. H., Greengard, P., Lin, M. T., Snyder, E. M., et al. (2005). β-amyloid accumulation in APP mutant neurons reduces PSD-95 and GluR1 in synapses. *Neurobiol. Dis.* 20, 187–198. doi: 10.1016/j.nbd.2005.02.008

Aono, H., Choudhury, M. E., Higaki, H., Miyanishi, K., Kigami, Y., Fujita, K., et al. (2017). Microglia may compensate for dopaminergic neuron loss in experimental Parkinsonism through selective elimination of glutamatergic synapses from the subthalamic nucleus. *Glia* 65, 1833–1847. doi: 10.1002/glia.23199

Araque, A., Parpura, V., Sanzgiri, R. P., and Haydon, P. G. (1999). Tripartite synapses: glia, the unacknowledged partner. *Trends Neurosci.* 22, 208–215. doi: 10.1016/s0166-2236(98)01349-6

Azevedo, E. P., Ledo, J. H., Barbosa, G., Sobrinho, M., Diniz, L., Fonseca, A. C., et al. (2013). Activated microglia mediate synapse loss and short-term memory deficits in a mouse model of transthyretin-related oculoleptomeningeal amyloidosis. *Cell Death Dis.* 4:e789. doi: 10.1038/cddis.2013.325

Bae, J. S., Simon, N. G., Menon, P., Vucic, S., and Kiernan, M. C. (2013). The puzzling case of hyperexcitability in amyotrophic lateral sclerosis. *J. Clin. Neurol.* 9, 65–74. doi: 10.3988/jcn.2013.9.2.65

Baglietto-Vargas, D., Moreno-Gonzalez, I., Sanchez-Varo, R., Jimenez, S., Trujillo-Estrada, L., Sanchez-Mejias, E., et al. (2010). Calretinin interneurons are early targets of extracellular amyloid-β pathology in PS1/AβPP Alzheimer mice hippocampus. *J. Alzheimers Dis.* 21, 119–132. doi: 10.3233/jad-2010-100066

Bahia El Idrissi, N., Bosch, S., Ramaglia, V., Aronica, E., Baas, F., and Troost, D. (2016). Complement activation at the motor end-plates in amyotrophic lateral sclerosis. *J. Neuroinflammation* 13:72. doi: 10.1186/s12974-016-0538-2

Bakker, A., Albert, M. S., Krauss, G., Speck, C. L., and Gallagher, M. (2015). Response of the medial temporal lobe network in amnestic mild cognitive impairment to therapeutic intervention assessed by fMRI and memory task performance. *Neuroimage Clin.* 7, 688–698. doi: 10.1016/j.nicl.2015.02.009

Bakker, A., Krauss, G. L., Albert, M. S., Speck, C. L., Jones, L. R., Stark, C. E., et al. (2012). Reduction of hippocampal hyperactivity improves cognition in amnestic mild cognitive impairment. *Neuron* 74, 467–474. doi: 10.1016/j.neuron.2012.03.023

Baumann, N., and Pham-Dinh, D. (2001). Biology of oligodendrocyte and myelin in the mammalian central nervous system. *Physiol. Rev.* 81, 871–927. doi: 10.1152/physrev.2001.81.2.871

Baxter, A. J., Brugha, T. S., Erskine, H. E., Scheurer, R. W., Vos, T., and Scott, J. G. (2015). The epidemiology and global burden of autism spectrum disorders. *Psychol. Med.* 45, 601–613. doi: 10.1017/S003329171400172X

Beach, T. G., Adler, C. H., Lue, L., Sue, L. I., Bachalakuri, J., Henry-Watson, J., et al. (2009). Unified staging system for Lewy body disorders: correlation with nigrostriatal degeneration, cognitive impairment and motor dysfunction. *Acta Neuropathol.* 117, 613–634. doi: 10.1007/s00401-009-0538-8

Béchade, C., Cantaut-Belarif, Y., and Bessis, A. (2013). Microglial control of neuronal activity. *Front. Cell. Neurosci.* 7:32. doi: 10.3389/fncel.2013.00032

Belinson, H., and Michaelson, D. M. (2009). ApoE4-dependent Aβ-mediated neurodegeneration is associated with inflammatory activation in the

hippocampus but not the septum. *J. Neural Transm.* 116, 1427–1434. doi: 10.1007/s00702-009-0218-9

Bellesi, M., de Vivo, L., Chini, M., Gilli, F., Tononi, G., and Cirelli, C. (2017). Sleep loss promotes astrocytic phagocytosis and microglial activation in mouse cerebral cortex. *J. Neurosci.* 37, 5263–5273. doi: 10.1523/jneurosci.3981-16.2017

Bellucci, A., Zaltieri, M., Navarria, L., Grigoletto, J., Missale, C., and Spano, P. (2012). From α-synuclein to synaptic dysfunctions: new insights into the pathophysiology of Parkinson's disease. *Brain Res.* 1476, 183–202. doi: 10.1016/j.brainres.2012.04.014

Bialas, A. R., Presumey, J., Das, A., van der Poel, C. E., Lapchak, P. H., Mesin, L., et al. (2017). Microglia-dependent synapse loss in type I interferon-mediated lupus. *Nature* 546, 539–543. doi: 10.1038/nature22821

Bie, B., Wu, J., Foss, J. F., and Naguib, M. (2019). Activation of mGluR1 mediates C1q-dependent microglial phagocytosis of glutamatergic synapses in Alzheimer's rodent models. *Mol. Neurobiol.* doi: 10.1007/s12035-019-1467-8 [Epub ahead of print].

Bishop, D. L., Misgeld, T., Walsh, M. K., Gan, W. B., and Lichtman, J. W. (2004). Axon branch removal at developing synapses by axosome shedding. *Neuron* 44, 651–661. doi: 10.1016/j.neuron.2004.10.026

Boillée, S., Yamanaka, K., Lobsiger, C. S., Copeland, N. G., Jenkins, N. A., Kassiotis, G., et al. (2006). Onset and progression in inherited ALS determined by motor neurons and microglia. *Science* 312, 1389–1392. doi: 10.1126/science.1123511

Braak, H., Del Tredici, K., Rub, U., de Vos, R. A., Jansen Steur, E. N., and Braak, E. (2003). Staging of brain pathology related to sporadic Parkinson's disease. *Neurobiol. Aging* 24, 197–211. doi: 10.1016/s0197-4580(02)00065-9

Brettschneider, J., Libon, D. J., Toledo, J. B., Xie, S. X., McCluskey, L., Elman, L., et al. (2012). Microglial activation and TDP-43 pathology correlate with executive dysfunction in amyotrophic lateral sclerosis. *Acta Neuropathol.* 123, 395–407. doi: 10.1007/s00401-011-0932-x

Brown, R., Lam, A. D., Gonzalez-Sulser, A., Ying, A., Jones, M., Chou, R. C., et al. (2018). Circadian and brain state modulation of network hyperexcitability in Alzheimer's disease. *eNeuro* 5:ENEURO.0426-17.2018. doi: 10.1523/eneuro.0426-17.2018

Browne, P., Chandraratna, D., Angood, C., Tremlett, H., Baker, C., Taylor, B. V., et al. (2014). Atlas of multiple sclerosis 2013: a growing global problem with widespread inequity. *Neurology* 83, 1022–1024. doi: 10.1212/wnl.0000000000000768

Bruijn, L. I., Becher, M. W., Lee, M. K., Anderson, K. L., Jenkins, N. A., Copeland, N. G., et al. (1997). ALS-linked SOD1 mutant G85R mediates damage to astrocytes and promotes rapidly progressive disease with SOD1-containing inclusions. *Neuron* 18, 327–338. doi: 10.1016/s0896-6273(00)80272-x

Busche, M. A., Eichhoff, G., Adelsberger, H., Abramowski, D., Wiederhold, K. H., Haass, C., et al. (2008). Clusters of hyperactive neurons near amyloid plaques in a mouse model of Alzheimer's disease. *Science* 321, 1686–1689. doi: 10.1126/science.1162844

Busche, M. A., Kekus, M., Adelsberger, H., Noda, T., Forstl, H., Nelken, I., et al. (2015). Rescue of long-range circuit dysfunction in Alzheimer's disease models. *Nat. Neurosci.* 18, 1623–1630. doi: 10.1038/nn.4137

Busche, M. A., and Konnerth, A. (2016). Impairments of neural circuit function in Alzheimer's disease. *Philos. Trans. R. Soc. Lond. B Biol. Sci.* 371:20150429. doi: 10.1098/rstb.2015.0429

Buzsáki, G., Geisler, C., Henze, D. A., and Wang, X. J. (2004). Interneuron diversity series: circuit complexity and axon wiring economy of cortical interneurons. *Trends Neurosci.* 27, 186–193. doi: 10.1016/j.tins.2004.02.007

Cady, J., Koval, E. D., Benitez, B. A., Zaidman, C., Jockel-Balsarotti, J., Allred, P., et al. (2014). TREM2 variant p.R47H as a risk factor for sporadic amyotrophic lateral sclerosis. *JAMA Neurol.* 71, 449–453. doi: 10.1001/jamaneurol.2013.6237

Canas, P. M., Simoes, A. P., Rodrigues, R. J., and Cunha, R. A. (2014). Predominant loss of glutamatergic terminal markers in a β-amyloid peptide model of Alzheimer's disease. *Neuropharmacology* 76, 51–56. doi: 10.1016/j.neuropharm.2013.08.026

Canet-Avilés, R. M., Wilson, M. A., Miller, D. W., Ahmad, R., McLendon, C., Bandyopadhyay, S., et al. (2004). The Parkinson's disease protein DJ-1 is neuroprotective due to cysteine-sulfinic acid-driven mitochondrial localization. *Proc. Natl. Acad. Sci. U S A* 101, 9103–9108. doi: 10.1073/pnas.0402959101

Cantaut-Belarif, Y., Antri, M., Pizzarelli, R., Colasse, S., Vaccari, I., Soares, S., et al. (2017). Microglia control the glycinergic but not the GABAergic synapses via prostaglandin E2 in the spinal cord. *J. Cell Biol.* 216, 2979–2989. doi: 10.1083/jcb.201607048

Chakrabarty, P., Ceballos-Diaz, C., Beccard, A., Janus, C., Dickson, D., Golde, T. E., et al. (2010). IFN-γ promotes complement expression and attenuates amyloid plaque deposition in amyloid β precursor protein transgenic mice. *J. Immunol.* 184, 5333–5343. doi: 10.4049/jimmunol.0903382

Chávez-Gutiérrez, L., Bammens, L., Benilova, I., Vandersteen, A., Benurwar, M., Borgers, M., et al. (2012). The mechanism of γ-Secretase dysfunction in familial Alzheimer disease. *EMBO J.* 31, 2261–2274. doi: 10.1038/emboj.2012.79

Chen, Z., Jalabi, W., Hu, W., Park, H. J., Gale, J. T., Kidd, G. J., et al. (2014). Microglial displacement of inhibitory synapses provides neuroprotection in the adult brain. *Nat. Commun.* 5:4486. doi: 10.1038/ncomms5486

Chen, X., Lin, R., Chang, L., Xu, S., Wei, X., Zhang, J., et al. (2013). Enhancement of long-term depression by soluble amyloid β protein in rat hippocampus is mediated by metabotropic glutamate receptor and involves activation of p38MAPK, STEP and caspase-3. *Neuroscience* 253, 435–443. doi: 10.1016/j.neuroscience.2013.08.054

Chen, C. C., Lu, J., Yang, R., Ding, J. B., and Zuo, Y. (2018). Selective activation of parvalbumin interneurons prevents stress-induced synapse loss and perceptual defects. *Mol. Psychiatry* 23, 1614–1625. doi: 10.1038/mp.2017.159

Chever, O., Dossi, E., Pannasch, U., Derangeon, M., and Rouach, N. (2016). Astroglial networks promote neuronal coordination. *Sci. Signal.* 9:ra6. doi: 10.1126/scisignal.aad3066

Chiaravalloti, N. D., and DeLuca, J. (2008). Cognitive impairment in multiple sclerosis. *Lancet Neurol.* 7, 1139–1151. doi: 10.1016/S1474-4422(08)70259-X

Choi, I., Kim, B., Byun, J. W., Baik, S. H., Huh, Y. H., Kim, J. H., et al. (2015). LRRK2 G2019S mutation attenuates microglial motility by inhibiting focal adhesion kinase. *Nat. Commun.* 6:8255. doi: 10.1038/ncomms9255

Choi, I., Kim, J., Jeong, H. K., Kim, B., Jou, I., Park, S. M., et al. (2013). PINK1 deficiency attenuates astrocyte proliferation through mitochondrial dysfunction, reduced AKT and increased p38 MAPK activation and downregulation of EGFR. *Glia* 61, 800–812. doi: 10.1002/glia.22475

Chung, W. S., Clarke, L. E., Wang, G. X., Stafford, B. K., Sher, A., Chakraborty, C., et al. (2013). Astrocytes mediate synapse elimination through MEGF10 and MERTK pathways. *Nature* 504, 394–400. doi: 10.1038/nature12776

Chung, W.-S., Verghese, P. B., Chakraborty, C., Joung, J., Hyman, B. T., Ulrich, J. D., et al. (2016). Novel allele-dependent role for APOE in controlling the rate of synapse pruning by astrocytes. *Proc. Natl. Acad. Sci. U S A* 113, 10186–10191. doi: 10.1073/pnas.1609896113

Chung, W. S., Welsh, C. A., Barres, B. A., and Stevens, B. (2015). Do glia drive synaptic and cognitive impairment in disease? *Nat. Neurosci.* 18, 1539–1545. doi: 10.1038/nn.4142

Clark, R. M., Blizzard, C. A., Young, K. M., King, A. E., and Dickson, T. C. (2017). Calretinin and Neuropeptide Y interneurons are differentially altered in the motor cortex of the $SOD1^{G93A}$ mouse model of ALS. *Sci. Rep.* 7:44461. doi: 10.1038/srep44461

Cleary, J. P., Walsh, D. M., Hofmeister, J. J., Shankar, G. M., Kuskowski, M. A., Selkoe, D. J., et al. (2005). Natural oligomers of the amyloid-β protein specifically disrupt cognitive function. *Nat. Neurosci.* 8, 79–84. doi: 10.1038/nn1372

Cognato, G. P., Agostinho, P. M., Hockemeyer, J., Müller, C. E., Souza, D. O., and Cunha, R. A. (2010). Caffeine and an adenosine A_{2A} receptor antagonist prevent memory impairment and synaptotoxicity in adult rats triggered by a convulsive episode in early life. *J. Neurochem.* 112, 453–462. doi: 10.1111/j.1471-4159.2009.06465.x

Colom-Cadena, M., Pegueroles, J., Herrmann, A. G., Henstridge, C. M., Muñoz, L., Querol-Vilaseca, M., et al. (2017). Synaptic phosphorylated α-synuclein in dementia with Lewy bodies. *Brain* 140, 3204–3214. doi: 10.1093/brain/awx275

Cooper-Knock, J., Green, C., Altschuler, G., Wei, W., Bury, J. J., Heath, P. R., et al. (2017). A data-driven approach links microglia to pathology and prognosis in amyotrophic lateral sclerosis. *Acta Neuropathol. Commun.* 5:23. doi: 10.1186/s40478-017-0424-x

Cope, E. C., LaMarca, E. A., Monari, P. K., Olson, L. B., Martinez, S., Zych, A. D., et al. (2018). Microglia play an active role in obesity-associated cognitive decline. *J. Neurosci.* 38, 8889–8904. doi: 10.1523/JNEUROSCI.0789-18.2018

Crimins, J. L., Rocher, A. B., and Luebke, J. I. (2012). Electrophysiological changes precede morphological changes to frontal cortical pyramidal neurons in the rTg4510 mouse model of progressive tauopathy. *Acta Neuropathol.* 124, 777–795. doi: 10.1007/s00401-012-1038-9

Cudkowicz, M. E., Titus, S., Kearney, M., Yu, H., Sherman, A., Schoenfeld, D., et al. (2014). Safety and efficacy of ceftriaxone for amyotrophic lateral sclerosis: a multi-stage, randomised, double-blind, placebo-controlled trial. *Lancet Neurol.* 13, 1083–1091. doi: 10.1016/s1474-4422(14)70222-4

Davalos, D., Grutzendler, J., Yang, G., Kim, J. V., Zuo, Y., Jung, S., et al. (2005). ATP mediates rapid microglial response to local brain injury *in vivo*. *Nat. Neurosci.* 8, 752–758. doi: 10.1038/nn1472

Day, M., Wang, Z., Ding, J., An, X., Ingham, C. A., Shering, A. F., et al. (2006). Selective elimination of glutamatergic synapses on striatopallidal neurons in Parkinson disease models. *Nat. Neurosci.* 9, 251–259. doi: 10.1038/nn1632

De Miranda, B. R., Rocha, E. M., Bai, Q., El Ayadi, A., Hinkle, D., Burton, E. A., et al. (2018). Astrocyte-specific DJ-1 overexpression protects against rotenone-induced neurotoxicity in a rat model of Parkinson's disease. *Neurobiol. Dis.* 115, 101–114. doi: 10.1016/j.nbd.2018.04.008

DeKosky, S. T., and Scheff, S. W. (1990). Synapse loss in frontal cortex biopsies in Alzheimer's disease: correlation with cognitive severity. *Ann. Neurol.* 27, 457–464. doi: 10.1002/ana.410270502

Del Tredici, K., Rüb, U., De Vos, R. A., Bohl, J. R., and Braak, H. (2002). Where does parkinson disease pathology begin in the brain? *J. Neuropathol. Exp. Neurol.* 61, 413–426. doi: 10.1093/jnen/61.5.413

Desplats, P., Lee, H. J., Bae, E. J., Patrick, C., Rockenstein, E., Crews, L., et al. (2009). Inclusion formation and neuronal cell death through neuron-to-neuron transmission of α-synuclein. *Proc. Natl. Acad. Sci. U S A* 106, 13010–13015. doi: 10.1073/pnas.0903691106

Di Filippo, M., Chiasserini, D., Gardoni, F., Viviani, B., Tozzi, A., Giampà, C., et al. (2013). Effects of central and peripheral inflammation on hippocampal synaptic plasticity. *Neurobiol. Dis.* 52, 229–236. doi: 10.1016/j.nbd.2012.12.009

Di Filippo, M., Portaccio, E., Mancini, A., and Calabresi, P. (2018). Multiple sclerosis and cognition: synaptic failure and network dysfunction. *Nat. Rev. Neurosci.* 19, 599–609. doi: 10.1038/s41583-018-0053-9

Di Liberto, G., Pantelyushin, S., Kreutzfeldt, M., Page, N., Musardo, S., Coras, R., et al. (2018). Neurons under T cell attack coordinate phagocyte-mediated synaptic stripping. *Cell* 175, 458.e19–471.e19. doi: 10.1016/j.cell.2018.07.049

Diógenes, M. J., Dias, R. B., Rombo, D. M., Vicente Miranda, H., Maiolino, F., Guerreiro, P., et al. (2012). Extracellular α-synuclein oligomers modulate synaptic transmission and impair LTP via NMDA-receptor activation. *J. Neurosci.* 32, 11750–11762. doi: 10.1523/jneurosci.0234-12.2012

Dionísio, P. E. A., Oliveira, S. R., Amaral, J., and Rodrigues, C. M. P. (2018). Loss of microglial parkin inhibits necroptosis and contributes to neuroinflammation. *Mol. Neurobiol.* doi: 10.1007/s12035-018-1264-9 [Epub ahead of print].

Doble, A. (1996). The pharmacology and mechanism of action of riluzole. *Neurology* 47, S233–S241. doi: 10.1212/wnl.47.6_suppl_4.233s

Duarte, J. M., Agostinho, P. M., Carvalho, R. A., and Cunha, R. A. (2012). Caffeine consumption prevents diabetes-induced memory impairment and synaptotoxicity in the hippocampus of NONcZNO10/LTJ mice. *PLoS One* 7:e21899. doi: 10.1371/journal.pone.0021899

Duregotti, E., Negro, S., Scorzeto, M., Zornetta, I., Dickinson, B. C., Chang, C. J., et al. (2015). Mitochondrial alarmins released by degenerating motor axon terminals activate perisynaptic Schwann cells. *Proc. Natl. Acad. Sci. U S A* 112, E497–E505. doi: 10.1073/pnas.1417108112

Durieux, A. M., Fernandes, C., Murphy, D., Labouesse, M. A., Giovanoli, S., Meyer, U., et al. (2015). Targeting glia with N-acetylcysteine modulates brain glutamate and behaviors relevant to neurodevelopmental disorders in C57BL/6J mice. *Front. Behav. Neurosci.* 9:343. doi: 10.3389/fnbeh.2015.00343

Dutta, R., Chang, A., Doud, M. K., Kidd, G. J., Ribaudo, M. V., Young, E. A., et al. (2011). Demyelination causes synaptic alterations in hippocampi from multiple sclerosis patients. *Ann. Neurol.* 69, 445–454. doi: 10.1002/ana.22337

Dutta, R., McDonough, J., Yin, X., Peterson, J., Chang, A., Torres, T., et al. (2006). Mitochondrial dysfunction as a cause of axonal degeneration in multiple sclerosis patients. *Ann. Neurol.* 59, 478–489. doi: 10.1002/ana.20736

Edison, P., Donat, C. K., and Sastre, M. (2018). *In vivo* imaging of glial activation in Alzheimer's disease. *Front. Neurol.* 9:625. doi: 10.3389/fneur.2018.00625

Engert, F., and Bonhoeffer, T. (1999). Dendritic spine changes associated with hippocampal long-term synaptic plasticity. *Nature* 399, 66–70. doi: 10.1038/19978

Ertürk, A., Wang, Y., and Sheng, M. (2014). Local pruning of dendrites and spines by caspase-3-dependent and proteasome-limited mechanisms. *J. Neurosci.* 34, 1672–1688. doi: 10.1523/jneurosci.3121-13.2014

Esposito, Z., Belli, L., Toniolo, S., Sancesario, G., Bianconi, C., and Martorana, A. (2013). Amyloid β, glutamate, excitotoxicity in Alzheimer's disease: are we on the right track? *CNS Neurosci. Ther.* 19, 549–555. doi: 10.1111/cns.12095

Ferraiuolo, L., Higginbottom, A., Heath, P. R., Barber, S., Greenald, D., Kirby, J., et al. (2011). Dysregulation of astrocyte-motoneuron cross-talk in mutant superoxide dismutase 1-related amyotrophic lateral sclerosis. *Brain* 134, 2627–2641. doi: 10.1093/brain/awr193

Ferretti, M. T., Merlini, M., Spani, C., Gericke, C., Schweizer, N., Enzmann, G., et al. (2016). T-cell brain infiltration and immature antigen-presenting cells in transgenic models of Alzheimer's disease-like cerebral amyloidosis. *Brain Behav. Immun.* 54, 211–225. doi: 10.1016/j.bbi.2016.02.009

Fields, R. D., Araque, A., Johansen-Berg, H., Lim, S. S., Lynch, G., Nave, K. A., et al. (2014). Glial biology in learning and cognition. *Neuroscientist* 20, 426–431. doi: 10.1177/1073858413504465

Filipello, F., Morini, R., Corradini, I., Zerbi, V., Canzi, A., Michalski, B., et al. (2018). The microglial innate immune receptor TREM2 is required for synapse elimination and normal brain connectivity. *Immunity* 48, 979.e8–991.e8. doi: 10.1016/j.immuni.2018.04.016

Fischer, L. R., Culver, D. G., Tennant, P., Davis, A. A., Wang, M., Castellano-Sanchez, A., et al. (2004). Amyotrophic lateral sclerosis is a distal axonopathy: evidence in mice and man. *Exp. Neurol.* 185, 232–240. doi: 10.1016/j.expneurol.2003.10.004

Fogarty, M. J., Mu, E. W., Noakes, P. G., Lavidis, N. A., and Bellingham, M. C. (2016). Marked changes in dendritic structure and spine density precede significant neuronal death in vulnerable cortical pyramidal neuron populations in the $SOD1^{G93A}$ mouse model of amyotrophic lateral sclerosis. *Acta Neuropathol. Commun.* 4:77. doi: 10.1186/s40478-016-0347-y

Fogarty, M. J., Mu, E. W. H., Lavidis, N. A., Noakes, P. G., and Bellingham, M. C. (2017). Motor areas show altered dendritic structure in an amyotrophic lateral sclerosis mouse model. *Front. Neurosci.* 11:609. doi: 10.3389/fnins.2017.00609

Fogarty, M. J., Noakes, P. G., and Bellingham, M. C. (2015). Motor cortex layer V pyramidal neurons exhibit dendritic regression, spine loss and increased synaptic excitation in the presymptomatic $hSOD1^{G93A}$ mouse model of amyotrophic lateral sclerosis. *J. Neurosci.* 35, 643–647. doi: 10.1523/jneurosci.3483-14.2015

Fonseca, M. I., Zhou, J., Botto, M., and Tenner, A. J. (2004). Absence of C1q leads to less neuropathology in transgenic mouse models of Alzheimer's disease. *J. Neurosci.* 24, 6457–6465. doi: 10.1523/jneurosci.0901-04.2004

Frakes, A. E., Ferraiuolo, L., Haidet-Phillips, A. M., Schmelzer, L., Braun, L., Miranda, C., et al. (2014). Microglia induce motor neuron death via the classical NF-κB pathway in amyotrophic lateral sclerosis. *Neuron* 81, 1009–1023. doi: 10.1016/j.neuron.2014.01.013

Frey, D., Schneider, C., Xu, L., Borg, J., Spooren, W., and Caroni, P. (2000). Early and selective loss of neuromuscular synapse subtypes with low sprouting competence in motoneuron diseases. *J. Neurosci.* 20, 2534–2542. doi: 10.1523/jneurosci.20-07-02534.2000

Fritschy, J. M., and Brünig, I. (2003). Formation and plasticity of GABAergic synapses: physiological mechanisms and pathophysiological implications. *Pharmacol. Ther.* 98, 299–323. doi: 10.1016/s0163-7258(03)00037-8

Frøyset, A. K., Edson, A. J., Gharbi, N., Khan, E. A., Dondorp, D., Bai, Q., et al. (2018). Astroglial DJ-1 over-expression up-regulates proteins involved in redox regulation and is neuroprotective *in vivo*. *Redox Biol.* 16, 237–247. doi: 10.1016/j.redox.2018.02.010

Fu, M., Yu, X., Lu, J., and Zuo, Y. (2012). Repetitive motor learning induces coordinated formation of clustered dendritic spines *in vivo*. *Nature* 483, 92–95. doi: 10.1038/nature10844

Gao, R., and Penzes, P. (2015). Common mechanisms of excitatory and inhibitory imbalance in schizophrenia and autism spectrum disorders. *Curr. Mol. Med.* 15, 146–167. doi: 10.2174/1566524015666150303003028

Garcia-Marin, V., Blazquez-Llorca, L., Rodriguez, J. R., Boluda, S., Muntane, G., Ferrer, I., et al. (2009). Diminished perisomatic GABAergic terminals on cortical neurons adjacent to amyloid plaques. *Front. Neuroanat.* 3:28. doi: 10.3389/neuro.05.028.2009

Geloso, M. C., Corvino, V., Marchese, E., Serrano, A., Michetti, F., and D'Ambrosi, N. (2017). The dual role of microglia in ALS: mechanisms and therapeutic approaches. *Front. Aging Neurosci.* 9:242. doi: 10.3389/fnagi.2017.00242

George, J., Cunha, R. A., Mulle, C., and Amédée, T. (2016). Microglia-derived purines modulate mossy fibre synaptic transmission and plasticity through P2X4 and A1 receptors. *Eur. J. Neurosci.* 43, 1366–1378. doi: 10.1111/ejn.13191

George, J., Gonçalves, F. Q., Cristóvão, G., Rodrigues, L., Meyer Fernandes, J. R., Gonçalves, T., et al. (2015). Different danger signals differently impact on microglial proliferation through alterations of ATP release and extracellular metabolism. *Glia* 63, 1636–1645. doi: 10.1002/glia.22833

Geracitano, R., Paolucci, E., Prisco, S., Guatteo, E., Zona, C., Longone, P., et al. (2003). Altered long-term corticostriatal synaptic plasticity in transgenic mice overexpressing human CU/ZN superoxide dismutase (GLY^{93}—>ALA) mutation. *Neuroscience* 118, 399–408. doi: 10.1016/s0306-4522(02)00809-6

Gomez-Arboledas, A., Davila, J. C., Sanchez-Mejias, E., Navarro, V., Nuñez-Diaz, C., Sanchez-Varo, R., et al. (2018). Phagocytic clearance of presynaptic dystrophies by reactive astrocytes in Alzheimer's disease. *Glia* 66, 637–653. doi: 10.1002/glia.23270

Gomide, V., and Chadi, G. (2005). Glial bFGF and S100 immunoreactivities increase in ascending dopamine pathways following striatal 6-OHDA-induced partial lesion of the nigrostriatal system: a sterological analysis. *Int. J. Neurosci.* 115, 537–555. doi: 10.1080/00207450590521064

González-Reyes, R. E., Nava-Mesa, M. O., Vargas-Sánchez, K., Ariza-Salamanca, D., and Mora-Munoz, L. (2017). Involvement of astrocytes in Alzheimer's disease from a neuroinflammatory and oxidative stress perspective. *Front. Mol. Neurosci.* 10:427. doi: 10.3389/fnmol.2017.00427

Gorter, R. P., Stephenson, J., Nutma, E., Anink, J., de Jonge, J. C., Baron, W., et al. (2018). Rapidly progressive amyotrophic lateral sclerosis is associated with microglial reactivity and small heat shock protein expression in reactive astrocytes. *Neuropathol. Appl. Neurobiol.* doi: 10.1111/nan.12525 [Epub ahead of print].

Gosselin, D., Skola, D., Coufal, N. G., Holtman, I. R., Schlachetzki, J. C. M., Sajti, E., et al. (2017). An environment-dependent transcriptional network specifies human microglia identity. *Science* 356:eaal3222. doi: 10.1126/science.aal3222

Graber, D. J., Hickey, W. F., and Harris, B. T. (2010). Progressive changes in microglia and macrophages in spinal cord and peripheral nerve in the transgenic rat model of amyotrophic lateral sclerosis. *J. Neuroinflammation* 7:8. doi: 10.1186/1742-2094-7-8

Gu, L., Kleiber, S., Schmid, L., Nebeling, F., Chamoun, M., Steffen, J., et al. (2014). Long-term *in vivo* imaging of dendritic spines in the hippocampus reveals structural plasticity. *J. Neurosci.* 34, 13948–13953. doi: 10.1523/JNEUROSCI.1464-14.2014

Guerreiro, R., Wojtas, A., Bras, J., Carrasquillo, M., Rogaeva, E., Majounie, E., et al. (2013). TREM2 variants in Alzheimer's disease. *N. Engl. J. Med.* 368, 117–127. doi: 10.1056/NEJMoa1211851

Guo, H., Lai, L., Butchbach, M. E., Stockinger, M. P., Shan, X., Bishop, G. A., et al. (2003). Increased expression of the glial glutamate transporter EAAT2 modulates excitotoxicity and delays the onset but not the outcome of ALS in mice. *Hum. Mol. Genet.* 12, 2519–2532. doi: 10.1093/hmg/ddg267

Gylys, K. H., Fein, J. A., Yang, F., Wiley, D. J., Miller, C. A., and Cole, G. M. (2004). Synaptic changes in Alzheimer's disease: increased amyloid-β and gliosis in surviving terminals is accompanied by decreased PSD-95 fluorescence. *Am. J. Pathol.* 165, 1809–1817. doi: 10.1016/S0002-9440(10)63436-0

Hakim, Y., Yaniv, S. P., and Schuldiner, O. (2014). Astrocytes play a key role in *drosophila* mushroom body axon pruning. *PLoS One* 9:e86178. doi: 10.1371/journal.pone.0086178

Handley, E. E., Pitman, K. A., Dawkins, E., Young, K. M., Clark, R. M., Jiang, T. C., et al. (2017). Synapse dysfunction of layer V pyramidal neurons precedes neurodegeneration in a mouse model of TDP-43 proteinopathies. *Cereb. Cortex* 27, 3630–3647. doi: 10.1093/cercor/bhw185

Harauzov, A., Spolidoro, M., DiCristo, G., De Pasquale, R., Cancedda, L., Pizzorusso, T., et al. (2010). Reducing intracortical inhibition in the adult visual cortex promotes ocular dominance plasticity. *J. Neurosci.* 30, 361–371. doi: 10.1523/JNEUROSCI.2233-09.2010

Hardy, J. A., and Higgins, G. A. (1992). Alzheimer's disease: the amyloid cascade hypothesis. *Science* 256, 184–185. doi: 10.1126/science.1566067

Harris, K. M., and Weinberg, R. J. (2012). Ultrastructure of synapses in the mammalian brain. *Cold Spring Harb. Perspect. Biol.* 4:a005587. doi: 10.1101/cshperspect.a005587

Hashimoto, K., and Kano, M. (2003). Functional differentiation of multiple climbing fiber inputs during synapse elimination in the developing cerebellum. *Neuron* 38, 785–796. doi: 10.1016/s0896-6273(03)00298-8

Henkel, J. S., Beers, D. R., Zhao, W., and Appel, S. H. (2009). Microglia in ALS: the good, the bad and the resting. *J. Neuroimmune Pharmacol.* 4, 389–398. doi: 10.1007/s11481-009-9171-5

Henry, A. G., Aghamohammadzadeh, S., Samaroo, H., Chen, Y., Mou, K., Needle, E., et al. (2015). Pathogenic LRRK2 mutations, through increased kinase activity, produce enlarged lysosomes with reduced degradative capacity and increase ATP13A2 expression. *Hum. Mol. Genet.* 24, 6013–6028. doi: 10.1093/hmg/ddv314

Hensch, T. K., and Fagiolini, M. (2005). Excitatory-inhibitory balance and critical period plasticity in developing visual cortex. *Prog. Brain Res.* 147, 115–124. doi: 10.1016/s0079-6123(04)47009-5

Henstridge, C. M., Hyman, B. T., and Spires-Jones, T. L. (2019). Beyond the neuron-cellular interactions early in Alzheimer disease pathogenesis. *Nat. Rev. Neurosci.* 20, 94–108. doi: 10.1038/s41583-018-0113-1

Henstridge, C. M., Pickett, E., and Spires-Jones, T. L. (2016). Synaptic pathology: a shared mechanism in neurological disease. *Ageing Res. Rev.* 28, 72–84. doi: 10.1016/j.arr.2016.04.005

Henstridge, C. M., Sideris, D. I., Carroll, E., Rotariu, S., Salomonsson, S., Tzioras, M., et al. (2018). Synapse loss in the prefrontal cortex is associated with cognitive decline in amyotrophic lateral sclerosis. *Acta Neuropathol.* 135, 213–226. doi: 10.1007/s00401-017-1797-4

Heurich, B., El Idrissi, N. B., Donev, R. M., Petri, S., Claus, P., Neal, J., et al. (2011). Complement upregulation and activation on motor neurons and neuromuscular junction in the SOD1 G93A mouse model of familial amyotrophic lateral sclerosis. *J. Neuroimmunol.* 235, 104–109. doi: 10.1016/j.jneuroim.2011.03.011

Hirsch, E. C., Breidert, T., Rousselet, E., Hunot, S., Hartmann, A., and Michel, P. P. (2006). The role of glial reaction and inflammation in Parkinson's disease. *Ann. N Y Acad. Sci.* 991, 214–228. doi: 10.1111/j.1749-6632.2003.tb07478.x

Holtmaat, A., and Svoboda, K. (2009). Experience-dependent structural synaptic plasticity in the mammalian brain. *Nat. Rev. Neurosci.* 10, 647–658. doi: 10.1038/nrn2699

Hong, S., Beja-Glasser, V. F., Nfonoyim, B. M., Frouin, A., Li, S., Ramakrishnan, S., et al. (2016). Complement and microglia mediate early synapse loss in Alzheimer mouse models. *Science* 352, 712–716. doi: 10.1126/science.aad8373

Hong, Y. K., and Chen, C. (2011). Wiring and rewiring of the retinogeniculate synapse. *Curr. Opin. Neurobiol.* 21, 228–237. doi: 10.1016/j.conb.2011.02.007

Horti, A. G., Naik, R., Foss, C. A., Minn, I., Misheneva, V., Du, Y., et al. (2019). PET imaging of microglia by targeting macrophage colony-stimulating factor 1 receptor (CSF1R). *Proc. Natl. Acad. Sci. U S A* 116, 1686–1691. doi: 10.1073/pnas.1812155116

Hua, J. Y., and Smith, S. J. (2004). Neural activity and the dynamics of central nervous system development. *Nat. Neurosci.* 7, 327–332. doi: 10.1038/nn1218

Ibata, K., Sun, Q., and Turrigiano, G. G. (2008). Rapid synaptic scaling induced by changes in postsynaptic firing. *Neuron* 57, 819–826. doi: 10.1016/j.neuron.2008.02.031

Ince, P. G., Slade, J., Chinnery, R. M., McKenzie, J., Royston, C., Roberts, G. W., et al. (1995). Quantitative study of synaptophysin immunoreactivity of cerebral cortex and spinal cord in motor neuron disease. *J. Neuropathol. Exp. Neurol.* 54, 673–679. doi: 10.1097/00005072-199509000-00009

Ingham, C. A., Hood, S. H., and Arbuthnott, G. W. (1989). Spine density on neostriatal neurones changes with 6-hydroxydopamine lesions and with age. *Brain Res.* 503, 334–338. doi: 10.1016/0006-8993(89)91686-7

Janelsins, M. C., Mastrangelo, M. A., Park, K. M., Sudol, K. L., Narrow, W. C., Oddo, S., et al. (2008). Chronic neuron-specific tumor necrosis factor-α expression enhances the local inflammatory environment ultimately leading

to neuronal death in 3xTg-AD mice. *Am. J. Pathol.* 173, 1768–1782. doi: 10.2353/ajpath.2008.080528

Janezic, S., Threlfell, S., Dodson, P. D., Dowie, M. J., Taylor, T. N., Potgieter, D., et al. (2013). Deficits in dopaminergic transmission precede neuron loss and dysfunction in a new Parkinson model. *Proc. Natl. Acad. Sci. U S A* 110, E4016–E4025. doi: 10.1073/pnas.1309143110

Jha, M. K., Jo, M., Kim, J. H., and Suk, K. (2018). Microglia-astrocyte crosstalk: an intimate molecular conversation. *Neuroscientist* doi: 10.1177/1073858418783959 [Epub ahead of print].

Ji, K., Akgul, G., Wollmuth, L. P., and Tsirka, S. E. (2013). Microglia actively regulate the number of functional synapses. *PLoS One* 8:e56293. doi: 10.1371/journal.pone.0056293

Jo, E. K., Kim, J. K., Shin, D. M., and Sasakawa, C. (2016). Molecular mechanisms regulating NLRP3 inflammasome activation. *Cell. Mol. Immunol.* 13, 148–159. doi: 10.1038/cmi.2015.95

Jonsson, T., Stefansson, H., Steinberg, S., Jonsdottir, I., Jonsson, P. V., Snaedal, J., et al. (2013). Variant of TREM2 associated with the risk of Alzheimer's disease. *N. Engl. J. Med.* 368, 107–116. doi: 10.1056/NEJMoa1211103

Jürgens, T., Jafari, M., Kreutzfeldt, M., Bahn, E., Brück, W., Kerschensteiner, M., et al. (2016). Reconstruction of single cortical projection neurons reveals primary spine loss in multiple sclerosis. *Brain* 139, 39–46. doi: 10.1093/brain/awv353

Kakegawa, W., Mitakidis, N., Miura, E., Abe, M., Matsuda, K., Takeo, Y. H., et al. (2015). Anterograde C1ql1 signaling is required in order to determine and maintain a single-winner climbing fiber in the mouse cerebellum. *Neuron* 85, 316–329. doi: 10.1016/j.neuron.2014.12.020

Kamiyama, T., Yoshioka, N., and Sakurai, M. (2006). Synapse elimination in the corticospinal projection during the early postnatal period. *J. Neurophysiol.* 95, 2304–2313. doi: 10.1152/jn.00295.2005

Kang, S. S., Ebbert, M. T. W., Baker, K. E., Cook, C., Wang, X., Sens, J. P., et al. (2018). Microglial translational profiling reveals a convergent APOE pathway from aging, amyloid and tau. *J. Exp. Med.* 215, 2235–2245. doi: 10.1084/jem.20180653

Karch, C. M., and Goate, A. M. (2015). Alzheimer's disease risk genes and mechanisms of disease pathogenesis. *Biol. Psychiatry* 77, 43–51. doi: 10.1016/j.biopsych.2014.05.006

Kaster, M. P., Machado, N. J., Silva, H. B., Nunes, A., Ardais, A. P., Santana, M., et al. (2015). Caffeine acts through neuronal adenosine A_{2A} receptors to prevent mood and memory dysfunction triggered by chronic stress. *Proc. Natl. Acad. Sci. U S A* 112, 7833–7838. doi: 10.1073/pnas.1423088112

Kawamata, T., Akiyama, H., Yamada, T., and McGeer, P. L. (1992). Immunologic reactions in amyotrophic lateral sclerosis brain and spinal cord tissue. *Am. J. Pathol.* 140, 691–707.

Keren-Shaul, H., Spinrad, A., Weiner, A., Matcovitch-Natan, O., Dvir-Szternfeld, R., Ulland, T. K., et al. (2017). A unique microglia type associated with restricting development of Alzheimer's disease. *Cell* 169, 1276–1290.e17. doi: 10.1016/j.cell.2017.05.018

Kim, J. M., Cha, S. H., Choi, Y. R., Jou, I., Joe, E. H., and Park, S. M. (2016). DJ-1 deficiency impairs glutamate uptake into astrocytes via the regulation of flotillin-1 and caveolin-1 expression. *Sci. Rep.* 6:28823. doi: 10.1038/srep28823

Kim, D. Y., Hao, J., Liu, R., Turner, G., Shi, F. D., and Rho, J. M. (2012). Inflammation-mediated memory dysfunction and effects of a ketogenic diet in a murine model of multiple sclerosis. *PLoS One* 7:e35476. doi: 10.1371/journal.pone.0035476

Klausberger, T., and Somogyi, P. (2008). Neuronal diversity and temporal dynamics: the unity of hippocampal circuit operations. *Science* 321, 53–57. doi: 10.1126/science.1149381

Ko, C. P., and Robitaille, R. (2015). Perisynaptic Schwann cells at the neuromuscular synapse: adaptable, multitasking glial cells. *Cold Spring Harb. Perspect. Biol.* 7:a020503. doi: 10.1101/cshperspect.a020503

Koffie, R. M., Hashimoto, T., Tai, H. C., Kay, K. R., Serrano-Pozo, A., Joyner, D., et al. (2012). Apolipoprotein E4 effects in Alzheimer's disease are mediated by synaptotoxic oligomeric amyloid-β. *Brain* 135, 2155–2168. doi: 10.1093/brain/aws127

Koffie, R. M., Hyman, B. T., and Spires-Jones, T. L. (2011). Alzheimer's disease: synapses gone cold. *Mol. Neurodegener.* 6:63. doi: 10.1186/1750-1326-6-63

Koffie, R. M., Meyer-Luehmann, M., Hashimoto, T., Adams, K. W., Mielke, M. L., Garcia-Alloza, M., et al. (2009). Oligomeric amyloid β associates with postsynaptic densities and correlates with excitatory synapse loss near senile plaques. *Proc. Natl. Acad. Sci. U S A* 106, 4012–4017. doi: 10.1073/pnas.0811698106

Kordower, J. H., Chu, Y., Hauser, R. A., Freeman, T. B., and Olanow, C. W. (2008). Lewy body-like pathology in long-term embryonic nigral transplants in Parkinson's disease. *Nat. Med.* 14, 504–506. doi: 10.1038/nm1747

Korn, T., Reddy, J., Gao, W., Bettelli, E., Awasthi, A., Petersen, T. R., et al. (2007). Myelin-specific regulatory T cells accumulate in the CNS but fail to control autoimmune inflammation. *Nat. Med.* 13, 423–431. doi: 10.1038/nm1564

Kotter, M. R., Li, W. W., Zhao, C., and Franklin, R. J. (2006). Myelin impairs CNS remyelination by inhibiting oligodendrocyte precursor cell differentiation. *J. Neurosci.* 26, 328–332. doi: 10.1523/JNEUROSCI.2615-05.2006

Kramer, M. L., and Schulz-Schaeffer, W. J. (2007). Presynaptic α-synuclein aggregates, not Lewy bodies, cause neurodegeneration in dementia with Lewy bodies. *J. Neurosci.* 27, 1405–1410. doi: 10.1523/JNEUROSCI.4564-06.2007

Krasemann, S., Madore, C., Cialic, R., Baufeld, C., Calcagno, N., El Fatimy, R., et al. (2017). The TREM2-APOE pathway drives the transcriptional phenotype of dysfunctional microglia in neurodegenerative diseases. *Immunity* 47, 566–581.e9. doi: 10.1016/j.immuni.2017.08.008

Lansita, J. A., Mease, K. M., Qiu, H., Yednock, T., Sankaranarayanan, S., and Kramer, S. (2017). Nonclinical development of ANX005: a humanized anti-C1q antibody for treatment of autoimmune and neurodegenerative diseases. *Int. J. Toxicol.* 36, 449–462. doi: 10.1177/1091581817740873

Laudisi, F., Spreafico, R., Evrard, M., Hughes, T. R., Mandriani, B., Kandasamy, M., et al. (2013). Cutting edge: the NLRP3 inflammasome links complement-mediated inflammation and IL-1β release. *J. Immunol.* 191, 1006–1010. doi: 10.4049/jimmunol.1300489

Lehrman, E. K., Wilton, D. K., Litvina, E. Y., Welsh, C. A., Chang, S. T., Frouin, A., et al. (2018). CD47 protects synapses from excess microglia-mediated pruning during development. *Neuron* 100, 120–134.e6. doi: 10.1016/j.neuron.2018.09.017

Lendvai, B., Stern, E. A., Chen, B., and Svoboda, K. (2000). Experience-dependent plasticity of dendritic spines in the developing rat barrel cortex *in vivo*. *Nature* 404, 876–881. doi: 10.1038/35009107

Li, J. Y., Englund, E., Holton, J. L., Soulet, D., Hagell, P., Lees, A. J., et al. (2008). Lewy bodies in grafted neurons in subjects with Parkinson's disease suggest host-to-graft disease propagation. *Nat. Med.* 14, 501–503. doi: 10.1038/nm1746

Li, S., Hong, S., Shepardson, N. E., Walsh, D. M., Shankar, G. M., and Selkoe, D. (2009). Soluble oligomers of amyloid β protein facilitate hippocampal long-term depression by disrupting neuronal glutamate uptake. *Neuron* 62, 788–801. doi: 10.1016/j.neuron.2009.05.012

Li, Y., Du, X. F., Liu, C. S., Wen, Z. L., and Du, J. L. (2012). Reciprocal regulation between resting microglial dynamics and neuronal activity *in vivo*. *Dev. Cell* 23, 1189–1202. doi: 10.1016/j.devcel.2012.10.027

Li, S., Jin, M., Koeglsperger, T., Shepardson, N. E., Shankar, G. M., and Selkoe, D. J. (2011). Soluble Aβ oligomers inhibit long-term potentiation through a mechanism involving excessive activation of extrasynaptic NR2B-containing NMDA receptors. *J. Neurosci.* 31, 6627–6638. doi: 10.1523/JNEUROSCI.0203-11.2011

Lichtman, J. W., and Colman, H. (2000). Synapse elimination and indelible memory. *Neuron* 25, 269–278. doi: 10.1016/s0896-6273(00)80893-4

Liddelow, S. A., and Barres, B. A. (2017). Reactive astrocytes: production, function and therapeutic potential. *Immunity* 46, 957–967. doi: 10.1016/j.immuni.2017.06.006

Liddelow, S. A., Guttenplan, K. A., Clarke, L. E., Bennett, F. C., Bohlen, C. J., Schirmer, L., et al. (2017). Neurotoxic reactive astrocytes are induced by activated microglia. *Nature* 541, 481–487. doi: 10.1038/nature21029

Lin, Y. T., Seo, J., Gao, F., Feldman, H. M., Wen, H. L., Penney, J., et al. (2018). APOE4 causes widespread molecular and cellular alterations associated with Alzheimer's disease phenotypes in human iPSC-derived brain cell types. *Neuron* 98, 1141.e7–1154.e7. doi: 10.1016/j.neuron.2018.06.011

Ling, S. C., Polymenidou, M., and Cleveland, D. W. (2013). Converging mechanisms in ALS and FTD: disrupted RNA and protein homeostasis. *Neuron* 79, 416–438. doi: 10.1016/j.neuron.2013.07.033

Liu, C. C., Liu, C. C., Kanekiyo, T., Xu, H., and Bu, G. (2013). Apolipoprotein E and Alzheimer disease: risk, mechanisms and therapy. *Nat. Rev. Neurol.* 9, 106–118. doi: 10.1038/nrneurol.2012.263

Lobsiger, C. S., Boillée, S., Pozniak, C., Khan, A. M., McAlonis-Downes, M., Lewcock, J. W., et al. (2013). C1q induction and global complement pathway activation do not contribute to ALS toxicity in mutant SOD1 mice. *Proc. Natl. Acad. Sci. U S A* 110, E4385–E4392. doi: 10.1073/pnas.1318309110

Lui, H., Zhang, J., Makinson, S. R., Cahill, M. K., Kelley, K. W., Huang, H. Y., et al. (2016). Progranulin deficiency promotes circuit-specific synaptic pruning by microglia via complement activation. *Cell* 165, 921–935. doi: 10.1016/j.cell.2016.04.001

Luk, K. C., Kehm, V., Carroll, J., Zhang, B., O'Brien, P., Trojanowski, J. Q., et al. (2012). Pathological α-synuclein transmission initiates Parkinson-like neurodegeneration in nontransgenic mice. *Science* 338, 949–953. doi: 10.1126/science.1227157

Lundgaard, I., Luzhynskaya, A., Stockley, J. H., Wang, Z., Evans, K. A., Swire, M., et al. (2013). Neuregulin and BDNF induce a switch to NMDA receptor-dependent myelination by oligodendrocytes. *PLoS Biol.* 11:e1001743. doi: 10.1371/journal.pbio.1001743

Manyam, N. V., Katz, L., Hare, T. A., Gerber, J. C. III., Grossman, M. H. (1980). Levels of γ-aminobutyric acid in cerebrospinal fluid in various neurologic disorders. *Arch. Neurol.* 37, 352–355. doi: 10.1001/archneur.1980.00500550054006

Martín, R., Bajo-Grañeras, R., Moratalla, R., Perea, G., and Araque, A. (2015). Circuit-specific signaling in astrocyte-neuron networks in basal ganglia pathways. *Science* 349, 730–734. doi: 10.1126/science.aaa7945

Mason, C. A., and Gregory, E. (1984). Postnatal maturation of cerebellar mossy and climbing fibers: transient expression of dual features on single axons. *J. Neurosci.* 4, 1715–1735. doi: 10.1523/jneurosci.04-07-01715.1984

Masuda-Suzukake, M., Nonaka, T., Hosokawa, M., Oikawa, T., Arai, T., Akiyama, H., et al. (2013). Prion-like spreading of pathological α-synuclein in brain. *Brain* 136, 1128–1138. doi: 10.1093/brain/awt037

Matsumoto, S., Goto, S., Kusaka, H., Ito, H., and Imai, T. (1994). Synaptic pathology of spinal anterior horn cells in amyotrophic lateral sclerosis: an immunohistochemical study. *J. Neurol. Sci.* 125, 180–185. doi: 10.1016/0022-510x(94)90032-9

Matsuzaki, M., Ellis-Davies, G. C., Nemoto, T., Miyashita, Y., Iino, M., and Kasai, H. (2001). Dendritic spine geometry is critical for AMPA receptor expression in hippocampal CA1 pyramidal neurons. *Nat. Neurosci.* 4, 1086–1092. doi: 10.1038/nn736

Matsuzaki, M., Honkura, N., Ellis-Davies, G. C., and Kasai, H. (2004). Structural basis of long-term potentiation in single dendritic spines. *Nature* 429, 761–766. doi: 10.1038/nature02617

McGeer, P. L., and McGeer, E. G. (2008). Glial reactions in Parkinson's disease. *Mov. Disord.* 23, 474–483. doi: 10.1002/mds.21751

McGeer, P. L., Walker, D. G., Pitas, R. E., Mahley, R. W., and McGeer, E. G. (1997). Apolipoprotein E4 (ApoE4) but not ApoE3 or ApoE2 potentiates β-amyloid protein activation of complement *in vitro*. *Brain Res.* 749, 135–138. doi: 10.1016/s0006-8993(96)01324-8

Mederos, S., González-Arias, C., and Perea, G. (2018). Astrocyte-neuron networks: a multilane highway of signaling for homeostatic brain function. *Front. Synaptic Neurosci.* 10:45. doi: 10.3389/fnsyn.2018.00045

Meiser, J., Delcambre, S., Wegner, A., Jäger, C., Ghelfi, J., d'Herouel, A. F., et al. (2016). Loss of DJ-1 impairs antioxidant response by altered glutamine and serine metabolism. *Neurobiol. Dis.* 89, 112–125. doi: 10.1016/j.nbd.2016.01.019

Michailidou, I., Jongejan, A., Vreijling, J. P., Georgakopoulou, T., de Wissel, M. B., Wolterman, R. A., et al. (2018). Systemic inhibition of the membrane attack complex impedes neuroinflammation in chronic relapsing experimental autoimmune encephalomyelitis. *Acta Neuropathol. Commun.* 6:36. doi: 10.1186/s40478-018-0536-y

Michailidou, I., Naessens, D. M., Hametner, S., Guldenaar, W., Kooi, E. J., Geurts, J. J., et al. (2017). Complement C3 on microglial clusters in multiple sclerosis occur in chronic but not acute disease: implication for disease pathogenesis. *Glia* 65, 264–277. doi: 10.1002/glia.23090

Michailidou, I., Willems, J. G., Kooi, E. J., van Eden, C., Gold, S. M., Geurts, J. J., et al. (2015). Complement C1q-C3-associated synaptic changes in multiple sclerosis hippocampus. *Ann. Neurol.* 77, 1007–1026. doi: 10.1002/ana.24398

Mikuni, T., Uesaka, N., Okuno, H., Hirai, H., Deisseroth, K., Bito, H., et al. (2013). Arc/Arg3.1 is a postsynaptic mediator of activity-dependent synapse elimination in the developing cerebellum. *Neuron* 78, 1024–1035. doi: 10.1016/j.neuron.2013.04.036

Minett, T., Classey, J., Matthews, F. E., Fahrenhold, M., Taga, M., Brayne, C., et al. (2016). Microglial immunophenotype in dementia with Alzheimer's pathology. *J. Neuroinflammation* 13:135. doi: 10.1186/s12974-016-0601-z

Miron, V. E., Boyd, A., Zhao, J. W., Yuen, T. J., Ruckh, J. M., Shadrach, J. L., et al. (2013). M2 microglia and macrophages drive oligodendrocyte differentiation during CNS remyelination. *Nat. Neurosci.* 16, 1211–1218. doi: 10.1038/nn.3469

Mitew, S., Kirkcaldie, M. T., Dickson, T. C., and Vickers, J. C. (2013). Altered synapses and gliotransmission in Alzheimer's disease and AD model mice. *Neurobiol. Aging* 34, 2341–2351. doi: 10.1016/j.neurobiolaging.2013.04.010

Morales, I., Sanchez, A., Rodriguez-Sabate, C., and Rodriguez, M. (2017). Striatal astrocytes engulf dopaminergic debris in Parkinson's disease: a study in an animal model. *PLoS One* 12:e0185989. doi: 10.1371/journal.pone.0185989

Mullett, S. J., and Hinkle, D. A. (2009). DJ-1 knock-down in astrocytes impairs astrocyte-mediated neuroprotection against rotenone. *Neurobiol. Dis.* 33, 28–36. doi: 10.1016/j.nbd.2008.09.013

Narayanan, R. K., Mangelsdorf, M., Panwar, A., Butler, T. J., Noakes, P. G., and Wallace, R. H. (2013). Identification of RNA bound to the TDP-43 ribonucleoprotein complex in the adult mouse brain. *Amyotroph. Lateral Scler. Frontotemporal Degener.* 14, 252–260. doi: 10.3109/21678421.2012.734520

Nash, Y., Schmukler, E., Trudler, D., Pinkas-Kramarski, R., and Frenkel, D. (2017). DJ-1 deficiency impairs autophagy and reduces α-synuclein phagocytosis by microglia. *J. Neurochem.* 143, 584–594. doi: 10.1111/jnc.14222

Nelson, S. B., and Valakh, V. (2015). Excitatory/inhibitory balance and circuit homeostasis in autism spectrum disorders. *Neuron* 87, 684–698. doi: 10.1016/j.neuron.2015.07.033

Neumann, M., Sampathu, D. M., Kwong, L. K., Truax, A. C., Micsenyi, M. C., Chou, T. T., et al. (2006). Ubiquitinated TDP-43 in frontotemporal lobar degeneration and amyotrophic lateral sclerosis. *Science* 314, 130–133. doi: 10.1126/science.1134108

Nguyen, M., and Krainc, D. (2018). LRRK2 phosphorylation of auxilin mediates synaptic defects in dopaminergic neurons from patients with Parkinson's disease. *Proc. Natl. Acad. Sci. U S A* 115, 5576–5581. doi: 10.1073/pnas.1717590115

Nishijima, H., Suzuki, S., Kon, T., Funamizu, Y., Ueno, T., Haga, R., et al. (2014). Morphologic changes of dendritic spines of striatal neurons in the levodopa-induced dyskinesia model. *Mov. Disord.* 29, 336–343. doi: 10.1002/mds.25826

Nistico, R., Mori, F., Feligioni, M., Nicoletti, F., and Centonze, D. (2014). Synaptic plasticity in multiple sclerosis and in experimental autoimmune encephalomyelitis. *Philos. Trans. R. Soc. Lond. B Biol. Sci.* 369:20130162. doi: 10.1098/rstb.2013.0162

Olmos-Alonso, A., Schetters, S. T., Sri, S., Askew, K., Mancuso, R., Vargas-Caballero, M., et al. (2016). Pharmacological targeting of CSF1R inhibits microglial proliferation and prevents the progression of Alzheimer's-like pathology. *Brain* 139, 891–907. doi: 10.1093/brain/awv379

Ophir, G., Meilin, S., Efrati, M., Chapman, J., Karussis, D., Roses, A., et al. (2003). Human apoE3 but not apoE4 rescues impaired astrocyte activation in apoE null mice. *Neurobiol. Dis.* 12, 56–64. doi: 10.1016/s0969-9961(02)00005-0

Ortinski, P. I., Dong, J., Mungenast, A., Yue, C., Takano, H., Watson, D. J., et al. (2010). Selective induction of astrocytic gliosis generates deficits in neuronal inhibition. *Nat. Neurosci.* 13, 584–591. doi: 10.1038/nn.2535

Ouali Alami, N., Schurr, C., Olde Heuvel, F., Tang, L., Li, Q., Tasdogan, A., et al. (2018). NF-γB activation in astrocytes drives a stage-specific beneficial neuroimmunological response in ALS. *EMBO J.* 37:e98697. doi: 10.15252/embj.201798697

Overmyer, M., Helisalmi, S., Soininen, H., Laakso, M., Riekkinen, P. Sr., and Alafuzoff, I. (1999). Astrogliosis and the ApoE genotype. an immunohistochemical study of postmortem human brain tissue. *Dement. Geriatr. Cogn. Disord.* 10, 252–257. doi: 10.1159/000017128

Palop, J. J., and Mucke, L. (2016). Network abnormalities and interneuron dysfunction in Alzheimer disease. *Nat. Rev. Neurosci.* 17, 777–792. doi: 10.1038/nrn.2016.141

Panatier, A., Vallée, J., Haber, M., Murai, K. K., Lacaille, J. C., and Robitaille, R. (2011). Astrocytes are endogenous regulators of basal transmission at central synapses. *Cell* 146, 785–798. doi: 10.1016/j.cell.2011.07.022

Paolicelli, R. C., Bolasco, G., Pagani, F., Maggi, L., Scianni, M., Panzanelli, P., et al. (2011). Synaptic pruning by microglia is necessary for normal brain development. *Science* 333, 1456–1458. doi: 10.1126/science.1202529

Paolicelli, R. C., and Ferretti, M. T. (2017). Function and dysfunction of microglia during brain development: consequences for synapses and neural circuits. *Front. Syn. Neurosci.* 9:9. doi: 10.3389/fnsyn.2017.00009

Paolicelli, R. C., Jawaid, A., Henstridge, C. M., Valeri, A., Merlini, M., Robinson, J. L., et al. (2017). TDP-43 depletion in microglia promotes amyloid clearance but also induces synapse loss. *Neuron* 95, 297.e6–308.e6. doi: 10.1016/j.neuron.2017.05.037

Parkhurst, C. N., Yang, G., Ninan, I., Savas, J. N., Yates, J. R. III., and Lafaille, J. J., et al. (2013). Microglia promote learning-dependent synapse formation through brain-derived neurotrophic factor. *Cell* 155, 1596–1609. doi: 10.1016/j.cell.2013.11.030

Parpura, V., Basarsky, T. A., Liu, F., Jeftinija, K., Jeftinija, S., and Haydon, P. G. (1994). Glutamate-mediated astrocyte-neuron signalling. *Nature* 369, 744–747. doi: 10.1038/369744a0

Pascual, O., Ben Achour, S., Rostaing, P., Triller, A., and Bessis, A. (2012). Microglia activation triggers astrocyte-mediated modulation of excitatory neurotransmission. *Proc. Natl. Acad. Sci. U S A* 109, E197–E205. doi: 10.1073/pnas.1111098109

Pellerin, L., Bouzier-Sore, A. K., Aubert, A., Serres, S., Merle, M., Costalat, R., et al. (2007). Activity-dependent regulation of energy metabolism by astrocytes: an update. *Glia* 55, 1251–1262. doi: 10.1002/glia.20528

Pellerin, L., and Magistretti, P. J. (1994). Glutamate uptake into astrocytes stimulates aerobic glycolysis: a mechanism coupling neuronal activity to glucose utilization. *Proc. Natl. Acad. Sci. U S A* 91, 10625–10659. doi: 10.1073/pnas.91.22.10625

Pellerin, L., Pellegri, G., Bittar, P. G., Charnay, Y., Bouras, C., Martin, J. L., et al. (1998). Evidence supporting the existence of an activity-dependent astrocyte-neuron lactate shuttle. *Dev. Neurosci.* 20, 291–299. doi: 10.1159/000017324

Penn, A. A., Riquelme, P. A., Feller, M. B., and Shatz, C. J. (1998). Competition in retinogeniculate patterning driven by spontaneous activity. *Science* 279, 2108–2112. doi: 10.1126/science.279.5359.2108

Penzes, P., Cahill, M. E., Jones, K. A., VanLeeuwen, J. E., and Woolfrey, K. M. (2011). Dendritic spine pathology in neuropsychiatric disorders. *Nat. Neurosci.* 14, 285–293. doi: 10.1038/nn.2741

Perea, G., Gómez, R., Mederos, S., Covelo, A., Ballesteros, J. J., Schlosser, L., et al. (2016). Activity-dependent switch of GABAergic inhibition into glutamatergic excitation in astrocyte-neuron networks. *Elife* 5:e20362. doi: 10.7554/eLife.20362

Peretti, D., Bastide, A., Radford, H., Verity, N., Molloy, C., Martin, M. G., et al. (2015). RBM3 mediates structural plasticity and protective effects of cooling in neurodegeneration. *Nature* 518, 236–239. doi: 10.1038/nature14142

Perez-Nievas, B. G., and Serrano-Pozo, A. (2018). deciphering the astrocyte reaction in Alzheimer's disease. *Front. Aging Neurosci.* 10:114. doi: 10.3389/fnagi.2018.00114

Pérez-Otaño, I., Larsen, R. S., and Wesseling, J. F. (2016). Emerging roles of GluN3-containing NMDA receptors in the CNS. *Nat. Rev. Neurosci.* 17, 623–635. doi: 10.1038/nrn.2016.92

Personius, K. E., and Balice-Gordon, R. J. (2000). Activity-dependent editing of neuromuscular synaptic connections. *Brain Res. Bull.* 53, 513–522. doi: 10.1016/s0361-9230(00)00384-1

Pfeiffer, T., Poll, S., Bancelin, S., Angibaud, J., Inavalli, V. K., Keppler, K., et al. (2018). Chronic 2P-STED imaging reveals high turnover of dendritic spines in the hippocampus *in vivo*. *Elife* 7:e34700. doi: 10.7554/elife.34700

Phan, J. A., Stokholm, K., Zareba-Paslawska, J., Jakobsen, S., Vang, K., Gjedde, A., et al. (2017). Early synaptic dysfunction induced by α-synuclein in a rat model of Parkinson's disease. *Sci. Rep.* 7:6363. doi: 10.1038/s41598-017-06724-9

Philips, T., and Robberecht, W. (2011). Neuroinflammation in amyotrophic lateral sclerosis: role of glial activation in motor neuron disease. *Lancet Neurol.* 10, 253–263. doi: 10.1016/s1474-4422(11)70015-1

Pickering, M., and O'Connor, J. J. (2007). Pro-inflammatory cytokines and their effects in the dentate gyrus. *Prog. Brain Res.* 163, 339–354. doi: 10.1016/s0079-6123(07)63020-9

Pieri, M., Albo, F., Gaetti, C., Spalloni, A., Bengtson, C. P., Longone, P., et al. (2003). Altered excitability of motor neurons in a transgenic mouse model of familial amyotrophic lateral sclerosis. *Neurosci. Lett.* 351, 153–156. doi: 10.1016/j.neulet.2003.07.010

Pilz, G. A., Carta, S., Stäuble, A., Ayaz, A., Jessberger, S., and Helmchen, F. (2016). Functional imaging of dentate granule cells in the adult mouse hippocampus. *J. Neurosci.* 36, 7407–7414. doi: 10.1523/JNEUROSCI.3065-15.2016

Poewe, W., Seppi, K., Tanner, C. M., Halliday, G. M., Brundin, P., Volkmann, J., et al. (2017). Parkinson disease. *Nat. Rev. Dis. Primers* 3:17013. doi: 10.1038/nrdp.2017.13

Potter, L. E., Paylor, J. W., Suh, J. S., Tenorio, G., Caliaperumal, J., Colbourne, F., et al. (2016). Altered excitatory-inhibitory balance within somatosensory cortex is associated with enhanced plasticity and pain sensitivity in a mouse model of multiple sclerosis. *J. Neuroinflammation* 13:142. doi: 10.1186/s12974-016-0609-4

Prince, M., Bryce, R., Albanese, E., Wimo, A., Ribeiro, W., and Ferri, C. P. (2013). The global prevalence of dementia: a systematic review and metaanalysis. *Alzheimers Dement.* 9, 63.e2–75.e2. doi: 10.1016/j.jalz.2012.11.007

Pun, S., Santos, A. F., Saxena, S., Xu, L., and Caroni, P. (2006). Selective vulnerability and pruning of phasic motoneuron axons in motoneuron disease alleviated by CNTF. *Nat. Neurosci.* 9, 408–419. doi: 10.1038/nn1653

Qiu, H., Lee, S., Shang, Y., Wang, W. Y., Au, K. F., Kamiya, S., et al. (2014). ALS-associated mutation FUS-R521C causes DNA damage and RNA splicing defects. *J. Clin. Invest.* 124, 981–999. doi: 10.1172/jci72723

Rajendran, L., and Paolicelli, R. C. (2018). Microglia-mediated synapse loss in Alzheimer's disease. *J. Neurosci.* 38, 2911–2919. doi: 10.1523/JNEUROSCI.1136-17.2017

Ramos, B., Baglietto-Vargas, D., del Rio, J. C., Moreno-Gonzalez, I., Santa-Maria, C., Jimenez, S., et al. (2006). Early neuropathology of somatostatin/NPY GABAergic cells in the hippocampus of a PS1×APP transgenic model of Alzheimer's disease. *Neurobiol. Aging* 27, 1658–1672. doi: 10.1016/j.neurobiolaging.2005.09.022

Rao, S. M., Leo, G. J., Bernardin, L., and Unverzagt, F. (1991). Cognitive dysfunction in multiple sclerosis. I. Frequency, patterns, and prediction. *Neurology* 41, 685–691. doi: 10.1212/wnl.41.5.685

Recasens, A., and Dehay, B. (2014). α-synuclein spreading in Parkinson's disease. *Front. Neuroanat.* 8:159. doi: 10.3389/fnana.2014.00159

Reemst, K., Noctor, S. C., Lucassen, P. J., and Hol, E. M. (2016). The indispensable roles of microglia and astrocytes during brain development. *Front. Hum. Neurosci.* 10:566. doi: 10.3389/fnhum.2016.00566

Ren, S. Q., Yao, W., Yan, J. Z., Jin, C., Yin, J. J., Yuan, J., et al. (2018). Amyloid β causes excitation/inhibition imbalance through dopamine receptor 1-dependent disruption of fast-spiking GABAergic input in anterior cingulate cortex. *Sci. Rep.* 8:302. doi: 10.1038/s41598-017-18729-5

Renton, A. E., Chio, A., and Traynor, B. J. (2014). State of play in amyotrophic lateral sclerosis genetics. *Nat. Neurosci.* 17, 17–23. doi: 10.1038/nn.3584

Rial, D., Lemos, C., Pinheiro, H., Duarte, J. M., Gonçalves, F. Q., Real, J. I., et al. (2015). Depression as a glial-based synaptic dysfunction. *Front. Cell. Neurosci.* 9:521. doi: 10.3389/fncel.2015.00521

Risher, W. C., Patel, S., Kim, I. H., Uezu, A., Bhagat, S., Wilton, D. K., et al. (2014). Astrocytes refine cortical connectivity at dendritic spines. *Elife* 3:e04047. doi: 10.7554/eLife.04047

Rizzo, F. R., Musella, A., De Vito, F., Fresegna, D., Bullitta, S., Vanni, V., et al. (2018). Tumor necrosis factor and interleukin-1β modulate synaptic plasticity during neuroinflammation. *Neural Plast.* 2018:8430123. doi: 10.1155/2018/8430123

Robin, L. M., Oliveira da Cruz, J. F., Langlais, V. C., Martin-Fernandez, M., Metna-Laurent, M., Busquets-Garcia, A., et al. (2018). Astroglial CB1 receptors determine synaptic D-serine availability to enable recognition memory. *Neuron* 98, 935.e5–944.e5. doi: 10.1016/j.neuron.2018.04.034

Rodrigues, R. J., Tomé, A. R., and Cunha, R. A. (2015). ATP as a multi-target danger signal in the brain. *Front. Neurosci.* 9:148. doi: 10.3389/fnins.2015.00148

Rodriguez, G. A., Tai, L. M., LaDu, M. J., and Rebeck, G. W. (2014). Human APOE4 increases microglia reactivity at Aβ plaques in a mouse model of Aβ deposition. *J. Neuroinflammation* 11:111. doi: 10.1186/1742-2094-11-111

Roses, A. D. (1996). Apolipoprotein E alleles as risk factors in Alzheimer's disease. *Annu. Rev. Med.* 47, 387–400. doi: 10.1146/annurev.med.47.1.387

Ross, C. A., and Poirier, M. A. (2004). Protein aggregation and neurodegenerative disease. *Nat. Med.* 10, S10–S17. doi: 10.1038/nm1066

Rothstein, J. D., Dykes-Hoberg, M., Pardo, C. A., Bristol, L. A., Jin, L., Kuncl, R. W., et al. (1996). Knockout of glutamate transporters reveals a major role for astroglial transport in excitotoxicity and clearance of glutamate. *Neuron* 16, 675–686. doi: 10.1016/s0896-6273(00)80086-0

Rothstein, J. D., Patel, S., Regan, M. R., Haenggeli, C., Huang, Y. H., Bergles, D. E., et al. (2005). β-lactam antibiotics offer neuroprotection by increasing glutamate transporter expression. *Nature* 433, 73–77. doi: 10.1038/nature03180

Rothstein, J. D., Van Kammen, M., Levey, A. I., Martin, L. J., and Kuncl, R. W. (1995). Selective loss of glial glutamate transporter GLT-1 in amyotrophic lateral sclerosis. *Ann. Neurol.* 38, 73–84. doi: 10.1002/ana.410380114

Rubenstein, J. L., and Merzenich, M. M. (2003). Model of autism: increased ratio of excitation/inhibition in key neural systems. *Genes Brain Behav.* 2, 255–267. doi: 10.1034/j.1601-183x.2003.00037.x

Saba, L., Viscomi, M. T., Caioli, S., Pignataro, A., Bisicchia, E., Pieri, M., et al. (2016). Altered functionality, morphology, and vesicular glutamate transporter expression of cortical motor neurons from a presymptomatic mouse model of amyotrophic lateral sclerosis. *Cereb. Cortex* 26, 1512–1528. doi: 10.1093/cercor/bhu317

Sanchez, P. E., Zhu, L., Verret, L., Vossel, K. A., Orr, A. G., Cirrito, J. R., et al. (2012). Levetiracetam suppresses neuronal network dysfunction and reverses synaptic and cognitive deficits in an Alzheimer's disease model. *Proc. Natl. Acad. Sci. U S A* 109, E2895–E2903. doi: 10.1073/pnas.1121081109

Sardinha, V. M., Guerra-Gomes, S., Caetano, I., Tavares, G., Martins, M., Reis, J. S., et al. (2017). Astrocytic signaling supports hippocampal-prefrontal theta synchronization and cognitive function. *Glia* 65, 1944–1960. doi: 10.1002/glia.23205

Sasaki, S., and Iwata, M. (1999). Ultrastructural change of synapses of Betz cells in patients with amyotrophic lateral sclerosis. *Neurosci. Lett.* 268, 29–32. doi: 10.1016/s0304-3940(99)00374-2

Sasaki, S., and Maruyama, S. (1994a). Decreased synaptophysin immunoreactivity of the anterior horns in motor neuron disease. *Acta Neuropathol.* 87, 125–128. doi: 10.1007/bf00296180

Sasaki, S., and Maruyama, S. (1994b). Synapse loss in anterior horn neurons in amyotrophic lateral sclerosis. *Acta Neuropathol.* 88, 222–227. doi: 10.1007/s004010050153

Schafer, D. P., Lehrman, E. K., Kautzman, A. G., Koyama, R., Mardinly, A. R., Yamasaki, R., et al. (2012). Microglia sculpt postnatal neural circuits in an activity and complement-dependent manner. *Neuron* 74, 691–705. doi: 10.1016/j.neuron.2012.03.026

Scheff, S. W., Neltner, J. H., and Nelson, P. T. (2014). Is synaptic loss a unique hallmark of Alzheimer's disease? *Biochem. Pharmacol.* 88, 517–528. doi: 10.1016/j.bcp.2013.12.028

Scheff, S. W., Price, D. A., Schmitt, F. A., and Mufson, E. J. (2006). Hippocampal synaptic loss in early Alzheimer's disease and mild cognitive impairment. *Neurobiol. Aging* 27, 1372–1384. doi: 10.1016/j.neurobiolaging.2005.09.012

Selimbeyoglu, A., Kim, C. K., Inoue, M., Lee, S. Y., Hong, A. S. O., Kauvar, I., et al. (2017). Modulation of prefrontal cortex excitation/inhibition balance rescues social behavior in CNTNAP2-deficient mice. *Sci. Transl. Med.* 9:eaah6733. doi: 10.1126/scitranslmed.aah6733

Selkoe, D. J. (2002). Alzheimer's disease is a synaptic failure. *Science* 298, 789–791. doi: 10.1126/science.1074069

Selnes, P., Stav, A. L., Johansen, K. K., Bjørnerud, A., Coello, C., Auning, E., et al. (2017). Impaired synaptic function is linked to cognition in Parkinson's disease. *Ann. Clin. Transl. Neurol.* 4, 700–713. doi: 10.1002/acn3.446

Sephton, C. F., Tang, A. A., Kulkarni, A., West, J., Brooks, M., Stubblefield, J. J., et al. (2014). Activity-dependent FUS dysregulation disrupts synaptic homeostasis. *Proc. Natl. Acad. Sci. U S A* 111, E4769–E4778. doi: 10.1073/pnas.1406162111

Serrano-Pozo, A., Muzikansky, A., Gomez-Isla, T., Growdon, J. H., Betensky, R. A., Frosch, M. P., et al. (2013). Differential relationships of reactive astrocytes and microglia to fibrillar amyloid deposits in Alzheimer disease. *J. Neuropathol. Exp. Neurol.* 72, 462–471. doi: 10.1097/nen.0b013e3182933788

Shankar, G. M., Bloodgood, B. L., Townsend, M., Walsh, D. M., Selkoe, D. J., and Sabatini, B. L. (2007). Natural oligomers of the Alzheimer amyloid-β protein induce reversible synapse loss by modulating an NMDA-type glutamate receptor-dependent signaling pathway. *J. Neurosci.* 27, 2866–2875. doi: 10.1523/JNEUROSCI.4970-06.2007

Shankar, G. M., Li, S., Mehta, T. H., Garcia-Munoz, A., Shepardson, N. E., Smith, I., et al. (2008). Amyloid-β protein dimers isolated directly from Alzheimer's brains impair synaptic plasticity and memory. *Nat. Med.* 14, 837–842. doi: 10.1038/nm1782

Shi, Q., Chowdhury, S., Ma, R., Le, K. X., Hong, S., Caldarone, B. J., et al. (2017). Complement C3 deficiency protects against neurodegeneration in aged plaque-rich APP/PS1 mice. *Sci. Transl. Med.* 9:eaaf6295. doi: 10.1126/scitranslmed.aaf6295

Shi, Q., Colodner, K. J., Matousek, S. B., Merry, K., Hong, S., Kenison, J. E., et al. (2015). Complement C3-deficient mice fail to display age-related hippocampal decline. *J. Neurosci.* 35, 13029–13042. doi: 10.1523/JNEUROSCI.1698-15.2015

Shi, Y., Yamada, K., Liddelow, S. A., Smith, S. T., Zhao, L., Luo, W., et al. (2017). ApoE4 markedly exacerbates tau-mediated neurodegeneration in a mouse model of tauopathy. *Nature* 549, 523–527. doi: 10.1038/nature24016

Shinozaki, Y., Nomura, M., Iwatsuki, K., Moriyama, Y., Gachet, C., and Koizumi, S. (2014). Microglia trigger astrocyte-mediated neuroprotection via purinergic gliotransmission. *Sci. Rep.* 4:4329. doi: 10.1038/srep04329

Sierra, A., Tremblay, M. E., and Wake, H. (2014). Never-resting microglia: physiological roles in the healthy brain and pathological implications. *Front. Cell. Neurosci.* 8:240. doi: 10.3389/fncel.2014.00240

Simons, M., and Nave, K. A. (2015). Oligodendrocytes: myelination and axonal support. *Cold Spring Harb. Perspect. Biol.* 8:a020479. doi: 10.1101/cshperspect.a020479

Sipe, G. O., Lowery, R. L., Tremblay, M. È., Kelly, E. A., Lamantia, C. E., and Majewska, A. K. (2016). Microglial P2Y12 is necessary for synaptic plasticity in mouse visual cortex. *Nat. Commun.* 7:10905. doi: 10.1038/ncomms10905

Smith, E. F., Shaw, P. J., and De Vos, K. J. (2017). The role of mitochondria in amyotrophic lateral sclerosis. *Neurosci. Lett.* doi: 10.1016/j.neulet.2017.06.052 [Epub ahead of print].

Snyder, E. M., Nong, Y., Almeida, C. G., Paul, S., Moran, T., Choi, E. Y., et al. (2005). Regulation of NMDA receptor trafficking by amyloid-β. *Nat. Neurosci.* 8, 1051–1058. doi: 10.1038/nn1503

Sofroniew, M. V., and Vinters, H. V. (2010). Astrocytes: biology and pathology. *Acta Neuropathol.* 119, 7–35. doi: 10.1007/s00401-009-0619-8

Sokolow, S., Henkins, K. M., Bilousova, T., Miller, C. A., Vinters, H. V., Poon, W., et al. (2012). AD synapses contain abundant Aβ monomer and multiple soluble oligomers, including a 56-kDa assembly. *Neurobiol. Aging* 33, 1545–1555. doi: 10.1016/j.neurobiolaging.2011.05.011

Soto, C., and Pritzkow, S. (2018). Protein misfolding, aggregation, and conformational strains in neurodegenerative diseases. *Nat. Neurosci.* 21, 1332–1340. doi: 10.1038/s41593-018-0235-9

Spangenberg, E. E., Lee, R. J., Najafi, A. R., Rice, R. A., Elmore, M. R., Blurton-Jones, M., et al. (2016). Eliminating microglia in Alzheimer's mice prevents neuronal loss without modulating amyloid-β pathology. *Brain* 139, 1265–1281. doi: 10.1093/brain/aww016

Spiller, K. J., Restrepo, C. R., Khan, T., Dominique, M. A., Fang, T. C., Canter, R. G., et al. (2018). Microglia-mediated recovery from ALS-relevant motor neuron degeneration in a mouse model of TDP-43 proteinopathy. *Nat. Neurosci.* 21, 329–340. doi: 10.1038/s41593-018-0083-7

Spires-Jones, T. L., and Hyman, B. T. (2014). The intersection of amyloid β and tau at synapses in Alzheimer's disease. *Neuron* 82, 756–771. doi: 10.1016/j.neuron.2014.05.004

Srinivasan, R., Sailasuta, N., Hurd, R., Nelson, S., and Pelletier, D. (2005). Evidence of elevated glutamate in multiple sclerosis using magnetic resonance spectroscopy at 3 T. *Brain* 128, 1016–1025. doi: 10.1093/brain/awh467

Stellwagen, D., and Malenka, R. C. (2006). Synaptic scaling mediated by glial TNF-α. *Nature* 440, 1054–1059. doi: 10.1038/nature04671

Strong, M. J., Abrahams, S., Goldstein, L. H., Woolley, S., McLaughlin, P., Snowden, J., et al. (2017). Amyotrophic lateral sclerosis—frontotemporal spectrum disorder (ALS-FTSD): revised diagnostic criteria. *Amyotroph. Lateral Scler. Frontotemporal. Degener.* 18, 153–174. doi: 10.1080/21678421.2016.1267768

Sunico, C. R., Domínguez, G., García-Verdugo, J. M., Osta, R., Montero, F., and Moreno-Lopez, B. (2011). Reduction in the motoneuron inhibitory/excitatory synaptic ratio in an early-symptomatic mouse model of amyotrophic lateral sclerosis. *Brain Pathol.* 21, 1–15. doi: 10.1111/j.1750-3639.2010.00417.x

Sunkaria, A., Bhardwaj, S., Halder, A., Yadav, A., and Sandhir, R. (2016). Migration and phagocytic ability of activated microglia during post-natal development is mediated by calcium-dependent purinergic signalling. *Mol. Neurobiol.* 53, 944–954. doi: 10.1007/s12035-014-9064-3

Surmeier, D. J., Ding, J., Day, M., Wang, Z., and Shen, W. (2007). D1 and D2 dopamine-receptor modulation of striatal glutamatergic signaling in striatal medium spiny neurons. *Trends Neurosci.* 30, 228–235. doi: 10.1016/j.tins.2007.03.008

Svahn, A. J., Don, E. K., Badrock, A. P., Cole, N. J., Graeber, M. B., Yerbury, J. J., et al. (2018). Nucleo-cytoplasmic transport of TDP-43 studied in real time: impaired microglia function leads to axonal spreading of TDP-43 in degenerating motor neurons. *Acta Neuropathol.* 136, 445–459. doi: 10.1007/s00401-018-1875-2

Takahashi, R. H., Capetillo-Zarate, E., Lin, M. T., Milner, T. A., and Gouras, G. K. (2013). Accumulation of intraneuronal β-amyloid 42 peptides is associated with early changes in microtubule-associated protein 2 in neurites and synapses. *PLoS One* 8:e51965. doi: 10.1371/journal.pone.0051965

Teismann, P., Tieu, K., Cohen, O., Choi, D. K., Wu, D. C., Marks, D., et al. (2003). Pathogenic role of glial cells in Parkinson's disease. *Mov. Disord.* 18, 121–129. doi: 10.1002/mds.10332

Tremblay, M. È., Lowery, R. L., and Majewska, A. K. (2010). Microglial interactions with synapses are modulated by visual experience. *PLoS Biol.* 8:e1000527. doi: 10.1371/journal.pbio.1000527

Terry, R. D., Masliah, E., Salmon, D. P., Butters, N., DeTeresa, R., Hill, R., et al. (1991). Physical basis of cognitive alterations in Alzheimer's disease: synapse loss is the major correlate of cognitive impairment. *Ann. Neurol.* 30, 572–580. doi: 10.1002/ana.410300410

Tomiyama, T., Matsuyama, S., Iso, H., Umeda, T., Takuma, H., Ohnishi, K., et al. (2010). A mouse model of amyloid β oligomers: their contribution to synaptic alteration, abnormal tau phosphorylation, glial activation, and neuronal loss *in vivo*. *J. Neurosci.* 30, 4845–4856. doi: 10.1523/JNEUROSCI.5825-09.2010

Tong, J., Huang, C., Bi, F., Wu, Q., Huang, B., Liu, X., et al. (2013). Expression of ALS-linked TDP-43 mutant in astrocytes causes non-cell-autonomous motor neuron death in rats. *EMBO J.* 32, 1917–1926. doi: 10.1038/emboj.2013.122

Toni, N., Buchs, P. A., Nikonenko, I., Bron, C. R., and Muller, D. (1999). LTP promotes formation of multiple spine synapses between a single axon terminal and a dendrite. *Nature* 402, 421–425. doi: 10.1038/46574

Torborg, C. L., and Feller, M. B. (2005). Spontaneous patterned retinal activity and the refinement of retinal projections. *Prog. Neurobiol.* 76, 213–235. doi: 10.1016/j.pneurobio.2005.09.002

Town, T., Tan, J., Flavell, R. A., and Mullan, M. (2005). T-cells in Alzheimer's disease. *Neuromolecular Med.* 7, 255–264. doi: 10.1385/NMM:7:3:255

Tremblay, M. È., Stevens, B., Sierra, A., Wake, H., Bessis, A., and Nimmerjahn, A. (2011). The role of microglia in the healthy brain. *J. Neurosci.* 31, 16064–16069. doi: 10.1523/JNEUROSCI.4158-11.2011

Turner, M. R., Cagnin, A., Turkheimer, F. E., Miller, C. C., Shaw, C. E., Brooks, D. J., et al. (2004). Evidence of widespread cerebral microglial activation in amyotrophic lateral sclerosis: an [^{11}C](R)-PK11195 positron emission tomography study. *Neurobiol. Dis.* 15, 601–609. doi: 10.1016/j.nbd.2003.12.012

Turrigiano, G. G. (2008). The self-tuning neuron: synaptic scaling of excitatory synapses. *Cell* 135, 422–435. doi: 10.1016/j.cell.2008.10.008

Turrigiano, G. G., Leslie, K. R., Desai, N. S., Rutherford, L. C., and Nelson, S. B. (1998). Activity-dependent scaling of quantal amplitude in neocortical neurons. *Nature* 391, 892–896. doi: 10.1038/36103

Turrigiano, G. G., and Nelson, S. B. (2004). Homeostatic plasticity in the developing nervous system. *Nat. Rev. Neurosci.* 5, 97–107. doi: 10.1038/nrn1327

Tzioras, M., Davies, C., Newman, A., Jackson, R., and Spires-Jones, T. (2018). Invited Review: APOE at the interface of inflammation, neurodegeneration and pathological protein spread in Alzheimer's disease. *Neuropathol. Appl. Neurobiol.* doi: 10.1111/nan.12529 [Epub ahead of print].

Ulrich, J. D., Ulland, T. K., Mahan, T. E., Nyström, S., Nilsson, K. P., Song, W. M., et al. (2018). ApoE facilitates the microglial response to amyloid plaque pathology. *J. Exp. Med.* 215, 1047–1058. doi: 10.1084/jem.20171265

Umeda, T., Kimura, T., Yoshida, K., Takao, K., Fujita, Y., Matsuyama, S., et al. (2017). Mutation-induced loss of APP function causes GABAergic depletion in recessive familial Alzheimer's disease: analysis of Osaka mutation-knockin mice. *Acta Neuropathol. Commun.* 5:59. doi: 10.1186/s40478-017-0461-5

Van den Bos, M. A. J., Higashihara, M., Geevasinga, N., Menon, P., Kiernan, M. C., and Vucic, S. (2018). Imbalance of cortical facilitatory and inhibitory circuits underlies hyperexcitability in ALS. *Neurology* 91, e1669–e1676. doi: 10.1212/wnl.0000000000006438

Vasek, M. J., Garber, C., Dorsey, D., Durrant, D. M., Bollman, B., Soung, A., et al. (2016). A complement-microglial axis drives synapse loss during virus-induced memory impairment. *Nature* 534, 538–543. doi: 10.1038/nature18283

Verkhratsky, A., Parpura, V., Pekna, M., Pekny, M., and Sofroniew, M. (2014). Glia in the pathogenesis of neurodegenerative diseases. *Biochem. Soc. Trans.* 42, 1291–1301. doi: 10.1042/bst20140107

Verret, L., Mann, E. O., Hang, G. B., Barth, A. M., Cobos, I., Ho, K., et al. (2012). Inhibitory interneuron deficit links altered network activity and cognitive dysfunction in Alzheimer model. *Cell* 149, 708–721. doi: 10.1016/j.cell.2012.02.046

Vesce, S., Bezzi, P., and Volterra, A. (1999). The active role of astrocytes in synaptic transmission. *Cell. Mol. Life Sci.* 56, 991–1000. doi: 10.1007/s000180050488

Viana da Silva, S., Haberl, M. G., Zhang, P., Bethge, P., Lemos, C., Gonçalves, N., et al. (2016). Early synaptic deficits in the APP/PS1 mouse model of Alzheimer's disease involve neuronal adenosine A_{2A} receptors. *Nat. Commun.* 7:11915. doi: 10.1038/ncomms11915

Voineagu, I., Wang, X., Johnston, P., Lowe, J. K., Tian, Y., Horvath, S., et al. (2011). Transcriptomic analysis of autistic brain reveals convergent molecular pathology. *Nature* 474, 380–384. doi: 10.1038/nature10110

Vossel, K. A., Ranasinghe, K. G., Beagle, A. J., Mizuiri, D., Honma, S. M., Dowling, A. F., et al. (2016). Incidence and impact of subclinical epileptiform activity in Alzheimer's disease. *Ann. Neurol.* 80, 858–870. doi: 10.1002/ana.24794

Walsh, D. M., Klyubin, I., Fadeeva, J. V., Cullen, W. K., Anwyl, R., Wolfe, M. S., et al. (2002). Naturally secreted oligomers of amyloid β protein potently inhibit hippocampal long-term potentiation *in vivo*. *Nature* 416, 535–539. doi: 10.1038/416535a

Wang, J. Y., Chen, F., Fu, X. Q., Ding, C. S., Zhou, L., Zhang, X. H., et al. (2014). Caspase-3 cleavage of dishevelled induces elimination of postsynaptic structures. *Dev. Cell* 28, 670–684. doi: 10.1016/j.devcel.2014.02.009

Watkins, L. M., Neal, J. W., Loveless, S., Michailidou, I., Ramaglia, V., Rees, M. I., et al. (2016). Complement is activated in progressive multiple sclerosis cortical grey matter lesions. *J. Neuroinflammation* 13:161. doi: 10.1186/s12974-016-0611-x

Wiesel, T. N., and Hubel, D. H. (1963). Effects of visual deprivation on morphology and physiology of cells in the cats lateral geniculate body. *J. Neurophysiol.* 26, 978–993. doi: 10.1152/jn.1963.26.6.978

Wishart, T. M., Parson, S. H., and Gillingwater, T. H. (2006). Synaptic vulnerability in neurodegenerative disease. *J. Neuropathol. Exp. Neurol.* 65, 733–739. doi: 10.1097/01.jnen.0000228202.35163.c4

Wolff, J. R., and Missler, M. (1993). Synaptic remodelling and elimination as integral processes of synaptogenesis. *APMIS Suppl.* 40, 9–23.

Wu, H. Y., Hudry, E., Hashimoto, T., Kuchibhotla, K., Rozkalne, A., Fan, Z., et al. (2010). Amyloid β induces the morphological neurodegenerative triad of spine loss, dendritic simplification, and neuritic dystrophies through calcineurin activation. *J. Neurosci.* 30, 2636–2649. doi: 10.1523/JNEUROSCI.4456-09.2010

Xie, L., and Yang, S. H. (2015). Interaction of astrocytes and T cells in physiological and pathological conditions. *Brain Res.* 1623, 63–73. doi: 10.1016/j.brainres.2015.03.026

Xu, T., Yu, X., Perlik, A. J., Tobin, W. F., Zweig, J. A., Tennant, K., et al. (2009). Rapid formation and selective stabilization of synapses for enduring motor memories. *Nature* 462, 915–919. doi: 10.1038/nature08389

Yamanaka, K., Chun, S. J., Boillee, S., Fujimori-Tonou, N., Yamashita, H., Gutmann, D. H., et al. (2008). Astrocytes as determinants of disease progression in inherited amyotrophic lateral sclerosis. *Nat. Neurosci.* 11, 251–253. doi: 10.1038/nn2047

Yang, J., Yang, H., Liu, Y., Li, X., Qin, L., Lou, H., et al. (2016). Astrocytes contribute to synapse elimination via type 2 inositol 1,4,5-trisphosphate receptor-dependent release of ATP. *Elife* 5:e15043. doi: 10.7554/eLife.15043

Yang, Y., and Zhou, Q. (2009). Spine modifications associated with long-term potentiation. *Neuroscientist* 15, 464–476. doi: 10.1177/1073858409340800

Zaja-Milatovic, S., Milatovic, D., Schantz, A. M., Zhang, J., Montine, K. S., Samii, A., et al. (2005). Dendritic degeneration in neostriatal medium spiny neurons in Parkinson disease. *Neurology* 64, 545–547. doi: 10.1212/01.wnl.0000150591.33787.a4

Zang, D. W., Lopes, E. C., and Cheema, S. S. (2005). Loss of synaptophysin-positive boutons on lumbar motor neurons innervating the medial gastrocnemius muscle of the SOD1$^{G93A\ G1H}$ transgenic mouse model of ALS. *J. Neurosci. Res.* 79, 694–699. doi: 10.1002/jnr.20379

Zhan, Y., Paolicelli, R. C., Sforazzini, F., Weinhard, L., Bolasco, G., Pagani, F., et al. (2014). Deficient neuron-microglia signaling results in impaired functional brain connectivity and social behavior. *Nat. Neurosci.* 17, 400–406. doi: 10.1038/nn.3641

Zhang, J. M., Wang, H. K., Ye, C. Q., Ge, W., Chen, Y., Jiang, Z. L., et al. (2003). ATP released by astrocytes mediates glutamatergic activity-dependent heterosynaptic suppression. *Neuron* 40, 971–982. doi: 10.1016/s0896-6273(03)00717-7

Zhou, Y., Lai, B., and Gan, W. B. (2017). Monocular deprivation induces dendritic spine elimination in the developing mouse visual cortex. *Sci. Rep.* 7:4977. doi: 10.1038/s41598-017-05337-6

Zhu, Y., Nwabuisi-Heath, E., Dumanis, S. B., Tai, L. M., Yu, C., Rebeck, G. W., et al. (2012). APOE genotype alters glial activation and loss of synaptic markers in mice. *Glia* 60, 559–569. doi: 10.1002/glia.22289

Zürcher, N. R., Loggia, M. L., Lawson, R., Chonde, D. B., Izquierdo-Garcia, D., Yasek, J. E., et al. (2015). Increased *in vivo* glial activation in patients with amyotrophic lateral sclerosis: assessed with [^{11}C]-PBR28. *Neuroimage Clin.* 7, 409–414. doi: 10.1016/j.nicl.2015.01.009

Conflict of Interest Statement: The authors declare that the research was conducted in the absence of any commercial or financial relationships that could be construed as a potential conflict of interest.

frontiers in Molecular Neuroscience

ORIGINAL RESEARCH
published: 16 May 2019
doi: 10.3389/fnmol.2019.00113

Comprehensive Modeling of Spinal Muscular Atrophy in *Drosophila melanogaster*

Ashlyn M. Spring[1], Amanda C. Raimer[1,2], Christine D. Hamilton[1], Michela J. Schillinger[3] and A. Gregory Matera[1,2,3,4,5]*

[1]Integrative Program in Biological and Genome Sciences, University of North Carolina, Chapel Hill, NC, United States, [2]Curriculum in Genetics and Molecular Biology, University of North Carolina, Chapel Hill, NC, United States, [3]Department of Biology, University of North Carolina, Chapel Hill, NC, United States, [4]Lineberger Comprehensive Cancer Center, University of North Carolina, Chapel Hill, NC, United States, [5]Department of Genetics, University of North Carolina, Chapel Hill, NC, United States

Spinal muscular atrophy (SMA) is a neurodegenerative disorder that affects motor neurons, primarily in young children. SMA is caused by mutations in the *Survival Motor Neuron 1 (SMN1)* gene. SMN functions in the assembly of spliceosomal RNPs and is well conserved in many model systems including mouse, zebrafish, fruit fly, nematode, and fission yeast. Work in *Drosophila* has focused on the loss of SMN function during larval stages, primarily using null alleles or strong hypomorphs. A systematic analysis of SMA-related phenotypes in the context of moderate alleles that more closely mimic the genetics of SMA has not been performed in the fly, leading to debate over the validity and translational value of this model. We, therefore, examined 14 *Drosophila* lines expressing SMA patient-derived missense mutations in *Smn*, with a focus on neuromuscular phenotypes in the adult stage. Animals were evaluated on the basis of organismal viability and longevity, locomotor function, neuromuscular junction structure, and muscle health. In all cases, we observed phenotypes similar to those of SMA patients, including progressive loss of adult motor function. The severity of these defects is variable and forms a broad spectrum across the 14 lines examined, recapitulating the full range of phenotypic severity observed in human SMA. This includes late-onset models of SMA, which have been difficult to produce in other model systems. The results provide direct evidence that SMA-related locomotor decline can be reproduced in the fly and support the use of patient-derived SMN missense mutations as a comprehensive system for modeling SMA.

Keywords: SMN1, SMN2, spinal muscular atrophy, SMA, invertebrate models, neuromuscular disease

OPEN ACCESS

Edited by:
Jaichandar Subramanian, University of Kansas, United States

Reviewed by:
Stefan Johan Helge Thor, Linköping University, Sweden
Udai Pandey, University of Pittsburgh Medical Center, United States

****Correspondence:***
Ashlyn M. Spring
ashlyns@email.unc.edu

Received: *12 November 2018*
Accepted: *18 April 2019*
Published: *16 May 2019*

Citation:
Spring AM, Raimer AC, Hamilton CD, Schillinger MJ and Matera AG (2019) Comprehensive Modeling of Spinal Muscular Atrophy in Drosophila melanogaster. Front. Mol. Neurosci. 12:113. doi: 10.3389/fnmol.2019.00113

INTRODUCTION

Spinal Muscular Atrophy (SMA) is a neurodegenerative disease that primarily affects motor neurons in the anterior horn of the spinal cord and is a leading genetic cause of death among infants (Pearn, 1980). Symptoms involve muscle weakness that progressively worsens to the point of paralysis. The diaphragm becomes involved in later stages, leading to difficulty breathing and persistent respiratory infection that is a typical cause of death (Crawford, 2017). SMA has a broad range of severity; symptomatic onset can occur *in utero* in the most severe

cases or in adulthood in the least severe. This spectrum has been subdivided into different "types" of SMA (Darras and Finkel, 2017; Talbot and Tizzano, 2017) based on age of onset: Type 0 (*in utero*), Type I (first 6 months), Type II (7–18 months), Type III (childhood onset after 18 months), and Type IV (adult onset). Although motor neurons are the most dramatically impacted cell-type in SMA, other tissues including the musculature, cardiovascular system, liver, pancreas, gastrointestinal tract, and immune system are also affected (Perez-Garcia et al., 2017).

SMA is most commonly caused by reduced levels of the Survival Motor Neuron (SMN) protein which is encoded in humans by two genes *(SMN1)* and *SMN2* (Lefebvre et al., 1995). SMN protein is ubiquitously expressed and canonically functions in the assembly of spliceosomal snRNPs (Matera et al., 2007; Matera and Wang, 2014; Gruss et al., 2017). SMN is also reported to have functions related to RNA trafficking, translation, endocytosis, cytoskeletal maintenance, and cellular signaling (Raimer et al., 2017; Singh et al., 2017; Chaytow et al., 2018; Price et al., 2018). There is currently one FDA-approved SMA treatment: an antisense oligonucleotide (ASO) called nusinersen that increases SMN protein production from *SMN2* (Shorrock et al., 2018). This therapeutic strategy prevents motor neuron dysfunction if treatment begins before or soon after symptomatic onset (Finkel et al., 2017; Mendell et al., 2017). In later-stage patients, ASO therapy halts degeneration but does not restore lost function (Mercuri et al., 2018). Thus, these patients remain at high risk of complication and death despite receiving treatment.

The approved method of ASO delivery (intrathecal injection) treats only the central nervous system. While this is sufficient to prevent motor neuron dysfunction and early death, it appears likely that secondary symptoms will arise with age in peripheral systems of ASO treated patients (Hua et al., 2015; Bowerman et al., 2017). Therefore, there is an emerging need for SMA models that can be rapidly adapted to new research challenges. In this vein, *Drosophila melanogaster* is a highly useful model. In addition to the general advantages of the fly (low cost, rapid generation time, high-quality genetic tools), this model system also has well-characterized organ systems and cellular pathways that are highly relevant to the study of classical and emerging peripheral phenotypes in SMA.

Drosophila has a single *Smn* gene that is conserved, both in terms of protein sequence (Chan et al., 2003) and molecular function (Rajendra et al., 2007). To date, work in the fly has focused primarily on assessing the effects of strong *Smn* depletion on organismal development (Rajendra et al., 2007; Shpargel et al., 2009) or larval synapses and musculature (Chan et al., 2003; Chang et al., 2008), reviewed in (Grice et al., 2013; Aquilina and Cauchi, 2018). Despite this body of work, the validity and translational value of the fly as a model for SMA continues to be called into question (Bowerman et al., 2017; Iyer et al., 2018). This appears to be due, at least in part, to the lack of a systematic and comprehensive analysis of SMA-related phenotypes at the organismal level. Here, we aim to fill this gap and more firmly establish the fly as a comprehensive system for the study of SMA by complementing the large body of existing work on the impact of *Smn* mutations on molecular, cellular, and neuromuscular phenotypes.

In addition, this work also fills a more general need in the field, namely, the modeling of intermediate forms of SMA. In many model systems, there are few effective models of SMA Types II and III (Burghes et al., 2017; O'Hern et al., 2017). In mouse, the many attempts to generate such models have almost invariably produced animals that are either severely affected, or completely unaffected in terms of neuromuscular phenotype (Le et al., 2005; Osborne et al., 2012). This is problematic not only for assessing intermediate forms of SMA but also because nearly all severe SMA models exhibit developmental delays or arrest. This fact makes dissection of specific SMA-related phenotypes from general stress and death responses in an organism difficult and has complicated analysis of transcriptomic profiling of pre-mRNA splicing and neuromuscular development and function (Winkler et al., 2005; McWhorter et al., 2008; Hammond et al., 2010; Garcia et al., 2013, 2016).

Here, we present a set of 14 SMA models that cover the full spectrum of SMA severity and, in many cases, circumvent problems of developmental delay. In these models, symptomatic onset occurs anywhere from early development to adulthood, suggesting that the platform effectively models the full spectrum of SMA Types. The larval stages appear particularly useful for examining pre- and early-onset SMA, as we observe reduced locomotor function in the absence of overt synaptic or muscular defects. Conversely, the adult stage is well suited for modeling onset and progression of SMA phenotypes, as we observed reduced lifespan and locomotor deficits at different times post-eclosion. Similar to human patients, loss of motor function in adult flies is progressive and displays early involvement of posterior limbs relative to anterior ones. These results provide evidence that this system is a valuable and effective tool for studying the full range of SMA pathogenesis.

MATERIALS AND METHODS

Fly Lines and Husbandry

Fly lines used: Smn^{X7}, Smn^{D}, *da-Gal4*, "C15" driver line: *elav(C155)-Gal4; sca-Gal4; BG57-Gal4*. From Bloomington: *TRiP.JF02057* (Smn-RNAi #1, Stock #26288), *TRiP.HMC03832* (Smn-RNAi #2, Stock #55158). With the exception of the Y208C mutant, generation of the transgenic Flag-tagged *Smn* lines used in this study has previously been described (Praveen et al., 2012, 2014). In brief, a 3 kB genomic DNA sequence including the entire *Smn* coding region along with 3' and 5' regulatory sequences was cloned into the pAttB transgenic vector (Bischof et al., 2007). A 3× Flag epitope tag was inserted at the N-terminus immediately following the start codon. Expression is driven by the native *Smn* promotor present in the 3 kB genomic fragment. Constructs for each *Smn* mutation, including Y208C, were inserted into the same chromosomal location (86Fb), located at band position 86F8 on chromosome 3 (Bischof et al., 2007). All of the constructs have been recombined with an Smn^{X7} null mutation, located at the endogenous locus (band 73A9) using standard methods (Praveen et al., 2012, 2014).

To generate lines expressing *Smn* missense mutations in the absence of endogenous *Smn*, virgin females from the Smn^{X7}/TM6B-GFP line were crossed to Smn^{X7}, Smn^{TG}/TM6B-GFP males at 25°C. To reduce stress from overpopulation and/or competition from heterozygous siblings, crosses were performed on molasses plates with yeast paste and GFP negative (Smn^{X7}, Smn^{TG}/Smn^{X7}) larvae were sorted into vials containing standard molasses fly food during the second instar larval stage. Sorted larvae were raised at 25°C until the desired developmental stage was reached.

Experiments involving *UAS-Smn-RNAi* were carried out at 29°C to maximize expression from the Gal4/UAS system and, therefore, the degree of *Smn* knockdown. The one exception to this is the adult locomotion assay performed on da-Gal4/Smn-RNAi #2. Raising these animals at 29°C dramatically reduces viability and is incompatible with survival to the adult stage. To circumvent this and produce viable adults we instead raised all animals for this experiment at 25°C. To maintain consistency across experiments, we also use molasses plates with yeast paste and subsequent sorting for all *Smn-RNAi* experiments.

Viability Assays

To assess viability, we sorted 35–50 late second/early third instar larvae into vials containing standard molasses fly food and waited for them to complete development. After sufficient time had passed to allow for animals to complete development, we counted the total number of pupal cases in each vial and the number of empty pupal cases, which corresponds to the number of eclosed adults. We calculated % viability at both the pupal and adult stages by dividing these values by the number of initial larvae and then multiplying by 100 [pupal viability = (# total pupae/# initial larvae)*100, adult viability = (# empty pupal cases/# initial larvae)*100]. Each vial is considered a biological replicate with respect to calculating averages and standard error. *n*-value represents the total number of larvae collected and assayed.

Determining the stage of pupal arrest involves an identical procedure for assessing pupal and adult viability with the exception of scoring the pupae. In this assay, we examined pupae under white light at 2× magnification and score them based on morphology as having arrested early in pupal development, in mid pupal development, late in pupal development, or as empty pupal cases (viable adults). These values were normalized to the total number of pupae.

Locomotion Assays

Larval Locomotion: the locomotion assay used here was adapted from a previously published protocol (Brooks et al., 2016). One to five larvae at either the early third or wandering third instar stage were placed onto the center of the locomotion stage (a large molasses plate) at room temperature. The stage was then placed in a recording chamber to control light and reflection and provide support for video recording. Once all larvae were actively crawling, movement was recorded as video for at least 1 min and 10 s on an iPhone 6S at minimum zoom. Two video recordings were taken for each set of larvae. Locomotion videos were transferred to a PC and converted to raw video.avi files in ffmpeg. Video length was trimmed to exactly 60 s by removing the first 2 s and final additional second to: (1) create videos of standard duration; and (2) eliminate from the analyzed frames small movements caused by starting and stopping the recording. Videos were opened and converted into binary images series in Fiji/ImageJ. The wrMTrck plugin for ImageJ (Husson et al., 2013) was used to assess larvae size, larval body length, average speed of movement in mm/s, and average speed normalized to larval size (body lengths/s).

Adult Locomotion: adult flies of various ages were placed in individual locomotion chambers consisting of 35 × 10 mm round tissue culture plates filled with 7.5 ml of clear agar to prevent movement in the Z-direction. Flies were given 5–6 h to adjust to the new environment and then free moving walking behavior was recorded and analyzed in the same manner described for the larval locomotion assay.

Western Blotting

Wandering third instar larval lysates were prepared by mechanically lysing whole animals in RIPA (50 mM Tris-HCL, pH 7.5, 150 mM NaCl, 1 mM EDTA, 1% NP-40) buffer with 10× protease inhibitor complex (Invitrogen). PAGE was carried out using a standard equipment system and Mini-Protean TGX Stain Free Precast Gels, which allow for imaging of total protein after transfer to a low fluorescence PVDF membrane. Transfer from gel to membrane was carried out using a standard Invitrogen system. Blots were blocked in 5% milk in 1× TBST for 2 h at room temperature, incubated in primary rabbit anti-SMN antibody (Praveen et al., 2012), diluted to 1:10,000 in 5% milk blocking solution) overnight at 4°C, and incubated in HRP-conjugated goat anti-rabbit secondary antibody (diluted to 1:5,000 in 1× TBST) for 2 h at room temperature. Blots were developed using the Amersham ECL Prime Western Blotting Detection Reagent and imaged in an Amersham Imager 600 using the chemiluminescence function. The intensities of total protein and SMN and were quantified using ImageQuant TL software.

Immunostaining

Third instar larvae were dissected in HL3 saline with the following components (and concentrations): NaCl (70 mM), KCl (5 mM), $MgCl_2$ (10 mM), NaHCO3 (10 mM), sucrose (115 mM = 3.9%), trehalose (4.2 mM = 0.16%), HEPES (5.0 mM = 0.12%), and $CaCl_2$ (0.5 mM, unless otherwise indicated). Dissected samples were subsequently fixed with Bouin's fixative (Ricca Chemical Company, Arlington, TX, USA) for 3 min. Fixed samples were washed in 1× PBST using standard procedures, and incubated in primary antibodies at 4°C for overnight. This was followed by additional washes and a 2-h incubation in secondary antibody at room temperature. Staining was performed using the following primary antibodies: mouse anti-Synapsin (3C11) 1:1,000 (concentrated antibody, Developmental Studies Hybridoma Bank, University of Iowa—DSHB); rabbit anti-Dlg 1:30,000 (Budnik et al., 1996). The following fluorophore-conjugated antibodies were also used: Alexa-488 goat anti-rabbit 1:5,000 and Alexa-546 donkey anti-mouse 1:5,000 (both from ThermoFisher/Invitrogen Life Technologies, Eugene OR, USA), and Alexa-647 goat anti-HRP

(Jackson ImmunoResearch Laboratoreis Inc., West Grove, PA, USA). Larval preparations were mounted in Antifade media and imaged on a Leica TCS SP5 AOBS UV/spectral confocal laser-scanning system mounted on an inverted DM IRE2 microscope. Boutons were counted manually in Fiji/ImageJ in z-stacks and were examined to ensure that any boutons overlapping in the z-direction were accounted for. Muscle surface area was determined by outlining muscle 6 and 7 manually in Fiji/ImageJ. Muscle surface area is a rough measure, as rearing conditions and differences in muscle stretching can cause variability in the phenotype. Rearing conditions (both temperature and larval population within a vial) were carefully controlled and variability in stretching during dissection was minimized as much as possible.

Longevity Assay

To assess longevity, newly eclosed adult flies were collected daily into vials containing molasses agar food. Animals were kept with no greater than 10 animals total to avoid stress from crowding and transferred to fresh vials every 2–3 days to avoid death due to non-optimal food conditions. The number of adults was recorded at the time of collection and once each week following collection until all animals had expired. Animals that escaped or were injured/killed during transfer were excluded from analysis.

Collecting Partially Eclosed Adults

Animals were crossed and larvae collected as described above. As animals entered the pupal stage and began to either arrest and die or proceed through development. Two to three days after pupal formation, viable pupae were transferred to an empty tissue culture dish for easy observation. Animals nearing the end of pupal development were observed for partial eclosion. Wild type flies eclose rapidly (within 1–10 s) under normal conditions. To be sure that Smn missense mutants were truly stuck in the partially eclosed state, we waited for 10 min following identification of potential partially-eclosed animals to see if they would complete eclosion. If they did not, we used fine forceps and microdissection scissors to remove partially eclosed animals from their pupal cases without damaging them. To control for the effects of possible stress during this assisted eclosion approach, we performed the same dissections/eclosion assist procedure on animals expressing wild type transgenic SMN that had completed pupal development but not yet eclosed.

Statistical Analysis

All statistical analyses were performed using GraphPad Prism 7. For all data except longevity curves, *p*-values are from one-way ANOVA with a Dunnet correction for multiple comparisons. Statistical significance for longevity curves was determined by the Logrank/Mantel-Cox test. Details for the statistical analysis used in each figure panel are described in figure legends and/or shown in **Supplementary Table S1**.

RESULTS

To maximize the range of phenotypic severity examined in this study, *Drosophila* lines carrying transgenic insertions of 14 different *Smn* alleles were examined, in addition to the Oregon R (OR) wild type lab strain. The inserted transgenes encode a wild type *Smn* allele (WT) along with 13 alleles for non-synonymous *Smn* point mutations. Each mutation in this allelic series produces SMN protein with a single residue change homologous to those of human SMA patients bearing small *SMN1* mutations (**Supplementary Table S2**). In this work, we will refer to these transgenic lines by the amino acid substitution produced in the fly SMN protein (D20V, for example). A single copy of each missense mutation allele is expressed in an *Smn* null background (see "Materials and Methods" for full genotype). Thus, the transgenic product is the sole form of SMN present in the animals after the maternal SMN contribution is fully depleted at the end of the second instar larval stage. For some *Smn* mutations, we have also generated stable, self-replicating lines with animals carrying the *Smn* transgene and two transheterozygous null mutations of the endogenous *Smn* gene. These flies lack maternally contributed wild type SMN at all stages of development.

It should be noted that expression of each of these transgenic *Smn* alleles is driven by the native 5' and 3' *Smn* flanking regions and inserted at an identical attP site on the third chromosome to standardize potential position effects. This genomic arrangement is reported to drive transgenic *Smn* expression at lower levels than the endogenous *Smn* gene (Praveen et al., 2012). The Smn^{WT} transgenic line serves both as a control for this lower level of SMN expression and, in some assays described here, displays mild phenotypic changes relative to the wild type lab strain Oregon R (OR). All but one of these *Smn* missense lines has been previously reported (Praveen et al., 2014). This work reports that these *Smn* alleles cause variable degrees of developmental arrest and reduced viability, suggesting that they could be useful in recapitulating the spectrum of SMA severity seen in human patients. Beyond this observation, the authors take a molecular approach and focus their analysis on the impact of these *Smn* point mutations on protein interactions within the SMN complex. Only the most severe alleles in the series (G206S, Y203C, and M194R) were assayed for reduced locomotor behavior as early third instar larvae. Beyond this, no phenotypic analysis of SMA-related phenotypes has previously been assessed in this allelic series.

Here, we fully characterize these *Smn* alleles in the context of organismal SMA-related phenotypes. We also report on an additional *Smn* allele based on a recently reported SMA mutation that produces a tyrosine to cysteine change at Y277 in the human (Y208 in *Drosophila*) SMN protein (**Supplementary Table S2**).

Smn Missense Mutations Reduce Viability Across Development

We first replicated the previously reported viability defects for each of these 14 lines, measured at the pupal and adult stages (**Figure 1A**). Consistent with previously published observations, our experiments produced a broad range of viability phenotypes. The most severe phenotype is full developmental arrest at the 2nd to 3rd instar transition, which was observed for the G206S, M194R, and Y203C alleles. Animals carrying any of the other 11 *Smn* alleles reach pupation at moderate to

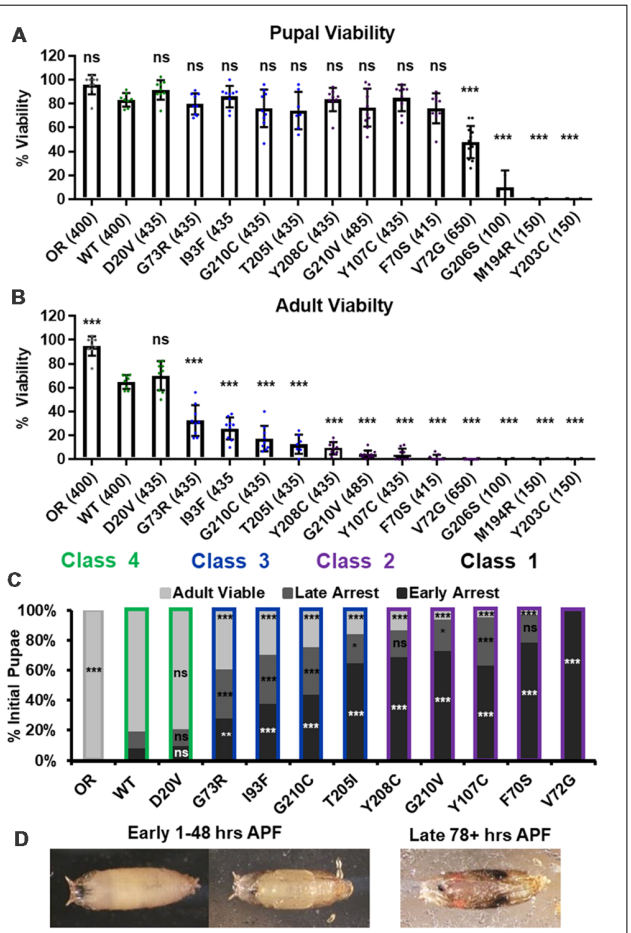

FIGURE 1 | Survival Motor Neuron (*Smn*) missense mutations produce a spectrum of viability defects. **(A,B)** Developmental viability of animals expressing *Smn* missense mutations at the pupal stage **(A)** and the adult stage **(B)**. % Viability is the proportion of animals that survive to the pupal/adult stage relative to the number of larvae initially collected. **(C)** Viability of animals carrying *Smn* missense mutations through pupal development. In the case, ns indicates a *p*-value of 0.99 and *** indicates a *p*-value of exactly 0.0001. **(D)** Representative images of the pupal stages assessed in **(C)**. Data: bars show average. Error bars show standard error. Data points represent biological replicates of 35–50 animals each, *n*-values (shown as numbers in parentheses next to genotypes) reflect the number of individual animals counted. *n*-values are the same for panels **(A–C)**. Statistical analysis: values above the data indicate significance vs. WT from one-way ANOVA using the Dunnet correction for multiple comparisons. ns: not significant ($p > 0.05$), *$p < 0.05$, **$p < 0.01$, ***$p < 0.001$.

normal levels, and all but one of them (V72G) produce viable adults to some degree (**Figure 1A**). The adult viability defects form a continuum that encompasses phenotypes from complete lethality (V72G) to nearly normal levels of viability (D20V and WT). This continuum is reminiscent of the spectrum of disease severity seen in SMA patients, indicating that this set of missense mutations has the potential to model a broad range of SMA Types.

A majority of these *Smn* alleles arrest during the pupal stage of development. To further explore this phenotype, we examined the timing of death during pupariation for each allele (**Figures 1B,C**). The pupal cases of developing *Drosophila* are transparent, so approximate staging can be performed visually using intact animals (**Figure 1C**). We observed arrest and death both early and late during pupal development for animals carrying all alleles except V72G, which causes arrest very shortly after pupariation (**Figures 1B,C**). Very few animals of any line arrested during the middle stages of pupation. Higher frequencies of arrest early in pupal development were observed for alleles that produce fewer viable adults.

Given the large number of individual genotypes described here, we organized these *Smn* alleles into four phenotypic classes based on gross viability phenotypes. Class I is the most severe, causing larval-stage arrest, and is comprised of G206S, M194R, and Y203C. Class II is comprised of the five most severe alleles that reach pupation: V72G, F70S, Y107C, G210V, and Y208C. A small fraction (2%–11%) of animals carrying Class II alleles eclose as adults. Class III alleles are more moderately affected, with ecolsion frequencies ranging from 20% to 45%. This class includes the T205I, G210C, I93F, and G73R alleles. Class IV includes the WT and D20V alleles, which are the least affected, displaying a moderate 20%–30% decrease in adult viability relative to the Oregon R strain. Throughout this manuscript, data for the *Smn* alleles are arranged in order of severity, and the color scheme for each Class is maintained for ease of reference.

Smn Missense Mutations Support Viability When Wild Type SMN Protein Is Completely Absent

In combination with previous observations, the range of severities observed in our viability assays suggests that most *Smn* missense mutations retain at least partial function. This conclusion is complicated by the presence of maternally contributed SMN that is present during embryonic and early larval development. We, therefore, attempted to generate stable fly lines expressing only *Smn* missense mutations. To do this, we sought to generate flies carrying two different *Smn* null alleles (Smn^{X7} and Smn^{D}) as well as one copy of each transgenic *Smn* allele (Smn^{TG}) for Class III and Class IV alleles. In all cases, adults of the desired genotype (Smn^{TG}, Smn^{X7}/Smn^{D}) were viable and sufficiently fertile to produce self-sustaining stocks. In later generations, animals in these stocks can carry either one or two copies of the *Smn* transgene and completely lack wild type SMN in all stages of life and development.

Having created these stocks, we assessed the functionality of *Smn* missense mutations by measuring developmental viability (**Supplementary Figure S1**). We found that, in all cases, expression of Class III and Class IV mutations is sufficient for robust pupal viability (**Supplementary Figure S1A**) and adult viability ranging from the moderate to wild type levels (**Supplementary Figure S1B**). This result definitively demonstrates that *Smn* missense mutations are functional in the absence of any wild type SMN protein.

Smn Missense Mutations Cause Defects in Larval Locomotion but Not NMJ Structure

Manipulations that strongly reduce SMN levels are known to cause larval locomotion defects. It is not clear, however, if the

moderate reduction of SMN function modeled by *Smn* missense alleles has the same functional impact as a strong reduction of wild type SMN. To address this, we performed larval locomotion assays on all lines at the early third instar stage (72 h post-egg lay) and in wandering third instar larvae for the 11 lines that reach this stage (**Figure 2**).

Larvae from all lines display reduced locomotion relative to Oregon R at the early third instar stage with the exception of G73R (**Figures 2A,B**). All three Class I alleles show a further decrease in crawling speed relative to the wild type transgenic line, as do the G210C, G210V, F70S, and Y107C lines. The rest of the mutant lines display no significant difference from the wild type transgenic control, suggesting that the mildly hypomorphic nature of these alleles is driving their locomotor defects (**Figures 2A,B**).

By the wandering third instar stage, all surviving lines exhibit locomotion defects. The Class IV alleles show a mild but statistically significant reduction in crawling speed relative to the Oregon R wild type train (**Figure 2D**). These two Class IV *Smn* alleles (WT and D20V) are not significantly different from one another, whereas all Class II and three alleles show a significant reduction in locomotion relative to both OR and the WT transgenic lines (**Figures 2D,E**). These differences are not due to overall changes in larval size, as this measure is unchanged in the wandering third instar larvae carrying transgenic *Smn* alleles (**Figure 2F**) and is controlled for within the analysis, by measuring locomotion in terms of body lengths per second (BLPS).

Given these locomotor deficits and previous reports of reduced NMJ size in the case of strong loss of SMN, we next immunostained and counted boutons at the muscle 6/7 NMJ in abdominal segment A2 for all lines that reach the wandering third instar stage. Surprisingly, we did not observe a dramatic change in bouton number for any of these alleles. All lines showed a slight but non-significant decrease in bouton number relative to Oregon R, with the exception of the I93F allele, which does reach statistical significance (**Supplementary Figures S2A,B**). These findings suggest that the locomotion defects observed in these larvae are likely due to functional changes in motor neurons or in other upstream central neurons such as interneurons. We also assessed the combined surface area of muscle 6/7 in segment A2 to look for signs of muscle degeneration. At the wandering third instar, we observed no changes in muscle area for any *Smn* allele (**Supplementary Figure S2C**). This indicates that the body wall muscles are not actively experiencing atrophy and that these larvae are in the early stages of symptomatic onset.

RNAi-Mediated *Smn* Knockdown Phenocopies *Smn* Missense Alleles

We next assessed potential tissue-specific roles of SMN in the observed phenotypes. To address this question, we used the *Gal4/UAS* system to drive two different constructs that produce shRNAs targeting RNAi-based knockdown of *Smn* under control of a *UAS* enhancer element (Perkins et al., 2015). These lines are *Smn-RNAi*^{JF02057} and *Smn-RNAi*^{HMC03832} and are referred to here as Smn-RNAi #1 and Smn-RNAi #2, respectively. Expression of these *UAS-RNAi* constructs is driven either ubiquitously with *da-Gal4* (*Daughterless*) or concurrently in both neurons and muscles using the "C15" driver line (Brusich et al., 2015), which contains three Gal4 constructs: two pan-neuronal drivers, *elav(C155)-Gal4* and *scabrous-Gal4*, and one muscle specific driver, *BG57-Gal4*. Crossing the C15 driver with the Smn-RNAi lines allows us to simultaneously deplete SMN in both muscles and neurons, the two cell types most closely linked to SMA pathology. Both Smn-RNAi lines have been used in previous publications, but have not been validated for their ability to reduce SMN protein expression (Atkinson et al., 2017; Mirra et al., 2017). To determine the strength of *Smn* knockdown, we measured SMN levels in wandering third instar larvae in which the two *Smn*-RNAi constructs were expressed using the *da*-Gal4 driver. This analysis reveals that both *Smn*-RNAi lines are capable of inducing significant knockdown of SMN (**Figures 3A,B**).

We first used these RNAi lines to assess pupal and adult viability (**Figures 3C,D**). Similar to the findings with the *Smn* allelic series, both ubiquitous and neuromuscular *Smn* knockdown caused a significant reduction in viability (**Figure 3C**). Ubiquitous knockdown causes an effect comparable to that of the V72G lines, strongly reducing pupal lethality and displaying complete lethality at the adult stage. In contrast, neuromuscular knockdown of *Smn* phenocopies the moderate Class III alleles, displaying fairly normal pupal viability and a moderate decline in adult viability (**Figure 3C**). These data suggest that neuronal and muscle tissues contribute to the viability defects observed following ubiquitous *Smn* knockdown and in animals ubiquitously expressing mutant *Smn* alleles.

We also examined locomotion in the context of *Smn* knockdown. Both ubiquitous and neuromuscular knockdown of *Smn* negatively impacted larval locomotion (**Figure 3E**). In the context of ubiquitous knockdown, the presence of the *Gal4* element alone did not impact the baseline locomotor phenotype. In contrast, *Gal4* expression in neuromuscular tissues from the C15 line caused a significant increase in crawling speed relative to the OR control (**Figure 3E**). Relative to this increase, expressing Smn-RNAi using the C15 driver line caused a significant decrease in locomotor speed (**Figure 3E**). A similar decrease in larval velocity was also observed in the context of ubiquitous *Smn* knockdown. Specifically, ubiquitous knockdown with Smn-RNA #1 causes a significant reduction in crawling speed (**Figure 3E**). Unlike the lines expressing *Smn* missense alleles, ubiquitous knockdown also caused a significant reduction in the size of the muscle 6/7 neuromuscular junction relative to the Oregon R wild type strain (**Supplementary Figure S2A**).

Overall, examination of SMA-related phenotypes in larvae reveals a spectrum of severities in the context of developmental viability and reveals a moderate reduction in locomotor behavior. However, we did not observe changes to larval NMJ structure or muscle size (**Supplementary Figure S2**). This is likely due to the relatively mild to intermediate nature of the *Smn* mutations examined here, the effects of maternally contributed SMN, and the short duration of the larval stages. In the context of our SMA models, there is likely not enough time for degenerative phenotypes to manifest in the larval stages. Therefore, to examine

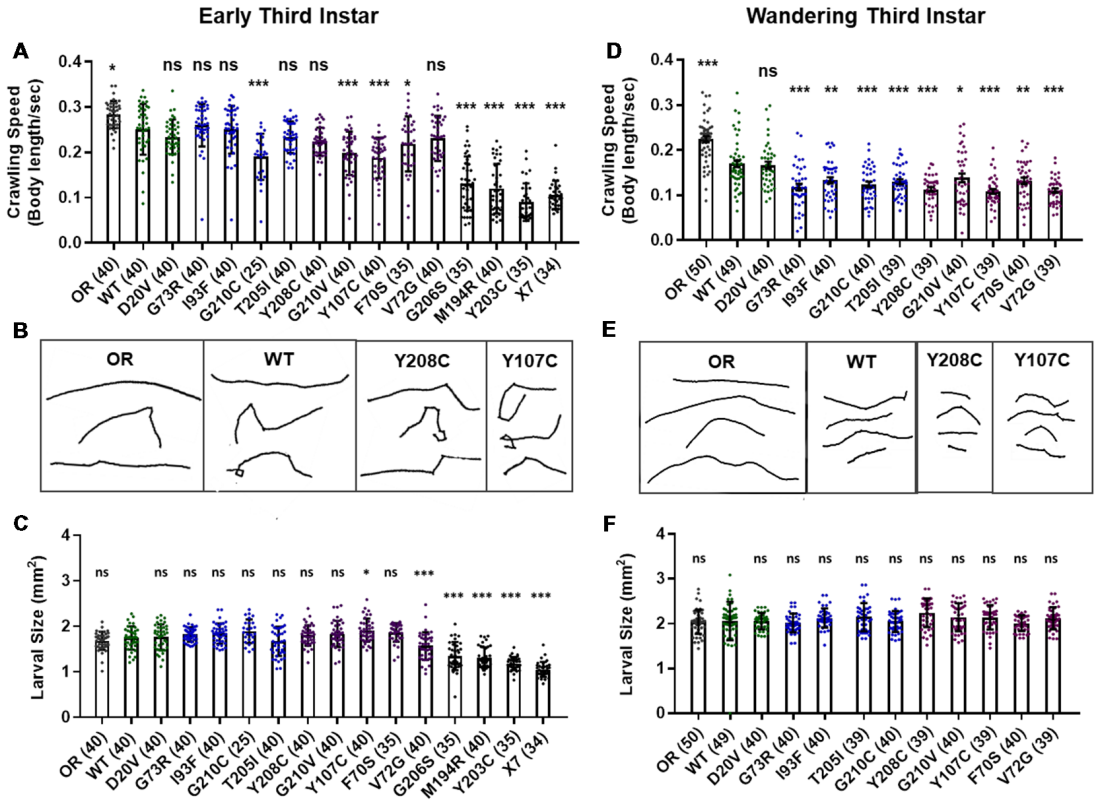

FIGURE 2 | *Smn* missense mutations or knockdown reduce larval locomotion. **(A)** Larval crawling speed, measured in body lengths/s, in early third instar larvae. **(B)** Representative traces for the data shown in **(A)**. **(C)** Larval size for the same animals measured in the locomotion assay in **(A)**. **(D)** Larval crawling speed, measured in body lengths per second, in wandering third instar larvae. **(E)** Representative traces for the data shown in **(D)**. **(F)** Larval size for the same animals measured in the locomotion assay in **(D)**. Data: bars show averages, points represent individual larvae, error bars represent standard error, *n*-values (# individual larvae) are shown in parentheses adjacent to genotype on x-axis. Statistical significance was determined by ANOVA (ns = not significant, $*p < 0.05$, $**p < 0.01$, $***p < 0.001$).

potential progressive degenerative phenotypes, we turned to the adult stages.

Smn Missense Mutations and Neuromuscular Knockdown Reduce Adult Longevity

Ten lines expressing transgenic *Smn* alleles produce viable adults to varying degrees (**Figure 1A**). We first used these adults to assess longevity, with the expectation that *Smn* mutations would shorten lifespan. Animals of the control Oregon R strain lived as long as 12 weeks, with 90% of individuals dying by 11 weeks of age (**Figures 4A–D**, gray line). The line expressing transgenic *Smn* (WT) is moderately hypomorphic and shows a significant decrease in longevity as compared to OR, with increased death occurring by week 4 in the case of WT (**Figures 4A–C**).

All other lines expressing missense *Smn* alleles show a further, statistically significant reduction in longevity relative to WT (**Figures 4A–D**). The Class IV mutation, D20V, begins to display impaired longevity relative to WT beginning at week 7 and 90% of animals carrying this mutation are decreased by 7.6 weeks of age (**Figures 4A,D**). The decrease in longevity is more pronounced for the Class III mutations G73R (**Figure 4A**), I93F, T205I, and G210C (**Figure 4B**), which begin to deviate from WT between 3 and 6 weeks of age (**Figures 4B,C**) and reach 90% death by 6–7 weeks (**Figure 4D**). The Class II mutations (G210V, Y208C, Y107C, and F70S) are the most severely impacted, with significant death occurring as early as the first week of life (**Figures 4C,D**).

We next sought to assess the possibility that the reduced longevity observed for missense *Smn* lines is related to neuromuscular health. To do so, we again turned to RNAi-mediated *Smn* knockdown in the neuromusculature. The C15 Gal4 driver line was used to express each of the two *UAS-Smn-RNAi* constructs in adult flies. To maximize shRNA expression, flies were raised at 29°C which increases the efficiency of the yeast-derived Gal4 protein as a transcriptional activator. Under these conditions, the OR strain displays reduced longevity/lifespan relative to other controls such as the Gal4 alone (C15/+) or the Smn-RNAi constructs alone (Smn-RNAi/+; **Figures 4E–G**). Neuromuscular expression of Smn-RNAi #1 moderately affected longevity relative to the C15/+ and Smn-RNAi #1/+ controls, although they outlived the OR controls (**Figures 4E,G**). The effect with Smn-RNAi #2 was much stronger, with all animals expiring within the first week

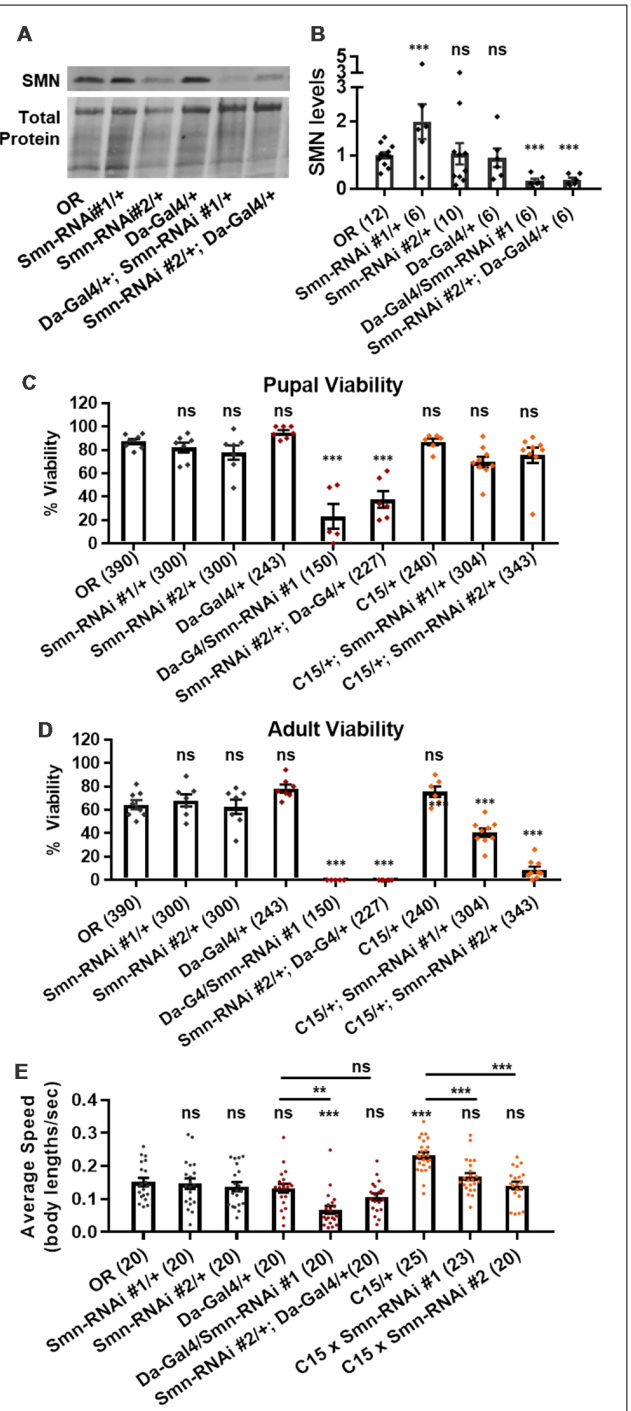

FIGURE 3 | Neuromuscular *Smn* knockdown reduces viability and larval locomotion. **(A)** Representative western blot of SMN levels and total protein (loading control). **(B)** Quantification of SMN levels on western blot replicates. SMN levels are divided by total protein levels to control for loading and normalized to OR for comparison between blots. **(C,D)** Developmental viability at the pupal stage **(C)** and adult stage **(D)** for animals expressing *Smn* missense mutations. % Viability is the proportion of animals the survive to the pupal/adult stage relative to the number of larvae initially collected. **(E)** Larval crawling speed, measured in body lengths/second, in early third instar larvae. Data: bars show average. Error bars show standard error. For **(A,B)**, data (*Continued*)

FIGURE 3 | Continued
points represent biological replicates of 30–50 animals each, *n*-values (shown in parentheses next to genotypes) reflect the number of individual animals counted. For **(C)**, data points and *n*-values (shown in parentheses next to genotypes) reflect the number of individual animals assayed. Statistical analysis: values above the data indicate significance vs. WT from one-way ANOVA using the Dunnet correction for multiple comparisons. ns: not significant ($p > 0.05$), $^{*}p < 0.05$, $^{**}p < 0.01$, $^{***}p < 0.001$.

of life (**Figures 4F,G**). These findings suggest that the longevity defects observed in the case of missense *Smn* alleles are due, at least in part, to loss of *SMN* function in neurons and muscles.

Smn Missense Alleles and Neuromuscular Knockdown Reduce Adult Locomotion

To more directly assess neuromuscular function in adult flies we performed an adult locomotion assay on free moving animals in a circular chamber with restricted vertical space to prevent flight. Flies were collected and assayed within 24–36 h after eclosing (**Figure 5**) and after aging for 5 and 6 weeks in certain cases (**Figure 6**). At 1 day of age, both Class IV alleles (WT and D20V) and two of the Class III alleles (G73R and I93F) showed robust locomotor behavior. These animals display walking speeds that are slightly faster than that of the Oregon R wild type strain and are not significantly different from one another (**Figures 5A,B**). The remaining Class III alleles (T205I and G210C) showed a moderate but significant decrease relative to the WT transgenic line. The Class II alleles showed robust and significant impairment in their locomotor behavior relative to both WT and Oregon R (**Figures 5A,B**).

Similar effects were observed for both ubiquitous and neuromuscular knockdown of *Smn* (**Figures 5C–E**). As was the case for larval locomotion, Gal4 expression alone leads to increased adult walking speeds. Relative to Gal4 controls, ubiquitous *Smn* knockdown using the Smn-RNAi #2 line produces a moderate but significant reduction in adult walking speed (**Figure 5C**). Neuromuscular *Smn* knockdown with Smn-RNAi #2 also reduces walking speed relative to both the C15 Gal4 line control and the Oregon R wild type strain. In this case, the reduction was dramatic, as many animals remained essentially stationary during the assay (**Figures 5D,E**). This finding suggests that the locomotor defects observed in animals expressing mutant *Smn* alleles are due to dysfunction in neuronal and/or muscular tissues. Collectively, these data suggest that the adult stage can be used to model SMA-related phenotypes in the fly.

Class IV and Class III Smn Missense Alleles Are Models for Late-Onset SMA

Three missense *Smn* alleles (D20V, G73R, and I93F) displayed robust adult locomotor behavior at 1 day of age (**Figures 5A,B**). In contrast, these lines also show reduced longevity as adults (**Figure 4**), mildly reduced viability (**Figure 1**), and impaired locomotion as larvae (**Figure 2**). These results indicated that these mutations have a relatively mild impact on *SMN* function and led us to hypothesize that these lines might be useful for modeling late-onset SMA. To test this, we aged flies carrying

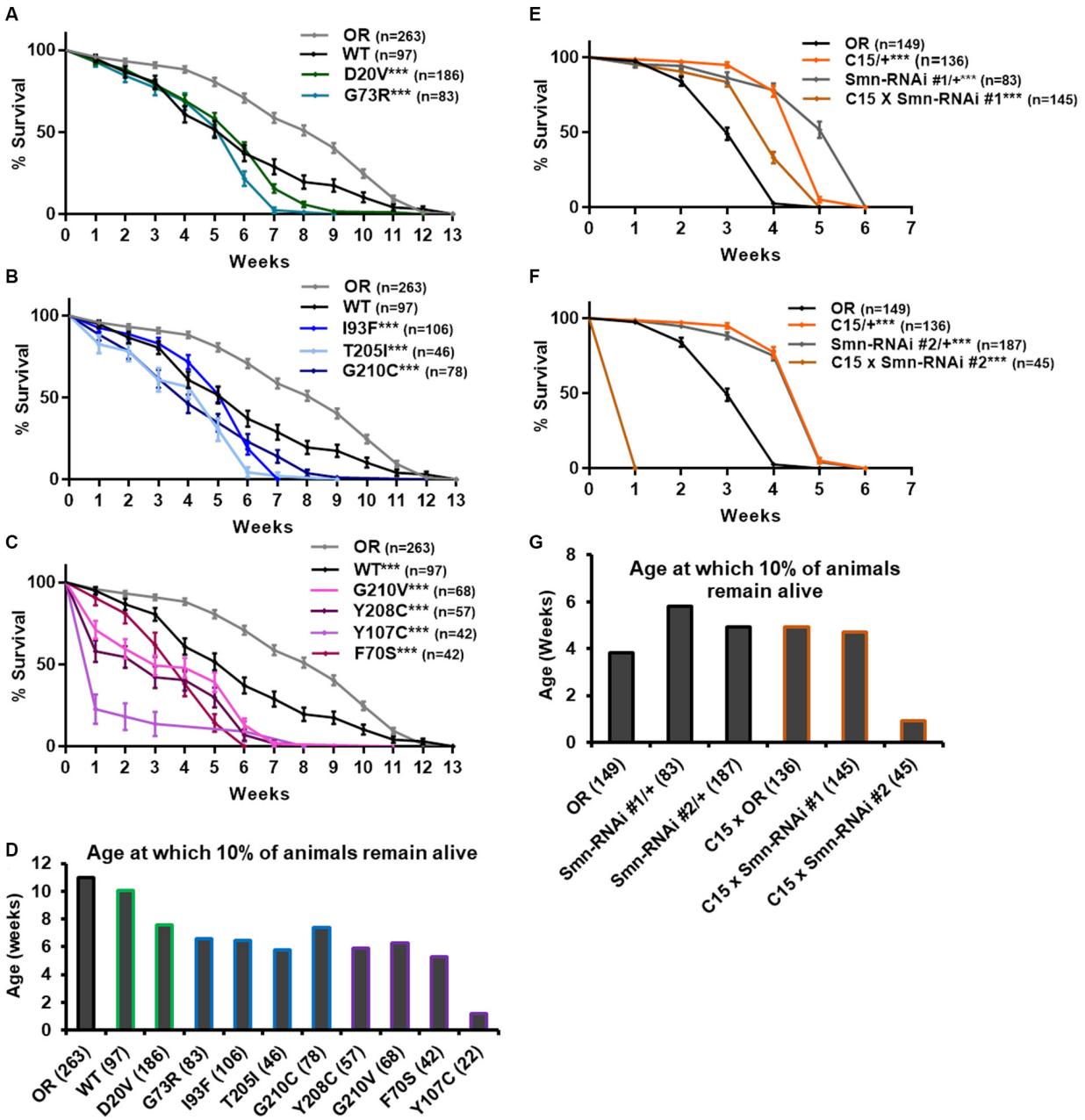

FIGURE 4 | *Smn* missense mutations and *Smn* knockdown reduce lifespan. **(A–C)** Survival curves for adult flies expressing *Smn* missense mutations. Data is split into three graphs for visual clarity. Colors correspond to phenotypic Class. **(D)** Lifespan measured as the age at which 10% of animals remain alive for each missense mutation. **(E,F)** Survival curves for adult flies expressing Smn-RNAi in all neurons and muscles. **(G)** Lifespan measured as the age at which 10% of animals remain alive for each RNAi condition and control. Shown next to genotypes, *n*-value (# of individual flies), *** indicates $p < 0.0001$ by Chi square analysis using the logrank rank/Mantel-Cox test.

each of these three mutations as well as animals expressing the WT *Smn* transgene and assayed adult walking behavior weekly (**Figure 6A**). By 5 weeks of age, flies expressing the D20V, G73R, or I93F mutant *Smn* all showed a significant reduction in walking speed relative to the animals expressing the WT *Smn* transgene (**Figures 6A,B,D**). This decline persisted into the 6th week of life (**Figures 6A,C,D**), but could not be effectively assessed beyond that point due to the limited number of animals that survive into the 7th week of life. Interestingly, this decline in locomotor function occurs 1–2 weeks prior to the time at which most of these flies began to die in the longevity assay (**Figure 4**), consistent with a causative link between the locomotor deficit

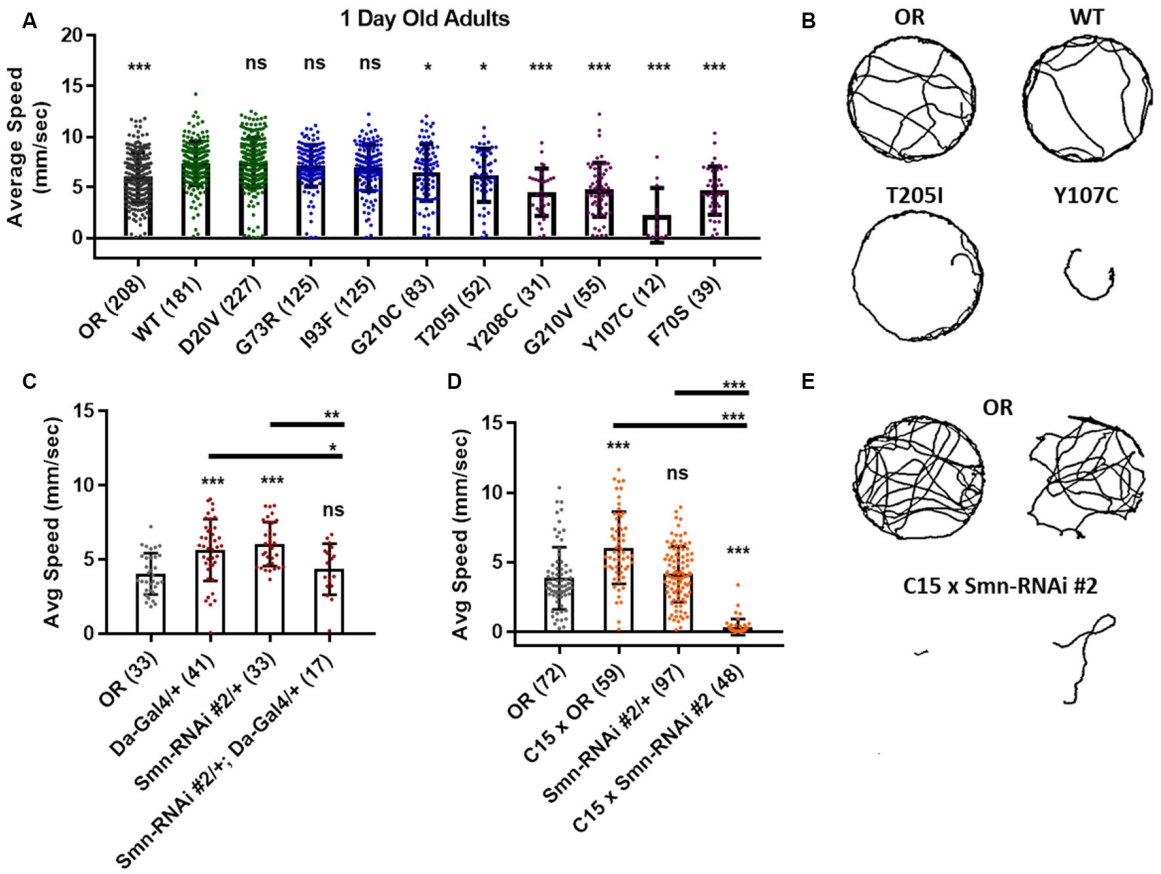

FIGURE 5 | *Smn* missense mutations or knockdown reduces free moving adult locomotion. **(A)** Adult walking speed, measured in mm/s, in adults 1 day after eclosion for animals expressing *Smn* missense mutations. **(B)** Representative traces for the data shown in **(A)**. **(C,D)** Adult waking speed, measured in mm/s, in adults 1 day after eclosion for animals expressing *Smn-RNAi* either ubiquitously with the da-Gal4 driver **(C)** or in both neurons and muscle using the C15 driver line **(D)**. **(E)** Representative traces for the data shown in **(D)**. Data: bars show average. Error bars show standard error. Data points and *n*-values (shown in parentheses next to genotypes) reflect the number of individual animals assayed. Statistical analysis: values above the data indicate significance vs. WT from one-way ANOVA using the Dunnet correction for multiple comparisons. ns: not significant ($p > 0.05$), $^{*}p < 0.05$, $^{**}p < 0.01$, $^{***}p < 0.001$.

and death. Based on this late-onset locomotor dysfunction, we conclude that these lines represent the first models of late-onset SMA that involve onset of dramatic impairment of locomotor function at an advanced age.

Smn Mutant Alleles and Knockdown Cause Progressive Loss of Motor Function

We analyzed the more severe Class II lines for progressive loss of motor function. We noticed that certain animals failed to fully eclose from their pupal cases and ultimately died (**Supplementary Figures S3A,B**). This phenotype was most prevalent for the intermediate Class III mutations and was less frequently observed for the more severe Class II mutations. This inverse relationship between allele severity and incidence of partial eclosion is likely due to the fact that most animals carrying Class II mutations arrest prior to reaching these later stages of development (**Figures 1A,B**).

We hypothesized that partial eclosion occurs in part due to severe muscle weakness in a subset of animals expressing missense *Smn*. To test this, we selected two lines, Y208C and G210V, which are both phenotypically severe in other assays yet produce enough late-stage animals to make analysis feasible. We monitored pupae for these lines on an hourly basis to identify animals that were unable to escape their pupal cases. Once identified, forceps and microdissection scissors were used to help these animals complete eclosion ("assisted eclosion"). We first put these animals through the adult locomotion assay and found that they had very low walking speeds and in many cases did not move at all (**Supplementary Figure S3C**). Additionally, the lifespan of these animals was dramatically reduced relative to both wild type and normally eclosing adults of the same genotype (**Supplementary Figure S3D**, **Figures 4C,D**). All animals examined died within 6 days of assisted eclosion (**Supplementary Figure S3D**). To ensure that our assisted eclosion techniques were not harming the animals or impairing their locomotor function or survival, we performed the same procedure on Smn^{WT} (WT) pharate adults. Analysis of lifespan and locomotor

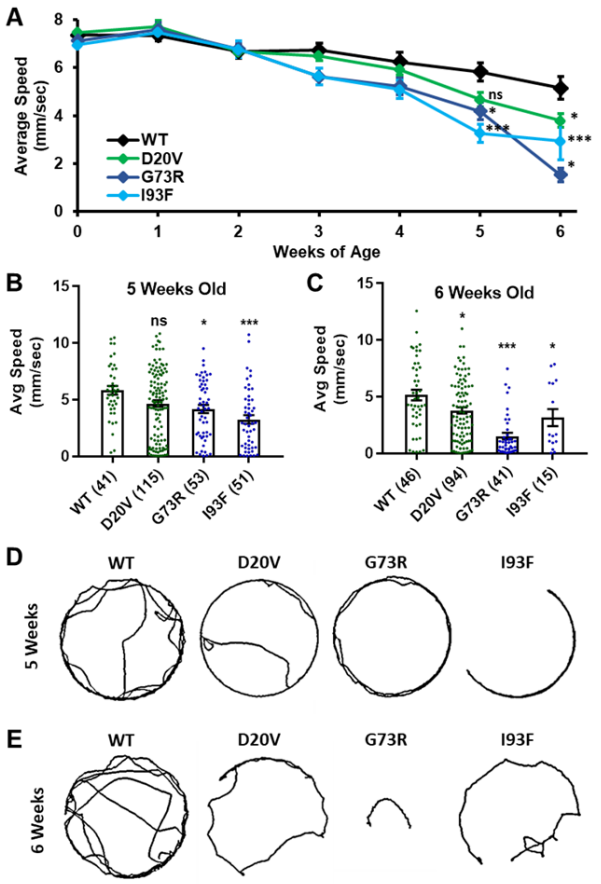

FIGURE 6 | Animals expressing mild *Smn* missense mutations develop late-onset locomotor defects as adults. **(A)** Adult walking speed, measured in mm/s, in adults ranging from 1 day of age (0 weeks) through 6 weeks of age for animals expressing the WT transgene or the D20V, G73R, I93F *Smn* missense mutations. **(B,C)** Adult walking speed (mm/s) for the same genotypes shown in **(A)** at either 5 weeks of age **(B)** or 6 weeks of age **(C)**. **(D)** Representative traces for the data shown in **(B)**. **(E)** Representative traces for the data shown in **(C)**. Data: in **(A)**, points show averages in **(B,C)**, bars show average. Error bars show standard error in all cases. Data points and *n*-values (shown in parentheses next to genotypes) reflect the number of individual animals assayed. Statistical analysis: values above the data indicate significance vs. WT from one-way ANOVA using the Dunnet correction for multiple comparisons. ns: not significant ($p > 0.05$), *$p < 0.05$, **$p < 0.01$, ***$p < 0.001$.

function of these animals was included for control purposes. As expected, the WT animals were unaffected by the manipulation (**Supplementary Figures S3C,D**).

Similar phenotypes were also observed for animals expressing neuromuscular knockdown of *Smn* with Smn-RNAi #2. These animals are able to eclose without assistance but display severe adult locomotor dysfunction in the adult walking assay 1 day after eclosion (**Figures 5F,G**). Neuromuscular *Smn* knockdown also leads to dramatically reduced lifespan almost identical to that seen for the partially eclosed animals examined, with all animals dying within 6 days of life (**Supplementary Figure S3E**).

Although walking speed was near zero for all of the mutant lines discussed above, qualitative observation suggested that these animals were not fully paralyzed and retained some degree of motor control over their legs at the time of assisted eclosion. To determine if motor control deteriorated over time in these animals, we turned to qualitative observation and scoring of locomotor function in a manner similar to the clinical analysis of human patients. For 10–30 individual animals per genotype, we monitored leg function under the stereoscope for 1–2 min and assigned a leg score for each of the three leg pairs. Scoring was performed on a scale of 0–10, with complete paralysis scored as 0 and normal function scored as 10. Scoring was performed every 4–8 h for the first 12 h of life, followed by observation every 24 h until death occurred. Using this method, we determined that partially eclosed flies expressing G210V and Y208C mutant *Smn* experience progressive loss of leg function over time (**Figure 7A**). This is the first report of progressive loss of motor function in any fly model of SMA.

Interestingly, individual leg pairs were differentially affected at the time of assisted eclosion. The most anterior pair initially presented with mild to moderate impairment, whereas the most posterior pair was more severely impaired. The function of all three leg pairs decreases over time, and the defects in the anterior and posterior limbs become more similar over time (**Figures 7B–D**). This is reminiscent of SMA disease progression in human patients who often develop muscle weakness in the legs prior to onset of in the arms.

Similar defects in leg function were observed upon examination of animals expressing Smn-RNAi #2 in neurons and muscles. Progressive loss of motor function was observed for all legs in aggregate (**Figure 7E**), and for individual leg pairs (**Figures 7F,G**). Additionally, we noted the same differential impact on individual leg pairs, with the anterior pair initially displaying much milder dysfunction than the most posterior pair (**Figures 7F,G**). None of these effects was observed for Oregon R controls reared and scored in the same manner (**Figures 7E,F**). Overall, the progressive loss of motor function and differential timing of affectation between posterior and anterior leg pairs suggests that these fly models of SMA are useful for modeling nuanced aspects of SMA onset and progression and suggest that highly specific mechanisms of SMA are conserved in fly.

CONCLUSION AND DISCUSSION

We carried out a systematic assessment of disease-related phenotypes in a set of *Drosophila* SMA models at multiple developmental stages. This work was performed in larvae and adult flies expressing one of 13 human patient-derived *Smn* missense mutations as well as flies expressing ubiquitous or neuromuscular-specific *Smn* knockdown. In larvae, we identified defects in developmental viability and locomotor function in the absence of overt muscle degeneration, leading to the conclusion that the larval stages are best suited to study of pre- and early onset stages of SMA. For the lines that reached the adult stage, we observed reduced longevity and locomotor defects with variable age of onset. Thus, the fly can be used to model progressive loss of motor function in SMA. We also report, for the first time in a model system, three alleles for late-onset (Type IV) SMA. Collectively, this set of SMA models provides a highly useful

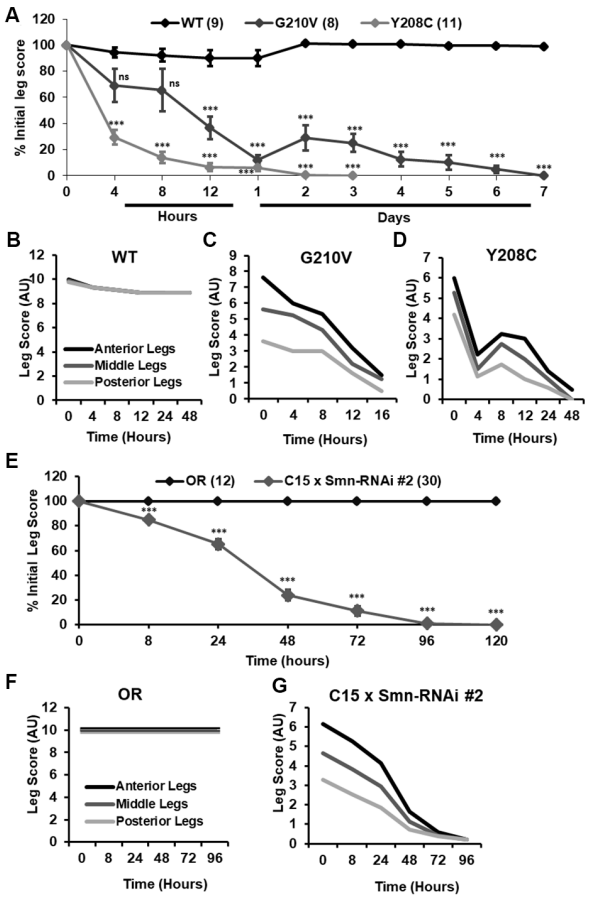

FIGURE 7 | Progressive loss of motor function is observed in the legs of partially eclosed *Smn* missense mutants and in animals expressing neuromuscular Smn knockdown. **(A)** Qualitative leg function scores (average or all three leg pairs) over time for partially eclosed animals expressing the wild type *Smn* transgene (n = 11) or the Y208C (n = 10) or G210V (n = 7) *Smn* missense mutations. **(B–D)** Qualitative leg function scores for each leg pair over time for same animals as in **(A)**. **(E)** Qualitative leg function scores (average or all three leg pairs) over time for animals expressing neuromuscular *Smn* knockdown. **(F,G)** Qualitative leg function scores for each leg pair over time for the same animals as in **(E)**. Statistical analysis: values above the data indicate significance vs.WT from one-way ANOVA using the Dunnet correction for multiple comparisons. ns: not significant ($p > 0.05$), $p < 0.05$, $p < 0.01$, $p < 0.001$.

system for studying all stages of SMA pathogenesis across the full spectrum of disease severity.

Modeling SMA in Adult Stage *Drosophila*

This study presents the first report of adult models of SMA in the fly, providing an opportunity to distinguish severe developmental complications from neuromuscular phenotypes. In typical cases, SMA patients appear healthy and normal at the time of birth with onset of impaired motor function occurring months or years after birth. Creating models that mimic this aspect of SMA has been difficult in the mouse, as most genetic manipulations that are sufficient to produce neuromuscular phenotypes also cause animals to be small, underdeveloped, and severely affected at the time of birth (Hsieh-Li et al., 2000; Monani et al., 2000). Pups for these models fail to grow significantly and die in the first weeks of life, reminiscent of Type 0 SMA in humans. Our Class III and IV fly models produce adults of normal size that appear otherwise healthy upon eclosion. These animals continue to mature as normal until they die between 1 and 7 weeks of life (control flies live for 12–13 weeks). Using animals that successfully progress through all developmental stages allows for separation of SMA phenotypes from gross developmental issues. This is important, as developmental arrest can independently affect mRNA processing and gene expression, nervous system development and growth, as well as many other phenotypes relevant to the study of SMA (Carrel et al., 2006; McWhorter et al., 2008; Garcia et al., 2013, 2016; Perez-Garcia et al., 2017). The ability to avoid these complications with genetic models that develop normally adds a valuable tool to the field of SMA research.

Modeling Intermediate Forms of SMA

Mouse models for late-onset SMA have been difficult to generate. Copy number changes in human *SMN2* transgenes or C >T mutation of the endogenous mouse *Smn* allele cause dramatic shifts in phenotype from mild and largely unaffected to very severe with onset of symptoms *in utero* and death between 4 and 14 days after birth (Hsieh-Li et al., 2000; Monani et al., 2000). Addition of partially functional SMN-producing genes, such as *SMNΔ7* or *SMN2* leads to a similar bifurcation of phenotypes (Le et al., 2005; Osborne et al., 2012). Depending on the gene dose, mice are either strongly affected at birth or completely rescued throughout life. This binary relationship between SMN dosage and phenotype in mice has led to a dearth of robust mouse models of intermediate SMA. Consequently, the processes that precede onset of neuromuscular dysfunction and motor neuron death have been difficult to study in murine systems.

In the fly, we observe a more continuous range of phenotypic severity across many assays in the context of hypomorphic SMN levels and partial function. The mildest *Smn* missense mutations we assessed (D20V, G73R, and I93F) are phenotypically wild type at the time of eclosion. By 5 weeks of age, however, flies carrying these mutations begin to show locomotor dysfunction and expire after 1–3 additional weeks of life. Based on these observations, we assert that these three *Smn* missense mutations model moderate, later-onset Type III and IV SMA. These models will be a useful tool in examining the full range of SMA disease progression from pre-onset changes to organismal death in a single biological context.

SMN Missense Mutations Are Partially Functional in the Absence of Wild Type SMN Protein

Together with previous work (Praveen et al., 2014; Garcia et al., 2016; Gray et al., 2018), the data presented here demonstrate that many SMN missense mutations retain partial function. As discussed above, the maternal contribution of SMN complicates this interpretation in early larval stages. By the beginning of the third instar larval stage, however, the maternal contribution

is fully depleted and complete lack of SMN rapidly leads to developmental arrest and death. In our models, transgenic *Smn* is expressed from the native promotor throughout the life of the organism. In this context, we observe survival to differential degrees and developmental stages for each *Smn* missense mutations. These findings demonstrate that *Smn* missense mutations specifically modify the null phenotype and are inconsistent with the notion that they extend viability due to secondary effects caused by non-specific stabilization of the maternal contribution.

Furthermore, we successfully generated stable, viable fly stocks that exclusively express certain missense alleles of *Smn* in an otherwise *Smn* null background (*Flag-Smn*^{TG}, *Smn*^{X7}/*Smn*^{D}). These animals are viable and fertile in the absence of any wild type SMN at any stage of their development, providing conclusive evidence that *Smn* missense mutations are at least partially functional. Given the conservation of SMN protein structure from invertebrates to vertebrates, we expect that this finding holds true in human patients as well. Our results contrast with those of a recent report using the SMNΔ7 mouse model, claiming that two mild patient-derived missense mutations (D44V and T274I) are non-functional in the absence of full-length SMN (Iyer et al., 2018). This assertion is based on a single finding: that mice expressing only *SMN* missense mutations do not survive to birth. While this result clearly indicates that these two *SMN* missense mutations are not fully functional, it by no means rules out the possibility of partial function.

Smn null mice arrest at the blastula stage of embryonic development (Schrank et al., 1997). Missense alleles that fully lack function would be expected to arrest at the same stage as the null allele. Unfortunately, neither this stage nor any other embryonic stage was assessed in the context of the D44V or T274I mutations to determine if *SMN* missense mutations partially rescue embryonic development (Iyer et al., 2018). Notably, all of the human *SMN* missense alleles analyzed in the mouse to date have been expressed from randomly-integrated, variable copy number, cDNA-based transgenes (Gavrilina et al., 2008; Workman et al., 2009; Iyer et al., 2018). Moreover, none of these studies uses a wild-type cDNA control, so it is difficult to compare the transgenic lines without the ability to control for expression levels, position effects, or secondary mutations caused by integration.

Indeed, transgenic rescue of embryonic lethality using human *SMN* constructs in the mouse is fraught with complication. Mice expressing two randomly-inserted cDNA copies of *SMN*Δ*7* die within 5 days of birth when crossed onto the FVB background (Monani et al., 2000). However, this same *SMN*Δ*7* transgene completely fails to rescue embryonic lethality when crossed onto a C57/BL6 background (Gogliotti et al., 2011; Osborne et al., 2012; Meier et al., 2018). Expressing one or two copies of human *SMN2* in an *Smn* null background is also insufficient to rescue embryonic lethality in mouse (Osborne et al., 2012). These results are in contrast to the effects of manipulating SMN expression from the endogenous mouse locus. Mice bearing a C > T mutation in exon 7 of the endogenous *Smn* gene (mimicking human *SMN2*) are fully viable and fertile (Gladman et al., 2010; Hammond et al., 2010). Further, these mice live a normal lifespan when the C > T allele is present in either the homozygous or hemizygous state, displaying mild adult-onset phenotypes (Gladman et al., 2010). This incongruity suggests that expression of randomly-inserted human *SMN* cDNAs is suboptimal in the context of restoring mouse viability. In fact, there is no evidence that a wild-type human *SMN* cDNA transgene can rescue mouse viability, as such a line has yet to be reported. For all of these reasons, additional work is needed in this area.

Concordance Between SMA Severity and *Drosophila* Phenotypes

The missense mutations examined here impact residues in the SMN protein that are well conserved from fly to human. Thus, we expect that mutating these residues will cause similar changes in SMN protein function and/or stability in both species. An indirect approach to assess this expectation is to compare the severity of SMA-related phenotypes in flies and SMA Type in humans. This analysis is somewhat complicated by several factors.

First, the diagnosis and classification of SMA have changed significantly over the 20-year period since the first *SMN1* missense mutations were reported. Thus, cross comparison of severity between patients diagnosed in different decades is imperfect. For example, a severe patient diagnosed with Type I SMA that was reported in the late 1990s might be diagnosed as a Type 0 patient in the 2010s. Similarly, a patient diagnosed as Type II two decades ago might be considered a Type III patient today.

Second, a major complicating factor is *SMN2* copy number. In several reports of missense mutations from the late 1990s, the *SMN2* copy number of the patient was neither assessed nor reported (**Supplementary Table S2**). Given the strong influence that *SMN2* copy number has on SMA severity, lack of this information prevents reasonable comparisons of human and fly SMA phenotypes. As mentioned above, genetic background is also known to modify SMA severity. Moreover, *SMN1* missense mutations are extremely rare and often reported in single patients or a pair of affected siblings whose disease severity is impacted by genetic background to an unknown degree.

From the perspective of the fly models, there are far fewer complicating genetic factors to consider. The 14 Flag-tagged *Smn* lines described here were generated in a single genetic background, with a single copy of the transgene inserted at the identical chromosomal location. This approach allows for direct, reliable comparison of phenotypic severity between patient mutations in the fly. An important caveat is that fly development includes multiple body plans (larval vs. adult) and stages of development (embryonic, larval, and pupal) prior to the adult stage and it is, therefore, difficult to directly compare to the relatively linear process of human development. For example, it is unclear how the onset of symptoms in larval stages compares to the age of onset in human development. Due to this uncertainty, phenotypic Class and SMA Type are not expected to align in terms of their number-designation. However, we do expect to see a correlation between human SMA Type and *Drosophila* Class designations, with the most

TABLE 1 | Alignment of phenotypic severity between human and fly.

Human protein	Fly protein	SMN2 Copy #	SMA Type	Fly phenotypic class
D44V	D20V	1	III	IV
G95R	G73R	1	III	III
I116F	I93F	1	I	III
T274I	T205I	1/2	II/III	III
Y277C	Y208C	1	II	II
W92S	F70S	3	I	II
V94G	V72G	3	II	II
M263R	M194R	2	I	I
Y272C	Y203C	1/2/3	I/II/III	I

*Smn missense mutations are shown in order of least severe to most severe, based on fly genotypes, with the corresponding information from human patients. The four missense mutations with unknown SMN2 copy number (Y107C, G206S, G210C, and G210V, shown in **Table 1**) have been excluded here to prevent potentially inaccurate comparisons.*

severe human mutations also being the most severe in fly and vice versa.

Indeed, the information in **Table 1** reveals that in almost every case, the severity observed in the fly is well aligned with human SMA Type. The one exception is the I93F/I116F mutant. Given that this mutation has only been observed in a single human patient, it is difficult to determine whether this residue may not be as functionally important for fly SMN as it is for human, or if confounding factors such as genetic background might enhance the SMA severity independent of *SMN1*.

In all other cases, we observe strong concordance between the phenotypic severity of fly and human. For example, the fly mutations Y203C and M194R cause the most severe phenotype in flies, phenocopying null alleles. The same is seen in human patients carrying Y272C and M263R mutations, which also phenocopy the *SMN1* null state in causing Type 1 SMA in the presence of 1 or 2 copies of *SMN2*. On the other end of the spectrum, the D44V, G95R, and T274I mutations appear to *improve* the SMA Type in patients, relative to the severity expected based on *SMN2* copy number. For example, humans hemizygous for both *SMN2* and $SMN1^{T274I}$ display a relatively mild, Type II phenotype. Flies expressing the corresponding mutations (D20V, G73R, and T205I) are also mildly affected, with G73R and D20V causing adult-onset of locomotor defects. Overall, when appropriately considering SMA Type and *SMN2* copy number, we conclude that SMN missense mutations modeled in the fly faithfully recapitulate the human phenotypes.

AUTHOR CONTRIBUTIONS

AS designed the study, performed the majority of experiments, and wrote and edited the manuscript. AR provided feedback on experimental design and performed experiments. CH and MS performed experiments. AM provided feedback on experimental design and edited the manuscript.

FUNDING

This work was supported by a grant from the US National Institute of General Medical Sciences (NIGMS; R01-GM118636, 2016; to AM). AS was supported by a Seeding Postdoctoral Innovators in Research and Education (SPIRE) fellowship from the National Institutes of Health (NIH; K12-GM000678; to D.T. Lysle).

ACKNOWLEDGMENTS

We thank C.A. Frank for providing the C15 Gal4 driver line. Note, a version of this manuscript has been posted on a pre-print server (Spring et al., 2018).

SUPPLEMENTARY MATERIAL

The Supplementary Material for this article can be found online at: https://www.frontiersin.org/articles/10.3389/fnmol.2019.00113/full#supplementary-material

FIGURE S1 | Survival Motor Neuron (*Smn* missense mutations are sufficient for viability in the absence of maternally contributed wild type SMN. **(A,B)** Developmental viability at the pupal stage **(A)** the adult stage **(B)** stable lines expressing only *Smn* missense mutations with maternal contribution of WT Smn present. Data: bars show average. Error bars show standard error. Data points represent biological replicates of 50 animals each, *n*-values (shown in parentheses next to genotypes) reflect the number of individual animals counted. Statistical analysis: values above the data indicate significance vs. WT from one-way ANOVA using the Dunnet correction for multiple comparisons. ns: not significant ($p > 0.05$), *$p < 0.05$, **$p < 0.01$, ***$p < 0.001$.

FIGURE S2 | Survival Motor Neuron (*Smn*) missense mutations or knockdown has modest effects on neuromuscular junction (NMJ) structure. **(A)** Bouton counts from the muscle 6/7 NMJ in wandering third instar larvae. **(B–B″)** Representative images for the data shown in **(A)** for the OR **(B)**, WT **(B′)**, and V72G **(B″)** gentypes. Red marks Discs Large (Dlg), green marks synapsin (syn), and blue marks neuronal membranes. **(C)** Muscle 6/7 combined area for the NMJs measured in **(A)**. Data: bars show average. Error bars show standard error. Data points and n-values (shown in parentheses next to genotypes) reflect the number of individual neuromuscular junctions **(A)** or muscles **(C)** assayed. Statistical analysis: values above the data indicate significance vs. WT from one-way ANOVA using the Dunnet correction for multiple comparisons. ns: not significant ($p > 0.05$), $p < 0.05$, $p < 0.01$, $p < 0.001$.

FIGURE S3 | *Smn* missense mutants exhibit defects in eclosion. **(A)** Percent of total larvae that complete pupal development but only partially eclose from their pupal case. **(B)** Representative images of the partial eclosion phenotype quantified in **(A)**. **(C)** Adult walking speed (mm/s) for partially eclosed animals expressing the wild type *Smn* transgene or the Smn missense mutations Y208C or G210V. **(D)** Survival curve for the same animals assayed in **(C)**. **(E)** Survival curve for animals expressing neuromuscular *Smn* knockdown. Data: bars show average. Error bars show standard error. Data points and *n*-values (shown in parentheses next to genotypes) reflect the number of individual animals assayed. Statistical analysis: for **(A,C)**, values above the data indicate significance vs. WT from one-way ANOVA using the Dunnet correction for multiple comparisons. For **(D,E)**, values next to each survival curve represent *p*-values generated by Chi square analysis using the logrank rank/Mantel-Cox test. ns: not significant ($p > 0.05$), *$p < 0.05$, **$p < 0.01$, ***$p < 0.001$.

TABLE S1 | Information on all statistical analysis. Statistical analysis was performed using GraphPad Prism 7 and includes corrections for multiple comparisons when appropriate.

TABLE S2 | SMN missense mutation information from human patients and fly. When multiple SMA types and *SMN2* copy numbers are present, the order of the information for each criterion corresponds such that the first SMA type shown corresponds to the first *SMN2* copy number listed for a given mutation and so on and forth.

REFERENCES

Aquilina, B., and Cauchi, R. J. (2018). Modelling motor neuron disease in fruit flies: lessons from spinal muscular atrophy. *J. Neurosci. Methods* 310, 3–11. doi: 10.1016/j.jneumeth.2018.04.003

Atkinson, D., Nikodinovic Glumac, J., Asselbergh, B., Ermanoska, B., Blocquel, D., Steiner, R., et al. (2017). Sphingosine 1-phosphate lyase deficiency causes Charcot-Marie-Tooth neuropathy. *Neurology* 88, 533–542. doi: 10.1212/WNL.0000000000003595

Bischof, J., Maeda, R. K., Hediger, M., Karch, F., and Basler, K. (2007). An optimized transgenesis system for *Drosophila* using germ-line-specific phiC31 integrases. *Proc. Natl. Acad. Sci. U S A* 104, 3312–3317. doi: 10.1073/pnas.0611511104

Bowerman, M., Becker, C. G., Yáñez-Munoz, R. J., Ning, K., Wood, M. J. A., Gillingwater, T. H., et al. (2017). Therapeutic strategies for spinal muscular atrophy: SMN and beyond. *Dis. Model. Mech.* 10, 943–954. doi: 10.1242/dmm.030148

Brooks, D. S., Vishal, K., Kawakami, J., Bouyain, S., and Geisbrecht, E. R. (2016). Optimization of wrMTrck to monitor *Drosophila* larval locomotor activity. *J. Insect. Physiol.* 93–94, 11–17. doi: 10.1016/j.jinsphys.2016.07.007

Brusich, D. J., Spring, A. M., and Frank, C. A. (2015). A single-cross, RNA interference-based genetic tool for examining the long-term maintenance of homeostatic plasticity. *Front. Cell. Neurosci.* 9:107. doi: 10.3389/fncel.2015.00107

Budnik, V., Koh, Y. H., Guan, B., Hartmann, B., Hough, C., Woods, D., et al. (1996). Regulation of synapse structure and function by the *Drosophila* tumor suppressor gene dlg. *Neuron* 17, 627–640. doi: 10.1016/s0896-6273(00)80196-8

Burghes, A. H. M., DiDonato, C. J., McGovern, V. L., and Arnold, W. D. (2017). "Mammalian models of spinal muscular atrophy," in *Spinal Muscular Atrophy: Disease Mechanisms and Therapy*, eds C. J. Sumner, S. Paushkin and C. P. Ko (San Diego: Academic Press), 241–260.

Carrel, T. L., McWhorter, M. L., Workman, E., Zhang, H., Wolstencroft, E. C., Lorson, C., et al. (2006). Survival motor neuron function in motor axons is independent of functions required for small nuclear ribonucleoprotein biogenesis. *J. Neurosci.* 26, 11014–11022. doi: 10.1523/JNEUROSCI.1637-06.2006

Chan, Y. B., Miguel-Aliaga, I., Franks, C., Thomas, N., Trülzsch, B., Sattelle, D. B., et al. (2003). Neuromuscular defects in a *Drosophila* survival motor neuron gene mutant. *Hum. Mol. Genet.* 12, 1367–1376. doi: 10.1093/hmg/ddg157

Chang, H. C., Dimlich, D. N., Yokokura, T., Mukherjee, A., Kankel, M. W., Sen, A., et al. (2008). Modeling spinal muscular atrophy in *Drosophila*. *PLoS One* 3:e3209. doi: 10.1371/journal.pone.0003209

Chaytow, H., Huang, Y. T., Gillingwater, T. H., and Faller, K. M. E. (2018). The role of survival motor neuron protein (SMN) in protein homeostasis. *Cell. Mol. Life Sci.* 75, 3877–3894. doi: 10.1007/s00018-018-2849-1

Crawford, T. O. (2017). "Standard of care for spinal muscular atrophy," in *Spinal Muscular Atrophy: Disease Mechanisms and Therapy*, eds C. J. Sumner, S. Paushkin and C. P. Ko (San Diego: Academic Press), 43–62.

Darras, B. T., and Finkel, R. S. (2017). "Natural history of spinal muscular atrophy," in *Spinal Muscular Atrophy: Disease Mechanisms and Therapy*, eds C. J. Sumner, S. Paushkin and C. P. Ko (San Diego: Academic Press), 399–421.

Finkel, R. S., Mercuri, E., Darras, B. T., Connolly, A. M., Kuntz, N. L., Kirschner, J., et al. (2017). Nusinersen versus sham control in infantile-onset spinal muscular atrophy. *N. Engl. J. Med.* 377, 1723–1732. doi: 10.1056/NEJMoa1702752

Garcia, E. L., Lu, Z., Meers, M. P., Praveen, K., and Matera, A. G. (2013). Developmental arrest of *Drosophila* survival motor neuron (Smn) mutants accounts for differences in expression of minor intron-containing genes. *RNA* 19, 1510–1516. doi: 10.1261/rna.038919.113

Garcia, E. L., Wen, Y., Praveen, K., and Matera, A. G. (2016). Transcriptomic comparison of *Drosophila* snRNP biogenesis mutants reveals mutant-specific changes in pre-mRNA processing: implications for spinal muscular atrophy. *RNA* 22, 1215–1227. doi: 10.1261/rna.057208.116

Gavrilina, T. O., McGovern, V. L., Workman, E., Crawford, T. O., Gogliotti, R. G., DiDonato, C. J., et al. (2008). Neuronal SMN expression corrects spinal muscular atrophy in severe SMA mice while muscle-specific SMN expression has no phenotypic effect. *Hum. Mol. Genet.* 17, 1063–1075. doi: 10.1093/hmg/ddm379

Gladman, J. T., Bebee, T. W., Edwards, C., Wang, X., Sahenk, Z., Rich, M. M., et al. (2010). A humanized Smn gene containing the SMN2 nucleotide alteration in exon 7 mimics SMN2 splicing and the SMA disease phenotype. *Hum. Mol. Genet.* 19, 4239–4252. doi: 10.1093/hmg/ddq343

Gogliotti, R. G., Lutz, C., Jorgensen, M., Huebsch, K., Koh, S., and Didonato, C. J. (2011). Characterization of a commonly used mouse model of SMA reveals increased seizure susceptibility and heightened fear response in FVB/N mice. *Neurobiol. Dis.* 43, 142–151. doi: 10.1016/j.nbd.2011.03.002

Gray, K. M., Kaifer, K. A., Baillat, D., Wen, Y., Bonacci, T. R., Ebert, A. D., et al. (2018). Self-oligomerization regulates stability of survival motor neuron protein isoforms by sequestering an SCF(Slmb) degron. *Mol. Biol. Cell* 29, 96–110. doi: 10.1091/mbc.e17-11-0627

Grice, S. J., Praveen, K., Matera, A. G., and Liu, J.-L. (2013). "Spinal muscular atrophy: insights from the fruit fly," in *Drosophila Melanogaster Models of Motor Neuron Disease*, ed. R. J. Cauchi (New York, NY: Nova Biomedical), 171–184.

Gruss, O. J., Meduri, R., Schilling, M., and Fischer, U. (2017). UsnRNP biogenesis: mechanisms and regulation. *Chromosoma* 126, 577–593. doi: 10.1007/s00412-017-0637-6

Hammond, S. M., Gogliotti, R. G., Rao, V., Beauvais, A., Kothary, R., and DiDonato, C. J. (2010). Mouse survival motor neuron alleles that mimic SMN2 splicing and are inducible rescue embryonic lethality early in development but not late. *PLoS One* 5:e15887. doi: 10.1371/journal.pone.0015887

Hsieh-Li, H. M., Chang, J. G., Jong, Y. J., Wu, M. H., Wang, N. M., Tsai, C. H., et al. (2000). A mouse model for spinal muscular atrophy. *Nat. Genet.* 24, 66–70. doi: 10.1038/71709

Hua, Y., Liu, Y. H., Sahashi, K., Rigo, F., Bennett, C. F., and Krainer, A. R. (2015). Motor neuron cell-nonautonomous rescue of spinal muscular atrophy phenotypes in mild and severe transgenic mouse models. *Genes Dev.* 29, 288–297. doi: 10.1101/gad.256644.114

Husson, S. J., Costa, W. S., Schmitt, C., and Gottschalk, A. (2013). Keeping track of worm trackers. *WormBook* doi: 10.1895/wormbook.1.156.1 [Epub ahead of print].

Iyer, C. C., Corlett, K. M., Massoni-Laporte, A., Duque, S. I., Madabusi, N., Tisdale, S., et al. (2018). Mild SMN missense alleles are only functional in the presence of SMN2 in mammals. *Hum. Mol. Genet.* 27, 3404–3416. doi: 10.1093/hmg/ddy251

Le, T. T., Pham, L. T., Butchbach, M. E., Zhang, H. L., Monani, U. R., Coovert, D. D., et al. (2005). SMNΔ7, the major product of the centromeric survival motor neuron (SMN2) gene, extends survival in mice with spinal muscular atrophy and associates with full-length SMN. *Hum. Mol. Genet.* 14, 845–857. doi: 10.1093/hmg/ddi078

Lefebvre, S., Burglen, L., Reboullet, S., Clermont, O., Burlet, P., Viollet, L., et al. (1995). Identification and characterization of a spinal muscular atrophy-determining gene. *Cell* 80, 155–165. doi: 10.1016/0092-8674(95)90460-3

Matera, A. G., Terns, R. M., and Terns, M. P. (2007). Non-coding RNAs: lessons from the small nuclear and small nucleolar RNAs. *Nat. Rev. Mol. Cell Biol.* 8, 209–220. doi: 10.1038/nrm2124

Matera, A. G., and Wang, Z. (2014). A day in the life of the spliceosome. *Nat. Rev. Mol. Cell Biol.* 15, 108–121. doi: 10.1038/nrm3742

McWhorter, M. L., Boon, K. L., Horan, E. S., Burghes, A. H., and Beattie, C. E. (2008). The SMN binding protein Gemin2 is not involved in motor axon outgrowth. *Dev. Neurobiol.* 68, 182–194. doi: 10.1002/dneu.20582

Meier, I. D., Walker, M. P., and Matera, A. G. (2018). Gemin4 is an essential gene in mice, and its overexpression in human cells causes relocalization of the SMN complex to the nucleoplasm. *Biol. Open* 7:bio032409. doi: 10.1242/bio.032409

Mendell, J. R., Al-Zaidy, S., Shell, R., Arnold, W. D., Rodino-Klapac, L. R., Prior, T. W., et al. (2017). Single-dose gene-replacement therapy for spinal muscular atrophy. *N. Engl. J. Med.* 377, 1713–1722. doi: 10.1056/NEJMoa1706198

Mercuri, E., Darras, B. T., Chiriboga, C. A., Day, J. W., Campbell, C., Connolly, A. M., et al. (2018). Nusinersen versus sham control in later-onset spinal muscular atrophy. *N. Engl. J. Med.* 378, 625–635. doi: 10.1056/NEJMoa1710504

Mirra, A., Rossi, S., Scaricamazza, S., Di Salvio, M., Salvatori, I., Valle, C., et al. (2017). Functional interaction between FUS and SMN underlies SMA-like splicing changes in wild-type hFUS mice. *Sci. Rep.* 7:2033. doi: 10.1038/s41598-017-02195-0

Monani, U. R., Sendtner, M., Coovert, D. D., Parsons, D. W., Andreassi, C., Le, T. T., et al. (2000). The human centromeric survival motor neuron gene (SMN2) rescues embryonic lethality in $Smn^{-/-}$ mice and results in a mouse with spinal muscular atrophy. *Hum. Mol. Genet.* 9, 333–339. doi: 10.1093/hmg/9.3.333

O'Hern, P., Garcia, E. L., Hao, L. T., Hart, A. C., Matera, A. G., and Beattie, C. E. (2017). "Nonmammalian animal models of spinal muscular atrophy," in *Spinal Muscular Atrophy: Disease Mechanisms and Therapy*, eds C. J. Sumner, S. Paushkin and C. P. Ko (San Diego: Academic Press), 221–239.

Osborne, M., Gomez, D., Feng, Z., McEwen, C., Beltran, J., Cirillo, K., et al. (2012). Characterization of behavioral and neuromuscular junction phenotypes in a novel allelic series of SMA mouse models. *Hum. Mol. Genet.* 21, 4431–4447. doi: 10.1093/hmg/dds285

Pearn, J. (1980). Classification of spinal muscular atrophies. *Lancet* 1, 919–922. doi: 10.1016/s0140-6736(80)90847-8

Perez-Garcia, M. J., Kong, L., Sumner, C. J., and Tizzano, E. F. (2017). "Developmental aspects and pathological findings in spinal muscular atrophy," in *Spinal Muscular Atrophy: Disease Mechanisms and Therapy*, eds C. J. Sumner, S. Paushkin and C. P. Ko (San Diego: Academic Press), 21–42.

Perkins, L. A., Holderbaum, L., Tao, R., Hu, Y., Sopko, R., McCall, K., et al. (2015). The transgenic RNAi project at harvard medical school: resources and validation. *Genetics* 201, 843–852. doi: 10.1534/genetics.115.180208

Praveen, K., Wen, Y., Gray, K. M., Noto, J. J., Patlolla, A. R., Van Duyne, G. D., et al. (2014). SMA-causing missense mutations in survival motor neuron (Smn) display a wide range of phenotypes when modeled in *Drosophila*. *PLoS Genet.* 10:e1004489. doi: 10.1371/journal.pgen.1004489

Praveen, K., Wen, Y., and Matera, A. G. (2012). A *Drosophila* model of spinal muscular atrophy uncouples snRNP biogenesis functions of survival motor neuron from locomotion and viability defects. *Cell Rep.* 1, 624–631. doi: 10.1016/j.celrep.2012.05.014

Price, P. L., Morderer, D., and Rossoll, W. (2018). RNp assembly defects in spinal muscular atrophy. *Adv. Neurobiol.* 20, 143–171. doi: 10.1007/978-3-319-89689-2_6

Raimer, A. C., Gray, K. M., and Matera, A. G. (2017). SMN—a chaperone for nuclear RNP social occasions? *RNA Biol.* 14, 701–711. doi: 10.1080/15476286.2016.1236168

Rajendra, T. K., Gonsalvez, G. B., Walker, M. P., Shpargel, K. B., Salz, H. K., and Matera, A. G. (2007). A *Drosophila melanogaster* model of spinal muscular atrophy reveals a function for SMN in striated muscle. *J. Cell Biol.* 176, 831–841. doi: 10.1083/jcb.200610053

Schrank, B., Götz, R., Gunnersen, J. M., Ure, J. M., Toyka, K. V., Smith, A. G., et al. (1997). Inactivation of the survival motor neuron gene, a candidate gene for human spinal muscular atrophy, leads to massive cell death in early mouse embryos. *Proc. Natl. Acad. Sci. U S A* 94, 9920–9925. doi: 10.1073/pnas.94.18.9920

Shorrock, H. K., Gillingwater, T. H., and Groen, E. J. N. (2018). Overview of current drugs and molecules in development for spinal muscular atrophy therapy. *Drugs* 78, 293–305. doi: 10.1007/s40265-018-0868-8

Shpargel, K. B., Praveen, K., Rajendra, T. K., and Matera, A. G. (2009). Gemin3 is an essential gene required for larval motor function and pupation in *Drosophila*. *Mol. Biol. Cell* 20, 90–101. doi: 10.1091/mbc.e08-01-0024

Singh, R. N., Howell, M. D., Ottesen, E. W., and Singh, N. N. (2017). Diverse role of survival motor neuron protein. *Biochim. Biophys. Acta* 1860, 299–315. doi: 10.1016/j.bbagrm.2016.12.008

Spring, A. M., Raimer, A. C., Hamilton, C. D., Schillinger, M. J., and Matera, A. G. (2018). Comprehensive modeling of Spinal Muscular Atrophy in *Drosophila melanogaster*. *bioRxiv* 394908. doi: 10.1101/394908

Talbot, K., and Tizzano, E. F. (2017). The clinical landscape for SMA in a new therapeutic era. *Gene Ther.* 24, 529–533. doi: 10.1038/gt.2017.52

Wang, C. H., Papendick, B. D., Bruinsma, P., and Day, J. K. (1998). Identification of a novel missense mutation of the SMN^T gene in two siblings with spinal muscular atrophy. *Neurogenetics* 1, 273–276. doi: 10.1007/s100480050040

Winkler, C., Eggert, C., Gradl, D., Meister, G., Giegerich, M., Wedlich, D., et al. (2005). Reduced U snRNP assembly causes motor axon degeneration in an animal model for spinal muscular atrophy. *Genes Dev.* 19, 2320–2330. doi: 10.1101/gad.342005

Workman, E., Saieva, L., Carrel, T. L., Crawford, T. O., Liu, D., Lutz, C., et al. (2009). A SMN missense mutation complements SMN2 restoring snRNPs and rescuing SMA mice. *Hum. Mol. Genet.* 18, 2215–2229. doi: 10.1093/hmg/ddp157

Conflict of Interest Statement: The authors declare that the research was conducted in the absence of any commercial or financial relationships that could be construed as a potential conflict of interest.

frontiers in Molecular Neuroscience

REVIEW
published: 05 June 2019
doi: 10.3389/fnmol.2019.00141

Hyperpolarization-Activated Cyclic Nucleotide-Gated Channels: An Emerging Role in Neurodegenerative Diseases

Xiaoli Chang[1,2], Jun Wang[1,2], Hong Jiang[1,2], Limin Shi[1,2] and Junxia Xie[1,2]**

[1] Department of Physiology, Shandong Provincial Key Laboratory of Pathogenesis and Prevention of Neurological Disorders and State Key Disciplines: Physiology, Medical College of Qingdao University, Qingdao, China, [2] Institute of Brain Science and Disease, Qingdao University, Qingdao, China

Neurodegenerative diseases such as Parkinson's disease (PD), Alzheimer's disease (AD), amyotrophic lateral sclerosis (ALS), and spinal muscular atrophy (SMA) are chronic, progressive, and age-associated neurological disorders characterized by neuronal deterioration in specific brain regions. Although the specific pathological mechanisms underlying these disorders have remained elusive, ion channel dysfunction has become increasingly accepted as a potential mechanism for neurodegenerative diseases. Hyperpolarization-activated cyclic nucleotide-gated (HCN) channels are encoded by the *HCN1-4* gene family and conduct the hyperpolarization-activated current (I_h). These channels play important roles in modulating cellular excitability, rhythmic activity, dendritic integration, and synaptic transmission. In the present review, we first provide a comprehensive picture of the role of HCN channels in PD by summarizing their role in the regulation of neuronal activity in PD-related brain regions. Dysfunction of I_h may participate in 1-methyl-4-phenylpyridinium (MPP^+)-induced toxicity and represent a pathogenic mechanism in PD. Given current reports of the critical role of HCN channels in neuroinflammation and depression, we also discussed the putative contribution of HCN channels in inflammatory processes and non-motor symptoms in PD. In the second section, we summarize how HCN channels regulate the formation of β-amyloid peptide in AD and the role of these channels in learning and memory. Finally, we briefly discuss the effects of HCN channels in ALS and SMA based on existing discoveries.

Keywords: Parkinson's disease, Alzheimer's disease, HCN channels, I_h, amyotrophic lateral sclerosis, spinal muscular atrophy

OPEN ACCESS

Edited by:
Jaichandar Subramanian, The University of Kansas, United States

Reviewed by:
Nazzareno D'Avanzo, Université de Montréal, Canada
Alan Seth Lewis, Vanderbilt University Medical Center, United States

***Correspondence:**
Limin Shi
slm0532@163.com
Junxia Xie
jxiaxie@public.qd.sd.cn

Received: *09 November 2018*
Accepted: *13 May 2019*
Published: *05 June 2019*

Citation:
Chang X, Wang J, Jiang H, Shi L and Xie J (2019) Hyperpolarization-Activated Cyclic Nucleotide-Gated Channels: An Emerging Role in Neurodegenerative Diseases. Front. Mol. Neurosci. 12:141. doi: 10.3389/fnmol.2019.00141

Abbreviations: 2VO, permanent bilateral occlusion of the common carotid arteries; 6-OHDA, 6-hydroxydopamine; Aβ, β-amyloid peptide; AD, Alzheimer's disease; ALS, amyotrophic lateral sclerosis; APP, amyloid-β precursor protein; calbindin, calcium-binding protein; cAMP, cyclic adenosine monophosphate; CCH, chronic cerebral hypoperfusion; Cm, capacitance values; CMA, chronic mild unpredictable stress; CSDS, chronic social defeat stress; CUS, chronic unpredictable stress; DAT, dopamine transporter; EPSPs, excitatory post-synaptic potentials; FL-APP, full-length APP; GP, globus pallidus; GPe, external globus pallidus; GPi, interior globus pallidus; HCN channels, hyperpolarization-activated cyclic nucleotide-gated channels; $HCN1^{-/-}$, HCN1 knockout; $HCN1^{f/f,cre}$, forebrain-restricted knockout; $HCN2^{-/-}$, HCN2 knockout; $HCN3^{-/-}$, HCN3 knockout; IFNs, interferons; IL-1β, interleukin 1β; IPSPs, inhibitory post-synaptic potentials; K-ATP, ATP-sensitive potassium channels; LPS, lipopolysaccharide; LTP, long-term potentiation; MPP^+, 1-methyl-4-phenylpyridinium; MPTP, 1-methyl-4-phenyl-1,2,3,6-tetrahydropyridine; PD, Parkinson's disease; Rm, membrane resistance; ROS, reactive oxygen species; SCRs, somatic calcium responses; sIPSC, spontaneous inhibitory postsynaptic potentials; SMA, spinal muscular atrophy; SNc, substantia nigra pars compacta; STN, subthalamic nucleus; TNF-α, tumor necrosis factor-α; TRIP8b, Rab8b-interacting protein; VAPB, vesicle-associated membrane protein B; VTA, ventral tegmental area; X11L, X11-like protein.

INTRODUCTION

Hyperpolarization-activated cyclic nucleotide-gated (HCN) channels are voltage-gated channels encoded by the *HCN1-4* gene family. These channels are primarily expressed in the heart and in the central and peripheral nervous systems (Moosmang et al., 1999, 2010; Notomi and Shigemoto, 2010). HCN channels conduct K^+ and Na^+ ions at a ratio of 3:1 to 5:1. They are activated by hyperpolarization of membrane voltage to −50 mV or below, and conduct the hyperpolarization-activated current, termed I_f in heart and I_h in neurons (Brown et al., 1979; Difrancesco, 1993; Ludwig et al., 1998; Santoro et al., 1998). cAMP can regulate the voltage-dependent activation of HCN channels in a subtype-specific manner, with HCN2 and HCN4 channels being highly susceptible to this molecule (He et al., 2014). Downregulation of cAMP suppresses I_h and shifts the HCN activation curve to lower voltage values (Biel et al., 2009). HCN channels play essential roles in the modulation of neuronal excitability, rhythmic neuronal activity, dendritic integration, and synaptic transmission, thus mediate multiple physiological functions. For example, HCN channels are able to regulate sleep and wakefulness (Kanyshkova et al., 2009; Zobeiri et al., 2018), learning and memory (Nolan et al., 2003; Nolan et al., 2004), and somatic sensation (Emery and Mcnaughton, 2011; Ding et al., 2018). Indeed, dysfunction of HCN channels is closely associated with several pathophysiological states, including epilepsy (Dibbens et al., 2010; Nava et al., 2014), neuropathic pain (Emery et al., 2012; Tibbs et al., 2016), and inflammatory pain (Emery et al., 2012; Stadler et al., 2014). Recent studies have also shown that HCN channels play a significant but complex role in neurodegenerative diseases.

Neurodegenerative diseases are chronic, progressive, and age-associated disorders, characterized by selective loss of neurons in specific brain regions. As the global population increases, the incidence of these diseases increases accordingly, and thus neurodegenerative diseases have become a serious public health issue. Nevertheless, their etiology and pathogenesis have not yet been fully elucidated, which hinders the identification of key therapeutics, and the evaluation of their potential application as therapeutic. The pathogenesis of neurological disease is closely associated with the dysfunction of neuronal excitability, rhythmicity, and signaling, which are generated and modulated by specific sets of proteins, including ion channels. HCN channels are widely expressed in the basal ganglia and hippocampus, where they control the electrical activities of substantia nigra pars compacta (SNc) dopaminergic neurons and hippocampal glutamatergic neurons (Okamoto et al., 2006; Sinha and Narayanan, 2015). In agreement with these findings, HCN channel dysfunction has been implicated in PD and AD (Chan et al., 2011; Saito et al., 2012). Changes of HCN channels are also observed in ALS and SMA (Lai et al., 2018; Silbernagel et al., 2018). Therefore, in this review, we focus on the roles of HCN channels in the pathogenesis of PD, AD, and other neurodegenerative diseases. We also discuss whether modulation of these channels could provide a new therapeutic target for the alleviation of symptoms related to these neurodegenerative diseases.

HCN CHANNELS AND PD

Parkinson's disease is the second most common neurodegenerative disorder, characterized by a progressive degeneration of dopaminergic neurons in the SNc. PD patients often suffer from an array of motor impairments, including rigidity, resting tremor, postural instability, and bradykinesia. Non-motor symptoms such as olfactory loss, anxiety and depression, sleep abnormalities, and constipation are also present during early stages of the disease (Singaram et al., 1995; Weisskopf et al., 2003; Bohnen et al., 2007; Postuma et al., 2017; Del Rey et al., 2018). Dopaminergic neurons in SNc send neurological projections to several brain regions and help to chemically differentiate the direct and indirect pathways. Previous reports have shown that HCN channels are widely expressed in multiple basal ganglia such as the SNc, the globus pallidus (GP), and the STN. Moreover, HCN channels are involved in the regulation of electrical activities of these neurons under physiological and pathological conditions (Santoro et al., 2000; Moosmang et al., 2010). To date, studies on HCN channels and PD have mainly focused on the following aspects: (1) alteration of HCN channel expression and function in PD animal models, (2) potential involvement of HCN channels in the neurotoxic effects of MPP^+, and (3) HCN channels as a mechanism for the selective vulnerability of SNc neurons. Given current reports of the critical role of HCN channels in neuroinflammation and depression, we also discuss their possible involvement in the inflammatory processes and non-motor symptoms of PD.

HCN CHANNELS REGULATE THE ELECTRICAL ACTIVITIES OF NEURONS IN THE BASAL GANGLIA

In the 1980s, I_h was first recorded in SNc dopaminergic neurons (Lacey et al., 1987, 1989). The current was observed to become slowly activated at approximately −70 mV and was fully activated at −129 to −140 mV (Lacey et al., 1989; Mercuri et al., 1995). The current was specifically blocked by ZD7288 within a specific concentration range (<100 μM) (Harris and Constanti, 1995; Seutin et al., 2001; Neuhoff et al., 2002). Later, mRNA expression of HCN2–HCN4 was examined in SNc dopaminergic neurons using single-cell RT-mPCR and *in situ* hybridization (Franz et al., 2000; Santoro et al., 2000), showing that both HCN2 and HCN4 are expressed at relatively higher levels than HCN3 (Mercuri et al., 1995; Franz et al., 2000; Gambardella et al., 2012). Under current-clamp conditions, dopaminergic neurons exhibit a pronounced rebound depolarization (sag) mediated by I_h in response to a series of hyperpolarizing current pulses. The presence of I_h or sag has been used as a key criterion for the identification of

dopaminergic neurons (Grace and Onn, 1989). In these neurons, I_h has a high density of expression around the axon-bearing dendrites, and is reduced with distance from the axon origin, which may affect synaptic integration (Engel and Seutin, 2015). Neuhoff et al. (2002) further reported that there were significant differences in HCN channel density in various subpopulations of dopaminergic neurons. Calbindin-negative SNc dopaminergic neurons, which were more vulnerable to neurotoxins, possessed a larger sag amplitude and I_h density than calbindin-positive neurons (Neuhoff et al., 2002). Neurons in the GP also respond to series of hyperpolarizing current pulses with a drop in current (sag). Studies have shown that HCN1–4 channels are expressed in the GP and STN. Among them, HCN2 is the major isoform in the GP (Chan et al., 2004), while HCN2 and HCN3 are more highly expressed in the STN (Atherton et al., 2010).

HCN channels have been reported to regulate the electrical activities of neurons in basal ganglia. SNc dopaminergic neurons display two predominant types of firing patterns *in vivo*: tonic irregular single-spike activity and phasic burst activity. *In vitro*, they only exhibit slow and regular spontaneous firing activity. The spontaneous firing activity of dopaminergic neurons was significantly inhibited after application of the HCN channels blocker ZD7288 (<100 μM) in acutely prepared mouse or rat midbrain slices (Seutin et al., 2001; Neuhoff et al., 2002; Okamoto et al., 2006). Chan et al. (2007) further observed that ZD7288 (50 μM) inhibited spontaneous firing activity in juvenile wild-type SNc dopaminergic neurons (less than postnatal 21 days), and was able to completely block firing in adult Cav1.3$^{-/-}$ SNc dopaminergic neurons. Pharmacological blockade of HCN channels also promoted burst firing in SNc dopaminergic neurons of mice, which led to the release of a large amount of dopamine (Mrejeru et al., 2011).

HCN channels also make an important contribution to the autonomous pacemaking in GP neurons (Chan et al., 2004; Surmeier et al., 2005). Application of ZD7288 (50 μM) or Cs^+ in acutely prepared mouse brain slices led to hyperpolarization and reduced firing rate and regularity (Chan et al., 2004). Subsequently, a novel computational model of GPe neurons confirmed that when HCN channels were blocked, the pacemaker activity of GPe neurons was reduced or abolished (Merrisonhort and Borisyuk, 2013). However, HCN channels could regulate firing of GP neurons bidirectionally *in vivo* (Chen et al., 2015). Using single-unit extracellular recordings, Chen et al. observed that micro-pressure ejection of ZD7288 and Cs^+ decreased the frequency of spontaneous firing in 21 out of 40 GP neurons recorded, but increased the firing rate in another 18 neurons. Similar results were obtained when using 8-Br-cAMP, an activator of HCN channels (Chen et al., 2015). Since GP neurons consist of two types of neurons, GP-TI and GP-TA (Mallet et al., 2012), the bidirectional modulation of HCN channel firing activity may be a result of the interplay between these two types of neurons. As for the effect of HCN channels on pacemaking activity in the STN neurons, previous articles have reported that the effect was negligible in rat brain slices (Bevan and Wilson, 1999; Do and Bean, 2003). However, Deng et al. (2015) revealed that HCN channels could bidirectionally regulate the firing of STN neurons *in vivo* by using single-unit extracellular recordings, which was similar to their previously published report in the GP.

HCN channels also regulate the oscillatory activity of basal ganglia neurons. Oscillation activities, mainly including alpha (8–12 Hz), beta (11–30 Hz), delta (1–3 Hz), and theta (2–7 Hz)-frequency bands, are prominent features of the neuronal network and are closely related to many brain behavioral and functional states (Hutchison et al., 2004). Theta activity has been reported to lead to a paroxysmal increase in freezing behavior in PD patients (Follett and Torresrussotto, 2012; Hu et al., 2018). HCN channels reportedly contribute to theta frequency membrane resonance in hyperpolarized mammalian SNc neurons, which may be involved in theta oscillation (Xue et al., 2012). This membrane resonance in the hyperpolarized potential ranging from −60 to −80 mV was completely abolished by application of ZD7288 (10 μM) (Xue et al., 2012). In the late stage PD, excessive synchronized oscillation and high-frequency bursts often occur in STN neurons (Obeso et al., 2000; Bevan et al., 2002; Syed et al., 2012). A recent study showed that the resonance in rat STN was also mediated by HCN channels, and application of ZD7288 (20 μM) could abolish it (Yan et al., 2012).

ALTERATION OF HCN CHANNEL EXPRESSION AND FUNCTION IN PD ANIMAL MODELS

Functional changes in HCN channels within the basal ganglia have been observed in several animal models of PD. Previous studies have shown a progressive downregulation of HCN channels in SNc neurons in MitoPark mice (Good et al., 2011), a transgenic model in which a mitochondrial mutation caused parkinsonism (Ekstrand et al., 2007). MitoPark mice exhibited reduced current amplitude and a more negative I_h activation curve at postnatal 7–8 weeks, whereas motor dysfunction was not observed until 12 weeks. Therefore, HCN channel downregulation in SNc dopaminergic neurons may be one of the earliest physiological changes related to PD in MitoPark mice (Good et al., 2011). The finding that functional changes occur in SNc dopaminergic neurons prior to the onset of distinct behavioral symptoms in animal models of PD and Parkinsonian patients suggests that I_h could play an important role in the early stages of disease. Consistent with the above results, reduced I_h amplitude and density were recently observed in SNc dopaminergic neurons in spontaneous α-synuclein overexpressing rats (Guatteo et al., 2016).

The amplitude of I_h in GP neurons was also significantly reduced in acute reserpine-treated mice (Chan et al., 2011). Similar results were obtained in mice and rats as a result of chronic injection of 6-OHDA, a classic neurotoxin that causes PD (Chan et al., 2011). In all of these models, the downregulation of HCN channel expression/activity contributed to the progressive decline in the autonomous pacemaker activity of GPe neurons. They further demonstrated that the protein and mRNA levels of the four HCN subunits were

reduced in the GPe, with HCN2 being the most affected. Moreover, dopamine depletion induced a significant reduction in tetratricopeptide repeat-containing TRIP8b mRNA. TRIP8b, a brain-specific cytoplasmic protein and an HCN channel auxiliary subunit in the mammalian brain, influences HCN channel surface expression and regulates their gating and kinetics (Zolles et al., 2009; Bankston et al., 2012). Thus, these results suggested that both transcriptional and trafficking-related mechanisms may be involved in the downregulation of HCN channels, producing a progressive loss of autonomous pacemaking in GPe neurons and exacerbating their rhythmic bursting (Chan et al., 2011).

Meurers and Dziewczapolski (2009) also studied the role of HCN channels in the GPi. They demonstrated that HCN3 mRNA was selectively upregulated by twofold in the entopeduncular nucleus/GPi of rats and mice with 6-OHDA-induced parkinsonism. In agreement with this change in mRNA expression, both HCN3 current amplitude and neuronal excitability were significantly increased in the lesioned animals (Meurers and Dziewczapolski, 2009). These data indicated a potential association of HCN channels with altered excitability of basal ganglia output neurons in PD. In addition, the role of HCN channels in the GP may depend on the subtype and distribution environment of the channels.

POTENTIAL INVOLVEMENT OF HCN CHANNELS IN THE NEUROTOXIC EFFECTS OF MPP$^+$

MPP^+ is a traditional neurotoxin that can induce Parkinsonian syndrome in experimental primates and rodents. It is converted from the pro-toxin MPTP to MPP^+ and then selectively uptaken by SNc dopaminergic neurons through the DAT. Once inside the cell, MPP^+ primarily inhibits mitochondrial complex I, leading to ATP depletion, oxidative stress, and eventual cell death (Nicklas et al., 1985; Smeyne and Jackson-Lewis, 2005; Huang et al., 2017). In addition to the classical mitochondrial impairment mechanism, several studies have also described the effects of MPP^+ on neuronal electrophysiological activities. Acute application of MPP^+ on midbrain slices led to hyperpolarization of SNc dopaminergic neurons and reduced their firing rate (Liss et al., 2005; Masi et al., 2013; Yee et al., 2014). However, the ionic mechanisms of this toxin on neuronal electrophysiological properties remain controversial. Previous work has attributed the effects of MPP^+ to the opening of ATP-sensitive potassium (K-ATP) channels, which is supported by the observation that MPP^+ caused mitochondrial failure and ATP depletion (Liss et al., 2005). Subsequently, Masi et al. (2013) demonstrated that MPP^+ still led to a rapid hyperpolarization along with a reduction in spontaneous firing activity, even after preincubation with the K-ATP channel blocker glybenclamide. They further proposed that the effects of MPP^+ were mediated by HCN channels (Masi et al., 2013), specifically that MPP^+ inhibited I_h, shifted the I_h activation curve toward negative potentials, and slowed the I_h activation kinetics. These effects occurred under K-ATP channel blockade and in the presence of 2 mM ATP, indicating that it was independent of mitochondrial mechanisms. Thus, they speculated that MPP^+ may directly interact with HCN channels (Masi et al., 2013). However, Yee et al. (2014) reported that MPP^+ inhibited the activity of dopaminergic neurons in distinct stages through different mechanisms. The early phase of inhibition was dependent on D2 autoreceptors, whereas the late phase was due to the activation of K-ATP channels. Although I_h was reduced by MPP^+ in their study, pharmacological blockade of HCN channels did not prevent the inhibitory effects of MPP^+. Thus, the inhibition of I_h by MPP^+ may promote hyperpolarization through activation of some channels, such as K-ATP channels (Yee et al., 2014).

In summary, current literature indicates that MPP^+ has acute inhibitory actions on nigral dopaminergic neurons. Although independent groups have explored ionic mechanisms in this context, results remain controversial. One should note that these studies used inconsistent concentrations of MPP^+ (range from 10 to 50 μM), electrophysiological recording methods, and drug administration methods. Further studies are required to assess the impact of HCN channels on the neurotoxicity of MPP^+.

HCN CHANNELS MAY BE AN ION CHANNEL MECHANISM UNDERLYING THE SELECTIVE VULNERABILITY OF SNc NEURONS

A hallmark of PD is the selective vulnerability of SNc dopaminergic neurons to damage and cell death and is contrasted with the relative resistance of dopaminergic neurons in the neighboring VTA to the disease (Ekstrand et al., 2007; Blesa and Przedborski, 2014; Brichta and Greengard, 2014). However, the mechanisms underlying this selective vulnerability remain unclear. The genetic profile of these regions only differs by 1–3% (Greene et al., 2005), indicating that the genetic factors may not account for this discrepancy. Recent research has begun to explore the role of electrophysiological determinants, proposing that specific types of ion channels, including HCN channels, may be the basis for this selective vulnerability (**Table 1**) (Dragicevic et al., 2015).

Compared to VTA dopaminergic neurons, SNc neurons exhibit a larger cell body size, lower Rm, higher Cm (Krashia et al., 2017), faster firing frequency (Werkman et al., 2001; Krashia et al., 2017), and a distinct sag in response to a series of hyperpolarizing current pulses (Neuhoff et al., 2002), which appeared to correlate with the larger I_h magnitude. Indeed, the distribution of HCN channels in midbrain dopaminergic neurons is consistent with a ventro-dorsal gradient. In other words, SNc neurons show a larger average I_h than VTA neurons (Krashia et al., 2017). Moreover, there is a higher percentage of I_h-negative dopaminergic neurons in the VTA (Masi et al., 2015). The I_h blocker ZD7288 ($<$100 μM) inhibited firing activity in the SNc, but this effect was negligible in the VTA of both mice and rats (Neuhoff et al., 2002; Khaliq and Bean, 2010; Krashia et al., 2017). It is worth noting that unilateral ZD7288

TABLE 1 | Comparison of electrophysiological parameters of dopaminergic neurons in the SNc and VTA.

Electrophysiological parameters	SNc ($\bar{X} \pm$ SEM)	VTA ($\bar{X} \pm$ SEM)	Selected references
Body size (μm^2)	176.29 ± 5.84	113.18 ± 3.57	Krashia et al., 2017
Rm (MΩ)	227 ± 10	697 ± 99	Krashia et al., 2017
Cm (pF)	57 ± 2	44 ± 4	Krashia et al., 2017
Sag (mV)	37.3 ± 0.72	31.0 ± 1.72	Neuhoff et al., 2002
I_h (pA)	299 ± 14	45 ± 9	Krashia et al., 2017
Firing frequency (Hz)	2.1 ± 0.2	1.5 ± 0.1	Werkman et al., 2001
	Significantly inhibited after pharmacologically blocking I_h	Negligible	Neuhoff et al., 2002; Krashia et al., 2017
EPSP	Obviously enhanced after pharmacologically blocking I_h	Negligible	Masi et al., 2013
IPSP	Significantly inhibited after pharmacologically blocking I_h	Negligible	Masi et al., 2013
SCR	Remarkably activated after pharmacologically blocking I_h	Negligible	Carbone et al., 2017

Rm, membrane resistance; Cm, capacitance values; EPSP, excitatory post-synaptic potential; IPSP, inhibitory post-synaptic potential; SCR, somatic calcium response.

injection into the SNc of adult rats prominently increased the number of apomorphine-induced rotations and reduced the immunofluorescence intensity of tyrosine hydroxylase-positive neurons. These effects were not observed in VTA neurons (Carbone et al., 2017).

Notably, I_h differentially regulates the responsiveness to excitatory synaptic inputs in SNc and VTA neurons. MPP^+ increased the temporal summation of evoked eEPSPs in SNc neurons *via* the inhibition of I_h (Masi et al., 2013). Direct pharmacological suppression of I_h through ZD7288 (50 μM) also increased the decay time and amplitude of eEPSPs, and this response was more prominent in SNc than in VTA neurons (Masi et al., 2015). ZD7288 also significantly reduced the amplitude of evoked inhibitory post-synaptic potentials (eIPSPs) (Carbone et al., 2017). Therefore, I_h blockage likely enhances synaptic excitability through a dual mechanism in SNc dopaminergic neurons, specifically, by potentiating excitatory inputs and weakening inhibitory inputs. More importantly, increased excitatory synaptic transmission led to the amplification of SCRs in SNc neurons, while this response was minimally affected in VTA neurons (Carbone et al., 2017). In addition, low intracellular ATP caused a significant negative shift in the I_h activation curve (Carbone et al., 2017), suggesting that I_h dysfunction may be linked to the mechanisms that trigger PD, such as mitochondrial failure and ATP depletion, and that I_h dysfunction may act in concert with SNc-specific synaptic connectivity to promote selective vulnerability (Masi et al., 2015).

Based on the evidence mentioned above, we proposed a model of the pathogenic cascade in SNc neurons during PD progression (**Figure 1**): with the participation of a causative agent, mitochondrial dysfunction results in a decrease in intracellular ATP levels, which in turn inhibits ATP-dependent I_h. MPP^+ may also directly interact with HCN channels, causing the inhibition of I_h, and thus reducing spontaneous firing. This leads to the amplification of SCRs by potentiating EPSP and depressing IPSP, which ultimately results in an imbalance of intracellular calcium homeostasis and selective degeneration of SNc dopaminergic neurons.

Importantly, some of the above results, such as the ability of I_h to affect EPSP and EPSP-driven SCRs, were obtained using the channel blocker ZD7288. It has previously been suggested that ZD7288 induced a I_h-independent reduction of synaptic transmission in hippocampal neurons (Vivien and Castillo, 2002), but this phenomenon has not been reported in SNc and VTA neurons. Therefore, the mechanism of action of ZD7288 in SNc synaptic transmission requires further verification to support our hypothesis.

PUTATIVE CONTRIBUTION OF HCN CHANNELS TO INFLAMMATORY PROCESSES IN PD

A common hallmark of neurodegenerative diseases is the presence of neuroinflammation (Griffin et al., 1998; Pott Godoy et al., 2008; Deguise and Kothary, 2017; Liu and Wang, 2017). Reactive microglia, which is the main glial cell type that participates in the inflammatory response in the brain, was first revealed in the SNc of postmortem human brain tissue as early as in 1988 (McGeer et al., 1988). Elevated cytokine IL-1β and TNF-α were detected in the SNc and striatum of PD patients and animal models (Nagatsu et al., 2000; Bartels and Leenders, 2007). Activated microglial cells secrete pro-inflammatory cytokines and produce ROS, and these inflammatory factors in turn induce the activation of astrocytes, which could not promote neuronal synapse formation, but rather released toxic factors that caused neuronal damage (De Virgilio et al., 2016; Fahmy et al., 2019).

Neuroinflammation has been reported to target specific sets of channel proteins, including HCN channels. To date, there is no report that relates the possible role of HCN channels to PD-related neuroinflammation. However, in non-PD-related brain regions, *in vivo* elevation of type I IFNs by viral brain infection or acutely applied recombinant type I IFNs to rat slices has been shown to reduce HCN1-mediated I_h in cortical pyramidal neurons (Stadler et al., 2014). More importantly, IFN-β hyperpolarized the cell membrane, reduced neuronal resonance, and modulated spontaneous EEG slow-wave activity depending on the presence of HCN1 and reversibly altered the physiological responses of cortical neuronal

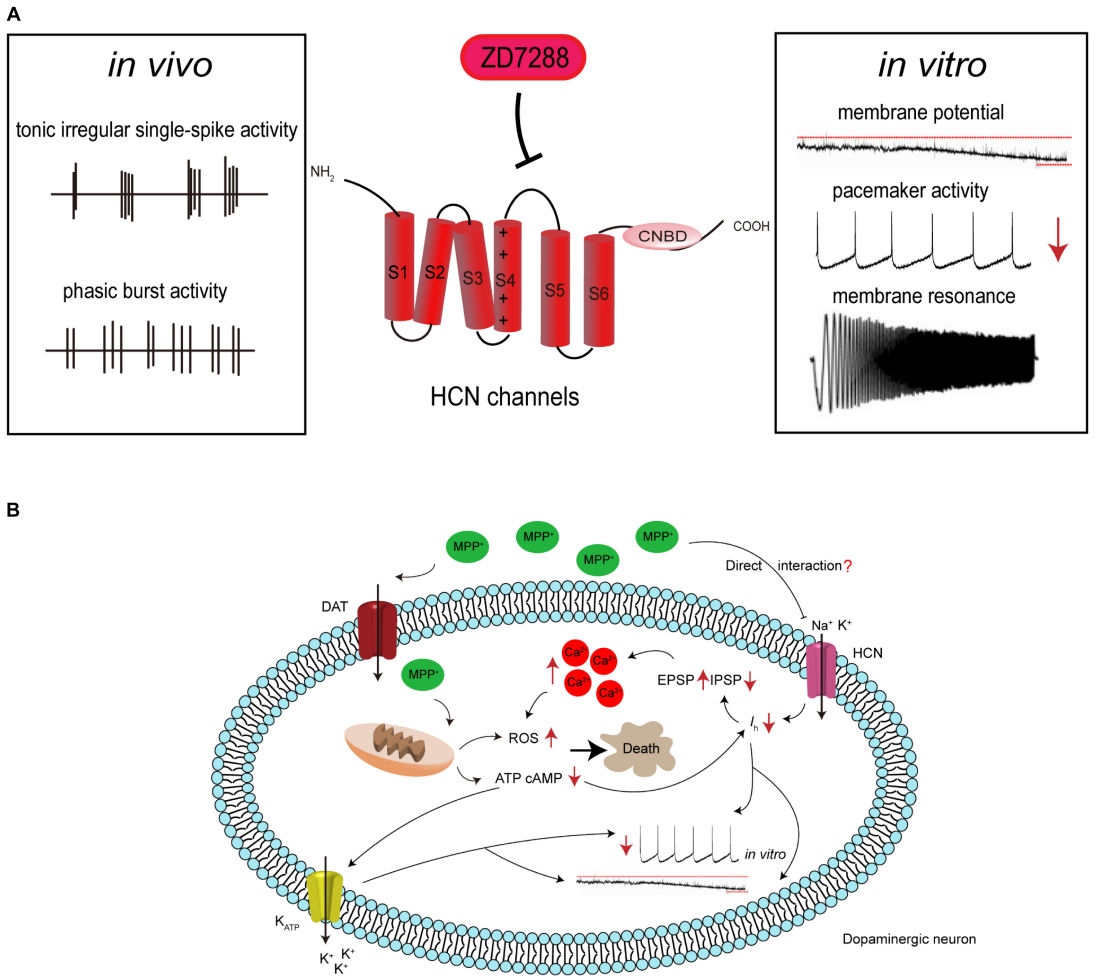

FIGURE 1 | Hypothetical HCN channel-related pathogenic cascade in SNc dopaminergic neurons in PD. **(A)** HCN channels modulate the electrophysiological activities of SNc dopaminergic neurons. Dopaminergic neurons display tonic irregular single-spike firing and phasic burst firing *in vivo*, and slow, regular, pacemaker activity *in vitro*. HCN channels blockade with ZD7288 reduces the amplitude of I_h, leading to cell membrane hyperpolarization, decreased firing activity, or even increased burst firing *in vitro*. HCN channels also regulate neuronal oscillatory activity. **(B)** Proposed mechanism for the involvement of HCN channels in the neurotoxic effects of MPP^+. MPP^+ accumulates in mitochondria, where it inhibits complex I, causing ATP depletion, increased ROS formation, and oxidative stress. The decreased cellular ATP and cAMP concentration leads to the opening of K-ATP channels and inhibition of HCN channels. This results in hyperpolarization of the cell membrane and reduction in the spontaneous firing of dopaminergic neurons. MPP^+ is also speculated to directly interact with HCN channels, causing I_h inhibition. This further leads to the amplification of SCRs by potentiating EPSP and depressing IPSP, which results in an imbalance of intracellular calcium homeostasis. This in turn potentiates oxidative stress and ultimately leads to cell death.

networks (Stadler et al., 2014). Similarly, a recent study by Federica and colleagues showed that bilateral stereotactic injection of LPS into rats' lateral ventricles could reduce HCN1 and TRIP8b protein levels, as well as I_h amplitude and kinetics in CA1 pyramidal neurons (Frigerio et al., 2018). Moreover, LPS treatment hyperpolarized the resting membrane potential, increased the input resistance, reduced resonance properties, and increased temporal summation of synaptic inputs, which was consistent with the inhibition of I_h. These data indicated that neuroinflammation can modulate the electrophysiological properties of neurons by affecting HCN channels and the related I_h current. Given the critical role of HCN channels in neuroinflammation, we boldly speculate that HCN channels could be involved in the progression of PD and even other neurodegenerative diseases *via* neuroinflammatory regulation.

PUTATIVE CONTRIBUTION OF HCN CHANNELS TO THE NON-MOTOR SYMPTOMS IN PD

Patients with PD are usually accompanied by numerous non-motor symptoms, such as depression, olfactory loss, sleep abnormalities, and constipation. To date, no studies are available concerning the possible impact of HCN channels on the non-motor symptoms of PD. However, growing evidence suggests that HCN channels and their auxiliary subunit TRIP8b

play an important role in the action of antidepressant and depression. Mice with reduced I_h in the hippocampal CA1 region resulting from whole-brain deletion of TRIP8b, HCN1, or HCN2 all demonstrated significant resistance to multiple tests of behavioral despair with high predictive validity for antidepressant efficacy (Lewis et al., 2011). In TRIP8b knockout mice, restoring TRIP8b expression in the dorsal CA1 region enhanced HCN protein expression and reversed the antidepressant-like behaviors (Han et al., 2017; Lyman et al., 2017). Kim et al. (2012) further observed that rats infused with lentiviral shRNA-HCN1 in the dorsal hippocampal CA1 region displayed antidepressant- and anxiolytic-like behaviors associated with widespread enhancement of hippocampal activity. Similar result was also confirmed in CUS, a widely accepted model for major depressive disorder. Deletion of HCN1 by shRNA-HCN1 in the dorsal CA1 region prevented the CUS-induced behavioral deficits (Kim et al., 2018).

Multiple lines of evidence implicate dysregulation in the brain's reward neural circuit in depression. Dysfunction of the dopamine reward system is thought to contribute to a hedonia and the loss of motivation common in depression (Berton et al., 2006; Nestler and Carlezon, 2006; Tye et al., 2013). I_h has also been reported to be increased in dopaminergic neurons of VTA in mice under CSDS, a well-established rodent model of depression (Cao et al., 2010; Friedman et al., 2014). However, I_h has been noted to be decreased in dopaminergic neurons of VTA in CMS, which is also a widely used depression model. A knockdown of HCN2 by lentiviral shRNA-HCN2 shRNA in the VTA produced depressive- and anxiety-like behavior, and overexpression of HCN2 in the VTA prevented the development of CMS-induced depressive-like behavior (Zhong et al., 2018). Thus, different HCN isoforms in different brain regions may play distinct roles in regulating depressive behavior.

In addition to the possible role of HCN channels and their auxiliary subunit in depression-like behavior, a possible link between HCN channels and the olfactory, sleep, and gastrointestinal functions in animal models is also noteworthy (Sun et al., 2003; Fried et al., 2010; Alicia et al., 2012; Wang et al., 2012; Shahi et al., 2014; Hu et al., 2016; Fisher et al., 2018). Because of the important diagnostic and therapeutic value of these non-motor symptoms in PD, perhaps the above studies provide a new perspective for further exploration of PD.

HCN CHANNELS AND AD

Alzheimer's disease is the most common neurodegenerative disease and is characterized by neuropsychiatric symptoms such as progressive memory impairment, cognitive dysfunction, personality changes, and language disorders, which seriously affect the patient's quality of life (Gotz et al., 2018). The accumulation of the β-amyloid peptide (Aβ) within the brain and hyperphosphorylated and cleaved forms of the microtubule-associated protein tau are two key pathological features of AD (O'Brien and Wong, 2011). Lesions caused by the accumulation of these proteins mainly affect the hippocampus, the associative cortices, and subcortical structures (Braak et al., 2011). HCN channels are widely distributed in these regions and may participate in the etiology of AD by affecting neuronal excitability and regulating Aβ generation (Cirrito et al., 2005; Saito et al., 2012).

THE RELATIONSHIP BETWEEN HCN CHANNELS AND AGE

Changes in HCN channels in AD-associated brain regions are closely related to age. Vasilyev and Barish (2002) published a pioneering study investigating the postnatal development of I_h in mouse hippocampal pyramidal neurons. Both I_h amplitude and HCN channels immunoreactivity appeared to increase with age from postnatal 1 to 20 days in CA1 and CA3 hippocampal pyramidal neurons. In addition, I_h activation became progressively more rapid over the 1- to 20-day interval (Vasilyev and Barish, 2002). Subcellular HCN channel distribution also varied with age. HCN1 expression was found in the dendrites of rat hippocampal pyramidal neurons 2 days after birth and remained the only subtype present in dendrites until 2 weeks after birth. HCN2 was clearly distributed in the neuronal soma of rat hippocampal pyramidal neurons neonatally and was detected in the dendrites of hippocampal pyramidal neurons from the third week (Brewster et al., 2007; Bender and Baram, 2008). As rat CA1 pyramidal neurons matured, HCN1 expression prominently increased, becoming the primary HCN channel subtype (Brewster et al., 2007). This information suggests that the different expression patterns of HCN channels and I_h between immature and mature neurons may promote changes in neuronal excitability, which affect neuronal physiology and possibly lead to a pathological state.

HCN1 levels have been described to decrease dramatically in the temporal lobe of cynomolgus monkeys during aging, and be also significantly diminished in the temporal lobe of sporadic AD patients (Saito et al., 2012). The latest evidence demonstrated that the HCN1l and its auxiliary subunit, TRIP8b, were distally enriched in CA1 pyramidal neurons in both WT and 1-month-old ADTg mice but absent in ADTg mice at 12 and 24 months. The neuronal sag and rebound slope, as subthreshold voltage signatures, changed and deteriorated with age (Musial et al., 2018), and trafficking the HCN1 channel to distant dendrites restored abnormal subthreshold voltage signaling.

ROLE OF HCN CHANNELS IN THE REGULATION OF Aβ GENERATION

Aβ is the main component of senile plaques, and its deposition may be a common pathway for all causative factors leading to AD. Aβ is generated by sequential cleavage of the transmembrane amyloid-β precursor protein (APP) by β-secretase and the γ-secretase complex. γ-secretase may cleave at either of two sites, forming two different lengths of Aβ including Aβ40 and the more neurotoxic Aβ42 (Selkoe, 2002; O'Brien and Wong, 2011). An increase in neuronal activity could enhance the production of Aβ (Kamenetz et al., 2003; Cirrito et al., 2005, 2008). Given

the critical role of HCN channels in neuronal excitability, correlations between HCN channels and Aβ generation have long been suspected. Recent findings showed enhanced Aβ generation in entorhinal cortex after blockade of HCN1, as well as in global HCN1$^{-/-}$ mice. In contrast, overexpression of HCN1 in Neuro2a cells decreased Aβ generation, whereas inhibition of the overexpressed HCN1 channel activity restored the level of Aβ production (Saito et al., 2012). HCN1$^{-/-}$ mice had a significantly higher resting membrane potential and input resistance measured from responses to either negative or positive current steps, indicating that loss of the HCN1 subunit enhanced neuronal excitability in entorhinal cortex (Nolan et al., 2007). Thus, HCN1 may be involved in Aβ generation by regulating neuronal excitability. Eslamizade et al. (2015) further observed that rats with injection of Aβ peptides into the frontal cortex exhibited decreased excitability in hippocampal pyramidal neurons, which was caused by upregulation of I_h mediated *via* increased HCN1 mRNA.

In addition to relying on alterations in neuronal excitability, HCN1-mediated Aβ generation was also influenced by X11. The latter is an adaptor protein which binds to HCN channels and regulates the trafficking and metabolism of APP (Borg et al., 1998; Ho et al., 2002; Kimura et al., 2004; Rogelj et al., 2006). Saito et al. found that I_h amplitude and density decreased sharply in the entorhinal cortex of mice lacking both X11- and X11L. Together with X11 and X11L, APP and HCN1 were co-immunoprecipitated from the entorhinal cortex. Therefore, HCN1 may form a complex with APP and X11 or X11L to regulate the generation of Aβ (Saito et al., 2012).

As a γ-secretase-associated protein, the HCN2 channel could also participate in the regulation of Aβ production. Silencing HCN2 in HEK cells overexpressing wild-type APP (HEK-APP cells) led to a prominent decrease in Aβ40 and Aβ42, as well as a reduction in α-secretase and β-secretase cleavage. In addition, while the FL-APP levels did not change significantly, its glycosylation decreased in HEK-APP cells after silencing of HCN2 (Frykman et al., 2016). Thus, HCN2 could affect APP maturation by modulating the glycosylation of APP. Previous work has shown that glycosylated APP was reduced in Neuro2a cells overexpressing X11L (Saito et al., 2011). Interestingly, the HCN2 channel formed a complex with X11L in rat brain and in a heterologous expression cell system (Kimura et al., 2004). Thus, HCN2 may also regulate the generation of Aβ by forming a complex with X11L (**Figure 2**).

ROLE OF HCN CHANNELS IN LEARNING AND MEMORY OF RELEVANCE TO AD

Progressive learning and memory impairment is a major clinical symptom of AD. These changes have been primarily linked to dysregulated Ca^{2+} signaling (Bezprozvanny and Mattson, 2008; Berridge, 2011, 2014). Previous work has shown that high HCN1 expression may interfere with the generation of Ca^{2+} spikes in hippocampal CA1 pyramidal neurons (Tsay et al., 2007). In hippocampal pyramidal neurons from HCN1$^{-/-}$ mice, the amplitude and duration of distal dendritic Ca^{2+} events have been found to be enhanced. This has also been observed after a blockade of HCN channels with ZD7288 (10 μM). This effect was attributed to a reduction in I_h, which resulted in resting membrane hyperactivation and increased input resistance (Tsay et al., 2007). This resembles the previously mentioned amplification of SCRs induced by blockade of I_h in the SNc (Carbone et al., 2017).

The role of HCN channels in learning and memory has also been examined directly in gene knockout mice (Nolan et al., 2003, 2004; Matt et al., 2011; Stieglitz et al., 2017). Nolan et al. first explored the role of HCN1 in motor learning and memory. Global HCN1$^{-/-}$ mice showed remarkable deficits in motor learning and memory, whereas those with HCN1$^{f/f,cre}$ did not have this deficit. These defects in motor learning and memory were hypothesized to result from the loss of HCN1 in cerebellar Purkinje cells, a key component of the cerebellar circuit (Nolan et al., 2003). Although the HCN1 did not participate in the spontaneous discharge activity of Purkinje cells, HCN1 stabilizes the integration characteristics of Purkinje cells by mediating the depolarizing inward current that counteracts hyperpolarizing inputs which would otherwise push the membrane potential below the threshold for spontaneous spiking. This mechanism would allow Purkinje cells to maintain a constant input–output relationship independently of the effects of previous inputs to the cerebellum (Nolan et al., 2003).

Later, Nolan et al. (2004) investigated the role of HCN1 in spatial learning and memory. In contrast to the results mentioned above, they found that HCN1$^{-/-}$ mice had enhanced spatial learning and memory (Nolan et al., 2004). Theta activity, which plays an important role in coding and storing spatial information, was selectively enhanced in hippocampal CA1 pyramidal neurons both in HCN1$^{-/-}$ and HCN1$^{f/f,cre}$ mice. Moreover, deletion of HCN1 from forebrain neurons enhanced hippocampal-dependent learning and memory, as well as LTP at the direct perforant path input to the distal dendrites of CA1 pyramidal neurons (Nolan et al., 2004). These results demonstrate that the same ion channel may have distinct functional roles in different forms of learning and memory, depending on the cell environment and the neuronal circuitry in which the channel is involved.

Matt et al. (2011) further found that LTP was significantly increased in the perforant path of HCN2$^{-/-}$ mice. In contrast to HCN1$^{f/f,cre}$ mice, LTP was not enhanced in mice with HCN2 selectively knocked out in hippocampal pyramidal neurons (HCN2^{PyrKO}). Assessment of the amplitude and frequency of spontaneous inhibitory postsynaptic potentials (sIPSP) showed that the inhibitory interneurons were damaged in HCN2$^{-/-}$ mice. LTP was remarkably enhanced when HCN2 was deleted from interneurons (Matt et al., 2011). Therefore, HCN2 appears to act on inhibitory interneurons in the hippocampal CA1 area to regulate LTP.

Interestingly, recent experimental results showed that global HCN3$^{-/-}$ mice had no significant motor or spatial learning deficits in comparison with control mice (Stieglitz et al., 2017), suggesting that different subtypes of HCN channels may play different roles in learning and memory.

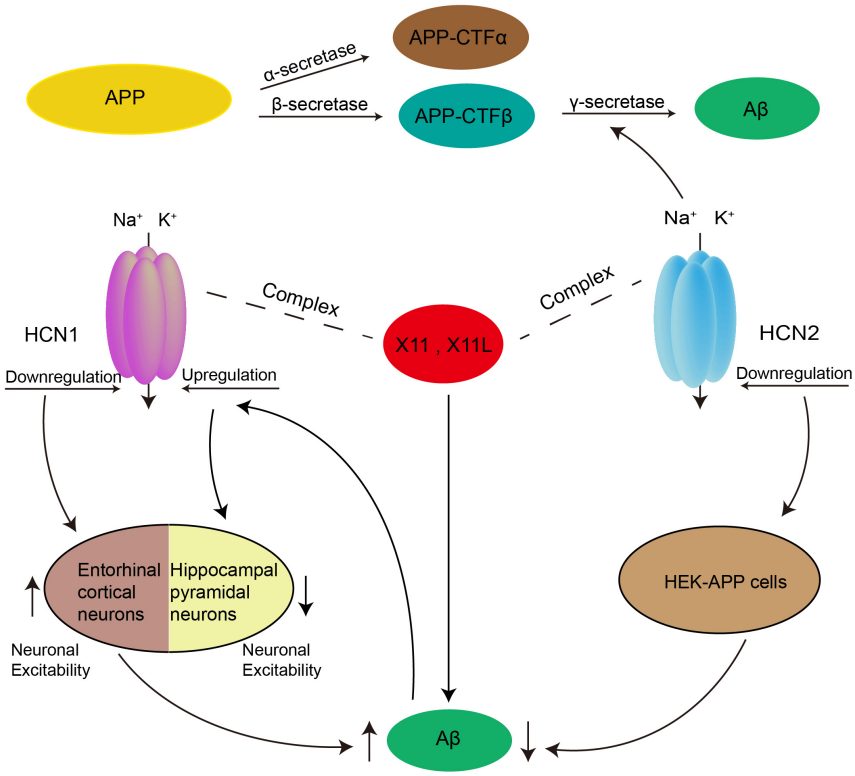

FIGURE 2 | Possible role of HCN channels in the generation of Aβ. Aβ is produced by two proteolytic enzymes, β- and γ-secretase. Downregulation of HCN1 channel could enhance the production of Aβ by increasing neuronal excitability in entorhinal cortex. Rats with injection of Aβ peptides into the frontal cortex exhibited decreased excitability in hippocampal pyramidal neurons, which was caused by upregulation of I_h mediated *via* increased HCN1. In addition, both HCN1 and HCN2 channels were able to form a complex with X11 or X11L proteins to regulate Aβ generation. The HCN2 channel can also participate in the regulation of Aβ production as a γ-secretase-associated protein, and by affecting APP maturation *via* modulation of the glycosylation of APP.

Notably, in an AD-related CCH animal model, HCN channels were also reported to be involved in spatial learning and memory (Li et al., 2014; Luo et al., 2015). CCH can promote learning and memory impairment and is a common risk factor for AD (de la Torre, 2004, 2010; Kalaria et al., 2012). Rats with 2VO also developed stable and long-term impairment of spatial learning and memory. Luo et al. (2015) found that rats, in the progressive phase of CCH, showed differentially altered HCN1 and HCN2 in the rat hippocampal CA1 region, and the HCN2/HCN1ratio increased throughout the process of chronic hypoperfusion. Specifically, the expression of HCN1 surface subunits was decreased at 4 weeks of 2VO, but exhibited no significant change at 8 or 12 weeks. In contrast to HCN1, HCN2 surface expression was increased at all time points of ischemia (Luo et al., 2015). In normal conditions, HCN1 subunit expression is more abundant than HCN2 in the hippocampal CA1 region. Therefore, the HCN1 subunit is more likely to form homologous channels. However, during the CCH process, due to the continuous increase of HCN2 subunits, the probability that HCN1 subunits will form heterologous channels with HCN2 subunits increases. Since the properties of homologous and heterologous channels differ, the hippocampal synaptic plasticity attributed to HCN channels is altered, which in turn leads to changes in spatial learning and memory. Thus, they proposed that in the early stages of CCH, the impairment of spatial motor memory in rats may be caused by common changes of HCN1 and HCN2, and later, the disorder was attributed to the upregulation of HCN2 expression. A similar phenomenon was also observed by Li et al. (2014) in the hippocampal CA1 area in rats after 5 weeks of 2VO, with reduced HCN1 expression and increased HCN2 expression. Moreover, Li et al. (2014) found that restoring the surface expression of HCN1 and HCN2 could ameliorate the impairment of spatial learning and memory. Together, these studies on learning and memory suggest novel avenues of research into the pathogenesis of AD (**Table 2**).

ROLE OF HCN CHANNELS IN OTHER NEURODEGENERATIVE DISEASES

HCN Channels and ALS

Amyotrophic lateral sclerosis is a universally fatal neurodegenerative disease characterized by progressive loss of corticospinal neurons, brainstem motor neurons, and spinal motor neurons, which leads to progressive weakness and paralysis. A recent study found that vesicle associated membrane protein B (VAPB), which modulates the surface

TABLE 2 | Roles of HCN channels in learning and memory of relevance to AD.

Models	Main findings	References
$HCN1^{-/-}$ mice	As I_h decreases, the resting membrane potential became hyperactivated and input resistance increased significantly, resulting in further enhancement of the amplitude and duration of distal dendritic Ca^{2+} events.	Tsay et al., 2007
$HCN1^{-/-}$ mice/$HCN1^{f/f,cre}$ mice	Theta activity was selectively enhanced in hippocampal CA1 pyramidal neurons.	Nolan et al., 2004
$HCN1^{f/f,cre}$ mice	LTP was significantly enhanced at the direct perforant path input to the distal dendrites of CA1 pyramidal neurons, as was spatial learning and memory.	Nolan et al., 2004
$HCN2^{-/-}$ mice	LTP was significantly enhanced.	Matt et al., 2011
Mice with deletion of HCN2 from interneurons	LTP was significantly enhanced.	Matt et al., 2011
$HCN3^{-/-}$ mice	There were no significant deficits in motor learning and spatial learning in comparison with control mice.	Stieglitz et al., 2017
2VO rats	Rats displayed a prolonged time to swim to the platform and altered expression patterns of HCN1 and HCN2 in the hippocampal CA1 area. Spatial learning and memory impairment could be improved when restoring the expression of HCN1 and HCN2.	Li et al., 2014; Luo et al., 2015

$HCN1^{-/-}$, HCN1 knockout; $HCN1^{f/f,cre}$, forebrain-restricted knockout; $HCN2^{-/-}$, HCN2 knockout; $HCN3^{-/-}$, HCN3 knockout; LTP, long-term potentiation; 2VO, permanent bilateral occlusion of the common carotid arteries.

expression and cellular localization of HCN1 and HCN2 channels, exhibited decreased expression in motor neurons of ALS8 patients, a typical form of familial ALS, as well as in the motor neurons of sporadic ALS patients (Anagnostou et al., 2010; Mitneneto et al., 2011; Silbernagel et al., 2018). Silbernagel et al. (2018) reported that HCN2 and VAPB were co-localized in both HCN2-transfected HeLa cells and VAPB-transfected HeLa cells. However, this co-localization was not observed in HeLa cells transfected with the $VAPB^{P56S}$ mutant (Silbernagel et al., 2018). Indeed, HCN2 current amplitude was noticeably decreased by VAPB modulation. Mutation or loss of VAPB led to a decrease in HCN activity and neuronal excitability in motor neurons, which are a main cell type involved in the pathogenesis of ALS (Silbernagel et al., 2018).

HCN Channels and SMA

Spinal muscular atrophy is an autosomal recessive motor neuron disorder, characterized by progressive muscle weakness, especially in the torso and proximal limbs (Russman, 2007). Currently, only two studies have examined the correlation between HCN channels and SMA. Similarly, to ALS, a mutation in VAPB has also been identified in SMA patients (Nishimura et al., 2004), establishing a potential connection between HCN channels and SMA, as VAPB modulates HCN channels. Recently, a marked enhancement of I_h amplitude as well as HCN channel expression was observed in the spinal cord and sciatic nerves of SMA mice. Furthermore, treatment with ZD7288 appeared to reduce early mortality, improve motor function, and restore neuromuscular junction architecture in SMA mice (Lai et al., 2018). These results provide initial evidence that HCN channels may play a role in SMA pathophysiology and could be a novel target for SMA treatment.

CONCLUSION

HCN channels are key regulators of neuronal excitability and network activity within the nervous system. Increasing evidence supports a model in which modifications in their physiological function contributes to the pathogenic mechanisms of several neurodegenerative diseases, implying that they may be a potential therapeutic target. This review, albeit simplistic, summarizes much of the research aimed at understanding the roles of HCN channels in animal models of PD, AD, and other neurodegenerative diseases, as well as in patients. To date, studies have reported reduced HCN1 expression in AD patients (Saito et al., 2012) as well as mutation or loss of VAPB, an HCN regulator protein in ALS (Anagnostou et al., 2010; Mitneneto et al., 2011) and SMA patients (Nishimura et al., 2004). However, gene variants/mutations in HCN channels or their regulatory proteins have not been identified in human patients with other neurodegenerative disorders. Presently, research concerning the role of HCN channels in neurodegenerative diseases is in its infancy, with a lack of probing for them as candidate genes. Interestingly, recent work has identified a mutation in the HCN2 gene, and augmentation of I_h in patients with genetic epilepsy with febrile seizures plus. This study provides evidence for the possible involvement of HCN channel mutations in familial forms of human epilepsy (Dibbens et al., 2010). Therefore, further research on the variations of HCN and their regulatory proteins may be an exciting area for future research, especially in patients with neurodegenerative diseases.

AUTHOR CONTRIBUTIONS

XC wrote the manuscript. JW, HJ, LS, and JX approved and revised the final manuscript.

FUNDING

This work was supported by the National Natural Science Foundation of China (31671054 and 81430024), the Postdoctoral Science Foundation of China (2017M610412 and 2018T110666), the Bureau of Science and Technology of Qingdao Municipality (17-1-1-44-jch), and Taishan Scholars Construction Project.

REFERENCES

Alicia, G. G., Enrique, T., Yolanda, L., Isabel, M., Laura, T., and Inmaculada, C. (2012). Ih current is necessary to maintain normal dopamine fluctuations and sleep consolidation in Drosophila. *PLoS One* 7:e36477. doi: 10.1371/journal.pone.0036477

Anagnostou, G., Akbar, M. T., Paul, P., Angelinetta, C., Steiner, T. J., and De, B. J. (2010). Vesicle associated membrane protein B (VAPB) is decreased in ALS spinal cord. *Neurobiol. Aging* 31, 969–985. doi: 10.1016/j.neurobiolaging.2008.07.005

Atherton, J. F., Kitano, K., Baufreton, J., Fan, K., Wokosin, D., Tkatch, T., et al. (2010). Selective participation of somatodendritic HCN channels in inhibitory but not excitatory synaptic integration in neurons of the subthalamic nucleus. *J. Neurosci.* 30, 16025–16040. doi: 10.1523/JNEUROSCI.3898-10.2010

Bankston, J. R., Camp, S. S., Dimaio, F., Lewis, A. S., Chetkovich, D. M., and Zagotta, W. N. (2012). Structure and stoichiometry of an accessory subunit TRIP8b interaction with hyperpolarization-activated cyclic nucleotide-gated channels. *Proc. Nat. Acad. Sci. U.S.A.* 109, 7899–7904. doi: 10.1073/pnas.1201997109

Bartels, A. L., and Leenders, K. L. (2007). Neuroinflammation in the pathophysiology of Parkinson's disease: evidence from animal models to human in vivo studies with [11C]-PK11195 PET. *Mov. Disord.* 22, 1852–1856. doi: 10.1002/mds.21552

Bender, R. A., and Baram, T. Z. (2008). Hyperpolarization activated cyclic-nucleotide gated (HCN) channels in developing neuronal networks. *Prog. Neurobiol.* 86, 129–140. doi: 10.1016/j.pneurobio.2008.09.007

Berridge, M. J. (2011). Calcium signalling and Alzheimer's disease. *Neurochem. Res.* 36, 1149–1156.

Berridge, M. J. (2014). Calcium regulation of neural rhythms, memory and Alzheimer's disease. *J. Physiol.* 592, 281–293. doi: 10.1113/jphysiol.2013.257527

Berton, O., Mcclung, C. A., Dileone, R. J., Krishnan, V., Renthal, W., Russo, S. J., et al. (2006). Essential role of BDNF in the mesolimbic dopamine pathway in social defeat stress. *Science* 311, 864–868. doi: 10.1126/science.1120972

Bevan, M. D., Magill, P. J., Terman, D., Bolam, J. P., and Wilson, C. J. (2002). Move to the rhythm: oscillations in the subthalamic nucleus–external globus pallidus network. *Trends Neurosci.* 25, 525–531. doi: 10.1016/s0166-2236(02)02235-x

Bevan, M. D., and Wilson, C. J. (1999). Mechanisms underlying spontaneous oscillation and rhythmic firing in rat subthalamic neurons. *J. Neurosci.* 19, 7617–7628. doi: 10.1523/jneurosci.19-17-07617.1999

Bezprozvanny, I., and Mattson, M. P. (2008). Neuronal calcium mishandling and the pathogenesis of Alzheimer's disease. *Trends Neurosci.* 31, 454–463. doi: 10.1016/j.tins.2008.06.005

Biel, M., Wahl-Schott, C., Michalakis, S., and Zong, X. (2009). Hyperpolarization-activated cation channels: from genes to function. *Physiol. Rev.* 89, 847–885. doi: 10.1152/physrev.00029.2008

Blesa, J., and Przedborski, S. (2014). Parkinson's disease: animal models and dopaminergic cell vulnerability. *Front. Neuroanat.* 8:155. doi: 10.3389/fnana.2014.00155

Bohnen, N. I., Gedela, S., Kuwabara, H., Constantine, G. M., Mathis, C. A., Studenski, S. A., et al. (2007). Selective hyposmia and nigrostriatal dopaminergic denervation in Parkinson's disease. *J. Neurol.* 254, 84–90. doi: 10.1007/s00415-006-0284-y

Borg, J. P., Yang, Y., De Taddeo-Borg, M., Margolis, B., and Turner, R. S. (1998). The X11alpha protein slows cellular amyloid precursor protein processing and reduces Abeta40 and Abeta42 secretion. *J. Biol. Chem.* 273, 14761–14766. doi: 10.1074/jbc.273.24.14761

Braak, H., Thal, D. R., Ghebremedhin, E., and Del Tredici, K. (2011). Stages of the pathologic process in Alzheimer disease: age categories from 1 to 100 years. *J. Neuropathol. Exp. Neurol.* 70, 960–969. doi: 10.1097/NEN.0b013e318232a379

Brewster, A. L., Chen, Y., Bender, R. A., Yeh, A., Shigemoto, R., and Baram, T. Z. (2007). Quantitative analysis and subcellular distribution of mRNA and protein expression of the hyperpolarization-activated cyclic nucleotide-gated channels throughout development in rat hippocampus. *Cereb. Cortex* 17, 702–712. doi: 10.1093/cercor/bhk021

Brichta, L., and Greengard, P. (2014). Molecular determinants of selective dopaminergic vulnerability in Parkinson's disease: an update. *Front. Neuroanat.* 8:152. doi: 10.3389/fnana.2014.00152

Brown, H. F., Difrancesco, D., and Noble, S. J. (1979). How does adrenaline accelerate the heart? *Nature* 280, 235–236. doi: 10.1038/280235a0

Cao, J. L., Covington, H. E., Friedman, A. K., Wilkinson, M. B., Walsh, J. J., Cooper, D. C., et al. (2010). Mesolimbic dopamine neurons in the brain reward circuit mediate susceptibility to social defeat and antidepressant action. *J. Neurosci.* 30, 16453–16458. doi: 10.1523/JNEUROSCI.3177-10.2010

Carbone, C., Costa, A., Provensi, G., Mannaioni, G., and Masi, A. (2017). The hyperpolarization-activated current determines synaptic excitability, calcium activity and specific viability of substantia nigra dopaminergic neurons. *Front Cell Neurosci.* 11:187. doi: 10.3389/fncel.2017.00187

Chan, C. S., Glajch, K. E., Gertler, T. S., Guzman, J. N., Mercer, J. N., Lewis, A. S., et al. (2011). HCN channelopathy in external globus pallidus neurons in models of Parkinson's disease. *Nat. Neurosci.* 14, 85–92. doi: 10.1038/nn.2692

Chan, C. S., Guzman, J. N., Ilijic, E., Mercer, J. N., Rick, C., Tkatch, T., et al. (2007). 'Rejuvenation' protects neurons in mouse models of Parkinson's disease. *Nature* 447, 1081–1086. doi: 10.1038/nature05865

Chan, C. S., Shigemoto, R., Mercer, J. N., and Surmeier, D. J. (2004). HCN2 and HCN1 channels govern the regularity of autonomous pacemaking and synaptic resetting in globus pallidus neurons. *J. Neurosci. Off. J. Soc. Neurosci.* 24, 9921–9932. doi: 10.1523/jneurosci.2162-04.2004

Chen, L., Xu, R., Sun, F. J., Xue, Y., Hao, X. M., Liu, H. X., et al. (2015). Hyperpolarization-activated cyclic nucleotide-gated (HCN) channels regulate firing of globus pallidus neurons *in vivo*. *Mol. Cell Neurosci.* 68, 46–55. doi: 10.1016/j.mcn.2015.04.001

Cirrito, J. R., Kang, J. E., Lee, J., Stewart, F. R., Verges, D. K., Silverio, L. M., et al. (2008). Endocytosis is required for synaptic activity-dependent release of amyloid-beta *in vivo*. *Neuron* 58, 42–51. doi: 10.1016/j.neuron.2008.02.003

Cirrito, J. R., Yamada, K. A., Finn, M. B., Sloviter, R. S., Bales, K. R., May, P. C., et al. (2005). Synaptic activity regulates interstitial fluid amyloid-beta levels *in vivo*. *Neuron* 48, 913–922. doi: 10.1016/j.neuron.2005.10.028

de la Torre, J. C. (2004). Is Alzheimer's disease a neurodegenerative or a vascular disorder? Data, dogma, and dialectics. *Lancet Neurol.* 3, 184–190. doi: 10.1016/s1474-4422(04)00683-0

de la Torre, J. C. (2010). The vascular hypothesis of Alzheimer's disease: bench to bedside and beyond. *Neurodegener. Dis.* 7, 116–121. doi: 10.1159/000285520

De Virgilio, A., Greco, A., Fabbrini, G., Inghilleri, M., Rizzo, M. I., Gallo, A., et al. (2016). Parkinson's disease: autoimmunity and neuroinflammation. *Autoimmun. Rev.* 15, 1005–1011.

Deguise, M. O., and Kothary, R. (2017). New insights into SMA pathogenesis: immune dysfunction and neuroinflammation. *Ann. Clin. Transl. Neurol.* 4, 522–530. doi: 10.1002/acn3.423

Del Rey, N. L., Quiroga-Varela, A., Garbayo, E., Carballo-Carbajal, I., Fernandez-Santiago, R., Monje, M. H. G., et al. (2018). Advances in Parkinson's Disease: 200 years later. *Front. Neuroanat.* 12:113. doi: 10.3389/fnana.2018.00113

Deng, W. S., Jiang, Y. X., Han, X. H., Xue, Y., Wang, H., Sun, P., et al. (2015). HCN channels modulate the activity of the subthalamic nucleus *in vivo*. *J. Mol. Neurosci.* 55, 260–268. doi: 10.1007/s12031-014-0316-5

Dibbens, L. M., Reid, C. A., Hodgson, B., Thomas, E. A., Phillips, A. M., Gazina, E., et al. (2010). Augmented currents of an HCN2 variant in patients with febrile seizure syndromes. *Ann. Neurol.* 67, 542–546. doi: 10.1002/ana.21909

Difrancesco, D. (1993). Pacemaker mechanisms in cardiac tissue. *Ann. Rev. Physiol.* 55, 455–472. doi: 10.1146/annurev.ph.55.030193.002323

Ding, W., You, Z., Shen, S., Yang, J., Lim, G., Doheny, J. T., et al. (2018). Increased HCN channel activity in the gasserian ganglion contributes to trigeminal neuropathic pain. *J. Pain* 19, 626–634. doi: 10.1016/j.jpain.2018.01.003

Do, M. T., and Bean, B. P. (2003). Subthreshold sodium currents and pacemaking of subthalamic neurons: modulation by slow inactivation. *Neuron* 39, 109–120. doi: 10.1016/s0896-6273(03)00360-x

Dragicevic, E., Schiemann, J., and Liss, B. (2015). Dopamine midbrain neurons in health and Parkinson's disease: emerging roles of voltage-gated calcium channels and ATP-sensitive potassium channels. *Neuroscience* 284, 798–814. doi: 10.1016/j.neuroscience.2014.10.037

Ekstrand, M. I., Terzioglu, M., Galter, D., Zhu, S., Hofstetter, C., Lindqvist, E., et al. (2007). Progressive parkinsonism in mice with respiratory-chain-deficient dopamine neurons. *Proc. Nat. Acad. Sci. U.S.A.* 104, 1325–1330. doi: 10.1073/pnas.0605208103

Emery, E. C., and Mcnaughton, P. A. (2011). HCN2 ion channels play a central role in inflammatory and neuropathic pain. *Science* 333, 1462–1466. doi: 10.1126/science.1206243

Emery, E. C., Young, G. T., and Mcnaughton, P. A. (2012). HCN2 ion channels: an emerging role as the pacemakers of pain. *Trends Pharmacol. Sci.* 33, 456–463. doi: 10.1016/j.tips.2012.04.004

Engel, D., and Seutin, V. (2015). High dendritic expression of Ih in the proximity of the axon origin controls the integrative properties of nigral dopamine neurons. *J. Physiol.* 593, 4905–4922. doi: 10.1113/JP271052

Eslamizade, M. J., Saffarzadeh, F., Mousavi, S. M., Meftahi, G. H., Hosseinmardi, N., Mehdizadeh, M., et al. (2015). Alterations in CA1 pyramidal neuronal intrinsic excitability mediated by Ih channel currents in a rat model of amyloid beta pathology. *Neuroscience* 305, 279–292. doi: 10.1016/j.neuroscience.2015.07.087

Fahmy, A. M., Boulais, J., Desjardins, M., and Matheoud, D. (2019). Mitochondrial antigen presentation: a mechanism linking Parkinson's disease to autoimmunity. *Curr. Opin. Immunol.* 58, 31–37. doi: 10.1016/j.coi.2019.02.004

Fisher, D. W., Luu, P., Agarwal, N., Kurz, J. E., and Chetkovich, D. M. (2018). Loss of HCN2 leads to delayed gastrointestinal motility and reduced energy intake in mice. *PLoS One* 13:e0193012. doi: 10.1371/journal.pone.0193012

Follett, K. A., and Torresrussotto, D. (2012). Deep brain stimulation of globus pallidus interna, subthalamic nucleus, and pedunculopontine nucleus for Parkinson's disease: which target? *Parkinsonism Relat. Disord.* 18, S165–S167.

Franz, O., Liss, B., Neu, A., and Roeper, J. (2000). Single-cell mRNA expression of HCN1 correlates with a fast gating phenotype of hyperpolarization-activated cyclic nucleotide-gated ion channels (Ih) in central neurons. *Eur. J. Neurosci.* 12, 2685–2693. doi: 10.1046/j.1460-9568.2000.00151.x

Fried, H. U., Kaupp, U. B., and Muller, F. (2010). Hyperpolarization-activated and cyclic nucleotide-gated channels are differentially expressed in juxtaglomerular cells in the olfactory bulb of mice. *Cell Tissue Res.* 339, 463–479. doi: 10.1007/s00441-009-0904-9

Friedman, A. K., Walsh, J. J., Juarez, B., Ku, S. M., Chaudhury, D., Wang, J., et al. (2014). Enhancing depression mechanisms in midbrain dopamine neurons achieves homeostatic resilience. *Science* 344, 313–319. doi: 10.1126/science.1249240

Frigerio, F., Flynn, C., Han, Y., Lyman, K., Lugo, J. N., Ravizza, T., et al. (2018). Neuroinflammation alters integrative properties of rat hippocampal pyramidal cells. *Mol. Neurobiol.* 55, 7500–7511. doi: 10.1007/s12035-018-0915-1

Frykman, S., Inoue, M., Ikeda, A., Teranishi, Y., Kihara, T., Lundgren, J. L., et al. (2016). Maturation and processing of the amyloid precursor protein is regulated by the potassium/sodium hyperpolarization-activated cyclic nucleotide-gated ion channel 2 (HCN2). *Biochem. Biophys. Res. Commun.* 483, 352–358. doi: 10.1016/j.bbrc.2016.12.140

Gambardella, C., Pignatelli, A., and Belluzzi, O. (2012). The h-current in the substantia nigra pars compacta neurons: a re-examination. *PLoS One* 7:e52329. doi: 10.1371/journal.pone.0052329

Good, C. H., Hoffman, A. F., Hoffer, B. J., Chefer, V. I., Shippenberg, T. S., Bäckman, C. M., et al. (2011). Impaired nigrostriatal function precedes behavioral deficits in a genetic mitochondrial model of Parkinson's disease. *FASEB J.* 25:1333. doi: 10.1096/fj.10-173625

Gotz, J., Bodea, L. G., and Goedert, M. (2018). Rodent models for Alzheimer disease. *Nat. Rev. Neurosci.* 19, 583–598. doi: 10.1038/s41583-018-0054-8

Grace, A. A., and Onn, S. P. (1989). Morphology and electrophysiological properties of immunocytochemically identified rat dopamine neurons recorded *in vitro*. *J. Neurosci.* 9, 3463–3481. doi: 10.1523/jneurosci.09-10-03463.1989

Greene, J. G., Dingledine, R., and Greenamyre, J. T. (2005). Gene expression profiling of rat midbrain dopamine neurons: implications for selective vulnerability in parkinsonism. *Neurobiol. Dis.* 18, 19–31. doi: 10.1016/j.nbd.2004.10.003

Griffin, W. S., Sheng, J. G., Royston, M. C., Gentleman, S. M., Mckenzie, J. E., Graham, D. I., et al. (1998). Glial-neuronal interactions in Alzheimer's disease: the potential role of a 'cytokine cycle' in disease progression. *Brain Pathol.* 8, 65–72. doi: 10.1111/j.1750-3639.1998.tb00136.x

Guatteo, E., Rizzo, F. R., Federici, M., Cordella, A., Ledonne, A., Latini, L., et al. (2016). Functional alterations of the dopaminergic and glutamatergic systems in spontaneous α-synuclein overexpressing rats. *Exp. Neurol.* 287, 21–33. doi: 10.1016/j.expneurol.2016.10.009

Han, Y., Heuermann, R. J., Lyman, K. A., Fisher, D., Ismail, Q. A., and Chetkovich, D. M. (2017). HCN-channel dendritic targeting requires bipartite interaction with TRIP8b and regulates antidepressant-like behavioral effects. *Mol. Psychiatry* 22, 458–465. doi: 10.1038/mp.2016.99

Harris, N. C., and Constanti, A. (1995). Mechanism of block by ZD 7288 of the hyperpolarization-activated inward rectifying current in guinea pig substantia nigra neurons *in vitro*. *J. Neurophysiol.* 74, 2366–2378. doi: 10.1152/jn.1995.74.6.2366

He, C., Chen, F., Li, B., and Hu, Z. (2014). Neurophysiology of HCN channels: from cellular functions to multiple regulations. *Prog. Neurobiol.* 112, 1–23. doi: 10.1016/j.pneurobio.2013.10.001

Ho, C. S., Marinescu, V., Steinhilb, M. L., Gaut, J. R., Turner, R. S., and Stuenkel, E. L. (2002). Synergistic effects of Munc18a and X11 proteins on amyloid precursor protein metabolism. *J. Biol. Chem.* 277, 27021–27028. doi: 10.1074/jbc.m201823200

Hu, B., Shi, Q., Guo, Y., Diao, X., Guo, H., Zhang, J., et al. (2018). The oscillatory boundary conditions of different frequency bands in Parkinson's disease. *J. Theor. Biol.* 451, 67–79. doi: 10.1016/j.jtbi.2018.04.040

Hu, R., Ferguson, K. A., Whiteus, C. B., Meijer, D. H., and Araneda, R. C. (2016). Hyperpolarization-activated currents and subthreshold resonance in granule cells of the olfactory bulb. *Eneuro* 3:ENEURO.0197-16.2016.

Huang, D., Xu, J., Wang, J., Tong, J., Bai, X., Li, H., et al. (2017). Dynamic changes in the nigrostriatal pathway in the MPTP mouse model of Parkinson's disease. *Parkinsons Dis.* 2017:9349487. doi: 10.1155/2017/9349487

Hutchison, W. D., Dostrovsky, J. O., Walters, J. R., Courtemanche, R., Boraud, T., Goldberg, J., et al. (2004). Neuronal oscillations in the basal ganglia and movement disorders: evidence from whole animal and human recordings. *J. Neurosci.* 24, 9240–9243. doi: 10.1523/jneurosci.3366-04.2004

Kalaria, R. N., Akinyemi, R., and Ihara, M. (2012). Does vascular pathology contribute to Alzheimer changes? *J. Neurol. Sci.* 322, 141–147. doi: 10.1016/j.jns.2012.07.032

Kamenetz, F., Tomita, T., Hsieh, H., Seabrook, G., Borchelt, D., Iwatsubo, T., et al. (2003). APP processing and synaptic function. *Neuron* 37, 925–937. doi: 10.1016/s0896-6273(03)00124-7

Kanyshkova, T., Pawlowski, M., Meuth, P., Dubé, C., Bender, R. A., Brewster, A. L., et al. (2009). Postnatal expression pattern of HCN channel isoforms in thalamic neurons: relationship to maturation of thalamocortical oscillations. *J. Neurosci. Off. J. Soc. Neurosci.* 29, 8847–8857. doi: 10.1523/JNEUROSCI.0689-09.2009

Khaliq, Z. M., and Bean, B. P. (2010). Pacemaking in dopaminergic ventral tegmental area neurons: depolarizing drive from background and voltage-dependent sodium conductances. *J. Neurosci. Off. J. Soc. Neurosci.* 30, 7401–7413. doi: 10.1523/JNEUROSCI.0143-10.2010

Kim, C. S., Brager, D. H., and Johnston, D. (2018). Perisomatic changes in h-channels regulate depressive behaviors following chronic unpredictable stress. *Mol. Psychiatry* 23, 892–903. doi: 10.1038/mp.2017.28

Kim, C. S., Chang, P. Y., and Johnston, D. (2012). Enhancement of dorsal hippocampal activity by knockdown of HCN1 channels leads to anxiolytic- and antidepressant-like behaviors. *Neuron* 75, 503–516. doi: 10.1016/j.neuron.2012.05.027

Kimura, K., Kitano, J., Nakajima, Y., and Nakanishi, S. (2004). Hyperpolarization-activated, cyclic nucleotide-gated HCN2 cation channel forms a protein assembly with multiple neuronal scaffold proteins in distinct modes of protein-protein interaction. *Genes Cells* 9, 631–640. doi: 10.1111/j.1356-9597.2004.00752.x

Krashia, P., Martini, A., Nobili, A., Aversa, D., D'amelio, M., Berretta, N., et al. (2017). On the properties of identified dopaminergic neurons in the mouse substantia nigra and ventral tegmental area. *Eur. J. Neurosci.* 45, 92–105. doi: 10.1111/ejn.13364

Lacey, M. G., Mercuri, N. B., and North, R. A. (1987). Dopamine acts on D2 receptors to increase potassium conductance in neurones of the rat substantia nigra zona compacta. *J. Physiol.* 392, 397–416. doi: 10.1113/jphysiol.1987.sp016787

Lacey, M. G., Mercuri, N. B., and North, R. A. (1989). Two cell types in rat substantia nigra zona compacta distinguished by membrane properties and the actions of dopamine and opioids. *J. Neurosci. Off. J. Soc. Neurosci.* 9:1233. doi: 10.1523/jneurosci.09-04-01233.1989

Lai, H. J., Chen, C. L., and Tsai, L. K. (2018). Increase of hyperpolarization-activated cyclic nucleotide-gated current in the aberrant excitability of spinal muscular atrophy. *Ann. Neurol.* 83, 494–507. doi: 10.1002/ana.25168

Lewis, A. S., Vaidya, S. P., Blaiss, C. A., Liu, Z., Stoub, T. R., Brager, D. H., et al. (2011). Deletion of the hyperpolarization-activated cyclic nucleotide-gated channel auxiliary subunit TRIP8b impairs hippocampal Ih localization and function and promotes antidepressant behavior in mice. *J. Neurosci.* 31, 7424–7440. doi: 10.1523/JNEUROSCI.0936-11.2011

Li, C. J., Lu, Y., Zhou, M., Zong, X. G., Li, C., Xu, X. L., et al. (2014). Activation of GABAB receptors ameliorates cognitive impairment via restoring the balance of HCN1/HCN2 surface expression in the hippocampal CA1 area in rats with chronic cerebral hypoperfusion. *Mol. Neurobiol.* 50, 704–720. doi: 10.1007/s12035-014-8736-3

Liss, B., Haeckel, O., Wildmann, J., Miki, T., Seino, S., and Roeper, J. (2005). K-ATP channels promote the differential degeneration of dopaminergic midbrain neurons. *Nat. Neurosci.* 8, 1742–1751. doi: 10.1038/nn1570

Liu, J., and Wang, F. (2017). Role of neuroinflammation in amyotrophic lateral sclerosis: cellular mechanisms and therapeutic implications. *Front. Immunol.* 8:1005. doi: 10.3389/fimmu.2017.01005

Ludwig, A., Zong, X., Jeglitsch, M., Hofmann, F., and Biel, M. (1998). A family of hyperpolarization-activated mammalian cation channels. *Nature* 393, 587–591. doi: 10.1038/31255

Luo, P., Lu, Y., Li, C., Zhou, M., Chen, C., Lu, Q., et al. (2015). Long-lasting spatial learning and memory impairments caused by chronic cerebral hypoperfusion associate with a dynamic change of HCN1/HCN2 expression in hippocampal CA1 region. *Neurobiol. Learn. Mem.* 123, 72–83. doi: 10.1016/j.nlm.2015.05.005

Lyman, K. A., Han, Y., and Chetkovich, D. M. (2017). Animal models suggest the TRIP8b-HCN interaction is a therapeutic target for major depressive disorder. *Expert Opin. Ther. Targets* 21, 235–237. doi: 10.1080/14728222.2017.1287899

Mallet, N., Micklem, B. R., Henny, P., Brown, M. T., Williams, C., Bolam, J. P., et al. (2012). Dichotomous organization of the external globus pallidus. *Neuron* 74, 1075–1086. doi: 10.1016/j.neuron.2012.04.027

Masi, A., Narducci, R., Landucci, E., Moroni, F., and Mannaioni, G. (2013). MPP(+) -dependent inhibition of Ih reduces spontaneous activity and enhances EPSP summation in nigral dopamine neurons. *Br. J. Pharmacol.* 169, 130–142. doi: 10.1111/bph.12104

Masi, A., Narducci, R., Resta, F., Carbone, C., Kobayashi, K., and Mannaioni, G. (2015). Differential contribution of Ih to the integration of excitatory synaptic inputs in substantia nigra pars compacta and ventral tegmental area dopaminergic neurons. *Eur. J. Neurosci.* 42, 2699–2706. doi: 10.1111/ejn.13066

Matt, L., Michalakis, S., Hofmann, F., Hammelmann, V., Ludwig, A., Biel, M., et al. (2011). HCN2 channels in local inhibitory interneurons constrain LTP in the hippocampal direct perforant path. *Cell Mol. Life Sci.* 68, 125–137. doi: 10.1007/s00018-010-0446-z

McGeer, P. L., Itagaki, S., Boyes, B. E., and Mcgeer, E. G. (1988). Reactive microglia are positive for HLA-DR in the substantia nigra of Parkinson's and Alzheimer's disease brains. *Neurology* 38, 1285–1291.

Mercuri, N. B., Bonci, A., Calabresi, P., Stefani, A., and Bernardi, G. (1995). Properties of the hyperpolarization-activated cation current Ih in rat midbrain dopaminergic neurons. *Eur. J. Neurosci.* 7, 462–469. doi: 10.1111/j.1460-9568.1995.tb00342.x

Merrisonhort, R., and Borisyuk, R. (2013). The emergence of two anti-phase oscillatory neural populations in a computational model of the Parkinsonian globus pallidus. *Front. Comput. Neurosci.* 7:173. doi: 10.3389/fncom.2013.00173

Meurers, B. H., and Dziewczapolski, G. A. (2009). Dopamine depletion induced up-regulation of HCN3 enhances rebound excitability of basal ganglia output neurons. *Neurobiol. Dis.* 34, 178–188. doi: 10.1016/j.nbd.2009.01.007

Mitneneto, M., Machadocosta, M., Marchetto, M. C. N., Bengtson, M. H., Joazeiro, C. A., Tsuda, H., et al. (2011). Downregulation of VAPB expression in motor neurons derived from induced pluripotent stem cells of ALS8 patients. *Hum. Mol. Genet.* 20, 3642–3652. doi: 10.1093/hmg/ddr284

Moosmang, S., Biel, M., Hofmann, F., and Ludwig, A. (1999). Differential distribution of four hyperpolarization-activated cation channels in mouse brain. *Biol. Chem.* 380, 975–980.

Moosmang, S., Stieber, J., Zong, X., Biel, M., Hofmann, F., and Ludwig, A. (2010). Cellular expression and functional characterization of four hyperpolarization-activated pacemaker channels in cardiac and neuronal tissues. *FEBS J.* 268, 1646–1652. doi: 10.1046/j.1432-1327.2001.02036.x

Mrejeru, A., Wei, A., and Ramirez, J. M. (2011). Calcium-activated non-selective cation currents are involved in generation of tonic and bursting activity in dopamine neurons of the substantia nigra pars compacta. *J. Physiol.* 589, 2497–2514. doi: 10.1113/jphysiol.2011.206631

Musial, T. F., Molina-Campos, E., Bean, L. A., Ybarra, N., Borenstein, R., Russo, M. L., et al. (2018). Store depletion-induced h-channel plasticity rescues a channelopathy linked to Alzheimer's disease. *Neurobiol. Learn. Mem.* 154, 141–157. doi: 10.1016/j.nlm.2018.06.004

Nagatsu, T., Mogi, M., Ichinose, H., and Togari, A. (2000). Changes in cytokines and neurotrophins in Parkinson's disease. *J. Neural Transm. Suppl.* 60, 277–290. doi: 10.1007/978-3-7091-6301-6_19

Nava, C., Dalle, C., Rastetter, A., Striano, P., Kovel, C. G., Nabbout, R., et al. (2014). De novo mutations in HCN1 cause early infantile epileptic encephalopathy. *Nat. Genet.* 46, 640–645. doi: 10.1038/ng.2952

Nestler, E. J., and Carlezon, W. A. Jr. (2006). The mesolimbic dopamine reward circuit in depression. *Biol. Psychiatry* 59, 1151–1159. doi: 10.1016/j.biopsych.2005.09.018

Neuhoff, H., Neu, A., Liss, B., and Roeper, J. (2002). I(h) channels contribute to the different functional properties of identified dopaminergic subpopulations in the midbrain. *J. Neurosci.* 22, 1290–1302. doi: 10.1523/jneurosci.22-04-01290.2002

Nicklas, W. J., Vyas, I., and Heikkila, R. E. (1985). Inhibition of NADH-linked oxidation in brain mitochondria by 1-methyl-4-phenyl-pyridine, a metabolite of the neurotoxin, 1-methyl-4-phenyl-1,2,5,6-tetrahydropyridine. *Life Sci.* 36, 2503–2508. doi: 10.1016/0024-3205(85)90146-8

Nishimura, A. L., Mitne-Neto, M., Silva, H. C., Richieri-Costa, A., Middleton, S., Cascio, D., et al. (2004). A mutation in the vesicle-trafficking protein VAPB causes late-onset spinal muscular atrophy and amyotrophic lateral sclerosis. *Am. J. Hum. Genet.* 75, 822–831. doi: 10.1086/425287

Nolan, M. F., Dudman, J. T., Dodson, P. D., and Santoro, B. (2007). HCN1 channels control resting and active integrative properties of stellate cells from layer II of the entorhinal cortex. *J. Neurosci.* 27, 12440–12451. doi: 10.1523/jneurosci.2358-07.2007

Nolan, M. F., Malleret, G., Dudman, J. T., Buhl, D. L., Santoro, B., Gibbs, E., et al. (2004). A behavioral role for dendritic integration: HCN1 channels constrain spatial memory and plasticity at inputs to distal dendrites of CA1 pyramidal neurons. *Cell* 119, 719–732. doi: 10.1016/s0092-8674(04)01055-4

Nolan, M. F., Malleret, G., Lee, K. H., Gibbs, E., Dudman, J. T., Santoro, B., et al. (2003). The hyperpolarization-activated HCN1 channel is important for motor learning and neuronal integration by cerebellar Purkinje cells. *Cell* 115, 551–564. doi: 10.1016/s0092-8674(03)00884-5

Notomi, T., and Shigemoto, R. (2010). Immunohistochemical localization of Ih channel subunits, HCN1–4, in the rat brain. *J. Comp. Neurol.* 471, 241–276. doi: 10.1002/cne.11039

O'Brien, R. J., and Wong, P. C. (2011). Amyloid precursor protein processing and Alzheimer's disease. *Ann. Rev. Neurosci.* 34, 185–204.

Obeso, J. A., Rodríguez-Oroz, M. C., Rodríguez, M., Lanciego, J. L., Artieda, J., Gonzalo, N., et al. (2000). Pathophysiology of the basal ganglia in Parkinson's disease. *Trends Neurosci.* 23, S8–S19.

Okamoto, T., Harnett, M. T., and Morikawa, H. (2006). Hyperpolarization-activated cation current (Ih) is an ethanol target in midbrain dopamine neurons of mice. *J. Neurophysiol.* 95, 619–626. doi: 10.1152/jn.00682.2005

Postuma, R. B., Gagnon, J. F., Pelletier, A., and Montplaisir, J. Y. (2017). Insomnia and somnolence in idiopathic RBD: a prospective cohort study. *NPJ Parkinsons Dis.* 3:9. doi: 10.1038/s41531-017-0011-7

Pott Godoy, M. C., Tarelli, R., Ferrari, C. C., Sarchi, M. I., and Pitossi, F. J. (2008). Central and systemic IL-1 exacerbates neurodegeneration and motor symptoms in a model of Parkinson's disease. *Brain* 131, 1880–1894. doi: 10.1093/brain/awn101

Rogelj, B., Mitchell, J. C., Miller, C. C. J., and Mcloughlin, D. M. (2006). The X11/Mint family of adaptor proteins. *Brain Res. Rev.* 52, 305–315. doi: 10.1016/j.brainresrev.2006.04.005

Russman, B. S. (2007). Spinal muscular atrophy: clinical classification and disease heterogeneity. *J. Child Neurol.* 22, 946–951. doi: 10.1177/0883073807305673

Saito, Y., Akiyama, M., Araki, Y., Sumioka, A., Shiono, M., Taru, H., et al. (2011). Intracellular trafficking of the amyloid β-protein precursor (APP) regulated by novel function of X11-like. *PLoS One* 6:e22108. doi: 10.1371/journal.pone.0022108

Saito, Y., Inoue, T., Zhu, G., Kimura, N., Okada, M., Nishimura, M., et al. (2012). Hyperpolarization-activated cyclic nucleotide gated channels: a potential molecular link between epileptic seizures and abeta generation in Alzheimer's disease. *Mol. Neurodegener.* 7:50. doi: 10.1186/1750-1326-7-50

Santoro, B., Chen, S., Luthi, A., Pavlidis, P., Shumyatsky, G. P., Tibbs, G. G. R., et al. (2000). Molecular and functional heterogeneity of hyperpolarization-activated pacemaker channels in the mouse CNS. *J. Neurosci.* 20, 5264–5275. doi: 10.1523/jneurosci.20-14-05264.2000

Santoro, B., Liu, D. T., Yao, H., Bartsch, D., Kandel, E. R., Siegelbaum, S. A., et al. (1998). Identification of a gene encoding a hyperpolarization-activated pacemaker channel of brain. *Cell* 93, 717–729. doi: 10.1016/s0092-8674(00)81434-8

Selkoe, D. J. (2002). Alzheimer's disease is a synaptic failure. *Science* 298, 789–791. doi: 10.1007/978-981-10-7757-9_11

Seutin, V., Massotte, L., Renette, M. F., and Dresse, A. (2001). Evidence for a modulatory role of Ih on the firing of a subgroup of midbrain dopamine neurons. *Neuroreport* 12, 255–258. doi: 10.1097/00001756-200102120-00015

Shahi, P. K., Choi, S., Zuo, D. C., Kim, M. Y., Park, C. G., Kim, Y. D., et al. (2014). The possible roles of hyperpolarization-activated cyclic nucleotide channels in regulating pacemaker activity in colonic interstitial cells of cajal. *J. Gastroenterol.* 49, 1001–1010. doi: 10.1007/s00535-013-0849-3

Silbernagel, N., Walecki, M., Schäfer, M. K., Kessler, M., Zobeiri, M., Rinné, S., et al. (2018). The VAMP-associated protein VAPB is required for cardiac and neuronal pacemaker channel function. *FASEB J.* doi: 10.1096/fj.201800246R [Epub ahead of print].

Singaram, C., Ashraf, W., Gaumnitz, E. A., Torbey, C., Sengupta, A., Pfeiffer, R., et al. (1995). Dopaminergic defect of enteric nervous system in Parkinson's disease patients with chronic constipation. *Lancet* 346, 861–864. doi: 10.1016/s0140-6736(95)92707-7

Sinha, M., and Narayanan, R. (2015). HCN channels enhance spike phase coherence and regulate the phase of spikes and LFPs in the theta-frequency range. *PNAS* 112, E2207–E2216. doi: 10.1073/pnas.1419017112

Smeyne, R. J., and Jackson-Lewis, V. (2005). The MPTP model of Parkinson's disease. *Brain Res. Mol. Brain Res.* 134, 57–66. doi: 10.1002/mds.27201

Stadler, K., Bierwirth, C., Stoenica, L., Battefeld, A., Reetz, O., Mix, E., et al. (2014). Elevation in type I interferons inhibits HCN1 and slows cortical neuronal oscillations. *Cereb. Cortex* 24, 199–210. doi: 10.1093/cercor/bhs305

Stieglitz, M. S., Fenske, S., Hammelmann, V., Becirovic, E., Schottle, V., Delorme, J. E., et al. (2017). Disturbed processing of contextual information in HCN3 channel deficient mice. *Front. Mol. Neurosci.* 10:436. doi: 10.3389/fnmol.2017.00436

Sun, Q. Q., Prince, D. A., and Huguenard, J. R. (2003). Vasoactive intestinal polypeptide and pituitary adenylate cyclase-activating polypeptide activate hyperpolarization-activated cationic current and depolarize thalamocortical neurons *in vitro*. *J. Neurosci.* 23, 2751–2758. doi: 10.1523/jneurosci.23-07-02751.2003

Surmeier, D. J., Mercer, J. N., and Chan, C. S. (2005). Autonomous pacemakers in the basal ganglia: who needs excitatory synapses anyway? *Curr. Opin. Neurobiol.* 15, 312–318. doi: 10.1016/j.conb.2005.05.007

Syed, E. C., Benazzouz, A., Taillade, M., Baufreton, J., Champeaux, K., Falgairolle, M., et al. (2012). Oscillatory entrainment of subthalamic nucleus neurons and behavioural consequences in rodents and primates. *Eur. J. Neurosci.* 36, 3246–3257. doi: 10.1111/j.1460-9568.2012.08246.x

Tibbs, G. R., Posson, D. J., and Goldstein, P. A. (2016). Voltage-gated ion channels in the PNS: novel therapies for neuropathic pain? *Trends Pharmacol. Sci.* 37, 522–542. doi: 10.1016/j.tips.2016.05.002

Tsay, D., Dudman, J. T., and Siegelbaum, S. A. (2007). HCN1 channels constrain synaptically evoked Ca2+ spikes in distal dendrites of CA1 pyramidal neurons. *Neuron* 56, 1076–1089. doi: 10.1016/j.neuron.2007.11.015

Tye, K. M., Mirzabekov, J. J., Warden, M. R., Ferenczi, E. A., Tsai, H. C., Finkelstein, J., et al. (2013). Dopamine neurons modulate neural encoding and expression of depression-related behaviour. *Nature* 493, 537–541. doi: 10.1038/nature11740

Vasilyev, D. V., and Barish, M. E. (2002). Postnatal development of the hyperpolarization-activated excitatory current Ih in mouse hippocampal pyramidal neurons. *J. Neurosci.* 22, 8992–9004. doi: 10.1523/jneurosci.22-20-08992.2002

Vivien, C., and Castillo, P. E. (2002). Assessing the role of Ih channels in synaptic transmission and mossy fiber LTP. *Proc. Nat. Acad. Sci. U.S.A.* 99, 9538–9543. doi: 10.1073/pnas.142213199

Wang, Y. P., Sun, B. Y., Li, Q., Dong, L., Zhang, G. H., Grundy, D., et al. (2012). Hyperpolarization-activated cyclic nucleotide-gated cation channel subtypes differentially modulate the excitability of murine small intestinal afferents. *World J. Gastroenterol.* 18, 522–531. doi: 10.3748/wjg.v18.i6.522

Weisskopf, M. G., Chen, H., Schwarzschild, M. A., Kawachi, I., and Ascherio, A. (2003). Prospective study of phobic anxiety and risk of Parkinson's disease. *Mov. Disord.* 18, 646–651. doi: 10.1002/mds.10425

Werkman, T. R., Kruse, C. G., Nievelstein, H., Long, S. K., and Wadman, W. J. (2001). In vitro modulation of the firing rate of dopamine neurons in the rat substantia nigra pars compacta and the ventral tegmental area by antipsychotic drugs. *Neuropharmacology* 40, 927–936. doi: 10.1016/s0028-3908(01)00015-6

Xue, W. N., Wang, Y., He, S. M., Wang, X. L., Zhu, J. L., and Gao, G. D. (2012). SK- and h-current contribute to the generation of theta-like resonance of rat substantia nigra pars compacta dopaminergic neurons at hyperpolarized membrane potentials. *Brain Struct. Funct.* 217, 379–394. doi: 10.1007/s00429-011-0361-6

Yan, Z. Q., Liu, S. M., Li, J., Wang, Y., Gao, L., Xie, R. G., et al. (2012). Membrane resonance and its ionic mechanisms in rat subthalamic nucleus neurons. *Neurosci. Lett.* 506, 160–165. doi: 10.1016/j.neulet.2011.10.072

Yee, A. G., Lee, S. M., Hunter, M. R., Glass, M., Freestone, P. S., and Lipski, J. (2014). Effects of the parkinsonian toxin MPP+ on electrophysiological properties of nigral dopaminergic neurons. *Neurotoxicology* 45, 1–11. doi: 10.1016/j.neuro.2014.08.009

Zhong, P., Vickstrom, C. R., Liu, X., Hu, Y., Yu, L., Yu, H. G., et al. (2018). HCN2 channels in the ventral tegmental area regulate behavioral responses to chronic stress. *eLife* 7, 11–15. doi: 10.7554/eLife.32420

Zobeiri, M., Chaudhary, R., Datunashvili, M., Heuermann, R. J., Luttjohann, A., Narayanan, V., et al. (2018). Modulation of thalamocortical oscillations by TRIP8b, an auxiliary subunit for HCN channels. *Brain Struct. Funct.* 223, 1537–1564. doi: 10.1007/s00429-017-1559-z

Zolles, G., Wenzel, D., Bildl, W., Schulte, U., and Hofmann, A. (2009). Association with the auxiliary subunit PEX5R/Trip8b controls responsiveness of HCN channels to camp and adrenergic stimulation. *Neuron* 62, 814–825. doi: 10.1016/j.neuron.2009.05.008

Conflict of Interest Statement: The authors declare that the research was conducted in the absence of any commercial or financial relationships that could be construed as a potential conflict of interest.

frontiers in Cellular Neuroscience

PERSPECTIVE
published: 10 July 2019
doi: 10.3389/fncel.2019.00314

Down-Regulation of Essential Synaptic Components by GI-Tract Microbiome-Derived Lipopolysaccharide (LPS) in LPS-Treated Human Neuronal-Glial (HNG) Cells in Primary Culture: Relevance to Alzheimer's Disease (AD)

*Yuhai Zhao[1,2], Nathan M. Sharfman[1], Vivian R. Jaber[1] and Walter J. Lukiw[1,3,4]**

[1] LSU Neuroscience Center, Louisiana State University Health Sciences Center, New Orleans, LA, United States, [2] Department of Anatomy and Cell Biology, Louisiana State University Health Sciences Center, New Orleans, LA, United States, [3] Department of Neurology, Louisiana State University Health Sciences Center, New Orleans, LA, United States, [4] Department of Ophthalmology, Louisiana State University Health Sciences Center, New Orleans, LA, United States

OPEN ACCESS

Edited by:
Jaichandar Subramanian,
University of Kansas, United States

Reviewed by:
Xinhua Zhan,
University of California, Davis, United States
Yuriy Pankratov,
University of Warwick, United Kingdom

***Correspondence:**
Walter J. Lukiw
wlukiw@lsuhsc.edu

Specialty section:
This article was submitted to Cellular Neuropathology, a section of the journal Frontiers in Cellular Neuroscience

Received: 16 April 2019
Accepted: 26 June 2019
Published: 10 July 2019

Citation:
Zhao Y, Sharfman NM, Jaber VR and Lukiw WJ (2019) Down-Regulation of Essential Synaptic Components by GI-Tract Microbiome-Derived Lipopolysaccharide (LPS) in LPS-Treated Human Neuronal-Glial (HNG) Cells in Primary Culture: Relevance to Alzheimer's Disease (AD). Front. Cell. Neurosci. 13:314. doi: 10.3389/fncel.2019.00314

Trans-synaptic neurotransmission of both electrical and neurochemical information in the central nervous system (CNS) is achieved through a highly interactive network of neuron-specific synaptic proteins that include pre-synaptic and post-synaptic elements. These elements include a family of several well-characterized integral- and *trans*-membrane synaptic core proteins necessary for the efficient operation of this complex signaling network, and include the *pre-synaptic proteins*: (i) neurexin-1 (NRXN-1); (ii) the synaptosomal-associated phosphoprotein-25 (SNAP-25); (iii) the phosphoprotein synapsin-2 (SYN-2); and the *post-synaptic elements:* (iv) neuroligin (NLGN), a critical cell adhesion protein; and (v) the SH3-ankyrin repeat domain, proline-rich cytoskeletal scaffolding protein SHANK3. All five of these pre- and post-synaptic proteins have been found to be significantly down-regulated in primary human neuronal-glial (HNG) cell co-cultures after exposure to *Bacteroides fragilis* lipopolysaccharide (BF-LPS). Interestingly, LPS has also been reported to be abundant in Alzheimer's disease (AD) affected brain cells where there are significant deficits in this same family of synaptic components. This "*Perspectives*" paper will review current research progress and discuss the latest findings in this research area. Overall these experimental results provide evidence (i) that gastrointestinal (GI) tract-derived Gram-negative bacterial exudates such as

BF-LPS express their neurotoxicity in the CNS in part through the directed down-regulation of neuron-specific neurofilaments and synaptic signaling proteins; and (ii) that this may explain the significant alterations in immune-responses and cognitive deficits observed after bacterial-derived LPS exposure to the human CNS.

Keywords: Alzheimer's disease (AD), *Bacteroides fragilis*, dysbiosis/microbiome, lipopolysaccharide (LPS), neurexin (NRXN)/SNAP-25, synapsin-2 (SYN-2), neurofilament light (NF-L) chain protein, neuroligin (NLGN)/SHANK3

OVERVIEW

Synaptic Protein Down-Regulation and Degeneration in Alzheimer's Disease (AD)

As the basic structural and functional components for inter-neuronal communication, synapses with sufficient, and consistent protein quality and quantity are essential for neural connectivity and functionality in the central nervous system (CNS) to maintain the continuous flow of functional neural information (Bae and Kim, 2017; Chen et al., 2019; Lee and Kim, 2019). Therefore, not too surprisingly, loss of critical synaptic components, synaptic disorganization, neuronal atrophy, and loss of synaptic contact, dysfunction at the pre-synaptic–post-synaptic interface and altered synapse-to-nucleus signaling have the highest correlation with cognitive deficits in progressive neurodevelopmental and inflammatory neurodegenerative disorders such as Alzheimer's disease (AD; Pogue and Lukiw, 2016; Marcello et al., 2018; Lee and Kim, 2019; Parra-Damas and Saura, 2019; Ramakrishna and Muddashetty, 2019).

Over the last several years multiple pre-synaptic and post-synaptic proteins including neurexin (NRXN), the synaptosomal-associated phosphoproteins SNAP-25 and synapsin-2 (SYN-2), the type 1 cell adhesion protein neuroligin (NLGN) and the proline-rich SH3-ankyrin repeat-containing cytoskeletal scaffolding protein SHANK3 have been identified and characterized: (i) as being critical to synaptic integrity, acting as key players in the modulation of synaptic neurotransmission, inter-neuronal signaling and synaptic plasticity; and (ii) as being down-regulated in AD and other progressive and lethal inflammatory neurodegenerative disorders of the human CNS (Guilmatre et al., 2014; Sindi and Dodd, 2015; Alexandrov et al., 2017; Bae and Kim, 2017; Itoh and Voskuhl, 2017; Chen et al., 2019; Karmakar et al., 2019; Lee and Kim, 2019; Lleó et al., 2019). Increasing evidence indicates that the combined down-regulation of these critical synaptic elements and synapse-associated proteins impairs *trans*-synaptic communication resulting in pathogenic neurotransmission that is accompanied by deficits in behavior, cognition, and memory formation.

The Human GI-Tract Microbiome and Gram-Negative Anaerobic Bacillus *Bacteroides fragilis*

Emerging evidence continues to suggest a contribution of the gastrointestinal (GI)-tract microbiome to human neurological health and disease (Bhattacharjee and Lukiw, 2013; Ghaisas et al., 2016; Barko et al., 2018; Awany et al., 2019). The GI-tract of *Homo sapiens* contains a complex microbiome consisting primarily of bacteria, with archaea, fungi, microbial eukaryotes, protozoa, viruses, and other microorganisms making up the balance (Giau et al., 2018; Zhao and Lukiw, 2018a,b; Awany et al., 2019; Ticinesi et al., 2019). Together with human host cells the microbiome comprises the entire meta-organism whose host interactions and symbiotic associations are significantly implicated in the biochemistry and neurochemistry of human health and disease (Hill and Lukiw, 2015; Youssef et al., 2015; Zhao et al., 2017c; Barko et al., 2018; Ticinesi et al., 2019). Microbiome-linked diseases include lethal, progressive, age-related, inflammatory neurodegenerative and synaptic disorders of the human CNS such as AD (Bhattacharjee and Lukiw, 2013; Yang and Chiu, 2017; Zhao et al., 2017a,b,c; Franceschi et al., 2019; Ticinesi et al., 2019). Interestingly, of the 52 currently recognized bacterial phyla, *H. sapiens* have co-evolved with just two dominant divisions: *Bacteroidetes*, representing ∼20–30% of all human GI-tract resident bacteria, and *Firmicutes* (about 70–80%), with *Actinobacteria* (∼3%), *Proteobacteria* (∼1%), and *Verrucomicrobia* (∼0.1%) making up the remaining divisions. These five major bacterial phyla represent the "*microbial-core*" of the human GI-tract microbiome (Youssef et al., 2015; Sarkar and Banerjee, 2019; Ticinesi et al., 2019). The vast majority of all human GI-tract microbiota consists of Gram-negative anaerobic bacteria, and *Bacteroidetes* species represent the most abundant Gram-negative anaerobic genus, outnumbering *Escherichia coli* in abundance by about one-hundred-to-one (Sears, 2009; Fathi and Wu, 2016). Interestingly, certain *Bacteroidetes* species such as *Bacteroides fragilis* (*B. fragilis*), as a normal commensal microbe of the human GI-tract, are thought to be usually advantageous to human health due to their abilities to biosynthesize and/or metabolize dietary fiber, complex sugars and polysaccharides, volatile fatty acids, and other nutrients, to function in the development, maintenance, and homeostasis of the host immune and digestive systems (Sears, 2009; Fathi and Wu, 2016; Lukiw, 2016). However, when enterotoxigenic strains of *Bacteroidetes* species including *B. fragilis* proliferate and their formidable array of secreted neurotoxins, including the classic neuro-inflammatory pattern recognition molecule LPS, leak through normally protective mucosal barriers of the GI-tract and blood–brain barrier (BBB) they can cause substantial inflammatory pathology both systemically and within vulnerable CNS compartments (Fathi and Wu, 2016; Lukiw, 2016; Zhao and Lukiw, 2018a,b; Barton et al., 2019; Batista et al., 2019; Sheppard et al., 2019).

BF-LPS, NEUROINFLAMMATION AND SYNAPTIC DISTURBANCES

The lipopolysaccharide of *Bacteroides fragilis* (BF-LPS) is one of the most neurotoxic and pro-inflammatory lipoglycans known (Sears, 2009; Lukiw, 2016; Batista et al., 2019; Sheppard et al., 2019). The pathogenic actions, pro-inflammatory mechanisms and neurodegeneration-promoting activities, however, of these secreted Gram-negative exotoxins on developing, adult or aging synaptic structure and function remain incompletely understood but currently significant progress is being made (Chugh et al., 2013; Fathi and Wu, 2016; Lukiw, 2016; Barko et al., 2018; Zhan et al., 2018; Zhao and Lukiw, 2018a,b; Awany et al., 2019; Barton et al., 2019; Lee and Kim, 2019; Sarkar and Banerjee, 2019; Sheppard et al., 2019; Wu et al., 2019). LPS-induced cognitive impairments appear to be, in part, the result of attenuated neocortical and/or hippocampal microglial activation, cytokine and reactive oxidative species (ROS) generation and oxidative stress damage, disruption of the BBB, the ROS-mediated oxidative destruction and loss of synaptic plasticity related proteins, up-regulated neuroinflammatory signaling or any combination of these (Li et al., 2015; Yang and Chiu, 2017; Barton et al., 2019; Batista et al., 2019; Sheppard et al., 2019; Wu et al., 2019).

EFFECTS OF LPS IN EXPERIMENTAL MODELS OF CNS INJURY AND NEURODEGENERATION

The intraperitoneal injection of LPS in experimental brain injury models elicits a rapid innate-immune-response and systemic inflammatory reaction with accompanying cognitive deficits (Chen et al., 2012, 2019; Zhao and Lukiw, unpublished). Interestingly both LPS-treated and chronically sleep-restricted mice exhibit higher brain expression of pro-inflammatory mediators and significant reductions in the levels of pre- and post-synaptic marker proteins (Kincheski et al., 2017; Batista et al., 2019; Chen et al., 2019; Sheppard et al., 2019). Hippocampal neurons from newborns are highly susceptible to LPS-induced brain inflammation affecting microglial-mediated synaptogenesis with disproportionate alterations in synaptic adhesion molecules and synaptic scaffolding proteins, and accompanying deficits in cognition (Hao et al., 2010; Chugh et al., 2013; Batista et al., 2019; Wu et al., 2019). Systemic inflammation as the result of LPS injection in neonatal mouse models or the use of the 5XFAD transgenic mouse model of AD has been further shown to increase the permeability of the BBB (Barton et al., 2019) and induce a significant spatial cognitive impairment as measured using Morris water maze tasks in LPS-treated animals later in adulthood (Peng et al., 2019). Prenatal exposure to LPS also results in cognitive deficits in offspring rodents as they age (Hao et al., 2010). LPS also induces a progressive neuro-inflammation, apoptosis, synaptic dysfunction cognitive impairment in aging murine models of neurodegeneration (Batista et al., 2019; Sheppard et al., 2019; Wu et al., 2019). Taken together these data indicate that LPS-mediated deficits in multiple synaptic components, LPS-induced synaptic dysfunction and altered synaptogenesis may be the common factor linking a progressive or developmental synaptic disorganization that is temporally associated with cognitive failure and/or age-related cognitive decline.

HNG CELLS – DNA ARRAY AND ELISA-BASED ASSAY OF β-ACTIN, NF-L AND SYNAPTIC GENE EXPRESSION

The culture and growth of human neuronal-glial (HNG) cells and preparation of LPS-enriched extracts from different Gram negative bacterial sources has been previously described in detail by our laboratory (Zhao et al., 2015, 2017a,b,c; Lukiw, 2016; Zhao and Lukiw, 2018a,b). The commercial source of HNG cells (Lonza, Houston TX, United States; Catalog #: PT-2599; see **Figures 1A–F**) is supplied as ampules of cryopreserved neurospheres isolated from human brain cortex; neurospheres are clusters of cells typically referred to as neural stem cells and progenitors (NSPCs), human brain-derived neural progenitor cells (hbdNPCs) or HNG cell co-cultures (Zhao et al., 2017a,b,c; Zhao and Lukiw, 2018a,b; Lonza, 2019). The analysis, verification and quantitation of the control β-actin filament, the down-regulated neuron-specific neurofilament light (NF-L) chain intermediate filament protein and this family of five pre- and post-synaptic messenger RNA (mRNA) and proteins described here were based on: (i) micro-fluidic DNA array analytical technologies for mRNA abundance, speciation and complexity (**Figure 2A**), and (ii) highly sensitive ELISA-based assays for the quantification of filament and synaptic protein levels (**Figure 2B**). Both of these methodologies have been extensively described and developed by our laboratory over the last 21 years (Colangelo et al., 2002; Cui et al., 2010; Lukiw et al., 2018; Zhao and Lukiw, 2018a,b).

β-ACTIN, NF-L AND SYNAPSE-ASSOCIATED PROTEINS: THEIR INTEGRATED FUNCTIONS AND METHODS OF DETECTION

β-actin (also known as ACTB; encoded at human chr 7p22.1) is a highly conserved 42 kDa polypeptide that polymerizes to produce microfilaments that form cross-linked networks in the cellular cytoplasm; interestingly β-actin is the most abundant 6 nm diameter microfilament in the synapse; β-actin proteins and filaments were detected using a ACTB/β-actin ELISA Kit; catalog number LS-F10737 (LifeSpan BioSciences, Seattle WA) with a detection range of 0.312–20 ng/ml. The neurofilament-light (NF-L) chain protein (also known as NEFL, NF68, NFL; encoded at human chr 8p21.2) is a 68 kDa polypeptide that forms a 10 nm diameter type IV intermediate filament specific to the neuronal cytoplasm;

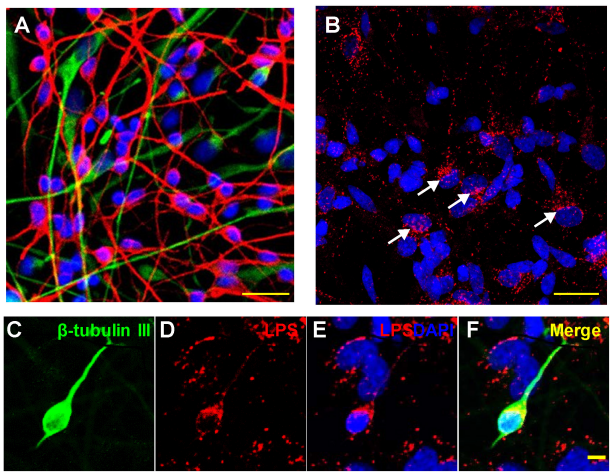

FIGURE 1 | Association of lipopolysaccharide (LPS) with human neuronal-glial (HNG) cells in primary co-culture; **(A)** HNG cells are a primary co-culture of neuronal [β-tubulin III (βTUBIII)-stained; red; λ_{max} = 690 nm] and glial (GFAP-stained; green; λ_{max} = 520 nm) human brain cells; cells are also stained for nuclei (DAPI-stained; blue; λ_{max} = 470 nm); cells shown are ∼2 weeks in culture; HNG cells are ∼60% neurons and ∼40% astroglia at ∼65% confluency; human primary neuronal and glial "support" cell co-cultures are utilized, because human neuronal cells do not culture well by themselves (Cui et al., 2010; Zhao et al., 2017b); HNG cells are electrically active and extremely sensitive to pro-inflammatory neurotoxins in the nM range (Lonza human cell systems; transplantation grade; Zhao et al., 2017b); yellow bar ∼20 um; HNG cells were exposed to 50 nM LPS for 36 h; **(B)** LPS (red; λ_{max} = 690 nm) and nuclei (blue; λ_{max} = 470 nm) stained HNG cells; four white arrows indicate perinuclear clustering of LPS as has been previously reported (Hill and Lukiw, 2015; Zhan et al., 2016, 2018; Yang and Chiu, 2017; Zhao et al., 2017a,c); panels **(C–F)** show details of LPS-neuronal cell interactions in a single neuron; LPS preferentially associates with neuronal nuclei and non-neuronal nuclei to a lesser extent (Zhao et al., 2017a,b,c; Zhao and Lukiw, 2018a,b); **(C)** β-TUBIII (green stain, λ_{max} = 520 nm) is a neuron-specific stain; a single neuron is highlighted; **(D)** LPS (red stain; λ_{max} = 690 nm) shows non-homogeneous clustering of LPS stain; **(E)** LPS (red stain; λ_{max} = 690 nm) and DAPI-stained nuclei (blue stain; λ_{max} = 470 nm) shows a "polarized" LPS affinity for the periphery of neuronal nuclei (see Zhao et al., 2017c); **(F)** merge of all signals; all yellow bars in **(A–F)** ∼20 um; LPS attraction for neuronal nuclei may be in part glial-cell modulated; there is recent evidence that perinuclear LPS may disrupt the normal transcriptional output of human neuronal nuclei for neuron-specific components such as the neurofilament light chain (NF-L) protein (Lukiw et al., 2018; Zhao et al., 2019).

together with microfilaments and microtubules NF-L forms the neuronal cytoskeleton and regulates axonal caliber and axonal conduction velocity; NF-L has long been known to exhibit significantly reduced expression in AD brain (McLachlan et al., 1988; Colangelo et al., 2002); NF-L filaments were detected using a human NF-L (NEFL) ELISA kit catalog number abx258398 (Abbexa Biosciences, Houston, TX) with a detection range of 15.6–1000 pg/ml. Neurexin-1 (NRXN; encoded at chr 2p16.3), is a large 162 kDa single-pass type I membrane protein that serves as a cell-surface receptor and binds neuroligins to form Ca^{2+}-dependent neurexin/neuroligin (NRXN/NLGN) complexes at CNS synapses; these are required for efficient neurotransmission and are involved in the formation of stable synaptic contacts; NRXN-1 was detected using a NRXN1 ELISA kit; Catalog Number ABIN2870172 (LifeSpan BioSciences); with a detection range of 0.312–20 ng/ml). The synaptosome associated protein 25 (SNAP25; encoded at human chr 20p12.2) is a 25 kDa synaptic vesicle membrane docking and fusion protein whose actions are mediated by SNAREs (soluble N-ethylmaleimide-sensitive factor attachment protein receptors) located on the synaptic vesicle membrane (v-SNAREs) and/or the target membrane (t-SNAREs); SNAP25 is a pre-synaptic plasma membrane protein involved in the regulation of neurotransmitter release; SNAP25 proteins were detected using a SNAP25 ELISA kit; Catalog Number LS-F17747-1 (LifeSpan BioSciences); with a detection range of 0.78–50 ng/ml. Synapsin-2 (SYN-2; encoded at chr 3p25.2) is a ∼54 kDa member of the synapsin gene family, encoding a neuronal phosphoprotein that associates with the cytoplasmic surface of synaptic vesicles; SYN-2 is implicated in synaptogenesis and the impairment of neurotransmitter release in multiple neuropsychiatric diseases (Alexandrov et al., 2017; Karmakar et al., 2019); SYN-2 was detected using a human SYN-2 ELISA kit Catalog Number MBS1603051 (MyBioSource, San Diego, CA) with a detection range of 0.55–50 ng/ml tissue suspension. The type 1 cell surface-cell adhesion protein neuroligin (NLGN; encoded at human chr 3q26.31) is a 94 kDa type 1 integral membrane protein of the type-B carboxylesterase/lipase family; NLGN is located on the post-synaptic membrane and acts as a ligand for β-neurexins (which are cell adhesion proteins located pre-synaptically); NLGNs affect the properties of neural networks by specifying synaptic functions and mediating synaptic signaling by recruiting and stabilizing key synaptic components; NLGN also plays a role in synapse function and synaptic signal transmission and mediates its signaling effects by recruiting and clustering other synaptic proteins, by promoting the initial formation of synapses and by triggering the *de novo* formation of pre-synaptic structures may be involved in the specification of excitatory synapses; synaptic adhesion molecules such as NLGN have an essential role in synaptic development (Chugh et al., 2013); NLGN was detected using a human neuroligin 1 (NLGN1) ELISA kit; Catalog Number MBS9313140 (MyBioSource) with a detection range of 6.25–200 ng/ml. The SH3 and multiple ankyrin repeat domain three post-synaptic protein SHANK3 (encoded at human chr 22q13.3) is a very large ∼186 kDa proline-rich post-synaptic cytoskeletal scaffolding protein that functions as an adapter protein at the post-synaptic density (PSD) of excitatory synapses that interconnects receptors of the post-synaptic membrane; these include NMDA-type and metabotropic glutamate receptors via complexes with GKAP/PSD-95 and Homer, respectively, and the β-actin-based micro-cytoskeleton; SHANK3 also plays a critical role in the structural and functional organization of the dendritic spine and synaptic junction and as such are key players in the modulation of *trans*-synaptic neurotransmission and synaptic plasticity (Guilmatre et al., 2014; Alexandrov et al., 2017; Marcello et al., 2018); levels of SHANK3 protein were detected and quantified using an ELISA kit specific for SHANK3; Catalog Number MBS900106 (MyBioSource) with a detection range of 15.6–1000 pg/ml.

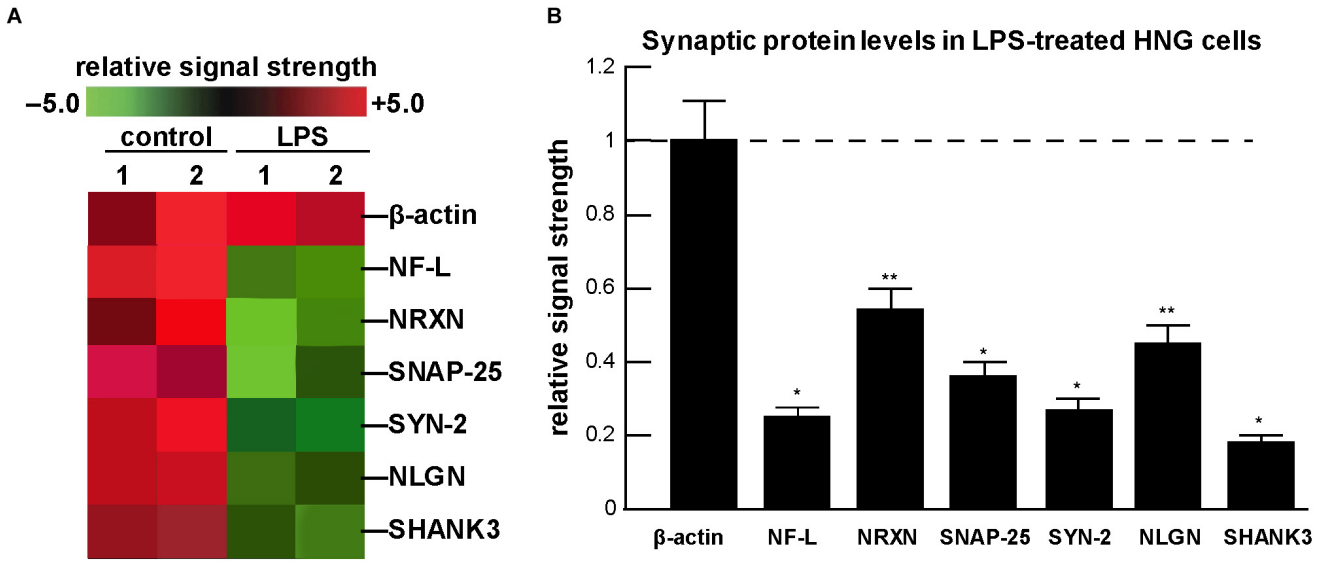

FIGURE 2 | Analysis of expression of neuronal-specific and/or synaptic genes and their proteins in HNG cells in the presence of lipopolysaccharide (LPS) using a GeneChip microarray and ELISA-based approach; **(A)** a typical computer-generated "cluster diagram" or "heat map" of mRNA-based expression data for selected neuron-specific mRNAs; in all experiments the control microfilament marker β-actin was not found to change; however, NF-L and five critical pre- and post-synaptic proteins analyzed were found to decrease from 0.18- to 0.54-fold of control; the results shown are a mean of 3 GeneChip analyses of 2 independent experiments (control) and 2 independent experiment (LPS); **(B)** using ELISA, neuron-specific filament and synaptic protein levels were quantified and compared against their control values; the control β-actin microfilament protein displayed unchanging levels and its expression was set at 1.0; the neuron-specific neurofilament-light (NF-L) polypeptide has long been known to be down-regulated in the limbic system of AD brain (McLachlan et al., 1988; Colangelo et al., 2002); the *pre-synaptic* proteins neurexin (NRXN); the synaptosomal-associated phosphoprotein-25 (SNAP-25); the phosphoprotein synapsin-2 (SYN-2); and the *post-synaptic* elements type 1 cell adhesion protein neuroligin (NLGN); and the SH3-ankyrin repeat domain, proline-rich post-synaptic-associated cytoskeletal protein SHANK3 were all found to be down-regulated after LPS-treatment of HNG cells; a dashed horizontal line at 1.0 is included for ease of comparison; results are shown as one mean and one standard deviation of $N = 3$–5 experiments for each determination of filament or synaptic element; $^{*}p < 0.001$; $^{**}p < 0.05$ (ANOVA). Taken together the results suggest an LPS-directed down-regulation of critical neuron-specific cytoskeletal and synaptic components in HNG co-cultures and this may explain, in part, the significant alterations and deficits in immune responses and cognition observed after bacterial-sourced LPS exposure to the human CNS.

DOWN-REGULATION OF NF-L AND PRE- AND POST-SYNAPTIC PROTEINS IN LPS-TREATED HNG CELLS

The neuron-specific NF-L intermediate filament protein, the pre-synaptic proteins NRXN-1, SNAP-25, SYN-2, and the post-synaptic proteins NLGN and SHANK3 constitute a critical mass of axonal filament support elements and synaptic signaling proteins whose deficits might be expected to lead to the inability of neurons and synapses to carry out both electrical- and neurochemical-based neurotransmission in the CNS, and hence contribute to deficits in cognition and memory formation in AD and in neurodegenerative disease models (Pogue and Lukiw, 2016; Marcello et al., 2018; Lee and Kim, 2019; Parra-Damas and Saura, 2019; Ramakrishna and Muddashetty, 2019). Why the expression of genes and proteins involved in the structure and function of the synapse appears to be targeted by the intensely pro-inflammatory LPS may be explained in part by the following multiple and highly interactive and dynamic factors:

(i) specific LPS-induced destabilizing effects on cell-adhesion proteins and vascular endothelial cells (Steven et al., 2017; Zhang et al., 2017; Hou et al., 2019; Sato et al., 2019);

(ii) LPS-mediated generation of ROS and the induction of significant amounts of oxidative stress which directly impacts the abundance and integrity of synapses, synaptogenesis and cognition in murine and related rodent models of neurodegeneration (Hao et al., 2010; Fujita-Hamabe and Tokuyama, 2012; Steven et al., 2017; Hou et al., 2019; Khan et al., 2019);

(iii) LPS-mediated disruption and opening of the BBB in transgenic AD mouse models (Barton et al., 2019; Sato et al., 2019);

(iv) LPS- and ROS-induced NF-kB (p50/p65) signaling, known to be a strong inducer of pro-inflammatory microRNAs (miRNAs) which target the 3′-untranslated regions (3'-UTR) of highly selective, AD-relevant mRNAs causing them to be down-regulated (Zhao and Lukiw, 2018b; Ramakrishna and Muddashetty, 2019; Zhao et al., 2019); interestingly, it has recently been shown that via NF-kB (p50/p65) signaling, BF-LPS up-regulates two pro-inflammatory miRNAs, miRNA-34a, and miRNA-146a, and these are known to down-regulate SHANK3 expression in in stressed HNG cells and in sporadic AD brain (Guilmatre et al., 2014; Alexandrov et al., 2017; Zhao and Lukiw, 2018b; Zhao et al., 2019);

(v) run-on transcription studies using HNG cells in primary culture employing an extremely sensitive endogenous RNA polymerase II activity driven incorporation of [$\alpha-^{32}$P]-uridine triphosphate (10^8 dpm/ml) into newly synthesized total RNA indicates that LPS at nanomolar concentrations strongly inhibits the transcriptional output of neuronal nuclei; this may contribute in part to the generalized down-regulation of gene expression for transcription factors and synaptic and neurotrophic markers as is widely observed in sporadic AD (Colangelo et al., 2002; Ginsberg et al., 2012; Garcia-Esparcia et al., 2017; Itoh and Voskuhl, 2017);

(vi) LPS, via synaptogenic targeting, has long been known to contribute to the impairment, alteration or shutting down of essential brain cell cognitive functions such as object recognition and spatial memory formation (Peng et al., 2019; Sarkar and Banerjee, 2019);

(vii) the progressive cognitive and functional impairment in AD and related forms of progressive inflammatory neurodegeneration is a reflection of progressive neuronal atrophy and synaptic loss; recent preclinical data suggests that LPS-activated microglia may contribute to the elimination of viable neurons and synapses by promoting a neurotoxic astrocytic phenotype known as A1, which can facilitate synaptic disruption and neuro-inflammation in response to peripherally applied LPS (Sfera et al., 2018; Sarkar and Banerjee, 2019);

(viii) a well-documented LPS-mediated neuro-inflammation, apoptosis, BBB disruption, synaptic dysfunction, and cognitive impairment, in multiple murine models of inflammatory neurodegeneration (Li et al., 2015; Barton et al., 2019; Batista et al., 2019; Khan et al., 2019; Lee and Kim, 2019; Peng et al., 2019; Wu et al., 2019);

(ix) LPS-directed synaptic dysfunction that may be related to the degradation of essential neuronal functions and/or part of a microbial immune-accommodation or evasion strategy directed toward immune tolerization and/or the triggering of an autoimmune response (Sfera et al., 2018; Zhao and Lukiw, 2018a; Barton et al., 2019; Sheppard et al., 2019);

(x) prenatal exposure to LPS that results in cognitive deficits in aging of offspring and LPS-induced cognitive impairment, neuro-inflammation, apoptosis, physiological barrier alteration, and synaptic dysfunction in multiple experimental animal models (Hao et al., 2010; Barton et al., 2019; Wu et al., 2019);

(xi) other yet unrecognized LPS-triggered neurological disruptions which significantly disturb homeostatic synaptic function that may be synergistic with other pathogenic factors involved in amyloidogenesis, neuronal atrophy and/or synaptic failure (Zhao and Lukiw, 2015; Kincheski et al., 2017; Zhao et al., 2017c; Sarkar and Banerjee, 2019); or (xii) any combination of these synapse-targeted pathogenic contributions via the actions of LPS.

CONCLUSION AND SUMMARY

The primary evidence of a potentially pathogenic link between microbial-derived neurotoxins of the human GI-tract microbiome, such as Gram-negative *B. fragilis*-derived LPS, and the contribution of LPS to the pathogenetic mechanisms of sporadic AD came over 6 years ago (Bhattacharjee and Lukiw, 2013). More recent evidence continues to strengthen our hypothesis that GI-tract-sourced, microbial-derived neurotoxins – now known to include Gram-negative bacterial-derived LPS, endotoxins and exotoxins (such as fragilysin), bacterial amyloids and bacterial-sourced small non-coding RNA (sncRNA) – have substantial potential to cross the aging and/or the diseased GI-tract and the BBB to gain access to CNS compartments, the parenchyma of brain cells and the neuronal cytoplasm to contribute to progressive pro-inflammatory neurodegeneration, altered synaptic organization and progressive loss of synaptic function. Activated microglial cells, astrocytes, and other types of glial cells appear to modulate many of these pathological activities of LPS, including LPS effects on neuronal nuclei (Chen et al., 2012, 2019; Zhao et al., 2017b; Lukiw et al., 2018). LPS-mediated synaptic alterations now appear to range from defective synaptogenesis during CNS development to increasingly altered cognitive abilities in AD and related neurological disorders which exhibit progressive inflammatory neurodegeneration (Chugh et al., 2013; Bae and Kim, 2017; Chen et al., 2019).

In summary, these combined results provide the first evidence that strongly pro-inflammatory, GI-tract microbiome-derived LPS induces both pre-synaptic and post-synaptic changes via the down-regulation of critical and specific synaptic components in primary HNG cell co-cultures, many of which are also observed in AD brain. The findings further support our idea that cytoskeletal-associated and synaptic molecules known to play essential roles in *trans*-synaptic communication: (i) are targeted by LPS and drive inflammatory neurodegenerative disease; and (ii) create specific alterations in neuronal synaptic transmission, and by doing so contribute to cognitive deficiencies characteristic of AD and the neurodegenerative disease process.

DATA AVAILABILITY

All datasets generated for this study are included in the manuscript and/or the supplementary files.

ETHICS STATEMENT

All acquisition, handling, experimental and analytical procedures involving human brain cell cultures (HNG cells) were carried out in an ethical manner in accordance with the ethics review board policies at brain and tissue donor institutions and at the Louisiana State University (LSU) Health Sciences Center. The ethical use of post-mortem human brain cells and their

analyses were also carried out in strict accordance with the Institutional Biosafety Committee and the Institutional Review Board Committee (IBC/IRBC) ethical guidelines IBC#18059 and IRBC#6774 at the LSU Health Sciences Center, New Orleans, LA, United States. The work in this research study was reviewed and approved by the IBC/IRB at the LSU Health Sciences Center, New Orleans, LA, United States.

AUTHOR CONTRIBUTIONS

WL compiled the research findings and wrote the final version of the manuscript. All authors performed the experiments, organized and compiled the data, and performed the statistical and bioinformatics analysis, and the literature searches.

FUNDING

Research on the GI-tract microbiome, human and murine small non-coding RNA (sncRNA) including microRNAs, pro-inflammatory, synaptic, and pathogenic signaling in the Lukiw laboratory involving the innate-immune response, neuroinflammation, and amyloidogenesis in human neurological disorders was supported through an unrestricted grant to the LSU Eye Center from Research to Prevent Blindness (RPB), the Louisiana Biotechnology Research Network (LBRN), the Alzheimer Association, and the NIH grants NEI EY006311, NIA AG18031, and NIA AG038834 (to WL).

ACKNOWLEDGMENTS

The analytical, experimental, and statistical work in this communication was presented in part at the Society for Neuroscience (SFN) Annual Meeting November 2018, San Diego, CA, United States and the SFN Annual Meeting October 2019 in Chicago, IL, United States. Sincere thanks are extended to the late Drs. J. M. Hill (Louisiana State University), T. P. A. Kruck (University of Toronto), C. Bergeron (University of Toronto) for neurofilament and synaptic protein antibody ELISA-based assay and helpful discussions on this research area and to C. Clement, J. G. Cui, C. Eicken, C. Hebel, Wenhong Li, and K. Navel for DNA array and ELISA assay, short post-mortem interval (PMI) human and other mammalian brain tissues or extracts and to D. Guillot and A. I. Pogue for expert technical assistance. All authors agreed on the content of this publication.

REFERENCES

Alexandrov, P. N., Zhao, Y., Jaber, V. R., Cong, L., and Lukiw, W. J. (2017). Deficits in the proline-rich synapse-associated SHANK3 protein in multiple neuropsychiatric disorders. *Front. Neurol.* 8:670. doi: 10.3389/fneur.2017.00670

Awany, D., Allali, I., Dalvie, S., Hemmings, S., Mwaikono, K. S., Thomford, N. E., et al. (2019). Host and microbiome genome-wide association studies. *Front. Genet.* 9:637. doi: 10.3389/fgene.2018.00637

Bae, J. R., and Kim, S. H. (2017). Synapses in neurodegenerative diseases. *BMB Rep.* 50, 237–246. doi: 10.5483/bmbrep.2017.50.5.038

Barko, P. C., McMichael, M. A., Swanson, K. S., and Williams, D. A. (2018). The gastrointestinal microbiome: a review. *J. Vet. Intern. Med.* 32, 9–25. doi: 10.1111/jvim.14875

Barton, S. M., Janve, V. A., McClure, R., Anderson, A., Matsubara, J. A., Gore, J. C., et al. (2019). Lipopolysaccharide induced opening of the blood brain barrier on aging 5XFAD mouse model. *J. Alzheimers Dis.* 67, 503–513. doi: 10.3233/JAD-180755

Batista, C. R. A., Gomes, G. F., Candelario-Jalil, E., Fiebich, B. L., and de Oliveira, A. C. P. (2019). Lipopolysaccharide-induced neuroinflammation as a bridge to understand neurodegeneration. *Int. J. Mol. Sci.* 20:E2293. doi: 10.3390/ijms20092293

Bhattacharjee, S., and Lukiw, W. J. (2013). Alzheimer's disease and the microbiome. *Front. Cell Neurosci.* 7:153. doi: 10.3389/fncel.2013.00153

Chen, Y., Fu, A. K. Y., and Ip, N. Y. (2019). Synaptic dysfunction in Alzheimer's disease: mechanisms and therapeutic strategies. *Pharmacol. Ther.* 195, 186–198. doi: 10.1016/j.pharmthera.2018.11.006

Chen, Z., Jalabi, W., Shpargel, K. B., Farabaugh, K. T., Dutta, R., Yin, X., et al. (2012). Lipopolysaccharide-induced microglial activation and neuroprotection against experimental brain injury is independent of hematogenous TLR4. *J. Neurosci.* 32, 11706–11715. doi: 10.1523/JNEUROSCI.0730-12.2012

Chugh, D., Nilsson, P., Afjei, S. A., Bakochi, A., and Ekdahl, C. T. (2013). Brain inflammation induces post-synaptic changes during early synapse formation in adult-born hippocampal neurons. *Exp. Neurol.* 250, 176–188. doi: 10.1016/j.expneurol.2013.09.005

Colangelo, V., Schurr, J., Ball, M. J., Pelaez, R. P., Bazan, N. G., and Lukiw, W. J. (2002). Gene expression profiling of 12633 genes in Alzheimer hippocampal CA1: transcription and neurotrophic factor down-regulation and up-regulation of apoptotic and pro-inflammatory signaling. *J. Neurosci. Res.* 70, 462–473. doi: 10.1002/jnr.10351

Cui, J. G., Li, Y. Y., Zhao, Y., Bhattacharjee, S., and Lukiw, W. J. (2010). Differential regulation of interleukin-1 receptor-associated kinase-1 (IRAK-1) and IRAK-2 by microRNA-146a and NF-kB in stressed human astroglial cells and in Alzheimer's disease. *J. Biol. Chem.* 285, 38951–38960. doi: 10.1074/jbc.M110.178848

Fathi, P., and Wu, S. (2016). Isolation, detection, and characterization of enterotoxigenic *Bacteroides fragilis* in clinical samples. *Open Microbiol. J.* 10, 57–63. doi: 10.2174/1874285801610010057

Franceschi, F., Ojetti, V., Candelli, M., Covino, M., Cardone, S., Potenza, A., et al. (2019). Microbes and Alzheimer' disease: lessons from H. pylori and GUT microbiota. *Eur. Rev. Med. Pharmacol. Sci.* 23, 426–430. doi: 10.26355/eurrev_201901_16791

Fujita-Hamabe, W., and Tokuyama, S. (2012). The involvement of cleavage of neural cell adhesion molecule in neuronal death under oxidative stress conditions in cultured cortical neurons. *Biol. Pharm. Bull.* 35, 624–628. . doi: 10.1248/bpb.35.624

Garcia-Esparcia, P., Sideris-Lampretsas, G., Hernandez-Ortega, K., Grau-Rivera, O., Sklaviadis, T., Gelpi, E., et al. (2017). Altered mechanisms of protein synthesis in frontal cortex in Alzheimer disease and a mouse model. *Am. J. Neurodegener. Dis.* 6, 15–25.

Ghaisas, S., Maher, J., and Kanthasamy, A. (2016). Gut microbiome in health and disease: linking the microbiome-gut-brain axis and environmental factors in the pathogenesis of systemic and neurodegenerative diseases. *Pharmacol. Ther.* 158, 52–62. doi: 10.1016/j.pharmthera.2015.11.012

Giau, V. V., Wu, S. Y., Jamerlan, A., An, S. S. A., Kim, S. Y., and Hulme, J. (2018). Gut microbiota and their neuro-inflammatory implications in Alzheimer's disease. *Nutrients* 10:E1765. doi: 10.3390/nu10111765

Ginsberg, S. D., Alldred, M. J., and Che, S. (2012). Gene expression levels assessed by CA1 pyramidal neuron and regional hippocampal dissections in Alzheimer's disease. *Neurobiol. Dis.* 45, 99–107. doi: 10.1016/j.nbd.2011.07.013

Guilmatre, A., Huguet, G., Delorme, R., and Bourgeron, T. (2014). The emerging role of SHANK genes in neuropsychiatric disorders. *Dev. Neurobiol.* 74, 113–122. doi: 10.1002/dneu.22128

Hao, L. Y., Hao, X. Q., Li, S. H., and Li, X. H. (2010). Prenatal exposure to lipopolysaccharide results in cognitive deficits in age-increasing offspring rats. *Neuroscience* 166, 763–770. doi: 10.1016/j.neuroscience.2010.01.006

Hill, J. M., and Lukiw, W. J. (2015). Microbial-generated amyloids and Alzheimer's disease (AD). *Front. Aging Neurosci.* 7:9. doi: 10.3389/fnagi.2015.00009

Hou, X., Yang, S., and Yin, J. (2019). Blocking the REDD1/TXNIP axis ameliorates LPS-induced vascular endothelial cell injury through repressing oxidative stress and apoptosis. *Am. J. Physiol. Cell Physiol.* 316, C104–C110. doi: 10.1152/ajpcell.00313.2018

Itoh, Y., and Voskuhl, R. R. (2017). Cell specificity dictates similarities in gene expression in multiple sclerosis, Parkinson's disease, and Alzheimer's disease. *PLoS One* 12:e0181349. doi: 10.1371/journal.pone.0181349

Karmakar, S., Sharma, L. G., Roy, A., Patel, A., and Pandey, L. M. (2019). Neuronal SNARE complex: A protein folding system with intricate protein-protein interactions, and its common neuropathological hallmark, SNAP25. *Neurochem. Int.* 122, 196–207. doi: 10.1016/j.neuint.2018.12.001

Khan, M. S., Ali, T., Kim, M. W., Jo, M. H., Chung, J. I., and Kim, M. O. (2019). Anthocyanins improve hippocampus-dependent memory function and prevent neurodegeneration via JNK/Akt/GSK3β signaling in LPS-treated adult mice. *Mol. Neurobiol.* 56, 671–687. doi: 10.1007/s12035-018-1101-1

Kincheski, G. C., Valentim, I. S., Clarke, J. R., Cozachenco, D., Castelo-Branco, M. T. L., Ramos-Lobo, A. M., et al. (2017). Chronic sleep restriction promotes brain inflammation and synapse loss, and potentiates memory impairment induced by amyloid-β oligomers in mice. *Brain Behav. Immun.* 64, 140–151. doi: 10.1016/j.bbi.2017.04.007

Lee, W., and Kim, S. H. (2019). Autophagy at synapses in neurodegenerative diseases. *Arch. Pharm. Res.* 42, 407–415. doi: 10.1007/s12272-019-01148-7

Li, R., Tong, J., Tan, Y., Zhu, S., Yang, J., and Ji, M. (2015). Low molecular weight heparin prevents lipopolysaccharide induced-hippocampus-dependent cognitive impairments in mice. *Int. J. Clin. Exp. Pathol.* 8, 8881–8891.

Lleó, A., Núñez-Llaves, R., Alcolea, D., Chiva, C., Balateu-Paños, D., Colom-Cadena, M., et al. (2019). Changes in synaptic proteins precede neurodegeneration markers in preclinical Alzheimer's disease cerebrospinal fluid. *Mol. Cell Proteo.* 18, 546–560. doi: 10.1074/mcp.RA118.001290

Lonza (2019). *Lonza Human Cell Systems*. Basel:Lonza.

Lukiw, W. J. (2016). *Bacteroides fragilis* lipopolysaccharide and inflammatory signaling in Alzheimer's disease. *Front. Microbiol.* 7:1544.

Lukiw, W. J., Cong, L., Jaber, V., and Zhao, Y. (2018). Microbiome-derived lipopolysaccharide (LPS) selectively inhibits neurofilament light chain (NF-L) gene expression in human neuronal-glial (HNG) cells in primary culture. *Front. Neurosci.* 12:896. doi: 10.3389/fnins.2018.00896

Marcello, E., Di Luca, M., and Gardoni, F. (2018). Synapse-to-nucleus communication: from developmental disorders to Alzheimer's disease. *Curr. Opin. Neurobiol.* 48, 160–166. doi: 10.1016/j.conb.2017.12.017

McLachlan, D. R. C., Lukiw, W. J., Wong, L., Bergeron, C., and Bech-Hansen, N. T. (1988). Selective messenger RNA reduction in Alzheimer's disease. *Brain Res.* 427, 255–261. doi: 10.1016/0169-328x(88)90048-4

Parra-Damas, A., and Saura, C. A. (2019). Synapse-to-nucleus signaling in neurodegenerative and neuropsychiatric disorders. *Biol* Psychiatrydoi: 10.1016/j.biopsych.2019.01.006 [Epub ahead of Print].

Peng, L., Zhu, M., Yang, Y., Weng, Y., Zou, W., Zhu, X., et al. (2019). Neonatal lipopolysaccharide challenge induces long-lasting spatial cognitive impairment and dysregulation of hippocampal histone acetylation in mice. *Neuroscience* 398, 76–87. doi: 10.1016/j.neuroscience.2018.12.001

Pogue, A. I., and Lukiw, W. J. (2016). Natural and synthetic neurotoxins in our environment: from Alzheimer's disease (AD) to autism spectrum disorder (ASD). *J. Alzheimers Dis. Parkinson.* 6:249.

Ramakrishna, S., and Muddashetty, R. S. (2019). Emerging role of microRNAs in dementia. *J. Mol. Biol.* 431, 1743–1762. doi: 10.1016/j.jmb.2019.01.046

Sarkar, R. S., and Banerjee, S. (2019). Gut microbiota in neurodegenerative disorders. *J. Neuroimmunol.* 328, 98–104. doi: 10.1016/j.jneuroim.2019.01.004

Sato, K., Tachikawa, M., Watanabe, M., Uchida, Y., and Terasaki, T. (2019). Selective protein expression changes of leukocyte-migration-associated cluster of differentiation antigens at the blood-brain barrier in a lipopolysaccharide-induced systemic inflammation mouse model without alteration of transporters, receptors or tight junction-related protein. *Biol. Pharm. Bull.* 42, 944–953. doi: 10.1248/bpb.b18-00939

Sears, C. L. (2009). Enterotoxigenic *Bacteroides fragilis*: a rogue among symbiotes. *Clin. Microbiol. Rev.* 22, 349–369. doi: 10.1128/CMR.00053-08

Sfera, A., Gradini, R., Cummings, M., Diaz, E., Price, A. I., and Osorio, C. (2018). Rusty microglia: trainers of innate immunity in Alzheimer's disease. *Front. Neurol.* 9:1062. doi: 10.3389/fneur.2018.01062

Sheppard, O., Coleman, M. P., and Durrant, C. S. (2019). Lipopolysaccharide-induced neuroinflammation induces presynaptic disruption through a direct action on brain tissue involving microglia-derived interleukin 1 beta. *J. Neuroinflam.* 16:106. doi: 10.1186/s12974-019-1490-8

Sindi, I. A., and Dodd, P. R. (2015). New insights into Alzheimer's disease pathogenesis: the involvement of neuroligins in synaptic malfunction. *Neurodegener. Dis. Manag.* 5, 137–145. doi: 10.2217/nmt.14.54

Steven, S., Dib, M., Roohani, S., Kashani, F., Münzel, T., and Daiber, A. (2017). Time response of oxidative/nitrosative stress and inflammation in LPS-induced endotoxaemia-a comparative study of mice and rats. *Int. J. Mol. Sci.* 18:E2176. doi: 10.3390/ijms18102176

Ticinesi, A., Tana, C., and Nouvenne, A. (2019). The intestinal microbiome and its relevance for functionality in older persons. *Curr. Opin. Clin. Nutr. Metab Care* 22, 4–12. doi: 10.1097/MCO.0000000000000521

Wu, X., Lv, Y. G., Du, Y. F., Hu, M., Reed, M. N., Long, Y., et al. (2019). Inhibitory effect of INT-777 on lipopolysaccharide-induced cognitive impairment, neuro-inflammation, apoptosis, and synaptic dysfunction in mice. *Prog. Neuropsychopharmacol. Biol. Psychiatry* 88, 360–374. doi: 10.1016/j.pnpbp.2018.08.016

Yang, N. J., and Chiu, I. M. (2017). Bacterial signaling to the nervous system through toxins and metabolites. *J. Mol. Biol.* 429, 587–605. doi: 10.1016/j.jmb.2016.12.023

Youssef, N. H., Couger, M. B., McCully, A. L., Criado, A. E., and Elshahed, M. S. (2015). Assessing the global phylum level diversity within the bacterial domain: a review. *J. Adv. Res.* 6, 269–282. doi: 10.1016/j.jare.2014.10.005

Zhan, X., Stamova, B., Jin, L. W., DeCarli, C., Phinney, B., and Sharp, F. R. (2016). Gram-negative bacterial molecules associate with Alzheimer disease pathology. *Neurology* 87, 2324–2332. doi: 10.1212/wnl.0000000000003391

Zhan, X., Stamova, B., and Sharp, F. R. (2018). Lipopolysaccharide associates with amyloid plaques, neurons and oligodendrocytes in Alzheimer's disease brain: a review. *Front. Aging Neurosci.* 10:42. doi: 10.3389/fnagi.2018.00042

Zhang, M., Pan, H., Xu, Y., Wang, X., Qiu, Z., and Jiang, L. (2017). Allicin decreases lipopolysaccharide-induced oxidative stress and inflammation in human umbilical vein endothelial cells through suppression of mitochondrial dysfunction and activation of Nrf2. *Cell Physiol. Biochem.* 41, 2255–2267. doi: 10.1159/000475640

Zhao, Y., Cong, L., Jaber, V. R., and Lukiw, W. J. (2017a). Microbiome-derived lipopolysaccharide enriched in the perinuclear region of Alzheimer's disease brain. *Front. Immunol.* 8:1064. doi: 10.3389/fimmu.2017.01064

Zhao, Y., Cong, L., and Lukiw, W. J. (2017b). Lipopolysaccharide (LPS) accumulates in neocortical neurons of Alzheimer's disease (AD) brain and impairs transcription in human neuronal-glial primary co-cultures. *Front. Aging Neurosci.* 9:407. doi: 10.3389/fnagi.2017.00407

Zhao, Y., Jaber, V., and Lukiw, W. J. (2017c). Secretory products of the human GI tract microbiome and their potential impact on Alzheimer's disease (AD): detection of lipopolysaccharide (LPS) in AD hippocampus. *Front. Cell Infect Microbiol.* 7:318. doi: 10.3389/fcimb.2017.00318

Zhao, Y., Dua, P., and Lukiw, W. J. (2015). Microbial sources of amyloid and relevance to amyloidogenesis and Alzheimer's disease (AD). *J. Alzheimers Dis. Parkinson.* 5:177.

Zhao, Y., Jaber, V. R., LeBeauf, A., Sharfman, N. M., and Lukiw, W. J. (2019). microRNA-34a (miRNA-34a) mediated down-regulation of the post-synaptic

cytoskeletal element SHANK3 in sporadic Alzheimer's disease (AD). *Front. Neurol.* 10:28. doi: 10.3389/fneur.2019.00028

Zhao, Y., and Lukiw, W. J. (2015). Microbiome-generated amyloid and potential impact on amyloidogenesis in Alzheimer's disease (AD). *J. Nat. Sci.* 1:e138.

Zhao, Y., and Lukiw, W. J. (2018a). *Bacteroidetes* neurotoxins and inflammatory neurodegeneration. *Mol. Neurobiol.* 55, 9100–9107. doi: 10.1007/s12035-018-1015-y

Zhao, Y., and Lukiw, W. J. (2018b). Microbiome-mediated upregulation of microRNA-146a in sporadic Alzheimer's disease. *Front. Neurol.* 9:145. doi: 10.3389/fneur.2018.00145

Conflict of Interest Statement: The authors declare that the research was conducted in the absence of any commercial or financial relationships that could be construed as a potential conflict of interest.

frontiers in Cellular Neuroscience

REVIEW
published: 13 August 2019
doi: 10.3389/fncel.2019.00368

The Role of Altered BDNF/TrkB Signaling in Amyotrophic Lateral Sclerosis

*Jonu Pradhan[1], Peter G. Noakes[1,2] and Mark C. Bellingham[1]**

[1] Faculty of Medicine, School of Biomedical Sciences, The University of Queensland, Brisbane, QLD, Australia, [2] Queensland Brain Institute, The University of Queensland, Brisbane, QLD, Australia

Brain derived neurotrophic factor (BDNF) is well recognized for its neuroprotective functions, via activation of its high affinity receptor, tropomysin related kinase B (TrkB). In addition, BDNF/TrkB neuroprotective functions can also be elicited indirectly via activation of adenosine 2A receptors (A_{2a}Rs), which in turn transactivates TrkB. Evidence suggests that alterations in BDNF/TrkB, including TrkB transactivation by A_{2a}Rs, can occur in several neurodegenerative diseases, including amyotrophic lateral sclerosis (ALS). Although enhancing BDNF has been a major goal for protection of dying motor neurons (MNs), this has not been successful. Indeed, there is emerging *in vitro* and *in vivo* evidence suggesting that an upregulation of BDNF/TrkB can cause detrimental effects on MNs, making them more vulnerable to pathophysiological insults. For example, in ALS, early synaptic hyper-excitability of MNs is thought to enhance BDNF-mediated signaling, thereby causing glutamate excitotoxicity, and ultimately MN death. Moreover, direct inhibition of TrkB and A_{2a}Rs has been shown to protect MNs from these pathophysiological insults, suggesting that modulation of BDNF/TrkB and/or A_{2a}Rs receptors may be important in early disease pathogenesis in ALS. This review highlights the relevance of pathophysiological actions of BDNF/TrkB under certain circumstances, so that manipulation of BDNF/TrkB and A_{2a}Rs may give rise to alternate neuroprotective therapeutic strategies in the treatment of neural diseases such as ALS.

Keywords: BDNF, TrkB receptors, A_{2a}R, motor neurons, ALS, MND

OPEN ACCESS

Edited by:
Marie-Eve Tremblay, Laval University, Canada

Reviewed by:
Francesco Ferrini, University of Turin, Italy
Yuriko Iwakura, Niigata University, Japan

****Correspondence:***
Mark C. Bellingham
mark.bellingham@uq.edu.au

Specialty section:
This article was submitted to Cellular Neurophysiology, a section of the journal Frontiers in Cellular Neuroscience

Received: *21 May 2019*
Accepted: *29 July 2019*
Published: *13 August 2019*

Citation:
Pradhan J, Noakes PG and Bellingham MC (2019) The Role of Altered BDNF/TrkB Signaling in Amyotrophic Lateral Sclerosis. Front. Cell. Neurosci. 13:368. doi: 10.3389/fncel.2019.00368

INTRODUCTION

Amyotrophic lateral sclerosis (ALS), the most common form of motor neuron disease (MND), is a fatal adult onset neurodegenerative disease resulting in progressive and preferential degeneration and death of upper motor neurons (UMNs, corticospinal neurons) of the motor cortex, and alpha lower motor neurons (LMNs) of the brain stem and the spinal cord (Cleveland and Rothstein, 2001; Turner et al., 2013). The incidence of ALS is 1.7 per 100,000 people each year (Pasinelli and Brown, 2006; Marin et al., 2017; Sandstedt et al., 2018). Only 10% of all ALS cases exhibit familial inheritance (fALS) (Turner et al., 2013) while the remaining 90% are sporadic (sALS). Mutations in the gene encoding Cu/Zn superoxide dismutase 1 (SOD1) were the first to be identified as a primary ALS mutation (Rosen et al., 1993) and have been also the most characterized, with several widely used mouse models of SOD1 mutations (Gurney et al., 1994). Overall, SOD1 mutations account for

20% of fALS and 1–2% of sALS, with more than 180 mutations identified within the SOD1 gene (Hayashi et al., 2016).

Despite decades of research, the pathogenic mechanism underlying death of UMNs and LMNs is still unclear. Numerous etiologies have been proposed, including oxidative stress, mitochondrial dysfunction, protein aggregation, RNA processing, autophagy, and glutamate excitotoxicity (Chico et al., 2017). Glutamate excitotoxicity, the focus of this review, results from a disruption of the finely tuned cellular response to input stimuli, resulting in excessive glutamate release from the pre-synaptic neuron, delayed clearance from the synaptic cleft or increased responsiveness by glutamate receptors post-synaptically (Rothstein et al., 1992; Hayashi et al., 2016). Excessive release of glutamate induced by Ca^{2+} dysregulation within the pre-synaptic compartment (Van Den Bosch et al., 2006; King et al., 2016), causes a prolonged state of activation of postsynaptic glutamate N-methyl-D-aspartate (NMDA) and alpha-amino-3-hydroxy-5-methyl-4-isoxazole propionate (AMPA) receptors. In addition to this, the Ca^{2+} buffering capacity of MNs in ALS is weakened at an early age, with impairment of the Ca^{2+} ATPase and Na^{+}/Ca^{2+} exchanger adding to the cytoplasmic Ca^{2+} load (DeJesus-Hernandez et al., 2011; Sirabella et al., 2018). Enhanced post-synaptic glutamate receptor activation is physiologically observed as synaptic hyper-activity of upper and lower MNs (van Zundert et al., 2008; Fogarty et al., 2015). Hyper-activity also raises the level of intracellular Ca^{2+} within the post-synaptic MN, potentially creating a toxic intracellular environment that can cause cell death (Le Masson et al., 2014; **Figure 1**).

Amyotrophic lateral sclerosis progresses relentlessly and, without effective intervention, 50% of the patients die within 3 to 5 years post-diagnosis, due to loss of their respiratory MNs (i.e., respiratory failure) (Brown and Al-Chalabi, 2017). The only FDA approved treatments so far are riluzole, which acts to reduce the release of glutamate and hence lower neuronal excitotoxicity (Bellingham, 2013b), and edaravone, an anti-oxidant compound. Unfortunately, riluzole only marginally enhances survival by a few months (Bensimon et al., 1994; Fang et al., 2018). In 2017 after more than 20 years, a second drug Radicava (edaravone) has been FDA approved to treat ALS; thus far, edaravone has also only been shown to slow the rate of clinical progression in ALS (Abe et al., 2014). This slow development of new treatments highlights the need to better understand the cellular and molecular mechanisms of ALS, so as to develop effective combination therapies to ameliorate this multi-factorial disease.

In addition to neuronal hyper-excitability in neuromotor circuits in ALS, the level of neuronal activity strongly influences the modification of neuronal circuits in the developing CNS, by stabilizing and strengthening coincident inputs and refining/removing weaker inputs (Goodman and Shatz, 1993; Stevens et al., 2007; Kutsarova et al., 2016). This developmental plasticity initially depends on the release of neurotransmitters from the pre-synaptic neuron (Andreae and Burrone, 2018), and thus factors that increase pre-synaptic activity will also increase synaptic plasticity. In ALS, upper and lower MNs in animal models of ALS have been shown to exhibit synaptic hyper-activity (van Zundert et al., 2008; Fogarty et al., 2015). In the case of lower MNs, hyperactivity of upper MNs could in turn result in enhanced glutamate release from their nerve terminal boutons at their synapses with lower MNs (**Figure 1**). Excessive release of glutamate from these pre-synaptic inputs onto lower MNs could lead to their death by excitotoxicity (King et al., 2016). Similar mechanisms may also operate for excitable synaptic connections made onto upper and lower MNs from other pre-motor excitatory inputs (van Zundert et al., 2008). To complicate matters, changes in neuronal circuit activity outside of what is considered a "normal physiological range" (i.e., "hyper-excitability;" Bae et al., 2013), can induce compensatory effects termed "synaptic homeostasis" (Turrigiano, 2012). For example, in $SOD1^{G93A}$ ALS model mice, while upper MNs have been shown to be hyper-active prior to their death, these neurons display reductions in dendritic length and spine density, suggesting a homeostatic response to heightened pre-synaptic activity (Fogarty et al., 2015; Saba et al., 2016). Alternatively, these morphological reductions may simply reflect the stressed state of the neurons as it progresses to death (Fogarty et al., 2016). Together these observations suggest that abnormal neuronal activity and death of upper and lower MNs in ALS are directly linked.

What might be the mechanism(s) that links abnormal neuronal activity to neuronal death? One proposed mechanism is the activity-dependent synthesis and release of neurotrophins (McAllister et al., 1996; Du et al., 2003; Cunha et al., 2010). Neurotrophins are secreted proteins and potent regulators of neuronal development, survival, neurogenesis and synaptic plasticity (Huang and Reichardt, 2001). They have long been targeted as prospective therapeutic agents for the treatment of neurodegenerative disorders, including ALS. The neurotrophin family constitutes nerve growth factor (NGF), brain derived neurotrophic factor (BDNF), neurotrophin-3 (NT-3), and neurotrophin-4/5 (NT-4/5). Amongst these, BDNF is abundantly expressed in the developing and adult nervous system (Murer et al., 2001) and has been extensively studied for its roles in neuronal survival (e.g., MNs) (Ringholz et al., 2005; Pansarasa et al., 2018), along with its ability to increase the release of glutamate at glutamatergic synapses (Rao and Finkbeiner, 2007; Mattson, 2008). Given these proposed roles for BDNF, namely its neurotrophic and possible neurotoxic roles, it becomes apparent that regulation of BDNF could open up new therapeutic strategies in the treatment of neurodegenerative disorders. This review focuses on the biology of BDNF and its proposed neurotrophic and neurotoxic roles in the pathogenesis and treatment of ALS.

BIOLOGY OF BDNF: FROM SYNTHESIS TO SECRETION

Brain derived neurotrophic factor is a member of the family of growth factors and was initially purified from pig brain (Barde et al., 1982). The expression of BDNF in human, rat and mouse is encoded by a single BDNF gene, whose transcription is regulated by several promoters (Sasi et al., 2017). The human BDNF gene consists of eleven 5′ untranslated (UTR) exons, compared to 9 exons found in rodents (rats and mice), and only one 3′ coding exon. These exons initiate transcription at

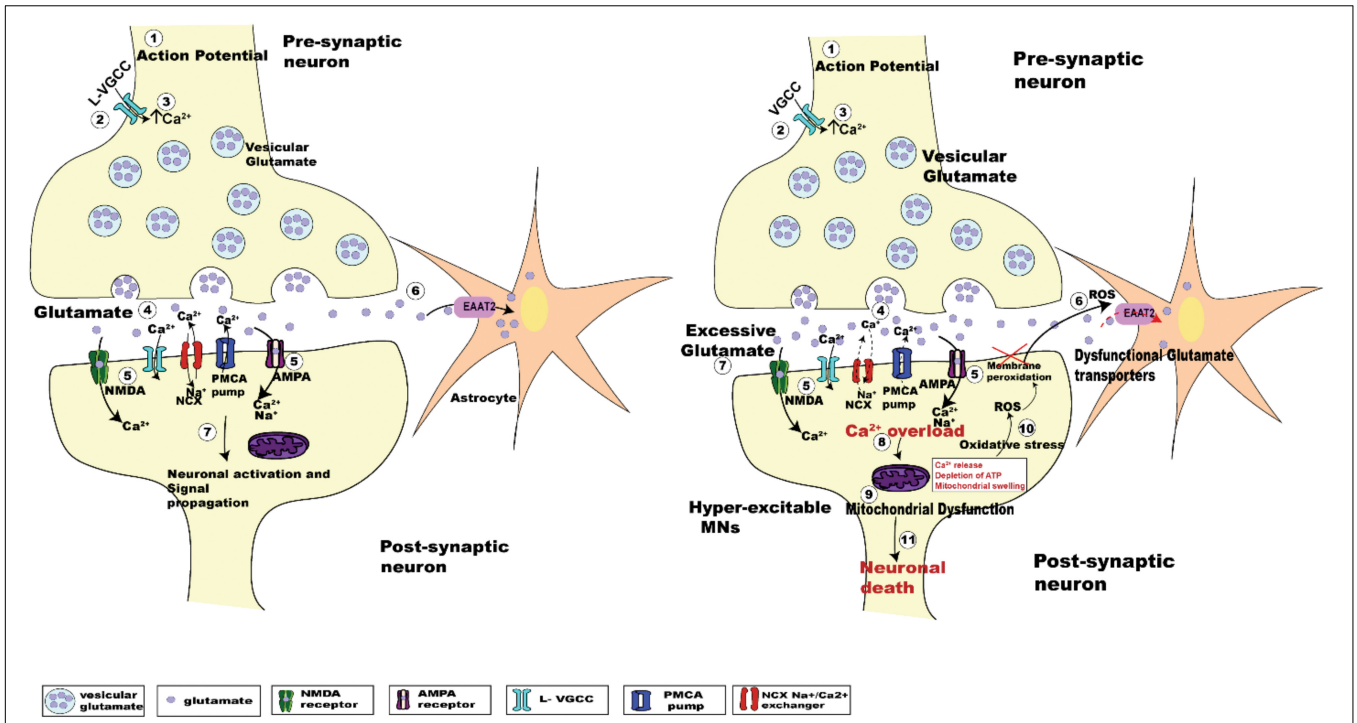

FIGURE 1 | Schematic diagrams showing the regulation of glutamatergic synaptic transmission at upper and lower MN synapses in normal and SOD1^{G93A} mice. The arrival of the action potential **(step 1)**, triggers the influx of Ca^{2+} ions into pre-synaptic terminal **(step 2)**, the rise in intracellular calcium **(step 3)** in turn triggers the fusion of synaptic vesicles with the pre-synaptic membrane to release glutamate (light purple dots) from the terminal **(step 4)**. Binding of glutamate to its postsynaptic receptors (NMDA, green; and AMPA, magenta; **step 5**), leads to the influx of Ca^{2+} ions. During this process, concentration of glutamate within the synaptic cleft is reduced by the uptake of glutamate into Astrocytes (orange star shaped cells) via EAAT2 glutamate transporters (pink; **step 6**). Within the post-synaptic neuron the influx of Ca^{2+} via glutamatergic receptors plus voltage gated Ca^{2+} channels, along with an influx of sodium (Na^{+}) ions lead to the activation of the postsynaptic neuron **(step 7)**. The subsequent lowering of Ca^{2+} post-synaptic transmission is managed by extrusion of calcium via ATP pumps (PMCA pumps) and Na^{+}/Ca^{2+} exchanger (NCX), plus calcium uptake into intracellular stores (ER and mitochondria) (Chio et al., 2012). The right panel shows the pathogenesis of glutamate induced excitotoxicity in ALS. Excessive glutamate released in the synaptic cleft triggers increased activation of the post-synaptic glutamate receptors (NMDA and AMPA receptors). This effect is enhanced due to dysfunctional glutamate transporters (EAAT2; **step 6**, *right panel*, red dashed arrow), which lengthen the persistence of glutamate within the synaptic cleft (**step 7**, *right panel*), which further activates glutamatergic receptors. Impaired Na^{+}/Ca^{2+} exchanger and ATP pumps in SOD1^{G93A} mice results in enhanced Ca^{2+} intracellularly (DeJesus-Hernandez et al., 2011; Sirabella et al., 2018). Generation of reactive oxygen species (ROS) causes neuronal membrane peri-oxidation impairing the glutamate transporters (EAAT2). The enhanced activation of these receptors leads to increased Ca^{2+} overload (**step 8**, *right panel*) in the post-synaptic neuron, which in turn leads to mitochondrial dysfunction (**step 9**, *right panel*), oxidative stress (**step 10**, *right panel*), and generation of reactive oxygen species (ROS) ultimately leading to motor neuron death (**step 11**, *right panel*).

the ATG start codon by alternate splicing to produce 17 BDNF mRNA transcripts and 9 BDNF 5′ promoters (Aid et al., 2007; Pruunsild et al., 2007). The transcription of BDNF is neuronal activity-dependent and regulated by membrane depolarization. An increase in intracellular calcium (Ca^{2+}) concentration via activation of NMDA glutamate receptors or L-type voltage gated calcium channels (L-VGCC) following a depolarizing stimulus initiates transcription of the BDNF gene, predominantly at exon IV (Tao et al., 1998; Zheng et al., 2011). The promoter of BDNF exon IV contains Ca^{2+} response elements (CaRE) – CaRE1 and CaRE3, which regulate transcription (Tao et al., 1998; Hong et al., 2008; Zheng et al., 2011). Cyclic AMP responsive element binding protein (CREB), a transcription factor, binds to these CaREs, which are phosphorylated by calcium/calmodulin (CaM)-dependent protein kinases, cAMP-dependent protein kinases and MAPK, activating the promoter and resulting in Ca^{2+} dependent transcription of BDNF mRNA at exon IV (Zheng et al., 2011).

Alternate splicing terminates transcription at two alternate polyadenylation points which shift the translation sites, giving rise to two distinct BDNF mRNA populations into specific neuronal compartments, allowing spatial and temporal translocation (Pruunsild et al., 2007; Notaras and van den Buuse, 2018). The short UTR BDNF transcripts are localized in the soma and maintain basal activity-dependent BDNF production. The long UTR BDNF transcript is targeted to the dendrites and displays robust translation on neuronal activation (An et al., 2008; Lau et al., 2010). BDNF localization is mostly somatodendritic (59%) within dense core vesicles (Tongiorgi, 2008; Dieni et al., 2012) with only 29% targeted to the dendrites (Adachi et al., 2005). The specific compartmental translation of BDNF mRNA at long or short 3′ UTR is also aided by binding to numerous microRNAs such as miR-30, resulting in degradation of BDNF transcripts (Bartel, 2004; Mellios et al., 2008) and negative regulation of BDNF synaptogenesis (Shi, 2015).

Translation of these distinct alternate BDNF mRNA transcripts gives rise to the precursor pre-pro BDNF in the endoplasmic reticulum (Foltran and Diaz, 2016; Kowianski et al., 2018), consisting of a signal peptide after the initiation codon and N-glycosylation site on the pro region. It is then translocated to the Golgi apparatus, where the signal peptide pre-sequence is cleaved off to form pro-BDNF (30 kDa) (Lessmann et al., 2003). The pro-BDNF is then further processed either intracellularly or extracellularly, via the Golgi apparatus, into the *trans*-Golgi network (TGN) where the pro domain is proteolytically cleaved off to form pro-domain and mature BDNF and is secreted into the extracellular space (hence forth termed "BDNF") (Foltran and Diaz, 2016; Kowianski et al., 2018; **Figure 2**). The pro domain has been identified as an independent ligand itself and encodes the single nucleotide polymorphism of methionine to valine substitution at position 66 in the BDNF gene (Egan et al., 2003; Dieni et al., 2012; Notaras and van den Buuse, 2018). Intracellular cleavage of pro-BDNF in the TGN occurs via furin, while its cleavage to form BDNF in secretory vesicles requires convertases. The final molecular weight of BDNF is 14 kDa, consisting of 119 amino acids (Lu et al., 2005). The pro-BDNF is also secreted extracellularly, and then cleaved by proteases such as plasmin and metalloproteinases (MMP2 and MMP9) to form BDNF (Hwang et al., 2005; Mizoguchi et al., 2011). The extracellularly secreted pro-domain, pro-BDNF and BDNF are all biologically active and perform their various physiological functions (**Figure 2**).

The packaging and secretion of pro domain, pro-BDNF and BDNF from within the TGN into dense core secretory vesicles occurs via the constitutive secretory pathway and a preferential tightly controlled regulated pathway (Goodman et al., 1996; Lu, 2003; Brigadski et al., 2005). BDNF is secreted both pre- and post-synaptically, and undergoes anterograde and retrograde transport via autocrine and paracrine mechanisms (Cunha et al., 2010). These mechanisms modulate synaptic transmission and synaptogenesis (Cunha et al., 2010) via Ca^{2+}-dependent mechanisms. BDNF is secreted pre-synaptically via increased intracellular influx of Ca^{2+} (Balkowiec and Katz, 2002). Post-synaptically, the secretion of BDNF is by regulated activity-dependent increases in Ca^{2+}, entering via ionotrophic glutamate receptors and voltage-gated Ca^{2+} channels (Hartmann et al., 2001), or Ca^{2+} release from intracellular stores (Griesbeck et al., 1999) and release occurs via endosome like vesicles where exogenous BDNF is recycled (Sasi et al., 2017). Altogether, the above described synthesis, processing and secretion of BDNF gives rise to three functionally active proteins: the pro domain of BDNF, pro-BDNF and BDNF (mature BDNF) (**Figure 2**; Hempstead, 2015). Once released, they interact with their respective receptors to exert their distinct physiological functions.

BDNF ISOFORMS AND THEIR RECEPTORS

The three products of the BDNF gene bind to specific receptors and regulate distinct biological functions. The pro-domain of BDNF binds to sortilin, a member of vacuolar protein sorting 10 protein (vps10p) of the sorting receptor family (Teng et al., 2005; Anastasia et al., 2013) to trigger specific functions in developing and adult neurons. The pro-domain acts by inducing growth cone retraction (Anastasia et al., 2013), facilitating long term synaptic depression (LTD) in developing neurons (Mizui et al., 2016), and modulating synaptic spine density and neuronal network plasticity via a cytochrome c caspase-3 mechanism in adult neurons (Guo et al., 2016). The pro-BDNF, comprising of the pro-domain and mature domain, act via preferential interactive binding to p75, a member of the tumor necrosis factor receptor family, and sortilin receptors, respectively (Teng et al., 2005; Kowianski et al., 2018) and with lower affinity binding to TrkB. The binding of pro-BDNF/p75/sortilin initiates the activation of c-Jun amino terminal kinase (JNK), Ras homolog gene family member A (RhoA), and nuclear factor kappa B (NF-κB) cascade (Reichardt, 2006; Anastasia et al., 2013; Kowianski et al., 2018). These signaling cascades (JNk, Ras, and NF-κB) in turn trigger a number of diverse cellular and morphological outcomes, such as neuronal apoptosis (Teng et al., 2005), neuronal growth cone development, and neuronal survival (Reichardt, 2006).

The third product, BDNF, binds with high affinity to TrkB of the Trk family of tyrosine kinases and with lower affinity to the p75 receptor (Chao and Hempstead, 1995; Reichardt, 2006). Activation of these two receptors is responsible for BDNF's known functions. In brief, BDNF/TrkB activation aids in neurogenesis, gliogenesis, neurite outgrowth, and enhanced neuronal survival (Huang and Reichardt, 2001; Vilar and Mira, 2016). In developing neuronal circuits, BDNF acts to regulate dendritic arborization and spine formation (Deinhardt and Chao, 2014; Gonzalez et al., 2016), and enhances long term synaptic potentiation (LTP) (Park and Poo, 2013; Leal et al., 2015). In mature neurons, BDNF is also required to sustain viability (Alcantara et al., 1997). BDNF mediates opposing actions on binding to the p75 receptor; while BDNF/TrkB enhances neuronal excitability and synaptic strength, BDNF/p75 acts to decrease excitability and synaptic strength and induce neuronal plasticity (Sasi et al., 2017), initiating JNK (Reichardt, 2006; Anastasia et al., 2013; Kowianski et al., 2018), triggering neuronal apoptosis (Teng et al., 2005), and NF-κB cascade regulating of neuronal growth cone development and navigation and neuronal survival. The TrkB and p75 receptor have somadendritic distribution (Bronfman and Fainzilber, 2004), where TrkB is localized to the pre- and post-synaptic membranes and intracellularly (Gomes et al., 2006; Song et al., 2017).

Brain derived neurotrophic factor undergoes slow exocytosis (Brigadski et al., 2005) following depolarization and stimulation of glutamate receptors (Righi et al., 2000; Kohara et al., 2001). Thus, activity-dependent BDNF secretion can be induced by numerous stimuli including high potassium, glutamate and the neurotrophin itself, dependent on intracellular Ca^{2+} increase (Blochl and Thoenen, 1995; Goodman et al., 1996; Canossa et al., 1997).

The TrkB Receptor

The TrkB receptor is encoded by a single TrkB gene, the NTRK2 gene encoding 24 exons located on chromosome 9q22 (Schneider and Schweiger, 1991; Nakagawara et al., 1995). TrkB

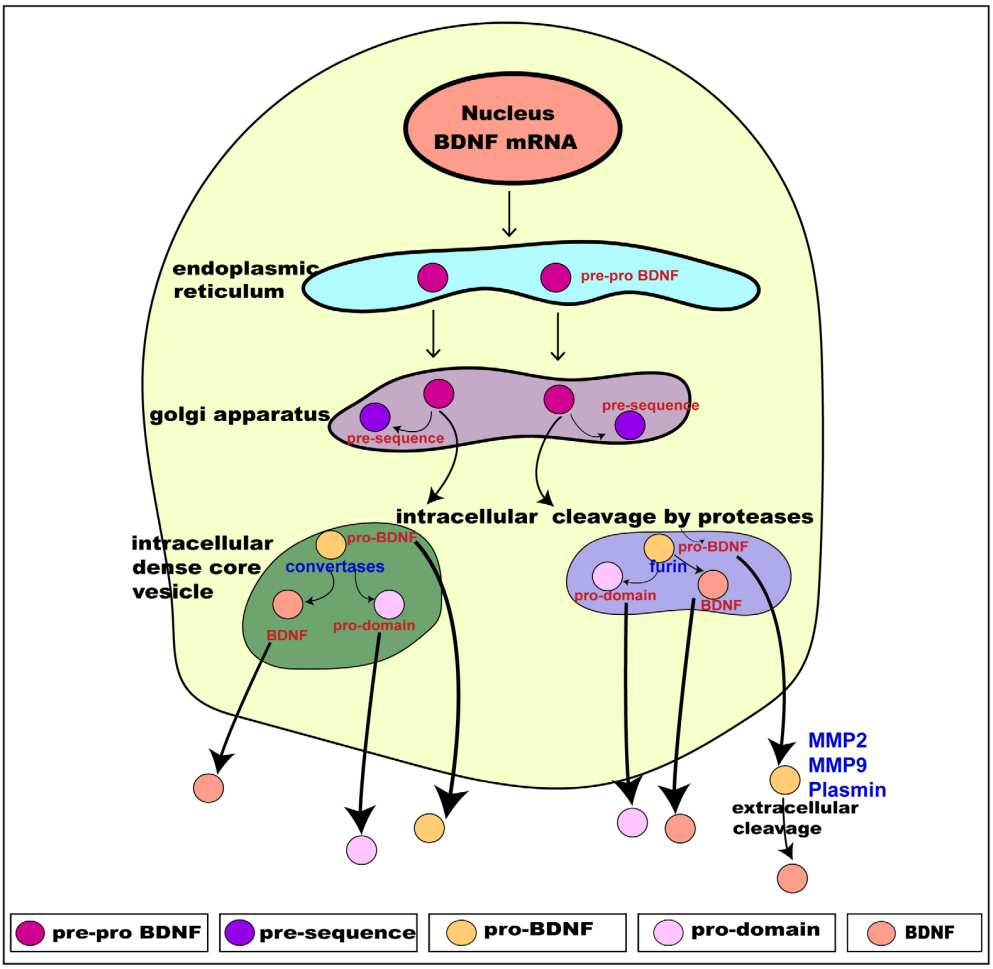

FIGURE 2 | Schematic presentation of BDNF synthesis from translation, intracellular processing through to its secretion. BDNF is synthesized from the BDNF gene in a multi-step process. Intracellularly, the pre-pro BDNF is produced in the endoplasmic reticulum which is then translocated toward the Golgi apparatus, where the pre-sequence is cleaved off to form pro- BDNF. The pro-BDNF is further processed, via the Golgi apparatus, into the *trans*-Golgi network (TGN) where the pro domain is cleaved off by proteases to form mature BDNF (BDNF). The pro-BDNF is proteolytically cleaved by furin or convertase and is intracellularly secreted as BDNF. Both pro-BDNF and BDNF are preferentially grouped and packaged into secretory dense core-vesicles and secreted extracellularly via exocytosis. The extracellularly secreted pro-BDNF is then processed and catalyzed by proteases such as plasmin and metalloproteinases (MMP2 and MMP9) to form BDNF. As a result, three functionally active isoforms, namely pro-domain, pro-BDNF and BDNF are secreted extracellularly. Adapted from Kowianski et al. (2018).

consists of three domains: – an extracellular ligand binding domain, a transmembrane domain and an intracellular tyrosine kinase domain. One full- length TrkB (TrkB) contains an extracellular transmembrane domain, consisting of a cysteine rich cluster followed by 3 leucine repeats, a cysteine cluster followed by 2 immunoglobulin (Ig1 and Ig2) domains; and an intracellular cytoplasmic tyrosine kinase domain acting as a phosphorylation dependent docking site (Schneider and Schweiger, 1991; Tejeda and Diaz-Guerra, 2017). The Ig domain in exon 12 directs binding specificity to its ligand, BDNF. Exon 15 encodes the transmembrane domain, and exon 20–24 the intracellular tyrosine kinase domain (Middlemas et al., 1991). The first five exons serve as the transcription initiation sites and display alternate splicing patterns (Stoilov et al., 2002). Exon five also serves as a ribosomal entry site, directing the start of translation and producing four isoforms of TrkB receptors in humans (Luberg et al., 2010; Sasi et al., 2017). Other splice variants are two truncated TrkB (TrkB-T1) isoforms, TrkB-T2, TrkB- Shc lacking tyrosine kinase domain, and a TrkB-TK with a non-viable catalytic domain. Truncated TrkB receptors (TrkB-T1 and TrkB-T2) are the product of alternate splicing at exon 18. These TrkB isoforms are activated on binding to BDNF to initiate downstream signaling.

BDNF/TrkB

Brain derived neurotrophic factor binds to the TrkB receptor, both TrkB-T and TrkB (full length) with similar affinity (Sasi et al., 2017). Exactly how TrkB receptor isoforms coordinate and produce a precise cellular and biological function is not yet clearly understood. BDNF binding to the TrkB-T isoform has been identified as a dominant negative

pathway (Fenner, 2012; Notaras and van den Buuse, 2018). More recently, the TrkB-T receptor has also been reported to have functions apart from dominant negative regulation, including the following: metabolite release (Baxter et al., 1997; Fenner, 2012); BDNF sequestration and translocation (Fryer et al., 1996); filopodia and neurite outgrowth (Fryer et al., 1997; Yacoubian and Lo, 2000; Fenner, 2012); and astrocytic cytoskeletal remodeling via Rho GTPase (Ohira et al., 2006; Fenner, 2012). Additionally, alterations in expression of TrkB-T has also been shown to alter neuronal viability, resulting in neurodegeneration (Vidaurre et al., 2012), indicating a biological function of TrkB-T. However, the mechanism driving the function of TrkB-T is not well understood. Given that this review focusses on the interaction of BDNF with the TrkB receptor, the following sections will only address BDNF-TrkB interactions together, independent of BDNF's non-TrkB functions.

Binding of BDNF to TrkB initiates two different categories of cascades: a fast acting BDNF/TrkB cascade that excites neurons or a slow acting occurring over minutes to hours. The action of BDNF markedly differs between these two categories (Kafitz et al., 1999; Ji et al., 2010). Additionally, evidence suggests that the well-studied effect of BDNF/TrkB on cell survival and plasticity are mediated by TrkB-FL (Klein et al., 1993; Carim-Todd et al., 2009). Once BDNF binds to TrkB, ligand-mediated dimerization of the complex occurs at the cell surface, followed by autophosphorylation of specific tyrosine residues in the cytoplasmic domain, leading to activation of three interconnected intrinsic intracellular cascades (Chao, 2003; Cunha et al., 2010; **Figure 3**).

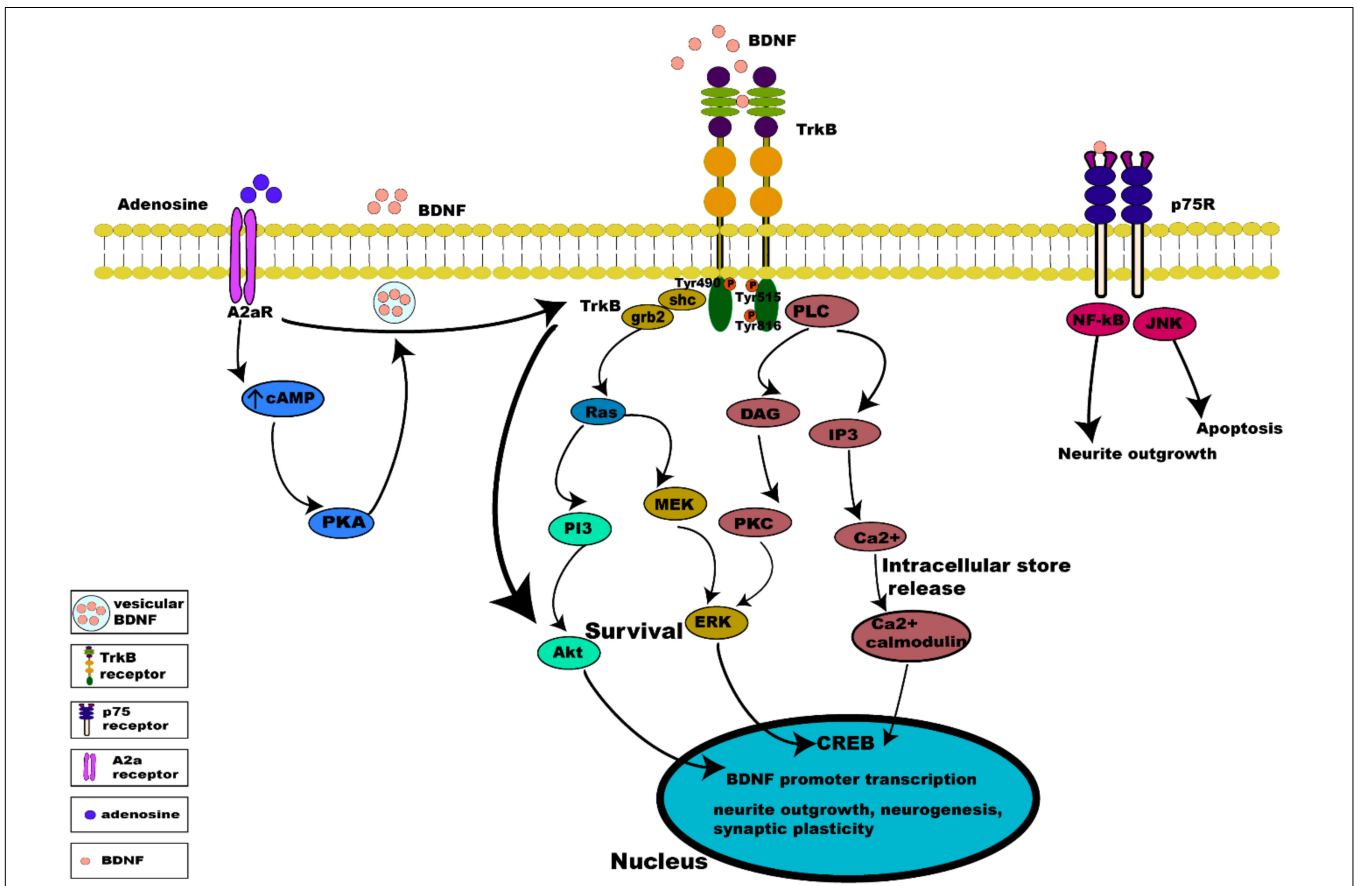

FIGURE 3 | Intrinsic intracellular signaling cascades of BDNF-TrkB and TrkB-A_{2a} receptors. BDNF-TrkB activation predominantly initiates MAPK, PI3K, and PLC γ signaling pathways. Activation of the TrkB receptor at its Tyr490 and Tyr515 residue recruits Shc adaptor protein leading to binding of growth factor receptor bound protein 2 (grb2) which binds with GTPase Ras to form a complex and initiate extracellular signal regulated kinase (ERK) activation which in turn activates the mitogen activated protein kinase MAPK/ERK pathway, which results in the activation of CREB transcription factor. Activation of Tyr515 residue also activates the PI3K signaling pathway, incorporating combined actions of Ras and activating the PI3/Akt and MEK/MAPK pathways. Both MAPK and PI3K signaling exert neurotrophic functions of survival, growth and differentiation, via activation transcription factors (CREB and C-myc). Phosphorylation of the TrkB receptor at its Tyr816 residue activates the phospholipase C γ (PLC γ) pathway, generating inositol-1, 4, 5-triphosphate (IP3) and diacylglycerol (DAG). The PLCγ/IP3 pathway results in calcium release from intracellular stores, in turn activating Ca^{2+}/CaMKII. DAG activates PKC, leading to synaptic plasticity. pro-BDNF/p75 initiates JNK signaling (Reichardt, 2006; Anastasia et al., 2013; Kowianski et al., 2018) triggering neuronal apoptosis (Teng et al., 2005), and the NF-κB signaling cascade regulation of neuronal growth cone development and navigation, and neuronal survival. Like BDNF, neuronal activity promotes release of adenosine which binds to A_{2a}Rs to activate adenylyl cyclase leading to production of cAMP further activating PKA downstream which controls Ca^{2+} dependent BDNF release. Activation of A_{2a}Rs also transactivates TrkB, initiating the TrkB-Akt pathway promoting neuronal survival.

THE MAPK PATHWAY

Activation of the TrkB receptor at its Tyr490 and Tyr515 residue causes the docking of Shc adaptor protein (Src- homology 2-domain) at these tyrosine sites and recruits growth factor receptor bound protein 2 (grb2) which binds with GTPase Ras to form a complex, and initiates extracellular signal regulated kinase (ERK) activation (Wheaton et al., 2007). ERK activation in turn activates the mitogen activated protein kinase MAPK/ERK pathway. MAPK/ERK kinases are able to phosphorylate and activate the transcription factor cAMP response element binding protein (CREB) (Huang and Reichardt, 2003; Begni et al., 2017). The phosphorylated CREB is then translocated into the nucleus, where it induces BDNF transcription by binding to BDNF promoters (Shaywitz and Greenberg, 1999). Binding to BDNF promoters drives BDNF expression to regulate neuronal survival, differentiation and synaptic plasticity (Patapoutian and Reichardt, 2001). In addition, this activation of BDNF expression induces activation of AMPA receptors on stimulation by BDNF (Song et al., 2013).

THE PI3K PATHWAY

Activation of the PI3K pathway incorporates combined actions of Ras at the Tyr515 residue, which activates multiple cascades, namely the PI3/Akt and MEK/MAPK pathways. Activation of the PI3K/Akt cascade regulates proteins such as BAD (Bcl-2 antagonist of cell death) and GSK-3β (glycogen synthase kinase 3β), essential for neuronal survival, growth and differentiation, and is activated by Ca^{2+} influx via L-type voltage gated calcium channels (L-VGCC) (Brunet et al., 2001). Activation of mammalian target of rapamycin (mTOR) by BDNF also enhances local BDNF translation to dendrites at active synapses via the PI3K pathway (Schratt et al., 2004).

THE PLC γ PATHWAY

The phosphorylation of the TrkB receptor at its Tyr816 residue activates the phospholipase C γ (PLC γ) pathway, generating inositol-1,4,5-triphosphate (IP_3), and diacylglycerol (DAG) which is important for survival, neurite outgrowth and synaptic plasticity. BDNF via the PLCγ/IP_3 pathway results in calcium release from intracellular stores activating CaMKII (Ca^{2+}/calmodulin dependent protein kinase) which in turn activates CREB phosphorylation (Minichiello et al., 2002; Tejeda and Diaz-Guerra, 2017). The generation of DAG on the other hand, activates PKC (Bellingham, 2013a) which is translocated to the membrane for further activation and phosphorylation of ERK leading to synaptic plasticity (Minichiello et al., 2002; Chao, 2003).

The BDNF-TrkB complex not only activates on its transmembrane surface (described above) but it also internalizes via endosomes (both early and late endosomes) to activate downstream pathways. This BDNF-TrkB signaling via endosome also determines the cellular fate of BDNF-TrkB complexes, which can be transported retrogradely, recycled back to the membrane, or prepared for degradation by lysosomes (Yamashita and Kuruvilla, 2016).

BDNF: ROLE IN SYNAPTIC TRANSMISSION

Synaptic transmission is a highly complex trans-neuronal process, occurring at the synapse between a pre-synaptic (axonal) terminal and a post-synaptic (typically dendritic) membrane. BDNF elicits rapid effects on synaptic transmission and membrane excitability, via activation of pathways in both the pre- and post-synaptic compartments. In the pre-synaptic compartment, BDNF causes release of glutamate and GABA, via the TrkB-ERK mediated pathway (Jovanovic et al., 2000). Enhanced glutamate release at glutamatergic synapses is mediated by an increase in docked vesicles at presynaptic active zones (Tyler and Pozzo-Miller, 2001). For example, BDNF application to hippocampal and cortical neuron cultures (Levine et al., 1995; Lessmann, 1998) and slice preparations (Kang and Schuman, 1995; Kang et al., 1997) potentiates excitatory neurotransmission, increasing glutamate release. Consequently, BDNF application onto brain slices induces hyper-excitability (Scharfman, 1997), which is consistent with observations in transgenic mice over-expressing BDNF (Croll et al., 1999). In the post-synaptic compartment, BDNF can also enhance synaptic responses by increasing the open probability of NMDA glutamate receptors (Rose et al., 2004). Hence, in the context of ALS, the increased neuronal activity observed in $hSOD1^{G93A}$ mice is capable of increasing BDNF secretion, which in turn can increase release of glutamate to trigger excitotoxicity, leading to MN degeneration. Indeed, BDNF has been shown to enhance MN death by glutamate excitotoxicity, via activation of TrkB (Hu and Kalb, 2003; Mojsilovic-Petrovic et al., 2006). Together, these observations highlight a possible role for BDNF in the death of MNs in ALS.

MECHANISMS OF BDNF-MODIFIED NEUROTRANSMISSION

Brain derived neurotrophic factor also modifies neurotransmission by altering the expression of pre-synaptic proteins that regulate neurotransmitter release (Andreae and Burrone, 2018). For example, in BDNF deficient mice, decreased synaptic transmission correlates with a drop in the number of docked synaptic vesicles (Carter et al., 2002). This is also correlated with decreases in synapsin, synaptophysin and synaptobrevin – presynaptic proteins required for vesicle docking and exocytosis at release sites (i.e., active zones) (Martinez et al., 1998; Pozzo-Miller et al., 1999; Jovanovic et al., 2000). These physiological and molecular changes are also present in TrkB knockout mice (Martinez et al., 1998). Thus, BDNF can stimulate synaptic transmission via three mechanisms: (1) increasing the number of synaptic vesicles at the active zone, (2) increasing the

postsynaptic receptor response, and (3) increasing the overall number of synapses per neuron (Bradley and Sporns, 1999).

TrkB RECEPTOR CAN BE ACTIVATED INDEPENDENT OF BDNF

Tropomysin related kinase B receptor is capable of autophosphorylation and activation of downward cascades independent of its ligand, BDNF. Activation of TrkB receptors in the absence of BDNF occurs via a mechanism known as trans-activation, which involves specific G protein coupled receptors (GPCR), such as the A_{2a} adenosine receptor ($A_{2a}R$) present both pre- and post-synaptically (Chao, 2003; Sebastiao et al., 2018). Adenosine is a key neuromodulator produced both extracellularly and intracellularly in neurons and glial cells (Moreau and Huber, 1999). Extracellularly, it is produced by ectonucleotidase degradation of ATP released by neurons and astrocytes, and intracellularly by production during breakdown of ATP during high energy demand, followed by transport into the extracellular space (Jacobson and Gao, 2006). Adenosine directly regulates synaptic transmission and plasticity, as well as modulating neurotransmission and neurotrophins (Sebastiao and Ribeiro, 2009). Pre-synaptically the activation of $A_{2a}Rs$ increases the release of glutamate (Ciruela et al., 2010; Cunha, 2016) and the activation of NMDA receptors (Azdad et al., 2009; Higley and Sabatini, 2010; Sarantis et al., 2015), thus facilitating LTP. Transactivation of TrkB by $A_{2a}Rs$ is mediated by the Src family of protein, such as Fyn (Lee and Chao, 2001), in a slow acting cascade occurring over minutes to hours. TrkB/$A_{2a}R$ interaction allows transactivation of a downstream protective TrkB-Akt pathway (Mojsilovic-Petrovic et al., 2006). Post-synaptic activation of $A_{2a}Rs$ also triggers calcium dependent processes, through L-type voltage gated calcium channels and NMDA receptors, activating adenylyl cyclase and leading to increased cAMP and PKA phosphorylation, which in turn influences Ca^{2+} dependent transcription of BDNF mRNA (Zheng et al., 2011) and BDNF secretion (Tebano et al., 2010) (summarized in **Figure 3**).

A study by Diogenes et al. (2004), demonstrated that BDNF alone without prior depolarization was devoid of effects on neurotransmission, while enhancement of synaptic transmission by BDNF in the hippocampus was facilitated by pre-synaptic activity-dependent adenosine release via $A_{2A}Rs$. This excitatory action of BDNF can be blocked by a TrkB inhibitor, an $A_{2A}R$ antagonist or by a PKA inhibitor, thus indicating that activation of $A_{2A}Rs$ facilitates BDNF modulation of synaptic transmission (Diogenes et al., 2004). Additionally, the role of $A_{2a}Rs$ in regulating BDNF function was further supported in a study using $A_{2a}R$ KO mice, which showed no increase in field EPSCs after BDNF application, whereas in normal hippocampus slices BDNF induced enhanced field EPSCs and EPSCs, and this effect was blocked by $A_{2a}R$ blockers, clearly indicating that activation of $A_{2a}Rs$ is required for normal BDNF levels and BDNF's potentiation of synaptic transmission (Tebano et al., 2008). Taking into account the enhanced glutamate present in MNs in ALS, the $A_{2a}Rs$ is considered as a potential neuroprotective therapeutic agent to ameliorate glutamate induced excitotoxicity in ALS, reinforcing the significance of TrkB transactivation.

In addition to TrkB transactivation by $A_{2a}Rs$, GPCR mediated TrkB transactivation also occurs via other mechanisms. For example, in embryonic cortical neurons TrkB is transactivated by activation of epidermal growth factor (EGF) leading to migration of early cortical neurons to form a differentiated cortical layer (Puehringer et al., 2013). Similarly in striatal neurons, activation of dopamine 1 (D1) receptors leads to transactivation of TrkB functioning in axonal growth and growth cone during neuronal development (Iwakura et al., 2008). Furthermore, in hippocampal mossy fiber neurons TrkB is transactivated by zinc, which is secreted along with glutamate in response to neuronal activity leading to potentiation of mossy fiber synapses, thus regulating synaptic plasticity (Huang et al., 2008). Hence, considering the role of BDNF/TrkB during development and pathological situations such as in neurodegenerative diseases, TrkB transactivation offers alternative methods to modulate BDNF/TrkB, opening new therapeutic avenues for the treatment of neurodegenerative disorders.

BDNF/TrkB INTERACTS WITH Ca^{2+} AND GLUTAMATE

The interplay between BDNF and glutamate has been well established in many previous studies. Glutamate is a major excitatory neurotransmitter in the central nervous system (CNS) known for its activity-dependent interplay with neurotrophic factors during development and in mature neurons. Post-synaptically, the effect of glutamate is mediated by activation of two major ionotrophic glutamate receptors; AMPA receptors and NMDA receptors (Rao and Finkbeiner, 2007; Mattson, 2008). Pre-synaptic depolarization results in glutamate release, activation of AMPA and NMDA receptors post-synaptically, and secretion of BDNF in the extracellular space (Nagappan and Lu, 2005). BDNF-induced pre-synaptic glutamate release is mediated via TrkB-ERK signaling (Jovanovic et al., 2000), and post-synaptic modulation of glutamate receptors occurs by phosphorylation of the NMDA receptor subunit NR2B (Cunha et al., 2010). Furthermore, BDNF also enhances AMPA receptor surface expression, thus increasing post-synaptic responses to glutamate (Narisawa-Saito et al., 2002; Cunha et al., 2010) – an effect mediated via ERK (Li and Keifer, 2009). BDNF treatment also leads to phosphorylation of NMDAR subunit NR1 (Slack and Thompson, 2002), altering NMDAR localization at synapses (Gomes et al., 2006).

In addition to these pre- and postsynaptic effects on glutamatergic transmission, TrkB activation also modulates ion channels that can alter neuronal excitability, including Na^+, Ca^{2+}, and K^+ channels through intracellular cascades (Blum et al., 2002; Tucker and Fadool, 2002). For example, BDNF/TrkB activation alters neuronal excitability by gating of Na^+ current via Nav1.9 (Blum et al., 2002). Metabotropic receptors such as $A_{2a}Rs$ also activate TrkB to induce release of intracellular Ca^{2+} from ER stores. This in turn activates a PLC cascade to

generate inositol triphosphate (IP3) which releases Ca^{2+} from IP3-sensitive stores, activating PKC.

Considering the interplay between the actions of BDNF and glutamate, there are several possible avenues leading to interactions between neuronal activity and BDNF. Synaptic hyper-excitability and increased intrinsic excitability of susceptible neurons in ALS are clearly observed in human patients (Bostock et al., 1998; Mogyoros et al., 1998; Kanai et al., 2006; Sirabella et al., 2018) and in animal models of ALS (van Zundert et al., 2008; Fogarty et al., 2015; Sirabella et al., 2018). The increased firing and synaptic activation of glutamate receptors would likely result in increased intracellular Ca^{2+}, enhancing BDNF release, which could trigger further release of glutamate. This proposed mechanism would perturb the neuron's ability to regulate its activity, leading to glutamate excitotoxicity and neuronal death (**Figure 4**).

BDNF/TrkB Crosstalk With Inhibitory Neurotransmission

Considering that the physiological functioning of neurons requires a balance between excitatory and inhibitory neurotransmission, hyper-excitability of MNs in ALS can also result from reduced inhibition. γ-aminobutyric acid (GABA) and glycine are the primary neurotransmitters regulating chloride (Cl^-) mediated inhibition in CNS by binding to their post-synaptic receptors. The strength of synaptic inhibition critically depends on intracellular Cl^- concentration, hence on Cl^- homeostasis (Rivera et al., 1999). A key regulator of Cl^- concentration, the potassium chloride cotransporter (KCC2) (Rivera et al., 1999) has been shown to be depleted in MNs (Boulenguez et al., 2010; Fuchs et al., 2010), contributing to the hyper-excitability of MNs. Furthermore, BDNF/TrkB has been shown to be associated with KCC2 regulation (Lee-Hotta et al., 2019) and BDNF/TrkB dependent KCC2 depletion has also been described in MNs (Fuchs et al., 2010; Lee-Hotta et al., 2019). Thus, BDNF/TrkB activation down regulates the expression of KCC2 thereby reducing the Cl^- extrusion capacity in MNs (Rivera et al., 2002, 2004), suppressing Cl^- dependent inhibition which as a result makes the neuron hyper-excitable. Also, the role of microglia induced synaptic inhibition cannot be ignored because KCC2 modulation is required to achieve synaptic balance (Fiumelli and Woodin, 2007; Ferrini and De Koninck, 2013). Indeed, BDNF is released not only from neurons but also from microglia, making BDNF/TrkB a major signaling point of interaction between microglia and neuron (Trang et al., 2011), eventually affecting Cl^- homeostasis (Rivera et al., 2002, 2004; Coull et al., 2005; Zhang et al., 2008). Besides, microglial activation and dysfunction observed in MNs of ALS mice contributes to the progression of disease (Brites and Vaz, 2014) making microglial BDNF a potential actor.

DETRIMENTAL EFFECTS OF BDNF/TrkB IN ALS

The ability of BDNF/TrkB to promote neuronal survival and resistance to toxic insults is well characterized (Kowianski et al., 2018). Several studies documented the neuroprotective effects of BDNF on glutamate induced excitotoxicity *in vivo* (Bemelmans et al., 2006; Henriques et al., 2010) and functional recovery of motor neurons *in vitro* following exogenous BDNF application (Shruthi et al., 2017). Contrary to the view stated in this review, potentiating BDNF has been one of the strategies to delay the disease progression of ALS. The modulation of TrkB via small molecule drug formulations to enhance BDNF signaling also enhanced neuronal survival in degenerating neurons *in vitro* (Guerzoni et al., 2017) and improved motor function and motor neuron loss in ALS model mice (Korkmaz et al., 2014). BDNF potentiation has also been demonstrated to enhance MN survival *in vitro* (Tsai et al., 2013) and in other neurodegenerative diseases (Aytan et al., 2018). Additionally, transactivating TrkB by A_{2a} receptors has also been reported to enhance survival of MNs in culture (Komaki et al., 2012). However, despite these neuroprotective effects observed there is also evidence to show that therapeutic interventions aimed at enhancing BDNF/TrkB are unable to promote survival or prevent death of neurons *in vivo* (The BDNF Study Group Phase III, 1999; Silani et al., 2001; Pansarasa et al., 2018). This suggests that the detrimental actions of BDNF also need to be considered. Under certain circumstances, many studies report that BDNF/TrkB can exert negative effects on MN survival, making MNs more vulnerable to insults (Hu and Kalb, 2003; Mojsilovic-Petrovic et al., 2006). Moreover, BDNF is potent at enhancing excitotoxic insult, by enhancing glutamatergic activity in neurons (Kafitz et al., 1999). Several studies report BDNF and TrkB to be key players in rendering MNs vulnerable to excitotoxic insult (Fryer et al., 2000; Hu and Kalb, 2003; Mojsilovic-Petrovic et al., 2005). Additionally, muscle from ALS patients expresses elevated levels of BDNF, suggesting the possible negative action of BDNF (Kust et al., 2002). Furthermore, BDNF can accelerate glutamate-induced death in rat neuroblastoma cells, and this effect was promoted by TrkB activation (Maki et al., 2015). BDNF also elicited glutamate excitotoxicity in cultured cortical neurons (Koh et al., 1995; Kim et al., 2003), and TrkB inhibition ameliorated these detrimental effects of BDNF (Kim et al., 2003). Additional evidence for the role of BDNF/TrkB in promoting neuronal death comes from a study, where exogenous nitic oxide (NO)/sodium nitroprusside-induced cell death in cortical neurons was enhanced by BDNF, and this effect was inhibited by TrkB antagonism (Ishikawa et al., 2000). Fryer et al. (1999, 2000) also demonstrated that BDNF enhanced glutamate excitotoxicity in cultured embryonic spinal cord MNs, and this response involved activation of TrkB. Furthermore, directly blocking TrkB activation protected embryonic cultured MNs from toxic insults thought to be involved in the pathogenesis of ALS, such as excitotoxicity and the presence of SOD1 mutations (Hu and Kalb, 2003; Mojsilovic-Petrovic et al., 2006; Jeong et al., 2011). Additionally, TrkB-T receptors have been shown to be enhanced in MNs in ALS and deletion of TrkB-T receptors delayed the progression of disease in $SOD1^{G93A}$ mice (Yanpallewar et al., 2012) which further adds to the role of TrkB in ALS. Similarly, impaired BDNF/TrkB signaling and altered TrkB-T isoform was observed in the neuromuscular

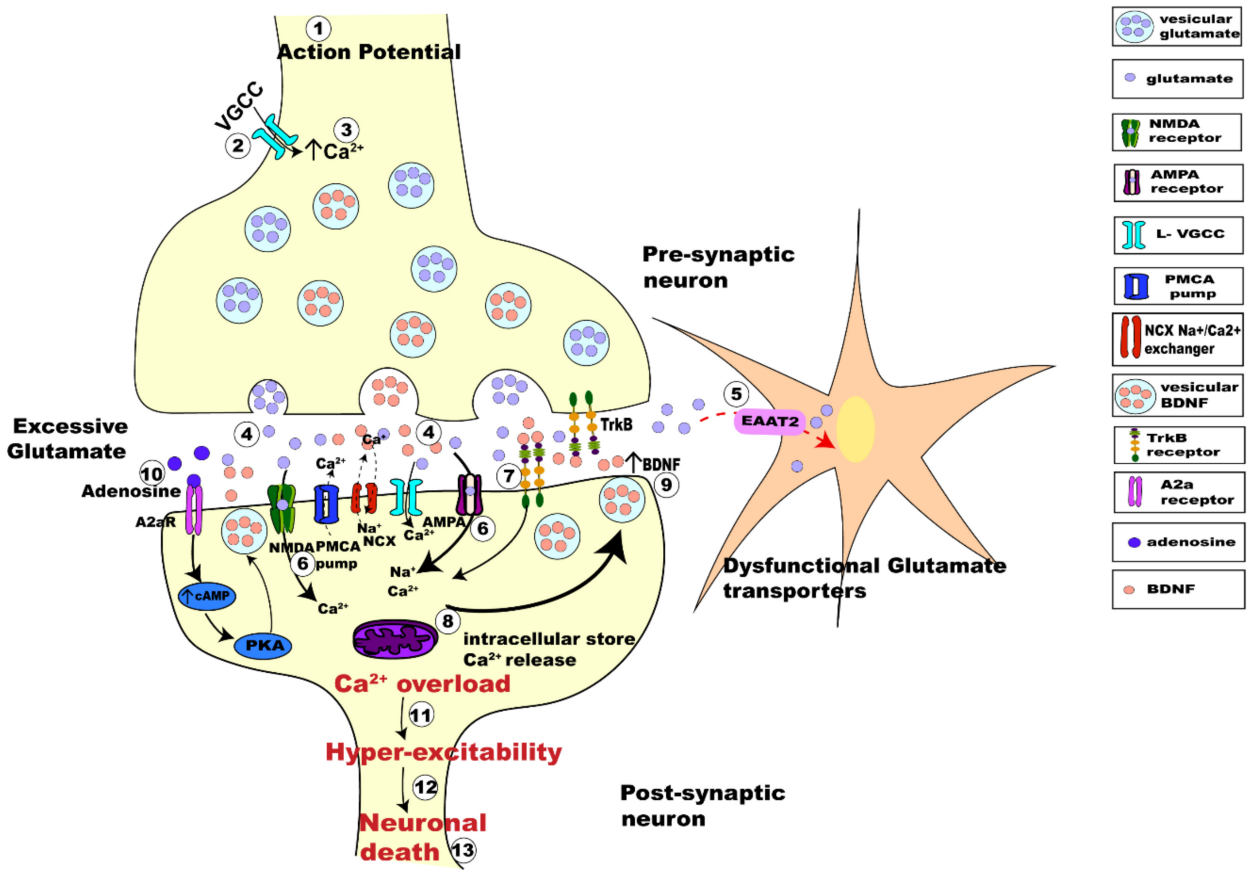

FIGURE 4 | Schematic figure representing activity-dependent interplay between glutamate-induced excitotoxicity and BDNF-TrkB signaling. The arrival of action potential **(step 1)**, triggers the influx of Ca^{2+} ions into pre-synaptic terminal **(step 2)**, the rise in intracellular calcium **(step 3)** in turn triggers the fusion of synaptic vesicles with pre-synaptic membrane to release glutamate (light purple dots) from the terminal **(step 4)**. Membrane depolarization also results in BDNF secretion (orange dots) **(step 4)** and release pre-synaptically into the synaptic cleft. Dysfunctional glutamate transporters (EAAT2) in ALS results in retention of excessive glutamate in the synaptic cleft **(step 5)**. Post-synaptically, Ca^{2+} enters through voltage gated calcium channels and via calcium-permeable glutamate receptors (NMDA, green; AMPA magenta; **step 6**). BDNF binding to TrkB alters the neuronal excitability of ion channels and also enhances post-synaptic glutamate receptor activation causing influx Ca^{2+} of ions post-synaptically **(step 7)**. Excessive glutamate in the synaptic-cleft over-activates its receptors increasing the intracellular Ca^{2+} furthermore **(step 8)**. Impaired Na^{+}/Ca^{2+} exchanger and ATP pumps in $SOD1^{G93A}$ mice results in enhanced Ca^{2+} intracellularly (DeJesus-Hernandez et al., 2011; Sirabella et al., 2018). Ca^{2+} released from the intracellular store adds to the Ca^{2+} concentration **(step 8)**. Enhanced Ca^{2+} in the post-synaptic neuron also triggers increased Ca^{2+} dependent secretion and release of BDNF extracellularly causing enhanced BDNF extracellularly **(step 9)**. *Trans*-activation of TrkB by A_{2a}Rs also triggers calcium dependent signaling, activating adenylyl cyclase and leading to increased cAMP and PKA phosphorylation, which in turn influences BDNF secretion **(step 10)**. This increased BDNF in the synaptic cleft binds to its receptors TrkB and repeats the process of Ca^{2+} influx and modulation of glutamate receptors, eventually leading to Ca^{2+} overload **(step 11)** making the neurons hyper-excitable **(step 12)** which eventually leads to neuronal death **(step 13)**.

junction of pre-symptomatic $SOD1^{G93A}$ mice (Just-Borras et al., 2019). Furthermore, removal of the TrkB-T receptor at the pre-symptomatic stage in $SOD1^{G93A}$ mice improved the disease symptoms rescuing hippocampal interneurons and regulating long term potentiation (Quarta et al., 2018) found to be enhanced in ALS (Spalloni et al., 2006).

In addition to the above BDNF-TrkB signaling effects, blocking A_{2a}Rs, which co-localize with and directly transactivate TrkB, protected cultured MNs from these detrimental effects (Mojsilovic-Petrovic et al., 2005, 2006; Ng et al., 2015; Cunha, 2016). Similarly the inhibition of TrkB or A_{2a}Rs also prevents toxicity following expression of the G85R or G37R SOD1 mutations, which are highly toxic to cultured MNs (Mojsilovic-Petrovic et al., 2006; Jeong et al., 2011). These pro-toxic effects of BDNF/TrkB are not merely an artifact of culturing embryonic MNs. It has also been shown that *in vivo* conditional deletion of TrkB in MNs of adult transgenic mice carrying a G85R SOD1 mutation attenuates SOD1 toxicity, resulting in extension of life span and motor function, slowing MN loss and causing persistence of neuromuscular junctions (Zhai et al., 2011). Furthermore, in a recent study utilizing $SOD1^{G93A}$ rats, phrenic motor neurons displayed an increased expression of BDNF and phosphorylated ERK at end stage disease, consistent with possibly increased BDNF function and basal protein levels (Nichols et al., 2017).

Hyper-activity induced activation of BDNF and TrkB have also been observed in other disease states, such as epilepsy and traumatic brain injury (Dai et al., 2010; Iughetti et al., 2018).

Upregulated expression of BDNF and TrkB has been well documented, resulting in alteration of excitability and neuronal network activity contributing to epileptogenesis (Scharfman, 1997; Iughetti et al., 2018). Enhancing BDNF expression or its systemic administration enhanced seizure activity in mice (Croll et al., 1999; Scharfman et al., 2002; Iughetti et al., 2018), while inhibiting TrkB reduced seizure development in these animals (Heinrich et al., 2011; Liu et al., 2014; Iughetti et al., 2018). Additionally, genetic or pharmacological inhibition of A_{2a}Rs in epilepsy has been shown to reduce seizures and neuronal damage (El Yacoubi et al., 2008, 2009). Despite these numerous reports, the concept of hyper-activity induced glutamate excitotoxicity resulting in overexpression of BDNF and TrkB activation in neuronal death still needs further investigation.

CONCLUSION

Amyotrophic lateral sclerosis is an incurable multi-factorial disease state where synaptic and intrinsic hyper-activity of MNs is a significant early factor (Mogyoros et al., 1998; Kanai et al., 2006; van Zundert et al., 2008; Fogarty et al., 2015). Therapeutic avenues until now have aimed at a reduction of this excitable state. Neuronal hyper-activity is plausibly a result of processes that take place simultaneously, one of them being the secretion of BDNF and activation of its receptor TrkB. Several lines of evidence show that increased BDNF-TrkB is evident in a number of neurodegenerative diseases, including ALS (Kust et al., 2002; Hu and Kalb, 2003; Nichols et al., 2017). This suggests that neuronal damage may be a result of excessive rather than a shortage of, neurotrophic support. A broader understanding of the factors that regulate altered neuronal activity and BDNF could help to identify new therapeutic targets in neurodegenerative diseases. Certainly, therapies that enhance endogenous BDNF have failed to produce any success in prevention or slowing of MN death in ALS. It is important to further investigate both pro- and anti-trophic functions of BDNF/TrkB in the hope of discovering novel therapeutic avenues to alleviate this devastating disease and other neurodegenerative conditions.

AUTHOR CONTRIBUTIONS

All authors contributed to the writing and editing of the manuscript.

FUNDING

This research was supported by an International Postgraduate Scholarship from the University of Queensland to JP, funding from the National Health and Medical Research Council to MB and PN (APP1065884), and funding from the Motor Neuron Disease Research Institute of Australia to MB.

REFERENCES

Abe, K., Itoyama, Y., Sobue, G., Tsuji, S., Aoki, M., Doyu, M., et al. (2014). Confirmatory double-blind, parallel-group, placebo-controlled study of efficacy and safety of edaravone (MCI-186) in amyotrophic lateral sclerosis patients. *Amyotroph. Lateral Scler. Frontotemporal Degener.* 15, 610–617. doi: 10.3109/21678421.2014.959024

Adachi, N., Kohara, K., and Tsumoto, T. (2005). Difference in trafficking of brain-derived neurotrophic factor between axons and dendrites of cortical neurons, revealed by live-cell imaging. *BMC Neurosci.* 6:42.

Aid, T., Kazantseva, A., Piirsoo, M., Palm, K., and Timmusk, T. (2007). Mouse and rat BDNF gene structure and expression revisited. *J. Neurosci. Res.* 85, 525–535. doi: 10.1002/jnr.21139

Alcantara, S., Frisen, J., Del Rio, J. A., Soriano, E., Barbacid, M., and Silos-Santiago, I. (1997). TrkB signaling is required for postnatal survival of CNS neurons and protects hippocampal and motor neurons from axotomy-induced cell death. *J. Neurosci.* 17, 3623–3633. doi: 10.1523/jneurosci.17-10-03623.1997

An, J. J., Gharami, K., Liao, G. Y., Woo, N. H., Lau, A. G., Vanevski, F., et al. (2008). Distinct role of long 3' UTR BDNF mRNA in spine morphology and synaptic plasticity in hippocampal neurons. *Cell* 134, 175–187. doi: 10.1016/j.cell.2008.05.045

Anastasia, A., Deinhardt, K., Chao, M. V., Will, N. E., Irmady, K., Lee, F. S., et al. (2013). Val66Met polymorphism of BDNF alters prodomain structure to induce neuronal growth cone retraction. *Nat. Commun.* 4:2490. doi: 10.1038/ncomms3490

Andreae, L. C., and Burrone, J. (2018). The role of spontaneous neurotransmission in synapse and circuit development. *J. Neurosci. Res.* 96, 354–359. doi: 10.1002/jnr.24154

Aytan, N., Choi, J. K., Carreras, I., Crabtree, L., Nguyen, B., Lehar, M., et al. (2018). Protective effects of 7,8-dihydroxyflavone on neuropathological and neurochemical changes in a mouse model of Alzheimer's disease. *Eur. J. Pharmacol.* 828, 9–17. doi: 10.1016/j.ejphar.2018.02.045

Azdad, K., Gall, D., Woods, A. S., Ledent, C., Ferre, S., and Schiffmann, S. N. (2009). Dopamine D2 and adenosine A2A receptors regulate NMDA-mediated excitation in accumbens neurons through A2A-D2 receptor heteromerization. *Neuropsychopharmacology* 34, 972–986. doi: 10.1038/npp.2008.144

Bae, J. S., Simon, N. G., Menon, P., Vucic, S., and Kiernan, M. C. (2013). The puzzling case of hyperexcitability in amyotrophic lateral sclerosis. *J. Clin. Neurol.* 9, 65–74. doi: 10.3988/jcn.2013.9.2.65

Balkowiec, A., and Katz, D. M. (2002). Cellular mechanisms regulating activity-dependent release of native brain-derived neurotrophic factor from hippocampal neurons. *J. Neurosci.* 22, 10399–10407. doi: 10.1523/jneurosci.22-23-10399.2002

Barde, Y. A., Edgar, D., and Thoenen, H. (1982). Purification of a new neurotrophic factor from mammalian brain. *Embo J.* 1, 549–553. doi: 10.1002/j.1460-2075.1982.tb01207.x

Bartel, D. P. (2004). MicroRNAs: genomics, biogenesis, mechanism, and function. *Cell* 116, 281–297.

Baxter, G. T., Radeke, M. J., Kuo, R. C., Makrides, V., Hinkle, B., Hoang, R., et al. (1997). Signal transduction mediated by the truncated trkB receptor isoforms, trkB.*T1* and trkB.T2. *J. Neurosci.* 17, 2683–2690. doi: 10.1523/jneurosci.17-08-02683.1997

Begni, V., Riva, M. A., and Cattaneo, A. (2017). Cellular and molecular mechanisms of the brain-derived neurotrophic factor in physiological and pathological conditions. *Clin. Sci.* 131, 123–138. doi: 10.1042/cs20160009

Bellingham, M. C. (2013a). "Pharmacological dissection of G protein-mediated second messenger cascades in neurons," in *Stimulation and Inhibition of Neurons*, eds P. M. Pilowsky, M. M. J. Farnham, and A. Y. Fong (Totowa, NJ: Humana Press), 61–106. doi: 10.1007/978-1-62703-233-9_5

Bellingham, M. C. (2013b). Pre- and postsynaptic mechanisms underlying inhibition of hypoglossal motor neuron excitability by riluzole. *J. Neurophysiol.* 110, 1047–1061. doi: 10.1152/jn.00587.2012

Bemelmans, A. P., Husson, I., Jaquet, M., Mallet, J., Kosofsky, B. E., and Gressens, P. (2006). Lentiviral-mediated gene transfer of brain-derived neurotrophic

factor is neuroprotective in a mouse model of neonatal excitotoxic challenge. *J. Neurosci. Res.* 83, 50–60. doi: 10.1002/jnr.20704

Bensimon, G., Lacomblez, L., and Meininger, V. (1994). A controlled trial of riluzole in amyotrophic lateral sclerosis. ALS/Riluzole study group. *N. Engl. J. Med.* 330, 585–591.

Blochl, A., and Thoenen, H. (1995). Characterization of nerve growth factor (NGF) release from hippocampal neurons: evidence for a constitutive and an unconventional sodium-dependent regulated pathway. *Eur. J. Neurosci.* 7, 1220–1228. doi: 10.1111/j.1460-9568.1995.tb01112.x

Blum, R., Kafitz, K. W., and Konnerth, A. (2002). Neurotrophin-evoked depolarization requires the sodium channel Na(V)1.9. *Nature* 419, 687–693. doi: 10.1038/nature01085

Bostock, H., Cikurel, K., and Burke, D. (1998). Threshold tracking techniques in the study of human peripheral nerve. *Muscle Nerve* 21, 137–158. doi: 10.1002/(sici)1097-4598(199802)21:2<137::aid-mus1>3.0.co;2-c

Boulenguez, P., Liabeuf, S., Bos, R., Bras, H., Jean-Xavier, C., Brocard, C., et al. (2010). Down-regulation of the potassium-chloride cotransporter KCC2 contributes to spasticity after spinal cord injury. *Nat. Med.* 16, 302–307. doi: 10.1038/nm.2107

Bradley, J., and Sporns, O. (1999). BDNF-dependent enhancement of exocytosis in cultured cortical neurons requires translation but not transcription. *Brain Res.* 815, 140–149. doi: 10.1016/s0006-8993(98)01112-3

Brigadski, T., Hartmann, M., and Lessmann, V. (2005). Differential vesicular targeting and time course of synaptic secretion of the mammalian neurotrophins. *J. Neurosci.* 25, 7601–7614. doi: 10.1523/jneurosci.1776-05.2005

Brites, D., and Vaz, A. R. (2014). Microglia centered pathogenesis in ALS: insights in cell interconnectivity. *Front. Cell. Neurosci.* 8:117. doi: 10.3389/fncel.2014.00117

Bronfman, F. C., and Fainzilber, M. (2004). Multi-tasking by the p75 neurotrophin receptor: sortilin things out? *EMBO Rep.* 5, 867–871. doi: 10.1038/sj.embor.7400219

Brown, R. H., and Al-Chalabi, A. (2017). Amyotrophic lateral sclerosis. *N. Engl. J. Med.* 377, 162–172.

Brunet, A., Datta, S. R., and Greenberg, M. E. (2001). Transcription-dependent and -independent control of neuronal survival by the PI3K-Akt signaling pathway. *Curr. Opin. Neurobiol.* 11, 297–305. doi: 10.1016/s0959-4388(00)00211-7

Canossa, M., Griesbeck, O., Berninger, B., Campana, G., Kolbeck, R., and Thoenen, H. (1997). Neurotrophin release by neurotrophins: implications for activity-dependent neuronal plasticity. *Proc. Natl. Acad. Sci. U.S.A.* 94, 13279–13286. doi: 10.1073/pnas.94.24.13279

Carim-Todd, L., Bath, K. G., Fulgenzi, G., Yanpallewar, S., Jing, D., Barrick, C. A., et al. (2009). Endogenous truncated TrkB.*T1* receptor regulates neuronal complexity and TrkB kinase receptor function in vivo. *J. Neurosci.* 29, 678–685. doi: 10.1523/JNEUROSCI.5060-08.2009

Carter, A. R., Chen, C., Schwartz, P. M., and Segal, R. A. (2002). Brain-derived neurotrophic factor modulates cerebellar plasticity and synaptic ultrastructure. *J. Neurosci.* 22, 1316–1327. doi: 10.1523/jneurosci.22-04-01316.2002

Chao, M. V. (2003). Neurotrophins and their receptors: a convergence point for many signalling pathways. *Nat. Rev. Neurosci.* 4, 299–309. doi: 10.1038/nrn1078

Chao, M. V., and Hempstead, B. L. (1995). p75 and Trk: a two-receptor system. *Trends Neurosci.* 18, 321–326. doi: 10.1016/0166-2236(95)93922-k

Chico, L., Modena, M., Lo Gerfo, A., Ricci, G., Caldarazzo Ienco, E., Ryskalin, L., et al. (2017). Cross-talk between pathogenic mechanisms in neurodegeneration: the role of oxidative stress in amyotrophic lateral sclerosis. *Arch. Ital. Biol.* 155, 131–141. doi: 10.12871/00039829201744

Chio, A., Calvo, A., Mazzini, L., Cantello, R., Mora, G., Moglia, C., et al. (2012). Extensive genetics of ALS: a population-based study in Italy. *Neurology* 79, 1983–1989. doi: 10.1212/wnl.0b013e3182735d36

Ciruela, F., Albergaria, C., Soriano, A., Cuffi, L., Carbonell, L., Sanchez, S., et al. (2010). Adenosine receptors interacting proteins (ARIPs): behind the biology of adenosine signaling. *Biochim. Biophys. Acta* 1798, 9–20. doi: 10.1016/j.bbamem.2009.10.016

Cleveland, D. W., and Rothstein, J. D. (2001). From Charcot to Lou Gehrig: deciphering selective motor neuron death in ALS. *Nat. Rev. Neurosci.* 2, 806–819. doi: 10.1038/35097565

Coull, J. A., Beggs, S., Boudreau, D., Boivin, D., Tsuda, M., Inoue, K., et al. (2005). BDNF from microglia causes the shift in neuronal anion gradient underlying neuropathic pain. *Nature* 438, 1017–1021. doi: 10.1038/nature04223

Croll, S. D., Suri, C., Compton, D. L., Simmons, M. V., Yancopoulos, G. D., Lindsay, R. M., et al. (1999). Brain-derived neurotrophic factor transgenic mice exhibit passive avoidance deficits, increased seizure severity and in vitro hyperexcitability in the hippocampus and entorhinal cortex. *Neuroscience* 93, 1491–1506. doi: 10.1016/s0306-4522(99)00296-1

Cunha, C., Brambilla, R., and Thomas, K. L. (2010). A simple role for BDNF in learning and memory? *Front. Mol. Neurosci.* 3:1. doi: 10.3389/neuro.02.001.2010

Cunha, R. A. (2016). How does adenosine control neuronal dysfunction and neurodegeneration? *J. Neurochem.* 139, 1019–1055. doi: 10.1111/jnc.13724

Dai, S. S., Zhou, Y. G., Li, W., An, J. H., Li, P., Yang, N., et al. (2010). Local glutamate level dictates adenosine A2A receptor regulation of neuroinflammation and traumatic brain injury. *J. Neurosci.* 30, 5802–5810. doi: 10.1523/JNEUROSCI.0268-10.2010

Deinhardt, K., and Chao, M. V. (2014). Shaping neurons: long and short range effects of mature and proBDNF signalling upon neuronal structure. *Neuropharmacology* 76(Pt C), 603–609. doi: 10.1016/j.neuropharm.2013.04.054

DeJesus-Hernandez, M., Mackenzie, I. R., Boeve, B. F., Boxer, A. L., Baker, M., Rutherford, N. J., et al. (2011). Expanded GGGGCC hexanucleotide repeat in noncoding region of C9ORF72 causes chromosome 9p-linked FTD and ALS. *Neuron* 72, 245–256. doi: 10.1016/j.neuron.2011.09.011

Dieni, S., Matsumoto, T., Dekkers, M., Rauskolb, S., Ionescu, M. S., Deogracias, R., et al. (2012). BDNF and its pro-peptide are stored in presynaptic dense core vesicles in brain neurons. *J. Cell Biol.* 196, 775–788. doi: 10.1083/jcb.201201038

Diogenes, M. J., Fernandes, C. C., Sebastiao, A. M., and Ribeiro, J. A. (2004). Activation of adenosine A2A receptor facilitates brain-derived neurotrophic factor modulation of synaptic transmission in hippocampal slices. *J. Neurosci.* 24, 2905–2913. doi: 10.1523/jneurosci.4454-03.2004

Du, J., Feng, L., Zaitsev, E., Je, H. S., Liu, X. W., and Lu, B. (2003). Regulation of TrkB receptor tyrosine kinase and its internalization by neuronal activity and Ca2+ influx. *J. Cell Biol.* 163, 385–395. doi: 10.1083/jcb.200305134

Egan, M. F., Kojima, M., Callicott, J. H., Goldberg, T. E., Kolachana, B. S., Bertolino, A., et al. (2003). The BDNF val66met polymorphism affects activity-dependent secretion of BDNF and human memory and hippocampal function. *Cell* 112, 257–269. doi: 10.1016/s0092-8674(03)00035-7

El Yacoubi, M., Ledent, C., Parmentier, M., Costentin, J., and Vaugeois, J. M. (2008). Evidence for the involvement of the adenosine A(2A) receptor in the lowered susceptibility to pentylenetetrazol-induced seizures produced in mice by long-term treatment with caffeine. *Neuropharmacology* 55, 35–40. doi: 10.1016/j.neuropharm.2008.04.007

El Yacoubi, M., Ledent, C., Parmentier, M., Costentin, J., and Vaugeois, J. M. (2009). Adenosine A2A receptor deficient mice are partially resistant to limbic seizures. *Naunyn Schmiedebergs Arch. Pharmacol.* 380, 223–232. doi: 10.1007/s00210-009-0426-8

Fang, T., Al Khleifat, A., Meurgey, J. H., Jones, A., Leigh, P. N., Bensimon, G., et al. (2018). Stage at which riluzole treatment prolongs survival in patients with amyotrophic lateral sclerosis: a retrospective analysis of data from a dose-ranging study. *Lancet Neurol.* 17, 416–422. doi: 10.1016/S1474-4422(18)30054-1

Fenner, B. M. (2012). Truncated TrkB: beyond a dominant negative receptor. *Cytokine Growth Factor Rev.* 23, 15–24. doi: 10.1016/j.cytogfr.2012.01.002

Ferrini, F., and De Koninck, Y. (2013). Microglia control neuronal network excitability via BDNF signalling. *Neural Plast.* 2013:429815. doi: 10.1155/2013/429815

Fiumelli, H., and Woodin, M. A. (2007). Role of activity-dependent regulation of neuronal chloride homeostasis in development. *Curr. Opin. Neurobiol.* 17, 81–86. doi: 10.1016/j.conb.2007.01.002

Fogarty, M. J., Mu, E. W., Noakes, P. G., Lavidis, N. A., and Bellingham, M. C. (2016). Marked changes in dendritic structure and spine density precede significant neuronal death in vulnerable cortical pyramidal neuron populations in the SOD1(G93A) mouse model of amyotrophic lateral sclerosis. *Acta Neuropathol. Commun.* 4:77. doi: 10.1186/s40478-016-0347-y

Fogarty, M. J., Noakes, P. G., and Bellingham, M. C. (2015). Motor cortex layer V pyramidal neurons exhibit dendritic regression, spine loss, and

increased synaptic excitation in the presymptomatic hSOD1(G93A) mouse model of amyotrophic lateral sclerosis. *J. Neurosci.* 35, 643–647. doi: 10.1523/JNEUROSCI.3483-14.2015

Foltran, R. B., and Diaz, S. L. (2016). BDNF isoforms: a round trip ticket between neurogenesis and serotonin? *J. Neurochem.* 138, 204–221. doi: 10.1111/jnc.13658

Fryer, H. J., Knox, R. J., Strittmatter, S. M., and Kalb, R. G. (1999). Excitotoxic death of a subset of embryonic rat motor neurons in vitro. *J. Neurochem.* 72, 500–513. doi: 10.1046/j.1471-4159.1999.0720500.x

Fryer, H. J., Wolf, D. H., Knox, R. J., Strittmatter, S. M., Pennica, D., O'leary, R. M., et al. (2000). Brain-derived neurotrophic factor induces excitotoxic sensitivity in cultured embryonic rat spinal motor neurons through activation of the phosphatidylinositol 3-kinase pathway. *J. Neurochem.* 74, 582–595. doi: 10.1046/j.1471-4159.2000.740582.x

Fryer, R. H., Kaplan, D. R., Feinstein, S. C., Radeke, M. J., Grayson, D. R., and Kromer, L. F. (1996). Developmental and mature expression of full-length and truncated TrkB receptors in the rat forebrain. *J. Comp. Neurol.* 374, 21–40. doi: 10.1002/(sici)1096-9861(19961007)374:1<21::aid-cne2>3.0.co;2-p

Fryer, R. H., Kaplan, D. R., and Kromer, L. F. (1997). Truncated trkB receptors on nonneuronal cells inhibit BDNF-induced neurite outgrowth in vitro. *Exp. Neurol.* 148, 616–627. doi: 10.1006/exnr.1997.6699

Fuchs, A., Ringer, C., Bilkei-Gorzo, A., Weihe, E., Roeper, J., and Schutz, B. (2010). Downregulation of the potassium chloride cotransporter KCC2 in vulnerable motoneurons in the SOD1-G93A mouse model of amyotrophic lateral sclerosis. *J. Neuropathol. Exp. Neurol.* 69, 1057–1070. doi: 10.1097/NEN.0b013e3181f4dcef

Gomes, R. A., Hampton, C., El-Sabeawy, F., Sabo, S. L., and Mcallister, A. K. (2006). The dynamic distribution of TrkB receptors before, during, and after synapse formation between cortical neurons. *J. Neurosci.* 26, 11487–11500. doi: 10.1523/jneurosci.2364-06.2006

Gonzalez, A., Moya-Alvarado, G., Gonzalez-Billaut, C., and Bronfman, F. C. (2016). Cellular and molecular mechanisms regulating neuronal growth by brain-derived neurotrophic factor. *Cytoskeleton* 73, 612–628. doi: 10.1002/cm.21312

Goodman, C. S., and Shatz, C. J. (1993). Developmental mechanisms that generate precise patterns of neuronal connectivity. *Cell* 72(Suppl.), 77–98. doi: 10.1016/s0092-8674(05)80030-3

Goodman, L. J., Valverde, J., Lim, F., Geschwind, M. D., Federoff, H. J., Geller, A. I., et al. (1996). Regulated release and polarized localization of brain-derived neurotrophic factor in hippocampal neurons. *Mol. Cell. Neurosci.* 7, 222–238. doi: 10.1006/mcne.1996.0017

Griesbeck, O., Canossa, M., Campana, G., Gartner, A., Hoener, M. C., Nawa, H., et al. (1999). Are there differences between the secretion characteristics of NGF and BDNF? Implications for the modulatory role of neurotrophins in activity-dependent neuronal plasticity. *Microsc. Res. Tech.* 45, 262–275. doi: 10.1002/(sici)1097-0029(19990515/01)45:4/5<262::aid-jemt10>3.0.co;2-k

Guerzoni, L. P., Nicolas, V., and Angelova, A. (2017). *In Vitro* modulation of TrkB receptor signaling upon sequential delivery of curcumin-DHA loaded carriers towards promoting neuronal survival. *Pharm. Res.* 34, 492–505. doi: 10.1007/s11095-016-2080-4

Guo, J., Ji, Y., Ding, Y., Jiang, W., Sun, Y., Lu, B., et al. (2016). BDNF pro-peptide regulates dendritic spines via caspase-3. *Cell Death Dis.* 7:e2264. doi: 10.1038/cddis.2016.166

Gurney, M. E., Pu, H., Chiu, A. Y., Dal Canto, M. C., Polchow, C. Y., Alexander, D. D., et al. (1994). Motor neuron degeneration in mice that express a human Cu,Zn superoxide dismutase mutation. *Science* 264, 1772–1775. doi: 10.1126/science.8209258

Hartmann, M., Heumann, R., and Lessmann, V. (2001). Synaptic secretion of BDNF after high-frequency stimulation of glutamatergic synapses. *EMBO J.* 20, 5887–5897. doi: 10.1093/emboj/20.21.5887

Hayashi, Y., Homma, K., and Ichijo, H. (2016). SOD1 in neurotoxicity and its controversial roles in SOD1 mutation-negative ALS. *Adv. Biol. Regul.* 60, 95–104. doi: 10.1016/j.jbior.2015.10.006

Heinrich, C., Lahteinen, S., Suzuki, F., Anne-Marie, L., Huber, S., Haussler, U., et al. (2011). Increase in BDNF-mediated TrkB signaling promotes epileptogenesis in a mouse model of mesial temporal lobe epilepsy. *Neurobiol. Dis.* 42, 35–47. doi: 10.1016/j.nbd.2011.01.001

Hempstead, B. L. (2015). Brain-derived neurotrophic factor: three ligands, many actions. *Trans. Am. Clin. Climatol. Assoc.* 126, 9–19.

Henriques, A., Pitzer, C., and Schneider, A. (2010). Neurotrophic growth factors for the treatment of amyotrophic lateral sclerosis: where do we stand? *Front. Neurosci.* 4:32. doi: 10.3389/fnins.2010.00032

Higley, M. J., and Sabatini, B. L. (2010). Competitive regulation of synaptic Ca2+ influx by D2 dopamine and A2A adenosine receptors. *Nat. Neurosci.* 13, 958–966. doi: 10.1038/nn.2592

Hong, E. J., Mccord, A. E., and Greenberg, M. E. (2008). A biological function for the neuronal activity-dependent component of Bdnf transcription in the development of cortical inhibition. *Neuron* 60, 610–624. doi: 10.1016/j.neuron.2008.09.024

Hu, P., and Kalb, R. G. (2003). BDNF heightens the sensitivity of motor neurons to excitotoxic insults through activation of TrkB. *J. Neurochem.* 84, 1421–1430. doi: 10.1046/j.1471-4159.2003.01599.x

Huang, E. J., and Reichardt, L. F. (2001). Neurotrophins: roles in neuronal development and function. *Annu. Rev. Neurosci.* 24, 677–736. doi: 10.1146/annurev.neuro.24.1.677

Huang, E. J., and Reichardt, L. F. (2003). Trk receptors: roles in neuronal signal transduction. *Annu. Rev. Biochem.* 72, 609–642. doi: 10.1146/annurev.biochem.72.121801.161629

Huang, Y. Z., Pan, E., Xiong, Z. Q., and Mcnamara, J. O. (2008). Zinc-mediated transactivation of TrkB potentiates the hippocampal mossy fiber-CA3 pyramid synapse. *Neuron* 57, 546–558. doi: 10.1016/j.neuron.2007.11.026

Hwang, J. J., Park, M. H., Choi, S. Y., and Koh, J. Y. (2005). Activation of the Trk signaling pathway by extracellular zinc. *Role of metalloproteinases. J. Biol. Chem.* 280, 11995–12001. doi: 10.1074/jbc.m403172200

Ishikawa, Y., Ikeuchi, T., and Hatanaka, H. (2000). Brain-derived neurotrophic factor accelerates nitric oxide donor-induced apoptosis of cultured cortical neurons. *J. Neurochem.* 75, 494–502. doi: 10.1046/j.1471-4159.2000.0750494.x

Iughetti, L., Lucaccioni, L., Fugetto, F., Predieri, B., Berardi, A., and Ferrari, F. (2018). Brain-derived neurotrophic factor and epilepsy: a systematic review. *Neuropeptides* 72, 23–29. doi: 10.1016/j.npep.2018.09.005

Iwakura, Y., Nawa, H., Sora, I., and Chao, M. V. (2008). Dopamine D1 receptor-induced signaling through TrkB receptors in striatal neurons. *J. Biol. Chem.* 283, 15799–15806. doi: 10.1074/jbc.M801553200

Jacobson, K. A., and Gao, Z. G. (2006). Adenosine receptors as therapeutic targets. *Nat. Rev. Drug Discov.* 5, 247–264.

Jeong, G. B., Mojsilovic-Petrovic, J., Boccitto, M., and Kalb, R. (2011). Signaling events in axons and/or dendrites render motor neurons vulnerable to mutant superoxide dismutase toxicity. *J. Neurosci.* 31, 295–299. doi: 10.1523/JNEUROSCI.4824-10.2011

Ji, Y., Lu, Y., Yang, F., Shen, W., Tang, T. T., Feng, L., et al. (2010). Acute and gradual increases in BDNF concentration elicit distinct signaling and functions in neurons. *Nat. Neurosci.* 13, 302–309. doi: 10.1038/nn.2505

Jovanovic, J. N., Czernik, A. J., Fienberg, A. A., Greengard, P., and Sihra, T. S. (2000). Synapsins as mediators of BDNF-enhanced neurotransmitter release. *Nat. Neurosci.* 3, 323–329. doi: 10.1038/73888

Just-Borras, L., Hurtado, E., Cilleros-Mane, V., Biondi, O., Charbonnier, F., Tomas, M., et al. (2019). Overview of impaired BDNF signaling, their coupled downstream serine-threonine kinases and SNARE/SM complex in the neuromuscular junction of the amyotrophic lateral sclerosis model SOD1-G93A mice. *Mol. Neurobiol.* [Epub ahead of print].

Kafitz, K. W., Rose, C. R., Thoenen, H., and Konnerth, A. (1999). Neurotrophin-evoked rapid excitation through TrkB receptors. *Nature* 401, 918–921. doi: 10.1038/44847

Kanai, K., Kuwabara, S., Misawa, S., Tamura, N., Ogawara, K., Nakata, M., et al. (2006). Altered axonal excitability properties in amyotrophic lateral sclerosis: impaired potassium channel function related to disease stage. *Brain* 129, 953–962. doi: 10.1093/brain/awl024

Kang, H., and Schuman, E. M. (1995). Long-lasting neurotrophin-induced enhancement of synaptic transmission in the adult hippocampus. *Science* 267, 1658–1662. doi: 10.1126/science.7886457

Kang, H., Welcher, A. A., Shelton, D., and Schuman, E. M. (1997). Neurotrophins and time: different roles for TrkB signaling in hippocampal long-term potentiation. *Neuron* 19, 653–664. doi: 10.1016/s0896-6273(00)80378-5

Kim, H. J., Hwang, J. J., Behrens, M. M., Snider, B. J., Choi, D. W., and Koh, J. Y. (2003). TrkB mediates BDNF-induced potentiation of neuronal necrosis

in cortical culture. *Neurobiol. Dis.* 14, 110–119. doi: 10.1016/s0969-9961(03)00103-7

King, A. E., Woodhouse, A., Kirkcaldie, M. T., and Vickers, J. C. (2016). Excitotoxicity in ALS: overstimulation, or overreaction? *Exp. Neurol.* 275(Pt 1), 162–171. doi: 10.1016/j.expneurol.2015.09.019

Klein, R., Smeyne, R. J., Wurst, W., Long, L. K., Auerbach, B. A., Joyner, A. L., et al. (1993). Targeted disruption of the trkB neurotrophin receptor gene results in nervous system lesions and neonatal death. *Cell* 75, 113–122. doi: 10.1016/0092-8674(93)90683-h

Koh, J. Y., Gwag, B. J., Lobner, D., and Choi, D. W. (1995). Potentiated necrosis of cultured cortical neurons by neurotrophins. *Science* 268, 573–575. doi: 10.1126/science.7725105

Kohara, K., Kitamura, A., Morishima, M., and Tsumoto, T. (2001). Activity-dependent transfer of brain-derived neurotrophic factor to postsynaptic neurons. *Science* 291, 2419–2423. doi: 10.1126/science.1057415

Komaki, S., Ishikawa, K., and Arakawa, Y. (2012). Trk and cAMP-dependent survival activity of adenosine A(2A) agonist CGS21680 on rat motoneurons in culture. *Neurosci. Lett.* 522, 21–24. doi: 10.1016/j.neulet.2012.06.003

Korkmaz, O. T., Aytan, N., Carreras, I., Choi, J. K., Kowall, N. W., Jenkins, B. G., et al. (2014). 7,8-Dihydroxyflavone improves motor performance and enhances lower motor neuronal survival in a mouse model of amyotrophic lateral sclerosis. *Neurosci. Lett.* 566, 286–291. doi: 10.1016/j.neulet.2014.02.058

Kowianski, P., Lietzau, G., Czuba, E., Waskow, M., Steliga, A., and Morys, J. (2018). BDNF: a key factor with multipotent impact on brain signaling and synaptic plasticity. *Cell Mol. Neurobiol.* 38, 579–593. doi: 10.1007/s10571-017-0510-4

Kust, B. M., Copray, J. C., Brouwer, N., Troost, D., and Boddeke, H. W. (2002). Elevated levels of neurotrophins in human biceps brachii tissue of amyotrophic lateral sclerosis. *Exp. Neurol.* 177, 419–427. doi: 10.1006/exnr.2002.8011

Kutsarova, E., Munz, M., and Ruthazer, E. S. (2016). Rules for shaping neural connections in the developing brain. *Front. Neural. Circuits* 10:111. doi: 10.3389/fncir.2016.00111

Lau, A. G., Irier, H. A., Gu, J., Tian, D., Ku, L., Liu, G., et al. (2010). Distinct 3'UTRs differentially regulate activity-dependent translation of brain-derived neurotrophic factor (BDNF). *Proc. Natl. Acad. Sci. U.S.A.* 107, 15945–15950. doi: 10.1073/pnas.1002929107

Le Masson, G., Przedborski, S., and Abbott, L. F. (2014). A computational model of motor neuron degeneration. *Neuron* 83, 975–988. doi: 10.1016/j.neuron.2014.07.001

Leal, G., Afonso, P. M., Salazar, I. L., and Duarte, C. B. (2015). Regulation of hippocampal synaptic plasticity by BDNF. *Brain Res.* 1621, 82–101. doi: 10.1016/j.brainres.2014.10.019

Lee, F. S., and Chao, M. V. (2001). Activation of Trk neurotrophin receptors in the absence of neurotrophins. *Proc. Natl. Acad. Sci. U.S.A.* 98, 3555–3560. doi: 10.1073/pnas.061020198

Lee-Hotta, S., Uchiyama, Y., and Kametaka, S. (2019). Role of the BDNF-TrkB pathway in KCC2 regulation and rehabilitation following neuronal injury: a mini review. *Neurochem. Int.* 128, 32–38. doi: 10.1016/j.neuint.2019.04.003

Lessmann, V. (1998). Neurotrophin-dependent modulation of glutamatergic synaptic transmission in the mammalian CNS. *Gen. Pharmacol.* 31, 667–674. doi: 10.1016/s0306-3623(98)00190-6

Lessmann, V., Gottmann, K., and Malcangio, M. (2003). Neurotrophin secretion: current facts and future prospects. *Prog. Neurobiol.* 69, 341–374. doi: 10.1016/s0301-0082(03)00019-4

Levine, E. S., Dreyfus, C. F., Black, I. B., and Plummer, M. R. (1995). Brain-derived neurotrophic factor rapidly enhances synaptic transmission in hippocampal neurons via postsynaptic tyrosine kinase receptors. *Proc. Natl. Acad. Sci. U.S.A* 92, 8074–8077. doi: 10.1073/pnas.92.17.8074

Li, W., and Keifer, J. (2009). BDNF-induced synaptic delivery of AMPAR subunits is differentially dependent on NMDA receptors and requires ERK. *Neurobiol. Learn. Mem.* 91, 243–249. doi: 10.1016/j.nlm.2008.10.002

Liu, G., Kotloski, R. J., and Mcnamara, J. O. (2014). Antiseizure effects of TrkB kinase inhibition. *Epilepsia* 55, 1264–1273. doi: 10.1111/epi.12671

Lu, B. (2003). BDNF and activity-dependent synaptic modulation. *Learn. Mem.* 10, 86–98. doi: 10.1101/lm.54603

Lu, B., Pang, P. T., and Woo, N. H. (2005). The yin and yang of neurotrophin action. *Nat. Rev. Neurosci.* 6, 603–614. doi: 10.1038/nrn1726

Luberg, K., Wong, J., Weickert, C. S., and Timmusk, T. (2010). Human TrkB gene: novel alternative transcripts, protein isoforms and expression pattern in the prefrontal cerebral cortex during postnatal development. *J. Neurochem.* 113, 952–964. doi: 10.1111/j.1471-4159.2010.06662.x

Maki, T., Arishima, K., Yamamoto, M., and Sakaue, M. (2015). TrkB is involved in the mechanism by which BDNF accelerates the glutamate-induced death of rat neuroblastoma B35 cells. *Neurol. Res.* 37, 30–34. doi: 10.1179/1743132814Y.0000000403

Marin, B., Boumediene, F., Logroscino, G., Couratier, P., Babron, M. C., Leutenegger, A. L., et al. (2017). Variation in worldwide incidence of amyotrophic lateral sclerosis: a meta-analysis. *Int. J. Epidemiol.* 46, 57–74. doi: 10.1093/ije/dyw061

Martinez, A., Alcantara, S., Borrell, V., Del Rio, J. A., Blasi, J., Otal, R., et al. (1998). TrkB and TrkC signaling are required for maturation and synaptogenesis of hippocampal connections. *J. Neurosci.* 18, 7336–7350. doi: 10.1523/jneurosci.18-18-07336.1998

Mattson, M. P. (2008). Glutamate and neurotrophic factors in neuronal plasticity and disease. *Ann. N. Y. Acad. Sci.* 1144, 97–112. doi: 10.1196/annals.1418.005

McAllister, A. K., Katz, L. C., and Lo, D. C. (1996). Neurotrophin regulation of cortical dendritic growth requires activity. *Neuron* 17, 1057–1064. doi: 10.1016/s0896-6273(00)80239-1

Mellios, N., Huang, H. S., Grigorenko, A., Rogaev, E., and Akbarian, S. (2008). A set of differentially expressed miRNAs, including miR-30a-5p, act as post-transcriptional inhibitors of BDNF in prefrontal cortex. *Hum. Mol. Genet.* 17, 3030–3042. doi: 10.1093/hmg/ddn201

Middlemas, D. S., Lindberg, R. A., and Hunter, T. (1991). trkB, a neural receptor protein-tyrosine kinase: evidence for a full-length and two truncated receptors. *Mol. Cell. Biol.* 11, 143–153. doi: 10.1128/mcb.11.1.143

Minichiello, L., Calella, A. M., Medina, D. L., Bonhoeffer, T., Klein, R., and Korte, M. (2002). Mechanism of TrkB-mediated hippocampal long-term potentiation. *Neuron* 36, 121–137. doi: 10.1016/s0896-6273(02)00942-x

Mizoguchi, H., Nakade, J., Tachibana, M., Ibi, D., Someya, E., Koike, H., et al. (2011). Matrix metalloproteinase-9 contributes to kindled seizure development in pentylenetetrazole-treated mice by converting pro-BDNF to mature BDNF in the hippocampus. *J. Neurosci.* 31, 12963–12971. doi: 10.1523/JNEUROSCI.3118-11.2011

Mizui, T., Ishikawa, Y., Kumanogoh, H., and Kojima, M. (2016). Neurobiological actions by three distinct subtypes of brain-derived neurotrophic factor: multi-ligand model of growth factor signaling. *Pharmacol. Res.* 105, 93–98. doi: 10.1016/j.phrs.2015.12.019

Mogyoros, I., Kiernan, M. C., Burke, D., and Bostock, H. (1998). Strength-duration properties of sensory and motor axons in amyotrophic lateral sclerosis. *Brain* 121(Pt 5), 851–859. doi: 10.1093/brain/121.5.851

Mojsilovic-Petrovic, J., Arneja, A., and Kalb, R. G. (2005). Enprofylline protects motor neurons from in vitro excitotoxic challenge. *Neurodegener. Dis.* 2, 160–165. doi: 10.1159/000089621

Mojsilovic-Petrovic, J., Jeong, G. B., Crocker, A., Arneja, A., David, S., Russell, D. S., et al. (2006). Protecting motor neurons from toxic insult by antagonism of adenosine A2a and Trk receptors. *J. Neurosci.* 26, 9250–9263. doi: 10.1523/jneurosci.1856-06.2006

Moreau, J. L., and Huber, G. (1999). Central adenosine A(2A) receptors: an overview. *Brain Res. Brain Res. Rev.* 31, 65–82. doi: 10.1016/s0165-0173(99)00059-4

Murer, M. G., Yan, Q., and Raisman-Vozari, R. (2001). Brain-derived neurotrophic factor in the control human brain, and in Alzheimer's disease and Parkinson's disease. *Prog. Neurobiol.* 63, 71–124. doi: 10.1016/s0301-0082(00)00014-9

Nagappan, G., and Lu, B. (2005). Activity-dependent modulation of the BDNF receptor TrkB: mechanisms and implications. *Trends Neurosci.* 28, 464–471. doi: 10.1016/j.tins.2005.07.003

Nakagawara, A., Liu, X. G., Ikegaki, N., White, P. S., Yamashiro, D. J., Nycum, L. M., et al. (1995). Cloning and chromosomal localization of the human TRK-B tyrosine kinase receptor gene (NTRK2). *Genomics* 25, 538–546. doi: 10.1016/0888-7543(95)80055-q

Narisawa-Saito, M., Iwakura, Y., Kawamura, M., Araki, K., Kozaki, S., Takei, N., et al. (2002). Brain-derived neurotrophic factor regulates surface expression of alpha-amino-3-hydroxy-5-methyl-4-isoxazoleproprionic acid receptors by enhancing the N-ethylmaleimide-sensitive factor/GluR2 interaction in developing neocortical neurons. *J. Biol. Chem.* 277, 40901–40910. doi: 10.1074/jbc.m202158200

Ng, S. K., Higashimori, H., Tolman, M., and Yang, Y. (2015). Suppression of adenosine 2a receptor (A2aR)-mediated adenosine signaling improves disease phenotypes in a mouse model of amyotrophic lateral sclerosis. *Exp. Neurol.* 267, 115–122. doi: 10.1016/j.expneurol.2015.03.004

Nichols, N. L., Satriotomo, I., and Allen, L. L. (2017). Mechanisms of enhanced phrenic long-term facilitation in SOD1(G93A) rats. *J. Neurosci.* 37, 5834–5845. doi: 10.1523/JNEUROSCI.3680-16.2017

Notaras, M., and van den Buuse, M. (2018). Brain-derived neurotrophic factor (BDNF): novel insights into regulation and genetic variation. *Neuroscientist* [Epub ahead of print],

Ohira, K., Homma, K. J., Hirai, H., Nakamura, S., and Hayashi, M. (2006). TrkB-T1 regulates the RhoA signaling and actin cytoskeleton in glioma cells. *Biochem. Biophys. Res. Commun.* 342, 867–874. doi: 10.1016/j.bbrc.2006.02.033

Pansarasa, O., Bordoni, M., Diamanti, L., Sproviero, D., Gagliardi, S., and Cereda, C. (2018). SOD1 in amyotrophic lateral sclerosis: "Ambivalent" behavior connected to the disease. *Int. J. Mol. Sci* 19:1345. doi: 10.3390/ijms19051345

Park, H., and Poo, M. M. (2013). Neurotrophin regulation of neural circuit development and function. *Nat. Rev. Neurosci.* 14, 7–23. doi: 10.1038/nrn3379

Pasinelli, P., and Brown, R. H. (2006). Molecular biology of amyotrophic lateral sclerosis: insights from genetics. *Nat. Rev. Neurosci.* 7, 710–723. doi: 10.1038/nrn1971

Patapoutian, A., and Reichardt, L. F. (2001). Trk receptors: mediators of neurotrophin action. *Curr. Opin. Neurobiol.* 11, 272–280. doi: 10.1016/s0959-4388(00)00208-7

Pozzo-Miller, L. D., Gottschalk, W., Zhang, L., Mcdermott, K., Du, J., Gopalakrishnan, R., et al. (1999). Impairments in high-frequency transmission, synaptic vesicle docking, and synaptic protein distribution in the hippocampus of BDNF knockout mice. *J. Neurosci.* 19, 4972–4983. doi: 10.1523/jneurosci.19-12-04972.1999

Pruunsild, P., Kazantseva, A., Aid, T., Palm, K., and Timmusk, T. (2007). Dissecting the human BDNF locus: bidirectional transcription, complex splicing, and multiple promoters. *Genomics* 90, 397–406. doi: 10.1016/j.ygeno.2007.05.004

Puehringer, D., Orel, N., Luningschror, P., Subramanian, N., Herrmann, T., Chao, M. V., et al. (2013). EGF transactivation of Trk receptors regulates the migration of newborn cortical neurons. *Nat. Neurosci.* 16, 407–415. doi: 10.1038/nn.3333

Quarta, E., Fulgenzi, G., Bravi, R., Cohen, E. J., Yanpallewar, S., Tessarollo, L., et al. (2018). Deletion of the endogenous TrkB.*T1* receptor isoform restores the number of hippocampal CA1 parvalbumin-positive neurons and rescues long-term potentiation in pre-symptomatic mSOD1(G93A) ALS mice. *Mol. Cell Neurosci.* 89, 33–41. doi: 10.1016/j.mcn.2018.03.010

Rao, V. R., and Finkbeiner, S. (2007). NMDA and AMPA receptors: old channels, new tricks. *Trends Neurosci.* 30, 284–291. doi: 10.1016/j.tins.2007.03.012

Reichardt, L. F. (2006). Neurotrophin-regulated signalling pathways. *Philos. Trans. R. Soc. Lond. B Biol. Sci.* 361, 1545–1564. doi: 10.1098/rstb.2006.1894

Righi, M., Tongiorgi, E., and Cattaneo, A. (2000). Brain-derived neurotrophic factor (BDNF) induces dendritic targeting of BDNF and tyrosine kinase B mRNAs in hippocampal neurons through a phosphatidylinositol-3 kinase-dependent pathway. *J. Neurosci.* 20, 3165–3174. doi: 10.1523/jneurosci.20-09-03165.2000

Ringholz, G. M., Appel, S. H., Bradshaw, M., Cooke, N. A., Mosnik, D. M., and Schulz, P. E. (2005). Prevalence and patterns of cognitive impairment in sporadic ALS. *Neurology* 65, 586–590. doi: 10.1212/01.wnl.0000172911.39167.b6

Rivera, C., Li, H., Thomas-Crusells, J., Lahtinen, H., Viitanen, T., Nanobashvili, A., et al. (2002). BDNF-induced TrkB activation down-regulates the K+-Cl- cotransporter KCC2 and impairs neuronal Cl- extrusion. *J. Cell Biol.* 159, 747–752. doi: 10.1083/jcb.200209011

Rivera, C., Voipio, J., Payne, J. A., Ruusuvuori, E., Lahtinen, H., Lamsa, K., et al. (1999). The K+/Cl- co-transporter KCC2 renders GABA hyperpolarizing during neuronal maturation. *Nature* 397, 251–255. doi: 10.1038/16697

Rivera, C., Voipio, J., Thomas-Crusells, J., Li, H., Emri, Z., Sipila, S., et al. (2004). Mechanism of activity-dependent downregulation of the neuron-specific K-Cl cotransporter KCC2. *J. Neurosci.* 24, 4683–4691. doi: 10.1523/jneurosci.5265-03.2004

Rose, C. R., Blum, R., Kafitz, K. W., Kovalchuk, Y., and Konnerth, A. (2004). From modulator to mediator: rapid effects of BDNF on ion channels. *Bioessays* 26, 1185–1194. doi: 10.1002/bies.20118

Rosen, D. R., Siddique, T., Patterson, D., Figlewicz, D. A., Sapp, P., Hentati, A., et al. (1993). Mutations in Cu/Zn superoxide dismutase gene are associated with familial amyotrophic lateral sclerosis. *Nature* 362, 59–62.

Rothstein, J. D., Martin, L. J., and Kuncl, R. W. (1992). Decreased glutamate transport by the brain and spinal cord in amyotrophic lateral sclerosis. *N. Engl. J. Med.* 326, 1464–1468. doi: 10.1056/nejm199205283262204

Saba, L., Viscomi, M. T., Caioli, S., Pignataro, A., Bisicchia, E., Pieri, M., et al. (2016). Altered functionality, morphology, and vesicular glutamate transporter expression of cortical motor neurons from a presymptomatic mouse model of amyotrophic lateral sclerosis. *Cereb. Cortex* 26, 1512–1528. doi: 10.1093/cercor/bhu317

Sandstedt, P., Littorin, S., Johansson, S., Gottberg, K., Ytterberg, C., and Kierkegaard, M. (2018). Disability and contextual factors in patients with amyotrophic lateral sclerosis - a three-year observational study. *J. Neuromuscul. Dis.* 5, 439–449. doi: 10.3233/JND-180322

Sarantis, K., Tsiamaki, E., Kouvaros, S., Papatheodoropoulos, C., and Angelatou, F. (2015). Adenosine A(2)A receptors permit mGluR5-evoked tyrosine phosphorylation of NR2B (Tyr1472) in rat hippocampus: a possible key mechanism in NMDA receptor modulation. *J. Neurochem.* 135, 714–726. doi: 10.1111/jnc.13291

Sasi, M., Vignoli, B., Canossa, M., and Blum, R. (2017). Neurobiology of local and intercellular BDNF signaling. *Pflugers Arch.* 469, 593–610. doi: 10.1007/s00424-017-1964-4

Scharfman, H. E. (1997). Hyperexcitability in combined entorhinal/hippocampal slices of adult rat after exposure to brain-derived neurotrophic factor. *J. Neurophysiol.* 78, 1082–1095. doi: 10.1152/jn.1997.78.2.1082

Scharfman, H. E., Goodman, J. H., Sollas, A. L., and Croll, S. D. (2002). Spontaneous limbic seizures after intrahippocampal infusion of brain-derived neurotrophic factor. *Exp. Neurol.* 174, 201–214. doi: 10.1006/exnr.2002.7869

Schneider, R., and Schweiger, M. (1991). A novel modular mosaic of cell adhesion motifs in the extracellular domains of the neurogenic trk and trkB tyrosine kinase receptors. *Oncogene* 6, 1807–1811.

Schratt, G. M., Nigh, E. A., Chen, W. G., Hu, L., and Greenberg, M. E. (2004). BDNF regulates the translation of a select group of mRNAs by a mammalian target of rapamycin-phosphatidylinositol 3-kinase-dependent pathway during neuronal development. *J. Neurosci.* 24, 7366–7377. doi: 10.1523/jneurosci.1739-04.2004

Sebastiao, A. M., Rei, N., and Ribeiro, J. A. (2018). Amyotrophic lateral sclerosis (ALS) and adenosine receptors. *Front. Pharmacol.* 9:267. doi: 10.3389/fphar.2018.00267

Sebastiao, A. M., and Ribeiro, J. A. (2009). Adenosine receptors and the central nervous system. *Handb. Exp. Pharmacol.* 193, 471–534. doi: 10.1007/978-3-540-89615-9_16

Shaywitz, A. J., and Greenberg, M. E. (1999). CREB: a stimulus-induced transcription factor activated by a diverse array of extracellular signals. *Annu. Rev. Biochem.* 68, 821–861. doi: 10.1146/annurev.biochem.68.1.821

Shi, J. (2015). Regulatory networks between neurotrophins and miRNAs in brain diseases and cancers. *Acta Pharmacol. Sin.* 36, 149–157. doi: 10.1038/aps.2014.135

Shruthi, S., Sumitha, R., Varghese, A. M., Ashok, S., Chandrasekhar Sagar, B. K., Sathyaprabha, T. N., et al. (2017). Brain-derived neurotrophic factor facilitates functional recovery from ALS-cerebral spinal fluid-induced neurodegenerative changes in the NSC-34 motor neuron cell line. *Neurodegener Dis.* 17, 44–58. doi: 10.1159/000447559

Silani, V., Braga, M., Cardin, V., and Scarlato, G. (2001). The pathogenesis of ALS: implications for treatment strategies. *Neurol. Neurochir. Pol.* 35, 25–39.

Sirabella, R., Valsecchi, V., Anzilotti, S., Cuomo, O., Vinciguerra, A., Cepparulo, P., et al. (2018). Ionic homeostasis maintenance in ALS: focus on new therapeutic targets. *Front. Neurosci.* 12:510. doi: 10.3389/fnins.2018.00510

Slack, S. E., and Thompson, S. W. (2002). Brain-derived neurotrophic factor induces NMDA receptor 1 phosphorylation in rat spinal cord. *Neuroreport* 13, 1967–1970. doi: 10.1097/00001756-200210280-00027

Song, M., Martinowich, K., and Lee, F. S. (2017). BDNF at the synapse: why location matters. *Mol. Psychiatry* 22, 1370–1375. doi: 10.1038/mp.2017.144

Song, R. S., Massenburg, B., Wenderski, W., Jayaraman, V., Thompson, L., and Neves, S. R. (2013). ERK regulation of phosphodiesterase 4 enhances dopamine-stimulated AMPA receptor membrane insertion. *Proc. Natl. Acad. Sci. U.S.A.* 110, 15437–15442. doi: 10.1073/pnas.1311783110

Spalloni, A., Geracitano, R., Berretta, N., Sgobio, C., Bernardi, G., Mercuri, N. B., et al. (2006). Molecular and synaptic changes in the hippocampus underlying superior spatial abilities in pre-symptomatic G93A+/+ mice overexpressing the human Cu/Zn superoxide dismutase (Gly93 –> ALA) mutation. *Exp. Neurol.* 197, 505–514. doi: 10.1016/j.expneurol.2005.10.014

Stevens, B., Allen, N. J., Vazquez, L. E., Howell, G. R., Christopherson, K. S., Nouri, N., et al. (2007). The classical complement cascade mediates CNS synapse elimination. *Cell* 131, 1164–1178. doi: 10.1016/j.cell.2007.10.036

Stoilov, P., Castren, E., and Stamm, S. (2002). Analysis of the human TrkB gene genomic organization reveals novel TrkB isoforms, unusual gene length, and splicing mechanism. *Biochem. Biophys. Res. Commun.* 290, 1054–1065. doi: 10.1006/bbrc.2001.6301

Tao, X., Finkbeiner, S., Arnold, D. B., Shaywitz, A. J., and Greenberg, M. E. (1998). Ca2+ influx regulates BDNF transcription by a CREB family transcription factor-dependent mechanism. *Neuron* 20, 709–726. doi: 10.1016/s0896-6273(00)81010-7

Tebano, M. T., Martire, A., Chiodi, V., Ferrante, A., and Popoli, P. (2010). Role of adenosine A(2A) receptors in modulating synaptic functions and brain levels of BDNF: a possible key mechanism in the pathophysiology of Huntington's disease. *ScientificWorldJournal* 10, 1768–1782. doi: 10.1100/tsw.2010.164

Tebano, M. T., Martire, A., Potenza, R. L., Gro, C., Pepponi, R., Armida, M., et al. (2008). Adenosine A(2A) receptors are required for normal BDNF levels and BDNF-induced potentiation of synaptic transmission in the mouse hippocampus. *J. Neurochem.* 104, 279–286.

Tejeda, G. S., and Diaz-Guerra, M. (2017). Integral characterization of defective BDNF/TrkB signalling in neurological and psychiatric disorders leads the way to new therapies. *Int. J. Mol. Sci.* 18, 268. doi: 10.3390/ijms18020268

Teng, H. K., Teng, K. K., Lee, R., Wright, S., Tevar, S., Almeida, R. D., et al. (2005). ProBDNF induces neuronal apoptosis via activation of a receptor complex of p75NTR and sortilin. *J. Neurosci.* 25, 5455–5463. doi: 10.1523/jneurosci.5123-04.2005

The BDNF Study Group Phase III, (1999). A controlled trial of recombinant methionyl human BDNF in ALS: the BDNF study group phase III. *Neurology* 52, 1427–1433.

Tongiorgi, E. (2008). Activity-dependent expression of brain-derived neurotrophic factor in dendrites: facts and open questions. *Neurosci. Res.* 61, 335–346. doi: 10.1016/j.neures.2008.04.013

Trang, T., Beggs, S., and Salter, M. W. (2011). Brain-derived neurotrophic factor from microglia: a molecular substrate for neuropathic pain. *Neuron Glia Biol.* 7, 99–108. doi: 10.1017/S1740925X12000087

Tsai, T., Klausmeyer, A., Conrad, R., Gottschling, C., Leo, M., Faissner, A., et al. (2013). 7,8-Dihydroxyflavone leads to survival of cultured embryonic motoneurons by activating intracellular signaling pathways. *Mol. Cell Neurosci.* 56, 18–28. doi: 10.1016/j.mcn.2013.02.007

Tucker, K., and Fadool, D. A. (2002). Neurotrophin modulation of voltage-gated potassium channels in rat through TrkB receptors is time and sensory experience dependent. *J. Physiol.* 542, 413–429. doi: 10.1113/jphysiol.2002.017376

Turner, M. R., Hardiman, O., Benatar, M., Brooks, B. R., Chio, A., De Carvalho, M., et al. (2013). Controversies and priorities in amyotrophic lateral sclerosis. *Lancet Neurol.* 12, 310–322. doi: 10.1016/S1474-4422(13)70036-X

Turrigiano, G. (2012). Homeostatic synaptic plasticity: local and global mechanisms for stabilizing neuronal function. *Cold Spring Harb. Perspect. Biol.* 4:a005736. doi: 10.1101/cshperspect.a005736

Tyler, W. J., and Pozzo-Miller, L. D. (2001). BDNF enhances quantal neurotransmitter release and increases the number of docked vesicles at the active zones of hippocampal excitatory synapses. *J. Neurosci.* 21, 4249–4258. doi: 10.1523/jneurosci.21-12-04249.2001

Van Den Bosch, L., Van Damme, P., Bogaert, E., and Robberecht, W. (2006). The role of excitotoxicity in the pathogenesis of amyotrophic lateral sclerosis. *Biochim. Biophys. Acta* 1762, 1068–1082.

van Zundert, B., Peuscher, M. H., Hynynen, M., Chen, A., Neve, R. L., Brown, R. H., et al. (2008). Neonatal neuronal circuitry shows hyperexcitable disturbance in a mouse model of the adult-onset neurodegenerative disease amyotrophic lateral sclerosis. *J. Neurosci.* 28, 10864–10874. doi: 10.1523/JNEUROSCI.1340-08.2008

Vidaurre, O. G., Gascon, S., Deogracias, R., Sobrado, M., Cuadrado, E., Montaner, J., et al. (2012). Imbalance of neurotrophin receptor isoforms TrkB-FL/TrkB-T1 induces neuronal death in excitotoxicity. *Cell Death Dis.* 3:e256. doi: 10.1038/cddis.2011.143

Vilar, M., and Mira, H. (2016). Regulation of neurogenesis by neurotrophins during adulthood: expected and unexpected roles. *Front. Neurosci.* 10:26. doi: 10.3389/fnins.2016.00026

Wheaton, M. W., Salamone, A. R., Mosnik, D. M., Mcdonald, R. O., Appel, S. H., Schmolck, H. I., et al. (2007). Cognitive impairment in familial ALS. *Neurology* 69, 1411–1417.

Yacoubian, T. A., and Lo, D. C. (2000). Truncated and full-length TrkB receptors regulate distinct modes of dendritic growth. *Nat. Neurosci.* 3, 342–349. doi: 10.1038/73911

Yamashita, N., and Kuruvilla, R. (2016). Neurotrophin signaling endosomes: biogenesis, regulation, and functions. *Curr. Opin. Neurobiol.* 39, 139–145. doi: 10.1016/j.conb.2016.06.004

Yanpallewar, S. U., Barrick, C. A., Buckley, H., Becker, J., and Tessarollo, L. (2012). Deletion of the BDNF truncated receptor TrkB.*T1* delays disease onset in a mouse model of amyotrophic lateral sclerosis. *PLoS One* 7:e39946. doi: 10.1371/journal.pone.0039946

Zhai, J., Zhou, W., Li, J., Hayworth, C. R., Zhang, L., Misawa, H., et al. (2011). The in vivo contribution of motor neuron TrkB receptors to mutant SOD1 motor neuron disease. *Hum. Mol. Genet.* 20, 4116–4131. doi: 10.1093/hmg/ddr335

Zhang, W., Liu, L. Y., and Xu, T. L. (2008). Reduced potassium-chloride co-transporter expression in spinal cord dorsal horn neurons contributes to inflammatory pain hypersensitivity in rats. *Neuroscience* 152, 502–510. doi: 10.1016/j.neuroscience.2007.12.037

Zheng, F., Zhou, X., Luo, Y., Xiao, H., Wayman, G., and Wang, H. (2011). Regulation of brain-derived neurotrophic factor exon IV transcription through calcium responsive elements in cortical neurons. *PLoS One* 6:e28441. doi: 10.1371/journal.pone.0028441

Conflict of Interest Statement: The authors declare that the research was conducted in the absence of any commercial or financial relationships that could be construed as a potential conflict of interest.

frontiers in Molecular Neuroscience

REVIEW
published: 04 October 2019
doi: 10.3389/fnmol.2019.00240

Role of Exosomes in Central Nervous System Diseases

Wanying Liu[1,2,3], Xiaodan Bai[1,2,3], Ao Zhang[4], Juanjuan Huang[1,2,3], Shixin Xu[1,2]* and Junping Zhang[1]**

[1] First Teaching Hospital of Tianjin University of Traditional Chinese Medicine, Tianjin, China, [2] Tianjin Key Laboratory of Translational Research of TCM Prescription and Syndrome, Tianjin, China, [3] Tianjin University of Traditional Chinese Medicine, Tianjin, China, [4] Epidemiology, College of Global Public Health, New York University, New York, NY, United States

There are many types of intercellular communication, and extracellular vesicles are one of the important forms of this. They are released by a variety of cell types, are heterogeneous, and can roughly be divided into microvesicles and exosomes according to their occurrence and function. Of course, exosomes do not just play a role in cell-to-cell communication. In the nervous system, exosomes can participate in intercellular communication, maintain the myelin sheath, and eliminate waste. Similarly, exosomes in the brain can play a role in central nervous system diseases, such as stroke, Alzheimer's disease (AD), Parkinson's disease (PD), prion disease, and traumatic encephalopathy (CTE), with both positive and negative effects (such as the transfer of misfolded proteins). Exosomes contain a variety of key bioactive substances and can therefore be considered as a snapshot of the intracellular environment. Studies have shown that exosomes from the central nervous system can be found in cerebrospinal fluid and peripheral body fluids, and that their contents will change with disease occurrence. Because exosomes can penetrate the blood brain barrier (BBB) and are highly stable in peripheral circulation, they can protect disease-related molecules well and therefore, using exosomes as a biomarker of central nervous system diseases is an attractive prospect as they can be used to monitor disease development and enable early diagnosis and treatment optimization. In this review, we discuss the current state of knowledge of exosomes, and introduce their pathophysiological roles in different diseases of the central nervous system as well as their roles and applications as a viable pathological biomarker.

Keywords: exosomes, central nervous system diseases, biomarkers, intercellular communication, stroke

OPEN ACCESS

Edited by:
Marie-Eve Tremblay, Laval University, Canada

Reviewed by:
Massimo Aureli, University of Milan, Italy
Maria Xilouri, Biomedical Research Foundation of the Academy of Athens, Greece

****Correspondence:***
Wanying Liu
L1527044942@163.com
Shixin Xu
shixinxu1973@outlook.com
Junping Zhang
tjzhtcm@163.com

Received: *02 June 2019*
Accepted: *19 September 2019*
Published: *04 October 2019*

Citation:
Liu W, Bai X, Zhang A, Huang J, Xu S and Zhang J (2019) Role of Exosomes in Central Nervous System Diseases. Front. Mol. Neurosci. 12:240. doi: 10.3389/fnmol.2019.00240

INTRODUCTION

In the early 1980s, the term "exosome" was used to describe vesicles released by various types of cultured cells with a diameter of 40 to 1000 nm. Over the next few years, the term was refined to describe vesicles originating from the endosome with a diameter between 30 and 100 nm (Luarte et al., 2016; Malm et al., 2016; Yuyama and Igarashi, 2016; Zagrean et al., 2018).

According to most of the current literature, vesicular bodies with a bilayer membrane structure which are detached from the cell membrane or secreted by the cells, are called extracellular vesicles (EV). EVs are highly heterologous, they can come from several cell types, are influenced by their microenvironment,and can be detected in various human secretions. All extracellular vesicles are formed by a shared mechanism and are thought to have a common role in cell-to-cell communication by promoting cellular exchange of proteins, DNA, and RNA (Malm et al., 2016; Osier et al., 2018).

Although exosomes are a subtype of extracellular vesicles (EVs) defined specifically by their diameter (Malm et al., 2016; Yuyama and Igarashi, 2016; Mrowczynski et al., 2019), some published studies use the term EVs to refer just to exosomes. EVs refers to the larger group to which exosomes belong and also includes the apoptotic body (measuring 0.5–5 μm, formed by apoptosis), and microvesicles (measuring 0.05–1 μm, created by part budding), while exosomes originate from endosomes (Tian et al., 2018). Early endosomes will be converted to late endosomes when their protein composition changes, upon maturation, intraluminal vesicles (ILVs) begin to constitute in the lumen of the vesicles via enfoldment of the limiting membrane. Then the ILVs sequester cytoplasmic molecules leading to their accumulation within the late endosome, causing the formation of multivesicular bodies (MVB). MVBs can undergo fusion with lysosomes and with the cellular plasma membrane and then release their contents into the extracellular space (**Figure 1**). Exosomes produced by various cell types are found in bodily fluids, such as blood, cerebrospinal fluid (CSF), saliva, and urine (Malm et al., 2016; Yuyama and Igarashi, 2016; Cesselli et al., 2018; Osier et al., 2018) and contain proteins, lipids, miRNAs, RNA and DNA. It is precisely because of the transfer of these contents that exosomes can affect intercellular communication under various physiological and pathological conditions (Yuyama and Igarashi, 2016). The most commonly used method to extract exosomes is ultracentrifugation (UC) and storage of them for more than 90 days should be at −80°C (Hong et al., 2018).

The theory that EV can transfer RNA between cells was proposed by the team of Ratajczak et al. (2006) (Clemmens and Lambert, 2018; Stahl and Raposo, 2018). All of these studies have made advances in EV-related research and highlighted the important role of EVs in cell biology, physiology [including stem cell maintenance (Samuelson and Vidal-Puig, 2018)], cancer, neuropathology (Osier et al., 2018; Stahl and Raposo, 2018), stroke, and cardiovascular disease (Stahl and Raposo, 2018). Studies have shown that drugs and comorbidities can affect the mechanisms of biogenesis and release of MVBs and exosomes, thus affecting this mode of intercellular communication. EVs can also play an important role in communication between, and within, key metabolic organs (Clemmens and Lambert, 2018; Samuelson and Vidal-Puig, 2018). Their role in neurological diseases is also particularly prominent, extracellular vesicles (i.e., exosomes in the broad sense) are secreted by several cells and present in the CSF, they are involved in signal transduction not only among neural cells but also among hematopoietic cells and in the peripheral nervous system. The main cause of neurodegenerative diseases is the spread of EVs and the relationship between neurophysiology and neurological disorders, centered on EV-mediated communication between nerves and glial cells, is a critical area of discussion and research. The major causative proteins of various neurodegenerative

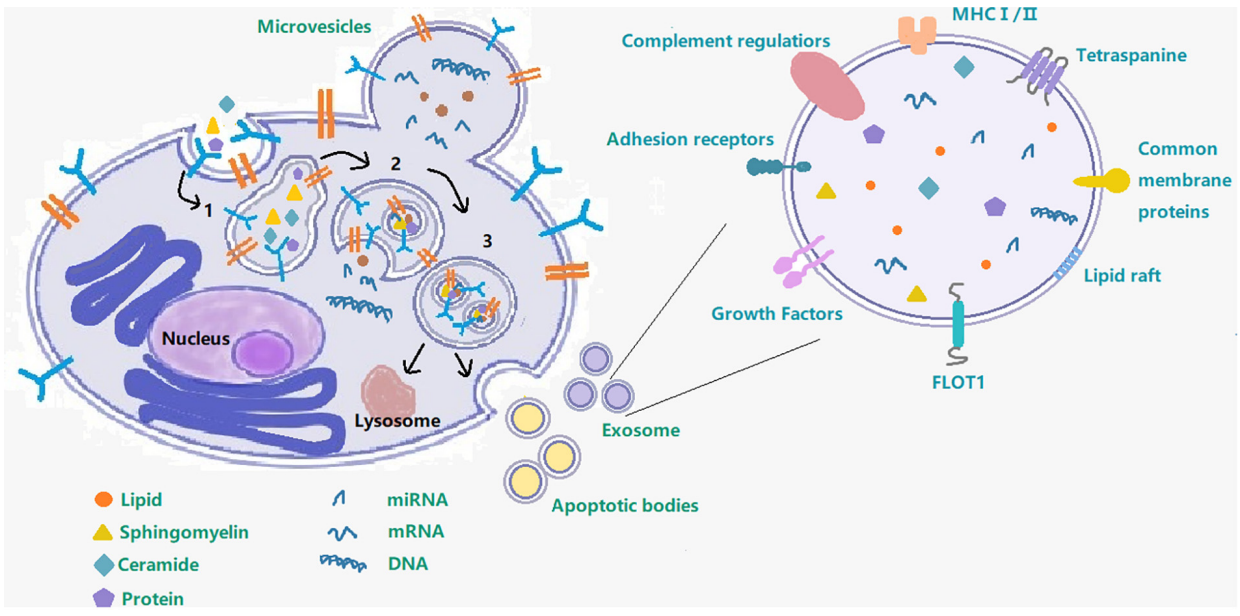

FIGURE 1 | Exosome– cargo, surface markers and endosomal pathway. This figure shows the process of exosome production and secretion. 1 Early endosome; 2 Late endosome; 3 Multivesicular body; following on, the multivesicular body will either fuse with the cell membrane to secrete exosomes out of the cell or fuse with lysosome.

diseases are encapsulated in EVs derived from CSF and there also appears to be a relationship between them (Kawahara and Hanayama, 2018). The characteristics of exosomes and their physiological and pathological effects make them both an ideal biomarker, and a potential drug delivery vehicle (including use as vectors for targeting gene therapy to specific cells (Clemmens and Lambert, 2018; Leone et al., 2018; Stahl and Raposo, 2018).

EXOSOMES IN STROKE

Stroke is a complex and life-threatening condition (Mirzaei et al., 2018), and one of the leading causes of death and disability worldwide with high mortality rates in both developing and developed countries. There is ample evidence that both genetic and environmental factors are related to the pathophysiology of stroke (Mirzaei et al., 2018). There are two stroke subtypes: ischemic and hemorrhagic, of which ischemic stroke accounts for about 87% of all strokes (Osier et al., 2018). Ischemic stroke is mainly caused by a thromboembolic occlusion or atherosclerosis of a major artery that supplies the brain, leading to cerebral ischemia and hypoxia (Malm et al., 2016; Zhang and Chopp, 2016). Cerebral hemorrhage is the cause of hemorrhagic stroke, which is usually caused by a weakened arterial wall (i.e., an aneurysm). The ischemic stroke lesion area can be divided into two main areas: the infarct core and the penumbra area (Hong et al., 2018). In the treatment of ischemic stroke, the main goal is to restore blood flow as soon as possible after the onset of symptoms. The two main methods for recanalization are intravenous thrombolysis [tissue plasminogen activator has become the only treatment for stroke patients within 4.5 h of onset (Zhang and Chopp, 2016)] and endovascular intracranial thrombectomy, which can extend patient life by rapidly reanalys of occluded blood vessels and re-establishing tissue perfusion within 12 h of onset (Zhang and Chopp, 2016). The window for treatment with these two methods is very narrow (Hong et al., 2018), and since a series of pathological events usually occurs before a stroke, we therefore need to find an appropriate method of stroke management. One of the main problems here is to identify effective biomarkers for diagnosis and monitoring the treatment of stroke patients (Mirzaei et al., 2018).

Biomarkers related to the treatment of diseases, including molecules, proteins, and RNA, have been obtained from a range of bodily fluids (Lausted et al., 2014). These biomarkers have some disadvantages, their low abundance and poor heterogeneity (i.e., it's not clear which groups these molecules come from), and exosomes have therefore gained more attention since they were discovered, in large part because of their heterogeneity and role in intercellular communication. Stroke recovery is carefully planned by a series of highly interactive processes involving neural stem cells and neurovascular units (Zhang and Chopp, 2016). Emerging data suggests that exosomes play an important role in these processes and mechanisms. After a stroke, exosomes can be synthesized and released from brain cells, and can be detected in peripheral blood or CSF by passing through the BBB. In addition to this, exosomes are also released into the bloodstream from blood cells and endothelial cells in response to stroke (Otero-Ortega et al., 2018). They are involved in increasing long-term neuroprotection after stroke, promoting nerve regeneration, enhancing neurological recovery, and modulating peripheral immune responses. At the same time, they also enhance angiogenesis, neurogenesis, and the remodeling of axon dendrites. The exosomes secreted by brain endothelial cells can also actively participate in brain reconstruction by communicating with brain cells (including neurons and glia) and distal cells in other organs during stroke recovery (Zhang and Chopp, 2016; **Figure 2**). In addition to beneficial effects, these exosomes can also have adverse effects on distal organs. The release of exosomes from damaged central nervous cells after stroke into the peripheral circulation will affect the spleen, increase the production of circulating pro-inflammatory cytokines, and recruit and activate T and B lymphocytes to regulate peripheral immune inflammatory response. These changes will also affect the heart, kidney, and intestine (Seifert and Offner, 2018; Wang et al., 2019). In the heart, the secretion of inflammatory cytokines by damaged brain cells stimulates the hypothalamus and increases the release of catecholamine, thereby increasing the risk of myocardial ischemia and tumorigenesis (Shoemaker and Goswami, 2015; Venkat et al., 2018). In kidneys, inflammatory mediators induced and secreted after stroke can increase the permeability of renal endothelial cells and make immune cells and inflammatory mediators enter, resulting in renal dysfunction (Wang et al., 2014; Li et al., 2015; Makin et al., 2015). In the intestinal tract, intestinal dysfunction after stroke is characterized by a decrease in the number of beneficial cells in the intestine and an increase in the opportunistic bacteria count. Abnormal bacterial metabolites can also affect the immune response which in turn may adversely affect recovery from stroke (Winek et al., 2016; Arya and Hu, 2018; Zhao et al., 2018; **Table 1**).

There are many kinds of exosomes and multiple reports about the proteins they contain, such as cystatin C and CD14, which are involved in the progress of brain atrophy in patients with vascular diseases and whose levels are also associated with the risk of vascular events in patients with coronary artery disease (Kanhai et al., 2014), and integrin alpha-IIb, talin-1 and coagulation cascade proteins which are also associated with vascular events in patients (Datta et al., 2014). Despite the variety and nature of goods contained in exosomes, studies have shown that the main role of the exosome lies in the transmission of related RNA signals, and exosomal miRNAs will vary between different periods of a stroke. MiRNA and RNA networks play major roles in the process of secretion-mediated brain repair and are key mediators in the pathogenesis and pathology of ischemic stroke. One example of this was the study by Collino et al. (2015) whose results showed that when exosomes were released by cells depleted of Drosha protein (producing a total downregulation of miRNAs) the therapeutic effect of the secretion on acute kidney injury was abolished (Luarte et al., 2016). MiRNA has therefore become the most reliable biomarker for the diagnosis, treatment, and prognosis of ischemic stroke. A lot of research on the miRNA and protein content of exosome has been carried out, including Kerr N's team, who used the multi-analyte automated microfluidic immunoassay platform Plex Assay to

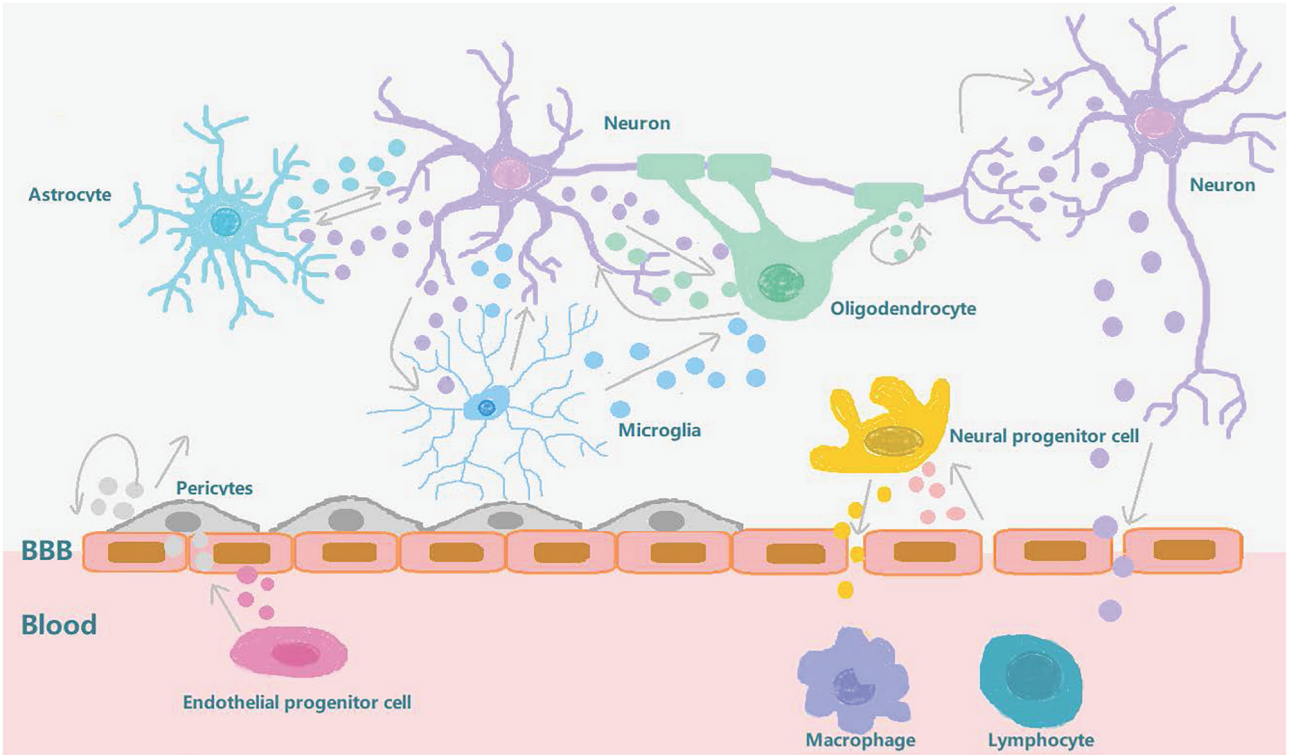

FIGURE 2 | Exosome involvement in brain reconstruction after stroke. After a stroke, the blood-brain barrier is destroyed and the pericytes interact with brain endothelial cells to promote angiogenesis and repair the BBB. The exosomes secreted by the pericytes can also provide nutrition and promote neurogenesis. The exosomes secreted by circulating endothelial progenitor cells can also act on cerebral endothelial cells to promote angiogenesis. Neurons, oligodendrocytes, and astrocytes interact to regulate synaptic plasticity. Neurons interact with microglia to regulate brain immune inflammation, and neurons and neural progenitor cells can secrete exosomes to regulate peripheral immunity after being stimulated by external substances which pass through the BBB. After stroke, brain endothelial cells secrete exosomes that stimulate neural progenitor cells to differentiate into oligodendrocytes to participate in myelination. In conclusion, exosomes can increase long-term neuroprotective effects after stroke, regulate peripheral immune response, and participate in brain reconstruction events such as enhanced angiogenesis and axonal dendritic remodeling.

detect the levels of caspase-1 inflammatory body proteins in serum and serum-derived EVs from stroke patients. This team has previously shown that inflammatory body proteins are a potential biomarker of CNS damage and also proved that, in the case of brain injury, EV can release inflammatory body proteins into the peripheral circulation. They also located caspase recruitment domains in apoptosis-related proteins (ASC). This can be used as a potential biomarker to help analyze the role of inflammatory bodies in the inflammatory responses following cerebral ischemia (Kerr et al., 2018).

Fan Chen et al. used *in vitro* and *in vivo* methods to study stroke. Wistar rats were exposed to a focal cerebral ischemia model using transient or permanent intraluminal occlusion to the middle cerebral artery (Osier et al., 2018). In *in vitro* culture, compared to DMEM normal controls, miR-126 levels in exosomes from brain endothelial cell were significantly reduced after oxygen-glucose deprivation. In the rat model, compared to levels before ischemic onset, both transient and permanent ischemia samples showed a rapid and significant reduction in exosomal miR-126 at 3 h, and by 24 h, miR-126 levels of exosomes mostly renormalized close to pre-ischemia baseline levels. Serum miR-126 levels were significantly reduced at 3 h of permanent ischemia but did not change significantly after transient ischemia or 24 h. The results showed that the exosomal miR-126 obtained from peripheral blood was more sensitive to the effects of cerebral ischemia and responded to both mild and severe ischemic attacks. However, total serum miR-126 may be a more specific indicator of ischemic severity (Chen et al., 2015; Osier et al., 2018). In another study, the release of miR-124 from brain tissue was considered to play a key role in stroke and there is further evidence that the expression of miR-124 in the central nervous system is 100 times higher than that in other organs and can thus be used as a biomarker (Mishima et al., 2007; Mirzaei et al., 2018). In a study by Wang W's team, 143 IS patients and 24 non-stroke patients were divided into four phases: hyperacute (HIS), acute (AIS), subacute (SIS), and recovery (RIS), and the expression of miR-30a-5p and miR-21-5p in plasma-derived exosomes in the different stages of ischemic stroke (IS) was examined. The data elucidated that the combination of miR-30a-5p and miR-21-5p can be used to distinguish between HIS, SIS, and RIS, and in the diagnosis of IS. It was hoped that miR-30a-5p might be a favorable biomarker for the diagnosis of HIS, providing a possibility for early clinical diagnosis (Wang W. et al., 2018) although, as Yang et al. pointed out, there are many circulating

TABLE 1 | Biomarkers in exosomes associated with stroke.

Source	Contents	Mechanism	Clinical application	References
Peripheral blood	cystatin C, CD14, alpha-lib and talin-1	Vascular event	Early diagnosis	Datta et al., 2014; Kanhai et al., 2014
Serum	caspase-1	Inflammation	Severity judgment	Kerr et al., 2018
Serum	miR-126	Angiogenesis	Severity judgment	Chen et al., 2015; Osier et al., 2018
Plasma	miR-124	Neurogenesis	Early diagnosis	Mishima et al., 2007; Mirzaei et al., 2018
Plasma	miR-30a-5p and miR-21-5p	Inflammation	Early diagnosis, severity judgment and prognosis	Hong et al., 2018; Jiang et al., 2018

caspase-1, inflammatory protein.

miRNAs that can be used as diagnostic markers for stroke, and for diagnosis. The results indicated that circulating miR-153, miR-128b, and miR-107, are up-regulated in the stroke group, and so can be used as important biomarkers for diagnosis (Yang et al., 2016). In addition to studies of miRNAs, current studies have expounded the role of other types of ncRNAs, including circular RNAs and long non-coding RNAs, in cerebral hemorrhage (ICH) strokes. These results show that, in the clinic, ncRNAs can be used in the predictive diagnosis of the extent of ICH-induced damage as an optional biomarker (Li et al., 2019).

There are a multiple reports and studies proving that RNA, found in the exosome, has the potential to become a powerful biomarker for stroke diagnosis, treatment, and prognosis. The value of the exosome as a biomarker in the treatment of stroke has also been determined and future research will need to identify specific sources of RNA in circulating and tissue secreted exosomes.

NEURODEGENERATIVE DISEASES

Neurodegenerative diseases are one of the major causes of death and disability, and one of the greatest burdens on the health care system (Luarte et al., 2016). Like cerebral apoplexy, exosomes may represent a promising prognostic biomarker and a therapeutic approach to traumatic brain injury and neurodegenerative diseases. Multiple studies have shown that exosomes can initiate and participate in the regulation of neuroinflammation, improve neurogenesis and neurogenic physiological location, and have potential significance for the treatment of certain neurological diseases (Yang Y. et al., 2017; Osier et al., 2018). These neurodegenerative diseases have similar clinical manifestations, but a common feature of a large number of these diseases is the accumulation of insoluble proteins (both extracellular and intracellular) and, as such, these diseases are also called cerebral proteinopathies (Hartmann et al., 2017). For example, AD is characterized by the aggregation of beta-amyloid protein and microtubule-associated protein Tau; PD by the accumulation of neuronal terminal protein alpha-synuclein; ALS by the accumulation of phosphorylated TDP43 (a transcription inhibitor) and superoxide dismutase 1 (SOD1), and Huntington's disease by the accumulation of mutant Huntington's protein (mHTT; Luarte et al., 2016).

These neurodegenerative diseases, which present different entities and pathogenesis, have many common features besides the aggregation of erroneously folded proteins. These include; overload of protein clearance pathways, impaired protein homeostasis, and dysfunction or loss of specific neuron populations (Kanata et al., 2018). The neurological dysfunction caused by progressive irreversible degeneration of neurons and synapses is a marker of this kind of disease (Hartmann et al., 2017). It has been shown that many types of cells in the CNS secrete exosomes, including oligodendrocytes, neurons, and astrocytes. Exosomes, as potential carriers, can play a role in the pathogenesis of neurodegenerative diseases and can also help transmission (Wu et al., 2017; **Table 2**). When released into circulation, they also become a convenient and efficient peripheral non-invasive biomarker for the prediction and diagnosis of various neurodegenerative diseases (Hartmann et al., 2017).

EXOSOMES IN ALZHEIMER'S DISEASE

Alzheimer's disease (AD) is the most common neurodegenerative disease, mainly occurring in the form of dementia, which is characterized by severe impairment of cognitive ability, mental state, and ability to carry out activities of daily life. The main pathological markers of AD are the accumulation of Aβ plaque and neurofibrillary tangles (NFT) formed by over-phosphorylation of tau protein. The pathological characteristics of AD can be divided into two types: amyloid plaques and NFTs. The accumulation of Aβ in oligomers (which can lead to amyloid plaque formation) occurs at the earliest stage of disease development (Reza-Zaldivar et al., 2018). Data has shown that about 5.5 million Americans are currently diagnosed with Alzheimer's disease, and the number is expected to rise to 13.8 million by 2050 (DeLeo and Ikezu, 2018). There is also growing evidence that exosomes are associated with the transmission of Aβ and Tau proteins, but their specific role in the process of Alzheimer's disease remains controversial. This is because some studies show that exosome transfer of these two proteins can participate in the process of neuronal microtubule decomposition, thus affecting axonal transport, resulting in cell death and neuron loss, but in other studies, exosomes seem to have the ability to reduce brain amyloid beta protein by being ingested by microglia. They can also transmit neuroprotective substances between cells (Malm et al., 2016; Xiao et al., 2017).

Experiments have shown that there are disease-related proteins (Pluta and Ulamek-Koziol, 2019) in exosomes isolated from plasma or CSF samples of patients with AD, which show that exosomes may be used as AD biomarkers. Goetz et al. and Fiandaca et al. found that neuronal exosomes isolated from the plasma of AD patients contained autolysosome proteins, and

TABLE 2 | Biomarkers in exosomes associated with neurodegenerative disease.

Name of disease	Source	Contents	Mechanism	Clinical application	References
Alzheimer's disease	Plasma and CSF	Aβ and NFT	Neuronal damage	Early diagnosis	Wang et al., 2017; Xiao et al., 2017
Alzheimer's disease	Plasma	REST, HSF-1, Lamp 1 and IRS	Neuronal damage	Early diagnosis	DeLeo and Ikezu, 2018; Pluta and Ulamek-Koziol, 2019
Alzheimer's disease	Serum	miR-135a, miR-193b and miR-384	Neuronal damage	Early diagnosis	Goetzl et al., 2015b
Parkinson's disease	CSF	α - SYN, DJ-1 miR-1, miR-485-5p, miR-153, miR-409-	Neuronal damage	Early diagnosis	Joshi et al., 2015; Li et al., 2019
Parkinson's disease	CSF	3p, miR-433, miR-136-3p, let-7g-3p, miR-19b-3p, miR-10a-5p, miR-132-5p, miR-370 and miR-873-3p	Neuronal damage	Early diagnosis	Yang J. et al., 2017
Prion Diseases	Plasma	PrPSc	Neuronal damage	Early diagnosis	Hartmann et al., 2017
Prion Diseases	Serum	miR-142-3p, miR-143-3p, miR-145a-5p, miR-451a, miR-146a-5p, miR-150-5p, miR-320, miR-let-7b, miR-141-3p, miR-429-3p and miR- 200 family	Neuronal damage and inflammation	Early diagnosis and severity judgment	Reza-Zaldivar et al., 2018; Shah et al., 2018
Amyotrophic lateral sclerosis	Peripheral blood and CSF	TDP-43	Neuronal damage and inflammation	Early diagnosis	Iguchi et al., 2016
Amyotrophic lateral sclerosis	Plasma	miR-183-5p, miR-9-5p, miR-193a-5p and miR- 15a-5p	Neuronal damage	Early diagnosis	Saucier et al., 2019
Huntington's disease	Plasma	mHtt	Neuronal damage	Early diagnosis and severity judgment	Wang et al., 2017; Denis et al., 2018
Huntington's disease	Plasma	miR-877-5p, miR-223-3p, miR-30d-5p, miR-128, miR-22-5p, miR-223-5p, miR-222-3p, miR-338-3p, miR-130b-3p, miR-628-3p, miR-361-5p, miR-425-5p	Neuronal damage	Early diagnosis	Kumar et al., 2017

CSF, cerebrospinal fluid; Aβ plaque, aggregation of beta-amyloid protein; NFT, neurofibrillary tangles; α-SYN, alpha-synuclein; DJ-1, oxidative stress sensor; PrPSc, misfolded prion protein; TDP-43, a protein that helps regulate gene expression; mHtt, produces mutant Huntington protein.

that LAMP1 levels had changed. Changes in P-tau and Aβ levels were also detected in exosomes isolated from patients' plasma samples, which proved that they could be used as predictors of AD long before the onset of AD (Malm et al., 2016). Goetzl et al. (2015a,b) and Kapogiannis et al. (2015) also found that there were some neurogenic exosome-related proteins in the plasma of AD patients, including repressor element 1-silencing transcription factor (REST), heat-shock factor 1 (HSF-1), Lamp 1 and phosphorylated type 1 insulin receptor substrate (IRS), and that their levels would change within 10 years prior to the formal diagnosis of AD. They are all therefore likely to be reliable biomarkers for predicting and diagnosing AD. Yang et al. (2018) compared the expression levels of miR-135a, miR-193b, and -384 in serum-derived exosomes of patients with Alzheimer's dementia (DAT), Parkinson's disease dementia (PDD), mild cognitive impairment (MCI) and vascular dementia (VaD). Their results showed that compared with the other two small RNAs, microRNA-384 was best able to differentiate AD, PDD and VaD. For the early diagnosis of AD, the combination of mir-384, mir-193b, and mir-135a seems to be more useful (Yang et al., 2018). These experiments not only prove the feasibility of the exosome as a biomarker for the early diagnosis of AD, but also prove that the exosome can provide a new direction for disease identification and prevention.

It seems that exosomes secreted by different brain tissue cells will play different roles in the development and change of AD (Joshi et al., 2015). For soluble Aβ42 species (monomers formed after cutting of amyloid precursors participate in the formation of amyloid plaques), microglia can internalize and degrade them, but they can also secrete exosomes that lead to the aggregation of extracellular soluble Aβ42 species, and neuronal astrocytes, or their exosomes, also promote the aggregation of soluble Aβ42. However, exosomes released by neurons can enhance the ability of microglia to scavenge Aβ42. These findings may be a manifestation of the postsynaptic diffusion mechanism of Aβ in AD (Dinkins et al., 2014; Joshi et al., 2014, 2015). This proves the complexity of the role of exosomes in AD and thus it is essential to further clarify the interaction between different EV populations and different forms of Aβ, and to understand the influence of different EV populations on the diffusion of Aβ assembly between cells to better provide accurate and effective markers for AD and improve the quality of life of patients.

EXOSOMES IN PARKINSON'S DISEASE

Parkinson's disease (PD) is the second most common neurodegenerative disease and the most common motor disorder of the central nervous system (CNS) and its incidence increases with aging (Leggio et al., 2017; Zagrean et al., 2018). The main clinical manifestations are; static tremor, muscle stiffness, slow movement, postural instability, and other symptoms caused by dyskinesia. These symptoms are caused by the imbalance between excitatory (acetylcholine) neurotransmitters and inhibitory (DA) neurotransmitters in the substantia nigra of PD patients (Wu et al., 2017). These motor symptoms do not occur immediately after imbalance. The first motor symptoms are observed only when the loss of DAergic neurons in SNpc reaches almost 70% and at least 80% of that DA in the striatum. In addition, PD patients also show a variety of non-motor symptoms, including dementia, and depression (Leggio et al., 2017).

It has been shown that misfolded and aggregated alpha-synuclein (α-syn) is the main component of Lewy bodies and axons in inherited and sporadic forms of PD (Leggio et al., 2017; Tofaris, 2017; Wu et al., 2017). The release of exosomes is closely related to intracellular protein transport along the endosomal-lysosomal pathway, so their biological functions may be related to PD. The cause of PD is also reflected at the molecular level, defective protein transport to endosomes and lysosomes has become a potentially unifying cellular pathway in the pathogenesis of sporadic PD. Because the release of exosomes is closely related to intracellular protein transport along the endosomal-lysosomal pathway, their biology may be relevant to PD (Zagrean et al., 2018).

Studies have shown that exosomes transmit toxic α-syn between cells and induce apoptosis, which is involved in the pathological development of PD. It has also been reported that exosomes have potential neuroprotective effects in PD (Wu et al., 2017). In addition to intercellular communication, exosomes also have the ability to eliminate misfolded proteins which hinder the formation of neural stem cells (Zagrean et al., 2018). Brain neurons and glial cells can also eliminate and reduce harmful metabolites and proteins (e.g., α-syn) in cells by exosome extravasation (Ohmichi et al., 2018). Some studies have shown that exosomes obtained from PD patients can attenuate the neuronal stress response, for example, Tomlinson PR and colleagues performed proteomic analysis of microvesicle preparations from PD patients with inherited and sporadic forms, and added microvesicles to cortical neurons of primary rats deprived of nutrition to observe their biological effects (Tomlinson et al., 2015).

At present, the diagnosis of PD still mainly depends on assessing motor symptoms according to the British Brain Bank Standard and the patient's response to dopaminergic drugs (Ohmichi et al., 2018). DAergic degeneration before the onset of PD symptoms lasts for about 8–17 years (Leggio et al., 2017), which means that there must be some compensatory mechanism in the early development of PD and therefore, searching for biomarkers of preclinical PD is key to treating and predicting the disease and differentiating it from other diseases with the same manifestations. Because oxidative stress and mitochondrial dysfunction influence the underlying mechanisms of misfolded α-syn aggregation (Picca et al., 2019), biomarkers such as DJ-1 (mitochondrial dysfunction-related) and α-syn have potential as clinical tools for early remission and accurate diagnosis of PD. However, for mitochondrial dysfunction, the main focus is on mitochondrial DNA (mtDNA) analysis with proinflammatory properties (West et al., 2015), as systemic inflammation and mitochondria in the CNS are not known under PD conditions. Whether the disorder is related (Picca et al., 2019). Since there are no defined ranges for α-syn levels in peripheral blood (Ohmichi et al., 2018) no reliable quantitative diagnostic tests for PD have been developed so far. As it is inconvenient to obtain invasive CSF or postmortem (brain tissue) samples to collect these biomarkers (Leggio et al., 2017), the development of specific, non-invasive biochemical markers for the disease is the logical direction to focus research on. Quantitative studies have been carried out on exosomes derived from brain cells in patients with PD to find the best biomarkers, these include neurone-, astrocyte-, and oligodendrocyte-derived exosomes (NDE, ADE, and ODE). One study showed that plasma NDE and ODE levels increased significantly in early stage PD patients and that ODE levels were positively correlated with the severity of the disease. This also demonstrated brain cells' ability to remove neurotoxic substances (Ohmichi et al., 2018).

With regard to using biomarkers for tracking the progress of PD, Yuki et al. performed protein profiling of plasma-derived exosomes from PD patients at Hoehn and Yahr (HY) stages II and III, and found that in HY stage III PD patients apolipoprotein A1 expression was significantly lower than in HY stage II PD patients. There was no significant difference in fibrinogen gamma chain expression between HY stage II and III PD patients. These results show that the plasma-derived exosome proteins; clusterin, complement C1r subcomponent, and apolipoprotein A1, and the fibrinogen gamma chain, are potential biomarker candidates for PD diagnosis, and exosomal apolipoprotein A1 can be used as a biomarker for tracking PD progression (Kitamura et al., 2018). The feasibility of using peripheral circulating exosomes as biomarkers has been further demonstrated. Recent studies have shown that brain insulin signaling can regulate neuronal survival through the mitogen-activated protein kinase (MAPK) and phosphoinositide 3-kinase-protein kinase B (Akt) downstream pathways, and plays a role in PD pathogenesis. It has also been shown that it is easier to assess time-dependent changes in PD by measuring insulin-signaling markers from brain-derived exosomes than neuroimaging and CSF studies (Athauda et al., 2019). Classical gene mutation is a cause of PD and gene regulation is a topic that attracts people's attention for study. There are abundant miRNAs in exosomes for diagnosis and treatment, such as miRNA - 124, - 7, - 126, - 155, and so on (Thome et al., 2016; Leggio et al., 2017; Yang J. et al., 2017; Titze-de-Almeida and Titze-de-Almeida, 2018). Gui et al. (2015) found 13 small RNAs in CSF-derived exosomes of PD patients with significant changes, including the KEGG pathway "Dopaminergic synapse," which was also significantly altered in PD patients with 9 miRNAs (miR-1, -153, -485-5p, -409-3p, -433, -136-3p, -19b-3p, -10a-5p and let-7g-3p) targeting 41 genes in the pathway map of Dopaminergic synapse and the KEGG pathway

"Cholinergic synapse" which was significantly enriched in PD patients with 11 miRNAs (miR-1, -153, -132-5p, -485-5p, -409-3p, -433, -370, -873-3p, -19b-3p, -10a-5p and let-7g-3p) targeting 40 genes in the Cholinergic synapse pathway. This was compared with the corresponding levels of miRNAs in AD patients, which proved the reliability of RNA molecules in the exosome as a biomarker and the robustness in distinguishing between PD and AD. These experiments prove that exosomes can be used to help develop new diagnostic and predictive tools.

At present, PD can't be cured, we can only alleviate the symptoms of patients and minimize the occurrence of dyskinesia. The pre-symptomatic stage of PD emphasizes the importance of early prediction and intervention of the disease (Wu et al., 2017) and it is clear that these experiments also reflect the potential of exosomes for use as biomarkers in AD.

EXOSOMES IN PRION DISEASES

Prion disease, also known as infectious spongiform encephalopathy (TSEs), is characterized by spongiform vacuolation and progressive loss of neuronal structure and function. It is a fatal neurodegenerative disease that occurs mainly in the central and peripheral nervous systems and can be transmitted in animals and humans. The existence of detectable misfolded prion protein (PrPSc) whose main structure is a beta-sheet conformation, is the main pathological feature of prion disease. It is produced by the misfolding of the normal prion protein (PrPC) which is mainly alpha-helical in structure.

PrPC can be highly expressed in exosomes (Hartmann et al., 2017) and disease-related forms of PrPC are also found in exosomes and can be ingested by immature cells. This indicates that exosomes carrying PrPSc can participate in the transmission of viruses between different tissues and promote the development of diseases. In addition, the exosome is also rich in cholesterol, sphingomyelin, and sphingomyelin GPI anchored proteins (which help PrPSc formation), which may also participate in protein sorting in the exosome. Studies have shown that injecting prion-infected exosomes into animals can successfully spread the disease (Cervenakova et al., 2016).

At present, the most well-known transmission routes of prions include cell-cell contact, tunnel nanotubes, and exosomes (Hartmann et al., 2017; Cheng et al., 2018; Heisler et al., 2018). Some studies have shown that PrPSc can come from different cell types, tissues and infection stages, resulting in different mechanisms or combinations of prion transmission, which is not fixed. In other words, there may be multiple prion transmission mechanisms (Guo et al., 2016).

Present research on the role of miRNAs in exosomes with infectious prions is not complete, however, in the late and clinical stages of prion infection, the up-regulation of miR-142-3p, miR-143-3p, miR-145a-5p, miR-451a, miR-146a-5p, miR-150-5p, miR-320 and miR-let-7b, as well as the down-regulation of miR-141-3p, miR-429-3p, all members of the miR-200 family and 182 other miRNA clusters, have all been demonstrated (Boese et al., 2016; Cheng et al., 2018; Shah et al., 2018). The involvement of miRNA in the regulation of complex gene networks may affect various mechanisms of prion disease development, but its key impact points and extent are still unclear.

MiRNAs are valuable as biomarkers of prion diseases, however, further high-throughput studies are needed to identify specific the miRNA(s) in bodily fluids which have potential as biomarkers for the diagnosis and treatment of prion diseases (Kanata et al., 2018). The up- or down-regulation of miRNA in prion-infected exosomes may also be altered in other neurodegenerative diseases, for example, miR-146a-5p, besides being down-regulated in prion diseases, can also be down-regulated in serum of patients with primary progression (PPMS) (Vistbakka et al., 2017), with PD (Wang et al., 2016), and in patients with AD.

Understanding the changes of PrPSc and other neurotoxic proteins *in vivo* and their relationship with exosome release, transport, and related miRNA will help us to manage prion-related diseases from multiple levels (Cheng et al., 2018).

EXOSOMES IN AMYOTROPHIC LATERAL SCLEROSIS

ALS is a serious neurological disease in which the cortex, brainstem, and spinal motor neurons are affected by prion-like misfolded proteins, e.g., superoxide dismutase-1 (SOD1) and TDP-43, resulting in neurodegeneration and is disease marked by protein dysfunction without RNA or DNA components (Lee et al., 2016; Maguire, 2017). Symptoms include weakness, muscle paralysis, atrophy, and eventually respiratory failure, leading to death. In addition to dysfunction of the motor system, 50% of ALS patients may also have mental illness (Maguire, 2017). The pathophysiology of ALS is complex and there is currently no definite analysis and explanation, nor effective therapy. Most experts believe that its influencing factors may include epigenetics, genetics, stress, poor diet, poor physical fitness, and various environmental factors (Maguire, 2017). Data show that about 5–10% of ALS patients are familial and we can observe important mutations in the SOD1, FUS, TARDBP, C9ORF72, and bone morphogenetic protein modifier genes, all of which increase the susceptibility for ALS, but it has been made clear that the SOD1 mutation is the main genetic factor of ALS (Bonafede et al., 2016; Sohrab et al., 2018). TDP-43 (a protein that helps regulate gene expression) is the main pathological feature of ALS and its level in brain tissue-derived exosomes of ALS patients increases. Central nervous system cells, such as motor neurons, are particularly sensitive to the dysfunction of TDP-43 and incorrect folding of TDP-43 also affects, to some extent, the function of mitochondria (Maguire, 2017).

It is known that exosomes are involved in the transmission of TDP-43 protein and Iguchi et al. believe that, although exosomes contribute to the transmission of TDP-43 proteinosis, they are also a key way to remove TDP-43 aggregates from the neurons and primary neurons of ALS patients. They inhibited the secretion of these exosomes by knocking out the GW4869 or RAB27A gene, which resulted in the aggregation of TDP-43

in the Neuro2a cells of TDP-43A315T transgenic mice. These results showed that the inhibition of exosomes aggravated the disease phenotype of TDP-43A315T mutant transgenic mice, and aggravated cognitive and motor neuron system dysfunction (Iguchi et al., 2016). The exosome has proved to be an important inflammatory mediator of blood mononuclear cells. In ALS, the exosome can carry TDP-43 protein into the external environment and be swallowed by mononuclear cells. Some cytokines, such as IL-6, IL-10, IL-1B and MCP-1, are also secreted reactively under the stimulation of exosomes containing TDP-43 and participate in peripheral immune regulation (Zondler et al., 2017). This illustrates that exosomes associated with ALS exist in the peripheral circulation and interact with other cells and that other substances contained in related exosomes have potential as a biomarker as ALS in addition to TDP-43 protein. As Saucier et al. noted, increased levels of 5 miRNAs were found in plasma-derived exosomes from patients with ALS, levels of 22 miRNAs were reduced, and individual related miRNAs such as miR-183-5p and miR-9-5p, were dysregulated. It has also been shown that miR-193a-5p and miR-15a-5p are associated with ALS progression and can contribute toward diagnosis (Saucier et al., 2019).

EXOSOMES IN HUNTINGTON'S DISEASE

Huntington's disease (HD) is a progressive dominant hereditary neurodegenerative disease. It is caused by abnormal amplification of CAG repeats in Huntington's gene (HTT) and produces mutant Huntington protein (mHTT). It has some neurotoxicity and is one of nine neurodegenerative diseases caused by polyglutamine (polyQ) amplification, however, the mechanism of how mHTT ultimately causes HD remains unclear. It is a great concern that there is no effective means of treatment at present (Zhang et al., 2016; Lee et al., 2017; Wang et al., 2017). Typical symptoms of HD include cognitive impairment and unconscious dance movements (Lee et al., 2017). Although it has been reported that mHTT can be transmitted across nerves through "tunneling nanotubes" and/or vesicle mechanisms, there is no data suggesting that mHTT is directly associated with the exosome during *trans*-nervous transmission (Zhang et al., 2016; Wang et al., 2017).

Zhang and his colleagues used a model culture system to overexpress the HTT-exon 1 polyQ-GFP construct in 293T cells, and showed that EVs contain polyQ-GFP protein and amplified duplicate RNA. Striatal mouse neurons could ingest these EVs, which led to an increase in polyQ-GFP RNA in the cells, although it did not exhibit any significant toxicity during the experimental period. They showed that EVs have the potential to deliver toxic amplified trinucleotide repetitive RNA and so more work needs to be done to assess the fate of the transferred RNA/protein and its potential toxicity to receptor cells. This also seems to indicate that exosomes can act as scavengers, eliminating polyQ proteins from cells to help reduce toxicity. These disease-related amplified RNAs in HD patients' bodily fluids would seem to be a good choice for finding biomarkers for monitoring disease progression and treatment (Zhang et al., 2016). In another study, statistical analysis revealed that 13 miRNAs were significantly up-regulated in plasma-derived exosomes of HD patients, such as miR-877-5p, miR-223-3p, miR-30d-5p, miR-128, miR-22-5p, miR-223-5p, miR-222-3p, miR-338-3p, miR-130b-3p, miR-628-3p, miR-361-5p, miR-425-5p, and miR-942 (Kumar et al., 2017).

EXOSOMES IN TRAUMATIC ENCEPHALOPATHY

Chronic traumatic encephalopathy (CTE) is one of the main causes of death and disability in the world (Xiong et al., 2017). Severe CTE can lead to long-term motor impairment, cognitive impairment and even death, however, the molecular mechanism of neuronal injury and recovery after CTE remains unclear (Huang et al., 2018; Wang and Han, 2019). Currently, the diagnosis of CTE relies on neuroimaging methods, such as magnetic resonance imaging (MRI) and CT scans, and the Glasgow Coma Scale (GCS) (Manek et al., 2018; Cheng et al., 2019). Of these the GCS is the most commonly used, but these diagnostic methods each have their own limitations and difficulties (Manek et al., 2018), which compels us to look for a more reliable diagnostic approach.

The symptoms of CTE can be recovered from in the first year after injury in most cases because about 90% of CTE patients have mild traumatic brain injury. Unfortunately, most patients experience repeated mild traumatic brain injury (mCTE) and thus present with long-term persistent symptoms and even perpetual cognitive dysfunction (Cheng et al., 2019; Karnati et al., 2019). At present, it is difficult to differentiate between, and make a correct diagnosis for, mCTE and CTE (Moyron et al., 2017), but it is certain that neurons, vascular injuries, and inflammatory reactions play key roles in the secondary injury process (Kenney et al., 2018; Ojo et al., 2019), and that the timing of each part is also characteristic (Agoston et al., 2017). There are ongoing efforts to study the pathophysiology mechanism (Manek et al., 2018; Cheng et al., 2019) and, accordingly, obtaining efficient and beneficial biomarkers is essential as they can be used to identify potential pathological changes (Karnati et al., 2019). Promising results have been achieved in the detection of markers from CSF. These biomarkers can be used to predict clinical outcomes, monitor the progression of disease and the persistent pathobiological changes in CTE (Atif and Hicks, 2019) and include markers such as S100β, tau proteins, Neuron-specific enolase (NSE), neurofilament heavy chain protein (NF-H), myelin basic protein (MBP), spectrin breakdown product, glial fibrillary acidic protein (GFAP) and its fragments, and pan C-terminal hydrolase L1 (UCHL1) (Taylor and Gercel-Taylor, 2014; Wang K.K. et al., 2018). However, the biomarkers in these cycles appear very unstable (Kawata et al., 2018; Cheng et al., 2019) and are not very useful in the diagnosis of mCTE.

In addition to these readily soluble proteins obtained by invasive methods, interesting exosomes were later discovered and easily quantified (Kenney et al., 2018). As they are part of intercellular communication mechanisms, they naturally contain a number of pathologically related biologically active substances.

Compared to previously found markers, exosomes can better protect the initial state of the contents from hydrolysis and better characterize the time line and severity of CTE due to its two-layer membrane structure (Agoston et al., 2017). In the pathological state, by analyzing the changes in proteomics and genomic profiles (Taylor and Gercel-Taylor, 2014; Karnati et al., 2019) and using cell-specific non-coding RNA (Agoston et al., 2017), we can identify the exosomes (such as form neurons and glial cells) which we need to assess the degree of damage and pathological changes of CTE faster and more accurately. This non-invasive diagnostic approach offers a novel and exciting path for painless diagnosis (Cheng et al., 2019) and opens a new field of study. Studies have indicated that gene expression in saliva-derived exosomes can be used as a biomarker for the diagnosis of mCTE and also demonstrated the existence of a variety of AD-related genes in mCTE patients (Cheng et al., 2019), moreover, exosomes containing Tau are not only a circulating biomarker of AD, they also exist as a biomarker of chronic traumatic encephalopathy after CTE (Ling et al., 2017; Manek et al., 2018). Kenney et al. measured amyloid beta (Aβ), total tau, and phosphorylated tau (p-tau) in plasma and plasma-derived exosomes from 195 veterans (some patients with chronic neuropsychological symptoms). When comparing the results of the mCTE and non-mCTE groups it was found that the exosomes of mCTE soldiers have elevated levels of p-tau and exosome tau, which suggests that blood-derived exosomes have the capacity to be biomarkers of mCTE, and also proved that mCTE is related to chronic neuropsychological symptoms (Kenney et al., 2018). As a promising CTE biomarker, exosomes, if used in conjunction with related physical examinations, will become useful in the early diagnosis and prediction of injury (Karnati et al., 2019).

CONCLUSION AND OVERVIEW

Exosomes can be used as both therapeutic means and ideal biological indicators in central nervous system diseases, and of course, this ability can apply to other diseases as well. The non-invasive nature of exosome analysis means that it can be safely used for prenatal evaluation of fetal central nervous system injury (Goetzl et al., 2019), and diagnostic testing of elderly patients (Cicognola et al., 2019).

Since exosomes released by brain cells can pass through the BBB and enter the peripheral body and CSFs, we should be able to isolate and analyze the cargo contained in these circulating exosomes. This should allow for the isolation of high-efficiency biomarkers, and provide possibilities for monitoring the pathological progress of nervous system diseases and assess treatment effects (Shi et al., 2019). Because exosomes are also modified and targeted, they are also used for treatment (Shi et al., 2019). To make use of these exosomes in the diagnosis of diseases we still need large-scale population studies and their specificity and sensitivity need to be confirmed by further clinical studies. Exosome separation methods and gold standards also needed to be developed to truly distinguish them from contaminating proteins and lipoprotein aggregates. We also need to differentiate exosomes secreted by brain cells to find out which exosome source is the best biomarker for various central nervous system diseases. These issues must be taken into account when aiming to improve the diagnostic value of exosomes (Malm et al., 2016; Wu et al., 2017).

While it is clear that this research area is still at an early stage, especially in the context of the diseases of the central nervous system as described in this review, it can also been seen that the isolation and characterization of exosomes, and the analysis of their contents have attracted considerable attention, causing a surge in recent research output. Further research in this emerging field will have a profound impact on the clinical diagnosis and, over time, treatment of more complex and cryptic diseases.

AUTHOR CONTRIBUTIONS

WL provided the idea of this article and wrote it for the first author. XB, AZ, JH, SX, and JZ was responsible for collecting and collating the data.

FUNDING

This work was supported by the National Natural Science Foundation of China (No. 81774059) and Natural Science Foundation of Tianjin City (No. 19JCZDJC37100).

REFERENCES

Agoston, D. V., Shutes-David, A., and Peskind, E. R. (2017). Biofluid biomarkers of traumatic brain injury. *Brain Inj.* 31, 1195–1203. doi: 10.1080/02699052.2017.1357836

Arya, A. K., and Hu, B. (2018). Brain-gut axis after stroke. *Brain Circ.* 4, 165–173. doi: 10.4103/bc.bc_32_18

Athauda, D., Gulyani, S., Karnati, H. K., Li, Y., Tweedie, D., Mustapic, M., et al. (2019). Utility of neuronal-derived exosomes to examine molecular mechanisms that affect motor function in patients with Parkinson disease: a secondary analysis of the exenatide-PD trial. *JAMA Neurol.* 76, 420–429. doi: 10.1001/jamaneurol.2018.4304

Atif, H., and Hicks, S. D. (2019). A review of MicroRNA biomarkers in traumatic brain injury. *J. Exp. Neurosci.* 13:1179069519832286. doi: 10.1177/1179069519832286

Boese, A. S., Saba, R., Campbell, K., Majer, A., Medina, S., Burton, L., et al. (2016). MicroRNA abundance is altered in synaptoneurosomes during prion disease. *Mol. Cell. Neurosci.* 71, 13–24. doi: 10.1016/j.mcn.2015.12.001

Bonafede, R., Scambi, I., Peroni, D., Potrich, V., Boschi, F., Benati, D., et al. (2016). Exosome derived from murine adipose-derived stromal cells: neuroprotective effect on in vitro model of amyotrophic lateral sclerosis. *Exp. Cell Res.* 340, 150–158. doi: 10.1016/j.yexcr.2015.12.009

Cervenakova, L., Saa, P., Yakovleva, O., Vasilyeva, I., de Castro, J., Brown, P., et al. (2016). Are prions transported by plasma exosomes? *Transfus. Apher. Sci.* 55, 70–83. doi: 10.1016/j.transci.2016.07.013

Cesselli, D., Parisse, P., Aleksova, A., Veneziano, C., Cervellin, C., Zanello, A., et al. (2018). Extracellular vesicles: how drug and pathology interfere with their biogenesis and function. *Front. Physiol.* 9:1394. doi: 10.3389/fphys.2018.01394

Chen, F., Du, Y., Esposito, E., Liu, Y., Guo, S., Wang, X., et al. (2015). Effects of focal cerebral ischemia on exosomal versus serum mir126. *Transl. Stroke Res.* 6, 478–484. doi: 10.1007/s12975-015-0429-3

Cheng, L., Zhao, W., and Hill, A. F. (2018). Exosomes and their role in the intercellular trafficking of normal and disease associated prion proteins. *Mol. Aspects Med.* 60, 62–68. doi: 10.1016/j.mam.2017.11.011

Cheng, Y., Pereira, M., Raukar, N., Reagan, J. L., Queseneberry, M., Goldberg, L., et al. (2019). Potential biomarkers to detect traumatic brain injury by the profiling of salivary extracellular vesicles. *J. Cell. Physiol.* 234, 14377–14388. doi: 10.1002/jcp.28139

Cicognola, C., Brinkmalm, G., Wahlgren, J., Portelius, E., Gobom, J., Cullen, N. C., et al. (2019). Novel tau fragments in cerebrospinal fluid: relation to tangle pathology and cognitive decline in Alzheimer's disease. *Acta Neuropathol.* 137, 279–296. doi: 10.1007/s00401-018-1948-2

Clemmens, H., and Lambert, D. W. (2018). Extracellular vesicles: translational challenges and opportunities. *Biochem. Soc. Trans.* 46, 1073–1082. doi: 10.1042/BST20180112

Collino, F., Bruno, S., Incarnato, D., Dettori, D., Neri, F., Provero, P., et al. (2015). AKI Recovery induced by mesenchymal stromal cell-derived extracellular vesicles carrying microRNAs. *J. Am. Soc. Nephrol.* 26, 2349–2360. doi: 10.1681/ASN.2014070710

Datta, A., Chen, C. P., and Sze, S. K. (2014). Discovery of prognostic biomarker candidates of lacunar infarction by quantitative proteomics of microvesicles enriched plasma. *PLoS One.* 9:e94663. doi: 10.1371/journal.pone.0094663

DeLeo, A. M., and Ikezu, T. (2018). Extracellular vesicle biology in Alzheimer's disease and related tauopathy. *J. Neuroimmune. Pharmacol.* 13, 292–308. doi: 10.1007/s11481-017-9768-z

Denis, H. L., Lamontagne-Proulx, J., St-Amour, I., Mason, S. L., Weiss, A., Chouinard, S., et al. (2018). Platelet-derived extracellular vesicles in Huntington's disease. *J. Neurol.* 265, 2704–2712. doi: 10.1007/s00415-018-9022-5

Dinkins, M. B., Dasgupta, S., Wang, G., Zhu, G., and Bieberich, E. (2014). Exosome reduction in vivo is associated with lower amyloid plaque load in the 5XFAD mouse model of Alzheimer's disease. *Neurobiol. Aging.* 35, 1792–1800. doi: 10.1016/j.neurobiolaging.2014.02.012

Goetzl, E. J., Boxer, A., Schwartz, J. B., Abner, E. L., Petersen, R. C., Miller, B. L., et al. (2015a). Altered lysosomal proteins in neural-derived plasma exosomes in preclinical Alzheimer disease. *Neurology* 85, 40–87. doi: 10.1212/WNL.0000000000001702

Goetzl, E. J., Boxer, A., Schwartz, J. B., Abner, E. L., Petersen, R. C., Miller, B. L., et al. (2015b). Low neural exosomal levels of cellular survival factors in Alzheimer's disease. *Ann. Clin. Transl. Neurol.* 2, 769–773. doi: 10.1002/acn3.211

Goetzl, L., Darbinian, N., and Merabova, N. (2019). Noninvasive assessment of fetal central nervous system insult: Potential application to prenatal diagnosis. *Prenat. Diagn.* 39, 609–615. doi: 10.1002/pd.5474

Gui, Y., Lin, H., Zhang, L., Lv, W., and Hu, X. (2015). Altered microRNA profiles in cerebrospinal fluid exosome in Parkinson disease and Alzheimer disease. *Oncotarget* 6, 37043–37053. doi: 10.18632/oncotarget.6158

Guo, B. B., Bellingham, S. A., and Hill, A. F. (2016). Stimulating the release of exosomes increases the intercellular transfer of prions. *J. Biol. Chem.* 291, 5128–5137. doi: 10.1074/jbc.M115.684258

Hartmann, A., Muth, C., Dabrowski, O., Krasemann, S., and Glatzel, M. (2017). Exosomes and the prion protein: more than one truth. *Front. Neurosci.* 11:194. doi: 10.3389/fnins.2017.00194

Heisler, F. F., Pechmann, Y., Wieser, I., Altmeppen, H. C., Veenendaal, L., Muhia, M., et al. (2018). Muskelin coordinates PrP(C) lysosome versus exosome targeting and impacts prion disease progression. *Neuron.* 99, 1155–1169.e9. doi: 10.1016/j.neuron.2018.08.010

Hong, S. B., Yang, H., Manaenko, A., Lu, J., Mei, Q., and Hu, Q. (2018). Potential of exosomes for the treatment of stroke. *Cell Transplant.* 28, 662–670. doi: 10.1177/0963689718816990

Huang, S., Ge, X., Yu, J., Han, Z., Yin, Z., Li, Y., et al. (2018). Increased miR-124-3p in microglial exosomes following traumatic brain injury inhibits neuronal inflammation and contributes to neurite outgrowth via their transfer into neurons. *FASEB J.* 32, 512–528. doi: 10.1096/fj.201700673R

Iguchi, Y., Eid, L., Parent, M., Soucy, G., Bareil, C., Riku, Y., et al. (2016). Exosome secretion is a key pathway for clearance of pathological TDP-43. *Brain* 139(Pt 12), 3187–3201. doi: 10.1093/brain/aww237

Jiang, M., Wang, H., Jin, M., Yang, X., Ji, H., Jiang, Y., et al. (2018). Exosomes from MiR-30d-5p-ADSCs reverse acute ischemic stroke-induced, autophagy-mediated brain injury by promoting M2 microglial/macrophage polarization. *Cell. Physiol. Biochem.* 47, 864–878. doi: 10.1159/000490078

Joshi, P., Benussi, L., Furlan, R., Ghidoni, R., and Verderio, C. (2015). Extracellular vesicles in Alzheimer's disease: friends or foes? focus on abeta-vesicle interaction. *Int. J. Mol. Sci.* 16, 4800–4813. doi: 10.3390/ijms16034800

Joshi, P., Turola, E., Ruiz, A., Bergami, A., Libera, D. D., Benussi, L., et al. (2014). Microglia convert aggregated amyloid-beta into neurotoxic forms through the shedding of microvesicles. *Cell Death Differ.* 21, 582–593. doi: 10.1038/cdd.2013.180

Kanata, E., Thune, K., Xanthopoulos, K., Ferrer, I., Dafou, D., Zerr, I., et al. (2018). MicroRNA alterations in the brain and body fluids of humans and animal prion disease models: current status and perspectives. *Front. Aging Neurosci.* 10:220. doi: 10.3389/fnagi.2018.00220

Kanhai, D. A., de Kleijn, D. P., Kappelle, L. J., Uiterwaal, C. S., van der Graaf, Y., Pasterkamp, G., et al. (2014). Extracellular vesicle protein levels are related to brain atrophy and cerebral white matter lesions in patients with manifest vascular disease: the SMART-MR study. *BMJ Open* 4:e003824. doi: 10.1136/bmjopen-2013-003824

Kapogiannis, D., Boxer, A., Schwartz, J. B., Abner, E. L., Biragyn, A., Masharani, U., et al. (2015). Dysfunctionally phosphorylated type 1 insulin receptor substrate in neural-derived blood exosomes of preclinical Alzheimer's disease. *FASEB J.* 29, 589–596. doi: 10.1096/fj.14-262048

Karnati, H. K., Garcia, J. H., Tweedie, D., Becker, R. E., Kapogiannis, D., and Greig, N. H. (2019). Neuronal enriched extracellular vesicle proteins as biomarkers for traumatic brain injury. *J. Neurotrauma.* 36, 975–987. doi: 10.1089/neu.2018.5898

Kawahara, H., and Hanayama, R. (2018). The role of exosomesextracellular vesicles in neural signal transduction. *Biol. Pharm. Bull.* 41, 1119–1125. doi: 10.1248/bpb.b18-00167

Kawata, K., Mitsuhashi, M., and Aldret, R. (2018). A preliminary report on brain-derived extracellular vesicle as novel blood biomarkers for sport-related concussions. *Front. Neurol.* 9:239. doi: 10.3389/fneur.2018.00239

Kenney, K., Qu, B. X., Lai, C., Devoto, C., Motamedi, V., Walker, W. C., et al. (2018). Higher exosomal phosphorylated tau and total tau among veterans with combat-related repetitive chronic mild traumatic brain injury. *Brain Inj.* 32, 1276–1284. doi: 10.1080/02699052.2018.1483530

Kerr, N., Garcia-Contreras, M., Abbassi, S., Mejias, N. H., Desousa, B. R., Ricordi, C., et al. (2018). Inflammasome proteins in serum and serum-derived extracellular vesicles as biomarkers of stroke. *Front. Mol. Neurosci.* 11:309. doi: 10.3389/fnmol.2018.00309

Kitamura, Y., Kojima, M., Kurosawa, T., Sasaki, R., Ichihara, S., Hiraku, Y., et al. (2018). Proteomic profiling of exosomal proteins for blood-based biomarkers in Parkinson's disease. *Neuroscience.* 392, 121–128. doi: 10.1016/j.neuroscience.2018.09.017

Kumar, S., Vijayan, M., Bhatti, J. S., and Reddy, P. H. (2017). MicroRNAs as peripheral biomarkers in aging and age-related diseases. *Prog. Mol. Biol. Transl. Sci.* 146, 47–94. doi: 10.1016/bs.pmbts.2016.12.013

Lausted, C., Lee, I., Zhou, Y., Qin, S., Sung, J., Price, N. D., et al. (2014). Systems approach to neurodegenerative disease biomarker discovery. *Annu. Rev. Pharmacol. Toxicol.* 54, 457–481. doi: 10.1146/annurev-pharmtox-011613-135928

Lee, M., Ban, J. J., Kim, K. Y., Jeon, G. S., Im, W., Sung, J. J., et al. (2016). Adipose-derived stem cell exosomes alleviate pathology of amyotrophic lateral sclerosis in vitro. *Biochem. Biophys. Res. Commun.* 479, 434–439. doi: 10.1016/j.bbrc.2016.09.069

Lee, S.-T., Im, W., Ban, J.-J., Lee, M., Jung, K.-H., Lee, S. K., et al. (2017). Exosome-based delivery of miR-124 in a huntington's disease model. *J. Mov. Disord.* 10, 45–52. doi: 10.14802/jmd.16054

Leggio, L., Vivarelli, S., L'Episcopo, F., Tirolo, C., Caniglia, S., Testa, N., et al. (2017). MicroRNAs in Parkinson's disease: from pathogenesis to novel diagnostic and therapeutic approaches. *Int. J. Mol. Sci.* 18:E2698. doi: 10.3390/ijms18122698

Leone, D. A., Rees, A. J., and Kain, R. (2018). Dendritic cells and routing cargo into exosomes. *Immunol. Cell Biol.* doi: 10.1111/imcb.12170 [Epub ahead of print].

Li, L., Wang, P., Zhao, H., and Luo, Y. (2019). Noncoding RNAs and intracerebral hemorrhage. *CNS Neurol. Disord. Drug Targets.* 18, 205–211. doi: 10.2174/1871527318666190204102604

Li, Z., Wang, A., Cai, J., Gao, X., Zhou, Y., Luo, Y., et al. (2015). Impact of proteinuria and glomerular filtration rate on risk of ischaemic and intracerebral hemorrhagic stroke: a result from the kailuan study. *Eur. J. Neurol.* 22, 355–360. doi: 10.1111/ene.12580

Ling, H., Morris, H. R., Neal, J. W., Lees, A. J., Hardy, J., Holton, J. L., et al. (2017). Mixed pathologies including chronic traumatic encephalopathy account for dementia in retired association football (soccer) players. *Acta Neuropathol.* 133, 337–352. doi: 10.1007/s00401-017-1680-3

Luarte, A., Batiz, L. F., Wyneken, U., and Lafourcade, C. (2016). Potential therapies by stem cell-derived exosomes in CNS diseases: focusing on the neurogenic niche. *Stem Cells Int.* 2016:5736059. doi: 10.1155/2016/5736059

Maguire, G. (2017). Amyotrophic lateral sclerosis as a protein level, non-genomic disease: therapy with S2RM exosome released molecules. *World J. Stem Cells* 9, 187–202. doi: 10.4252/wjsc.v9.i11.187

Makin, S. D., Cook, F. A., Dennis, M. S., and Wardlaw, J. M. (2015). Cerebral small vessel disease and renal function: systematic review and meta-analysis. *Cerebrovasc. Dis.* 39, 39–52. doi: 10.1159/000369777

Malm, T., Loppi, S., and Kanninen, K. M. (2016). Exosomes in Alzheimer's disease. *Neurochem. Int.* 97, 193–199. doi: 10.1016/j.neuint.2016.04.011

Manek, R., Moghieb, A., Yang, Z., Kumar, D., Kobessiy, F., Sarkis, G. A., et al. (2018). Protein biomarkers and neuroproteomics characterization of microvesicles/exosomes from human cerebrospinal fluid following traumatic brain injury. *Mol. Neurobiol.* 55, 6112–6128. doi: 10.1007/s12035-017-0821-y

Mirzaei, H., Momeni, F., Saadatpour, L., Sahebkar, A., Goodarzi, M., Masoudifar, A., et al. (2018). MicroRNA: relevance to stroke diagnosis, prognosis, and therapy. *J. Cell Physiol.* 233, 856–865. doi: 10.1002/jcp.25787

Mishima, T., Mizuguchi, Y., Kawahigashi, Y., Takizawa, T., and Takizawa, T. (2007). RT-PCR-based analysis of microRNA (miR-1 and -124) expression in mouse CNS. *Brain Res.* 1131, 37–43. doi: 10.1016/j.brainres.2006.11.035

Moyron, R. B., Gonda, A., Selleck, M. J., Luo-Owen, X., Catalano, R. D., O'Callahan, T., et al. (2017). Differential protein expression in exosomal samples taken from trauma patients. *Proteomics Clin. Appl.* 11. doi: 10.1002/prca.201700061

Mrowczynski, O. D., Zacharia, B. E., and Connor, J. R. (2019). Exosomes and their implications in central nervous system tumor biology. *Prog. Neurobiol.* 172, 71–83. doi: 10.1016/j.pneurobio.2018.06.006

Ohmichi, T., Mitsuhashi, M., Tatebe, H., Kasai, T., Ali El-Agnaf, O. M., and Tokuda, T. (2018). Quantification of brain-derived extracellular vesicles in plasma as a biomarker to diagnose Parkinson's and related diseases. *Parkinsonism Relat. Disord.* 61, 82–87. doi: 10.1016/j.parkreldis.2018.11.021

Ojo, J. O., Algamal, M., Leary, P., Abdullah, L., Mouzon, B., Evans, J. E., et al. (2019). converging and differential brain phospholipid dysregulation in the pathogenesis of repetitive mild traumatic brain injury and Alzheimer's disease. *Front. Neurosci.* 13:103. doi: 10.3389/fnins.2019.00103

Osier, N., Motamedi, V., Edwards, K., Puccio, A., Diaz-Arrastia, R., Kenney, K., et al. (2018). Exosomes in acquired neurological disorders: new insights into pathophysiology and treatment. *Mol. Neurobiol.* 55, 9280–9293. doi: 10.1007/s12035-018-1054-4

Otero-Ortega, L., Laso-Garcia, F., Gomez-de Frutos, M., Fuentes, B., Diekhorst, L., Diez-Tejedor, E., et al. (2018). Role of exosomes as a treatment and potential biomarker for stroke. *Transl. Stroke Res.* 10, 241–249. doi: 10.1007/s12975-018-0654-7

Picca, A., Guerra, F., Calvani, R., Bucci, C., Lo Monaco, M. R., Bentivoglio, A. R., et al. (2019). Mitochondrial-derived vesicles as candidate biomarkers in Parkinson's disease: rationale, design and methods of the exosomes in parkinson disease (EXPAND) Study. *Int. J. Mol. Sci.* 20:E2373. doi: 10.3390/ijms20102373

Pluta, R., and Ulamek-Koziol, M. (2019). Lymphocytes, platelets, erythrocytes, and exosomes as possible biomarkers for Alzheimer's disease clinical diagnosis. *Adv. Exp. Med. Biol.* 1118, 71–82. doi: 10.1007/978-3-030-05542-4_4

Ratajczak, J., Miekus, K., Kucia, M., Zhang, J., Reca, R., Dvorak, P., et al. (2006). Embryonic stem cell-derived microvesicles reprogram hematopoietic progenitors: evidence for horizontal transfer of mRNA and protein delivery. *Leukemia* 20, 847–856. doi: 10.1038/sj.leu.2404132

Reza-Zaldivar, E. E., Hernandez-Sapiens, M. A., Minjarez, B., Gutierrez-Mercado, Y. K., Marquez-Aguirre, A. L., and Canales-Aguirre, A. A. (2018). Potential effects of MSC-derived exosomes in neuroplasticity in Alzheimer's disease. *Front. Cell. Neurosci.* 12:317. doi: 10.3389/fncel.2018.00317

Samuelson, I., and Vidal-Puig, A. J. (2018). Fed-exosome: extracellular vesicles and cell-cell communication in metabolic regulation. *Essays Biochem.* 62, 165–175. doi: 10.1042/EBC20170087

Saucier, D., Wajnberg, G., Roy, J., Beauregard, A. P., Chacko, S., Crapoulet, N., et al. (2019). Identification of a circulating miRNA signature in extracellular vesicles collected from amyotrophic lateral sclerosis patients. *Brain Res.* 1708, 100–108. doi: 10.1016/j.brainres.2018.12.016

Seifert, H. A., and Offner, H. (2018). The splenic response to stroke: from rodents to stroke subjects. *J. Neuroinflammation* 15:195. doi: 10.1186/s12974-018-1239-9

Shah, S. Z. A., Zhao, D., Hussain, T., Sabir, N., and Yang, L. (2018). Regulation of microRNAs-mediated autophagic flux: a new regulatory avenue for neurodegenerative diseases with focus on prion diseases. *Front. Aging Neurosci.* 10:139. doi: 10.3389/fnagi.2018.00139

Shi, M., Sheng, L., Stewart, T., Zabetian, C. P., and Zhang, J. (2019). New windows into the brain: Central nervous system-derived extracellular vesicles in blood. *Prog. Neurobiol.* 175, 96–106. doi: 10.1016/j.pneurobio.2019.01.005

Shoemaker, J. K., and Goswami, R. (2015). Forebrain neurocircuitry associated with human reflex cardiovascular control. *Front. Physiology.* 6:240. doi: 10.3389/fphys.2015.00240

Sohrab, S. S., Suhail, M., Ali, A., Kamal, M. A., Husen, A., Ahmad, F., et al. (2018). Role of viruses, prions and miRNA in neurodegenerative disorders and dementia. *Virusdisease.* 29, 419–433. doi: 10.1007/s13337-018-0492-y

Stahl, P. D., and Raposo, G. (2018). Exosomes and extracellular vesicles: the path forward. *Essays Biochem.* 62, 119–124. doi: 10.1042/EBC20170088

Taylor, D. D., and Gercel-Taylor, C. (2014). Exosome platform for diagnosis and monitoring of traumatic brain injury. *Philos. Trans. R. Soc. Lond. B Biol. Sci.* 369:20130503. doi: 10.1098/rstb.2013.0503

Thome, A. D., Harms, A. S., Volpicelli-Daley, L. A., and Standaert, D. G. (2016). microRNA-155 regulates alpha-synuclein-induced inflammatory responses in models of Parkinson disease. *J. Neurosci.* 36, 2383–2390. doi: 10.1523/JNEUROSCI.3900-15.2016

Tian, T., Zhang, H. X., He, C. P., Fan, S., Zhu, Y. L., Qi, C., et al. (2018). Surface functionalized exosomes as targeted drug delivery vehicles for cerebral ischemia therapy. *Biomaterials* 150, 137–149. doi: 10.1016/j.biomaterials.2017.10.012

Titze-de-Almeida, R., and Titze-de-Almeida, S. S. (2018). miR-7 replacement therapy in Parkinson's disease. *Curr. Gene Ther.* 18, 143–153. doi: 10.2174/1566523218666180430121323

Tofaris, G. K. (2017). A critical assessment of exosomes in the pathogenesis and stratification of Parkinson's disease. *J. Parkinsons Dis.* 7, 569–576. doi: 10.3233/JPD-171176

Tomlinson, P. R., Zheng, Y., Fischer, R., Heidasch, R., Gardiner, C., Evetts, S., et al. (2015). Identification of distinct circulating exosomes in Parkinson's disease. *Ann. Clin. Transl. Neurol.* 2, 353–361. doi: 10.1002/acn3.175

Venkat, P., Chen, J., and Chopp, M. (2018). Exosome-mediated amplification of endogenous brain repair mechanisms and brain and systemic organ interaction in modulating neurological outcome after stroke. *J. Cereb. Blood Flow Metab.* 38, 2165–2178. doi: 10.1177/0271678X18782789

Vistbakka, J., Elovaara, I., Lehtimäki, T., and Hagman, S. (2017). Circulating microRNAs as biomarkers in progressive multiple sclerosis. *Mult. Scler.* 23, 403–412. doi: 10.1177/1352458516651141

Wang, B., and Han, S. (2019). Modified exosomes reduce apoptosis and ameliorate neural deficits induced by traumatic brain injury. *ASAIO J.* 65, 285–292. doi: 10.1097/MAT.0000000000000810

Wang, G., Huang, Y., Wang, L. L., Zhang, Y. F., Xu, J., Zhou, Y., et al. (2016). MicroRNA-146a suppresses ROCK1 allowing hyperphosphorylation of tau in Alzheimer's disease. *Sci. Rep.* 6:26697. doi: 10.1038/srep26697

Wang, J. K. T., Langfelder, P., Horvath, S., and Palazzolo, M. J. (2017). Exosomes and homeostatic synaptic plasticity are linked to each other and to huntington's, Parkinson's, and other neurodegenerative diseases by database-enabled analyses of comprehensively curated datasets. *Front. Neurosci.* 11:149. doi: 10.3389/fnins.2017.00149

Wang, K. K., Yang, Z., Zhu, T., Shi, Y., Rubenstein, R., Tyndall, J. A., et al. (2018). An update on diagnostic and prognostic biomarkers for traumatic brain injury. *Expert Rev. Mol. Diagn.* 18, 165–180. doi: 10.1080/14737159.2018.1428089

Wang, W., Li, D. B., Li, R. Y., Zhou, X., Yu, D. J., Lan, X. Y., et al. (2018). Diagnosis of hyperacute and acute ischaemic stroke: the potential utility of exosomal MicroRNA-21-5p and MicroRNA-30a-5p. *Cerebrovasc. Dis.* 45, 204–212. doi: 10.1159/000488365

Wang, X., Luo, Y., Wang, Y., Wang, C., Zhao, X., Wang, D., et al. (2014). Comparison of associations of outcomes after stroke with estimated GFR using Chinese modifications of the MDRD study and CKD-EPI creatinine equations: results from the china national stroke registry. *Am. J. Kidney Dis.* 63, 59–67. doi: 10.1053/j.ajkd.2013.08.008

Wang, Z., He, D., Zeng, Y. Y., Zhu, L., Yang, C., Lu, Y. J., et al. (2019). The spleen may be an important target of stem cell therapy for stroke. *J. Neuroinflammation* 16:20. doi: 10.1186/s12974-019-1400-0

West, A. P., Khoury-Hanold, W., Staron, M., Tal, M. C., Pineda, C. M., Lang, S. M., et al. (2015). Mitochondrial DNA stress primes the antiviral innate immune response. *Nature* 520, 553–557. doi: 10.1038/nature14156

Winek, K., Engel, O., Koduah, P., Heimesaat, M. M., Fischer, A., Bereswill, S., et al. (2016). Depletion of cultivatable gut microbiota by broad-spectrum antibiotic pretreatment worsens outcome after murine stroke. *Stroke* 47, 1354–1363. doi: 10.1161/STROKEAHA.115.011800

Wu, X., Zheng, T., and Zhang, B. (2017). Exosomes in Parkinson's disease. *Neurosci. Bull.* 33, 331–338. doi: 10.1007/s12264-016-0092-z

Xiao, T., Zhang, W., Jiao, B., Pan, C. Z., Liu, X., and Shen, L. (2017). The role of exosomes in the pathogenesis of Alzheimer' disease. *Transl. Neurodegener.* 6:3. doi: 10.1186/s40035-017-0072-x

Xiong, Y., Mahmood, A., and Chopp, M. (2017). Emerging potential of exosomes for treatment of traumatic brain injury. *Neural. Regen. Res.* 12, 19–22. doi: 10.4103/1673-5374.198966

Yang, J., Zhang, X., Chen, X., Wang, L., and Yang, G. (2017). Exosome mediated delivery of miR-124 promotes neurogenesis after ischemia. *Mol. Ther. Nucleic Acids* 7, 278–287. doi: 10.1016/j.omtn.2017.04.010

Yang, Y., Ye, Y., Su, X., He, J., Bai, W., and He, X. (2017). MSCs-derived exosomes and neuroinflammation, neurogenesis and therapy of traumatic brain injury. *Front. Cell. Neurosci.* 11:55. doi: 10.3389/fncel.2017.00055

Yang, T. T., Liu, C. G., Gao, S. C., Zhang, Y., and Wang, P. C. (2018). The serum exosome derived MicroRNA-135a, -193b, and -384 were potential Alzheimer's disease biomarkers. *Biomed. Environ. Sci.* 31, 87–96. doi: 10.3967/bes2018.011

Yang, Z. B., Li, T. B., Zhang, Z., Ren, K. D., Zheng, Z. F., Peng, J., et al. (2016). The diagnostic value of circulating brain-specific MicroRNAs for ischemic stroke. *Intern. Med.* 55, 1279–1286. doi: 10.2169/internalmedicine.55.5925

Yuyama, K., and Igarashi, Y. (2016). Physiological and pathological roles of exosomes in the nervous system. *Biomol. Concepts* 7, 53–68. doi: 10.1515/bmc-2015-2033

Zagrean, A. M., Hermann, D. M., Opris, I., Zagrean, L., and Popa-Wagner, A. (2018). Multicellular crosstalk between exosomes and the neurovascular unit after cerebral ischemia. therapeutic implications. *Front. Neurosci.* 12:811. doi: 10.3389/fnins.2018.00811

Zhang, X., Abels, E. R., Redzic, J. S., Margulis, J., Finkbeiner, S., and Breakefield, X. O. (2016). Potential transfer of polyglutamine and CAG-Repeat RNA in extracellular vesicles in huntington's disease: background and evaluation in cell culture. *Cell. Mol. Neurobiol.* 36, 459–470. doi: 10.1007/s10571-016-0350-7

Zhang, Z. G., and Chopp, M. (2016). Exosomes in stroke pathogenesis and therapy. *J. Clin. Investigat.* 126, 1190–1197. doi: 10.1172/jci81133

Zhao, L., Xiong, Q., Stary, C. M., Mahgoub, O. K., Ye, Y., Gu, L., et al. (2018). Bidirectional gut-brain-microbiota axis as a potential link between inflammatory bowel disease and ischemic stroke. *J. Neuroinflammation* 15:339. doi: 10.1186/s12974-018-1382-3

Zondler, L., Feiler, M. S., Freischmidt, A., Ruf, W. P., Ludolph, A. C., Danzer, K. M., et al. (2017). Impaired activation of ALS monocytes by exosomes. *Immunol. Cell Biol.* 95, 207–214. doi: 10.1038/icb.2016.89

Conflict of Interest: The authors declare that the research was conducted in the absence of any commercial or financial relationships that could be construed as a potential conflict of interest.

frontiers in Molecular Neuroscience

ORIGINAL RESEARCH
published: 24 March 2020
doi: 10.3389/fnmol.2020.00043

Interference With Complex IV as a Model of Age-Related Decline in Synaptic Connectivity

Martin Kriebel[1†], *Julia Ebel*[1†], *Florian Battke*[2], *Stefan Griesbach*[2] *and Hansjürgen Volkmer*[1*]

[1]*Department of Molecular Biology and Neurobiology, NMI Natural and Medical Sciences Institute at the University of Tübingen, Reutlingen, Germany,* [2]*CeGaT GmbH, Tübingen, Germany*

Age-related impairment of mitochondrial function may negatively impact energy-demanding processes such as synaptic transmission thereby triggering cognitive decline and processes of neurodegeneration. Here, we present a novel model for age-related mitochondrial impairment based on partial inhibition of cytochrome c oxidase subunit 4 (Cox4) of complex IV of the respiratory chain. miRNA-mediated knockdown of Cox4 correlated with a marked reduction in excitatory and inhibitory synaptic marker densities *in vitro* and *in vivo* as well as an impairment of neuronal network activity in primary neuronal cultures. Transcriptome analysis identified the deregulation of gene clusters, which link induced mitochondrial perturbation to impaired synaptic function and plasticity as well as processes of aging. In conclusion, the model of Cox4 deficiency reflects aspects of age-related dementia and might, therefore, serve as a novel test system for drug development.

Keywords: cytochrome c oxidase, Cox4, mitochondria, aging, synaptic connectivity, neurodegeneration

OPEN ACCESS

Edited by:
Marie-Eve Tremblay, Laval University, Canada

Reviewed by:
Luca Peruzzotti-Jametti, University of Cambridge, United Kingdom
Jorge Valero, Achucarro Basque Center for Neuroscience, Spain

***Correspondence:**
Hansjürgen Volkmer
volkmer@nmi.de

[†]These authors have contributed equally to this work

Received: *25 November 2019*
Accepted: *04 March 2020*
Published: *24 March 2020*

Citation:
Kriebel M, Ebel J, Battke F, Griesbach S and Volkmer H (2020) Interference With Complex IV as a Model of Age-Related Decline in Synaptic Connectivity. Front. Mol. Neurosci. 13:43. doi: 10.3389/fnmol.2020.00043

INTRODUCTION

A large and complex set of parameters contributes to cellular aging including genomic instability, epigenetic alterations, deregulated nutrient sensing, and impaired proteostasis (López-Otín et al., 2013). Additionally, an age-dependent decline in mitochondrial function may lead to a decrease in cellular energy supply and dysregulation of calcium homeostasis. Mitochondrial deficits are therefore expected to have a strong impact on energy-demanding processes such as synaptic transmission and might represent a contributing factor for aspects of neurodegeneration (Grimm and Eckert, 2017), e.g., synaptic dysfunction. In line with this, neurodegenerative diseases such as Alzheimer's disease (AD) and Parkinson's disease (PD) have been linked to mitochondrial dysfunction that might exacerbate the impact of aging. Likewise, brains from animal models for aging display a decrease in oxygen consumption as well as ATP production, both tightly linked to proper mitochondrial function (Xu et al., 2007; Hiona et al., 2010; Stefanatos and Sanz, 2018).

In the case of animal models of familial AD (FAD), that rely on inherited mutations driving the pathology, mitochondrial impairments occur already early with respect to disease progression suggesting mitochondrial physiology as an interesting therapeutic target (Hauptmann et al., 2009; Yao et al., 2009). Accordingly, a FAD model shows a decreased expression of subunit 4 of cytochrome c oxidase (Cox), also termed complex IV, decreased Cox activity and decreased mitochondrial respiration in parallel with an increase in oxidative stress (Yao et al., 2009).

Importantly, activity of Cox was also shown to be reduced in patients diagnosed with MCI or AD (Mutisya et al., 1994; Parker and Parks, 1995; Bosetti et al., 2002; Cardoso et al., 2004; Valla et al., 2006; Selfridge et al., 2013).

Cox is composed of 13 subunits encoded by three mitochondrial and ten nuclear genes. The complex is the terminal component of the mitochondrial respiratory chain and serves for the transfer of electrons to oxygen. Cox4 was previously suggested to be essential for the assembly of the cytochrome c oxidase complex and therefore indispensable for proper respiration and concomitant ATP production (Li et al., 2006).

Here, we characterize a model for age-related neurodegeneration based on the downregulation of Cox4. We show that the model exhibits synaptic loss and altered neuronal network activity. Furthermore, transcriptomic profiling revealed deregulation of gene clusters for synaptic function and plasticity as well as processes of aging.

MATERIALS AND METHODS

Construction of Lentiviral and AAV miRNA Expression Vectors

Target sequences for the miRNA-mediated knockdown of Cox4 isoform 1 were identified with the help of the Block-iT™ RNAi Designer[1]. Target sequences chosen were AT AGTCTTCACTCTTCACAAC for miCox79 and TTCTTG TTGTAGTCCCACTTG for miCox474. Synthetic double-stranded polynucleotides harboring the target sequences in a sense-loop-antisense configuration were designed and ligated into pcDNA™6.2-GW/miR (Thermo Fisher Scientific, Waltham, MA, USA). All constructs were validated by sequencing before site-specific Gateway® recombination (Thermo Fisher Scientific, Waltham, MA, USA) was applied to transfer miRNA knockdown cassettes from newly generated pcDNA™6.2-GW/miR vectors or a negative control miRNA from pcDNA™6.2-GW/miR-neg control plasmid (Thermo Fisher Scientific, Waltham, MA, USA) into pLenti04C/SEW or pAAV-C1.3_mCherry_attR_WPRE. pLenti04C/SEW was based on pLenti6/V5-DEST® (Thermo Fisher Scientific, Waltham, MA, USA), pAAV_C1.3_mCherry_attR_WPRE was generated from pAAV-CaMKIIa-hM3D(Gq)-mCherry (gift from Bryan Roth; Addgene plasmid #50476[2]; RRID:Addgene_50476).

For the generation of pLenti04C/SEW, CMV promoter sequences were exchanged for a functional mouse α-CaMKII promoter fragment *via* restriction cloning using ClaI and SpeI restriction sites on pLenti6/V5-DEST®. V5-epitope, EM7 promoter and Blasticidin resistance from pLenti6/V5-DEST® were replaced by an expression cassette driving EGFP expression under the control of a rat synapsin I promoter and WPRE using XhoI (PspXI) and Bpu1102I restriction sites (Dittgen et al., 2004). For the generation of pAAV-C1.3_mCherry_attR_WPRE from pAAV-CaMKIIa-hM3D(Gq)-mCherry, hM3D sequences were first removed by BamHI digest and subsequent re-ligation of the vector. A Gateway® recombination compatible cassette from pLenti6/V5-DEST® containing attR1 and attR2 sites was inserted 3' to the mCherry sequence using EcoRV and HindIII restriction sites.

[1]https://rnaidesigner.invitrogen.com/rnaiexpress/
[2]http://n2t.net/addgene:50476

Preparation, Culture, and Treatment of Primary Neurons

Primary hippocampal or cortical neurons were prepared from E18 rat embryos of either sex by trypsin digestion and subsequent trituration of respective tissues (Goetze et al., 2003; Kriebel et al., 2011). Cells were seeded in serum-free MEM with B27 supplement (Thermo Fisher Scientific, Waltham, MA, USA) on polyethyleneimine (PEI) coated 6-Well cell culture plates (Corning), 96-well μCLEAR® or SENSOPLATE microplates (Greiner Bio-One) at a density of 2.0×10^5 cells/cm^2. At 1 day *in vitro* (DIV1), the plating medium was replaced by fresh serum-free MEM with B27 supplement. Cultures were maintained at 37°C, 5% CO_2 in either serum-free MEM with B27 supplement or in BrainPhys™ Neuronal Medium containing SM1 supplement (STEMCELL Technologies) depending on the downstream application. A 50% medium change was performed every other day.

Lentiviral suspensions generated by lipofection of HEK239FT with lentiviral expression vectors and packaging plasmids pLP1, pLP2 and pLP/VSVG (Thermo Fisher Scientific, Waltham, MA, USA) were used to transduce cultured neurons at MOIs up to 10 at DIV2. After the transduction of mouse neuroblastoma Neuro-2a cells with lentiviral miRNA vectors coexpressing EGFP, biological titers (TU/ml) were determined by flow cytometry and detection of transduced, EGFP-positive cells. Each viral suspension was additionally tested by the transduction of primary rat neurons to assure quantitative transduction before *in vivo* application. AAV suspensions were produced by the Viral-Core-Facility (VCF) of the Charité—Universitätsmedizin Berlin after the provision of corresponding AAV miRNA expression vectors. The transduction of cultured neurons was carried out at DIV2 at MOI of 1×10^4. SB216763 was applied at a concentration of 5 μM for 24 h.

Stereotaxic Injection of Lentiviral Suspensions

Adult female Sprague–Dawley rats (250 g at the time of surgery; Janvier) were kept in compliance with the European Union recommendations for the care and use of laboratory animals and as approved by the responsible German regional council, respectively. For stereotaxic injection of lentiviral suspensions, animals were deeply anesthetized with 2–5% isoflurane/oxygen, followed by s.c. injection of metamizole (50 mg/kg) for intraoperative analgesia at least 30 min before the start of surgical procedures. Bilateral injections of 2.5 μl of lentiviral suspensions (2×10^7 TU/ml) into the dorsal dentate gyrus (AP: −2.9 mm, ML: ±2.5 mm, DV: −4.3 mm; all coordinates relative to Bregma) were conducted using a Lab Standard™ Stereotaxic Instrument (Stoelting) connected to a 701 RN Hamilton syringe (10 μl, 30 gauge, pst 4; CS-Chromatographie Service). Injection speed was set to 0.2 μl/min. To assure sufficient postoperative

analgesia, 2 mg/kg meloxicam was administered by s.c. injection at the end of surgical procedures.

For fixation of brain tissue, animals were deeply anesthetized with ketamine (100 mg/kg i.p.) and xylazine (10 mg/kg i.p.) and transcardially perfused with 100 ml of PBS followed by 250 ml of freshly prepared 4% paraformaldehyde/PBS. Brain tissue was collected and additionally fixed in 4% paraformaldehyde/PBS at 4°C for 60 min.

Quantitative RT-PCR

Total RNA of primary rat neurons quantitatively transduced on DIV2 by lentiviral or AAV suspensions was prepared at DIV14 using RNeasy Mini Kit (Qiagen) according to manufacturer's guidelines. DNase digestion as well as cDNA synthesis were performed according to manufacturer's protocols using RQ1 DNase (Promega) as well as M-MuLV reverse transcriptase (New England Biolabs). Quantitative real-time PCR was performed on the 7500 Fast Real-Time PCR System (Thermo Fisher Scientific, Waltham, MA, USA). The following TaqMan® Gene Expression Assays (Thermo Fisher Scientific, Waltham, MA, USA) were used: GAPDH (VIC-MGB), Rn01775763_g1; Cox4 isoform 1 (FAM-MGB), Rn00665001-g1.

Determination of Cell Viability, Induction of Apoptosis, ATP Content and Mitochondrial Membrane Potential

Cell viability and induction of apoptosis were determined using the ApoLive-Glo™ Multiplex Assay (Promega) according to the manufacturer's guidelines. ATP content was determined using the CellTiter-Glo® Luminescent Cell Viability Assay (Promega) according to the manufacturer's protocols. For both assays, primary rat neurons cultivated in 96-well μCLEAR® microplates were transduced with lentiviral suspensions at DIV2 and cultivated until DIV16. Where applicable, cultures were treated with picomolar concentrations of rotenone 30 min before measurement. Fluorescence and luminescence were detected with a Pherastar microplate reader (BMG Labtech).

Changes in mitochondrial membrane potential (MMP) of rat primary neurons were assessed using JC-10 (Enzo Life Sciences, Farmingdale, NY, USA). Neuronal cultures in 96-well μCLEAR® microplates were transduced with lentiviral suspensions at DIV2, cultivated until DIV14 and incubated with 4 μM JC-10 in culture medium containing 0.02% Pluronic F127 (Merck) for 20 min. JC-10 emission ratio (590 nm/525 nm) was determined with an EnVision 2102 Multilabel Reader. FCCP (Merck) was added to the cultures after JC-10 labeling before fluorescence measurements.

Immunocytochemistry, Immunohistochemistry

Primary rat neurons cultured in 96-well SENSOPLATE microplates were fixed at DIV16 using 4% paraformaldehyde/PBS for 10 min at room temperature. After blocking and permeabilization for 30 min at room temperature in 0.2% Triton X-100/PBS containing 1× Blocking Reagent for ELISA (Merck) cells were incubated overnight at 4°C with primary antibodies diluted in blocking solution. Subsequently, cells were washed three times in PBS before fluorescently labeled secondary antibodies (1:500; Cy3/Cy5-coupled goat anti-mouse and goat anti-rabbit, respectively; Dianova) were added for 2 h at room temperature. Nuclei were stained using Hoechst Dye 33258 (1:1,000 in PBS; Merck). The following primary antibodies were used: monoclonal mouse anti-Cox4 (Cell Signaling Technology, Danvers, MA, USA, Cat. No. 11967), monoclonal mouse anti-gephyrin (Synaptic Systems, Cat. No. 147021), monoclonal mouse anti-MAP2 (Merck, Cat. No. M1406), polyclonal rabbit anti-MAP2 (Merck, Cat. No. AB5622), monoclonal mouse anti-NeuN (Merck, Cat. No. MAB377), polyclonal rabbit anti-PSD95 (Abcam, Cat. No. ab18258), monoclonal rabbit anti-PSD95 (Cell Signaling Technology, Danvers, MA, USA), polyclonal rabbit anti-VGAT (Synaptic Systems, Cat. No. 131003), monoclonal mouse anti-VGlutI (Synaptic Systems, Cat. No. 135511).

Perfusion-fixed brains were washed in PBS and cut into free-floating sections using a vibrating microtome set at 70 μm section thickness (Vibratom VT1000S; Leica Biosystems). After permeabilization for 1 h at room temperature in 0.6% Triton X-100/PBS slices were blocked in 1× Blocking Reagent for ELISA (Merck) for 1 h before being incubated with primary antibodies overnight at room temperature. Further immunohistochemical staining of brain slices followed the procedure described above for primary cells. Specimens were coverslipped on microscopic slides using Dako Fluorescent Mounting Medium (Dako).

Image Acquisition and Analysis

Confocal fluorescence microscopy was performed using a Zeiss LSM510 Meta confocal microscope equipped with a 63× Plan-Apochromat oil immersion objective, NA 1.4 (Carl Zeiss Microscopy). Confocal image stacks of stained neuronal cultures and hippocampal slices were recorded with LSM510 software [microns per pixel (x, y, z): 0.28 μm, 0.28 μm, 0.5 μm] with excitation and emission settings kept constant during the recording of sample material from different experimental groups.

Determination of Cox4 Immunoreactivity *in vitro*

Protein expression levels of Cox4 *in vitro* were quantified with ZEN 2 (Carl Zeiss Microscopy) in confocal images of lentivirally transduced primary neuronal cultures immunocytochemically stained against Cox4. To this end, mean gray value intensities of Cox4 immunoreactivity in 50 μm^2 somatic regions of interest (ROI) of EGFP positive neurons were quantified with the help of ZEN's measure function. ROIs were placed in neuronal cytoplasm in confocal z-planes which showed maximum diameters of neuronal somata.

Determination of Cox4 Immunoreactivity *in vivo*

Quantification of Cox4 expression *in vivo* was carried out on confocal z-stacks of lentivirally transduced hippocampal tissue immunohistochemically stained for Cox4 and labeled with the nuclear dye Hoechst 33258. Image stacks were loaded into Imaris 8 (Bitplane) and 3-dimensional ROIs of EGFP positive neuronal cell somata were generated using Imaris' surface

creation functionality. Respective ROIs were used to mask EGFP fluorescent signals and to subsequently generate a new image channel representative of the somatic EGFP signal ($EGFP^{soma}$) determined by the ROIs selected. To exclude nuclear regions from the downstream quantification of Cox4 immunoreactivity, additional ROIs for neuronal nuclei (positive for Hoechst 33258) were generated using Imaris' surface tool and subtracted from the $EGFP^{soma}$ image channel resulting in another image channel devoid of nuclear regions ($EGFP^{cytoplasm}$). Three-dimensional ROIs of the $EGFP^{cytoplasm}$ image channels generated using Imaris' surface tool were finally used to quantify mean gray value intensities of Cox4 immunoreactivity and to generate another image channel representing Cox4 immunoreactivity located inside the cytoplasm of EGFP positive neurons.

Determination of Neuronal Survival *in vivo*

Quantification of Draq5 positive nuclei in the granule cell layer of the dentate gyrus was carried out using Imaris' spots creation functionality. Confocal image stacks of the hippocampal granule cell layer immunohistochemically stained for NeuN and labeled with the nuclear dye Draq5 were loaded into Imaris. Appropriate values for expected spot size were set (7 μm) and nuclei were individually detected as spots in defined ROIs [x, y, z (μm): 70, 135, 30] inside the granule cell layer. To initially investigate whether all nuclei present in the granule cell layer were of neuronal origin, the colocalization of Draq5 signals and the neuronal marker NeuN was analyzed. First, the number of Draq5 signals was determined as described above. Resulting spot structures were used to mask the NeuN channel creating a new image channel. The new image channel was then used to run a second round of spot detection detecting only NeuN positive cell nuclei (see also **Supplementary Figure S5**). The reliability of the method described above was confirmed by comparing the results of a manual count with those of the automated determination. Analysis of five different confocal z-stacks yielded an accuracy of the automated protocol of 98.99% [±1.36 (SEM)].

Quantification of Clusters of Synaptic Marker Proteins

Quantification of immunocytochemically/immunohistochemically labeled clusters of synaptic marker proteins was carried out using confocal z-stacks of either additionally MAP2 stained primary rat neuronal cultures or hippocampal tissue, both transduced with respective lentiviral suspensions. Twenty micrometer segments of proximal dendrites were defined as ROIs using Imaris' surface creation tool and either MAP2 immunoreactivity (primary neurons) or EGFP expression (hippocampal tissue). The position of ROIs was solely based on MAP2 immunoreactivity or EGFP fluorescence to avoid any bias towards the distribution of synaptic marker protein staining. Generated ROIs were used to mask image channels of stained synaptic marker proteins allowing for the isolation of the corresponding immunoreactivity located in the previously defined ROI. The number of synaptic marker protein clusters was then determined using the Imaris' surface creation tool, which was applied to the ROI-specific immunoreactive signals of the synaptic marker protein analyzed.

Calcium Imaging

Cal520®-AM (AAT Bioquest) was originally dissolved in DMSO containing 20% (v/v) Pluronic® F-127 to yield stock solutions of 10 mM. At DIV14, primary rat neurons cultivated in 96-well μCLEAR® microplates and transduced with AAV suspensions on DIV2 were labeled by incubation with 1 μM Cal520®-AM in culture medium for 30 min. Subsequently, calcium transients, i.e., temporal changes in green fluorescence, were recorded in complete culture medium using an FDSS/μCell (Hamamatsu). Raw data was analyzed using FDSS software and Origin 2015 (OriginLab Corporation, Northampton, MA, USA).

Western Blotting

Primary rat neurons were cultivated in 6-well plates and harvested in lysis buffer (10 mM Tris-HCL pH 7.5, 100 mM EDTA, 10 mM NaCl, 0.5% (v/v) Triton-X-100, 0.5% (w/v) Sodium deoxycholate) on ice at DIV16. Protein concentrations were determined with the Pierce™ BCA Protein Assay Kit (Thermo Fisher Scientific, Waltham, MA, USA) according to manufacturer's guidelines. Lysates were separated by SDS-PAGE and transferred to a nitrocellulose membrane followed by incubation with the following primary antibodies: monoclonal mouse anti-gephyrin (1:1,000; Synaptic Systems), monoclonal mouse anti-β-actin (1:10,000; Merck). Bound primary antibodies were detected using fluorescently labeled, mouse-specific secondary antibodies (Dianova). Corresponding fluorescent signals were acquired with a Typhoon Trio Variable Mode Imager (GE Healthcare).

Transcriptome Sequencing

For transcriptome sequencing, primary rat neurons were lysed in RLT buffer at DIV16 and total RNA was extracted using the RNeasy Mini Kit (Qiagen). The quality and quantity of RNA were measured using an RNA 6000 Nanochip on the 2100 BioAnalyzer (Agilent Technologies). Thirty nanogram of total RNA was converted to cDNA using the Ovation RNA-Seq System V2 (Nugen Technologies) according to manufacturer's protocols. This cDNA was used to construct libraries for next-generation sequencing using Ovation Rapid DR Multiplex System (Nugen Technologies) according to the manufacturer's protocols. Sequencing was performed on HiSeq2500 instruments (Illumina) with paired-end sequencing, 100 bp read length, yielding an average of 75 million read pairs per sample.

Detection of Differentially Expressed Transcripts

Sequencing data were processed with bcl2fastq (version 1.8.2, Illumina) to demultiplex sequencing reads. Sequencing adapters were trimmed using Skewer [version 0.1.116 (Jiang et al., 2014)]. The trimmed reads were mapped to the rat reference genome (RNor5, Illumina iGenomes) using STAR [version 2.3.0e_r291 (Dobin et al., 2013)] with default parameters. Transcription was quantified on Ensembl transcripts [release 75 (Flicek et al., 2014)] and differential expression computed using Cuffdiff [version 2.1.1 (Trapnell et al., 2013)] based on the pooled dispersion model and geometric library size

normalization. Differentially expressed genes were identified at a significance threshold of $p < 0.05$ (FDR-corrected p-values) in two comparisons: (1) miCox79 vs. miCTR; and (2) miCox474 vs. miCTR. Mayday (Battke et al., 2010) was used for the heatmap generation. Venn diagrams were generated using InteractiVenn (Heberle et al., 2015).

Statistics

Statistical analyses (unpaired *t*-test, Mann–Whitney test, multiple *t*-tests, one-way ANOVA, Kruskal–Wallis test, *post hoc*-tests where applicable) were performed with GraphPad Prism 7 (GraphPad Software). Unless stated otherwise, experiments were carried out three times. Apart from the quantifications *in vivo*, results shown are representative of one of three experiments conducted, which all replicated the respective experimental findings. For analyses *in vivo*, three rats per experimental condition, i.e., lentiviral suspension applied, were used. Error bars indicate the standard error of the mean (SEM).

All experimental procedures described were conducted according to standard biosecurity and institutional safety procedures.

RESULTS

RNAi-Mediated Knockdown of Cox4 for Modeling Mitochondrial Impairment

A decline of complex IV activity has been detected in individuals diagnosed with MCI (Mutisya et al., 1994; Cardoso et al., 2004). To generate a corresponding model of age-related mitochondrial impairment, we, therefore, chose to interfere with the expression of subunit 4 (Cox4) of cytochrome c oxidase, a subunit reported being essential for assembly and respiratory function of complex IV (Li et al., 2006). Lentiviral vectors were employed that expressed Cox4-specific miRNAs, namely miCox79 or miCox474, or a control miRNA under the control of a mouse CaMKII promoter, which restricts miRNA expression to neurons. Furthermore, the expression of EGFP under the control of a rat synapsin promoter allowed for the identification of successfully transduced cells *in vitro* and *in vivo* (**Figures 1A**, **4A**). Knockdown efficacies of either miCox79 or miCox474 were first determined by qRT-PCR after the quantitative transduction of rat primary neurons *in vitro*. miCox79 and miCox474 significantly reduced Cox4 mRNA levels to 34% and 73% of control transduced cells (miCTR; **Figure 1B**). The functionality of both miCox79 and miCox474 was confirmed on the protein level utilizing quantitative immunocytochemistry using an antibody specific for Cox4 (**Figure 1C**).

A salient problem of interference with components of the mitochondrial respiratory chain is a potential effect on general cellular viability. Decreased viability may systemically and unspecifically affect cell survival and thereby preclude the analysis of drugs designed to modulate cellular physiology, e.g., intracellular signaling pathways. An analysis of cell viability and induction of apoptosis (**Figures 1D,E**), overall ATP content and MMP (**Supplementary Figures S1A,B**) in cultures of rat primary neurons revealed no significant differences between Cox4 knockdown and control. However, ATP content was significantly decreased by up to 15% after coincubation with a minimum of 20 pM of the complex I inhibitor rotenone (**Figure 1F**). In conclusion, our observations argue for a mild impairment of mitochondrial function after partial Cox4 knockdown, which was detectable after additional treatment with rotenone as a second stressor.

Cox4 Knockdown Impairs Synaptic Connectivity

Synaptic loss is a hallmark of neurodegenerative diseases and is mechanistically linked to early symptoms like MCI in the case of AD. We, therefore, determined cluster densities of synaptic marker proteins Gephyrin and PSD95 on dendritic segments of rat primary neurons after knockdown of Cox4. Quantitative immunocytochemistry revealed that miRNAs for Cox4 knockdown decreased Gephyrin cluster densities, indicative for GABAergic postsynaptic components, to 60% and 66%, respectively. PSD95 cluster densities, indicative for glutamatergic postsynaptic components, were decreased to 49% and 44% (**Figures 2A–C**). The significant reduction of synaptic marker densities by two independent miRNAs targeting Cox4 excluded potential off-target effects.

To additionally confirm that the observed reduction in synaptic marker densities is not due to an unspecific, toxic effect of mitochondrial impairment caused by knockdown of Cox4, the efficacy of drugs suggested to modulate clustering of Gephyrin was tested. We chose the GSK3β antagonist SB216763 since GSK3β is known to negatively regulate Gephyrin clustering (Wuchter et al., 2012; Tyagarajan et al., 2013). Likewise, the AMPK inhibitor compound c was applied to potentially upregulate mTOR activity. AMPK, which is a negative regulator of mTOR, the latter being required for Gephyrin clustering, becomes activated upon mitochondrial deficits (Wuchter et al., 2012; Beuter et al., 2016). Neither SB216763 nor compound c significantly modulated Gephyrin cluster densities in rat primary neurons expressing miCTR. By contrast, inhibition of GSK3β by SB216763 significantly rescued the effect of Cox4 knockdown on Gephyrin cluster density number, while compound c remained ineffective (**Figure 2D**, **Supplementary Figure S2**).

The observed reduction in Gephyrin clustering might be a consequence of reduced Gephyrin expression and/or enhanced cleavage by the calcium-dependent protease calpain after the Cox4 knockdown (Tyagarajan et al., 2013). However, Western Blot analysis revealed that Gephyrin protein levels remained unaffected after knockdown of Cox4 (**Supplementary Figure S3**).

In summary, partial knockdown of Cox4 expression *in vitro* reduced the densities of excitatory as well as inhibitory synaptic markers. Furthermore, the observed decrease in Gephyrin cluster density is explained most likely by dissociation of Gephyrin scaffolds from postsynapses rather than a depletion of Gephyrin molecules.

The observed loss of essential synaptic components might result in neuronal network perturbations at the functional level. Therefore, calcium transients were measured in rat primary

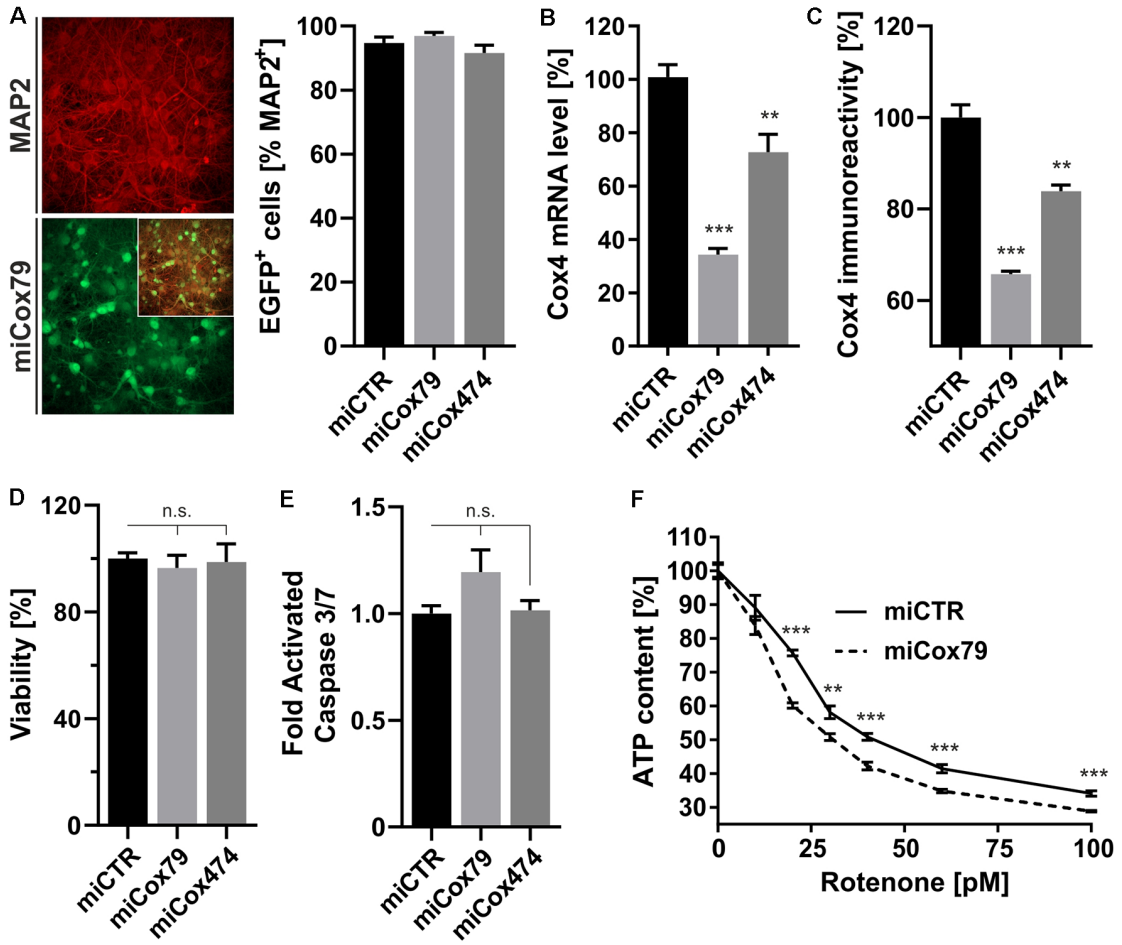

FIGURE 1 | Neuron-specific knockdown of Cytochrome C Oxidase subunit 4 (Cox4). **(A)** Determination of lentiviral transduction efficiency, i.e., percentage of cells positive for both virally expressed EGFP and neuronal marker Microtubule-associated protein 2 (MAP2). Micrographs depict confocal images of a rat primary neuronal culture transduced with Lenti04CmiCox79/SEW (miCox79) and counterstained for MAP2. $n = 10$ images for all groups. **(B,C)** Knockdown of rat Cox4 expression as assessed by quantitative real-time PCR **(B)** and single-cell quantitative immunocytochemistry **(C)** in lentivirally transduced primary rat neurons *in vitro*. One-way ANOVA, Dunnett's multiple comparisons test. $^{***}p < 0.001$; $^{**}p < 0.01$. $n = 6$ wells for all groups **(B)**. Kruskal–Wallis test, Dunn's multiple comparisons test. $^{***}p < 0.001$; $^{**}p < 0.01$. $n = 25$ cells for all groups **(C)**. **(D,E)** Determination of cell viability and activated caspase 3/7 (ApoLive-Glo™ Multiplex Assay) in cultures of rat primary neurons after lentiviral transduction with either miCTR, miCox79 or miCox474 expressing lentiviral vectors. One-way ANOVA, Dunnett's multiple comparisons test. n.s., not significant. $n = 6$ wells for all groups. **(F)** Determination of ATP content in primary rat neurons transduced with miCTR or miCox79 expressing lentiviral vectors and treated with picomolar concentrations of rotenone for 30 min before measurement. Multiple *t*-tests. $^{***}p < 0.001$; $^{**}p < 0.01$. $n = 6$ wells for all groups.

neurons loaded with the synthetic calcium sensor Cal520®-AM. miCox79 and miCTR sequences were expressed after transduction *via* AAV vectors (**Figure 3A**). Coexpression of mCherry (transduction control) and functionality of miCox79 was assured using fluorescence microscopy and qRT-PCR analysis of transduced cultures (**Figure 3B**, **Supplementary Figure S4**). At 14 DIV, control cultures displayed robust network activity as shown by rhythmic and synchronized peaks (**Figure 3C**, upper panel). In the presence of Cox4 knockdown (**Figure 3C**, lower panel), the rhythmicity of network activity decreased while network synchronicity was retained. Accordingly, calculation of the coefficient of variation (CV) of peak-to-peak interval revealed a significant increase in the case of Cox4 knockdown, while no difference was found between untransduced and miCTR transduced cultures (**Figure 3D**). Determination of peak rates (peaks/minutes) showed no significant differences between untreated and miCTR or miCox79 expressing cultures (**Figure 3F**), pointing towards high peak frequencies in episodes of elevated network activity in the case of Cox4 knockdown (**Figure 3C**, lower panel). Indeed, quantification of peak-to-peak intervals filtered for intervals shorter than 10 s to address episodes of elevated network activity revealed a highly significant decrease in the duration of peak-to-peak intervals for miCox79 expressing cultures when compared to either untreated or control transduced cultures (**Figure 3E**). In summary, the decrease in synaptic density after knockdown of Cox4 described above coincides with decreased network rhythmicity.

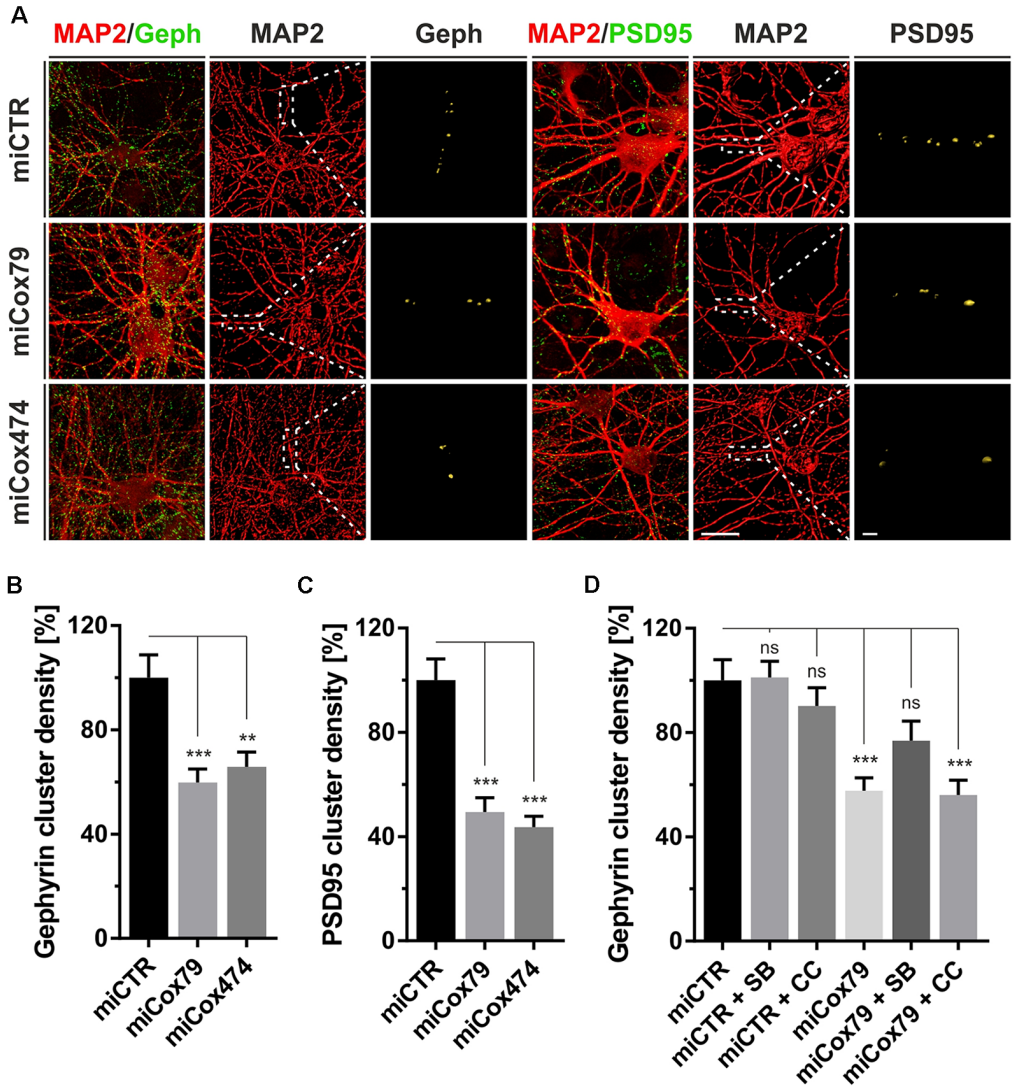

FIGURE 2 | Synaptic loss *in vitro* after knockdown of Cox4. **(A)** Micrographs of cultured primary rat neurons transduced with lentiviral suspensions for the expression of either miCTR, miCox79, or miCox474 and stained for neuronal markers MAP2, Gephyrin (Geph), and PSD95, respectively. The respective left images (EGFP/Geph, EGFP/PSD95) represent maximum intensity projections (MIP) of confocal z-stacks. The remaining tiles depict neuronal cultures after surface rendering using immunofluorescent signals of marker proteins indicated. Segmentation of Gephyrin and PSD95 positive immunofluorescent signals was carried out on 20 μm segments of primary dendrites (dashed boxes). Scale bars, 20 μm, and 2 μM, respectively. **(B,C)** Quantification of Gephyrin and PSD95 cluster densities on 20 μm segments of primary dendrites of hippocampal neurons transduced as indicated. $n = 39$ dendritic segments for all groups. Kruskal–Wallis test, Dunn's multiple comparisons test. $^{***}p < 0.001$; $^{**}p < 0.01$. **(D)** Quantification of Gephyrin cluster densities on 20 μm segments of primary dendrites. Hippocampal neurons were transduced with lentiviral suspensions and treated with pharmacological inhibitors as indicated. SB, SB216763 (GSK3 inhibitor); CC, Compound C (AMPK inhibitor). Kruskal–Wallis test, Dunn's multiple comparisons test. $^{***}p < 0.001$. ns, not significant. $n = 40$ dendritic segments for all groups.

Knockdown of Cox4 Induces Synaptic Loss *in vivo*

Employing stereotaxic injections of lentiviral suspensions into the dentate gyrus of the hippocampus of adult female rats we wanted to further examine potential effects of a knockdown of Cox4 with respect to neuronal survival or synaptic connectivity *in vivo*. Successful transduction of hippocampal neurons and subsequent neuronal expression of EGFP led to prominent labeling of the dentate gyrus which allowed for a clear identification of its granule cell layer and molecular layer (**Figure 4A**). We detected a spread of viral transduction, i.e., EGFP-positive neurons, 1–2 mm in the anterior-posterior direction. Using quantitative immunohistochemistry, the successful knockdown of Cox4 was confirmed in somata of transduced granule cells (66% and 87% of residual Cox4 immunoreactivity for miCox79 and mi474, respectively; **Figures 4B,C**). Of note and underlining the findings *in vitro*, partial Cox4 knockdown did not show any detectable impact on neuronal survival *in vivo* 4 weeks after lentiviral transduction (**Figures 4D–G**) as assessed by

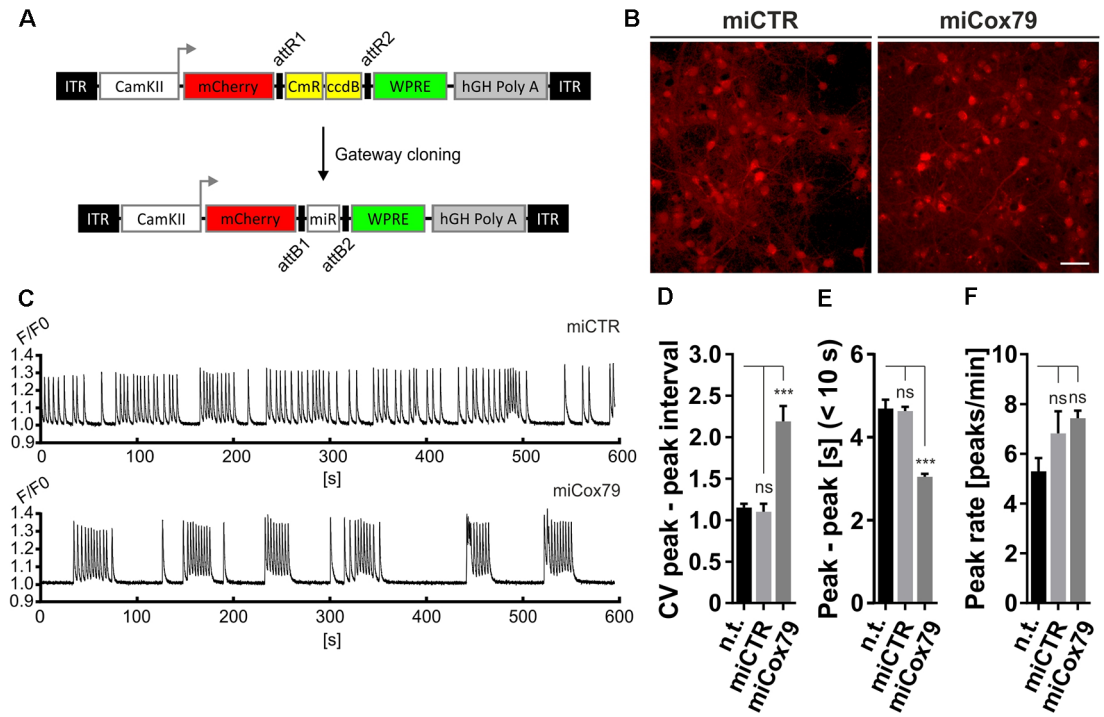

FIGURE 3 | Altered network rhythmicity after knockdown of Cox4. **(A)** Structure of AAV constructs for bicistronic expression of mCherry and miRNA sequences under the control of a functional mouse α-CaMKII promoter fragment. Respective miRNA sequences are transferred by Gateway cloning. ccdB, ccdB gene; CmR, Chloramphenicol resistance; ITR, inverted terminal repeats; WPRE, Woodchuck Hepatitis Virus Posttranscriptional Regulatory Element. **(B)** Successful transduction of rat primary neurons using both AAV_C1.3_mCherry_miCTR_W (miCTR) and AAV_C1.3_mCherry_mi79_W (miCox79) viral suspensions as assessed by mCherry expression. Scale bar, 50 μm. **(C)** Recordings of intracellular calcium levels indicative of neuronal network activity after transduction of primary rat neurons with either miCTR or miCox79 expressing AAVs. Intracellular calcium transients were detected using Cal-520® AM. Each graph depicts the Cal-520® AM intensity (F/F0 ratio) recorded from one well of a 96-Well plate using Hamamatsu's FDSS/μCELL. **(D–F)** Quantification of peak-to-peak interval coefficient of variation (CV), peak-to-peak interval [s] filtered for intervals <10 s, and average peak rate (peaks/min) from recorded cultures transduced as indicated. One-way ANOVA, Dunnett's multiple comparisons test, $n = 6$ wells for all groups in **(D,F)**. **(E)** Kruskal–Wallis test, Dunn's multiple comparisons test, $n = 168$ (n.t.), 367 (miCTR), and 321 (miCox79) from six wells each. $^{***}p < 0.001$. ns, not significant; n.t., not treated.

the number of neuronal somata in the granule cell layer. We further assessed whether the phenotype of reduced synaptic connectivity could be reproduced *in vivo*. To this end, brain slices obtained from stereotaxically injected rats were prepared for immunohistochemistry 4 weeks after surgery and stained for inhibitory as well as excitatory pre- and postsynaptic markers. Z-stacks of the dendritic trees of hippocampal granule neurons extending into the molecular layer of the dentate gyrus were recorded by confocal laser scan microscopy and submitted to 3D reconstruction and quantification of clusters of synaptic marker proteins (**Figure 5**). Concurrent to our findings in primary cultures *in vitro*, both miCox79 and miCox474 significantly reduced the densities of postsynaptic Gephyrin (75% and 71%) and PSD95 clusters (62% and 61%) compared to controls (**Figures 5C,D**). Moreover, presynaptic clusters of VGAT (67% and 78%) and VGluT (71% and 68%) were also diminished in number (**Figures 5E,F**). Thus, pre- and post-synaptic markers of excitatory and inhibitory synapses were significantly reduced after Cox4 knockdown *in vivo*. In conclusion, our *in vivo* findings strongly corroborate the *in vitro* phenotype of impaired synaptic connectivity and underscore the validity of the *in vitro* test system.

Transcriptome Analysis

We analyzed the transcriptomes of lentivirally transduced primary neuronal cultures to further assess phenotypic changes after the Cox4 knockdown. As compared to controls (miCTR), miCox79 and miCox474 significantly induced upregulation of 612 and 207 annotated genes, respectively. 567 (miCox79) and 274 genes (miCox474) were found to be significantly downregulated (**Figure 6B**, **Supplementary Table S1**). Of note, 173 downregulated and 104 upregulated transcripts were independently identified in both miCox79 and miCox474 samples. This already accounted for 63% of all downregulated and 50% of all upregulated transcripts found in miCox474. In addition, plotting of the top 10 downregulated and top 10 upregulated genes for miCox79 and miCox474 revealed clear segregation from transcriptomic signatures of miCTR treated samples (**Figure 6A**). As expected, Cox4 expression was downregulated after the expression of

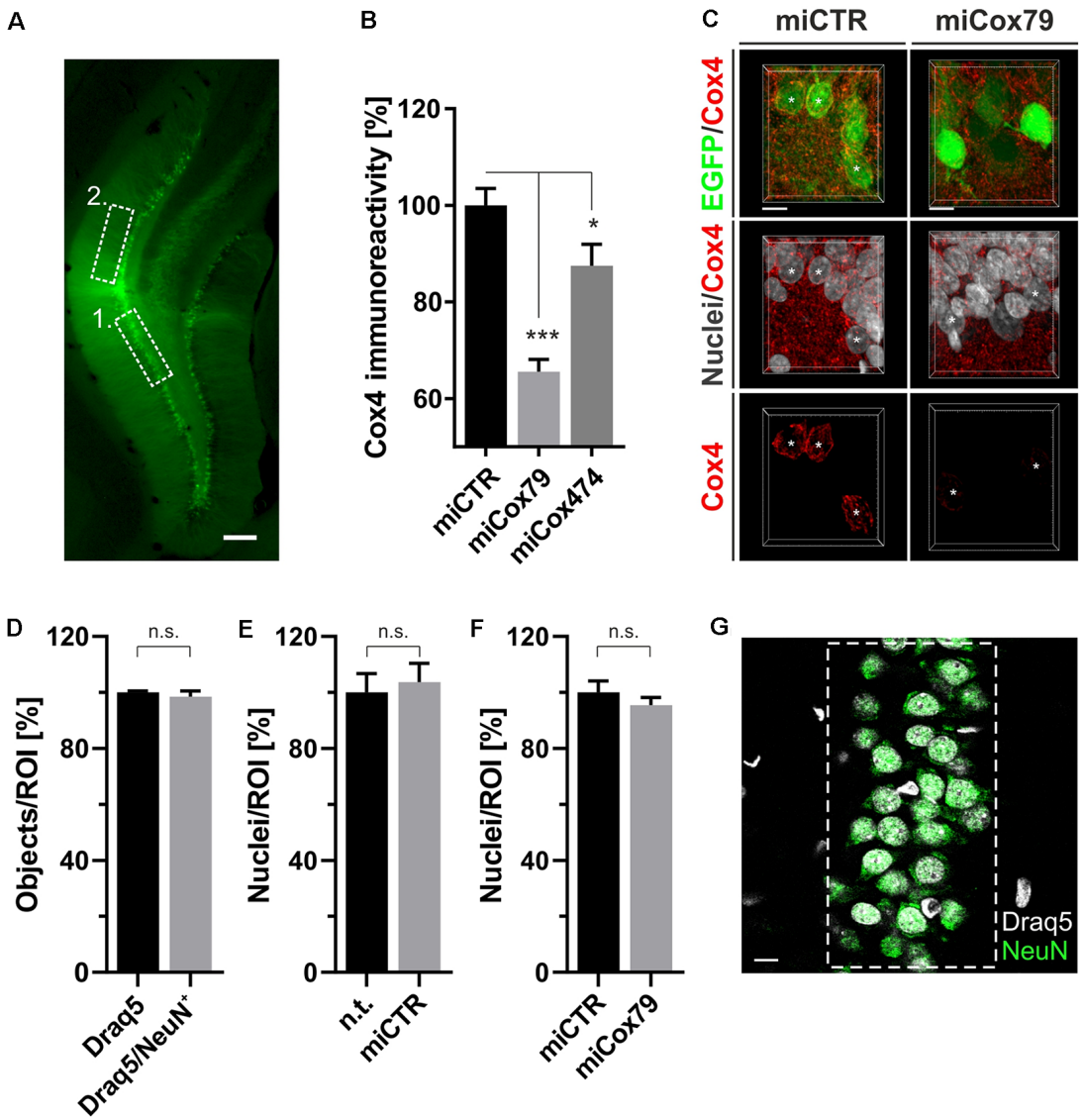

FIGURE 4 | (A) Successful transduction of granule cells of the dentate gyrus *in vivo* as shown by EGFP expression after injection of Lenti04CmiCTR/SEW. Dashed boxes indicate the areas of analysis for 1. Determination of Cox4 expression **(B,C)** and neuronal survival **(D–G)**, i.e., the granule cell layer, and 2. assessment of synaptic connectivity (**Figure 5**), i.e., the molecular layer of the suprapyramidal blade. Scale bar, 200 μm. **(B)** Knockdown of rat Cox4 expression as assessed by single-cell quantitative immunohistochemistry in hippocampal granule cells after stereotaxic injection of respective lentiviral suspensions *in vivo*. One-way ANOVA, Dunnett's multiple comparisons test. ***$p < 0.001$; *$p < 0.05$. $n = 40$ cells for miCTR, $n = 42$ cells for miCox79, and $n = 25$ cells for miCox474. **(C)** MIP of confocal image stacks from hippocampal granule cells after transduction with miCTR or miCox79 expressing lentiviral vectors. Asterisks mark successfully transduced granule cells (EGFP positive) selected for quantification of Cox4 immunoreactivity. Scale bars, 10 μm. **(D)** High percentage of neuronal cells (98%) in the granule cell layer of the dentate gyrus of the rat, as shown by the NeuN labeling of Draq5 stained nuclei. Unpaired *t*-test. n.s., not significant. $n = 3$ animals. Average number of nuclei detected per animal (12 confocal stacks): 653 (Draq5), 629 (Draq5/NeuN). Neuronal cell numbers are not affected under either control **(E)** or Cox4 knockdown conditions **(F)**. Unpaired *t*-test. $n = 3$ animals for both groups in **(E,F)**. n.s., not significant. Average number of nuclei detected per animal (12 confocal stacks) in **(E)**: 648 [n.t. (not treated)], 672 (miCTR). Average number of nuclei detected per animal (15 confocal stacks) in **(F)**: 857 (miCTR), 820 (miCox79). **(G)** Dashed box indicates the region of interest (ROI) delineating the granule cell layer which was used for quantifications in **(D–F)**. Scale bar, 10 μm.

both miCox79 or miCox474. Moreover, we also identified further deregulated genes related to complex IV after expression of miCox79, the miRNA with higher efficacy over miCox474 (downregulated: Cox14, UniProtKB=Q5XFV8); upregulated: Cox6A2, UniProtKB=P10817; Cox11, UniProtKB=M0RE03; Cox18, UniProtKB=D4A568).

Deregulated genes were assigned to gene ontology (GO) clusters with the help of the PANTHER classification tool[3] [(Mi et al., 2013); annotation data sets: biological process complete, cellular component complete; GO Ontology database

[3]http://www.pantherdb.org

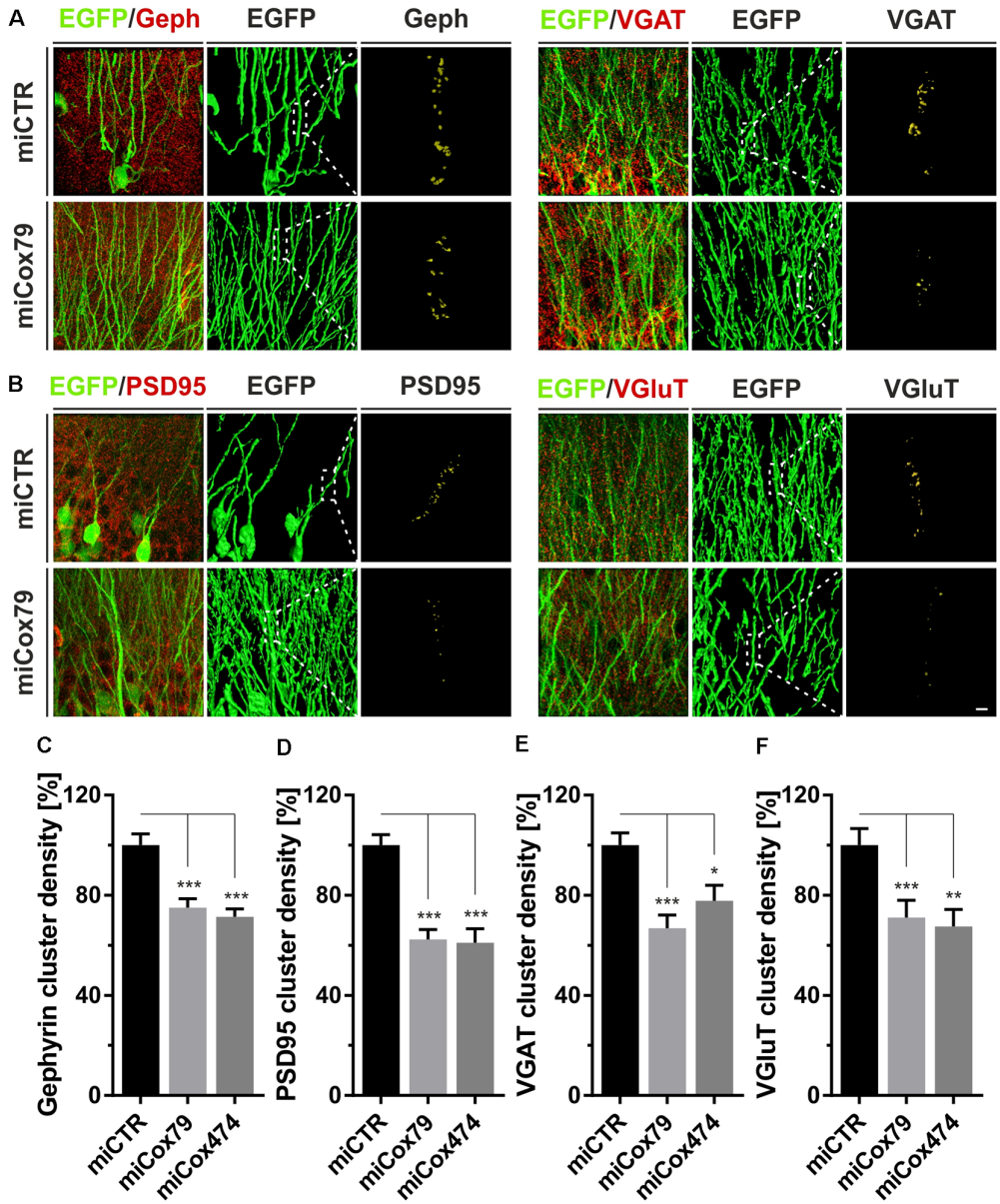

FIGURE 5 | Synaptic loss *in vivo* after knockdown of Cox4. Micrographs of hippocampal granule neurons transduced with lentivirus expressing EGFP and miCTR or miCox79 and stained for synaptic markers Gephyrin (Geph) and VGAT **(A)** or PSD95 and VGluT **(B)**. The respective left images (EGFP/Geph, EGFP/VGAT, EGFP/PSD95, EGFP/VGluT) represent MIP of confocal z-stacks. The remaining tiles depict hippocampal granule neurons after surface rendering using immunofluorescent signals of the marker proteins indicated. Segmentation of synaptic markers was carried out on 20 μm dendritic segments (dashed boxes). Scale bar, 2 μm. **(C–F)** Quantification of Gephyrin, PSD95, VGAT, and VGluT cluster densities on 20 μm segments of primary dendrites of hippocampal granule neurons transduced as indicated. Shown are combined results from three (miCTR, miCox79) and two animals (miCox474), respectively. Kruskal–Wallis test, Dunn's multiple comparisons test. ***$p < 0.001$; **$p < 0.01$; *$p < 0.05$. **(C)** $n = 150$ for miCTR and miCox79, $n = 145$ for miCox474; **(D–F)** $n = 90$ for miCTR and miCox79, $n = 60$ for miCox474.

released 2020-01-03]. GO clusters obtained (FDR < 0.05; **Supplementary Table S1**) were aligned between miCox79 and miCox474 treated samples to identify clusters significantly and independently enriched after application of both miRNAs pointing towards a specific effect of Cox4 knockdown. 456 common GO clusters for biological processes emerged using either (miCox79, miCox474) list of downregulated genes, 71 GO clusters were identified for cellular components. These numbers made up 77% and 92% of all clusters identified for miCox474, respectively. In comparison, only three common GO clusters for biological processes and nine common GO clusters for cellular components were found based on upregulated genes (60% and 90% of all clusters identified for miCox474, respectively).

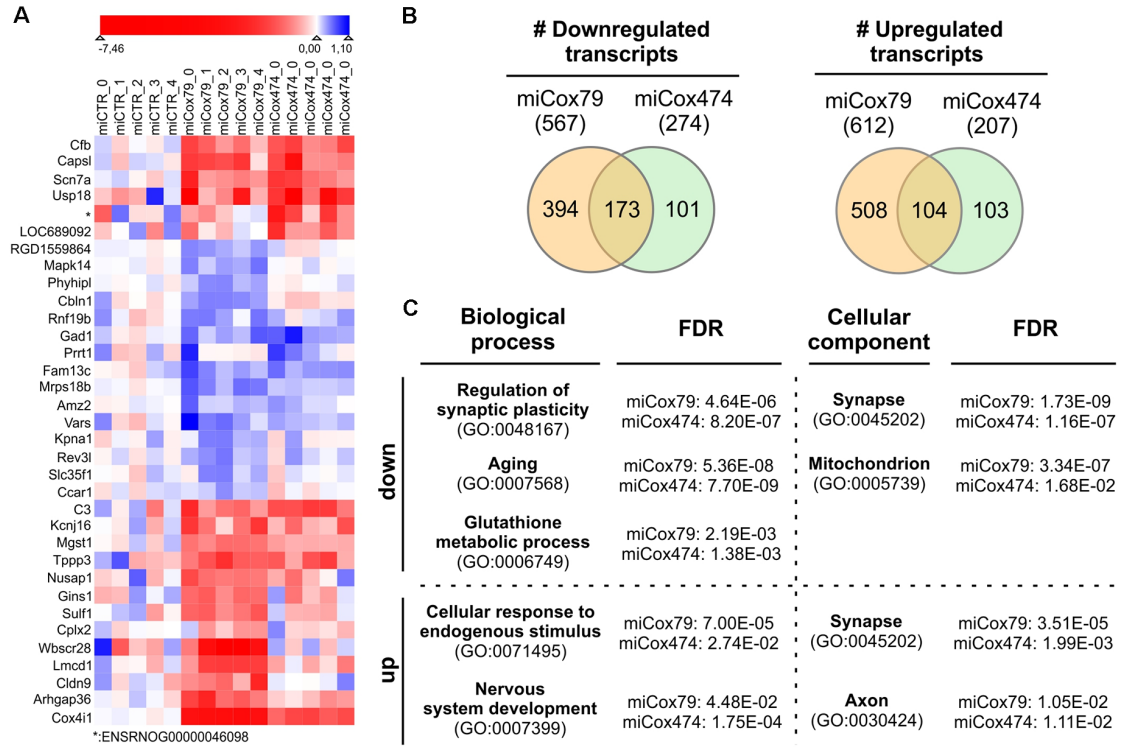

FIGURE 6 | Transcriptomic alterations after knockdown of Cox4. **(A)** Heatmap of top differentially expressed genes. The top 10 downregulated and top 10 upregulated genes (by fold change between conditions) were selected both for miCox79 and miCox474. Due to overlap in the lists between the miCox79 and miCox474 conditions, 34 genes are included in the plot. Individual replicates are shown for each condition, log2 foldchange normalized to the average of the expression in all miCTR replicates is shown on a sigmoid red-blue gradient. Genes are sorted by hierarchical clustering on normalized log2 fold changes (euclidean distance). *no gene symbol associated. **(B)** Venn diagrams showing the distribution of differentially expressed transcripts following miCox79 or miCox474 treatment compared to control (miCTR). **(C)** PANTHER gene ontology (GO) analysis (statistical overrepresentation test) based on mRNAs significantly deregulated after the Cox4 knockdown. Selected GO clusters from annotation data set "biological process" and "cellular component" are shown, that were identified in both miCox79 and miCox474 datasets [Fisher's exact test, false discovery rate (FDR) calculation]. For a complete list of GO clusters identified for miCox79 and miCox474 see **Supplementary Table S1**. down/up, GO clusters identified based on a list of downregulated and upregulated transcripts, respectively.

GO clusters found after assignment of downregulated genes were linked to synaptic function, cellular responses to oxidative stress, as well as aging. This is in line with our working hypothesis that an age-related decline of mitochondrial function is linked to synaptic impairments that are faithfully reproduced in our model (**Figure 6C**). Findings in the annotation data set biological process complete was paralleled by the GO cluster "synapse" (GO:0045202) for cellular components. Besides, genes belonging to the GO cluster "mitochondrion" (GO:0005739) were identified as significantly overrepresented in both miCox79 and miCox474 lists of downregulated genes. Concerning upregulated genes, the appearance of the cluster "synapse" (GO:0045202) underlines a dysregulation of genes involved in synaptic functioning as GO clusters for synaptic functions and cellular compartment were also identified in lists of downregulated genes.

DISCUSSION

Here, we present a novel model for age-related neurodegeneration based on mitochondrial impairment through partial inhibition of Cox4 expression. The model displays construct validity by interfering with complex IV known to be impaired in AD. Face validity is suggested by reduced synapse numbers and transcriptomic profiles that highlight aspects of age-related neuronal dysfunction. Thus, the Cox4 knockdown model appears to be a useful tool for phenotypic drug testing in the context of neuronal malfunction caused by mitochondrial impairment.

Aging is linked to mitochondrial dysfunction and concomitant cognitive decline (Trifunovic and Larsson, 2008). Therefore, interference with mitochondrial function and synaptic stability appears to be a reasonable starting point for the development of a new model for age-related dementia. Reduced synaptic connectivity in conjunction with a loss in spatial memory is the most salient symptom associated with dementia in general and AD (Lithfous et al., 2013; Spires-Jones and Hyman, 2014). Further, the course of AD is characterized by a loss of synaptic plasticity and connectivity before cell death occurs (Terry et al., 1991; Coleman and Yao, 2003). Our Cox4 knockdown model shows reduction of synaptic markers in conjunction with altered neuronal network rhythmicity

in vitro suggesting a representation of impaired synaptic connectivity as observed in neurodegenerative phenotypes. Direct measurements of mitochondrial function and integrity like ATP content or MMP did not show major abnormalities under basic load. However, co-treatment of neuronal cultures with picomolar concentrations of the complex I inhibitor rotenone revealed reduced levels of ATP in the presence of Cox4 knockdown. Synaptic transmission is considered a cellular process with a particularly high-energy demand. Failure of mitochondria to respond to peaks of energy demand because of a diminished spare respiratory capacity might lead to synaptic malfunction and subsequent synaptic loss as observed in our model *in vitro* as well as *in vivo*. Our *in vitro* model is likely to reflect pathogenic phenotypes only partially due to an early developmental stage of the neurons cultured as well as an unknown absolute and spatial representation of interneurons. However, results obtained using calcium imaging document alterations in synaptic transmission, i.e., overall network rhythmicity, after synaptic loss. At his stage, however, it is unclear, whether this parameter is predictive for the action of drugs.

In a previous report, a similar strategy to reduce complex IV activity was applied (Diaz et al., 2012). The Cox10 subunit of cytochrome c oxidase was deleted in conditional knockout mice after CRE expression under the control of the CaMKII promoter. These mice showed reduced survival starting at month 4 after birth and died between months 8 and 12 probably due to cortical atrophy. Accordingly, Cox10 interference was considered as a model for encephalopathy and was not applicable as a model for age-related dementia. Our model based on partial Cox4 downregulation in mature, tightly integrated neurons appeared to be less harmful since no loss of transduced neurons was observed *in vivo* throughout the investigation. Possible effects of Cox4 knockdown at later stages than tested in this report would have to be determined in subsequent studies. Likewise, an application of Cox10 interference for the development of *in vitro* test systems remains to be assessed.

Transcriptomic analysis disclosed changes in gene expression after the Cox4 knockdown that nicely correlated with our findings regarding impaired synaptic connectivity *in vitro* and *in vivo*. Deregulated transcripts identified in both miCox79 and miCox474 groups comprised important players of synaptic plasticity such as the transcription factor Egr1, the motor protein Myo6 enriched at the postsynaptic density and the serine proteinase tissue-type plasminogen activator (Plat). For Egr1, decreased expression has been reported in aged animals and models of AD correlating with associated deficits in synaptic plasticity (Koldamova et al., 2014; Penner et al., 2016). Also, analysis of post-mortem brain tissue from non-demented controls and individuals with AD revealed changes in Egr1 expression corresponding with disease progression (Hu et al., 2019). Interference with Myo6 function, necessary for proper postsynaptic AMPA receptor trafficking, was shown to reduce synaptic numbers and impair AMPA receptor recruitment to postsynaptic sites (Wu et al., 2002; Osterweil et al., 2005; Nash et al., 2010). Likewise, a role for the stabilization of postsynaptic AMPA receptors has been assigned to Plat and the tPA-plasmin system (Diaz et al., 2019), the activity of which is decreased in aged individuals and existing models of AD (Ledesma et al., 2000; Melchor et al., 2003).

Besides further emphasizing our model's phenotype of altered synaptic connectivity, clusters of deregulated genes also shared additional similarities with gene expression patterns observed in AD. These comprised key players of the glutathione metabolic process, e.g., members of the Gst-superfamily, which have been reported to show decreased activity also in AD possibly leading to increased oxidative stress, a process that precedes AD hallmarks like the formation of senile plaques (Lovell et al., 1998; Ansari and Scheff, 2010). In this regard, further studies would be required to determine the degree of cellular oxidative stress after the Cox4 knockdown.

Since, our model did not display neuronal loss and showed responsiveness to pharmacological treatment as exemplified by inhibition of GSK3β, phenotypes observed are unlikely to be the consequence of decreased general cellular viability. We, therefore, propose partial knockdown of Cox4 as a novel strategy to model early phases of age-related neurodegeneration characterized by impaired synaptic connectivity.

DATA AVAILABILITY STATEMENT

The transcriptomic data generated for this study can be found in the NIH Sequence Read Archive (SRA; https://www.ncbi.nlm.nih.gov/sra/PRJNA591113).

ETHICS STATEMENT

The animal study was reviewed and approved by Regierungspräsidium Tübingen, Konrad-Adenauer-Str. 20, 72072 Tübingen.

AUTHOR CONTRIBUTIONS

MK constructed lentiviral and AAV expression vectors, determined corresponding knockdown efficacies, performed ATP and MMP (JC-10) quantifications, calcium measurements, and PANTHER GO analyses and contributed to manuscript writing. JE performed stereotaxic injections, determination of neuronal numbers *in vivo*, analyses of synaptic marker densities *in vitro* and *in vivo*, Western Blot experiments, and ATP quantifications. FB and SG conducted transcriptome sequencing and detection of differentially expressed transcripts. HV wrote the manuscript and contributed to the study design. All authors contributed to manuscript revision, read, and approved the submitted version.

FUNDING

This work was funded by grants EuroTransBio MitoModels (Bundesministerium für Bildung und Forschung, reference number 0315774B) and Eurostars A-ADAM (Bundesministerium für Bildung und Forschung, reference number 01QE1703C).

ACKNOWLEDGMENTS

We thank Christine Dürr for technical assistance. We are very grateful for important discussions with Robert Wronski, QPS Austria GmbH.

SUPPLEMENTARY MATERIAL

The Supplementary Material for this article can be found online at: https://www.frontiersin.org/articles/10.3389/fnmol.2020.00043/full#supplementary-material.

REFERENCES

Ansari, M. A., and Scheff, S. W. (2010). Oxidative stress in the progression of Alzheimer disease in the frontal cortex. *J. Neuropathol. Exp. Neurol.* 69, 155–167. doi: 10.1097/NEN.0b013e3181cb5af4

Battke, F., Symons, S., and Nieselt, K. (2010). Mayday-integrative analytics for expression data. *BMC Bioinformatics* 11:121. doi: 10.1186/1471-2105-11-121

Beuter, S., Ardi, Z., Horovitz, O., Wuchter, J., Keller, S., Saha, R., et al. (2016). Receptor tyrosine kinase EphA7 is required for interneuron connectivity at specific subcellular compartments of granule cells. *Sci. Rep.* 6:29710. doi: 10.1038/srep29710

Bosetti, F., Brizzi, F., Barogi, S., Mancuso, M., Siciliano, G., Tendi, E. A., et al. (2002). Cytochrome c oxidase and mitochondrial F1F0-ATPase (ATP synthase) activities in platelets and brain from patients with Alzheimer's disease. *Neurobiol. Aging* 23, 371–376. doi: 10.1016/s0197-4580(01)00314-1

Cardoso, S. M., Proença, M. T., Santos, S., Santana, I., and Oliveira, C. R. (2004). Cytochrome c oxidase is decreased in Alzheimer's disease platelets. *Neurobiol. Aging* 25, 105–110. doi: 10.1016/s0197-4580(03)00033-2

Coleman, P. D., and Yao, P. J. (2003). Synaptic slaughter in Alzheimer's disease. *Neurobiol. Aging* 24, 1023–1027. doi: 10.1016/j.neurobiolaging.2003.09.001

Diaz, A., Jeanneret, V., Merino, P., Mccann, P., and Yepes, M. (2019). Tissue-type plasminogen activator regulates p35-mediated Cdk5 activation in the postsynaptic terminal. *J. Cell Sci.* 132:jcs224196. doi: 10.1242/jcs.224196

Diaz, F., Garcia, S., Padgett, K. R., and Moraes, C. T. (2012). A defect in the mitochondrial complex III, but not complex IV, triggers early ROS-dependent damage in defined brain regions. *Hum. Mol. Genet.* 21, 5066–5077. doi: 10.1093/hmg/dds350

Dittgen, T., Nimmerjahn, A., Komai, S., Licznerski, P., Waters, J., Margrie, T. W., et al. (2004). Lentivirus-based genetic manipulations of cortical neurons and their optical and electrophysiological monitoring *in vivo*. *Proc. Natl. Acad. Sci. U S A* 101, 18206–18211. doi: 10.1073/pnas.0407976101

Dobin, A., Davis, C. A., Schlesinger, F., Drenkow, J., Zaleski, C., Jha, S., et al. (2013). STAR: ultrafast universal RNA-seq aligner. *Bioinformatics* 29, 15–21. doi: 10.1093/bioinformatics/bts635

Flicek, P., Amode, M. R., Barrell, D., Beal, K., Billis, K., Brent, S., et al. (2014). Ensembl 2014. *Nucleic Acids Res.* 42, D749–D755. doi: 10.1093/nar/gkt1196

Goetze, B., Grunewald, B., Kiebler, M. A., and Macchi, P. (2003). Coupling the iron-responsive element to GFP-an inducible system to study translation in a single living cell. *Sci. STKE* 2003:PL12. doi: 10.1126/stke.2003.204.pl12

Grimm, A., and Eckert, A. (2017). Brain aging and neurodegeneration: from a mitochondrial point of view. *J. Neurochem.* 143, 418–431. doi: 10.1111/jnc.14037

Hauptmann, S., Scherping, I., Dröse, S., Brandt, U., Schulz, K. L., Jendrach, M., et al. (2009). Mitochondrial dysfunction: an early event in Alzheimer pathology accumulates with age in AD transgenic mice. *Neurobiol. Aging* 30, 1574–1586. doi: 10.1016/j.neurobiolaging.2007.12.005

Heberle, H., Meirelles, G. V., Da Silva, F. R., Telles, G. P., and Minghim, R. (2015). InteractiVenn: a web-based tool for the analysis of sets through Venn diagrams. *BMC Bioinformatics* 16:169. doi: 10.1186/s12859-015-0611-3

Hiona, A., Sanz, A., Kujoth, G. C., Pamplona, R., Seo, A. Y., Hofer, T., et al. (2010). Mitochondrial DNA mutations induce mitochondrial dysfunction, apoptosis and sarcopenia in skeletal muscle of mitochondrial DNA mutator mice. *PLoS One* 5:e11468. doi: 10.1371/journal.pone.0011468

Hu, Y. T., Chen, X. L., Huang, S. H., Zhu, Q. B., Yu, S. Y., Shen, Y., et al. (2019). Early growth response-1 regulates acetylcholinesterase and its relation with the course of Alzheimer's disease. *Brain Pathol.* 29, 502–512. doi: 10.1111/bpa.12688

Jiang, H., Lei, R., Ding, S. W., and Zhu, S. (2014). Skewer: a fast and accurate adapter trimmer for next-generation sequencing paired-end reads. *BMC Bioinformatics* 15:182. doi: 10.1186/1471-2105-15-182

Koldamova, R., Schug, J., Lefterova, M., Cronican, A. A., Fitz, N. F., Davenport, F. A., et al. (2014). Genome-wide approaches reveal EGR1-controlled regulatory networks associated with neurodegeneration. *Neurobiol. Dis.* 63, 107–114. doi: 10.1016/j.nbd.2013.11.005

Kriebel, M., Metzger, J., Trinks, S., Chugh, D., Harvey, R. J., Harvey, K., et al. (2011). The cell adhesion molecule neurofascin stabilizes axo-axonic GABAergic terminals at the axon initial segment. *J. Biol. Chem.* 286, 24385–24393. doi: 10.1074/jbc.M110.212191

Ledesma, M. D., Da Silva, J. S., Crassaerts, K., Delacourte, A., De Strooper, B., and Dotti, C. G. (2000). Brain plasmin enhances APP alpha-cleavage and Aα degradation and is reduced in Alzheimer's disease brains. *EMBO Rep.* 1, 530–535. doi: 10.1093/embo-reports/kvd107

Li, Y., Park, J. S., Deng, J. H., and Bai, Y. (2006). Cytochrome c oxidase subunit IV is essential for assembly and respiratory function of the enzyme complex. *J. Bioenerg. Biomembr.* 38, 283–291. doi: 10.1007/s10863-006-9052-z

Lithfous, S., Dufour, A., and Despres, O. (2013). Spatial navigation in normal aging and the prodromal stage of Alzheimer's disease: insights from imaging and behavioral studies. *Ageing Res. Rev.* 12, 201–213. doi: 10.1016/j.arr.2012.04.007

López-Otín, C., Blasco, M. A., Partridge, L., Serrano, M., and Kroemer, G. (2013). The hallmarks of aging. *Cell* 153, 1194–1217. doi: 10.1016/j.cell.2013.05.039

Lovell, M. A., Xie, C., and Markesbery, W. R. (1998). Decreased glutathione transferase activity in brain and ventricular fluid in Alzheimer's disease. *Neurology* 51, 1562–1566. doi: 10.1212/wnl.51.6.1562

Melchor, J. P., Pawlak, R., and Strickland, S. (2003). The tissue plasminogen activator-plasminogen proteolytic cascade accelerates amyloid-α (Aα) degradation and inhibits Aα-induced neurodegeneration. *J. Neurosci.* 23, 8867–8871. doi: 10.1523/jneurosci.23-26-08867.2003

Mi, H., Muruganujan, A., Casagrande, J. T., and Thomas, P. D. (2013). Large-scale gene function analysis with the PANTHER classification system. *Nat. Protoc.* 8, 1551–1566. doi: 10.1038/nprot.2013.092

Mutisya, E. M., Bowling, A. C., and Beal, M. F. (1994). Cortical cytochrome oxidase activity is reduced in Alzheimer's disease. *J. Neurochem.* 63, 2179–2184. doi: 10.1046/j.1471-4159.1994.63062179.x

Nash, J. E., Appleby, V. J., Correa, S. A., Wu, H., Fitzjohn, S. M., Garner, C. C., et al. (2010). Disruption of the interaction between myosin VI and SAP97 is associated with a reduction in the number of AMPARs at hippocampal synapses. *J. Neurochem.* 112, 677–690. doi: 10.1111/j.1471-4159.2009.06480.x

Osterweil, E., Wells, D. G., and Mooseker, M. S. (2005). A role for myosin VI in postsynaptic structure and glutamate receptor endocytosis. *J. Cell Biol.* 168, 329–338. doi: 10.1083/jcb.200410091

Parker, W. D. Jr., and Parks, J. K. (1995). Cytochrome c oxidase in Alzheimer's disease brain: purification and characterization. *Neurology* 45, 482–486. doi: 10.1212/wnl.45.3.482

Penner, M. R., Parrish, R. R., Hoang, L. T., Roth, T. L., Lubin, F. D., and Barnes, C. A. (2016). Age-related changes in Egr1 transcription and DNA methylation within the hippocampus. *Hippocampus* 26, 1008–1020. doi: 10.1002/hipo.22583

Selfridge, J. E., E, L., Lu, J., and Swerdlow, R. H. (2013). Role of mitochondrial homeostasis and dynamics in Alzheimer's disease. *Neurobiol. Dis.* 51, 3–12. doi: 10.1016/j.nbd.2011.12.057

Spires-Jones, T. L., and Hyman, B. T. (2014). The intersection of amyloid beta and tau at synapses in Alzheimer's disease. *Neuron* 82, 756–771. doi: 10.1016/j.neuron.2014.05.004

Stefanatos, R., and Sanz, A. (2018). The role of mitochondrial ROS in the aging brain. *FEBS Lett.* 592, 743–758. doi: 10.1002/1873-3468.12902

Terry, R. D., Masliah, E., Salmon, D. P., Butters, N., Deteresa, R., Hill, R., et al. (1991). Physical basis of cognitive alterations in Alzheimer's disease: synapse loss is the major correlate of cognitive impairment. *Ann. Neurol.* 30, 572–580. doi: 10.1002/ana.410300410

Trapnell, C., Hendrickson, D. G., Sauvageau, M., Goff, L., Rinn, J. L., and Pachter, L. (2013). Differential analysis of gene regulation at transcript resolution with RNA-seq. *Nat. Biotechnol.* 31, 46–53. doi: 10.1038/nbt.2450

Trifunovic, A., and Larsson, N. G. (2008). Mitochondrial dysfunction as a cause of ageing. *J. Intern. Med.* 263, 167–178. doi: 10.1111/j.1365-2796.2007.01905.x

Tyagarajan, S. K., Ghosh, H., Yévenes, G. E., Imanishi, S. Y., Zeilhofer, H. U., Gerrits, B., et al. (2013). Extracellular signal-regulated kinase and glycogen synthase kinase 3beta regulate gephyrin postsynaptic aggregation and GABAergic synaptic function in a calpain-dependent mechanism. *J. Biol. Chem.* 288, 9634–9647. doi: 10.1074/jbc.M112.442616

Valla, J., Schneider, L., Niedzielko, T., Coon, K. D., Caselli, R., Sabbagh, M. N., et al. (2006). Impaired platelet mitochondrial activity in Alzheimer's disease and mild cognitive impairment. *Mitochondrion* 6, 323–330. doi: 10.1016/j.mito.2006.10.004

Wu, H., Nash, J. E., Zamorano, P., and Garner, C. C. (2002). Interaction of SAP97 with minus-end-directed actin motor myosin VI. Implications for AMPA receptor trafficking. *J. Biol. Chem.* 277, 30928–30934. doi: 10.1074/jbc.M203735200

Wuchter, J., Beuter, S., Treindl, F., Herrmann, T., Zeck, G., Templin, M. F., et al. (2012). A comprehensive small interfering RNA screen identifies signaling pathways required for gephyrin clustering. *J. Neurosci.* 32, 14821–14834. doi: 10.1523/JNEUROSCI.1261-12.2012

Xu, J., Shi, C., Li, Q., Wu, J., Forster, E. L., and Yew, D. T. (2007). Mitochondrial dysfunction in platelets and hippocampi of senescence-accelerated mice. *J. Bioenerg. Biomembr.* 39, 195–202. doi: 10.1007/s10863-007-9077-y

Yao, J., Irwin, R. W., Zhao, L., Nilsen, J., Hamilton, R. T., and Brinton, R. D. (2009). Mitochondrial bioenergetic deficit precedes Alzheimer's pathology in female mouse model of Alzheimer's disease. *Proc. Natl. Acad. Sci. U S A* 106, 14670–14675. doi: 10.1073/pnas.0903563106

Conflict of Interest: FB and SG were employed by the company CeGaT GmbH.

The remaining authors declare that the research was conducted in the absence of any commercial or financial relationships that could be construed as a potential conflict of interest.

frontiers in Cellular Neuroscience

BRIEF RESEARCH REPORT
published: 15 October 2020
doi: 10.3389/fncel.2020.558181

Sex Differences of Microglia and Synapses in the Hippocampal Dentate Gyrus of Adult Mouse Offspring Exposed to Maternal Immune Activation

Chin Wai Hui[1], Haley A. Vecchiarelli[2], Étienne Gervais[1], Xiao Luo[1†], Félix Michaud[1], Lisa Scheefhals[3], Kanchan Bisht[1†], Kaushik Sharma[1†], Lisa Topolnik[1,4] and Marie-Ève Tremblay[1,2,5,6,7]**

[1] Axe neurosciences, Centre de Recherche, Centre Hospitalier Universitarie de Qu-Université Laval, Québec, QC, Canada, [2] Division of Medical Sciences, University of Victoria, Victoria, BC, Canada, [3] Master Neuroscience and Cognition, Faculty of Science, Utrecht University, Utrecht, Netherlands, [4] Department of Biochemistry, Microbiology, and Bioinformatics, Faculty of Science and Engineering, Université Laval, Québec, QC, Canada, [5] Department of Molecular Medicine, Faculty of Medicine, Université Laval, Québec, QC, Canada, [6] Neurology and Neurosurgery Department, McGill University, Montréal, QC, Canada, [7] Department of Biochemistry and Molecular Biology, The University of British Columbia, Vancouver, BC, Canada

Schizophrenia is a psychiatric disorder affecting ∼1% of humans worldwide. It is earlier and more frequently diagnosed in men than woman, and men display more pronounced negative symptoms together with greater gray matter reductions. Our previous findings utilizing a maternal immune activation (mIA) mouse model of schizophrenia revealed exacerbated anxiety-like behavior and sensorimotor gating deficits in adult male offspring that were associated with increased microglial reactivity and inflammation in the hippocampal dentate gyrus (DG). However, both male and female adult offspring displayed stereotypy and impairment of sociability. We hypothesized that mIA may lead to sex-specific alterations in microglial pruning activity, resulting in abnormal synaptic connectivity in the DG. Using the same mIA model, we show in the current study sex-specific differences in microglia and synapses within the DG of adult offspring. Specifically, microglial levels of cluster of differentiation (CD)68 and CD11b were increased in mIA-exposed females. Sex-specific differences in excitatory and inhibitory synapse densities were also observed following mIA. Additionally, inhibitory synaptic tone was increased in DG granule cells of both males and females, while changes in excitatory synaptic transmission occurred only in females with mIA. These findings suggest that phagocytic and complement pathways may together contribute to a sexual dimorphism in synaptic pruning and neuronal dysfunction in mIA, and may propose sex-specific therapeutic targets to prevent schizophrenia-like behaviors.

Keywords: microglia, schizophrenia, maternal immune activation, complement, dentate gyrus, phagocytosis, mice

OPEN ACCESS

Edited by:
Maria Angeles Arevalo, Cajal Institute (CSIC), Spain

Reviewed by:
Dilja Krueger-Burg, University Medical Center Göttingen, Germany
Andreas Vlachos, University of Freiburg, Germany

****Correspondence:***
Lisa Topolnik
lisa.topolnik@bcm.ulaval.ca
Marie-Ève Tremblay
evetremblay@uvic.ca

†Present address:
Xiao Luo, Krembil Research Institute, University Health Network, Toronto, ON, Canada
Kanchan Bisht and Kaushik Sharma, Center for Brain Immunology and Glia, University of Virginia School of Medicine, Charlottesville, VA, United States

Specialty section:
This article was submitted to Non-Neuronal Cells, a section of the journal Frontiers in Cellular Neuroscience

Received: *01 May 2020*
Accepted: *14 September 2020*
Published: *15 October 2020*

Citation:
Hui CW, Vecchiarelli HA, Gervais É, Luo X, Michaud F, Scheefhals L, Bisht K, Sharma K, Topolnik L and Tremblay M-È (2020) Sex Differences of Microglia and Synapses in the Hippocampal Dentate Gyrus of Adult Mouse Offspring Exposed to Maternal Immune Activation. Front. Cell. Neurosci. 14:558181. doi: 10.3389/fncel.2020.558181

INTRODUCTION

Schizophrenia is a psychiatric disorder that affects ∼1% of humankind. It is more frequently diagnosed in men than women; additionally, men are more likely to have an earlier age of disease onset and experience more negative symptoms (Mendrek and Mancini-Marïe, 2016). Microglia, yolk-sac derived innate immune cells that inhabit the brain early during development, potentially contribute to these sex differences. Microglia are required for proper brain development, plasticity and homeostasis (Tian et al., 2017). Their pruning of synapses can be mediated through the complement (C) 3/C1q pathway (Stevens et al., 2007; Paolicelli et al., 2011; Schafer et al., 2012), which may contribute to an inadequate synaptic maintenance when abnormally active in disease (Druart and Le Magueresse, 2019). In response to changes in homeostasis, microglia can acquire reactive phenotypes, in which they increase their secretion of inflammatory cytokines and neurotrophic factors, as well as modify their phagocytic activity (Kettenmann et al., 2011; Cherry et al., 2014). Microglial alterations were reported throughout the *post-mortem* brains of schizophrenia patients, specifically an increase in ionized calcium binding adaptor molecule (IBA) 1-immunopositive (+) cells (Mongan et al., 2019). Animal models of schizophrenia induced by maternal immune activation (mIA) show microglial alterations (Juckel et al., 2011; Ratnayake et al., 2012; Pratt et al., 2013; Van den Eynde et al., 2014; Giovanoli et al., 2016). Our previous work revealed overall sex differences in microglial density, and, utilizing a polyinosinic:polycytidylic acid (poly I:C) mIA mouse model, increased morphological index (soma area/arborization area) and interactions with synapses in the hippocampal dentate gyrus (DG) of adult male offspring, correlating with schizophrenia-like behavioral deficits (Hui et al., 2018).

In addition to sex differences in schizophrenia, there is significant sexual dimorphism in embryonic migration, gene expression and function of microglia throughout life (Bordeleau et al., 2019). Microglial density and morphology differ between sexes in the rat hippocampus: at embryonic day (E) 17 there are no sex differences, but at postnatal (P) 0, females show increased numbers of ameboid and stout microglia; whereas at P4, males have more ameboid, stout and non-ramified microglia; then at P30 and P60, females display more abundant microglia with longer or ramified processes (Schwarz et al., 2012). Microglial phagolysosomal activity is sexually dimorphic in the mouse hippocampus: females at P3 have greater numbers of microglia with phagocytic cups in which cluster of differentiation (CD) 68, a marker of phagolysosomal activity, colocalizes with neuronal elements (Nelson et al., 2017); while females at P8 and males at P28 have greater staining intensity for CD68 (Weinhard et al., 2018). Based on these findings, we hypothesized that mIA induced with poly I:C may lead to sex-specific alterations in microglial phagocytosis, resulting in abnormal synaptic pruning in the DG, leading to the behavioral outcomes observed at adulthood. The DG is a region that is greatly affected by schizophrenia, as neuroimaging reports show reduced volumes in patients and animal models (Tavitian et al., 2019). There is also a potential arrestment of maturation of granule cells (GCs) in the DG in both patients with and potentially in animal models of schizophrenia (Tavitian et al., 2019), which may be the result of defective synaptic elimination (Feinberg, 1982). We examined in this study changes in microglial phagocytic markers, complement system, neuronal oxidative stress, as well as synaptic density and activity in the DG of adult male and female mouse offspring exposed to mIA at E9.5.

Abbreviations: ACSF, artificial cerebrospinal fluid; C, complement; CD, cluster of differentiation; CR3, complement receptor 3; DAPI, 4′,6-diamidino-2-phenylindole; DG, dentate gyrus; E, embryonic; GABA, gamma aminobutyric acid; GC, granule cells; GFAP, glial fibrillary acidic protein; GL, granule cell layer; IBA, ionized calcium binding adaptor molecule; i.p., intraperitoneal; MAP, microtubule-associated protein; mEPSC, miniature excitatory post-synaptic currents; mIA, maternal immune activation; mIPSC, miniature inhibitory post-synaptic currents; P, postnatal; PBS, phosphate buffered saline; PFA, paraformaldehyde; PL, polymorphic layer; poly I:C, polyinosinic:polycytidylic acid; ROI, region of interest; RT, room temperature; S, supplementary; SEM, standard error of the mean; TBS, tris buffered saline; TEM, transmission electron microscope; VGAT, vesicular GABA transporter; VGLUT, vesicular glutamate transporter; 3-NT, 3-nitrotyrosine.

MATERIALS AND METHODS

Animals

Animals were housed under a 12 h light–dark cycle at 22–25°C, with free access to food and water. Experimental animals were generated from C57Bl/6 mice (Charles River). All experiments were approved by Université Laval's animal ethics committees, according to the Canadian Council on Animal Care's guidelines.

Poly I:C Maternal Immune Activation Model

Infection was simulated by intraperitoneal (i.p) injection of poly I:C potassium salt (Sigma-Aldrich, P9582) (5 mg/kg in sterile saline) at E9.5 as described (Hui et al., 2018). A vehicle control group received sterile saline. Each analysis included animals from three to five litters. Two to five mice per sex/group were housed together until behavioral testing from P60 to P80 followed by sacrifice 48 h later (cohorts 1 and 2; detailed in Hui et al., 2018), or sacrifice at P80–90 (cohort 3 for electrophysiology). Cohorts 1 and 2 mice were anesthetized with ketamine-xylazine (80/10 mg/mL), then cohort 1 mice were transcardially perfused with ice-cold phosphate buffered saline (PBS; 50 mM, pH 7.4). Right hemisphere hippocampi were dissected and kept at −80°C for molecular studies. Left hemispheres were fixed by immersion in 4% paraformaldehyde (PFA; Electron Microscopy Sciences) at 4°C overnight. Cohort 2 mice were transcardially perfused with 0.2% glutaraldehyde (Electron Microscopy Sciences)/4% PFA.

Fluorescent Immunohistochemistry

Left hemispheres were sectioned longitudinally at 30 μm using a cryostat. Sections containing the dorsal hippocampal DG (Bregma 0.36–1.00) (Paxinos and Watson, 1998) were processed for fluorescent immunohistochemistry. Sections were incubated in 0.1 M citrate buffer at 85°C for 8–10 min

for antigen retrieval. After the slides cooled, they were washed with PBS and incubated in blocking buffer for 1 h at room temperature (RT). Sections were then incubated with primary antibodies overnight at 4°C, rinsed in PBS and incubated with secondary antibodies for 2 h at RT (see **Supplementary Table S1** for antibody information). Sections were then washed in PBS, counter-stained with 4′,6-diamidino-2-phenylindole (DAPI) (1:20,000; Thermo Fisher Scientific) and coverslipped in Fluoromount-G (SouthernBiotech).

Confocal Imaging

All imaging analyses were performed by an investigator unaware of experimental conditions.

Confocal Imaging and Quantitative Analysis of Microglia, Astrocytes and Neurons

Using a Quorum WaveFX Spinning disc confocal microscope, *Z*-stacks (∼50 slices, Δz = 0.5 μm) were acquired at 20x magnification with an ORCA-R2 camera (Hamamatsu, 1,344 × 1,024 pixels) in two regions of interest (ROI) in the DG for each section, covering the GCs layer (GL) and polymorphic layer (PL). Two sections per animal were imaged and the results averaged. Focus stacking was performed with Volocity (Version 5.4, PerkinElmer). Colocalization of CD68 in IBA1+ microglia was assayed with ImageJ (National Institutes of Health). Twenty to thirty microglia were analyzed per animal. The analysis focused on cell bodies, as staining was diffuse in processes. Data are presented as CD68 counts per IBA1+ microglial cell. Signal intensity was assayed for glial fibrillary acidic protein (GFAP), C1q, C3, CD11b, and 3-nitrotyrosine (3-NT) using ImageJ. For each combination of antibodies, sections were imaged with the same laser intensity and were quantified using the area measurement tool keeping the threshold values constant. Data are expressed as percent area.

Confocal Imaging for Synaptic Density and Staining Intensity Analysis

Confocal imaging of the DG was performed with a Carl Zeiss LSM-800 laser scanning confocal microscope. *Z*-stacks (15 steps (Δz = 0.33 μm) were acquired using a Plan-Apochromat 63×/1.4 oil immersion objective (1,024 × 1,024 pixels). Two regions of interest (ROI) were imaged in the PL of two to three sections per animal. Synaptic puncta analysis was performed manually with ImageJ in locations devoid of DAPI staining. For inhibitory puncta analysis, a ROI of 30 × 30 μm was selected. Vesicular gamma aminobutyric acid (GABA) transporter (VGAT) and gephyrin puncta were counted individually before merging channels to count overlapping puncta. For excitatory puncta analysis, a ROI of 20 × 20 μm was selected. Maximum intensity projections were created from 4 *z*-steps. All puncta were counted in individual channels for Homer1 and vesicular glutamate transporter (VGLUT) 1 before merging channels to identify overlap. See **Supplementary Materials and Methods** for additional information.

Tissue Preparation and Immunoperoxidase Signaling for Electron Microscopy

Fifty micrometer transverse sections from Bregma 2.12–1.64 (Paxinos and Watson, 1998) were cut using a vibratome. They were processed as described (Bisht et al., 2016). Briefly, sections were washed in Tris-buffered saline (TBS), quenched, and processed for CD68 immunostaining. They were blocked and incubated overnight in primary antibody (**Supplementary Table S1**) at 4°C, washed, incubated with secondary antibody for 1.5 h at RT, and then incubated with ABC Vectastain (1:100; Vector Laboratories, #PK−6100), diaminobenzidine (0.05%) and hydrogen peroxide (0.015%). The sections were post-fixed in 1% osmium tetroxide, dehydrated in ethanol, and embedded with Durcupan at 55°C for 72 h. Areas of the DG (PL and GL) were cut at 70–80 nm using an ultramicrotome (Leica Ultracut UC7). Ultrathin sections were examined at 80 kV with a FEI Tecnai Spirit G2 transmission electron microscope (TEM). Imaging was performed at 6,800X, using an ORCA-HR digital camera (10 MP; Hamamatsu). Dark neuronal cell bodies and dendrites were identified ultrastructurally as described previously (Tremblay et al., 2012; Audoy-Rémus et al., 2015). Their density was expressed as numbers per mm^2 of screened tissue surface, using the systematic approach developed for dark microglia analysis (Bisht et al., 2016; Hui et al., 2018).

Gene Expression Analysis Using Quantitative Real-Time PCR

Tissue was homogenized using the QIAzol lysis reagent (Qiagen) and total RNA was extracted by phenol-chloroform method. One microgram of total RNA was reverse transcribed into cDNA using the iScript cDNA synthesis kit (BioRad). Real-time PCR was performed with the SsoAdvanced universal SYBR Green supermix kit (BioRad) in a Lightcycler 480II (Roche). Primers (**Supplementary Table S2**) were designed using NCBI Primer Blast (Hui et al., 2018). Relative expression was calculated with the $2^{-\Delta\Delta CT}$ method using *Gapdh* for normalization (Yuan et al., 2006).

Electrophysiological Patch-Clamp Recordings

Cohort 3 mice were anesthetized with ketamine-xylazine (10/100 mg/mL) and perfused intracardially with an ice-cold sucrose-based solution (**Supplementary Table S3**). Transverse hippocampal slices (300 μm) were obtained using a vibratome (Microm HM 650V, Thermo Scientific) in the same sucrose-based solution oxygenated with 95%O_2/5%CO_2, and transferred into the heated oxygenated recovery solution (**Supplementary Table S3**) until use.

For electrophysiological recordings, slices were transferred to the recording chamber perfused continuously with an oxygenated artificial cerebrospinal fluid (ACSF) and maintained at near physiological temperature (**Supplementary Table S3**). The GCs within the DG were visually identified using a Nikon (Eclipse FN1) microscope with infrared differential

interference contrast microscopy using a 40× (NA 0.8) water-immersion objective. Patch pipettes (3.5–6 MΩ) were made from borosilicate glass capillaries using a Flaming/Brown micropipette puller (Sutter Instrument Co.). Whole-cell patch-clamp recordings (5–10 min) were performed in voltage-clamp at −70 mV for miniature excitatory post-synaptic currents (mEPSCs) and at +10 mV for miniature inhibitory post-synaptic currents (mIPSCs). The passive membrane properties were taken immediately upon membrane rupture. The same intracellular solution (**Supplementary Table S3**) and ACSF with tetrodotoxin (TTX; 1 μM; Alomone Labs; for blocking action potentials) were utilized in all experiments. Data acquisition (digitized at 10 kHz; Digidata 1550A, Molecular Devices) was performed using the MultiClamp 700B amplifier and the pCLAMP 10.5 software (Molecular Devices). The resting membrane potential was taken immediately upon membrane rupture. The input resistance and the membrane capacitance were detected automatically during the first minute of whole-cell configuration using a 5 mV square pulse in Membrane Test of Clampex 10.7 software. More than 200 events per neuron were selected using an automated template search algorithm in Clampfit. All events were counted for frequency analysis as described previously (David and Topolnik, 2017). Anatomical analysis of biocytin-filled neurons was also performed (**Supplementary Materials and Methods**).

Statistics

Data were analyzed using Prism (GraphPad, Version 8), Clampfit 10.7, Excel, IGOR Pro (Wavematrics) and Statistica (Tibco). Two-way ANOVAs with *post hoc* analyses using Bonferroni corrections were used to determine interactions between poly I:C exposure and sex effects. Outliers were determined using the ROUT test (Q = 0.1%; GraphPad) for cohort 1 and 2 animals. For cohort 3 animals, data distributions were tested for normality using Shapiro-Wilcoxon test, and Kolmogorov-Smirnov test was used for comparison of pooled data from individual cells. $p < 0.05$ was considered statistically significant. All data are reported as mean ± standard error of the mean (SEM).

RESULTS

mIA Increases CD68 Levels in IBA1+ Microglia of Female but Not Male Offspring

We first assessed microglial phagolysosomal activity by immunofluorescent confocal microscopy against CD68 in the DG of adult offspring. In response to mIA, IBA1+ microglia had increased numbers of CD68 puncta in female vs. male offspring, in both the GL and PL (**Figures 1A–C**), indicating an increased phagocytic activity in the DG of female offspring. The baseline levels of CD68 also differed between sexes, with males showing greater immunoreactivity than females in the GL and PL of saline offspring (**Figures 1A–C**). Immunocytochemical TEM confirmed the localization of CD68 protein in microglial soma and processes from mIA and control offspring, across the GL and PL. CD68 staining was particularly found on endosomes, lysosomes and the plasma membrane, suggesting extracellular digestion or "exophagy" (**Figure 1D**). CD68 was not found, however, in GFAP+ astrocytes (**Figure 1E**). These data indicate that microglia from mIA-exposed female but not male offspring display increased phagolysosomal activity in the DG, with more pronounced changes observed in the PL.

mIA Is Associated With Changes in the Complement System in Male and Female Offspring

One hemisphere of the whole hippocampus of adult offspring was examined by quantitative real-time PCR. Overall, there were no changes with mIA or between sexes in the expression of genes related to synaptic development or maintenance (*Stx1a*, *Vamp2*, *Snap25*, *Bdnf*, *Fmr1*, and *Shank2*) (**Supplementary Table S4**). For genes involved in phagocytosis or synaptic pruning, there was a reduction with mIA in the expression of complement system components *C1q* (**Figure 2A**) and *C3* (**Figure 2B**), without changes in the expression of *Axl*, *MerTK*, *Gas6,* and *C4a* (**Supplementary Table S4**).

We then used immunofluorescent staining to examine by confocal microscopy protein levels of complement components in the DG of adult offspring. C1q staining did not localize to IBA1+ microglia (**Supplementary Figure S1A**) or GFAP+ astrocytes (**Supplementary Figure S1B**). Complementary to gene expression, C1q protein levels in microtubule-associated protein (MAP) 2+ neurons were lower in mIA-exposed offspring (**Figures 2C–D**). C3 protein levels, unlike gene expression data, were also greater in mIA-exposed offspring (**Figures 2E–H**). Confocal microscopy additionally revealed that C3 protein localizes to GFAP+ astrocytes (**Figure 2E**), while GFAP staining intensity was increased in mIA-exposed offspring (**Figure 2G**). Proteins levels of complement receptor 3 (CR3)'s component CD11b were assayed, revealing increased staining in mIA-exposed offspring and overall in females (**Figures 2I,J**). Together these data reveal alterations of the complement system following mIA, without a clear pattern emerging regarding sex differences, except for greater levels of CD11b in females.

mIA Increases the Density of Excitatory and Inhibitory Synapses in Males While Reducing Excitatory Synapses in Females

To provide functional insights into these changes in phagolysosomal activity and the complement system, we measured synaptic density by immunofluorescent confocal microscopy, in the PL of adult offspring. Inhibitory synapses were assessed via colocalization of VGAT (presynaptic) and gephyrin (post-synaptic) (**Figures 3A,B**). Excitatory synapses were assessed by colocalization of VGLUT1 (presynaptic) and Homer1 (post-synaptic) (**Figures 3A,C**). There was potential increased density (**Figure 3D**) and staining intensity (**Supplementary Figures S3A,B**) of inhibitory synapses with mIA in males but not females; additionally, there were potential baseline sex differences in inhibitory synapses, with males having fewer than females (**Figure 3D**). For excitatory synapses,

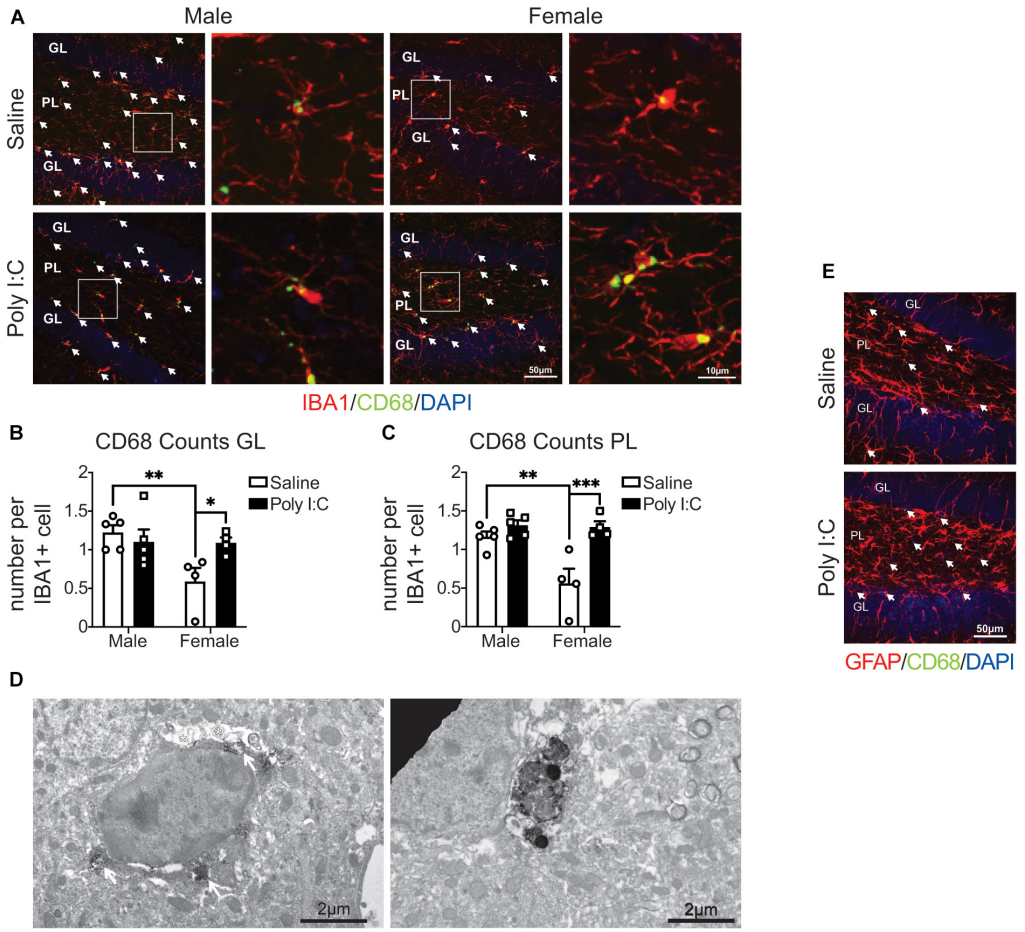

FIGURE 1 | Male (left); female (right); saline (black outlined white bars with black outlined circles); poly I:C (black bars with black outline squares). n = 4–5 animals/group. *$p < 0.05$; **$p < 0.01$; ***$p < 0.001$. CD68 levels were increased in IBA1+ microglia in the hippocampal DG of female mice exposed to maternal poly I:C. **(A)** Representative images (20x) (left of each pair) and 5x magnified pictures (100x) (right of each pair) of IBA1+ microglia containing CD68 puncta from each condition (left half: males, right half: females; saline: top, poly I:C: bottom). Each image was from the DG and includes the granule cell layer (GL) and polymorphic layer (PL). IBA1+ microglia are shown in red, CD68 puncta in green and DAPI stained nuclei in blue. Scale bar = 50 μm (20x) and 10 μm (100x). **(B)** CD68 puncta counts per IBA1+ microglia in the GL. There was an increase in CD68 counts in female offspring exposed to poly I:C [interaction: $F(1, 14) = 5.41$, $p = 0.04$; $p = 0.05$], but not male offspring ($p > 0.99$). There were less microglial CD68 puncta in females than males from saline exposed dams ($p = 0.009$), but not poly I:C exposed dams ($p > 0.99$). There was also a main effect of sex [$F(1, 14) = 5.88$, $p = 0.03$] with males having greater CD68 counts in total; but not between saline and poly I:C [$F(1, 14) = 2.02$, $p = 0.18$]. **(C)** CD68 counts per IBA1+ microglia in the PL. As with the GL, there was an increase in CD68 levels in females prenatally exposed to poly I:C [interaction: $F(1, 14) = 7.99$, $p = 0.01$; $p = 0.0006$], contrary to males ($p > 0.99$). Males whose dams were exposed to saline had greater CD68 levels than females ($p = 0.002$), but there were no sex differences in the poly I:C exposed offspring ($p > 0.99$). There was a main effect of sex [$F(1, 14) = 9.14$, $p = 0.009$], with males having greater CD68 counts overall, and of poly I:C administration also leading to greater CD68 puncta counts overall [$F(1, 14) = 18.09$, $p = 0.0008$]. **(D)** Representative electron micrograph (left) confirming the association of CD68 to lysosomes inside microglial cell bodies in mice exposed to mIA. White arrows indicate CD68 signal surrounding lysosomes and white asterisks represent CD68 signal adjacent to extracellular digestion. Scale bar = 2 μm. Representative electron micrograph (right) (6,800x) showing CD68 staining in a microglial process. Scale bar = 2 μm. **(E)** CD68 signal did not colocalize with GFAP+ astrocytes. Representative image from saline and poly I:C conditions. Each image was taken of the DG and included the GL and PL. GFAP+ astrocytes are show in red, CD68 puncta in green and indicated by white arrows, and DAPI stained nuclei in blue. Scale bar = 50 μm.

between males and females and following mIA, there was a potential interaction; pattern-wise, males showed an increase, and females a decrease in their density (**Figure 3E**); for staining intensity, there was only an effect of mIA on VGLUT1 but no effect on Homer1 (**Supplementary Figures S2C,D**). Similarly, there were baseline sex differences, with females having more excitatory synapses than males (**Figure 3E**). These data indicate that following mIA, there is a dynamic synaptic reorganization taking place in the PL, where inhibitory and excitatory synapses both increase in male offspring, and where inhibitory synapses are unchanged while excitatory synapses decrease in female offspring.

mIA Increases Dark Neurons Without Affecting 3-NT Levels in Both Sexes

To determine whether these changes of synapses are associated with altered neuronal health, we next examined the occurrence

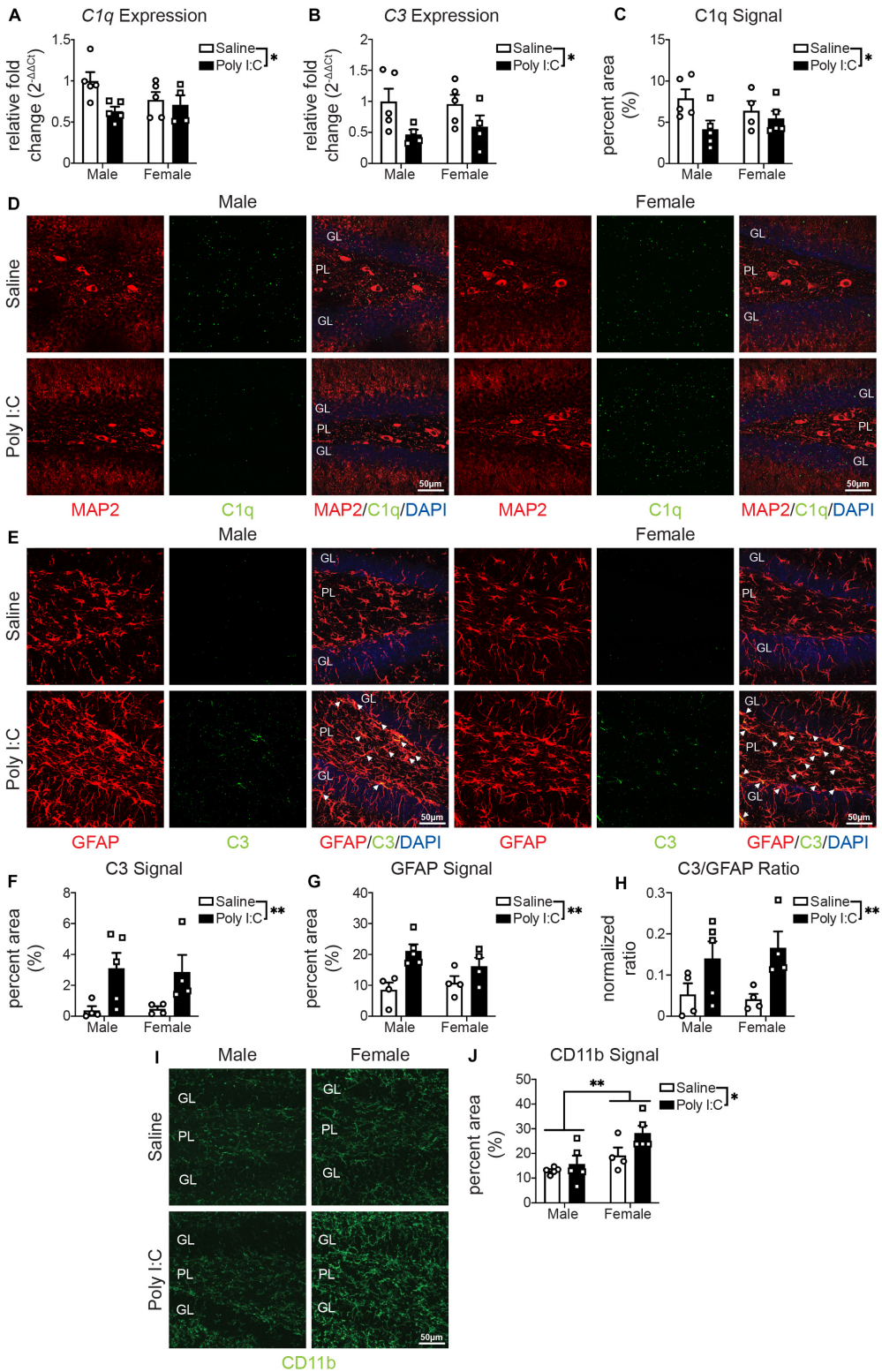

FIGURE 2 | Male (left); female (right); saline (black outlined white bars with black outlined circles); poly I:C (black bars with black outline squares). n = 4–5 animals per group. $^{*}p < 0.05$, $^{**}p < 0.01$. mIA led to decreased expression of *C1q* and *C3* in the hippocampus, reduced levels of C1q and increased levels of C3 in the DG in a sex independent manner, while increasing CD11b levels in the DG of female offspring. **(A)** Relative expression of *C1q* in the DG. There was an overall reduction from maternal poly I:C exposure [$F(1, 15) = 5.19$, $p = 0.04$]. There was not an overall effect of sex [$F(1, 15) = 0.65$, $p = 0.43$] or interaction between the two factors [$F(1, 15) = 2.70$, $p = 0.12$]. **(B)** Relative expression of *C3* in the DG. As with C1q, there was an overall reduction in offspring whose dams were exposed to

(Continued)

FIGURE 2 | Continued
poly I:C [$F(1, 14) = 7.16$, $p = 0.02$]. There was not an effect of sex [$F(1, 14) = 0.06$, $p = 0.81$] or an interaction between the two [$F(1, 14) = 0.25$, $p = 0.63$]. **(C)** C1q levels were lower in offspring whose dams were exposed to poly I:C [$F(1, 15) = 4.89$, $p = 0.04$]. There was not an overall effect of sex [$F(1, 15) = 0.009$, $p = 0.93$] or interaction between the two [$F(1, 15) = 1.81$, $p = 0.20$]. **(D)** Representative images (left half: males, right half: females; saline: top, poly I:C: bottom) of C1q levels in the hippocampal DG (MAP2 (neurons; red, left); C1q (green, middle); merged [MAP2 (red)/C1q (green)/DAPI stained nuclei (blue); right)]. Each image was from the DG and includes the granule cell layer (GL) and polymorphic layer (PL). Scale bar = 50 μm. **(E)** Representative images (left half: males, right half: females; saline: top, poly I:C: bottom) of C3 levels in the DG [GFAP (astrocytes; red, left); C3 (green, middle); merged (GFAP (red)/C3 (green)/DAPI stained nuclei (blue); right)]. Each image was from the DG and includes the GL and PL. Scale bar = 50 μm. **(F)** C3 levels were greater in offspring from poly I:C exposed mothers [$F(1, 13) = 10.01$, $p = 0.008$]. There was not an effect of sex [$F(1, 13) = 0.008$, $p = 0.93$] or an interaction between the two [$F(1, 13) = 0.04$, $p = 0.84$]. **(G)** GFAP levels were also greater in offspring following maternal poly I:C administration [$F(1, 13) = 14.65$, $p = 0.002$]. There was not an effect of sex [$F(1, 13) = 2.37$, $p = 0.15$] or interaction between the two [$F(1, 13) = 0.33$, $p = 0.57$]. **(F)** The levels of C3 in GFAP+ positive cells was also greater in offspring when dams were exposed to poly I:C [$F(1, 13) = 9.65$, $p = 0.008$]. There was not an effect of sex [$F(1, 13) = 0.31$, $p = 0.59$] or an interaction between the two [$F(1, 13) = 0.04$, $p = 0.84$]. **(H)** Representative images of CD11b (green) levels in the DG (left: males, right half: females; saline: top, poly I:C: bottom). Each image was from the DG and includes the GL and PL. Scale bar = 50 μm. **(I)** CD11b levels were greater in offspring following maternal poly I:C administration [$F(1, 15) = 4.61$, $p = 0.05$]; furthermore, female offspring, from dams who were exposed to either saline or poly I:C had greater CD11b levels [$F(1, 15) = 11.57$, $p = 0.004$]. There was not an interaction between the two [$F(1, 15) = 1.34$, $p = 0.26$].

of dark neurons in the DG of adult offspring. Dark neurons are recognized by cellular stress markers: increased nuclear and cytoplasmic condensation, loss of heterochromatin pattern, as well as dilation of endoplasmic reticulum/Golgi apparatus; and are not necrotic or apoptotic (Turmaine et al., 2000; Tremblay et al., 2012; Henry et al., 2018). In the GL, the density of dark neuronal soma/dendrites was unchanged following mIA (**Figures 3F,G**). In the PL, however, there was a general effect of mIA increasing the numbers of dark neuronal soma/dendrites (**Figures 3F,H**). By immunofluorescent confocal microscopy, the levels of 3-NT, a biomarker of reactive nitrogen species formation (Walker et al., 2001), was also examined in the DG of adult offspring. 3-NT was only observed in MAP2+ neurons. There was no effect of mIA on 3-NT levels in both males and females (**Figures 3I,J**). These data combined point to potential neuronal stress following mIA, without any change in the oxidative stress marker 3-NT in neurons of the DG.

mIA Induces Sex-Specific Alterations in mIPSCs and mEPSCs of GCs

Lastly, we investigated whether the observed changes in microglia and synapses are associated with functional or morphological alterations in the DG GCs of adult offspring. While no changes were revealed in the passive membrane properties (**Supplementary Table S5**) or the morphological features of GCs (**Supplementary Figure S3**), both mEPSCs and mIPSCs showed sex-specific differences. Specifically, while the amplitude of mIPSCs was increased in both males and females exposed to mIA, the frequency of mIPSCs was only increased in males (**Figures 4A,B**), consistent with a higher inhibitory synapse density in the PL of males (**Figure 3A**). Contrastingly, there was no effect of mIA on mEPSCs in males (**Figure 4C**). However, with mIA, mEPSC amplitude was increased while frequency was decreased in females (**Figure 4D**), which could be associated with a loss of excitatory synapses, and compensatory increase in conductance at the surviving contacts. Together, these results revealed an increased inhibitory tone in both sexes, as well as female offspring-specific changes in GCs excitatory synaptic transmission following maternal exposure to poly I:C.

DISCUSSION

This study highlights sex differences in microglial phagolysosomal activity, complement system, neuronal health, and excitatory and inhibitory synapse density and activity, in the DG of adult offspring exposed to mIA with poly I:C. Most of the observed changes were likely sex independent, including the alterations in C1q and C3 expression and levels; increase in dark neuron and dendrite density; and increase in mIPSC amplitude. However, a number of changes were sex specific, including the increase in CD68 and CD11b levels (both in general and following mIA) observed in female offspring, and the reorganization of inhibitory and excitatory synapses number and activity following mIA.

CD68 is a marker of phagolysosomal activity that is often used to assess the reactivity of microglia (Korzhevskii and Kirik, 2016). In our data, CD68 was exclusively expressed by IBA1+ cells, which likely represented microglia, but could also be infiltrating macrophages (González Ibanez et al., 2019). This is the first example of baseline sex differences in CD68 levels measured in the DG at adulthood; but there are previous reports of sex differences in which microglial CD68 is greater in females among hippocampus CA1 and forebrain regions earlier in development (Weinhard et al., 2018; Yanguas-Casás et al., 2018). Specifically, females had lower CD68 levels that increased with mIA, whereas males had stable levels that remained unchanged following mIA. This could indicate a ceiling, where the amount of CD68 is already higher in males, and thus is unable to manifest a sustained response to mIA at the time point analyzed in this study; or an earlier, transient change in phagolysosomal activity in males. Alternatively, we previously observed an increased density of dark microglia, which downregulate IBA1 and display high phagocytic activity, in males with mIA (Hui et al., 2018), it is possible that males could recruit different microglial subsets. This change in CD68 levels in females could be related to the mIA-induced reductions in excitatory synapses and mEPSC frequency.

In addition to mounting an increase in CD68 following exposure to mIA, females had greater CD11b levels, both basally and in response to mIA. This pattern was observed in the hippocampus of an Alzheimer's disease model (Gallagher et al.,

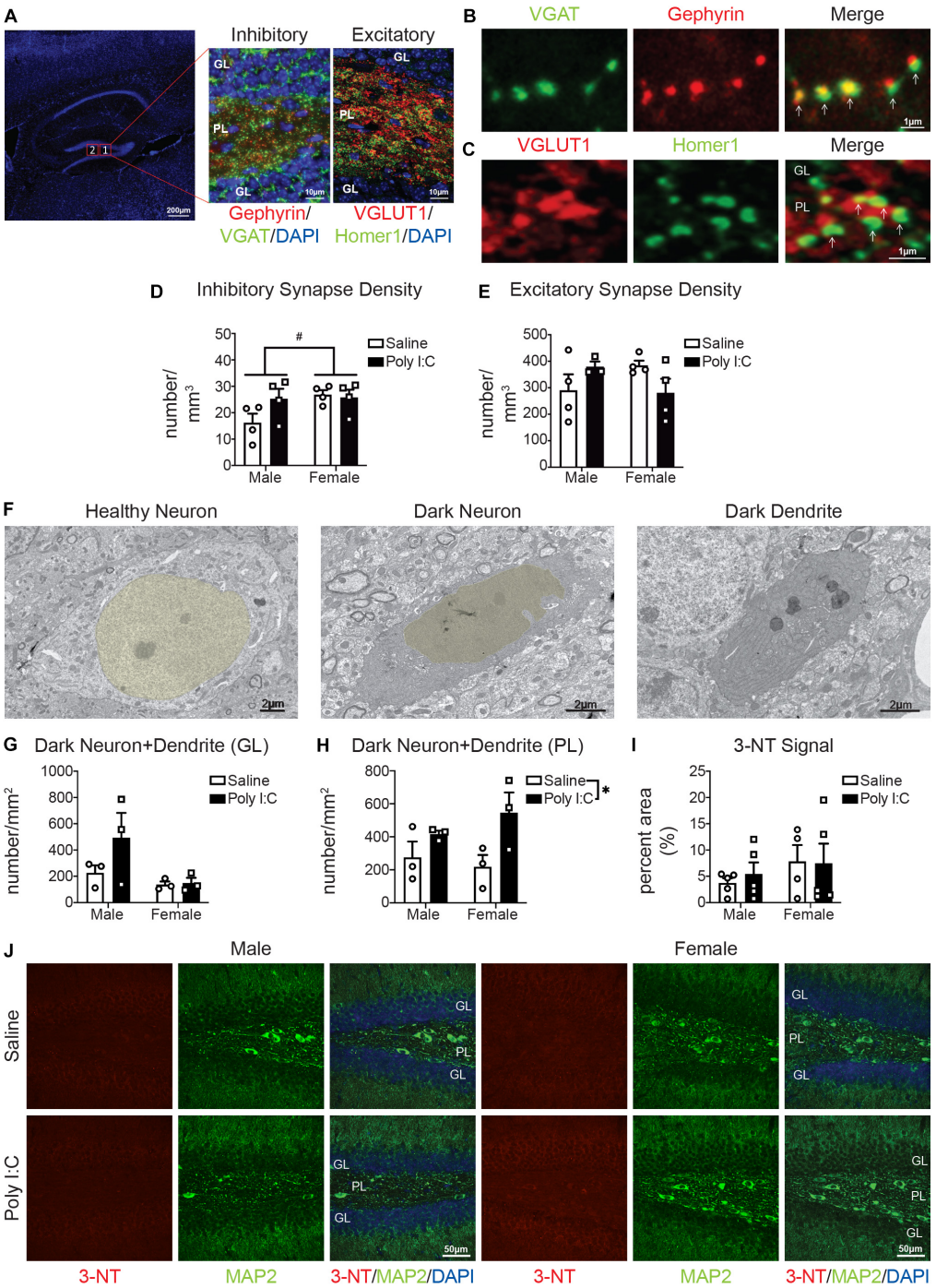

FIGURE 3 | Male (left); female (right); saline (black outlined white bars with black outlined circles); poly I:C (black bars with black outline squares). n = 3–5 animals per group. $^{\#}p < 0.1$; $^{*}p < 0.05$. Maternal poly I:C administration led to increased excitatory and inhibitory synapse levels in the PL in males, but reduced excitatory synapse levels in females, as well as increased dark neurons in the PL, without changing levels of the neuronal oxidative stress marker, 3-NT in the DG.
(A) Representative image of inhibitory and excitatory markers in the DG. Overview of the DG (left) (DAPI stained nuclei in blue; scale bar = 200 μm). Magnified images (63x) containing the polymorphic layer (PL) of the DG. The middle shows a representative image of inhibitory puncta (VGAT in green; Gephyrin in red; and DAPI stained nuclei in blue; scale bar = 10 μm). The right image shows a representative image of excitatory puncta (VGLUT in red; Homer1 in green; DAPI stained nuclei in blue; scale bar = 10 μm). **(B)** Representative images (63x) of components of inhibitory synapses (left, VGAT in green; middle, Gephyrin in red; right, merged; scale bar = 1 μm). **(C)** Representative images (63x) of components of excitatory synapses (left, VGLUT in red; middle, Homer1 in green; right, merged; scale bar = 1 μm). **(D)** There were potential baseline sex differences in inhibitory synapses between males and females [main effect, sex, $F(1, 12) = 3.31$, $p = 0.09$; $p = 0.06$], with males having less than females, but not following mIA ($p > 0.99$). There was no significant effect of poly I:C on excitatory synapses [interaction, $F(1, 12) = 2.72$,

(Continued)

FIGURE 3 | Continued
$p = 0.13$]; main effect, poly I:C [$F(1, 12) = 1.71$, $p = 0.22$]; males ($p = 0.12$); females ($p > 0.99$). **(E)** There were potential differences in excitatory synapses between males and females and following maternal poly I:C administration [interaction, $F(1, 12) = 4.61$, $p = 0.06$], although specific comparisons revealed no significant changes (males saline vs. poly I:C, $p = 0.41$; females saline vs. poly I:C, $p = 0.23$; saline males vs. females, $p = 0.30$; poly I:C males vs. females, $p = 0.32$), the pattern was males had lower levels compared to females at baseline, which was increased following poly I:C, whereas females had reduced levels following poly I:C. **(F)** Representative electron micrographs (6,800x) from the PL showing a healthy neuron (nucleus pseudocolored yellow; left), dark neuron (nucleus pseudocolored yellow; middle) and a dark dendrite (right). Scale bar = 2 μm. **(G)** There was no overall effect of maternal poly I:C administration or sex differences on the density of dark neuronal soma/dendrites in the granule cell layer (GL) of the DG [interaction, $F(1, 8) = 1.57$, $p = 0.25$; main effect of sex, $F(1, 8) = 4.53$, $p = 0.07$; main effect of poly I:C, $F(1, 8) = 1.88$, $p = 0.21$]. **(H)** In the polymorphic layer (PL) of the DG, maternal poly I:C administration increased dark neuronal soma and dendrites numbers [main effect, $F(1, 8) = 7.47$, $p = 0.03$]. There was not an effect of sex [main effect, $F(1, 8) = 0.18$, $p = 0.68$] or interaction between the two [$F(1, 8) = 1.19$, $p = 0.31$]. **(I)** There was no overall effect of maternal poly I:C administration or sex differences on the levels of 3-NT in the DG [interaction, $F(1, 15) = 0.15$, $p = 0.70$; main effect of sex, $F(1, 15) = 1.31$, $p = 0.27$; main effect of poly I:C, $F(1, 15) = 0.07$, $p = 0.80$]. **(J)** Representative images from each condition (left half: males, right half: females; saline: top, poly I:C: bottom) of dentate gyri with immunohistochemistry for 3-NT (oxidative stress marker; red, left), MAP2 (neuronal markers; green, middle) and merged [3-NT (red)/MAP2 (green)/DAPI (nuclei; blue)]. Each image was from the DG and includes the GL and PL. Scale bar = 50 μm.

2013). CD11b is part of CR3, and phagocytosis can be triggered by iC3b's (C3's cleavage product) interaction with CR3 (Fu et al., 2012). In our work, we saw reductions in hippocampal expression of *C1q* and *C3* following mIA, across sexes, and also with protein levels of C1q, in neurons. These reductions could reflect a decrease in complement-mediated synaptic elimination (Stevens et al., 2007; Druart and Le Magueresse, 2019; Sellgren et al., 2019; Magdalon et al., 2020; Tenner, 2020). However, unlike the gene expression, C3 protein levels are increased with mIA across both sexes. These differences could highlight differences between DG and whole hippocampus; or could be protein driving gene regulation. C3 is located further downstream along the classical complement cascade, but is also activated by the alternative and lectin complement cascades (Druart and Le Magueresse, 2019). It is possible that increases in these multiple pathways drive synapse elimination differently across neuronal subtypes or regions. A parsimonious explanation may be that in males the mIA-induced reduction of neuronal C1q leads to reduced microglia-mediated synapse elimination (as inhibitory and excitatory synapses were more abundant in the PL with mIA), whereas in females there is an increase in C3, and greater still an increase in CD11b, that leads to elimination of excitatory synapses with mIA. Interestingly, C3 levels in our data were increased in GFAP+ astrocytes. Astrocytic C3 production may modulate synaptic density, as observed in models of Alzheimer's disease (Lian et al., 2015, 2016; Luchena et al., 2018), amyotrophic lateral sclerosis (Heurich et al., 2011), perioperative neurocognitive disorder (Xiong et al., 2018) and diabetes (Zhao et al., 2018). We now show that there may be a similar phenomenon in the mIA model of schizophrenia.

As we previously observed altered microglial homeostasis and activation states (Hui et al., 2018), we investigated whether synaptic density changed after mIA. Imbalances in excitatory and inhibitory synaptic activities, notably in the hippocampus, are recognized as pathophysiological mechanisms in schizophrenia (Harrison et al., 2003; Coyle et al., 2012; Nakazawa et al., 2012; Tamminga et al., 2012; Li et al., 2015; Roberts et al., 2015; Matosin et al., 2016). In our data, for male offspring, we observed increased levels of mature inhibitory and excitatory synapses in the hippocampal DG, specifically the PL, following mIA. Furthermore, we saw an increase in only mIPSCs (amplitude and frequency) but not mEPSCs in DG GCs of male offspring. Therefore, it appears that despite potential increases in both mature inhibitory and excitatory synapses density in the PL, there is a net increase in functional inhibitory drive onto DG GCs in males. It is also possible that changes in excitatory synapses in the PL represent increased excitation of mossy cells or GABAergic interneurons that inhibit GCs (Scharfman, 2016). In addition, these data indicate that the perforant path, which is the major excitatory input to GCs (Witter, 2007; Treves et al., 2008), remains functionally unaltered in male offspring. Whereas in female animals, we observed no change in mature inhibitory synapses in the PL following mIA, but a potential reduction in mature glutamatergic synapses. There was also a concomitant increase in the amplitude of both mIPSCs and mEPSCs, and a decrease in mEPSC frequency. We cannot exclude a loss in functional excitatory synapses followed by a compensatory increase in the neurotransmitter content per quanta or in the density of the post-synaptic glutamate receptors (Pinheiro and Mulle, 2008) in female offspring. Future work is required to delineate specific changes with regards to pre- and post-synaptic site and specific inputs; as well as whether these effects are due to differences in microglial phagocytic activity. Additionally, as both excitatory and inhibitory currents on DG GCs are increased in females (perhaps compensatory evening out the output of these cells), but only inhibitory drive onto GCs is increased in males, this may contribute to sex differences in behavior observed following mIA (i.e., the prepulse inhibition deficits observed only in males) (Hui et al., 2018).

Our data reveals sex-dependent and -independent changes in the complement system and DG synapses following mIA. Despite some changes as a result of mIA, differences in other parameters may lead to sexual dimorphisms in structural and behavioral outcomes. For example, in males, changes in C1q but not CD68 could indicate less microglia-mediated synapse elimination, as there are perhaps increased synapse number in the PL and increased inhibitory input onto GCs. Contrastingly, in females, there were increases in CD68 and CD11b throughout the DG, potentially contributing to the potential reduction in excitatory synapses in the PL as well a decrease in GC mEPSC frequency, perhaps indicative of activity-dependent synaptic pruning. Through understanding the mechanisms underlying these sexual dimorphisms, we hope to provide new insights into novel therapies for schizophrenia or other diseases in which mIA is an environmental risk factor.

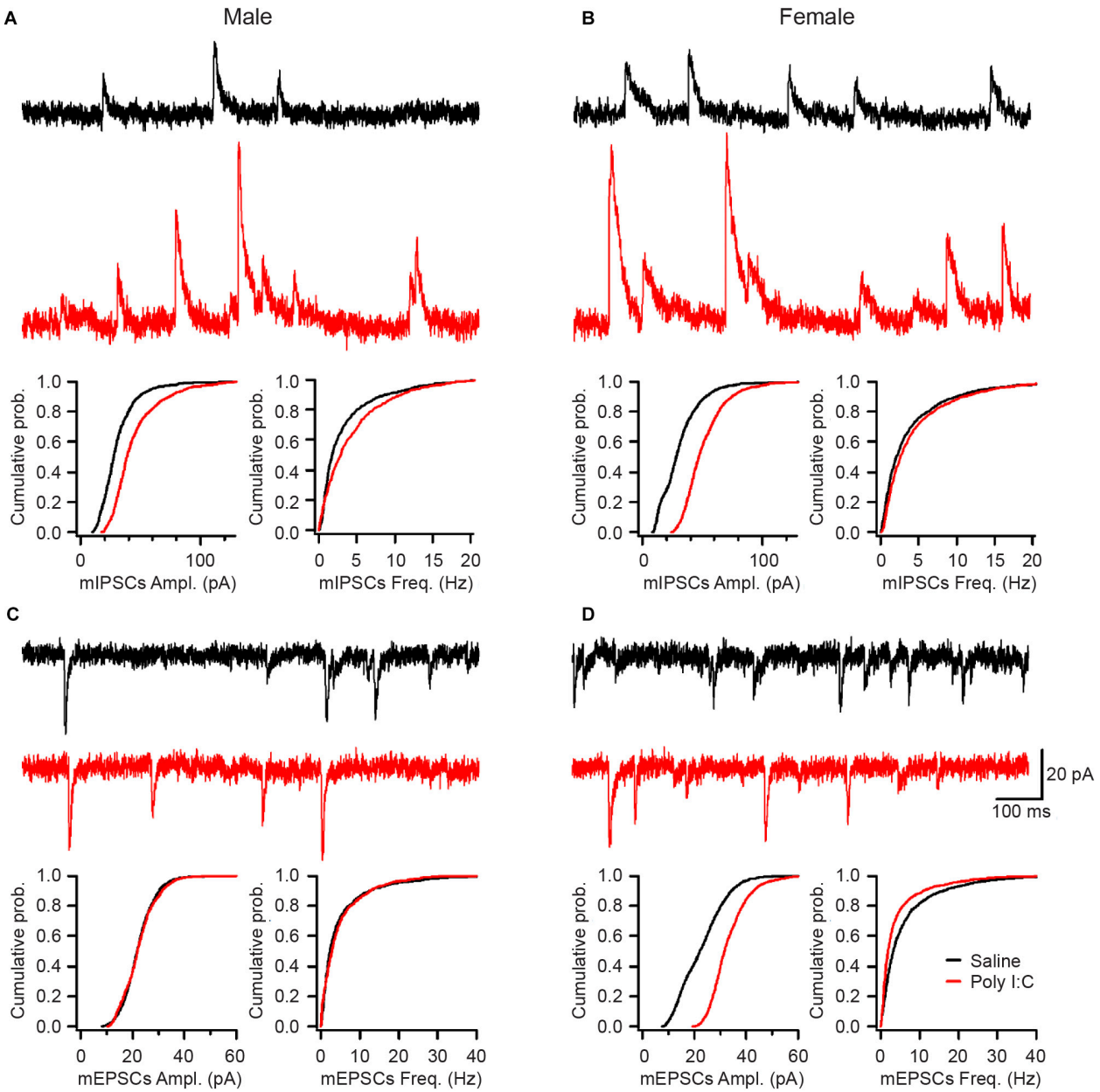

FIGURE 4 | Saline (top, black; male: n = 7 cells/5 mice; female: n = 9 cells/6 mice) or poly I:C (bottom, red; male: n = 5 cells/4 mice; female: n = 10 cells/5 mice). mIA led to increased mIPSC amplitude in GC of both males and females, together with increased mIPSC frequency in males, while increasing mEPSC amplitude but decreasing mEPSC frequency in females, without altering mEPSCs in males. **(A–D)** Representative traces from the GCs of the DG for miniature inhibitory post-synaptic currents (mIPSCs) in male **(A)** and female **(B)** offspring whose dams were exposed to saline or poly I:C. Representative traces from the DG GCs for miniature excitatory post-synaptic currents (mEPSCs) in male **(C)** and female **(D)** offspring whose dams were exposed to saline (top, black) or poly I:C (bottom, red). Scale bars indicate 20 pA (vertical) and 100 ms (horizontal). **(A)** Maternal poly I:C exposure increased the amplitude (median: saline, 27.6 pA; poly I:C, 38.6 pA; $p <$ 0.0001) and frequency (median: saline, 1.75 Hz; poly I:C, 2.85 Hz; $p < 0.0001$) of mIPSCs in male offspring. **(B)** As with males, in female offspring of dams exposed to poly I:C, there was an increase in the amplitude (median: saline, 28.3 pA; poly I:C, 47.0 pA; p 0.0001), but not the frequency of mIPSCs (median: saline, 2.10 Hz; poly I:C, 2.60 Hz; $p > 0.05$). **(C)** There was no effect of maternal poly I:C administration in male offspring on either the amplitude (median: saline, 23.6 pA; poly I:C, 21.0 pA; $p > 0.05$) or frequency (median: saline, 5.4 Hz; poly I:C, 5.9 Hz; $p > 0.05$) of miniature excitatory post-synaptic currents (mEPSCs). **(D)** Maternal poly I:C exposure increased the amplitude (median: saline, 22.2 pA; poly I:C, 31.7 pA; p 0.0001) but decreased the frequency (median: saline, 3.25 Hz; poly I:C, 1.90 Hz; p 0.01) of mEPSCs in females.

DATA AVAILABILITY STATEMENT

The raw data supporting the conclusions of this article will be made available by the authors, without undue reservation, to any qualified researcher.

ETHICS STATEMENT

The animal study was reviewed and approved by the Université Laval's Animal Ethics Committees, according to the Canadian Council on Animal Care's guidelines.

AUTHOR CONTRIBUTIONS

CH, LS, LT, and M-ÈT designed the study. CH, XL, ÉG, LS, KB, and KS conducted the experiments. CH, HV, XL, ÉG, FM, LS, LT, and M-ÈT analyzed the data. CH, HV, LS, LT, and M-ÈT contributed to writing and editing the manuscript. CH, HV, and ÉG prepared the figures. All authors contributed to the article and approved the submitted version.

FUNDING

This work was supported by the NARSAD Young Investigator Grant from the Brain and Behavior Research Foundation to M-ÈT, a CIHR Foundation Scheme grant (FDN341846) to M-ÈT and LT, CIHR (Operating Grants: MOP-137072-592 and MOP-142447) and NSERC (Discovery Grant: 342292-2012-RGPIN) awards to LT, a FRQS Postdoctoral Training Award to CH and a CIHR Fellowship to HV. M-ÈT is a Canada Research Chair – Tier 2 in Neurobiology of Aging and Cognition.

ACKNOWLEDGMENTS

We acknowledge that Université Laval stands on the unceded land of the Huron-Wendat peoples; and that the University of Victoria exists on the territory of the Lekwungen peoples and that the Songhees, Esquimalt and WSÁNEÆ peoples have relationships to this land. We are grateful to Julie-Christine Lévesque at the Bioimaging Platform of CRCHU de Québec-Université Laval for technical assistance, Nathalie Vernoux for guidance with the experiments and Dimitry Topolnik for electrophysiological equipment maintenance.

SUPPLEMENTARY MATERIAL

The Supplementary Material for this article can be found online at: https://www.frontiersin.org/articles/10.3389/fncel.2020.558181/full#supplementary-material

REFERENCES

Audoy-Rémus, J., Bozoyan, L., Dumas, A., Filali, M., Lecours, C., Lacroix, S., et al. (2015). GPR84 deficiency reduces microgliosis, but accelerates dendritic degeneration and cognitive decline in a mouse model of Alzheimer's disease. *Brain Behav. Immun.* 46, 112–120. doi: 10.1016/j.bbi.2015.01.010

Bisht, K., Sharma, K. P., Lecours, C., Sánchez, M. G., El Hajj, H., Milior, G., et al. (2016). Dark microglia: a new phenotype predominantly associated with pathological states. *Glia* 64, 826–839. doi: 10.1002/glia.22966

Bordeleau, M., Carrier, M., Luheshi, G. N., and Tremblay, M. -È. (2019). Microglia along sex lines: from brain colonization, maturation and function, to implication in neurodevelopmental disorders. *Semin. Cell Dev. Biol.* 94, 152–163. doi: 10.1016/j.semcdb.2019.06.001

Cherry, J. D., Olschowka, J. A., and O'Banion, M. K. (2014). Neuroinflammation and M2 microglia: the good, the bad, and the inflamed. *J. Neuroinflammation* 11:98. doi: 10.1186/1742-2094-11-98

Coyle, J. T., Basu, A., Benneyworth, M., Balu, D., and Konopaske, G. (2012). Glutamatergic synaptic dysregulation in schizophrenia: therapeutic implications. *Handb. Exp. Pharmacol.* 213, 267–295. doi: 10.1007/978-3-642-25758-2_10

David, L. S., and Topolnik, L. (2017). Target-specific alterations in the VIP inhibitory drive to hippocampal GABAergic cells after status epilepticus. *Exp. Neurol.* 292, 102–112. doi: 10.1016/j.expneurol.2017.03.007

Druart, M., and Le Magueresse, C. (2019). Emerging roles of complement in psychiatric disorders. *Front. Psychiatry* 10:573. doi: 10.3389/fpsyt.2019.00573

Feinberg, I. (1982). Schizophrenia: caused by a fault in programmed synaptic elimination during adolescence? *J. Psychiatr. Res.* 17, 319–334. doi: 10.1016/0022-3956(82)90038-3

Fu, H., Liu, B., Frost, J. L., Hong, S., Jin, M., Ostaszewski, B., et al. (2012). Complement component C3 and complement receptor type 3 contribute to the phagocytosis and clearance of fibrillar Aβ by microglia. *Glia* 60, 993–1003. doi: 10.1002/glia.22331

Gallagher, J. J., Minogue, A. M., and Lynch, M. A. (2013). Impaired performance of female APP/PS1 mice in the Morris water maze is coupled with increased Aβ accumulation and microglial activation. *Neurodegener. Dis.* 11, 33–41. doi: 10.1159/000337458

Giovanoli, S., Weber-Stadlbauer, U., Schedlowski, M., Meyer, U., and Engler, H. (2016). Prenatal immune activation causes hippocampal synaptic deficits in the absence of overt microglia anomalies. *Brain Behav. Immun.* 55, 25–38. doi: 10.1016/j.bbi.2015.09.015

González Ibanez, F., Picard, K., Bordelau, M., Sharma, K., Bisht, K., and Tremblay, M. -È. (2019). Immunofluorescence staining using IBA1 and TMEM119 for microglial density, morphology and peripheral myeloid cell infiltration analysis in mouse brain. *J. Vis. Exp.* 152:e60510. doi: 10.3791/60510

Harrison, P. J., Law, A. J., and Eastwood, S. L. (2003). Glutamate receptors and transporters in the hippocampus in schizophrenia. *Ann. N. Y. Acad. Sci.* 1003, 94–101. doi: 10.1196/annals.1300.006

Henry, M. S., Bisht, K., Vernoux, N., Gendron, L., Torres-Berrio, A., Drolet, G., et al. (2018). Delta opioid receptor signaling promotes resilience to stress under the repeated social defeat paradigm in mice. *Front. Mol. Neurosci.* 11:100. doi: 10.3389/fnmol.2018.00100

Heurich, B., El Idrissi, N. B., Donev, R. M., Petri, S., Claus, P., Neal, J., et al. (2011). Complement upregulation and activation on motor neurons and neuromuscular junction in the SOD1 G93A mouse model of familial amyotrophic lateral sclerosis. *J. Neuroimmunol.* 235, 104–109. doi: 10.1016/j.jneuroim.2011.03.011

Hui, C. W., St-Pierre, A., El Hajj, H., Remy, Y., Hébert, S. S., Luheshi, G. N., et al. (2018). Prenatal immune challenge in mice leads to partly sex-dependent behavioral, microglial, and molecular abnormalities associated with schizophrenia. *Front. Mol. Neurosci.* 11:13. doi: 10.3389/fnmol.2018.00013

Juckel, G., Manitz, M. P., Brüne, M., Friebe, A., Heneka, M. T., and Wolf, R. J. (2011). Microglial activation in a neuroinflammational animal model of schizophrenia–a pilot study. *Schizophr. Res.* 131, 96–100. doi: 10.1016/j.schres.2011.06.018

Kettenmann, H., Hanisch, U.-K., Noda, M., and Verkhratsky, A. (2011). Physiology of microglia. *Physiol. Rev.* 91, 461–553. doi: 10.1152/physrev.00011.2010

Korzhevskii, D. E., and Kirik, O. V. (2016). Brain microglia and microglial markers. *Neurosci. Behav. Physiol.* 46, 284–290. doi: 10.1007/s11055-016-0231-z

Li, W., Ghose, S., Gleason, K., Begovic, A., Perez, J., Bartko, J., et al. (2015). Synaptic proteins in the hippocampus indicative of increased neuronal activity in CA3 in schizophrenia. *Am. J. Psychiatry* 172, 373–382. doi: 10.1176/appi.ajp.2014.14010123

Lian, H., Litvinchuk, A., Chiang, A. C.-A., Aithmitti, N., Jankowsky, J. L., and Zheng, H. (2016). Astrocyte-microglia cross talk through complement activation modulates amyloid pathology in mouse models of Alzheimer's disease. *J. Neurosci.* 36, 577–589. doi: 10.1523/JNEUROSCI.2117-15.2016

Lian, H., Yang, L., Cole, A., Sun, L., Chiang, A. C.-A., Fowler, S. W., et al. (2015). NFκB-activated astroglial release of complement C3 compromises neuronal morphology and function associated with Alzheimer's disease. *Neuron* 85, 101–115. doi: 10.1016/j.neuron.2014.11.018

Luchena, C., Zuazo-Ibarra, J., Alberdi, E., Matute, C., and Capetillo-Zarate, E. (2018). Contribution of neurons and glial cells to complement-mediated synapse removal during development, aging and in Alzheimer's disease. *Mediators Inflamm.* 2018:2530414. doi: 10.1155/2018/2530414

Magdalon, J., Mansur, F., Teles, E., Silva, A. L., de Goes, V. A., Reiner, O., et al. (2020). Complement system in brain architecture and neurodevelopmental disorders. *Front. Neurosci.* 14:23. doi: 10.3389/fnins.2020.00023

Matosin, N., Fernandez-Enright, F., Lum, J. S., Engel, M., Andrews, J. L., Gassen, N. C., et al. (2016). Molecular evidence of synaptic pathology in the CA1 region in schizophrenia. *NPJ Schizophr.* 2:16022. doi: 10.1038/npjschz.2016.22

Mendrek, A., and Mancini-Marïe, A. (2016). Sex/gender differences in the brain and cognition in schizophrenia. *Neurosci. Biobehav. Rev.* 67, 57–78. doi: 10.1016/j.neubiorev.2015.10.013

Mongan, D., Ramesar, M., Föcking, M., Cannon, M., and Cotter, D. (2019). Role of inflammation in the pathogenesis of schizophrenia: a review of the evidence, proposed mechanisms and implications for treatment. *Early Interv. Psychiatry* 14, 385–397. doi: 10.1111/eip.12859

Nakazawa, K., Zsiros, V., Jiang, Z., Nakao, K., Kolata, S., Zhang, S., et al. (2012). GABAergic interneuron origin of schizophrenia pathophysiology. *Neuropharmacology* 62, 1574–1583. doi: 10.1016/j.neuropharm.2011.01.022

Nelson, L. H., Warden, S., and Lenz, K. M. (2017). Sex differences in microglial phagocytosis in the neonatal hippocampus. *Brain Behav. Immun.* 64, 11–22. doi: 10.1016/j.bbi.2017.03.010

Paolicelli, R. C., Bolasco, G., Pagani, F., Maggi, L., Scianni, M., Panzanelli, P., et al. (2011). Synaptic pruning by microglia is necessary for normal brain development. *Science* 333, 1456–1458. doi: 10.1126/science.1202529

Paxinos, G., and Watson, C. (1998). *The Rat Brain in Stereotaxic Coordinates*. Cambridge, MA: Academic Press.

Pinheiro, P. S., and Mulle, C. (2008). Presynaptic glutamate receptors: physiological functions and mechanisms of action. *Nat. Rev. Neurosci.* 9, 423–436. doi: 10.1038/nrn2379

Pratt, L., Ni, L., Ponzio, N. M., and Jonakait, G. M. (2013). Maternal inflammation promotes fetal microglial activation and increased cholinergic expression in the fetal basal forebrain: role of interleukin-6. *Pediatr. Res.* 74, 393–401. doi: 10.1038/pr.2013.126

Ratnayake, U., Quinn, T. A., Castillo-Melendez, M., Dickinson, H., and Walker, D. W. (2012). Behaviour and hippocampus-specific changes in spiny mouse neonates after treatment of the mother with the viral-mimetic Poly I:C at mid-pregnancy. *Brain Behav. Immun.* 26, 1288–1299. doi: 10.1016/j.bbi.2012.08.011

Roberts, R. C., Barksdale, K. A., Roche, J. K., and Lahti, A. C. (2015). Decreased synaptic and mitochondrial density in the postmortem anterior cingulate cortex in schizophrenia. *Schizophr. Res.* 168, 543–553. doi: 10.1016/j.schres.2015.07.016

Schafer, D. P., Lehrman, E. K., Kautzman, A. G., Koyama, R., Mardinly, A. R., Yamasaki, R., et al. (2012). Microglia sculpt postnatal neural circuits in an activity and complement-dependent manner. *Neuron* 74, 691–705. doi: 10.1016/j.neuron.2012.03.026

Scharfman, H. E. (2016). The enigmatic mossy cell of the dentate gyrus. *Nat. Rev. Neurosci.* 17, 562–575. doi: 10.1038/nrn.2016.87

Schwarz, J. M., Sholar, P. W., and Bilbo, S. D. (2012). Sex differences in microglial colonization of the developing rat brain. *J. Neurochem.* 120, 948–963. doi: 10.1111/j.1471-4159.2011.07630.x

Sellgren, C. M., Gracias, J., Watmuff, B., Biag, J. D., Thanos, J. M., Whittredge, P. B., et al. (2019). Increased synapse elimination by microglia in schizophrenia patient-derived models of synaptic pruning. *Nat. Neurosci.* 22, 374–385. doi: 10.1038/s41593-018-0334-7

Stevens, B., Allen, N. J., Vazquez, L. E., Howell, G. R., Christopherson, K. S., Nouri, N., et al. (2007). The classical complement cascade mediates CNS synapse elimination. *Cell* 131, 1164–1178. doi: 10.1016/j.cell.2007.10.036

Tamminga, C. A., Southcott, S., Sacco, C., Wagner, A. D., and Ghose, S. (2012). Glutamate dysfunction in hippocampus: relevance of dentate gyrus and CA3 signaling. *Schizophr. Bull.* 38, 927–935. doi: 10.1093/schbul/sbs062

Tavitian, A., Song, W., and Schipper, H. M. (2019). Dentate gyrus immaturity in schizophrenia. *Neuroscientist* 25, 528–547. doi: 10.1177/1073858418824072

Tenner, A. J. (2020). Complement-mediated events in Alzheimer's disease: mechanisms and potential therapeutic targets. *J. Immunol.* 204, 306–315. doi: 10.4049/jimmunol.1901068

Tian, L., Hui, C. W., Bisht, K., Tan, Y., Sharma, K., Chen, S., et al. (2017). Microglia under psychosocial stressors along the aging trajectory: consequences on neuronal circuits, behavior, and brain diseases. *Prog. Neuropsychopharmacol. Biol. Psychiatry* 79, 27–39. doi: 10.1016/j.pnpbp.2017.01.007

Tremblay, M. -È., Zettel, M. L., Ison, J. R., Allen, P. D., and Majewska, A. K. (2012). Effects of aging and sensory loss on glial cells in mouse visual and auditory cortices. *Glia* 60, 541–558. doi: 10.1002/glia.22287

Treves, A., Tashiro, A., Witter, M. P., and Moser, E. I. (2008). What is the mammalian dentate gyrus good for? *Neuroscience* 154, 1155–1172. doi: 10.1016/j.neuroscience.2008.04.073

Turmaine, M., Raza, A., Mahal, A., Mangiarini, L., Bates, G. P., and Davies, S. W. (2000). Nonapoptotic neurodegeneration in a transgenic mouse model of Huntington's disease. *Proc. Natl. Acad. Sci. U.S.A.* 97, 8093–8097. doi: 10.1073/pnas.110078997

Van den Eynde, K., Missault, S., Fransen, E., Raeymaekers, L., Willems, R., Drinkenburg, W., et al. (2014). Hypolocomotive behaviour associated with increased microglia in a prenatal immune activation model with relevance to schizophrenia. *Behav. Brain Res.* 258, 179–186. doi: 10.1016/j.bbr.2013.10.005

Walker, L. M., York, J. L., Imam, S. Z., Ali, S. F., Muldrew, K. L., and Mayeux, P. R. (2001). Oxidative stress and reactive nitrogen species generation during renal ischemia. *Toxicol. Sci.* 63, 143–148. doi: 10.1093/toxsci/63.1.143

Weinhard, L., Neniskyte, U., Vadisiute, A., di Bartolomei, G., Aygün, N., Riviere, L., et al. (2018). Sexual dimorphism of microglia and synapses during mouse postnatal development. *Dev. Neurobiol.* 78, 618–626. doi: 10.1002/dneu.22568

Witter, M. P. (2007). The perforant path: projections from the entorhinal cortex to the dentate gyrus. *Prog. Brain Res.* 163, 43–61. doi: 10.1016/s0079-6123(07)63003-9

Xiong, C., Liu, J., Lin, D., Zhang, J., Terrando, N., and Wu, A. (2018). Complement activation contributes to perioperative neurocognitive disorders in mice. *J. Neuroinflammation* 15:254.

Yanguas-Casás, N., Crespo-Castrillo, A., de Ceballos, M. L., Chowen, J. A., Azcoitia, I., Arevalo, M. A., et al. (2018). Sex differences in the phagocytic and migratory activity of microglia and their impairment by palmitic acid. *Glia* 66, 522–537. doi: 10.1002/glia.23263

Yuan, J. S., Reed, A., Chen, F., and Stewart, C. N. (2006). Statistical analysis of real-time PCR data. *BMC Bioinformatics* 7:85. doi: 10.1186/1471-2105-7-85

Zhao, Y., Luo, C., Chen, J., Sun, Y., Pu, D., Lv, A., et al. (2018). High glucose-induced complement component 3 up-regulation via RAGE-p38MAPK-NF-κB signalling in astrocytes: in vivo and in vitro studies. *J. Cell. Mol. Med.* 22, 6087–6098. doi: 10.1111/jcmm.13884

Conflict of Interest: The authors declare that the research was conducted in the absence of any commercial or financial relationships that could be construed as a potential conflict of interest.

frontiers in Cellular Neuroscience

REVIEW
published: 17 December 2020
doi: 10.3389/fncel.2020.592607

Synaptic Loss in Alzheimer's Disease: Mechanistic Insights Provided by Two-Photon *in vivo* Imaging of Transgenic Mouse Models

Jaichandar Subramanian[1]*, *Julie C. Savage*[2†] and *Marie-Ève Tremblay*[3,4,5,6]*

[1] Department of Pharmacology & Toxicology, University of Kansas, Lawrence, KS, United States, [2] Axe Neurosciences, Centre de Recherche du CHU de Québec, Université Laval, Québec City, QC, Canada, [3] Neurology and Neurosurgery Department, McGill University, Montreal, QC, Canada, [4] Department of Molecular Medicine, Université Laval, Québec City, QC, Canada, [5] Division of Medical Sciences, University of Victoria, Victoria, BC, Canada, [6] Department of Biochemistry and Molecular Biology, The University of British Columbia, Vancouver, BC, Canada

Synapse loss is the strongest correlate for cognitive decline in Alzheimer's disease. The mechanisms underlying synapse loss have been extensively investigated using mouse models expressing genes with human familial Alzheimer's disease mutations. In this review, we summarize how multiphoton *in vivo* imaging has improved our understanding of synapse loss mechanisms associated with excessive amyloid in the living animal brain. We also discuss evidence obtained from these imaging studies for the role of cell-intrinsic calcium dyshomeostasis and cell-extrinsic activities of microglia, which are the immune cells of the brain, in mediating synapse loss.

Keywords: dendritic spines, microglia, two-photon, *in vivo* imaging, amyloid mouse models

OPEN ACCESS

Edited by:
Carole Escartin, UMR9199 Laboratory of Neurodegenerative Diseases Mechanisms, Therapies, Imaging, France

Reviewed by:
Jochen Herms, German Center for Neurodegenerative Diseases (DZNE) and Zentrum für Neuropathologie (ZNP) Ludwig-Maximilians-University Munich, Germany
Estibaliz Capetillo-Zarate, University of the Basque Country, Spain

***Correspondence:**
Jaichandar Subramanian
jaichandar@ku.edu
Marie-Ève Tremblay
evetremblay@uvic.ca

†Present address:
Julie C. Savage, Convelo Therapeutics, Cleveland, OH, United States

Specialty section:
This article was submitted to Cellular Neuropathology, a section of the journal Frontiers in Cellular Neuroscience

Received: *07 August 2020*
Accepted: *25 November 2020*
Published: *17 December 2020*

Citation:
Subramanian J, Savage JC and Tremblay M-È (2020) Synaptic Loss in Alzheimer's Disease: Mechanistic Insights Provided by Two-Photon in vivo Imaging of Transgenic Mouse Models. Front. Cell. Neurosci. 14:592607. doi: 10.3389/fncel.2020.592607

INTRODUCTION

Immunohistochemistry of *postmortem* brain from Alzheimer's disease (AD) patients revealed that synapse loss is the strongest correlate for the cognitive deficit (Terry et al., 1991; DeKosky et al., 1996; Scheff and Price, 2006; Scheff et al., 2007; de Wilde et al., 2016). Mouse models that express familial AD-associated mutations in genes coding for amyloid precursor protein and presenilin that increase amyloid levels in the brain or that express mutated Tau leading to neurofibrillary tangles provide an entry point to study mechanisms of synapse loss associated with prominent AD related pathologies, such as amyloid plaques and neurofibrillary tangles (Jankowsky and Zheng, 2017). Morphological and electrophysiological studies done on *ex vivo* and *postmortem* preparations from these mice have confirmed that human familial AD associated mutations cause synaptic dysfunction, ranging from impaired plasticity to increased loss of synapses (Selkoe, 2002; Knobloch and Mansuy, 2008; Spires-Jones and Knafo, 2012; Yu and Lu, 2012; Pozueta et al., 2013; Forner et al., 2017). *Postmortem* preparations only offer a snapshot of pathology that does not capture dynamic events that precede or follow the observed deficits. *Ex vivo* preparations, on the other hand, allow for monitoring dynamic events but not in the context of the intact neural circuitry of a living brain. In addition, the functions of microglia, which are the immune cells of the brain, are severely affected by experimental procedures (Hellwig et al., 2013; Gosselin et al., 2017).

The advent of fluorescence labeling technologies and two-photon microscopy enabled direct visualization of synapse dynamics *in vivo* in the living mouse brain (Grutzendler et al., 2002; Trachtenberg et al., 2002). Typically, neurons are sparsely labeled with a fluorescent cell fill to

visualize the morphology of subcellular structures, such as dendritic spines (postsynapse) or axonal boutons (presynapse). Fluorescence labeling is achieved by expressing fluorescent proteins through transgene integration, viral delivery, or *in utero* electroporation. Optical access to fluorescently labeled neurons is achieved by replacing part of the skull with a glass coverslip or thinning it. Though two-photon excitation provides higher depth resolution than traditional single-photon excitation, it is still limited to ∼450 μm from the surface of the brain (Takasaki et al., 2020). Therefore, non-invasive two-photon imaging studies are restricted to superficial layers of the cortex, however synaptic imaging in the hippocampus has been achieved using more invasive approaches, such as removal of overlying cortical tissue or micro-endoscopy (Mizrahi et al., 2004; Gu et al., 2014; Attardo et al., 2015). Two-photon imaging in mouse models of AD has allowed for the interrogation of synaptic dysfunction associated with amyloid and tau pathology in the intact circuitry of living animals (**Tables 1**, **2**). More importantly, *in vivo* imaging of synapses allows for chronic monitoring of synaptic changes in the same neurons over time, thereby enabling the visualization of synaptic dynamics. In this review, we focus on how *in vivo* imaging using two-photon microscopy has revealed the properties and mechanisms of synapse loss in mouse models of AD, emphasizing mouse models of amyloidosis. Due to the depth limitations of two-photon imaging, most of these studies tracked synaptic changes in the somatosensory cortex (unless otherwise mentioned).

AMYLOID ASSOCIATED NEURITE PATHOLOGY

After its development for *in vivo* imaging (Grutzendler et al., 2002; Trachtenberg et al., 2002), two-photon microscopy was quickly adopted to visualize neurite dystrophy associated with amyloidosis (D'Amore et al., 2003). The initial study confirmed findings from *postmortem* AD patient brains (Onorato et al., 1989) and amyloid mouse models (Richardson and Burns, 2002) that plaques alter the trajectory of neurites and are associated with their dystrophy (D'Amore et al., 2003). Consistently, many subsequent *in vivo* imaging studies confirmed the existence of dystrophic neurites (variably defined as swelling >2.5 μm or a volume 2-fold over normal neurites) near plaques (Tsai et al., 2004; Brendza et al., 2005; Spires et al., 2005; Spires-Jones et al., 2007, 2011; Kuchibhotla et al., 2008; Meyer-Luehmann et al., 2008; Bittner et al., 2010, 2012; Wu et al., 2010; Zou et al., 2015, 2016; Schmid et al., 2016; Blazquez-Llorca et al., 2017; Peters et al., 2018). The presence of dystrophic neurites near plaques could either mean that plaques cause neurite dystrophy or dystrophic neurites promote plaque formation. Addressing this question requires monitoring the dynamics of neurites and plaques over time, which is not possible with traditional imaging approaches on *postmortem* brain slices. Longitudinal imaging of dystrophic neurites and plaques shows that plaque formation precedes dystrophic neurites (Meyer-Luehmann et al., 2008; Blazquez-Llorca et al., 2017; Peters et al., 2018). In one of the mouse models, APPswe/PS1E9 mice, dystrophic dendrites were present in regions with no apparent plaques (Meyer-Luehmann et al., 2008). Longitudinal imaging of these regions did not identify any *de novo* plaque formation near the dystrophic dendrites. Interestingly, during this time, some of the neurites returned to normalcy or disappeared. Only 60% of the dystrophic neurites remained stable over 2 weeks (Meyer-Luehmann et al., 2008). If dystrophic neurites do not promote plaque formation, it is more likely that plaques increase the abundance of dystrophic neurites. This possibility is supported by the observations that the appearance of dystrophic neurites follows plaque appearance (Meyer-Luehmann et al., 2008; Blazquez-Llorca et al., 2017). The curvature of neurites across the plaque continues to increase following plaque formation, with damaged neurites appearing in the subsequent days (Tsai et al., 2004; Meyer-Luehmann et al., 2008). Only ∼25% of neurites near plaque developed dystrophy, and more detailed analyses of their dynamics revealed that they are highly stable with a mean lifetime of 76 days (Blazquez-Llorca et al., 2017). The volume of dystrophy is highly variable, and interestingly, is also highly dynamic, with dystrophies undergoing both shrinkage and expansion (Blazquez-Llorca et al., 2017). Plaques smaller than 4 μm are not associated with dystrophic neurites, and as the plaque size increased, the extent of dystrophy also increased (Blazquez-Llorca et al., 2017; Peters et al., 2018).

Though dystrophic neurites do not appear to promote plaque formation, they may still contribute to the growth of preformed plaque. Plaque growth occurs over a long period, exhibiting sigmoidal growth kinetics (Christie et al., 2001; Yan et al., 2009; Burgold et al., 2011, 2014; Condello et al., 2011; Hefendehl et al., 2011; Bittner et al., 2012). One of the contributing factors for plaque growth is the local concentration of the enzyme BACE-1, whose cleavage of amyloid precursor protein results in amyloid peptides present in the plaque (Hussain et al., 1999; Sinha et al., 1999; Vassar et al., 1999; Yan et al., 1999; Lin et al., 2000). BACE-1 levels are increased in dystrophic neurites in cultured neurons and brain sections of AD patients, and 5XFAD amyloid mouse model (Zhang et al., 2009; Kandalepas et al., 2013; Sadleir et al., 2016), and therefore, dystrophic neurites can contribute to plaque growth. Consistent with this idea, inhibition of BACE-1 decreased the growth rate of plaques (Peters et al., 2018), which, in turn, reduced the formation of dystrophic neurites associated with plaque (Peters et al., 2018). The vicious cycle of amyloid plaque growth, the formation of neurite dystrophy, and accumulation of BACE-1 in dystrophic neurites also results in the formation of satellite plaques (Peters et al., 2018). Interestingly, the deletion of the gene coding for microtubule binding protein Tau reduces the accumulation of BACE-1 in dystrophic neurites and reduces the formation of satellite plaques (Peters et al., 2019). Thus, *in vivo* two-photon imaging approaches have allowed us to understand the kinetics of plaque formation and growth and its relevance to the appearance of dystrophic neurites in a manner not feasible with traditional *postmortem* analyses.

AMYLOID ASSOCIATED DENDRITIC SPINE PATHOLOGY

Dystrophic neurites near plaques have a reduced density of dendritic spines (Spires et al., 2005). Since neurite dystrophy is

TABLE 1 | Studies examining dendritic spine and neurite pathology in mouse models of amyloidosis using *in vivo* two-photon microscopy that are discussed in this review.

Model strain	Method of neuronal labeling	Age at imaging	Brain region imaged	Interval between imaging sessions	Dendritic spine/bouton changes (compared to control)	Presence of neurite dystrophy	References
PDAPP	Alexafluor-594-Dextran	19–22 months	Non-specified cortical regions	–	–	Yes	D'Amore et al., 2003
PSAPP	Crossed with Thy1-YFP transgenic mice	6 months	Non-specified cortex	2–4 days, 1–2 weeks, 4–5 weeks	Increased spine gain and loss but loss greater than gain	Yes	Tsai et al., 2004
Tg2576	Viral delivery of GFP	21–24 months	Somatosensory cortex	1 week	–	Yes	Spires et al., 2005
Tg2576	Viral delivery of GFP	8–10 months; 18–24 months	Somatosensory cortex	Minutes to 1 hour	Increased spine loss in 18–24 but not 8–10 months		Spires-Jones et al., 2007
Tg2576; PS1ΔE9; APP/PS1; PS1M146V	Viral delivery of a calcium indicator YC3.6	Tg2576: 17–20 months; PS1ΔE9: 5- 6 months; APP/PS1: 3–3.5 months.	Somatosensory cortex	–	Elevated intracellular calcium and disrupted calcium compartmentalization.	Yes	Kuchibhotla et al., 2008
APPswe/PS1d9; Tg2576; PDAPP	Crossed with Thy1-YFP transgenic mice	5–6 months	Non-specified cortex	One day or one week	–	Yes	Meyer-Luehmann et al., 2008
3xTg-AD	Crossed with Thy1-YFP transgenic mice	4-6, 8–10, 13–15 and 18–20 months	Somatosensory cortex	Few days	8–10 month - no change, 13–15 and 18–20 month - increased spine gain and loss	Yes	Bittner et al., 2010
APP1PS1	Viral delivery of GFP	6 month	Somatosensory cortex	–	–	Yes	Wu et al., 2010
APP PS1	Crossed with Thy1-YFP transgenic mice	3–4 months and 18–19 months	Somatosensory cortex	One week	Increased spine loss but same spine gain	–	Bittner et al., 2012
5X-FAD	Crossed with Thy1-YFP transgenic mice	3–4 months	Somatosensory cortex	Few days	Not reported.	No gross deficit observed.	Buskila et al., 2013
APP PS1 mice	Crossed with Thy1-GFP transgenic mice	3–4 months	Somatosensory cortex	One week	Increased spine gain and loss	–	Liebscher et al., 2014
APP23 and APPswe/PS1deltaE9	Crossed with Thy1-GFP transgenic mice	4–5 months	Somatosensory cortex	One week	Decreased spine gain and no change in loss.	–	Zou et al., 2015
APPPS1	Crossed with GAD1-GFP mice	4–11 months	Hippocampus	Weekly, monthly	Increased spine loss with age. Decreased spine stabilization after learning.	–	Schmid et al., 2016
APPswe/PS1deltaE9	Crossed with Thy1-GFP transgenic mice	4–5 months	Somatosensory cortex	One week	Enriched environment does not change spine turnover whereas it is increased in controls.	–	Zou et al., 2016
APP swe/PS1deltaE9	Viral delivery of calcium sensor GCaMP6	3 months	Primary motor cortex	Hours	Longer duration calcium transients in dendrites, decreased spine size in dendrites with long duration calcium currents.	–	Bai et al., 2017

(Continued)

TABLE 1 | Continued

Model strain	Method of neuronal labeling	Age at imaging	Brain region imaged	Interval between imaging sessions	Dendritic spine/bouton changes (compared to control)	Presence of neurite dystrophy	References
APPswe/PSen1ΔE9	Crossed with Thy1-GFP transgenic mice	3–4 months; 10–11 months	Somatosensory cortex	2 weeks	Increase in both spine gain and loss.	–	Heiss et al., 2017
APPswe/PS1deltaE9 and APP-PS1	Crossed with Thy1-GFP transgenic mice	APPswe/PS1deltaE9: 7–13 months; APP-PS1: 3–10 months	Somatosensory cortex	One week	–	Yes	Blazquez-Llorca et al., 2017
APP-PS1	Crossed with VGLUT1^{venus} knockin mice	3–7 months	Somatosensory cortex	One week	Bouton density reduced closer to plaque	Yes	Peters et al., 2018
APP-PS1	Crossed with VGLUT1^{venus} knockin mice	3–6 months	Somatosensory cortex	One week	–	Yes	Peters et al., 2019
J20	Viral delivery of GFP	7–10 and 11–14 months	Somatosensory cortex	One week	Bouton but not spine density reduced	No	Stephen et al., 2019

increased after plaque appearance, is the reduction in synapses triggered only after plaque formation? One of the consensuses from the different *in vivo* imaging studies performed in mouse models of amyloidosis is that the density of dendritic spines is lower within 50 μm from the plaque compared to farther away from the plaque or non-transgenic controls (Spires-Jones et al., 2007; Kuchibhotla et al., 2008; Zou et al., 2015) but see Stephen et al. (2019). Though less pronounced, a reduction in spine density (Spires et al., 2005; Bittner et al., 2010) or a reduction in mature spine morphology (Zou et al., 2015) compared to non-transgenic controls was observed in dendrites > 50 μm away from plaque. A smaller reduction in spine density farther away from plaque could be due to reduced local concentration of soluble amyloid compared to the vicinity of a plaque. The reduction in spine density did not correlate with the size of the plaque (Spires et al., 2005), supporting the idea that soluble amyloid in the periphery of the plaque rather than the plaque itself is responsible for synapse loss (Mucke et al., 2000; Koffie et al., 2009). Consistently, spine loss is observed in *ex vivo* preparations following exposure to amyloid peptides (Hsieh et al., 2006; Shrestha et al., 2006; Shankar et al., 2007), and *in vivo* 1 day after the injection of soluble amyloid in non-transgenic mice (Arbel-Ornath et al., 2017).

Soluble amyloid is present even in the absence of plaques; therefore, if soluble amyloid alone were sufficient for spine loss, one would expect a significant reduction in spine loss prior to plaque formation. Longitudinal imaging of spines before and following *de novo* plaque formation reveals that spine density begins to reduce only 4.5 weeks after plaque formation (Bittner et al., 2012). Consistently, multiple imaging studies show normal spine density before plaque formation (Spires-Jones et al., 2007; Kuchibhotla et al., 2008; Bittner et al., 2010). Though these observations tend to support a role for amyloid plaque itself in spine loss, a more parsimonious explanation is that spine loss requires a high enough concentration of amyloid peptides that becomes available at an age when plaques are formed in the strains used for *in vivo* imaging (Maia et al., 2013). The less dramatic effect of soluble amyloid in transgenic mouse models of amyloidosis on overt spine loss *in vivo* compared to *ex vivo* preparations indicates possible resistance to spine loss when the buildup of amyloid is gradual compared to a sudden spike used in bath applications of *ex vivo* preparations. In addition, the lack or alteration of clearance mechanisms, such as microglial phagocytosis (Mandrekar et al., 2009), may exacerbate the synaptotoxic effect of amyloid in *ex vivo* preparations. These explanations, however, are at odds with the findings that brain slices from some mouse models of amyloidosis show synapse loss prior to plaque formation (Hsia et al., 1999; Moechars et al., 1999; Mucke et al., 2000; Lanz et al., 2003; Jacobsen et al., 2006). One plausible explanation for this discrepancy is that the brain regions examined for synapse loss using *in vivo* imaging (mostly, somatosensory cortex) and brain slices (mostly, hippocampus) are not the same. The vulnerability of synapses or the local concentration of amyloid could differ between brain regions and contribute to the plaque dependence for spine loss in brain regions imaged using two-photon microscopy. However, this may not be the sole reason because, in 3xTg-AD mouse strain,

TABLE 2 | Studies examining dendritic spine and neurite pathology in mouse models of Tauopathy using *in vivo* two-photon microscopy that are discussed in this review.

Model strain	Method of neuronal labeling	Age at imaging	Brain region imaged	Interval between imaging sessions	Dendritic spine/bouton changes (compared to control)	Presence of neurite dystrophy	References
rTg4510	Crossed with Thy1-YFP transgenic mice	9–10 months	Somatosensory cortex	–	Reduced spine density	–	Kopeikina et al., 2013a
P301S Tau	Crossed with Thy1-YFP transgenic mice	4 months	Somatosensory cortex	3–4 days	Reduced spine density. Decreased spine gain and slightly decreased loss	–	Hoffmann et al., 2013
rTg4510	Viral delivery of calcium indicator YC3.6	8–9 months	Somatosensory cortex	–	Reduced spine density did not correlate with calcium levels in parent dendrite	–	Kopeikina et al., 2013b
rTg4510	Viral delivery of GFP	4, 5, and 6.5 months	Somatosensory cortex	One week	Reduced spine density. Both gain and loss are increased. Bouton turnover decreased.	–	Jackson et al., 2017
rTg4510	Viral delivery of GFP	4,5,6 and 7 months	Somatosensory cortex	One week	Reduced spine and bouton density. Spine turnover increased and bouton turnover decreased.	–	Jackson et al., 2017

spine loss was observed in brain slices of the hippocampus and frontal cortex only after plaque formation, though these areas did not exhibit a characteristic plaque-distance dependence for spine loss (Bittner et al., 2010).

Pre- and postsynaptic terminals may exhibit differential plaque distance dependent vulnerability. The evidence for the vulnerability of presynaptic terminals in amyloid mouse models has been contradictory. Some histological studies found evidence for the loss of synaptophysin (Rutten et al., 2005; Dong et al., 2007; Tampellini et al., 2010) whereas others have not (King and Arendash, 2002; Rutten et al., 2003; Boncristiano et al., 2005; Hong et al., 2016), even in the same amyloid mouse model. *In vivo* imaging of presynaptic boutons in amyloid model mice show increased dynamics of boutons near the plaque compared to farther away from the plaque (Liebscher et al., 2014; Blazquez-Llorca et al., 2017; Stephen et al., 2019). The plaque distance-dependent synaptic loss and dystrophy holds up even when a presynaptic protein (Vglut1) is directly visualized *in vivo* (Peters et al., 2018). One of the reasons for the lack of consensus with respect to loss of presynaptic terminals in amyloid models could be due to variations in the sampling of different cell types between studies.

The plaque distance dependence of synapse loss observed in *in vivo* imaging studies using amyloid mouse models is in stark contrast to the observed loss of synapses affecting both pre- and postsynaptic elements across *postmortem* cortex (Terry et al., 1991; DeKosky et al., 1996; Sze et al., 1997; Scheff and Price, 2006; Scheff et al., 2007; de Wilde et al., 2016), despite plaques occupying only 5–10% of cortical volume in AD patients (Terry, 2000). Multiple differences between AD patients and mouse models of amyloidosis can account for the difference in plaque distance-dependent effect on synapses. One remarkable feature of mouse models of amyloidosis is that they exhibit limited or no neuronal death (Wirths and Bayer, 2010; Jankowsky and Zheng, 2017). The death of a neuron whose axons travel far will be accompanied by synapse loss farther from the soma. Thus, the lack of synapse loss farther away from plaque could be a consequence of limited or no plaque-associated cell death in these mouse models. Another possibility for preferential loss of synapses closer to plaques is that most mouse models of amyloidosis do not display the Tau pathology observed in human AD patients. When Tau mutation is combined with amyloidosis, as in the triple transgenic 3xTg-AD mice, spine loss was observed closer to and farther away from the plaque (Bittner et al., 2010).

SPINE LOSS AND COGNITIVE DECLINE

If spine loss increases only at the age when plaques are present, then one would expect cognitive deficits to be apparent only after plaque formation. However, cognitive deficits are observed before plaque formation in many amyloid mouse models (Holcomb et al., 1998; Wisniewski and Sigurdsson, 2010). In one of the strains, APP23, where cognitive decline precedes plaque formation, it was found that amyloid precursor protein accumulates intracellularly, and the amount of intracellular accumulation correlates with spine loss (Zou et al., 2015). Another caveat in reconciling cognitive studies with *in vivo* spine imaging studies is that most *in vivo* imaging studies in amyloid mouse models are restricted to the somatosensory cortex. Typically used cognitive tests, such as spatial or contextual memory tasks, may not elicit synaptic remodeling in the somatosensory cortex. In contrast, changes to sensory experience have been shown to cause synaptic remodeling in the somatosensory cortex (Trachtenberg et al., 2002). In the one of the amyloid mouse models, synaptic remodeling elicited by exposure to an enriched environment is disrupted in the somatosensory cortex before plaque appearance when spine density is normal (Zou et al., 2016; Heiss et al., 2017).

One of the main reasons most *in vivo* imaging studies are restricted to the somatosensory cortex is that it is easily accessible for non-invasive imaging. Imaging hippocampus, located ∼1 mm deep in the brain, is out of the range for conventional two-photon imaging. Two-photon imaging of dendritic spines in the hippocampus is achieved by microendoscopy or by removing the

overlying cortex (Mizrahi et al., 2004; Gu et al., 2014; Attardo et al., 2015). To date, to our knowledge, spine imaging *in vivo* in the hippocampus has not been performed in excitatory neurons of amyloid mouse models. However, a group of inhibitory neurons in the hippocampus, positive for somatostatin, that possess dendritic spines, has been studied using *in vivo* two-photon imaging in an amyloid mouse model (Schmid et al., 2016). The density of spines on these interneurons is reduced near the plaque. This reduction is due to a decrease in input from cholinergic neurons, which are lost due to cell death. In these somatostatin positive interneurons, new spines are formed in response to fear conditioning; however, this process is disrupted in the amyloid model (Schmid et al., 2016).

Most *in vivo* imaging studies use dendritic spines as a proxy for excitatory synapses. The maturation status of the spine is inferred from their shape, stability, and age. Newly formed spines are usually thin and are transient. If they persist for more than 4 days, they are highly likely to carry synapses (Knott et al., 2006). Mature persistent spines resemble mushroom-like structures and are called mushroom spines (Bourne and Harris, 2007). Though age, shape, and stability of dendritic spines could be a good predictor for the maturation status of a synapse, they are not entirely reliable. Spines that persist for 4 days may not contain synaptic proteins associated with mature synapses (Subramanian et al., 2019). Even if the plaque-associated spine loss observed in the superficial cortical regions is globally true, structural alterations, such as changes to AMPA receptors concentration, not captured by imaging spine alone could underlie cognitive decline. Therefore, synaptic abnormalities associated with cognitive decline may not require overt spine loss and the mechanisms could differ depending on the brain region and the model strains.

MECHANISMS OF AMYLOID ASSOCIATED SPINE LOSS

In adult mice, spine formation and elimination are balanced to maintain spine density (Villa et al., 2016; Subramanian et al., 2019). A reduction in the density of spines under amyloid pathology could result from the decreased formation of new spines or increased elimination of preexisting spines or both. No consensus has emerged on whether amyloid pathology triggers spine reduction by regulating formation or elimination. *In vivo* imaging studies have found increased spine elimination with no change in formation or smaller increase in formation (Tsai et al., 2004; Spires-Jones et al., 2007; Bittner et al., 2012), decreased spine formation with no change or an increase in elimination (Zou et al., 2015), or an increase in both formation and elimination (Bittner et al., 2010; Liebscher et al., 2014; Heiss et al., 2017). How could an increase in both formation and elimination result in reduced spine density? Newly formed dendritic spines could mature into stable synapses or disappear without forming synapses (Subramanian et al., 2019). If amyloid pathology reduces synapse stabilization, neurons will continue to make futile attempts to form synapses, whereas under non-pathological conditions, due to synapse stabilization, there would be fewer futile attempts. Each futile attempt will be counted as a dynamic event, and therefore, APP mice would have higher spine dynamics and yet have lower spine density.

How could amyloid pathology induce neurite dystrophy and spine loss? Calcium signaling regulates synaptic plasticity and dendritic arbor development (Konur and Ghosh, 2005), and growing evidence suggests that amyloid pathology disrupts neuronal calcium homeostasis (Holscher, 1998; Kawahara, 2004; Small, 2009; Brawek and Garaschuk, 2014; Popugaeva et al., 2017). Consistent with *ex vivo* preparations (Mattson et al., 1992; Guo et al., 1999; Demuro et al., 2005; Smith et al., 2005; Mattson, 2007), *in vivo* imaging of calcium reveals that dendrites closer to plaque have increased intracellular neuronal calcium in the intact brain of amyloid mouse models (Kuchibhotla et al., 2008). Before plaque formation, dendritic calcium levels in an amyloid mouse model are not different from non-transgenic mice (Kuchibhotla et al., 2008). In non-transgenic mice, calcium concentration within the spine does not correlate with that of the parent dendrite, whereas under amyloid pathology, there is a linear relationship between the two, suggesting that the compartmentalization of calcium in spines is lost (Kuchibhotla et al., 2008). Amyloid peptides can increase intracellular calcium within an hour after exposure, but spine loss occurs only 24 h later (Arbel-Ornath et al., 2017). Interestingly, spines that shrink following the application of amyloid peptide in the motor cortex are the ones that were activated during the prolonged dendritic calcium current elicited by the amyloid peptide (Bai et al., 2017).

A ROLE FOR TAU IN SYNAPSE LOSS

The *in vivo* imaging studies described thus far are mostly focused on how amyloidosis associated with familial AD cases influence synapses. The effect of accumulation of hyper-phosphorylated Tau, another prominent AD-related pathology, on synaptic structure integrity is relatively less studied using *in vivo* two-photon imaging. The effect of overexpressing mutant Tau on synapse density has yielded mixed results in the histological analysis (Shahani et al., 2006; Eckermann et al., 2007; Yoshiyama et al., 2007; Hoover et al., 2010; Rocher et al., 2010; Crimins et al., 2011; Jaworski et al., 2011; Kremer et al., 2011; Alldred et al., 2012). In contrast, there is consensus among *in vivo* two-photon imaging studies that dendritic spine density is reduced in Tau mouse models (Bittner et al., 2010; Hoffmann et al., 2013; Kopeikina et al., 2013a,b; Jackson et al., 2017, 2020). The first *in vivo* imaging study describing the effect of Tau on synapses was done in triple transgenic 3xTg-AD mice that also had mutations associated with amyloidosis (Bittner et al., 2010). However, later studies using Tau models also showed a decrease in spine density. In a Tau model with P301S mutation, spine gain is reduced and is not matched by an equivalent reduction in spine loss, whereas, in the control mice, formation and elimination of spines are balanced. As a consequence, spine density is reduced in the Tau mutant model. Interestingly, the spine deficits are present at an age when no neurofibrillary tangles are apparent, and Tau itself is not localized to dendritic spines (Hoffmann et al., 2013). *In vivo* imaging also revealed decreased spine density in 8–9 month-old rTg4510 mouse model with P301L mutation. Surprisingly, in the same study, array tomography revealed no difference in synaptic density compared to wild-type control mice (Kopeikina

et al., 2013a). Later *in vivo* imaging studies using this model confirmed a progressive decline in spine density between 4 and 6.5 months of age (Jackson et al., 2017, 2020). The decline in spine density is not uniform in all dendrites, with some dendrites exhibiting complete loss of spines. Higher turnover of dendritic spines, in some instances, is followed by the loss of associated dendritic branches. Over 6 months, ∼35% of the dendrites are lost. In contrast, the axonal loss is preceded by a decreased turnover of boutons. The loss of synapses in this model also occurred at an age when neurofibrillary tangles are not yet present (Jackson et al., 2017, 2020). Interestingly, unlike amyloid models, spine loss in the rTg4510 model is not associated with elevated intracellular neuronal calcium (Kopeikina et al., 2013b).

Multiple cellular pathologies, such as intracellular calcium homeostasis, mitochondrial dysfunction, energy metabolism, and reactive oxygen species, associated with amyloidosis, have been imaged *in vivo* using two-photon microscopy (McLellan et al., 2003; Xie et al., 2013; Arbel-Ornath et al., 2017; Bai et al., 2017; Gomez et al., 2018; Lerdkrai et al., 2018; Calvo-Rodriguez et al., 2020). However, the dynamics of synapse loss in relation to these different cellular deficits resulting from amyloidosis remains to be explored by *in vivo* two-photon imaging. Synapse loss may not occur solely due to these cell-intrinsic factors. Growing evidence indeed suggests that microglial phagocytosis may be a key player in synaptic loss in amyloid and/or Tau mouse models. Below, we discuss how two-photon *in vivo* imaging has also uncovered a novel role for microglia during amyloid and Tau pathology.

MICROGLIAL IMPLICATION IN AD: INSIGHTS FROM TWO-PHOTON *IN VIVO* IMAGING STUDIES

Microglia, which are the resident innate immune cells of the brain, have been intimately associated with AD since the disease was first described. In his landmark studies, Dr. Alois Alzheimer described glial cells developing excess fibers and containing "adipose saccules" (Alzheimer et al., 1995). Over 80 years later, studies conducted on *postmortem* AD brain samples revealed that microglia surrounding plaques express elevated levels of histocompatibility antigens and the pro-inflammatory cytokine IL-1 (Rogers et al., 1988; Griffin et al., 1989; Overmyer et al., 1999). Ultrastructural studies further uncovered microglia's intimate relationship with plaques, and even posited that microglia were responsible for amyloid deposition (Wisniewski et al., 1989; Perlmutter et al., 1990). Though it was later discovered that neurons produce amyloid precursor protein and amyloid (Wisniewski et al., 1989; Alzheimer et al., 1995), the role of microglia in AD has remained largely elusive. Over the past 30 years, microglia in the AD brain have vacillated between valiant protectors, powerless observers, and indiscriminate destroyers. In this section of the review, we cover the insights into their roles in synaptic loss that were provided using two-photon *in vivo* imaging (**Table 3**) and complementary techniques.

LOSS OF MICROGLIAL PHAGOCYTIC ABILITIES IN AD

Two-photon *in vivo* studies in the APP/PS1ΔE9 and Tg2576 models demonstrated that removing microglia during the chronic disease stage causes significant growth of existing plaques (Zhao et al., 2017). Combining these data with the fact that microglia (including the dark microglia, a subset identified by its markers of cellular stress including the condensation state of its cytoplasm and nucleoplasm resulting in a dark appearance under electron microscopy; Bisht et al., 2016) are occasionally seen containing amyloid deposits led to conclude that while microglia may be competent phagocytes, they are unable to control amyloid levels late during AD pathology. Of note, the dark microglia are rare in the healthy mature brain, but increase in number up to 10-fold with pathological conditions that include chronic stress, aging and amyloid deposition (in APP/PS1ΔE9 mice; Bisht et al., 2016). This microglial subset discovered with electron microscopy displays hyper-ramified processes that extensively ensheath and engulf synaptic elements (pre- and postsynaptic), suggesting their role in the pathological remodeling of neuronal circuits in AD (Stratoulias et al., 2019; St-Pierre et al., 2020).

While neuroinflammation is a main hallmark of AD, alongside amyloid deposition and tangle formation, prolonged exposure to pro-inflammatory cytokines inhibits microglial phagocytic ability (Koenigsknecht and Landreth, 2004). Two-photon imaging in APP/PS1ΔE9 mouse slices demonstrated that microglia lose their mobility and phagocytic capabilities as plaque deposition increases (Krabbe et al., 2013). Slice culture studies further determined that microglia from aged APP/PS1ΔE9 and 5XFAD mice have reduced phagocytic capacity, possibly due to an impaired MerTK signaling (Savage et al., 2015). Work by others has determined that acute exposure to amyloid does not affect microglial phagocytic competence, whereas prolonged exposure in later disease stages results in reduced phagocytosis (Wendt et al., 2017). Together these data suggest that while microglial response to amyloid may be beneficial in the short-term, chronic exposure to amyloid may stunt microglia and prevent them from performing their normal phagocytic duties required to clear the brain from toxic or inflammatory debris.

Environmental enrichment has been shown using two-photon *in vivo* imaging to increase microglial amyloid clearing capacities thus preventing prion-like seeding of amyloid in a mouse model, while also reversing the deficits in neurogenesis and memory (Ziegler-Waldkirch et al., 2018). Environmental enrichment is well-known to promote beneficial neuroprotective microglial activities (Savage and Tremblay, 2019). However, increasing microglial phagocytosis with other strategies should be undertaken with extreme caution, as microglia could phagocytose the incorrect cargo. The same complement-mediated pathway which prunes excess synapses during normal brain development causes mistargeted phagocytosis of synapses early in mouse models of amyloid pathology, before plaques are deposited (Hong et al., 2016). Inhibiting C1q, C3, or microglial complement receptor CR3 in amyloid mouse models was

TABLE 3 | Studies examining microglial interactions with neuronal or synaptic loss in mouse models of amyloid or Tau pathology using *in vivo* two-photon microscopy that are discussed in this review.

Model strain	Method of neuronal labeling	Age at imaging	Brain region imaged	Interval between imaging sessions	Neuronal/synaptic changes (compared to control)	Presence of neurite dystrophy	Reference
3xTg-AD	Crossed with CX3CR1-GFP and Thy1-YFP transgenic mice	4–6 months	Somatosensory cortex	7 days	Reduced neuronal loss in the absence of CX3CR1 (knockout)	–	Fuhrmann et al., 2010
5xFAD	Crossed with Thy1-YFP and CX3CR1-GFP	10–12 months	Somatosensory cortex	5 days	Increased neurite dystrophy in the absence of microglial coverage	Yes	Condello et al., 2015
APP-PS1	Crossed with Thy1-YFP and CX3CR1-iDTR to deplete microglia	>12 months	Motor, somatosensory, and visual cortices	7 days	Increased loss of spines and shaft atrophy associated with amyloid plaques during microglial depletion	Yes	Zhao et al., 2017

shown to prevent synaptic loss, as well as cognitive impairment (Hammond et al., 2019). The microglial receptor TREM2, which displays various genetic variants in AD and is expressed by dark microglia, was also shown to mediate synaptic pruning during normal development, in cooperation with astrocytes (Filipello et al., 2018; Jay et al., 2019). Determining the outcome of TREM2 gene loss, haplodeficiency or variants on microglia-mediated synaptic loss in mouse models of amyloid and Tau pathology is an important topic of investigation (Yuan et al., 2016; Gratuze et al., 2020).

Similarly, fractalkine signaling between the neuronal chemokine fractalkine and its unique receptor CX3CR1, which is expressed by microglia, is a main mode of neuron-microglia communication in the brain. During normal physiological conditions, fractalkine signaling plays key roles in synaptic maturation, pruning, and plasticity, and mediates the adaptation of the brain and behavior to environmental challenges (Paolicelli et al., 2014; Tay et al., 2017). In AD pathology, evidence from complementary techniques revealed that fractalkine signaling is detrimental during amyloid pathology, yet beneficial in Tau pathology (Lee et al., 2010; Chen et al., 2016; Bemiller et al., 2018). *In vivo*, two-photon imaging indicates that 3xTg-AD mice deficient in fractalkine signaling are protected from neuronal loss, contrary to 3xTg-AD controls with an intact fractalkine signaling (Fuhrmann et al., 2010). In the 3xTg-AD mice, microglia were also shown to display an increased process velocity around the disappearing neurons, suggesting a possible involvement in their elimination, at early stages of pathology still devoid of plaques and Tau pathology (Fuhrmann et al., 2010). Similarly, using two-photon *in vivo* imaging in a zebrafish model of Tau pathology, in which neurons express $hTau^{P301L}$, microglia were recently shown to transform their morphology (retraction and reduced number of processes, enlarged cell bodies), while increasing their migration and phagocytic activity toward dying neurons. Nevertheless, microglial phagocytosis failed in this context to remove all the dying neurons (Hassan-Abdi et al., 2019).

EMERGENCE OF NEUROPROTECTIVE PHENOTYPES

While microglia are not sufficient to prevent AD pathology, synaptic loss, and cognitive impairment, they nonetheless form a barrier around plaques and slow disease progression, at least early on during disease pathogenesis. A major avenue of therapeutic research is focused on restoring proper microglial metabolism and physiological function, thus enabling them to clear amyloid, remove apoptotic neurons as well as provide trophic support for synaptic maintenance. Two-photon *in vivo* imaging of healthy mice revealed that microglia play an important role in the formation of dendritic spines, through their secretion of brain-derived neurotrophic factor, which is required for motor learning (Parkhurst et al., 2013). Microglia were also well-shown to dynamically contact pre- and postsynaptic elements by two-photon *in vivo* imaging during normal physiological conditions, and these interactions were frequently followed by the elimination of dendritic spines during experience-dependent plasticity (Tremblay et al., 2010). Whether microglia could exert similar beneficial roles at synapses in AD remains to be determined.

Recent studies identified a number of neuroprotective microglial phenotypes present on a subset of microglia within the AD brain, and these provide further potential for specific, microglia-targeted therapeutics. Two-photon *in vivo* imaging in 5XFAD mice revealed that microglia "wall off" plaques and likely promote neuronal and/or synaptic survival in regions affected by the amyloid pathology (Condello et al., 2015). In fact, dystrophic neurons were much more commonly seen in regions near plaques that were not covered by microglia, as these regions contained increased levels of toxic amyloid oligomeric and protofibrillar species. Microglial ability to seal off amyloid plaques from the surrounding neuropil is dependent on TREM2, as knockout mice had significantly reduced plaque area covered by microglia, while displaying increased plaque-associated neuronal dystrophy (Yuan et al., 2016).

Recent technical advances in the field now allow researchers to study populations of microglia from specific brain microenvironments, and thus characterize differences between microglia associated with plaques and those from nearby brain regions. These studies have begun to uncover the specifically and differentially-regulated transcriptome of microglial cells associated or not with plaques. When plaque-associated microglia were microdissected from amyloid mouse models, transcriptomic analysis identified increased genes associated with priming (i.e., immunological alert) and cellular metabolism as well as lysosomal activity (Kamphuis et al., 2016; Yin et al., 2017). While two-photon *in vivo* imaging of the primed microglia in particular and their dynamics at synapses is currently lacking, these studies indicate that plaque-associated microglia are not dystrophic or senescent, but rather highly active cells attempting to digest the amyloid, as supported by ultrastructural studies (El Hajj et al., 2019). These data support the idea that microglia surrounding plaques prevent plaque growth by removing oligomeric and protofibrillar amyloid from their immediate surroundings.

Additional work using single-cell RNAseq uncovered a disease-associated microglial (DAM) subtype in amyloid mouse models and human brain tissues (Keren-Shaul et al., 2017). A similar subtype was subsequently named the microglia-associated with neurodegeneration (MGnD) (Krasemann et al., 2017). These disease-associated subsets lose homeostatic microglial markers and upregulate genes associated with phagocytosis of apoptotic cells. The authors posit that MGnD microglia require contact with, if not phagocytosis of, dystrophic neurons like those associated with plaques, while depending on Trem2 and Apoe expression (Krasemann et al., 2017). These disease-associated phenotypes echo the ultrastructurally-defined dark microglia, but further *in vivo* research is required to determine the independent or concerted implication of these different microglial types in synaptic loss.

CONCLUSION AND PERSPECTIVES

In vivo imaging approach using two-photon *in vivo* microscopy has found that dendritic spines are destabilized by the extracellular deposition or intracellular accumulation of amyloid. Cell intrinsic factors, such as elevated calcium, and extrinsic factors, like microglial phenotypic transformation elicited by the amyloid or Tau pathology, disrupt dendritic spine stability and might specifically trigger synaptic loss. Future two-photon imaging studies to simultaneously visualize the dynamics of axon terminals, dendritic spines, synaptic proteins, intracellular calcium, and microglia, together with amyloid and Tau pathology, *in vivo* in mouse models, will provide novel insights into the dynamic events preceding and causing loss of pre- and postsynaptic elements.

AUTHOR CONTRIBUTIONS

JS and M-ÈT designed and wrote the manuscript. JCS contributed to the section on microglia. All authors contributed to the article and approved the submitted version.

FUNDING

This work was supported by a grant from the National Institutes of Health (Grant No. R01AG064067) to JS and a Canadian Institutes of Health Research–Foundation (Grant No. 353750) to M-ÈT. M-ÈT holds a Canada Research Chair (Tier 2) in Neurobiology of Aging and Cognition.

REFERENCES

Alldred, M. J., Duff, K. E., and Ginsberg, S. D. (2012). Microarray analysis of CA1 pyramidal neurons in a mouse model of tauopathy reveals progressive synaptic dysfunction. *Neurobiol. Dis.* 45, 751–762. doi: 10.1016/j.nbd.2011.10.022

Alzheimer, A., Stelzmann, R. A., Schnitzlein, H. N., and Murtagh, F. R. (1995). An english translation of alzheimer's 1907 paper, "Uber eine eigenartige Erkankung der Hirnrinde". *Clin. Anat.* 8, 429–431. doi: 10.1002/ca.980080612

Arbel-Ornath, M., Hudry, E., Boivin, J. R., Hashimoto, T., Takeda, S., Kuchibhotla, K. V., et al. (2017). Soluble oligomeric amyloid-beta induces calcium dyshomeostasis that precedes synapse loss in the living mouse brain. *Mol. Neurodegener.* 12:27. doi: 10.1186/s13024-017-0169-9

Attardo, A., Fitzgerald, J. E., and Schnitzer, M. J. (2015). Impermanence of dendritic spines in live adult CA1 hippocampus. *Nature* 523, 592–596. doi: 10.1038/nature14467

Bai, Y., Li, M., Zhou, Y., Ma, L., Qiao, Q., Hu, W., et al. (2017). Abnormal dendritic calcium activity and synaptic depotentiation occur early in a mouse model of alzheimer's disease. *Mol. Neurodegener.* 12:86. doi: 10.1186/s13024-017-0228-2

Bemiller, S. M., Maphis, N. M., Formica, S. V., Wilson, G. N., Miller, C. M., Xu, G., et al. (2018). Genetically enhancing the expression of chemokine domain of CX3CL1 fails to prevent tau pathology in mouse models of tauopathy. *J. Neuroinflammation* 15:278. doi: 10.1186/s12974-018-1310-6

Bisht, K., Sharma, K. P., Lecours, C., Sanchez, M. G., El Hajj, H., Milior, G., et al. (2016). Dark microglia: a new phenotype predominantly associated with pathological states. *Glia* 64, 826–839. doi: 10.1002/glia.22966

Bittner, T., Burgold, S., Dorostkar, M. M., Fuhrmann, M., Wegenast-Braun, B. M., Schmidt, B., et al. (2012). Amyloid plaque formation precedes dendritic spine loss. *Acta Neuropathol.* 124, 797–807. doi: 10.1007/s00401-012-1047-8

Bittner, T., Fuhrmann, M., Burgold, S., Ochs, S. M., Hoffmann, N., Mitteregger, G., et al. (2010). Multiple events lead to dendritic spine loss in triple transgenic alzheimer's disease mice. *PLoS ONE* 5:e15477. doi: 10.1371/journal.pone.0015477

Blazquez-Llorca, L., Valero-Freitag, S., Rodrigues, E. F., Merchan-Perez, A., Rodriguez, J. R., Dorostkar, M. M., et al. (2017). High plasticity of axonal pathology in alzheimer's disease mouse models. *Acta Neuropathol. Commun.* 5:14. doi: 10.1186/s40478-017-0415-y

Boncristiano, S., Calhoun, M. E., Howard, V., Bondolfi, L., Kaeser, S. A., Wiederhold, K. H., et al. (2005). Neocortical synaptic bouton number is maintained despite robust amyloid deposition in APP23 transgenic mice. *Neurobiol. Aging* 26, 607–613. doi: 10.1016/j.neurobiolaging.2004.06.010

Bourne, J., and Harris, K. M. (2007). Do thin spines learn to be mushroom spines that remember? *Curr. Opin. Neurobiol.* 17, 381–386. doi: 10.1016/j.conb.2007.04.009

Brawek, B., and Garaschuk, O. (2014). Network-wide dysregulation of calcium homeostasis in alzheimer's disease. *Cell Tissue Res.* 357, 427–438. doi: 10.1007/s00441-014-1798-8

Brendza, R. P., Bacskai, B. J., Cirrito, J. R., Simmons, K. A., Skoch, J. M., Klunk, W. E., et al. (2005). Anti-Abeta antibody treatment promotes the rapid recovery of amyloid-associated neuritic dystrophy in PDAPP transgenic mice. *J. Clin. Invest.* 115, 428–433. doi: 10.1172/JCI23269

Burgold, S., Bittner, T., Dorostkar, M. M., Kieser, D., Fuhrmann, M., Mitteregger, G., et al. (2011). *In vivo* multiphoton imaging reveals gradual growth of newborn amyloid plaques over weeks. *Acta Neuropathol.* 121, 327–335. doi: 10.1007/s00401-010-0787-6

Burgold, S., Filser, S., Dorostkar, M. M., Schmidt, B., and Herms, J. (2014). *In vivo* imaging reveals sigmoidal growth kinetic of beta-amyloid plaques. *Acta Neuropathol. Commun.* 2:30. doi: 10.1186/2051-5960-2-30

Buskila, Y., Crowe, S. E., and Ellis-Davies, G. C. (2013). Synaptic deficits in layer 5 neurons precede overt structural decay in 5xFAD mice. *Neuroscience* 254, 152–159. doi: 10.1016/j.neuroscience.2013.09.016

Calvo-Rodriguez, M., Hou, S. S., Snyder, A. C., Kharitonova, E. K., Russ, A. N., Das, S., et al. (2020). Increased mitochondrial calcium levels associated with neuronal death in a mouse model of alzheimer's disease. *Nat. Commun.* 11:2146. doi: 10.1038/s41467-020-16074-2

Chen, P., Zhao, W., Guo, Y., Xu, J., and Yin, M. (2016). CX3CL1/CX3CR1 in alzheimer's disease: a target for neuroprotection. *Biomed. Res. Int.* 2016:8090918. doi: 10.1155/2016/8090918

Christie, R. H., Bacskai, B. J., Zipfel, W. R., Williams, R. M., Kajdasz, S. T., Webb, W. W., et al. (2001). Growth arrest of individual senile plaques in a model of alzheimer's disease observed by *in vivo* multiphoton microscopy. *J. Neurosci.* 21, 858–864. doi: 10.1523/JNEUROSCI.21-03-00858.2001

Condello, C., Schain, A., and Grutzendler, J. (2011). Multicolor time-stamp reveals the dynamics and toxicity of amyloid deposition. *Sci. Rep.* 1:19. doi: 10.1038/srep00019

Condello, C., Yuan, P., Schain, A., and Grutzendler, J. (2015). Microglia constitute a barrier that prevents neurotoxic protofibrillar Abeta42 hotspots around plaques. *Nat. Commun.* 6:6176. doi: 10.1038/ncomms7176

Crimins, J. L., Rocher, A. B., Peters, A., Shultz, P., Lewis, J., and Luebke, J. I. (2011). Homeostatic responses by surviving cortical pyramidal cells in neurodegenerative tauopathy. *Acta Neuropathol.* 122, 551–564. doi: 10.1007/s00401-011-0877-0

D'Amore, J. D., Kajdasz, S. T., McLellan, M. E., Bacskai, B. J., Stern, E. A., and Hyman, B. T. (2003). *In vivo* multiphoton imaging of a transgenic mouse model of alzheimer disease reveals marked thioflavine-S-associated alterations in neurite trajectories. *J. Neuropathol. Exp. Neurol.* 62, 137–145. doi: 10.1093/jnen/62.2.137

de Wilde, M. C., Overk, C. R., Sijben, J. W., and Masliah, E. (2016). Meta-analysis of synaptic pathology in alzheimer's disease reveals selective molecular vesicular machinery vulnerability. *Alzheimers. Dement.* 12, 633–644. doi: 10.1016/j.jalz.2015.12.005

DeKosky, S. T., Scheff, S. W., and Styren, S. D. (1996). Structural correlates of cognition in dementia: quantification and assessment of synapse change. *Neurodegeneration* 5, 417–421. doi: 10.1006/neur.1996.0056

Demuro, A., Mina, E., Kayed, R., Milton, S. C., Parker, I., and Glabe, C. G. (2005). Calcium dysregulation and membrane disruption as a ubiquitous neurotoxic mechanism of soluble amyloid oligomers. *J. Biol. Chem.* 280, 17294–17300. doi: 10.1074/jbc.M500997200

Dong, H., Martin, M. V., Chambers, S., and Csernansky, J. G. (2007). Spatial relationship between synapse loss and beta-amyloid deposition in Tg2576 mice. *J. Comp. Neurol.* 500, 311–321. doi: 10.1002/cne.21176

Eckermann, K., Mocanu, M. M., Khlistunova, I., Biernat, J., Nissen, A., Hofmann, A., et al. (2007). The beta-propensity of Tau determines aggregation and synaptic loss in inducible mouse models of tauopathy. *J. Biol. Chem.* 282, 31755–31765. doi: 10.1074/jbc.M705282200

El Hajj, H., Savage, J. C., Bisht, K., Parent, M., Vallieres, L., Rivest, S., et al. (2019). Ultrastructural evidence of microglial heterogeneity in alzheimer's disease amyloid pathology. *J. Neuroinflammation* 16:87. doi: 10.1186/s12974-019-1473-9

Filipello, F., Morini, R., Corradini, I., Zerbi, V., Canzi, A., Michalski, B., et al. (2018). The microglial innate immune receptor TREM2 is required for synapse elimination and normal brain connectivity. *Immunity 48*, 979–991.e978. doi: 10.1016/j.immuni.2018.04.016

Forner, S., Baglietto-Vargas, D., Martini, A. C., Trujillo-Estrada, L., and LaFerla, F. M. (2017). Synaptic impairment in alzheimer's disease: a dysregulated symphony. *Trends Neurosci.* 40, 347–357. doi: 10.1016/j.tins.2017.04.002

Fuhrmann, M., Bittner, T., Jung, C. K., Burgold, S., Page, R. M., Mitteregger, G., et al. (2010). Microglial Cx3cr1 knockout prevents neuron loss in a mouse model of alzheimer's disease. *Nat. Neurosci.* 13, 411–413. doi: 10.1038/nn.2511

Gomez, C. A., Fu, B., Sakadzic, S., and Yaseen, M. A. (2018). Cerebral metabolism in a mouse model of alzheimer's disease characterized by two-photon fluorescence lifetime microscopy of intrinsic NADH. *Neurophotonics* 5:045008. doi: 10.1117/1.NPh.5.4.045008

Gosselin, D., Skola, D., Coufal, N. G., Holtman, I. R., Schlachetzki, J. C. M., Sajti, E., et al. (2017). An environment-dependent transcriptional network specifies human microglia identity. *Science* 356:eaal3222. doi: 10.1126/science.aal3222

Gratuze, M., Leyns, C. E., Sauerbeck, A. D., St-Pierre, M. K., Xiong, M., Kim, N., et al. (2020). Impact of TREM2R47H variant on tau pathology-induced gliosis and neurodegeneration. *J. Clin. Invest.* 30, 4654–4968. doi: 10.1172/JCI138179

Griffin, W. S., Stanley, L. C., Ling, C., White, L., MacLeod, V., Perrot, L. J., et al. (1989). Brain interleukin 1 and S-100 immunoreactivity are elevated in down syndrome and alzheimer disease. *Proc. Natl. Acad. Sci. U.S.A.* 86, 7611–7615. doi: 10.1073/pnas.86.19.7611

Grutzendler, J., Kasthuri, N., and Gan, W. B. (2002). Long-term dendritic spine stability in the adult cortex. *Nature* 420, 812–816. doi: 10.1038/nature01276

Gu, L., Kleiber, S., Schmid, L., Nebeling, F., Chamoun, M., Steffen, J., et al. (2014). Long-term *in vivo* imaging of dendritic spines in the hippocampus reveals structural plasticity. *J. Neurosci.* 34, 13948–13953. doi: 10.1523/JNEUROSCI.1464-14.2014

Guo, Q., Sebastian, L., Sopher, B. L., Miller, M. W., Ware, C. B., Martin, G. M., et al. (1999). Increased vulnerability of hippocampal neurons from presenilin-1 mutant knock-in mice to amyloid beta-peptide toxicity: central roles of superoxide production and caspase activation. *J. Neurochem.* 72, 1019–1029. doi: 10.1046/j.1471-4159.1999.0721019.x

Hammond, T. R., Marsh, S. E., and Stevens, B. (2019). Immune signaling in neurodegeneration. *Immunity* 50, 955–974. doi: 10.1016/j.immuni.2019.03.016

Hassan-Abdi, R., Brenet, A., Bennis, M., Yanicostas, C., and Soussi-Yanicostas, N. (2019). Neurons expressing pathological tau protein trigger dramatic changes in microglial morphology and dynamics. *Front. Neurosci.* 13:1199. doi: 10.3389/fnins.2019.01199

Hefendehl, J. K., Wegenast-Braun, B. M., Liebig, C., Eicke, D., Milford, D., Calhoun, M. E., et al. (2011). Long-term *in vivo* imaging of beta-amyloid plaque appearance and growth in a mouse model of cerebral beta-amyloidosis. *J. Neurosci.* 31, 624–629. doi: 10.1523/JNEUROSCI.5147-10.2011

Heiss, J. K., Barrett, J., Yu, Z., Haas, L. T., Kostylev, M. A., and Strittmatter, S. M. (2017). Early activation of experience-independent dendritic spine turnover in a mouse model of alzheimer's disease. *Cereb. Cortex* 27, 3660–3674. doi: 10.1093/cercor/bhw188

Hellwig, S., Heinrich, A., and Biber, K. (2013). The brain's best friend: microglial neurotoxicity revisited. *Front. Cell. Neurosci.* 7:71. doi: 10.3389/fncel.2013.00071

Hoffmann, N. A., Dorostkar, M. M., Blumenstock, S., Goedert, M., and Herms, J. (2013). Impaired plasticity of cortical dendritic spines in P301S tau transgenic mice. *Acta Neuropathol. Commun.* 1:82. doi: 10.1186/2051-5960-1-82

Holcomb, L., Gordon, M. N., McGowan, E., Yu, X., Benkovic, S., Jantzen, P., et al. (1998). Accelerated alzheimer-type phenotype in transgenic mice carrying both mutant amyloid precursor protein and presenilin 1 transgenes. *Nat. Med.* 4, 97–100. doi: 10.1038/nm0198-097

Holscher, C. (1998). Possible causes of alzheimer's disease: amyloid fragments, free radicals, and calcium homeostasis. *Neurobiol. Dis.* 5, 129–141. doi: 10.1006/nbdi.1998.0193

Hong, S., Beja-Glasser, V. F., Nfonoyim, B. M., Frouin, A., Li, S., Ramakrishnan, S., et al. (2016). Complement and microglia mediate early synapse loss in alzheimer mouse models. *Science* 352, 712–716. doi: 10.1126/science.aad8373

Hoover, B. R., Reed, M. N., Su, J., Penrod, R. D., Kotilinek, L. A., Grant, M. K., et al. (2010). Tau mislocalization to dendritic spines mediates synaptic dysfunction independently of neurodegeneration. *Neuron* 68, 1067–1081. doi: 10.1016/j.neuron.2010.11.030

Hsia, A. Y., Masliah, E., McConlogue, L., Yu, G. Q., Tatsuno, G., Hu, K., et al. (1999). Plaque-independent disruption of neural circuits in alzheimer's disease mouse models. *Proc. Natl. Acad. Sci. U.S.A.* 96, 3228–3233. doi: 10.1073/pnas.96.6.3228

Hsieh, H., Boehm, J., Sato, C., Iwatsubo, T., Tomita, T., Sisodia, S., et al. (2006). AMPAR removal underlies Abeta-induced synaptic depression and dendritic spine loss. *Neuron* 52, 831–843. doi: 10.1016/j.neuron.2006.10.035

Hussain, I., Powell, D., Howlett, D. R., Tew, D. G., Meek, T. D., Chapman, C., et al. (1999). Identification of a novel aspartic protease (Asp 2) as beta-secretase. *Mol. Cell. Neurosci.* 14, 419–427. doi: 10.1006/mcne.1999.0811

Jackson, J. S., Johnson, J. D., Meftah, S., Murray, T. K., Ahmed, Z., Fasiolo, M., et al. (2020). Differential aberrant structural synaptic plasticity in axons and dendrites ahead of their degeneration in tauopathy. *bioRxiv [Preprint]*. doi: 10.1101/2020.04.29.067629

Jackson, J. S., Witton, J., Johnson, J. D., Ahmed, Z., Ward, M., Randall, A. D., et al. (2017). Altered synapse stability in the early stages of tauopathy. *Cell Rep.* 18, 3063–3068. doi: 10.1016/j.celrep.2017.03.013

Jacobsen, J. S., Wu, C. C., Redwine, J. M., Comery, T. A., Arias, R., Bowlby, M., et al. (2006). Early-onset behavioral and synaptic deficits in a mouse model of alzheimer's disease. *Proc. Natl. Acad. Sci. U.S.A.* 103, 5161–5166. doi: 10.1073/pnas.0600948103

Jankowsky, J. L., and Zheng, H. (2017). Practical considerations for choosing a mouse model of alzheimer's disease. *Mol. Neurodegener.* 12:89. doi: 10.1186/s13024-017-0231-7

Jaworski, T., Lechat, B., Demedts, D., Gielis, L., Devijver, H., Borghgraef, P., et al. (2011). Dendritic degeneration, neurovascular defects, and inflammation precede neuronal loss in a mouse model for tau-mediated neurodegeneration. *Am. J. Pathol.* 179, 2001–2015. doi: 10.1016/j.ajpath.2011.06.025

Jay, T. R., von Saucken, V. E., Munoz, B., Codocedo, J. F., Atwood, B. K., Lamb, B. T., et al. (2019). TREM2 is required for microglial instruction of astrocytic synaptic engulfment in neurodevelopment. *Glia* 67, 1873–1892. doi: 10.1002/glia.23664

Kamphuis, W., Kooijman, L., Schetters, S., Orre, M., and Hol, E. M. (2016). Transcriptional profiling of CD11c-positive microglia accumulating around amyloid plaques in a mouse model for alzheimer's disease. *Biochim. Biophys. Acta* 1862, 1847–1860. doi: 10.1016/j.bbadis.2016.07.007

Kandalepas, P. C., Sadleir, K. R., Eimer, W. A., Zhao, J., Nicholson, D. A., and Vassar, R. (2013). The alzheimer's beta-secretase BACE1 localizes to normal presynaptic terminals and to dystrophic presynaptic terminals surrounding amyloid plaques. *Acta Neuropathol.* 126, 329–352. doi: 10.1007/s00401-013-1152-3

Kawahara, M. (2004). Disruption of calcium homeostasis in the pathogenesis of alzheimer's disease and other conformational diseases. *Curr. Alzheimer Res.* 1, 87–95. doi: 10.2174/1567205043332234

Keren-Shaul, H., Spinrad, A., Weiner, A., Matcovitch-Natan, O., Dvir-Szternfeld, R., Ulland, T. K., et al. (2017). A unique microglia type associated with restricting development of alzheimer's disease. *Cell* 169, 1276–1290.e1217. doi: 10.1016/j.cell.2017.05.018

King, D. L., and Arendash, G. W. (2002). Maintained synaptophysin immunoreactivity in Tg2576 transgenic mice during aging: correlations with cognitive impairment. *Brain Res.* 926, 58–68. doi: 10.1016/S0006-8993(01)03294-2

Knobloch, M., and Mansuy, I. M. (2008). Dendritic spine loss and synaptic alterations in alzheimer's disease. *Mol. Neurobiol.* 37, 73–82. doi: 10.1007/s12035-008-8018-z

Knott, G. W., Holtmaat, A., Wilbrecht, L., Welker, E., and Svoboda, K. (2006). Spine growth precedes synapse formation in the adult neocortex *in vivo*. *Nat. Neurosci.* 9, 1117–1124. doi: 10.1038/nn1747

Koenigsknecht, J., and Landreth, G. (2004). Microglial phagocytosis of fibrillar beta-amyloid through a beta1 integrin-dependent mechanism. *J. Neurosci.* 24, 9838–9846. doi: 10.1523/JNEUROSCI.2557-04.2004

Koffie, R. M., Meyer-Luehmann, M., Hashimoto, T., Adams, K. W., Mielke, M. L., Garcia-Alloza, M., et al. (2009). Oligomeric amyloid beta associates with postsynaptic densities and correlates with excitatory synapse loss near senile plaques. *Proc. Natl. Acad. Sci. U.S.A.* 106, 4012–4017. doi: 10.1073/pnas.0811698106

Konur, S., and Ghosh, A. (2005). Calcium signaling and the control of dendritic development. *Neuron* 46, 401–405. doi: 10.1016/j.neuron.2005.04.022

Kopeikina, K. J., Polydoro, M., Tai, H. C., Yaeger, E., Carlson, G. A., Pitstick, R., et al. (2013a). Synaptic alterations in the rTg4510 mouse model of tauopathy. *J. Comp. Neurol.* 521, 1334–1353. doi: 10.1002/cne.23234

Kopeikina, K. J., Wegmann, S., Pitstick, R., Carlson, G. A., Bacskai, B. J., Betensky, R. A., et al. (2013b). Tau causes synapse loss without disrupting calcium homeostasis in the rTg4510 model of tauopathy. *PLoS ONE* 8:e80834. doi: 10.1371/journal.pone.0080834

Krabbe, G., Halle, A., Matyash, V., Rinnenthal, J. L., Eom, G. D., Bernhardt, U., et al. (2013). Functional impairment of microglia coincides with Beta-amyloid deposition in mice with alzheimer-like pathology. *PLoS ONE* 8:e60921. doi: 10.1371/journal.pone.0060921

Krasemann, S., Madore, C., Cialic, R., Baufeld, C., Calcagno, N., El Fatimy, R., et al. (2017). The TREM2-APOE pathway drives the transcriptional phenotype of dysfunctional microglia in neurodegenerative diseases. *Immunity* 47, 566–581.e569. doi: 10.1016/j.immuni.2017.08.008

Kremer, A., Maurin, H., Demedts, D., Devijver, H., Borghgraef, P., and Van Leuven, F. (2011). Early improved and late defective cognition is reflected by dendritic spines in Tau.P301L mice. *J. Neurosci.* 31, 18036–18047. doi: 10.1523/JNEUROSCI.4859-11.2011

Kuchibhotla, K. V., Goldman, S. T., Lattarulo, C. R., Wu, H. Y., Hyman, B. T., and Bacskai, B. J. (2008). Abeta plaques lead to aberrant regulation of calcium homeostasis *in vivo* resulting in structural and functional disruption of neuronal networks. *Neuron* 59, 214–225. doi: 10.1016/j.neuron.2008.06.008

Lanz, T. A., Carter, D. B., and Merchant, K. M. (2003). Dendritic spine loss in the hippocampus of young PDAPP and Tg2576 mice and its prevention by the ApoE2 genotype. *Neurobiol. Dis.* 13, 246–253. doi: 10.1016/S0969-9961(03)00079-2

Lee, S., Varvel, N. H., Konerth, M. E., Xu, G., Cardona, A. E., Ransohoff, R. M., et al. (2010). CX3CR1 deficiency alters microglial activation and reduces beta-amyloid deposition in two alzheimer's disease mouse models. *Am. J. Pathol.* 177, 2549–2562. doi: 10.2353/ajpath.2010.100265

Lerdkrai, C., Asavapanumas, N., Brawek, B., Kovalchuk, Y., Mojtahedi, N., Olmedillas Del Moral, M., et al. (2018). Intracellular Ca^{2+} stores control *in vivo* neuronal hyperactivity in a mouse model of alzheimer's disease. *Proc. Natl. Acad. Sci. U.S.A.* 115, E1279–E1288. doi: 10.1073/pnas.1714409115

Liebscher, S., Page, R. M., Kafer, K., Winkler, E., Quinn, K., Goldbach, E., et al. (2014). Chronic gamma-secretase inhibition reduces amyloid plaque-associated instability of pre- and postsynaptic structures. *Mol. Psychiatry* 19, 937–946. doi: 10.1038/mp.2013.122

Lin, X., Koelsch, G., Wu, S., Downs, D., Dashti, A., and Tang, J. (2000). Human aspartic protease memapsin 2 cleaves the beta-secretase site of beta-amyloid precursor protein. *Proc. Natl. Acad. Sci. U.S.A.* 97, 1456–1460. doi: 10.1073/pnas.97.4.1456

Maia, L. F., Kaeser, S. A., Reichwald, J., Hruscha, M., Martus, P., Staufenbiel, M., et al. (2013). Changes in amyloid-beta and Tau in the cerebrospinal fluid of transgenic mice overexpressing amyloid precursor protein. *Sci. Transl. Med.* 5:194re192. doi: 10.1126/scitranslmed.3006446

Mandrekar, S., Jiang, Q., Lee, C. Y., Koenigsknecht-Talboo, J., Holtzman, D. M., and Landreth, G. E. (2009). Microglia mediate the clearance of soluble Abeta through fluid phase macropinocytosis. *J. Neurosci.* 29, 4252–4262. doi: 10.1523/JNEUROSCI.5572-08.2009

Mattson, M. P. (2007). Calcium and neurodegeneration. *Aging Cell* 6, 337–350. doi: 10.1111/j.1474-9726.2007.00275.x

Mattson, M. P., Cheng, B., Davis, D., Bryant, K., Lieberburg, I., and Rydel, R. E. (1992). β-Amyloid peptides destabilize calcium homeostasis and render human cortical neurons vulnerable to excitotoxicity. *J. Neurosci.* 12, 376–389. doi: 10.1523/JNEUROSCI.12-02-00376.1992

McLellan, M. E., Kajdasz, S. T., Hyman, B. T., and Bacskai, B. J. (2003). *In vivo* imaging of reactive oxygen species specifically associated with thioflavine S-positive amyloid plaques by multiphoton microscopy. *J. Neurosci.* 23, 2212–2217. doi: 10.1523/JNEUROSCI.23-06-02212.2003

Meyer-Luehmann, M., Spires-Jones, T. L., Prada, C., Garcia-Alloza, M., de Calignon, A., Rozkalne, A., et al. (2008). Rapid appearance and local toxicity of amyloid-beta plaques in a mouse model of alzheimer's disease. *Nature* 451, 720–724. doi: 10.1038/nature06616

Mizrahi, A., Crowley, J. C., Shtoyerman, E., and Katz, L. C. (2004). High-resolution *in vivo* imaging of hippocampal dendrites and spines. *J. Neurosci.* 24, 3147–3151. doi: 10.1523/JNEUROSCI.5218-03.2004

Moechars, D., Dewachter, I., Lorent, K., Reverse, D., Baekelandt, V., Naidu, A., et al. (1999). Early phenotypic changes in transgenic mice that overexpress different mutants of amyloid precursor protein in brain. *J. Biol. Chem.* 274, 6483–6492. doi: 10.1074/jbc.274.10.6483

Mucke, L., Masliah, E., Yu, G. Q., Mallory, M., Rockenstein, E. M., Tatsuno, G., et al. (2000). High-level neuronal expression of abeta 1-42 in wild-type human amyloid protein precursor transgenic mice:

synaptotoxicity without plaque formation. *J. Neurosci.* 20, 4050–4058. doi: 10.1523/JNEUROSCI.20-11-04050.2000

Onorato, M., Mulvihill, P., Connolly, J., Galloway, P., Whitehouse, P., and Perry, G. (1989). Alteration of neuritic cytoarchitecture in alzheimer disease. *Prog. Clin. Biol. Res.* 317, 781–789.

Overmyer, M., Helisalmi, S., Soininen, H., Laakso, M., Riekkinen, P. Sr., and Alafuzoff, I. (1999). Reactive microglia in aging and dementia: an immunohistochemical study of postmortem human brain tissue. *Acta Neuropathol.* 97, 383–392. doi: 10.1007/s004010051002

Paolicelli, R. C., Bisht, K., and Tremblay, M. E. (2014). Fractalkine regulation of microglial physiology and consequences on the brain and behavior. *Front. Cell. Neurosci.* 8:129. doi: 10.3389/fncel.2014.00129

Parkhurst, C. N., Yang, G., Ninan, I., Savas, J. N., Yates, J. R. III, Lafaille, J. J., et al. (2013). Microglia promote learning-dependent synapse formation through brain-derived neurotrophic factor. *Cell* 155, 1596–1609. doi: 10.1016/j.cell.2013.11.030

Perlmutter, L. S., Barron, E., and Chui, H. C. (1990). Morphologic association between microglia and senile plaque amyloid in alzheimer's disease. *Neurosci. Lett.* 119, 32–36. doi: 10.1016/0304-3940(90)90748-X

Peters, F., Salihoglu, H., Pratsch, K., Herzog, E., Pigoni, M., Sgobio, C., et al. (2019). Tau deletion reduces plaque-associated BACE1 accumulation and decelerates plaque formation in a mouse model of alzheimer's disease. *EMBO J.* 38:e102345. doi: 10.15252/embj.2019102345

Peters, F., Salihoglu, H., Rodrigues, E., Herzog, E., Blume, T., Filser, S., et al. (2018). BACE1 inhibition more effectively suppresses initiation than progression of beta-amyloid pathology. *Acta Neuropathol.* 135, 695–710. doi: 10.1007/s00401-017-1804-9

Popugaeva, E., Pchitskaya, E., and Bezprozvanny, I. (2017). Dysregulation of neuronal calcium homeostasis in alzheimer's disease - a therapeutic opportunity? *Biochem. Biophys. Res. Commun.* 483, 998–1004. doi: 10.1016/j.bbrc.2016.09.053

Pozueta, J., Lefort, R., and Shelanski, M. L. (2013). Synaptic changes in alzheimer's disease and its models. *Neuroscience* 251, 51–65. doi: 10.1016/j.neuroscience.2012.05.050

Richardson, J. A., and Burns, D. K. (2002). Mouse models of alzheimer's disease: a quest for plaques and tangles. *ILAR J.* 43, 89–99. doi: 10.1093/ilar.43.2.89

Rocher, A. B., Crimins, J. L., Amatrudo, J. M., Kinson, M. S., Todd-Brown, M. A., Lewis, J., et al. (2010). Structural and functional changes in tau mutant mice neurons are not linked to the presence of NFTs. *Exp. Neurol.* 223, 385–393. doi: 10.1016/j.expneurol.2009.07.029

Rogers, J., Luber-Narod, J., Styren, S. D., and Civin, W. H. (1988). Expression of immune system-associated antigens by cells of the human central nervous system: relationship to the pathology of alzheimer's disease. *Neurobiol. Aging* 9, 339–349. doi: 10.1016/S0197-4580(88)80079-4

Rutten, B. P., Van der Kolk, N. M., Schafer, S., van Zandvoort, M. A., Bayer, T. A., Steinbusch, H. W., et al. (2005). Age-related loss of synaptophysin immunoreactive presynaptic boutons within the hippocampus of APP751SL, PS1M146L, and APP751SL/PS1M146L transgenic mice. *Am. J. Pathol.* 167, 161–173. doi: 10.1016/S0002-9440(10)62963-X

Rutten, B. P., Wirths, O., Van de Berg, W. D., Lichtenthaler, S. F., Vehoff, J., Steinbusch, H. W., et al. (2003). No alterations of hippocampal neuronal number and synaptic bouton number in a transgenic mouse model expressing the beta-cleaved C-terminal APP fragment. *Neurobiol. Dis.* 12, 110–120. doi: 10.1016/S0969-9961(02)00015-3

Sadleir, K. R., Kandalepas, P. C., Buggia-Prevot, V., Nicholson, D. A., Thinakaran, G., and Vassar, R. (2016). Presynaptic dystrophic neurites surrounding amyloid plaques are sites of microtubule disruption, BACE1 elevation, and increased Abeta generation in alzheimer's disease. *Acta Neuropathol.* 132, 235–256. doi: 10.1007/s00401-016-1558-9

Savage, J. C., Jay, T., Goduni, E., Quigley, C., Mariani, M. M., Malm, T., et al. (2015). Nuclear receptors license phagocytosis by trem2+ myeloid cells in mouse models of alzheimer's disease. *J. Neurosci.* 35, 6532–6543. doi: 10.1523/JNEUROSCI.4586-14.2015

Savage, J. C., and Tremblay, M. E. (2019). Studying laboratory mice - into the wild. *Trends Neurosci.* 42, 566–568. doi: 10.1016/j.tins.2019.05.004

Scheff, S. W., and Price, D. A. (2006). Alzheimer's disease-related alterations in synaptic density: neocortex and hippocampus. *J. Alzheimers. Dis.* 9, 101–115. doi: 10.3233/JAD-2006-9S312

Scheff, S. W., Price, D. A., Schmitt, F. A., DeKosky, S. T., and Mufson, E. J. (2007). Synaptic alterations in CA1 in mild alzheimer disease and mild cognitive impairment. *Neurology* 68, 1501–1508. doi: 10.1212/01.wnl.0000260698.46517.8f

Schmid, L. C., Mittag, M., Poll, S., Steffen, J., Wagner, J., Geis, H. R., et al. (2016). Dysfunction of somatostatin-positive interneurons associated with memory deficits in an alzheimer's disease model. *Neuron* 92, 114–125. doi: 10.1016/j.neuron.2016.08.034

Selkoe, D. J. (2002). Alzheimer's disease is a synaptic failure. *Science* 298, 789–791. doi: 10.1126/science.1074069

Shahani, N., Subramaniam, S., Wolf, T., Tackenberg, C., and Brandt, R. (2006). Tau aggregation and progressive neuronal degeneration in the absence of changes in spine density and morphology after targeted expression of alzheimer's disease-relevant tau constructs in organotypic hippocampal slices. *J. Neurosci.* 26, 6103–6114. doi: 10.1523/JNEUROSCI.4245-05.2006

Shankar, G. M., Bloodgood, B. L., Townsend, M., Walsh, D. M., Selkoe, D. J., and Sabatini, B. L. (2007). Natural oligomers of the alzheimer amyloid-beta protein induce reversible synapse loss by modulating an NMDA-type glutamate receptor-dependent signaling pathway. *J. Neurosci.* 27, 2866–2875. doi: 10.1523/JNEUROSCI.4970-06.2007

Shrestha, B. R., Vitolo, O. V., Joshi, P., Lordkipanidze, T., Shelanski, M., and Dunaevsky, A. (2006). Amyloid beta peptide adversely affects spine number and motility in hippocampal neurons. *Mol. Cell. Neurosci.* 33, 274–282. doi: 10.1016/j.mcn.2006.07.011

Sinha, S., Anderson, J. P., Barbour, R., Basi, G. S., Caccavello, R., Davis, D., et al. (1999). Purification and cloning of amyloid precursor protein beta-secretase from human brain. *Nature* 402, 537–540. doi: 10.1038/990114

Small, D. H. (2009). Dysregulation of calcium homeostasis in alzheimer's disease. *Neurochem. Res.* 34, 1824–1829. doi: 10.1007/s11064-009-9960-5

Smith, I. F., Green, K. N., and LaFerla, F. M. (2005). Calcium dysregulation in alzheimer's disease: recent advances gained from genetically modified animals. *Cell Calcium* 38, 427–437. doi: 10.1016/j.ceca.2005.06.021

Spires, T. L., Meyer-Luehmann, M., Stern, E. A., McLean, P. J., Skoch, J., Nguyen, P. T., et al. (2005). Dendritic spine abnormalities in amyloid precursor protein transgenic mice demonstrated by gene transfer and intravital multiphoton microscopy. *J. Neurosci.* 25, 7278–7287. doi: 10.1523/JNEUROSCI.1879-05.2005

Spires-Jones, T., and Knafo, S. (2012). Spines, plasticity, and cognition in alzheimer's model mice. *Neural Plast* 2012:319836. doi: 10.1155/2012/319836

Spires-Jones, T. L., de Calignon, A., Meyer-Luehmann, M., Bacskai, B. J., and Hyman, B. T. (2011). Monitoring protein aggregation and toxicity in alzheimer's disease mouse models using *in vivo* imaging. *Methods* 53, 201–207. doi: 10.1016/j.ymeth.2010.12.009

Spires-Jones, T. L., Meyer-Luehmann, M., Osetek, J. D., Jones, P. B., Stern, E. A., Bacskai, B. J., et al. (2007). Impaired spine stability underlies plaque-related spine loss in an alzheimer's disease mouse model. *Am. J. Pathol.* 171, 1304–1311. doi: 10.2353/ajpath.2007.070055

Stephen, T. L., Tamagnini, F., Piegsa, J., Sung, K., Harvey, J., Oliver-Evans, A., et al. (2019). Imbalance in the response of pre- and post-synaptic components to amyloidopathy. *Sci. Rep.* 9:14837. doi: 10.1038/s41598-019-50781-1

St-Pierre, M. K., Simoncicova, E., Bogi, E., and Tremblay, M. E. (2020). Shedding light on the dark side of the microglia. *ASN Neuro* 12:1759091420925335. doi: 10.1177/1759091420925335

Stratoulias, V., Venero, J. L., Tremblay, M. E., and Joseph, B. (2019). Microglial subtypes: diversity within the microglial community. *EMBO J.* 38:e101997. doi: 10.15252/embj.2019101997

Subramanian, J., Michel, K., Benoit, M., and Nedivi, E. (2019). CPG15/neuritin mimics experience in selecting excitatory synapses for stabilization by facilitating PSD95 recruitment. *Cell Rep. 28,* 1584–1595.e1585. doi: 10.1016/j.celrep.2019.07.012

Sze, C. I., Troncoso, J. C., Kawas, C., Mouton, P., Price, D. L., and Martin, L. J. (1997). Loss of the presynaptic vesicle protein synaptophysin in hippocampus correlates with cognitive decline in alzheimer disease. *J. Neuropathol. Exp. Neurol.* 56, 933–944. doi: 10.1097/00005072-199708000-00011

Takasaki, K., Abbasi-Asl, R., and Waters, J. (2020). Superficial bound of the depth limit of two-photon imaging in mouse brain. *eNeuro* 7:ENEURO.0255-19.2019. doi: 10.1523/ENEURO.0255-19.2019

Tampellini, D., Capetillo-Zarate, E., Dumont, M., Huang, Z., Yu, F., Lin, M. T., et al. (2010). Effects of synaptic modulation on beta-amyloid, synaptophysin, and memory performance in alzheimer's disease transgenic mice. *J. Neurosci.* 30, 14299–14304. doi: 10.1523/JNEUROSCI.3383-10.2010

Tay, T. L., Savage, J. C., Hui, C. W., Bisht, K., and Tremblay, M. E. (2017). Microglia across the lifespan: from origin to function in brain development, plasticity and cognition. *J. Physiol.* 595, 1929–1945. doi: 10.1113/JP272134

Terry, R. D. (2000). Cell death or synaptic loss in alzheimer disease. *J. Neuropathol. Exp. Neurol.* 59, 1118–1119. doi: 10.1093/jnen/59.12.1118

Terry, R. D., Masliah, E., Salmon, D. P., Butters, N., DeTeresa, R., Hill, R., et al. (1991). Physical basis of cognitive alterations in alzheimer's disease: synapse loss is the major correlate of cognitive impairment. *Ann. Neurol.* 30, 572–580. doi: 10.1002/ana.410300410

Trachtenberg, J. T., Chen, B. E., Knott, G. W., Feng, G., Sanes, J. R., Welker, E., et al. (2002). Long-term *in vivo* imaging of experience-dependent synaptic plasticity in adult cortex. *Nature* 420, 788–794. doi: 10.1038/nature01273

Tremblay, M. E., Lowery, R. L., and Majewska, A. K. (2010). Microglial interactions with synapses are modulated by visual experience. *PLoS Biol.* 8:e1000527. doi: 10.1371/journal.pbio.1000527

Tsai, J., Grutzendler, J., Duff, K., and Gan, W. B. (2004). Fibrillar amyloid deposition leads to local synaptic abnormalities and breakage of neuronal branches. *Nat. Neurosci.* 7, 1181–1183. doi: 10.1038/nn1335

Vassar, R., Bennett, B. D., Babu-Khan, S., Kahn, S., Mendiaz, E. A., Denis, P., et al. (1999). Beta-secretase cleavage of alzheimer's amyloid precursor protein by the transmembrane aspartic protease BACE. *Science* 286, 735–741. doi: 10.1126/science.286.5440.735

Villa, K. L., Berry, K. P., Subramanian, J., Cha, J. W., Oh, W. C., Kwon, H. B., et al. (2016). Inhibitory synapses are repeatedly assembled and removed at persistent sites *in vivo*. *Neuron* 89, 756–769. doi: 10.1016/j.neuron.2016.01.010

Wendt, S., Maricos, M., Vana, N., Meyer, N., Guneykaya, D., Semtner, M., et al. (2017). Changes in phagocytosis and potassium channel activity in microglia of 5xFAD mice indicate alterations in purinergic signaling in a mouse model of alzheimer's disease. *Neurobiol. Aging* 58, 41–53. doi: 10.1016/j.neurobiolaging.2017.05.027

Wirths, O., and Bayer, T. A. (2010). Neuron loss in transgenic mouse models of alzheimer's disease. *Int. J. Alzheimers. Dis.* 2010:723782. doi: 10.4061/2010/723782

Wisniewski, H. M., Wegiel, J., Wang, K. C., Kujawa, M., and Lach, B. (1989). Ultrastructural studies of the cells forming amyloid fibers in classical plaques. *Can. J. Neurol. Sci.* 16, 535–542. doi: 10.1017/S0317167100029887

Wisniewski, T., and Sigurdsson, E. M. (2010). Murine models of alzheimer's disease and their use in developing immunotherapies. *Biochim. Biophys. Acta* 1802, 847–859. doi: 10.1016/j.bbadis.2010.05.004

Wu, H. Y., Hudry, E., Hashimoto, T., Kuchibhotla, K., Rozkalne, A., Fan, Z., et al. (2010). Amyloid beta induces the morphological neurodegenerative triad of spine loss, dendritic simplification, and neuritic dystrophies through calcineurin activation. *J. Neurosci.* 30, 2636–2649. doi: 10.1523/JNEUROSCI.4456-09.2010

Xie, H., Guan, J., Borrelli, L. A., Xu, J., Serrano-Pozo, A., and Bacskai, B. J. (2013). Mitochondrial alterations near amyloid plaques in an alzheimer's disease mouse model. *J. Neurosci.* 33, 17042–17051. doi: 10.1523/JNEUROSCI.1836-13.2013

Yan, P., Bero, A. W., Cirrito, J. R., Xiao, Q., Hu, X., Wang, Y., et al. (2009). Characterizing the appearance and growth of amyloid plaques in APP/PS1 mice. *J. Neurosci.* 29, 10706–10714. doi: 10.1523/JNEUROSCI.2637-09.2009

Yan, R., Bienkowski, M. J., Shuck, M. E., Miao, H., Tory, M. C., Pauley, A. M., et al. (1999). Membrane-anchored aspartyl protease with alzheimer's disease beta-secretase activity. *Nature* 402, 533–537. doi: 10.1038/990107

Yin, Z., Raj, D., Saiepour, N., Van Dam, D., Brouwer, N., Holtman, I. R., et al. (2017). Immune hyperreactivity of Abeta plaque-associated microglia in alzheimer's disease. *Neurobiol. Aging* 55, 115–122. doi: 10.1016/j.neurobiolaging.2017.03.021

Yoshiyama, Y., Higuchi, M., Zhang, B., Huang, S. M., Iwata, N., Saido, T. C., et al. (2007). Synapse loss and microglial activation precede tangles in a P301S tauopathy mouse model. *Neuron* 53, 337–351. doi: 10.1016/j.neuron.2007.01.010

Yu, W., and Lu, B. (2012). Synapses and dendritic spines as pathogenic targets in alzheimer's disease. *Neural Plast* 2012:247150. doi: 10.1155/2012/247150

Yuan, P., Condello, C., Keene, C. D., Wang, Y., Bird, T. D., Paul, S. M., et al. (2016). TREM2 Haplodeficiency in mice and humans impairs the microglia barrier function leading to decreased amyloid compaction and severe axonal dystrophy. *Neuron* 90, 724–739. doi: 10.1016/j.neuron.2016.05.003

Zhang, X. M., Cai, Y., Xiong, K., Cai, H., Luo, X. G., Feng, J. C., et al. (2009). Beta-secretase-1 elevation in transgenic mouse models of alzheimer's disease is associated with synaptic/axonal pathology and amyloidogenesis: implications for neuritic plaque development. *Eur. J. Neurosci.* 30, 2271–2283. doi: 10.1111/j.1460-9568.2009.07017.x

Zhao, R., Hu, W., Tsai, J., Li, W., and Gan, W. B. (2017). Microglia limit the expansion of beta-amyloid plaques in a mouse model of alzheimer's disease. *Mol. Neurodegener.* 12:47. doi: 10.1186/s13024-017-0188-6

Ziegler-Waldkirch, S., d'Errico, P., Sauer, J. F., Erny, D., Savanthrapadian, S., Loreth, D., et al. (2018). Seed-induced Abeta deposition is modulated by microglia under environmental enrichment in a mouse model of alzheimer's disease. *EMBO J.* 37, 167–182. doi: 10.15252/embj.201797021

Zou, C., Montagna, E., Shi, Y., Peters, F., Blazquez-Llorca, L., Shi, S., et al. (2015). Intraneuronal APP and extracellular Abeta independently cause dendritic spine pathology in transgenic mouse models of alzheimer's disease. *Acta Neuropathol.* 129, 909–920. doi: 10.1007/s00401-015-1421-4

Zou, C., Shi, Y., Ohli, J., Schuller, U., Dorostkar, M. M., and Herms, J. (2016). Neuroinflammation impairs adaptive structural plasticity of dendritic spines in a preclinical model of alzheimer's disease. *Acta Neuropathol.* 131, 235–246. doi: 10.1007/s00401-015-1527-8

Conflict of Interest: The authors declare that the research was conducted in the absence of any commercial or financial relationships that could be construed as a potential conflict of interest.

Advantages of publishing in Frontiers

OPEN ACCESS
Articles are free to read for greatest visibility and readership

FAST PUBLICATION
Around 90 days from submission to decision

HIGH QUALITY PEER-REVIEW
Rigorous, collaborative, and constructive peer-review

TRANSPARENT PEER-REVIEW
Editors and reviewers acknowledged by name on published articles

Frontiers
Avenue du Tribunal-Fédéral 34
1005 Lausanne | Switzerland

Visit us: www.frontiersin.org
Contact us: frontiersin.org/about/contact

REPRODUCIBILITY OF RESEARCH
Support open data and methods to enhance research reproducibility

DIGITAL PUBLISHING
Articles designed for optimal readership across devices

FOLLOW US
@frontiersin

IMPACT METRICS
Advanced article metrics track visibility across digital media

EXTENSIVE PROMOTION
Marketing and promotion of impactful research

LOOP RESEARCH NETWORK
Our network increases your article's readership